Integrability, Defects, and Flows in 2 and 4 Dimensional Quantum Field Theories

Dissertation

zur Erlangung des Doktorgrades
an der Fakultät für Mathematik,
Informatik und Naturwissenschaften

Fachbereich Physik
der Universität Hamburg

Vorgelegt von
Federico Ambrosino

Hamburg
2025

Gutachter/innen der Dissertation:	Prof. Dr. Jörg Teschner Prof. Dr. Volker Schomerus
Zusammensetzung der Prüfungskommission:	Prof. Dr. Elisabetta Gallo Prof. Dr. Sven-Olaf Moch Prof. Dr. Elli Pomoni Prof. Dr. Jörg Teschner Prof. Dr. Volker Schomerus
Vorsitzende/r der Prüfungskommission:	Prof. Dr. Sven-Olaf Moch
Datum der Disputation:	29.10.2025
Vorsitzender Fach-Promotionsausschusses PHYSIK:	Prof. Dr. Wolfgang J. Parak
Leiter des Fachbereichs PHYSIK:	Prof. Dr. Markus Drescher
Dekan der Fakultät MIN:	Prof. Dr. -Ing. Norbert Ritter

Abstract

This thesis investigates the interplay between integrability, defects, and renormalization group (RG) flows, in quantum field theories in 2 and 4 dimensions.

In the first part, we study the analytic properties and integrable structure of the meson spectrum in the large N_c limit of two-dimensional QCD. In this regime, the integral equation governing meson masses is shown to be equivalent to a TQ-Baxter equation, characteristic of integrable models. This reformulation gives access to the analytic structure of the spectrum in the complex plane of the quark masses. We demonstrate that the description via a spectral curve persists in a broader class of "generalized QCD" models with BF-type interactions, enabling the identification of new infrared phases and critical points.

The second part focuses on the symmetries and renormalization group flows of perturbed two-dimensional Conformal Field Theories (CFTs). We propose a new class of non-linear integral equations that encode the finite-size spectrum along RG flows between Virasoro minimal models, motivated by anomaly matching of non-invertible symmetries. Furthermore, we characterize a family of non-topological yet conserved defects in perturbed CFTs. These defects give rise to conserved charges along the RG flow, and extend topological symmetries. Applying this framework to minimal models, we establish the existence of infinite sets of non-local commuting charges, beyond previously known integrable deformations.

The final part examines the Schur quantization of four-dimensional $\mathcal{N} = 2$ supersymmetric theories and its interplay with RG flows, along with related mathematical and physical problems. We construct the quantization of the complex Teichmüller space, which describes the outcome of Schur quantization for class $\mathcal{S}$ theories. The quantum analytic Langlands correspondence emerges as a special case of Schur quantization. In a particular limit, this correspondence yields a geometric characterization of the spectrum of the quantum Hitchin integrable system in terms of real opers. Using the Separation of Variables method for the Gaudin integrable model, we provide a proof of the analytic Langlands correspondence for genus-zero curves.

Zusammenfassung

Diese Dissertation untersucht das Zusammenspiel zwischen Integrierbarkeit, Symmetrien, Korrespondenzen und Renormierungsgruppenflüssen (RG-Flüsse) in Quantenfeldtheorien in zwei und vier Dimensionen.

Im ersten Teil analysieren wir die analytischen Eigenschaften und die integrable Struktur des Mesonspektrums im Limes großer N_c der zweidimensionalen QCD. In diesem Regime zeigt sich, dass die Integralgleichung, welche die Mesonenmassen bestimmt, einer TQ-Baxter-Gleichung entspricht, wie sie aus integrablen Modellen bekannt ist. Diese Reformulierung ermöglicht den Zugang zur analytischen Struktur des Spektrums in der komplexen Ebene der Quarkmassen. Wir zeigen, dass diese emergente Integrierbarkeit auch in einer erweiterten Klasse von „verallgemeinerten QCD"-Modellen mit BF-artigen Wechselwirkungen erhalten bleibt, wodurch neue Infrarotphasen und kritische Punkte identifiziert werden können.

Der zweite Teil befasst sich mit den Symmetrien und Renormierungsgruppenflüssen deformierter zweidimensionaler konformer Feldtheorien (CFTs). Wir schlagen eine neue Klasse nichtlinearer Integralgleichungen vor, die das Spektrum endlicher Volumina entlang von RG-Flüssen zwischen Virasoro-Minimalmodellen kodieren. Diese Gleichungen sind motiviert durch Anomalieabgleiche nicht-invertierbarer Symmetrien. Darüber hinaus charakterisieren wir eine Familie nicht-topologischer, jedoch erhaltener Defekte in deformierten CFTs. Diese Defekte erzeugen erhaltene Ladungen entlang des RG-Flusses, erweitern die Kategorie topologischer Symmetrien und kodieren nichttriviale dynamische Informationen. Durch Anwendung dieses Rahmens auf Minimalmodelle zeigen wir die Existenz unendlich vieler nicht-lokaler kommutierender Ladungen, auch in Fällen jenseits der bisher bekannten integrablen Deformationen.

Der letzte Teil behandelt die Schur-Quantisierung von vierdimensionalen $\mathcal{N} = 2$ supersymmetrischen Theorien und ihr Zusammenspiel mit RG-Flüssen sowie verwandten mathematischen und physikalischen Problemen. Wir konstruieren die Quantisierung des komplexen Teichmüller-Raums, welcher das Ergebnis der Schur-Quantisierung für Theorien der Klasse $\mathcal{S}$ beschreibt. Die quantenanalytische Langlands-Korrespondenz ergibt sich dabei als Spezialfall der Schur-Quantisierung. In einem bestimmten Grenzfall liefert diese Korrespondenz eine geometrische Charakterisierung des einwertigen Spektrums des quantenmechanischen Hitchin-Integrablesystems in Form realer Oper. Wir verwenden die Methode der Separation der Variablen für Gaudin-Systeme, um einen Beweis der analytischen Langlands-Korrespondenz für Kurven vom Geschlecht Null zu liefern.

Declaration on Oath

I hereby declare and affirm that this doctoral dissertation is my own work and that I have not used any aids and sources other than those indicated.

If electronic resources based on generative artificial intelligence (gAI) were used in the course of writing this dissertation, I confirm that my own work was the main and value-adding contribution and that complete documentation of all resources used is available in accordance with good scientific practice. I am responsible for any erroneous or distorted content, incorrect references, violations of data protection and copyright law or plagiarism that may have been generated by the gAI.

Hamburg, 04.08.2025



Acknowledgments

First and foremost, I would like to express my gratitude to my advisor, Jörg Teschner, for his guidance, patience, and constant flow of ideas throughout my PhD journey. His mentorship and integrity has shaped not only the direction of my research but also the way I approach scientific questions. I would also like to sincerely thank Shota Komatsu, for his dedication, support and infinite insights, before and during the entirety of this PhD. Your help has been invaluable. The merit goes to all my collaborators - D. Gaiotto, G. Watts, I. Runkel, S. Negro, T. Procházka, R. Luo, Y. Zhang, and Y-N. Wang - for all the fun and interesting discussions across all possible timezones; I have learned so much from any of you.

A wonderful group of postdocs and PhD students has contributed to making DESY such an exciting and rich scientific environment. It would be impossible to acknowledge each and every one of you by name, but I want to especially thank Sophie, Alessio, Carlos & Ana, Deniz, Sebastian, Gabriele, and Lorenzo, that shared each and every step of this process with me and, Davide, Enrico, Philine, Guido, Jonah, Francesco and many others who made this experience so much more than just physics. Sharing lunches, coffee breaks, and everyday life in and outside the office with you all has been a true pleasure. Thank you all — your presence made this journey memorable.
I am also indebted to the Journal Club for all the physics I learned by presenting (basically) every week. A special thank goes to the DESY canteen that made me appreciate the delight of a well balanced home-cooked meal.

During these three years, I was lucky enough to have had several incredible opportunities to visit and interact with amazing physicist and people from all over the world, from Brazil to the US and Canada: I am truly indebted to all the people that made this possible. I want to mention especially some friends sprinkled among many continents - Enrico, Andrea, Bernardo, Gabriel, Alessandro - for the unwavering help, advices and a lot of fun at many points of this journey, Jack - for the amazing time in NYC and DC - Aiden, Anna, Alessandro, Sasha for a truly wonderful time at TASI, and many more.

I also want to thank my right arm and hand that decided to break while preparing this thesis. I surely will blame them for all the mistakes a reader may find in this work. If this thesis has taken shape it is for the support of my mother and Sophie. Without your help through such an difficult time (left-)handing my thesis would have been impossible.

To my mum and dad, my brother, my nonno and all my family: thanks for always supporting, understanding, and believing in me.

Finally, to my *Freundin* Sophie: you have been by my side since the very first day, and filled every single step of this journey with joy. Your support, care, and love have meant more than I can put into words. I am grateful we shared this together — you are the one who made this PhD a truly wonderful experience.

Author's contributions

This thesis is based on original contributions by the author. Specifically:

- Part I is based on:
  - ⋆ F. Ambrosino and S. Komatsu, *2d QCD and integrability. Part I. 't Hooft model*, *JHEP* **0**2 (2025) 126, [arXiv:2312.15598]
  - ⋆ F. Ambrosino and S. Komatsu, *2d QCD and Integrability. Part II. Generalized QCD*, [arXiv:2406.11078].
- Part II is based on:
  - ⋆ F. Ambrosino and S. Negro, *Minimal Model Renormalization Group Flows: Non-invertible Symmetries and Non-perturbative Description*, *Phys. Rev. Lett.* **1**35 (2025), no. 2 021602, [arXiv:2501.07511]
  - ⋆ F. Ambrosino, I. Runkel, and G. M. T. Watts, *Non-local charges from perturbed defects via SymTFT in 2d CFT*, [arXiv:2504.05277], accepted at J Phys A
  - ⋆ F. Ambrosino, T. Procházka, *RCFT with $\mathcal{W}$-algebra symmetry: non-invertible symmetries & flows*, [arXiv:2601.18667]
- Part III is based on:
  - ⋆ F. Ambrosino and D. Gaiotto, *Renormalization Group flow in Schur quantization*, [arXiv:2503.16685], submitted at JHEP
  - ⋆ F. Ambrosino and J. Teschner, *Analytic Langlands correspondence from* SoV, [arXiv:2510.06991]

The author has also contributed to the following publication, that has not been included in this thesis:

- F. Ambrosino, R. Luo, Y.-N. Wang, and Y. Zhang, *Understanding fermionic generalized symmetries*, *Phys. Rev. D* **1**10 (2024), no. 10 105020, [arXiv:2404.12301]

Contents

Abstract i
Declaration on Oath iv
Acknowledgments v
Author's contributions vi

Contents **vii**

1 General Introduction **3**
1.1 Strongly coupled quantum fields and where to find them 4
1.2 General outlook 5
1.3 Overview of the thesis 12

I Two dimensional QCD and Integrability **23**

2 Introduction **25**

3 The 't Hooft model **29**
3.1 A two-dimensional model for mesons 30
3.2 't Hooft equation as a TQ-system 36
3.3 Meson spectrum at complex quark mass and critical points 46
3.4 Extracting spectral data 53
3.5 Application to non-perturbative topological string 66

4 Generalized QCD **71**
4.1 Generalized QCD in the large N limit 72
4.2 Generalized 't Hooft equation as a TQ-system 76
4.3 Analytical structure of the spectrum and critical points 81
4.4 Mesons spectrum in the large representation limit 95

5 Outlook **103**

A Supplement to Part I **107**
A.1 Recurrence relation for integrals 107
A.2 Derivation of the bound state equation in the large representation limit 108

A.3 Numerical methods for analytical continuation 110
A.4 Non-critical spontaneous symmetry breaking of $\mathcal{PT}$-symmetry . . . 111

II Symmetries and flows of deformed 2d CFTs 115

6 Introduction 117

7 Non-invertible symmetries and flows between minimal models 121
7.1 Primer on Virasoro minimal models. 122
7.2 RG flows between Virasoro Minimal Models 123
7.3 Description via NLIE 126

8 Conserved Defects in 2D CFTs 135
8.1 SymTFT and non-local conserved charges 139
8.2 Non-local commuting charges in minimal models 154
8.3 Local conserved charges 166

9 Outlook 175

B Supplement to Part II 181
B.1 Detailed description of some RG flows 181
B.2 F-matrix in the case $\boldsymbol{x} \otimes \boldsymbol{x} \cong \mathbf{1}$ 184
B.3 Bulk commutation condition and mutual commutativity for $\mathcal{D} = \mathbf{1} \oplus x$185
B.4 Details of the calculation of a local conserved current 189

III The Analytic Langland Correspondance and Schur Quantization of 4d $\mathcal{N} = 2$ QFT 191

10 Introduction 193

11 The Langlands Correspondance 199
11.1 The many faces of the Langlands Correspondence 199
11.2 Quantum Analytic Langlands: a tale of two CFTs 211
11.3 Analytic Langlands correspondence from SoV 216

12 RG flows in Schur Quantization 233
12.1 Schur meets RG 234
12.2 Schur pairing and the Schur index 241
12.3 Schur Quantization 248
12.4 A minimal sequence of examples: rank 2 lattice 255
12.5 Adding Flavor: the $\mathcal{N} = 2^*$ $SU(2)$ example 265
12.6 The Spectrum Generator for RG flows triggered by large masses. . . 271

12.7 Towards higher ranks: examples with $SU(3)$ gauge group 285
12.8 Applications to the theory of quantum groups 289
12.9 Partial RG flows and $SL(2)$ character varieties 294
12.10Quantization of the Teichmüller space 296

13 Outlook **303**

C Supplement to Part III **307**
C.1 A primer on H_3^+ and Liouville CFT 307
C.2 Spectral problem on the annulus 310

Bibliography **319**

Chapter 1

General Introduction

Considerate la vostra semenza:
fatti non foste a viver come bruti,
ma per seguir virtute e canoscenza

Canto XXVI, Inferno, Dante

A comprehensive non-perturbative understanding of the low-energy behavior of strongly coupled four-dimensional gauge theories–particularly the mechanisms underlying color confinement–remains one of the most profound and challenging problems in Quantum Field Theory (QFT). In this regime, the coupling constant becomes large, causing traditional perturbative methods to break down and necessitating alternative, often highly sophisticated, approaches.

Approaching the study of quantum field theories (QFTs) from a non-perturbative perspective will be the *leitmotiv* of this thesis. In our investigations, we combine the power of symmetries and dualities with techniques from exactly solvable models—such as integrable and conformal field theories—to gain access to the spectra and renormalization group flows of QFTs in various dimensions.
The long-standing goal of solving strongly coupled gauge theories lies well beyond our current capabilities. As such, we are compelled to explore fundamentally new approaches to tackle these enduring problems. It is our responsibility to both refine established methods and develop entirely new, original ideas and techniques.
To this end, it is often essential to analyze models that exhibit features of strongly coupled physics but in controlled settings that permit analytic and quantitative treatment. New ideas and insights are best developed and tested in these tractable contexts, where we typically have access to a richer set of tools and approaches.
The hope is that the methods and concepts developed in the context of solvable or highly symmetric models will eventually shed light on the dynamics of more realistic, less tractable systems. This is the philosophy we follow in this thesis.

1.1 Strongly coupled quantum fields and where to find them

Strongly coupled systems are ubiquitous in nature. As a source of enduring motivation, let us briefly highlight several instances where where we are forced upon non-perturbative QFTs.
This overview is deliberately non-technical and aims to convey the flavor of how seemingly unrelated physical systems–ranging from high-energy particle physics to cold dilute atomic gases, passing through gravitational theories in Anti-de Sitter (AdS) space –can all give rise to strongly coupled quantum fields.
Despite their diversity, these systems share a common and formidable challenge: their dynamics cannot be fully captured by small perturbations around a classical background. Instead, they demand fundamentally new methods and insights, grounded in non-perturbative approaches.

Particle physics. From a phenomenological standpoint, the importance of strongly coupled dynamics in particle physics is evident. Non-Abelian gauge theories that describe the strong interaction are well understood in the high-energy regime, thanks to asymptotic freedom. In this limit, experimental measurements and theoretical predictions exhibit remarkable agreement.
However, the low-energy regime remains far more elusive. Describing phenomena such as confinement, mass generation, and dynamical symmetry breaking requires a complete resummation of both perturbative and non-perturbative effects—a task that lies well beyond the reach of conventional techniques.

Condensed matter. Strong coupling also plays a central role in condensed matter systems, where many-body problems often give rise to rich emergent phenomena that admit a continuum field theory description. A prominent example is high-temperature superconductivity, in which electron-electron interactions are too strong to be treated perturbatively (e.g. cfr. [8,9] and references therein). In these materials, the standard Bardeen-Cooper-Schrieffer (BCS) theory[10]– describing conventional superconductors–breaks down. Instead, the physics likely involves strong correlations, spin fluctuations, or even emergent gauge fields.
Similarly, at quantum critical points, quantum fluctuations dominate across all energy scales, leading to strongly coupled behavior. Near such points, systems exhibit scale invariance and universal features that are effectively described by strongly coupled Conformal Field Theories (CFTs).

Quantum gravity. Another compelling motivation for studying strongly coupled gauge theories lies in their deep and surprising connection to gravity.

Gauge/gravity duality [11] provides a powerful framework that posits an equivalence between certain strongly coupled gauge theories and weakly coupled gravitational theories in higher-dimensional spacetimes. The most celebrated example is

the AdS/CFT correspondence[12], which relates supersymmetric, strongly coupled conformal gauge theories (with a large gap) in the 't Hooft limit to perturbative string theory on backgrounds that are asymptotically Anti-de Sitter (AdS).
In this regime, the gravitational description becomes classical, and the duality enables the computation of strongly coupled gauge-theoretic observables—such as Wilson loops—in terms of geometric quantities in supergravity. Conversely, the gauge theory side offers a non-perturbative definition of certain quantum gravity theories. This duality thus opens an invaluable window into the non-perturbative regime of quantum gravity.

Relation to geometry. Quantum Field Theories (QFTs) have profoundly influenced and inspired modern developments in mathematics, particularly in areas such as enumerative geometry, algebraic geometry, and the study of moduli spaces. A famous example is mirror symmetry[13], originally postulated within string theory, which has since established deep and unexpected connections[14,15] between complex and symplectic geometry.
Supersymmetric theories, integrable models, and two-dimensional conformal field theories (CFTs) have also have profound relations to various aspects of the Geometric Langlands program[16–22], as we will witness throughout this thesis. This dialogue has led to a rich and fruitful dialogue, advancing parallel developments in both physics and mathematics.

1.2 General outlook

We are not groping in the dark when it comes to exact non-perturbative results.

The path towards a complete understanding of gauge theories across dimensions is a challenging and intricate one. Yet, there is no reason for despair: over the years, a wide array of powerful tools—both numerical and analytical—have been developed to access physical observables in interacting quantum field theories.
In this section, we provide a bird's-eye view of the main themes and questions addressed in this thesis, setting the stage for the more detailed discussions to follow in subsequent chapters. A comprehensive account of our specific results is deferred to the next section.

1.2.1 Solvable models: a window to strongly coupled physics

Extended symmetries. Models endowed with extended symmetries–whether spacetime or internal–serve as ideal testing grounds for exact methods in quantum field theory.

Conformal Field Theories (CFTs) are the most prominent example of QFTs with such enhanced symmetries. These theories are invariant under coordinate transformations that preserve angles, i.e., conformal transformations. By definition, CFTs describe quantum field theories at exact fixed points of the renormalization

group (RG) flow, where the notion of a small coupling expansion often breaks down or is entirely absent.
Nevertheless, their extended symmetry provides a powerful framework[23] in which correlation functions and scaling dimensions are tightly constrained by conformal invariance alone[24–26]. In two dimensions, conformal field theories attain an even more exceptional status[27]: conformal symmetry is enhanced to the infinite-dimensional Virasoro algebra, rendering many of these theories exactly solvable and showcasing the analytical power of symmetry in its purest form.

Supersymmetry (SUSY) offers an alternative and highly effective pathway to accessing non-perturbative physics. The additional structure imposed by supersymmetry often leads to remarkable analytic control, enabling exact computations of physical quantities such as beta functions, anomalous dimensions, and vacuum structures—even at strong coupling.
SUSY also provides a powerful framework for studying inherently non-perturbative phenomena such as instantons, monopoles, and solitons [28,29]. In many cases, it protects certain special states—known as BPS states—from acquiring quantum corrections, thereby making them exactly computable. Moreover, supersymmetry plays a central role in uncovering deep dualities, such as Seiberg duality[30] and S-duality[31–33], which relate strongly and weakly coupled theories in non-trivial ways.

Theories with large global or gauge symmetries–such as the $O(N)$ model[34] or planar gauge theories[35]–also provide controlled settings for exploring non-perturbative physics. One particularly powerful approach is the large-N expansion, pioneered by 't Hooft[35,36], which has proven very effective in analyzing non-perturbative phenomena such as confinement, string-like flux tubes, and the planar limit structure of gauge theories. More recently, significant attention has been devoted to studying the regime of large quantum numbers[37–40]—such as large spin, charge, or angular momentum. In these limits, the collective behavior of the system often becomes semi-classical, allowing for tractable analytic approaches and revealing universal features across different theories.

Low-dimensional toy models. Complementary to the approach of leveraging symmetry is the study of lower-dimensional quantum field theories, which offer simplified yet profoundly rich settings in which many non-perturbative features of higher-dimensional gauge theories can manifest in analytically tractable ways.
Two-dimensional models—such as the $\mathbb{CP}^N$ sigma model[41], the Gross-Neveu model[42], and the 't Hooft model[43]—exhibit hallmark phenomena like asymptotic freedom, instantons, and the generation of a mass gap, mirroring some of the features of four-dimensional QCD. Even one-dimensional quantum mechanical systems, such as supersymmetric quantum mechanics[44] and the Sachdev-Ye-Kitaev (SYK) model[45,46], have proven influential. The former provides a clean framework for studying BPS spectra and computing Witten indices, while the

latter has garnered significant attention for its rich connections to quantum chaos, holography, and emergent conformal symmetry in the infrared.
By reducing dimensionality, these models suppress many technical complexities while preserving essential physical mechanisms—such as confinement, duality, and topological structure—making them indispensable theoretical laboratories for probing quantum field theories.

Integrability. Quantum integrable systems occupy a important role in many areas of theoretical physics. These are typically models that possess a large—often infinite—number of conserved quantities. The theory of integrable systems has not only played a foundational role in our field for over a century, but it also serves as a key theme throughout this thesis.

Famous integrable spin chains, such as the XXX spin chain [47]and the Hubbard model [48], appear in a wide range of contexts—from statistical mechanics to $\mathcal{N} = 4$ super Yang-Mills theory[49]. In integrable quantum field theories[50], the conserved charges are frequently associated with infinite towers of higher-spin symmetries. As a result, strict integrability is compatible only with two-dimensional kinematics in interacting QFTs. This restriction simplifies the dynamics dramatically: multi-particle interactions reduce to a sequence of exactly solvable two-body scatterings, with the two-body S-matrix satisfying the celebrated Yang-Baxter equation [51,52]. Two-dimensional integrable models are thus highly constrained and solvable, featuring purely elastic (no particle production) and factorized scattering. Their spectra are non-chaotic and are often captured by Baxter-type TQ systems a.k.a. quantum spectral curves.
Integrable systems sits at very special corners of the space of two-dimensional QFTs, saturating unitary $SS^\dagger = 1$, as beautifully illustrated by S-matrix bootstrap program [53,54]. Notable examples include the sine-Gordon model, and some special deformations of Minimal Models of 2d CFT [55], as we will encounter in this thesis.

1.2.2 Extended operators in QFTs

Extended operators are observables associated not with points in spacetime, like local operators, but with extended geometrical objects such as lines, surfaces, or higher-dimensional manifolds. These operators probe non-local aspects of a QFT that cannot be captured by correlation functions of local operators.
Prominent examples include Wilson lines, which trace the holonomy of gauge fields along curves and serve as order parameters for confinement, and 't Hooft operators, which introduce prescribed singularities in the gauge field configuration that mimic the presence of magnetic monopoles. More generally, QFTs admit operators supported on manifolds of arbitrary codimension, each of which captures distinct and often subtle features of the theory. A complete understanding of a QFT must therefore include a systematic treatment of such extended operators at

all energy scales.
In condensed matter physics, extended operators play also an important role. Defects—such as impurities, vortices, dislocations, or domain walls—are localized in specific regions of space and are directly relevant to experimental observations. A paradigmatic example is the Kondo effect[56,57], in which a magnetic impurity behaves as a quantum defect embedded in a sea of conduction electrons, leading to rich and non-trivial many-body dynamics.

Supersymmetric defects. A BPS defect is a localized operator or configuration in a supersymmetric field theory that preserves part of the bulk supersymmetry. These defects saturate a Bogomol'nyi–Prasad–Sommerfield (BPS)-like bound, making them highly constrained. Often, they obey short multiplet conditions, are protected from acquiring quantum corrections, and remain invariant under renormalization group (RG) flow. Among the most studied examples are BPS Wilson and 't Hooft line operators, characterized by their electric and magnetic charges[58,59]. These BPS line defects play a central role in in low energy description of $\mathcal{N} = 2$ theories, where they act as both probes and sources for BPS states in the Coulomb branch of the moduli space of vacua[60].
$\mathcal{N} = 2$ theories also admit protected surface operators of codimension 2 and 4[61]. These defects are associated with rich geometric structures, including Hitchin systems and connections to the analytic Langlands program[62].

Conformal defects. Defects in conformal field theories (CFTs) [63–65] can naturally be understood as low energy fixed points of renormalization group (RG). Just as a bulk CFT describes a scale-invariant fixed point in the full spacetime, a conformal defect corresponds to the IR description of the defect at the end of a combined bulk-defect RG flow, where local perturbations have flowed to a scale-invariant configuration.
For instance, a defect may arise by introducing a relevant operator localized along a line or surface. At long distances, the system flows to a defect CFT, characterized by its own spectrum and correlation functions, subject to the constraints of the residual conformal symmetry. This defines an important class of defects that we will encounter and study in detail throughout this thesis.

Topological defects as generalized global symmetries. Ordinary global symmetries in Lagrangian quantum field theory are often presented as groups transformations acting on the fields of the theory that leave the action invariant and under which local (point-like) operators are charged. However, this formulation has notable limitations: it tightly binds the notion of symmetry to a particular Lagrangian description and does not naturally accommodate quantum effects such as anomalies.
Recent developments across high-energy physics, condensed matter theory, quantum

information, and mathematics have led to a revival of the understanding of global symmetries[66]. This modern perspective provides a unifying framework for describing dualities, anomalies, topological obstructions, and other non-perturbative phenomena. The key insight driving this revolution is the realization that in QFT, topological operators of arbitrary codimension can implement generalized notions of global symmetry.
Topological defects are extended operators invariant under small deformations of their support. Codimension-1 topological operators that fuse according to a group law correspond to ordinary (invertible) both discrete and continuous symmetries. However, this new framework vastly generalizes the notion of symmetry to include a rich landscape of structures: higher-form symmetries, higher-group symmetries, non-invertible symmetries, and many others[67,68].
All the constraints and selection rules associated with these generalized symmetries are now accessible and can be systematically applied to extract powerful non-perturbative data. As we will see in this thesis, several of these modern ideas play a central role in our analysis.

1.2.3 Dualities, correspondences and integrability in $\mathcal{N} = 2$ theories

One of the most intriguing non-perturbative phenomena in theoretical physics is the existence of *dualities*. Dualities play an important role in our understanding of quantum field theories, and we have already encountered several noteworthy examples. Broadly speaking, a duality refers to a precise and quantitative correspondence between (a subset of) observables associated with two different descriptions of a theory. These descriptions may involve distinct Lagrangians, field content, or regimes, yet describe the same underlying physics. More precisely, two theories are said to be dual if the same physical observables can be expressed in terms of different sets of variables. This means that although the formulations may appear unrelated, they yield equivalent physical predictions[30,69].
The existence of dualities poses a fundamental challenge to the notion that a quantum field theory is uniquely defined by its Lagrangian. Many of the most striking dualities in QFT find geometric descriptions from embedding into String Theory, which offers a unifying framework where different field theories emerge as effective descriptions of various brane configurations or compactifications[70,71].
In this context, dualities between quantum field theories often reflect deeper string-theoretic symmetries—such as the equivalence of different brane setups (e.g. the Hanany–Witten transition[72]), the modular properties of compactification manifolds (as in T-duality[73]), or dualities between distinct string theories themselves (as in S-duality).

In some cases two seemingly different Lagrangian descriptions can flow to the same infrared physics, sharing identical spectra, correlation functions, and operator algebras. Those are often referred to as IR dualities and concern the IR description in terms of a particular low energy effective actions, that is not an intrinsic property

of the theory. The most prominent example of an IR duality is the Electro-Magnetic (EM) duality of a gauge theory admitting an IR effective description as an abelian gauge theory coupled to matter $S[A, \tau, q]$. In this case, the same low-energy theory admits dual descriptions via the pairs $(F, \tau, q) \leftrightarrow (\star F, -1/\tau, \tilde{q})$. This is an instance of a strong-weak duality, and often involves complicated non-perturbative relations between the matter observables q and $\tilde{q}$.

There are even more fundamental (UV) dualities generalizing the emergent IR EM duality to the full UV QFT. Those often lie under the umbrella-term of S-dualities. One of the most famous one is the Montonen-Olive conjecture[31,74] of a duality between $\mathcal{N} = 4$ SYM with gauge group and complexified coupling (G, τ) and the dual pair[1] $({}^L G, -1/\tau)$, where ${}^L G$ is the Langlands-dual group of G. This instance of S-duality in $\mathcal{N} = 4$ SYM also provides a remarkable relation with the Geometric Langlands Program[16]. As shown in [17], this connection arises via the mirror symmetry of categories of boundary conditions in a topologically twisted version of the theory.

$\mathcal{N} = 2$ dualities. 4d supersymmetric $\mathcal{N} = 2$ theories offer a beautiful realization of these universal features of QFTs[75]. Theories with 8 supercharges are highly constrained at long distances, where they exhibit a beautiful connection to quantum integrable systems and geometry.

Seiberg-Witten (SW) theory [32,76] encodes very elegantly the IR EM dualities. As a prototypical example, consider the SW solution of an $\mathcal{N} = 2$ $SU(N)$ theory: in the coulomb branch the abelian $U(1)^D$ low energy theory is encoded in a single holomorphic function (the *prepotential*) $\mathcal{F}(\boldsymbol{a})$ encoding all the couplings $\boldsymbol{\tau}$ as well as the low-energy effective action. Furthermore the prepotential realizes the special Kähler geometry of the Coulomb branch. The EM dualities are then beautifully encoded in the monodromy data around singular points in moduli space. Many $\mathcal{N} = 2$ theories also admit a description of the special geometry via a SW curve. In this description the symplectic pairs is realized by the periods of the canonical differential λ_{SW} on the SW curve over a basis of its intersecting cycles. In this description EM duality manifests elegantly as a change of basis.

Also UV dualities are beautifully encoded in the rich landscape of $\mathcal{N} = 2$ theories. The work [77] greatly expanded the S-duality of $\mathcal{N} = 4$ SYM by constructing a vast class of Lagrangian $\mathcal{N} = 2$ theories, now known as class $\mathcal{S}$, via the compactification of six-dimensional $(2, 0)$ theory on a punctured Riemann surfaces $\mathcal{C}$. Different pants decomposition of $\mathcal{C}$ correspond to distinct UV Lagrangian frame, all sharing the same low energy dynamics governed by the geometry of $\mathcal{C}$, generalizing EM duality.

AGT correspondence. These developments, in combination with supersymmetric localization techniques, led the foundation for the *Alday–Gaiotto–Tachikawa* (AGT) correspondence [78]. This remarkable duality asserts a precise matching between

[1] When G is not simply laces, the relation involves the lacing number $\tau \leftrightarrow -1/(n_G \tau)$

the Nekrasov partition functions of four-dimensional $\mathcal{N} = 2$ gauge theories of Class $\mathcal{S}$ on the Ω-background, and the conformal blocks of two-dimensional Liouville (or more generally, Toda) CFT on the same Riemann surface $\mathcal{C}$.
The correspondence has been further enriched to include BPS line and surface operators in the gauge theory, which map to specific insertions or modifications in the associated two-dimensional CFT. This deep and intricate bridge between four-dimensional supersymmetric gauge theories and two-dimensional CFT has led to highly non-trivial results.

Quantum integrable systems from the Coulomb branch. The special geometry of the low-energy description, defines a classical integrable model with base space the Coulomb branch of the $\mathcal{N} = 2$ theory, describing its moduli space of vacua in a S^1 compactification[60]. For theories of class $\mathcal{S}$, this is the moduli spaces of Higgs bundles, associated to the Hitchin integrable system. The SW curve corresponds exactly to the spectral curve of the integrable system.
As the 4d theory is placed on Ω-background many interesting quantum properties emerge. In the Nekrasov-Shatashivili limit, the SW prepotential is upgraded to a twisted superpotential $\mathcal{Y}(\boldsymbol{a}, \boldsymbol{\tau})$, that plays the role of the Yang-Yang potential providing *Bethe-ansatz*–like equations $\partial_{a_i}\mathcal{Y}(\boldsymbol{a}, \boldsymbol{\tau}) \in 2\pi i\mathbb{Z}$ encoding the spectrum of quantum integrable models $\partial_{\tau_r}\mathcal{Y}(\boldsymbol{a}, \boldsymbol{\tau}) = E_r$. This connection to QFT provides invaluable insights on the notoriously hard problem of finding exact quantization conditions for several integrable models beyond the semi-classical limit.

Quantization of the Hitchin System and Langlands. As we have briefly discussed, class $\mathcal{S}$ theories on the full Ω-background lead naturally to quantization conditions for the Hitchin integrable system. This consists in the spectral problem for a system of commuting Hamiltonians associated to the data of a classical group, taking the form $\mathrm{H}_r\,\Psi = E_r\,\Psi$. The quantization of Hitchin system is tangled with the Geometric Langlands Correspondence since the work of Beilinson and Drinfeld[16]. More recently, as we will discuss in this thesis, the problem of quantizing the Hitchin system, has motivated a refined *analytic* version of the correspondence introducing aspects of harmonic analysis into the already rich Geometric program[19–21,79,80]. Analytic Langlands conjectures a correspondence between the single valued spectrum of the Hitchin system and set of certain differential operators called *opers* with real monodromy[81]. Remarkably, this arises as the critical level limit of the Separation of Variables (SoV) transform between two 2d CFTs: the H_3^+ WZW model and Liouville CFT[82]. This bigger correspondence lead [22] in turn to the formulation of a *quantum* version of analytic Langlands with endless ramifications in gauge theory, CFTs as well as Complex Chern-Simons (CS) theory[83].

BPS walls and framed BPS states. As one moves in the moduli space the spectrum of BPS states may change in a sharply discontinuous way. These jumps occur across special loci known as *walls of marginal stability*[32,84,85]. There the central charges of two or more BPS states become aligned in phase, and the energy of a bound state made from these constituents becomes equal to the sum of the individual masses. This makes the composite marginally bound, and it disappear from the BPS spectrum as one crosses a wall. While the BPS spectrum jumps, the full Hilbert space and dynamics of the theory remain continuous at the interface.

Framed BPS states arise when a BPS line defect is inserted along the time direction. The framed BPS spectrum consists of states in the modified Hilbert space by the defect that saturate a BPS-*like* bound. These are solitonic configurations interpolating between different vacua at spatial infinity, with the defect acting as a source. Moving in the moduli space, framed BPS states can form or decay, according to the wall crossing phenomena. The cumulative effect of these wall crossings is encoded in the spectrum generator S. For framed states, the spectrum generator acts as a transformation governed by the Kontsevich–Soibelman wall crossing formula [86], which expresses the invariance of S under continuous deformations of the moduli and encodes how BPS indices rearrange across walls of marginal stability.

Schur quantization. In gauge theory, Schur quantization[83] defines a quantum mechanical system whose operator algebra describes the fusion of $\frac{1}{2}$-BPS line defects, and provides a quantization of the Coulomb branch variety. The natural pairing in this quantum theory is the decorated Schur index $I_{a,b}(\mathfrak{q})$ [87], defined to be the Witten index counting local operators living at the junctions between the line defects. The properties of these quantum mechanical systems are inherited by the parent 4d SQFTs, and in this thesis we will see how this formalism will be used to extend known results about the low energy theory [5,88–90], and their spectrum of BPS states. In particular it provides new computational tools to compute the spectrum generator S. There is a rich interplay between Schur quantization, quantum analytic Langlands and CS theory: they all provide description for the same Hilbert space of states though a intricate chain of dualities.

1.3 Overview of the thesis

In this thesis we will see many of the general features and ideas we have presented in the previous section at interplay in a very non trivial fashion. The *red thread* bridging the different topics and models discussed in this thesis, from 2d QCD down to the Coulomb branch of 4d $\mathcal{N} = 2$ supersymmetric QFTs is illustrating how levering on the synergic combination of dualities, symmetries, and techniques from the theory of exactly solvable models, leads to interesting constraints and control on RG flows, spectrum and dynamics.

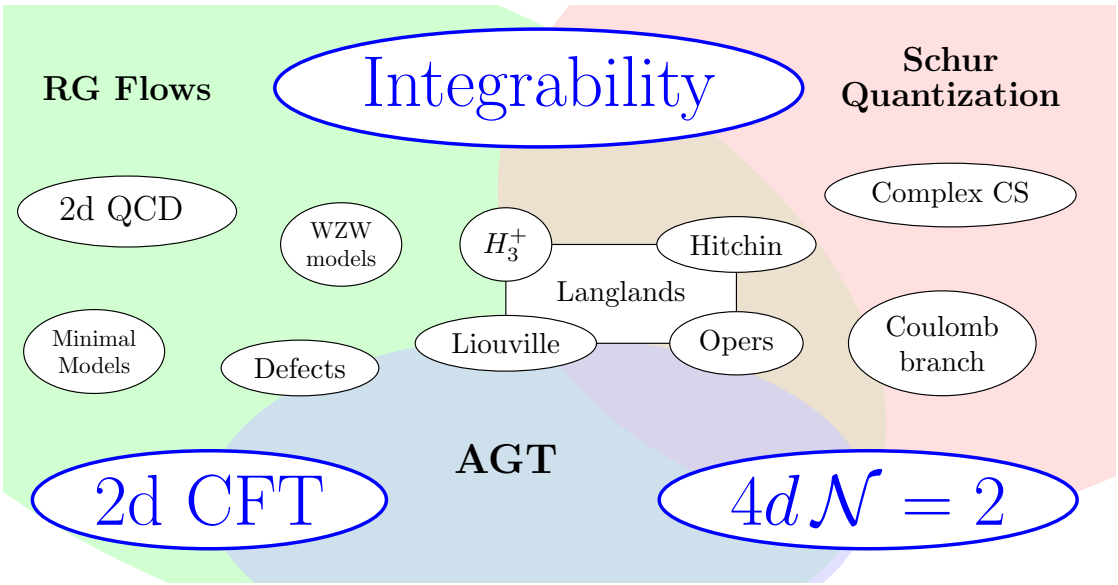


Figure 1.1: An incomplete and schematic account of the web of dualities, relations, flows and correspondences intertwining the various models and techniques of this thesis.

All these apparently completely distinct models are surprisingly connected by an incredibly ramified web of relations. This is really emblematic of the complexity and richness of QFTs and their mathematical structure. We will see at various instances in the course of this thesis such interplay at full work. In Fig 1.1 we try to give a schematic and partial impression of such network of connections. This shall serve as a guide to help the reader to navigate the thesis. We defer to 1.3.2, a more detailed account of a unified perspective on this thesis, after having introduced in detail the content of this work.

1.3.1 Overview of the content

Let us give an account of the content and main results in this thesis. This dissertation is naturally split in three different self-contained parts. Each of the parts, contains a specific introduction as well as an outlook chapter where various future directions and works are summarized.

Part I

In the first part we study integrable structures in the 't Hooft model and generalization thereof. This is based on two publications [1,2] coauthored by the author.

The 't Hooft model [91] is one of the most prominent toy models for confining gauge theory. It consist in the 2d version of an $SU(N_c)$ gauge theory coupled to a fundamental fermion(s).

In 2d vector particles have no propagating degrees of freedom, therefore the dynamics is a very crude simplification of real QCD in our universe, where gluons carry transverse polarizations. Yet, as illustrated by 't Hooft in the seminal paper [91], the 2 dimensional version of QCD maintains some qualitative features of its higher dimensional counterpart for what pertains to the spectrum of mesons, notably the existence of straight "*Regge*"-like trajectories. Mesons are $q\bar{q}$ quark–anti-quark bound states and are inherently non-perturbative objects arising from infinite resummation of interaction between their quark constituents. At large N_c, because of the simplifications of the planar limit [35], such infinite resummation can be performed analytically. This leads to a Schrödinger-like equation encoding spectrum and wavefunctions for mesons, that now is widely referred to as *'t Hooft equation*.

In Chapter 3, we start our discussion by revisiting this story using tools of integrability. Following the approach of [92] we reformulate the single flavour mesons' spectral problem a TQ-Baxter equation. This is a difference equation of the form:

$$\mathbb{Q}(\nu + 2i) + \mathbb{Q}(\nu - 2i) = \mathbb{T}(\nu)\mathbb{Q}(\nu)$$

that typically encodes the spectrum of integrable models, and is a remarkable how such a structure arises in this limit of 2d QCD. By recasting the problem into a TQ-system one unlocks access to analytic structures and critical points of the theory in the complex quark-mass plane[2].

In Chapter 4 we find that, these integrability structure persists in a very broad extension of the 't Hooft model known as generalized QCD_2 [95]. This family of theories is obtained from 2d QCD, by replacing the gauge field kinetic term with the unconventional BF interaction: $\operatorname{tr} B \wedge F - \operatorname{tr} V(B)$. For the choice of $V(B)$ in polynomial form we determined the generalized TQ-system in closed form, and we characterized the potentials admitting a discrete spectrum of mesons. From the analytical properties of the transfer matrix $\mathbb{T}$, we uncover a new interesting space of multicritical fixed point describing the IR phases of the generalized models. We also discuss the large isospin limit of an $SU(2)$ theory coupled to fermions in isospin J representation. Also in this limit, the generalized QCD theory admits stable meson states, and we derive the associated Bethe-Salpeter equation, generalizing the recent discussion of [96].

Part II

In Part II we continue the analysis of 2d QFTs. This is based on two publications [4,5] coauthored by the author, as well as one in preparation [97].

In Part I, we considered toy models of 2d QFTs obtained by taking the planar limit where the gauge symmetry becomes very large. In Part II, we instead consider

[2] cfr. also to more recent developments in [93,94], where these techniques are employed to derive full asympotic expansions and are extended to the multi-flavour case.

another very important class of solvable models in 2d that are characterized by having extended conformal symmetry. In two dimensions, conformal coordinate transformations consists of arbitrary holomorphic and antiholomorphic maps: $z \mapsto f(z)\,, \bar{z} \mapsto f(\bar{z})\,,$ where $z, \bar{z}$ are complex coordinate on the plane. This leads to an enhancement of the conformal algebra $SO(2,2)$ to the infinite-dimensional Virasoro algebra, making 2d CFTs even more constrained than CFTs in higher dimensions.

CFTs they are very special QFTs. They lie at the fixed points of the RG flow, and correspond to a description of a QFTs at arbitrary small (UV CFTs) or large distances (IR CFTs). The goal of this part of the thesis is to study the breaking of conformality due to deforming an UV CFT by one (or more) of its relevant operator(s), schematically as:

$$\mathcal{H}(\lambda_I) = \mathcal{H}_{\text{CFT}} + \lambda_I \int \mathrm{d}x\ \phi_I\,, \qquad \Delta_{\phi_I} < 2\,,$$

where $\mathcal{H}_{\text{CFT}}$ is the UV Hamiltonian, defining a QFT with Hamiltonian $\mathcal{H}(\lambda_I)$ for any value of the scale(s) λ_I .

In Chapter 7 we take the concrete approach of considering flows from Minimal Models in the UV. Minimal models are the simplest 2d CFTs and are characterized by having only a finite number of primary fields and rational central charge. Depending on the relevant deformations, RG flows from Minimal Model are constrained by non-invertible symmetries and or integrability. Non-invertible symmetries are global symmetries generated by the set of Verlinde line defects. By identifying which lines commute with deformations (i.e. what are the preserved symmetries), [98] proposed an infinite number of new RG flows between Virasoro Minimal Models[3]. To describe these flows non-perturbatively, we conjecture and test a novel family of non-linear integral equations (NLIEs) that capture the finite-size spectrum at finite value of the deformation. NLIEs of such form were only known to exist for a special subset of integrable perturbations preserving (part of) the infinite Virasoro algebra of the CFT. In those special cases integrability manifests itself with the existence of infinitely many commuting conserved charges. In all the new cases of [98][3, Section 4], such local charges are not known to exists . This suggest the following question:
Do we really know what is the set of conserved charges of a deformed 2d CFT?

Chapter 8 is dedicated to making progress in addressing this question. We have encountered already a class of conserved charges: those are topological line operators $\mathcal{D}$ commuting with the deformations $[\mathcal{D}, \phi] = 0$. One can consider more general defects $\mathcal{D}(\mu\psi + \bar{\mu}\,\overline{\psi})$ obtained by perturbing a conformal defect $\mathcal{D}$ by one of its defect fields ψ. Here building on [99–101], we construct a new class of

[3] In the Outlook for Part II (Chapter 9) we present some preliminary results from the upcoming work [97] where the ideas of [98] are applied and extended to find infinitely many new RG flows between $\mathcal{W}_N$ minimal models.

translational invariant defects $\mathcal{D}(\mu\psi + \bar{\mu}\,\overline{\psi})$ that are not topological but conserved in the deformed CFT, i.e. they commute with the full perturbed Hamiltonian

$$[\mathcal{H}(\lambda_I), \mathcal{D}(\mu\psi + \bar{\mu}\,\overline{\psi})] = 0$$

but not with the stress energy tensor. This condition is much more general than the one above, and indeed the set of topological lines is a strict subgroup of the translationally invariant ones[101]. We first study translational invariant defects in generic CFTs using the Symmetry Topological Field Theory (SymTFT) framework, and then we apply them to the study of Virasoro Minimal Models. Here, we find that translationally invariant defects provide infinitely many commuting non-local conserved charges that were not known before, including perturbations that were not known to be integrable in the literature.

Part III

Part III is an important linking point for all the topics and ideas discussed for far, providing a bridge between supersymmetric theories in 4 dimensions and their moduli spaces of vacua, and 2d CFTs, line operators, integrability and geometry. This part is based on the publication [5] coauthored by the author (together with the companion papers [22,83]) and a work to appear soon [6].

In Section 1.2.3, we have given a brief account of how the Hitchin integrable system describes of the moduli space of Coulomb vacua of class $\mathcal{S}$ $4d\,\mathcal{N} = 2$, and its quantization may be encoded in the twisted superpotential upon considering the Nekrasov-Shatashvili limit of the theory on Ω-background. The quantization of the Hitchin system is also a paramount problem in geometry and representation theory and, as proposed in the seminal work of Beilinson and Drinfeld [16], plays an important role in the context of the Geometric Langlands correspondence. More recently, an Analytic version of Langlands was conjectured [20,79,80] based on the work [19]. This will be the subject of Chapter 11. Analytic Langlands is formulated as an equivalence between two objects that can be associated to a Riemann surface $\mathcal{C}$: it conjectures a one-to-one correspondence between the single valued and L^2-normalizable solutions Ψ of the pair of complex conjugate eigenvalue equations associated to the quantum Hitchin Hamiltonians:

$$\mathrm{H}_r\Psi = E_r\Psi\,, \qquad \overline{\mathrm{H}}_r\Psi = \overline{E}_r\Psi$$

and the set of *real opers*:

$$\left(\partial_u^2 + t_\eta(u)\right)\chi(u) = 0\,, \qquad \left(\partial_{\bar{u}}^2 + t_{\bar{\eta}}(\bar{u})\right)\overline{\chi}(\bar{u}) = 0\,.$$

being a particular set projective connections with real monodromy. The state of the art is a proof [20,80] for a 4 and 5 punctured sphere and rank 1. In this thesis [6] we propose a preliminary version of a proof for genus 0 and any number of

punctures that is based on the Separation of Variables method for the Gaudin integrable model. In CFTs, Hitchin eigenvalue equations arise in the critical level limit of the system of Knizhnik–Zamolodchikov (KZ) equations satisfied by the correlation functions of 2d CFTs associated with an affine Lie algebra symmetry. For rank 1, the SoV Hitchin-oper (Gaudin-Whittaker) correspondence, is lifted to the SoV transform between H_3^+ WZW-Liouville correlation functions[82].

This observation rooted the development of quantum Analytic Langlands [19, 22,102] as a natural deformation of its critical level counterpart. Quantum Analytic Langlands produces a quantum theory where partition functions of the H_3^+ WZW model are interpreted as the wave-functions of a spherical vector in the quantization of complex Chern-Simons theory. Remarkably, this Hilbert space of states can be identified with the quantum mechanical system produced by the Schur Quantization of the Coulomb branch of certain 4d $\mathcal{N} = 2$ theories. In this relation the algebra of line operators coincides with the Skein algebra of Wilson lines in CS theory.

In Chapter 12 we apply the formalism of Schur Quantization to the low energy phases of 4d $\mathcal{N} = 2$ theories. The spectrum of BPS particles is robust and only jumps across certain walls of marginal stability in the IR moduli space. In the IR formulas for the (decorated) Schur indices[89,90], originally formulated only for conformal SQFTs, can be also employed for non-conformal theories, and admit a factorized form in terms of *bosonic* quantum dilogarithms. There is a non-trivial interplay between RG flows and Schur quantization. We consider (supersymmetric) RG flows between two theories $T_1 \to T_2$ preserving the $SU(2)$ R-symmetry. These induce a corresponding map on the algebra of BPS line operators $\mathcal{A}_1 \to \mathcal{A}_2$ that is represented unitarily on the Schur Hilbert space by normal unbounded operators. The RG map is not directly lifted to a map of the Schur quantization of the two theories. Indeed, while superconformal indices are often RG flow invariant, this is not always the case. For instance, RG flows involving the decoupling of very massive degrees of freedom, cannot always preserve the Schur index, that manifestly receives contribution from the massive fields. One of the results of the work [5] is associating to any RG flow a spectrum generator S intertwining the Schur correlation functions in the UV and IR (as well as the dualization map, but for simplicity let us postpone this to 12):

$$I^{(2)}_{\mathrm{RG}(a)\cdot S,\mathrm{RG}(b)\cdot S} = I^{(1)}_{a,b} \ ,$$

where $\mathrm{RG}(a)$ is the image of the line operator $a \in \mathcal{A}_1$ in $\mathcal{A}_2$. As a consequence, upon leveraging on multi-step flows, new computational tools to obtain the spectrum generator are presented[5].

Furthermore, once this is specified to Class $\mathcal{S}$ theories, Schur quantization provides the tools to quantize the (complex) Teichmüller space of the underlying curve. In this case the algebra of BPS line operators is isomorphic to the algebra of quantised functions on the moduli space of flat connections on Riemann surfaces,

a.k.a. the Teichmüller space. As a result, for the rank 1 case, we provide a construction of the complex Teichmüller space associated to the (doubled) quantum $SL(2,\mathbb{C})$ group in the Schur regime. Furthermore, we solve the spectral problem for the Wilson Line in the annulus, furnishing a key building block for the unitary equivalence between UV and IR Schur quantization.

1.3.2 Unifying perspective and connections

It is impossible to give a full account of all the connections stretching between the different models, themes and techniques that we discuss in this thesis. Here, we try to highlight some aspects in addition of the ones already mentioned in the previous sections, hoping to at least convey a flavor of the underlying structure. The diagram in Figure 1.1 serves as a map, highlighting a rich network of correspondences that intertwine solvable models in two dimensions, supersymmetric gauge theories in four dimensions, and the geometric structures arising from their moduli spaces.

Integrability, originally developed in the context of highly constrained solvable models, emerges throughout this thesis across all the three parts. Integrable structures appear in surprising and seemingly disconnected settings. The spectral equations of generalized 2d QCD, defects and perturbations of 2d CFTs, the quantization of moduli spaces of vacua of $\mathcal{N} = 2$ SQFTs, and the Langlands correspondence all reveal connection to integrable models. Integrability emerges here as a unifying language that threads together diverse areas of QFT and geometry. As a key instance: the oper equation is exactly the Baxter-TQ equation for Gaudin model, exactly how the Baxter TQ-equation captures the meson spectrum in 2d QCD.

Another central conceptual bridge is the BPS/CFT correspondence, through which 2d CFTs recur as structural components within the BPS sectors of 4d supersymmetric gauge theories. We have already illustrated an instance of this: the AGT correspondence. Let us mention another important one for this thesis.

From a generic 4d $\mathcal{N} = 2$ superconformal theory one can define a subsector of protected *Schur* operators who lie in a fixed plane $\mathbb{R}^2 \subset \mathbb{R}^4$ and defines a (non-unitary) 2d vertex operator algebra [103,104](VOA) (a.k.a. chiral algebra). We will say more about this in Chapter 9, but let us anticipate that for some special 4d theories, this chiral algebra sector is exactly given by the non-unitary Minimal Models studied in Part II. Furthermore, the Schur index in this sector exactly coincides with the vacuum character of the VOA.

Defects are another unifying thread that run through the entire thesis, appearing in a wide variety of guises and playing both structural and dynamical roles. In 2d CFTs, topological line defects such as Verlinde lines encode non-invertible symmetries and are used to organize RG flows between Minimal Models, while the translational invariant ones serve as probe for novel integrable structures and further conserved charges. In 4d $\mathcal{N} = 2$ supersymmetric theories the algebra of

BPS line defects encodes the IR dynamics and enters prominently in our discussion through Schur quantization. Remarkably, for class $\mathcal{S}$ theories the algebra of these line operators map onto the Skein algebra of Wilson lines in 3d Chern–Simons theory and of lines in 2d CFTs.

Let us mention a last instance where we see an interplay of the ideas we discussed here at work. Indeed, the full integrable structure of class $\mathcal{S}$ $\mathcal{N} = 2$ theories on the Ω-background is revealed through a rich interplay with defects[4], 2d CFTs, and quantum analytic Langlands . Quantization conditions for special class of Hitchin system arises in Nekrasov–Shatashvili (NS) limit[106] (corresponding to the critical level) as already briefly discussed. Upon considering class $\mathcal{S}$ theories on the full 4-Ellipsoid background (cfr. discussion in Part III introduction), it is natural to conjecture that the integrable structure of the NS limit, is lifted to the insertion of surface operators in the supersymmetric partition function on the four ellipsoid, further refined by the insertion of line operators[61,62,106]. These line insertions act as spectrum-generating operators in quantum Langlands and correspond, on the CFT side, to Verlinde lines acting on correlation functions of the WZW model (that are dual in AGT to surface defects). This illustrates a remarkable interplay between integrability, defects, Langlands, CFTs and SQFTs.

This provides only a small account of the rich structure underlying this thesis. The reader may find further points of contact upon delving into the detailed developments in each part.

1.3.3 List of Contributions

Let us give an account of the original contributions from the author

- Part I is mainly based on the original works [1,2] coauthored with S. Komatsu.
  - ⋆ Chapter 3 presents the results in [1, Section 2-4 and 6]. Building on [92], we derive the TQ-system for the single flavor 't Hooft, extract perturbative analytical expansions, and discuss analytical properties.
  - ⋆ Chapter 4 presents the results in [2, Section 2-5]. We apply the formalism just described to Generalized QCD, introduced first in [95]. Fixing $V(B) = \sum v_n B^n$, we derive the corresponding TQ system in close form for any polynomial potential. We describe theories admitting discrete positive spectrum and describe general properties of the IR phases. For cubic potential we discuss in detail the analytic structure of mesons' spectra and characterize critical points. We derive 't Hooft equation for $SU(2)$ generalized QCD coupled to fermions in large isospin J representations of the gauge group.

[4] We thank J. Teschner for sharing with us the slides from [105], presenting these insights

- Part II is mainly based on the original works: [3] coauthored with S. Negro, [4] coauthored with I. Runkel and G. M. T. Watts, and contains a plot from the upcoming work [97] with T. Procházka.
  - ⋆ Chapter 7 illustrates the results of [3]. There, we conjecture new NLIE description for the RG flows between minimal models presented in [98]. We test this conjecture against conformal perturbation theory both in the UV and in the IR, and against the constraints from non-invertible symmetries.
  - ⋆ Chapter 8 presents the original results in [4, Section 2-4]. We give a characterization of translational invariant defects in perturbed 2d CFTs via a the *bulk commutation condition* condition formulated in the SymTFT of the unperturbed theory. We apply this construction in details to the case Virasoro Minimal Models.
  - ⋆ In the outlook (Chapter 9) we also present a preliminary plot (Figure 9.1) from the upcoming work [97], where we extend the analysis of [98] to $\mathcal{W}_N$ Minimal Models.
- Part III is mainly based on the work [5] coauthored D. Gaiotto and an upcoming work [6] with J. Teschner.
  - ⋆ In Chapter 11 the novel original content, based on the upcoming work of the author with J. Teschner[6], is presented in Section 11.3. There we present a preliminary proof for analytic Langlands in genus 0 and rank 1 based on the SOV method. This includes a proof of the unitarity of the SoV map, as well as a proof of the Hecke eigenvalue property[5] The rest of the Chapter furnishes background on analytic Langlands..
  - ⋆ Chapter 12 presents the results of [5, Sections 2-9 & Appendix B]. The formalism of the Schur quantization to the IR of 4d $\mathcal{N} = 2$ theories is applied both to Lagrangian and non-Lagrangian theories. This employs the known formulas for the Schur index. Among the author's main contributions is the construction of the quantum complex Teichmüller space in the Schur quantization regime. We find that the special function, playing the role of the Faddeev Quantum Dilogarithm in this context, is the same special function entering in the solution of the Wilson Line spectral problem on the annulus. The latter determines the intertwiner providing the building block to relate UV and IR Schur quantization.

[5] We thank J. Teschner for having shared a set of unpublished notes discussing preliminary ideas in merit.

Part I

Two dimensional QCD and Integrability

Chapter 2

Introduction

Understanding the mechanism of confinement in gauge theories remains one of the most challenging and intriguing open problems in quantum field theory. To deepen our comprehension of the fundamental dynamics underlying confinement, it is often useful to analyze simplified "toy models" that share key features with more complex theories. These models provide a controlled setting where analytical methods can be more effectively applied.

Following this spirit, the first part of this thesis focuses on the 1+1-dimensional version of QCD with quarks in the fundamental representation of the gauge group. This model is one of the most celebrated toy models for confining gauge theories, and it has been extensively studied both analytically and numerically over the years (see [107] and references therein for a review).

When considering the double-scaling limit—sending the number of colors N_c to infinity while keeping the 't Hooft coupling $g = g^2_{\mathrm{YM}} N_c$ fixed—the theory becomes particularly tractable. In this regime, widely known as the *'t Hooft model* (first introduced in [91]), only Feynman diagrams that can be drawn on a two-dimensional sphere contribute at leading order, while all others are suppressed. This simplification reveals many emergent features of two-dimensional QCD that are not apparent from the Lagrangian alone [35]. Some of these features—such as the absence of deconfined quark states and the Regge-like structure of the meson spectrum—are shared with four-dimensional QCD, making the 't Hooft model a particularly valuable low-dimensional analog for understanding mesons QCD_4.

In recent years, there has been renewed interest in the study of *adjoint QCD* in two dimensions—that is, two-dimensional Yang-Mills theory coupled to quarks in the adjoint representation of the gauge group [108–122]. This model serves as a compelling toy model for confining flux tubes, as adjoint quarks can introduce rich dynamics without causing the flux tubes to break[1]. Intriguingly, there is evidence suggesting that the dynamics of the confining flux tube may become integrable in certain limits [125–129]. To investigate this possibility more concretely, it is

[1] This is true only for massive quarks. As discussed in [118,123,124], the theory does not confine when the quark masses vanish.

instructive to examine the integrable structures within simpler, solvable theories such as the 't Hooft model.

Mesons in the 't Hooft model.

Remarkably the problem of determining the mass spectrum of mesons and their wavefunctions in the 't Hooft model can be reformulated as an eigenvalue problem, which we present here for reference, deferring a comprehensive explanation of its significance to Chapter 3:

$$2\pi^2\lambda_n\,\phi_n(x) = \left[\frac{\alpha_1}{x} + \frac{\alpha_2}{1-x}\right]\phi_n(x) - \int_0^1 \mathrm{d}y\,\mathcal{P}\frac{1}{(x-y)^2}\,\phi_n(y) \tag{2.0.1}$$

Here $\alpha_{1,2}$ and λ_n are related to the quark masses $m_{1,2}$ and the meson mass M_n by

$$\alpha_{1,2} = \frac{\pi m_{1,2}^2}{g} - 1\,, \qquad \lambda_n = \frac{M_n^2}{\pi g}\,, \tag{2.0.2}$$

with g being the 't Hooft coupling $g = g_{\mathrm{YM}}^2 N_c$. This eigenproblem, often referred to as *'t Hooft Equation*, can be solved numerically with arbitrary precision and accuracy. The main benchmark characteristics of this theory that we have listed above can be directly inferred by direct numerical solution of (2.0.1) [91,130,131]. However, we believe that the eigenproblem (2.0.1) deserves a more thorough analytical treatment.

More precisely, we illustrate [1] that 't Hooft equation can be can be transformed into a finite-difference operator that has the same structure as a Baxter TQ-relation:

$$Q(\nu+2i) + Q(\nu-2i) - 2Q(\nu) = \frac{-4\pi\lambda}{\frac{2\alpha}{\pi} + \nu\coth\left(\frac{\pi}{2}\nu\right)}\,Q(\nu), \qquad \alpha = \frac{\alpha_1+\alpha_2}{2} \tag{2.0.3}$$

On top of unveiling a very interesting structure typical of integrable systems, this reformulation of the problem is particularly suitable for analytical methods.

Generalized QCD

Notably, this emergent structure is not specific to the 't Hooft model. In [2], we consider an extension of the 't Hooft model[43] known as the generalized Yang-Mills (gYM_2), obtained by replacing the kinetic term for the field strength F with a BF coupling involving an adjoint scalar field B and introducing an arbitrary potential $V(B)$ for it:

$$\mathcal{L} = \frac{N}{8\pi}\,\mathrm{Tr}\,B\wedge F - \frac{N}{4\pi}V(B) + \overline{\psi}_a\left(i\gamma^\mu D_\mu - m_a\right)\psi_a \tag{2.0.4}$$

As with the 't Hooft model, for a class of potentials $V(B)$ as we determine in the following, the generalized QCD at large N_c has stable mesonic bound states with a discrete spectrum. Thanks to the simplification that occurs at large N_c, the mass spectrum can be computed explicitly by solving integral equations that generalize the one for the 't Hooft model. For this very large class of models, we demonstrate that, employing the same spectral representation, the associated bound state 't Hooft equation can be casted into the exact same form of (3.0.1), which turns out to be remarkably simple and universal:

$$Q(\nu+2i)+Q(\nu-2i)-2Q(\nu)=T(\nu)Q(\nu)\,, \tag{2.0.5}$$

where the dependence on the potential $V(B)$ is contained entirely in the transfer matrix $T(\nu)$, which can be computed in a closed form for any given potential. See (4.2.17) for details. As in the 't Hooft model, this reformulation potentially enables systematic asymptotic expansions of the mass spectrum and the wavefunctions although we leave its detailed study for the future work. Leveraging this reformulation, we obtain various analytical expansions and we illustrate that upon tuning the coefficients of $V(B)$, several mesons can become simultaneously massless, realizing "multi-critical points". These results illustrate a very rich IR structure of this theory that would be worth further investigation.

Contents of Part I

3 The 't Hooft model **29**
3.1 A two-dimensional model for mesons 30
3.2 't Hooft equation as a TQ-system 36
3.3 Meson spectrum at complex quark mass and critical points 46
3.4 Extracting spectral data 53
3.5 Application to non-perturbative topological string 66

4 Generalized QCD **71**
4.1 Generalized QCD in the large N limit 72
4.2 Generalized 't Hooft equation as a TQ-system 76
4.3 Analytical structure of the spectrum and critical points 81
4.4 Mesons spectrum in the large representation limit 95

5 Outlook **103**

A Supplement to Part I **107**
A.1 Recurrence relation for integrals 107
A.2 Derivation of the bound state equation in the large representation limit 108
A.3 Numerical methods for analytical continuation 110
A.4 Non-critical spontaneous symmetry breaking of $\mathcal{PT}$-symmetry . . . 111

Chapter 3

The 't Hooft model

In this Chapter we study mesons' spectrum in the 't Hooft model. We illustrate [1] that the 't Hooft equation is equivalent to the following TQ-equation:

$$Q(\nu+2i)+Q(\nu-2i)-2Q(\nu)=\frac{-4\pi\lambda}{\frac{2\alpha}{\pi}+\nu\coth\left(\frac{\pi}{2}\nu\right)}Q(\nu),\qquad \alpha=\frac{\alpha_1+\alpha_2}{2} \tag{3.0.1}$$

For $\alpha_1=\alpha_2$[1] starting from the TQ system, we can construct expressions for the following spectral sums:

$$G_+^{(s)}(\alpha)=\sum_{n=0}^{\infty}\frac{1}{\lambda_{2n}^s}\,,\qquad\qquad G_-^{(s)}(\alpha)=\sum_{n=0}^{\infty}\frac{1}{\lambda_{2n+1}^s}\,, \tag{3.0.2}$$

Such results for $\alpha=0$ have been obtained by Fateev, Lukyanov and Zamolodchikov [92]. We will extend those results by developing a systematic perturbation in the mass parameter α. Another noteworthy result that we can extract from the TQ-system is an asymptotic approximation for the meson wavefunctions, which, although being constructed to be only asymptotic, turn out to approximate remarkably well the numerical solutions. These results are potentially useful for the evaluation of scattering amplitudes of mesons, which are known to be given by overlaps of meson wavefunctions [107,130,132].

In addition to this, we deduce important properties of the model that we anticipate here: as a function of the complex parameter α, $\lambda(\alpha)$ exhibits a square-root branch point at $\alpha_1=\alpha_2=-1$ where the chiral symmetry becomes exact and a massless meson emerges. One of the pivotal advantages of recasting 't Hooft equation in ν-space is that it makes straightforward to extend the analysis to the complex plane of the masses $\alpha\in\mathbb{C}$. Indeed, we illustrate that as we analytically continue onto the second sheet beyond the chiral-symmetry branch cut, there are infinitely many branch-point singularities accumulating at $\lambda=\infty$ at special values of the (complex) masses corresponding to which one of the even eigenvalues turns zero.

[1] The same problem with $\alpha_1\neq\alpha_2$ was discussed more recently in [94]

Furthermore, similar spectral problems of integral operators and TQ-systems appear in the context of topological string [133–137]; we comment on possible applications of our techniques in Section 3.5.

Outline. In Section 3.1, we review the derivation of the 't Hooft equation, which determines the spectrum of mesons. In Section 3.2, we explain how to rewrite the 't Hooft equation into a TQ-Baxter equation and extend it to arbitrary values of the meson mass λ by introducing an inhomogeneous term to the 't Hooft equation. This can be achieved systematically using the framework of the inhomogeneous Fredholm equation. In Section 3.3, we discuss the properties of the meson spectrum as we analytically continue the quark masses to complex values. In particular, we show that the complex quark mass plane contains infinitely many branch cuts, each of which starts from a point where one of the mesons becomes massless. We suggest that each of those points describes a "critical point"; namely their infrared dynamics is described by a nontrivial CFT. Further results, both numerical and analytical, as well as the results for wavefunctions are provided in Section [1, Section 5] but are omitted here. In Section 3.4, we explain how to extract the spectral data as a formal power series in α from the TQ-equation, as following from the discussion in [92] for a special quark mass. We refer the reader to the works [93,138] where the authors have presented full analytic solutions that do not require an expansion as a formal power series for the even more general case $\alpha_1 \neq \alpha_2$. The techniques employed here are likely to be useful in other setups in which the inhomogeneous Fredholm equation and TQ-equations show up, such as non-perturbative topological string discussed in Section 3.5.

3.1 A two-dimensional model for mesons

3.1.1 Conventions

Before starting our discussion, let us summarize notations and conventions. We work with two-dimensional Minkwoski metric $g^{00} = -g^{11} = 1$, and we take the γ-matrices $\gamma^0 = \left(\begin{smallmatrix} 0 & 1 \\ 1 & 0 \end{smallmatrix}\right)$, $\gamma^1 = \left(\begin{smallmatrix} 0 & -1 \\ 1 & 0 \end{smallmatrix}\right)$. We define lightcone coordinates as: $x^{\pm} = \frac{1}{\sqrt{2}}(x^0 \pm x^1)$, $p_{\pm} = \frac{1}{\sqrt{2}}(p_0 \pm p_1)$. In this coordinates, the γ-matrix algebra takes the form $\{\gamma_+, \gamma_-\} = 2$, $\gamma_+^2 = \gamma_-^2 = 0$.

3.1.2 Derivation of the 't Hooft equation

We now review the key features of the 't Hooft model that will be useful for our discussion. For more details, see the original paper [91], which is quite pedagogical. 't Hooft considered an $SU(N)$ YM theory in two dimensions coupled to fundamental massive fermions. In the large number of colors limit $N \to \infty$ the theory admits a double scaling limit taken for the 't Hooft coupling $g = g_{\mathrm{YM}}^2 N$ being fixed. The

Lagrangian is the standard YM Lagrangian with $a = 1, \cdots, N_f$ being the flavour index:

$$\mathcal{L} = -\frac{1}{4}\operatorname{Tr} F \wedge \star F + \overline{\Psi}_a(i\not{D} - m_a)\Psi_a \tag{3.1.1}$$

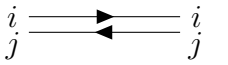
As customary in 2-dimensional theories, we take lightcone coordinates, where the theory greatly simplifies upon fixing lightcone gauge $A_- = 0$ as the field strength is linear in the fields, there are no ghosts and non-linear interactions between gauge fields are set to zero. Denoting $A_+ = A$, in this gauge the Lagrangian is:

$$\mathcal{L} = -\frac{1}{2}(\partial_- A)^2 + \overline{\Psi}_a(i\gamma_\mu\partial^\mu - m_a - g_{\rm YM}\gamma_- A)\Psi_a \tag{3.1.2}$$

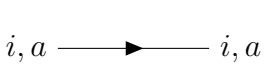
Exact quark propagator. The lightcone gauge leads to a drastic simplification of Feynman rules. Since the quark-antiquark-gluon vertex only involves γ_- satisfying $\gamma_+^2 = \gamma_-^2 = 0$ and $\gamma_+\gamma_-\gamma_+ = 2\gamma_+$, the terms proportional to $ip_+\gamma_- + m_a$ in the quark propagator (highlighted in red below) do not contribute when they appear in internal legs[2]:

$$\langle\overline{\Psi}_a(p)\,\Psi_a(-p)\rangle = \frac{ip_-\gamma_+ + ip_+\gamma_- + m_a}{2p_+p_- - m_a^2 + i\epsilon}\,, \tag{3.1.3}$$

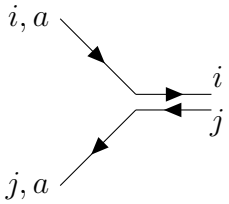
As a result, we can focus on the component proportional to γ_+ and the Feynman rules simplify to



$$\langle A(p)\,A(-p)\rangle = -i\frac{1}{p_-^2}\,, \tag{3.1.4}$$



$$\langle\overline{\Psi}_a(p)\,\Psi_a(-p)\rangle = \frac{ip_-}{2p_-p_+ - m_a^2 + i\epsilon}\,, \tag{3.1.5}$$

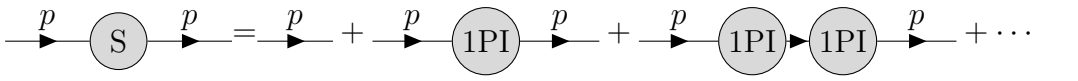


$$\langle\overline{\Psi}_a\,\Psi_a\,A\rangle = -2ig_{\rm YM}\,, \tag{3.1.6}$$

while fermionic loops are subleading in a $1/N$ expansion and are absent in the planar limit. These simplifications make it possible to obtain an explicit expression for the full (non-perturbative) fermion propagator $S(p)$ obtained by a resummation

[2]These terms do give non-vanishing contributions if the fermion propagators show up in the external legs. We can however project them out by multiplying γ_-'s from outside. In the subsequent analysis, we implicitly perform such a projection.

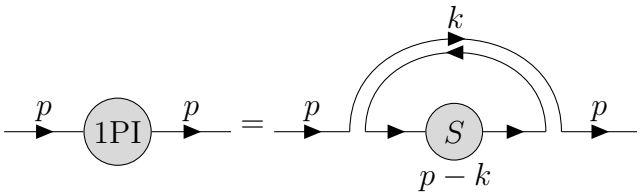
of the 1PI contribution $\Sigma(m_a, p)$:



$$= \frac{ip_-}{2p_+p_- - m_a^2 - p_-\Sigma(m_a, p) + i\epsilon} \tag{3.1.7}$$

In the planar limit, the 1PI contribution can be bootstrapped through the Dyson equation:

$$\Sigma(m_a, p) =$$



(3.1.8)

that can be remarkably solved explicitly in this case (see [91] for a derivation) leading to

$$\begin{aligned} \Sigma(m_a, p) &= \frac{g}{\pi}\left(\frac{\mathrm{sgn}(p_-)}{\rho} - \frac{1}{p_-}\right) \\ S(p) &= \frac{ip_-}{2p_+p_- - m^2 + g/\pi - g|p_-|/(\rho\pi)} \end{aligned} \tag{3.1.9}$$

where ρ is an IR regulator that must be introduced to cancel the infrared divergence. The introduction of this sharp cutoff should be regarded as an intermediate step since, in any gauge-invariant observables, factors containing ρ cancel in the limit $\rho \to 0$. On the other hand, any UV divergence is absent (upon symmetric regularisation) as a consequence of the super-renomalizability of QCD_2.

The form of the propagator illustrates the confining nature of the interaction: upon sending $\rho \to 0$, the pole of the full propagator, i.e. the effective mass that re-summes all the quantum corrections, is moved to ∞, signalling the absence of on-shell free quark states in this model. One can also understand it directly from the Lagrangian (3.1.2) by integrating out the gauge field and obtaining a confining linear potential between quarks:

$$\begin{aligned} A(x_+, x_-) &= -\sum_a \frac{g}{2}\int \mathrm{d}y_- \, |y_- - x_-| \, j_a(x_+, y_-), \qquad j_a = \overline{\Psi}_a\Psi_a \\ \mathcal{L} &\supset \int dx_1\, dx_2\, j^0(x_0, x_1)|x_1 - y_1|\, j^0(x_0, y_1) \end{aligned} \tag{3.1.10}$$

These arguments already capture the qualitative behavior of the quark-antiquark states and lead to the expectation that, in the quark-antiquark vertex, only bound state are formed and the spectrum is purely discrete.

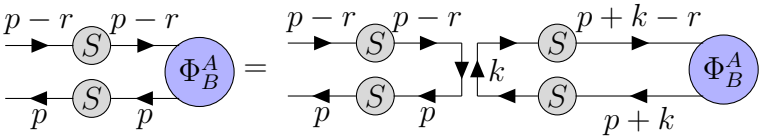
Bethe-Salpeter equation. The remarkable feature of this model is that we can go beyond this rudimentary analysis and construct explicitly the meson states. Generically, bound states arise as a result of summing up infinitely many interaction diagrams between their constituents. Such a resummation leads to the so-called *Bethe-Salpeter equation*, which can be viewed as a Schrödinger equation for bound states. Its derivation is standard textbook-material by now and we briefly review it here. In quantum field theory, the spectrum of particles can be read off from poles of the Green function. This statement, well-known for the one-particle spectrum, holds true also for bound states. Namely, two-particle bound states appear as poles of the two-particle Green function $\mathcal{G}^{(4)} \equiv \mathcal{G}^{(4)}(x_1, x_2; x_3, x_4)$. The Green function satisfies an *inhomogeneous* Dyson equation analogous to (3.1.8),

$$\begin{aligned}\mathcal{G}^{(4)}(x_1, x_2; x_3, x_4) &= S(x_1 - x_3)\, S(x_2 - x_4) \\ &+ \int \mathrm{d}^2 y_1 \cdots \mathrm{d}^2 y_4\, S(x_1 - y_1)\, S(x_2 - y_2)\, K(y_1, y_2; y_3, y_4)\, \mathcal{G}^{(4)}(y_3, y_4; x_3, x_4)\end{aligned} \tag{3.1.11}$$

where $K(y_1, y_2; y_3, y_4)$ is the full irreducible interaction kernel and S in the full two-point function of the constituents of the meson (the S we computed above). As stated above, $\mathcal{G}^{(4)}(x_1, x_2; x_3, x_4)$ will have poles in momentum space corresponding to the mass of the bound state M^2, so that, in the vicinity of a pole, the Green function can be approximated as $\mathcal{G}^{(4)}(p, r, P) \sim \frac{\overline{\Phi}(r,p)\Phi(p,r)}{P^2 - M^2}$ where Φ is bound state wavefunction[3]. Then, the 4-point Dyson equation near the pole reduces to the following *homogeneous* Dyson equation,

$$\Phi(p, r) = S(p)\, S(p - r) \int \mathrm{d}^2 k\, K(k, p, r)\, \Phi(p + k, r) \tag{3.1.12}$$

which is known as the Bethe-Salpeter equation. In general, $K(k, p, r)$ is a complicated object, containing all the interactions among the constituents. Normally, one then approximates the full interaction kernel by considering only a subset of diagrams. The most common approximation is the so-called rainbow-ladder approximation in which one only resums rainbow diagrams for each constituents and ladder diagrams between constituents. Normally, this is just a (non-systematic) approximation scheme. However, in the planar limit, it gives an exact answer since fermionic loops are suppressed by $1/N_c$

$\Phi^A_B(p, r) =$ 

(3.1.13)

[3] More precisely, it is a transition amplitude between the constituents and the bound state: $\langle \Omega | \overline{\psi}\, \psi | \Phi \rangle$.

and contains the full quantum dynamics of the quark-antiquark bound states. Explicitly, it takes the form:

$$\Phi_B^A(p,r) = -\frac{4g}{i}\, S(p)S(p-r) \int \frac{\mathrm{d}k_+\, \mathrm{d}k_-}{(2\pi)^2}\, \frac{\Phi_B^A(p+k,r)}{k_-^2} \tag{3.1.14}$$

with $S(p)$ being the full propagator in (3.1.9). Although it is not possible to solve analytically for this equation, it can be recast into a one dimensional eigenvalues problem. Namely, upon employing the variables:

$$\alpha_{a,b} = \frac{\pi\, m_{a,b}^2}{g} - 1, \qquad 2r_+\, r_- = \pi g \lambda, \qquad x = \frac{p_-}{r_-}, \quad x \in [0,1], \tag{3.1.15}$$

the "average" function $\phi_b^a(x) = \int \mathrm{d}p_+\, \Phi_b^a(p,r)$ is readily shown to satisfy the following equation[91]:

$$2\pi^2 \lambda\, \phi_b^a(x) = \left(\frac{\alpha_a}{x} + \frac{\alpha_b}{1-x}\right) \phi_b^a(x) - \fint_0^1 \mathrm{d}y\, \frac{\phi_b^a(y)}{(y-x)^2} =: \mathcal{H}\, \phi_b^a(x) \tag{3.1.16}$$

widely referred to as the 't Hooft equation[4].

Boundary condition and hermiticity. The eigenproblem (3.1.16) is the main focus of our work and therefore its characteristics deserve a thorough discussion. The behavior of the wavefunction close to the boundaries at $x = 0$ and 1 cannot be simply deduced from the equation itself; rather it requires careful analysis on the regularity near the boundaries and the hermiticity of the Hamiltonian.

Assume that the solutions have a power-law behavior near the boundaries of$[0,1]$:

$$\phi_b^a(x \sim 0) \simeq x^{\beta_a}, \qquad \phi_b^a(x \sim 1) \simeq (1-x)^{\beta_b}\,. \tag{3.1.17}$$

As shown in [91], the hermiticity of the Hamiltonian requires the wave function to vanish at the boundaries i.e. $\beta_i \geq 0$. In addition, it turns out that one needs to impose $\beta_i < 1$. To see this, let us analyze the behavior of (3.1.16) near $x = 0$. The first term on the RHS, $\alpha_a \frac{\phi(x)}{x}$, behaves as $\propto x^{\beta_1 - 1}$. To reproduce the LHS, which decays faster as x^{β_1}, it needs to be cancelled by the integral term, which can be approximated as

$$-\fint_0^1 \mathrm{d}y\, \frac{\phi(y)}{(x-y)^2} \overset{x\sim 0}{\sim} \begin{cases} \pi\beta_1 \cot(\pi\beta_1) x^{\beta_1 - 1} & \beta_1 < 1\,, \\ \mathcal{O}(1) & \beta_1 \geq 1\,. \end{cases} \tag{3.1.18}$$

As shown above, for $\beta_1 < 1$ the boundary behavior is singular and can be computed simply by substituting $\phi(x) = x^{\beta_1}$ to the integral. On the other hand, for $\beta_1 \geq 1$ the

[4]Since in the planar limit fermion loops are suppressed, 't Hooft equation depends on the flavour symmetry only through the masses of the quarks pairwise. In addition, since this equation describes gauge-invariant bound states, any dependence on the regulator ρ has disappeared.

integral is dominated by the behavior of ϕ away from $x \sim 0$, and is generically $\mathcal{O}(1)$. Thus, requiring the cancellation forces us to take $\beta_1 < 1$. A similar analysis at $x \sim 1$ shows that $\beta_2 < 1$ as well. To be more precise, the cancellation is guaranteed if β_i satisfies the following[5] :

$$\alpha_i + \pi\beta_i \cot(\pi\beta_i) = 0, \qquad 0 \leq \beta_i < 1 \qquad (i = a, b)\,. \tag{3.1.19}$$

See also §29 of [139] or recent discussions in [96]. For any fixed $\alpha_i \geq -1$, the solution to these conditions (3.1.19) is unique and it unambiguously determines the boundary behavior[6].

For this space of functions with the boundary conditions, the "Hamiltonian" $\mathcal{H}$ is Hermitian and positive definite [91]:

$$(\phi, \mathcal{H}\,\psi) = \int_0^1 \mathrm{d}x \left[\frac{\alpha_1 + 1}{x} + \frac{\alpha_2 + 1}{1 - x}\right] \phi^*(x)\,\psi(x) + \frac{1}{2}\int_0^1 \mathrm{d}x \int_0^1 \mathrm{d}y\, \frac{(\phi^*(x) - \phi^*(y))\,(\psi(x) - \psi(y))}{(x - y)^2} \tag{3.1.20}$$

Furthermore, the divergence of the potential at boundary of the box guarantees that the spectrum is purely discrete and non-degenerate. This confirms our expectations and shows that the spectrum of QCD_2 (at least at the leading order in $1/N$) only contains mesonic bound states and no free quark states, as the latter would be associated with a continuous spectrum. We remark that as a function of $\alpha_i \in \mathbb{C}$, the Hamiltonian is explicitly not-Hermitian. For $\mathbb{R} \ni \alpha < -1$, i.e. for purely imaginary quark masses, the scalar product is not longer positive definite and the Hamiltonian in this case is non-Hermitian as well.

Charge conjugation/parity. Solving the (discrete) eigenproblem defined by (3.1.16), allows us to extract the physical spectrum of mesons in the 't Hooft model: the eigenfunction $(\phi_b^a)_n$ correspond to the n-th excited bound state of the quark-antiquark meson and the corresponding eigenvalues μ_n^2 is related to the invariant mass of the bound state. The eigenstates can be chosen to be real $\phi^*(x) = \phi(x)$, given that the equation is real and the spectrum is non-degenerate. Solutions of (3.1.16) are also eigenstates of the charge conjugation $\mathcal{C}$, which is an exact symmetry of $\mathcal{H}$ and acts as a parity in x-space[7]:

$$(\phi_a^b)_n(x) = (-1)^n (\phi_b^a)_n(1 - x)\,. \tag{3.1.21}$$

[5]For integral equations of the Cauchy kind on a finite interval on the complex plane, which only contains first-order poles (unlike ours which contains second-order poles), the boundary behavior of solutions is well-studied [139]. The most general boundary condition in such cases is $\beta_i = \mathrm{Re}\ \beta_i + i\,\mathrm{Im}\ \beta_i$ with $-1 \leq \mathrm{Re}\ \beta_i \leq 0$, $\mathrm{Im}\ \beta_i \in \mathbb{R}$. Our results can be retrieved from it by imposing the reality condition and performing a simple differentiation [96] since the double pole principal value regularization (Hadamard regularization) is nothing but the derivative of the Cauchy principal value, i.e. $\fint_a^b \frac{f(t)}{(t-x)^2} = \frac{\mathrm{d}}{\mathrm{d}x} \fint_a^b \frac{f(t)}{t-x}$. Complex boundary conditions will show up also in our analysis, as we extend the problem to imaginary masses ($\alpha_i < -1$).

[6]For $\alpha_i > -1$, the exponents are strictly positive, and henceforth (3.1.17) correspond to Dirichlet boundary conditions in the box $[0, 1]$. On the other hand for $\alpha = -1$, the eigenfunction does not vanish at the boundary.

[7]To see that this is the correct parity in the box, one can go to the "Regge" limit $\mu^2 \to \infty$ where $\phi_n \sim \sin(n\pi x)$.

3.2 't Hooft equation as a TQ-system

For many years, the eigensystem (3.1.16) has been investigated either by means of numerical methods or by the WKB approximation (for instance [140]). Although this approach has been fruitful in illustrating many interesting features of the model, here we pursue the approach initiated in [92] that illustrates rich and emergent analytical structures that can be used to construct explicit analytical solutions in terms of asymptotic series. The paper [92] focused on the special case $\alpha_1 = \alpha_2 = 0$[8]. Here, we extend their results to the more general case $\alpha_1 = \alpha_2 \neq 0$, following closely the arguments in [92]. Some of our results apply also to the most general case of $\alpha_1 \neq \alpha_2$.

3.2.1 Spectral representation

The crucial idea is considering a suitably defined "Fourier space" (or the "Mellin space") defined by the Fourier transform with respect to the "rapidity" variable[9] $\theta = \frac{1}{2}\log\left(\frac{x}{1-x}\right)$:

$$\Psi(\nu) = \mathcal{F}[\phi(x)](\nu) = \int_0^1 \frac{\mathrm{d}x}{2x(1-x)} \left(\frac{x}{1-x}\right)^{\frac{i\nu}{2}} \phi(x) = \int_{-\infty}^{+\infty} \mathrm{d}\theta\, e^{i\nu\theta}\phi(\theta) \tag{3.2.1}$$

Being a Fourier transform, this integral transformation can be inverted as follows:

$$\phi(x) = \mathcal{F}^{-1}[\Psi(\nu)](x) = \int_{-\infty}^{+\infty} \frac{\mathrm{d}\nu}{2\pi} \left(\frac{x}{1-x}\right)^{-\frac{i\nu}{2}} \Psi(\nu) \tag{3.2.2}$$

It is worth noting that essentially the same rewriting was used in the analysis of the so-called ladder-limit of Wilson loop in $\mathcal{N} = 4$ super Yang-Mills [142–144], in order to reformulate the Bethe-Salpeter equation governing the spectrum of operators into the Baxter TQ-system.

't Hooft equation in the spectral space. Let us express (3.1.16) in the ν-space. To do that, it is convenient to multiply $x(1-x)$ to (3.1.16). Then upon going to rapidity space, $x = \frac{1}{1+e^{-2\theta}}$, we can just apply the usual properties of the Fourier transform, together with the identity:

$$x(1-x)\int_{-\infty}^{+\infty} \frac{\mathrm{d}\nu}{2\pi} \oint_0^1 \mathrm{d}y\, \frac{1}{(x-y)^2}\left(\frac{y}{1-y}\right)^{i\frac{\nu}{2}} \Psi(\nu) = \mathcal{F}^{-1}\left[\frac{\pi\nu}{2}\coth\left(\frac{\pi}{2}\nu\right)\Psi(\nu)\right], \tag{3.2.3}$$

to obtain the following form of (3.1.16) in the ν-space:

$$\begin{aligned}\lambda\int_{-\infty}^{+\infty} \mathrm{d}\nu'\, \frac{\pi(\nu-\nu')}{2\sinh\left(\frac{\pi}{2}(\nu-\nu')\right)}\Psi_b^a(\nu') = &\left[\nu\coth\left(\frac{\pi}{2}\nu\right) + \frac{\alpha_1+\alpha_2}{\pi}\right]\Psi_b^a(\nu) \\ &+ \int_{-\infty}^{+\infty} \mathrm{d}\nu'\,\mathcal{P}\frac{i(\alpha_2-\alpha_1)}{2\sinh\left(\frac{\pi}{2}(\nu-\nu')\right)}\Psi_b^a(\nu')\,.\end{aligned} \tag{3.2.4}$$

[8] Recall that this does not correspond to any special physical limit of the problem but simplifies greatly the eigenproblem.

[9] This representation was considered also in [141].

The factor of i multiplying the term proportional to the mass difference is crucial. Charge-conjugation $\mathcal{C}$, that is an exact symmetry of the system for real values of α, is readily shown to act in ν-space with complex conjugation of the wavefunctions:

$$\left(\Psi_a^b\right)_n^*(\nu) = \int_0^1 \frac{\mathrm{d}x}{2x(1-x)} \left(\frac{x}{1-x}\right)^{-\frac{i\nu}{2}} (\phi_b^a)_n (1-x) = (-1)^n (\Psi_b^a)_n (\nu) \,. \tag{3.2.5}$$

Then, the complex conjugate of (3.2.4) is satisfied by $(\Psi_b^a)(\nu)$ rather than $\left(\Psi_a^b\right)(\nu)$, and the factor of i in the last term takes care of exchanging the masses of the two quark constituents $\alpha_a \leftrightarrow \alpha_b$ under the complex conjugation.

Let us now specialize to $\alpha_1 = \alpha_2 = \alpha$ and use the notation $\Psi_a^a(\nu) = \Psi(\nu)$. We then arrive at the following form of the 't Hooft equation in the ν-space

$$\lambda \int_{-\infty}^{+\infty} \mathrm{d}\nu' \, \frac{\pi(\nu-\nu')}{2\sinh\left(\frac{\pi}{2}(\nu-\nu')\right)} \Psi(\nu') = \left[\nu \coth\left(\frac{\pi}{2}\nu\right) + \frac{2\alpha}{\pi}\right] \Psi(\nu) \,. \tag{3.2.6}$$

The solutions $\Psi(\nu)$ have to decay at $\nu \to \pm\infty$ to guarantee that the norm of the eigenfunctions is finite; we will refine this below by showing that the decay is actually exponential.

A key advantage of recasting the problem in the ν-space (3.2.6) is that this transformation turns a highly singular kernel affected by a (double-pole) principal-value prescription to a regular one. In fact, upon redefining further the function Ψ as:

$$\phi(\nu) = \sqrt{f(\nu)}\, \Psi(\nu), \qquad f(\nu) = \nu \coth\left(\frac{\pi}{2}\nu\right) + \frac{2\alpha}{\pi}, \tag{3.2.7}$$

the equation (3.2.6) takes a form of a homogeneous Fredholm equation of the second kind, a well-studied subject in mathematics: [145,146]:

$$\phi(\nu) = \lambda \int_{-\infty}^{\infty} \mathrm{d}\nu' \, \kappa(\nu,\nu') \, \phi(\nu'), \qquad \kappa(\nu,\nu') := \frac{\pi(\nu-\nu')}{2\sinh\left(\frac{\pi}{2}(\nu-\nu')\right)} \frac{1}{\sqrt{f(\nu)\, f(\nu')}} \,. \tag{3.2.8}$$

For $\alpha > -1$, the kernel $\kappa(\nu,\nu')$ defines a Hilbert–Schmidt integral operator[10][145]. This follows from the following properties of $f(\nu)$,

$$\frac{\partial f(\nu)}{\partial(\frac{2\alpha}{\pi})} = \nu \coth\left(\frac{\pi}{2}\nu\right) + 1 > 0 \quad \forall \nu, \qquad \min_{\nu\in\mathbb{R}} f(\nu)\Big|_{\alpha=-1} = 0 \,, \tag{3.2.9}$$

which guarantees that $f(\nu)$ never vanishes in the considered ranges of α_i and $\kappa(\nu,\nu')$ has a finite $L^2(\mathbb{R}^2)$ norm. This, together with (fast) decaying of the wavefunctions at infinity, is sufficient to show the uniqueness of the solution of (3.2.8) in $L^2(\mathbb{R})$ [145]. By contrast, the analysis for $\alpha = -1$ is more subtle as we will discuss below.

[10]Note the similarities with the kernel in (2.1) of [147], also considered in [148]. See also related works [134,135,149,150] and references therein,

Parity and norm. The Fourier-space function also enjoys similar parity properties, as illustrated by the simple calculation:

$$\begin{aligned}\Psi_n(-\nu) &= \int_{-\infty}^{+\infty} \mathrm{d}x\, \frac{\phi_n(x)}{x(1-x)} \left(\frac{x}{1-x}\right)^{-\frac{i\nu}{2}} = \int_{-\infty}^{+\infty} \mathrm{d}x\, \frac{\phi_n(1-x)}{x(1-x)} \left(\frac{x}{1-x}\right)^{\frac{i\nu}{2}} \\ &= (-1)^n\, \Psi_n(\nu);\end{aligned} \tag{3.2.10}$$

As discussed in [91], the wave functions $\phi_n(x)$ form an orthonormal and complete set in the considered Hilbert space of functions. This can be rephrased in ν-space as:

$$\lambda_n\, \delta_{nm} = \lambda_n \int_0^1 \mathrm{d}x\, \phi_n(x)\, \phi_m^*(x) = \tag{3.2.11}$$

$$\begin{aligned}&= \lambda_n \int_{-\infty}^{+\infty} \frac{\mathrm{d}\nu}{2\pi} \int_{-\infty}^{+\infty} \frac{\mathrm{d}\mu}{2\pi}\, \Psi_n(\nu)\, \Psi_m^*(\mu) \int_0^1 \mathrm{d}x \left(\frac{x}{1-x}\right)^{\frac{i}{2}(\nu-\mu)} \\ &= \lambda_n \int_{-\infty}^{+\infty} \frac{\mathrm{d}\nu}{2\pi} \int_{-\infty}^{+\infty} \frac{\mathrm{d}\mu}{2\pi}\, \Psi_n(\nu)\, \Psi_m^*(\mu)\, \frac{\pi(\nu-\mu)}{2\sinh\left(\frac{\pi}{2}(\nu-\mu)\right)} \\ &\overset{(3.2.6)}{=} \int_{-\infty}^{+\infty} \frac{\mathrm{d}\mu}{2\pi} \frac{f(\mu)}{2\pi}\, \Psi_n(\mu)\, \Psi_m^*(\mu)\end{aligned} \tag{3.2.12}$$

The measure $f(\mu)$ is the same as the one defined in (3.2.7). Another important fact is the asymptotic behavior of the $\Psi(\nu)$: in order to guarantee finiteness of the $\mathbb{L}^2$-norm, $\Psi(\nu)$ needs to decay at least polynomially fast on the real axis.

Massless quarks. At $\alpha = -1$, the quarks are exactly massless and the theory possesses exact chiral symmetry. $f(\nu)$ has a (double) zero in $\nu = 0$ and the conditions above are not satisfied. Indeed we can see that, for $\alpha = -1$ and $\lambda = 0$, (3.2.6) reduces to:

$$\left[\nu \coth\left(\frac{\pi}{2}\nu\right) - \frac{2}{\pi}\right] \Psi(\nu) = 0 \tag{3.2.13}$$

and both $\Psi(\nu) = \delta(\nu)$ and $\Psi(\nu) = \delta'(\nu)$ solve the equation above. While the first solution in x-space is just the constant $\phi(x) = 1$, the second correspond to a logarithmic solution $\mathcal{F}[\delta'(\nu)] = i \log\left(\frac{x}{1-x}\right)$, with finite $\mathbb{L}^2[0,1]$ norm:

$$\int_0^1 \left(\log\left(\frac{x}{1-x}\right)\right)^2 = \frac{\pi^2}{3}\,. \tag{3.2.14}$$

Although the solution diverges logarithmically at the boundaries, it can be verified explicitly that it solves the 't Hooft equation in x-space with $\lambda = 0$:

$$⨍_0^1 \mathrm{d}x\, \frac{\log\left(\frac{x}{1-x}\right)}{(x-y)^2} = \lim_{\epsilon\to 0^+} \frac{1}{2} \left[\int_0^1 \mathrm{d}x\, \frac{\log\left(\frac{x}{1-x}\right)}{(x-y+i\epsilon)^2} + \int_0^1 \mathrm{d}x\, \frac{\log\left(\frac{x}{1-x}\right)}{(x-y-i\epsilon)^2}\right] \tag{3.2.15}$$

$$= -\lim_{\epsilon\to 0^+} \frac{1}{2} \left[\frac{\log(-y+i\epsilon) - \log(1-y+i\epsilon)}{(1-y+i\epsilon)(y-i\epsilon)} + \frac{\log(y+i\epsilon) - \log(-1+y+i\epsilon)}{(1-y-i\epsilon)(y+i\epsilon)}\right] \tag{3.2.16}$$

Now, given that $y \in (0,1)$, we have to be careful while performing the limit $\epsilon \to 0^+$ to take the correct logarithmic branch:

$$\lim_{\epsilon\to 0^+} \log(-\zeta + i\epsilon) = \log\left(\zeta\, e^{+i\pi}\right) = \log(\zeta) + i\pi; \qquad \zeta = y, (1-y) > 0 \tag{3.2.17}$$

Thus, we have

$$\fint_0^1 \mathrm{d}x\, \frac{\log\left(\frac{x}{1-x}\right)}{(x-y)^2} = -\frac{\log\left(\frac{y}{1-y}\right)}{y(1-y)}\,, \tag{3.2.18}$$

from which we deduce that the 't Hooft equation (3.1.16) with $\alpha = -1$ is satisfied by $\log\left(\frac{x}{1-x}\right)$. Nevertheless this solution does not correspond to a physical mesonic state. This degeneracy between physical and unphysical solutions leads to interesting analytic structure of the spectrum (as a function of mass squared) as we will discuss thoroughly in section 3.3.

Bethe-Salpeter approximation in Ising Field Theory. Before proceeding further, let us point out a similarity with the so-called *Ising field theory* (IFT), i.e. Ising CFT perturbed by both magnetic field and temperature. In the "rapidity" variable, the 't Hooft equation (3.1.16) takes the form

$$\left(\frac{\pi^2\lambda}{2\cosh^2\theta} - \frac{\alpha_a+\alpha_b}{2} + \frac{\alpha_a-\alpha_b}{2}\tanh\theta\right)\phi_a^b(\theta) = -2\fint_{-\infty}^{+\infty}\mathrm{d}\varphi\,\frac{1}{\sinh^2(\theta-\varphi)}\phi_a^b(\varphi)\,. \tag{3.2.19}$$

In the equal mass limit, this equation is similar to the Bethe-Salpeter approximation of IFT [151]. In a small external magnetic field approximation of IFT, the stable particles in the spectrum share similarities with bound states in QCD_2 behaving exactly as mesons (see [151]). In this limit, one can expand around the free theory of Majorana fermions with mass m and obtains the Bethe-Salpeter equation by looking at the eigenstates of the perturbed Hamiltonian $H_{\text{free}} + h\int\sigma$ that are only of the form of two-particle state, and ignoring all the higher-particle contributions:

$$\left(m^2 - \frac{M^2}{\cosh^2\theta}\right)\Psi(\theta) = f_0\fint_{-\infty}^{+\infty}\frac{\mathrm{d}\theta'}{2\pi}\left(2\frac{\cosh(\theta-\theta')}{\sinh^2(\theta-\theta')} + \frac{1}{4}\frac{\sinh\theta\,\sinh\theta'}{\cosh^2\theta\,\cosh^2\theta'}\right)\Psi(\theta') \tag{3.2.20}$$

(Here f_0 is the "string tension" scale and is proportional to the strength of the magnetic field h.) This equation determines the spectrum of the *Ising mesons* that share many interesting features with the ones of the 't Hooft model. Higher-particle states will contribute at higher order in h, with the two particle sector being the dominant in $h \to 0$. In this sense, h plays the same role of $1/N$ in the 't Hooft model. In the beautiful recent work [138] the method of [92,93] as been extended also to cover IFT.

3.2.2 TQ-relation

Let us consider again the 't Hooft equation with equal masses (3.2.6), that we display here for convenience:

$$\lambda \int_{-\infty}^{+\infty} \mathrm{d}\nu' \, \frac{\pi(\nu-\nu')}{2\sinh\left(\frac{\pi}{2}(\nu-\nu')\right)} \, \Psi(\nu') = \underbrace{\left[\nu \coth\left(\frac{\pi}{2}\nu\right) + \frac{2\alpha}{\pi}\right]}_{=:f(\nu)} \Psi(\nu) \, . \tag{3.2.21}$$

The function $\sqrt{f(\nu)}\Psi(\nu)$ is a solution to a Fredholm equation of the second kind with a Hilbert-Schmidt kernel. In particular the right hand side $f(\nu)\Psi(\nu)$ does not have any singularities in the strip $(-2i, 2i)$ where we can analytically continue both the l.h.s. and the r.h.s. of the equation[11]. Then, the *Q-function* defined by

$$Q(\nu) = \sinh\left(\frac{\pi}{2}\nu\right) f(\nu)\, \Psi(\nu) \tag{3.2.22}$$

does not have any singularity in the strip $[-2i, 2i]$, grows slower than an exponential at $\nu \to \pm\infty$ on the real line, and satisfies the related integral equation:

$$Q(\nu) = \lambda \sinh\left(\frac{\pi}{2}\nu\right) \int_{-\infty}^{+\infty} \mathrm{d}\nu' \, \frac{\pi(\nu-\nu')}{2\sinh\left(\frac{\pi}{2}(\nu-\nu')\right)} \frac{Q(\nu')}{\sinh\left(\frac{\pi}{2}\nu'\right) f(\nu')} \, , \tag{3.2.23}$$

Furthermore, it follows from the absence of poles of $f(\nu)\,\Psi(\nu)$ as well as (3.2.23) that

$$Q(0) = Q(\pm 2i) = 0 \, , \tag{3.2.24}$$

where $\sinh\left(\frac{\pi}{2}\nu\right)$ vanishes. The equation (3.2.24) can be regarded as the "quantization" condition as we will discuss in Section 3.2.3.

We can extend the asymptotic behavior of the Q-functions to the entire strip $[-2i, 2i]$. To do so, we use (3.2.23) to verify that the Fourier transform of $\mathcal{Q}(\nu) := \frac{Q(\nu)}{\sinh\left(\frac{\pi}{2}\nu\right)}$,

$$\widehat{\mathcal{Q}}(y) := \mathcal{F}\left[\mathcal{Q}(\nu)\right](y) = \int_{-\infty}^{+\infty} \mathrm{d}\nu \, \frac{Q(\nu)}{\sinh\left(\frac{\pi}{2}\nu\right)} e^{i\nu y} \, , \qquad \widehat{\mathcal{Q}}_\xi(y) := \mathcal{F}[\mathcal{Q}(\nu + i\xi)](y) \, , \tag{3.2.25}$$

satisfies the following relation:

$$\widehat{\mathcal{Q}}_\xi(y) = \lambda \frac{\pi e^{-y\xi}}{\cosh^2(y)} \mathcal{F}\left[\mathcal{Q}/f\right](y) = \lambda \frac{\pi e^{-y\xi}}{\cosh^2(y)} \mathcal{F}\left[\Psi\right](y) \, . \tag{3.2.26}$$

Since $\Psi(\nu)$ is $\mathbb{L}^2$ and decays at least polynomially on the real axis, (3.2.26) implies automatically that also $\widehat{\mathcal{Q}}_\xi(y)$ and consequently $\mathcal{Q}(\nu + i\xi)$ are $\mathbb{L}^2$ for any $|\xi| < 2$. We thus deduce that $\mathcal{Q}(\nu)$ decays at least polynomially for any $\mathrm{Im}\ \nu \in [-2i, 2i]$ at $|\mathrm{Re}\ \nu| \to \infty$. Upon evaluating (3.2.26) at $\xi = \pm 2$, one can easily show

$$\widehat{\mathcal{Q}}_2(y) + \widehat{\mathcal{Q}}_{-2}(y) = -2\widehat{\mathcal{Q}}(y) + (4\pi\lambda)\, \mathcal{F}\left[\mathcal{Q}/f\right](y) \, . \tag{3.2.27}$$

[11] If we analytically continue outside of the strip, the integral kernel gets modified because of poles crossing the integration contour. We will discuss this in detail in Section 3.3.

This is the Fourier transform of the following difference equation[12],

$$\mathcal{Q}(\nu+2i)+\mathcal{Q}(\nu-2i)+2\mathcal{Q}(\nu)=\frac{4\pi\lambda}{f(\nu)}\mathcal{Q}(\nu)\,, \tag{3.2.28}$$

which can be further rewritten in terms of the original Q-function as follows[13]:

$$\boxed{Q(\nu+2i)+Q(\nu-2i)-2Q(\nu)=\frac{-4\pi\lambda}{\nu\coth\left(\frac{\pi}{2}\nu\right)+\frac{2\alpha}{\pi}}\,Q(\nu)} \tag{3.2.29}$$

This illustrates the advantage of going into the ν-space. Here the integral equation was recast into the finite-difference equation having the form of the so-called *TQ-Baxter* equation, which appears in the study of integrable systems. To each solution $\Psi(\nu)$ of (3.2.6) decaying at least polynomially at $|\mathrm{Re}\,\nu|\to\infty$, there is an associated solution $Q(\nu)$ of (3.2.29) analytic in the strip $(-2i,2i)$, and growing slower than any exponential at $|\mathrm{Re}\,\nu|\to\infty$. This asymptotic behavior, together with the quantization condition (3.2.24), determines the discrete spectrum of the 't Hooft equation.

From TQ back to 't Hooft. With the aforementioned asymptotic behavior, the converse is also true: any solution $Q(\nu)$ to the TQ-system subject to the asymptotic conditions gives a solution to (3.2.6). This can be proven[14] by noting that if $Q(\nu)$ satisfies (3.2.29), the difference between the l.h.s. and r.h.s. of (3.2.23),

$$h(\nu)=Q(\nu)-\lambda\sinh\left(\frac{\pi}{2}\nu\right)\int_{-\infty}^{+\infty}\mathrm{d}\nu'\,\frac{\pi(\nu-\nu')}{2\sinh\left(\frac{\pi}{2}(\nu-\nu')\right)}\frac{Q(\nu')}{\sinh\left(\frac{\pi}{2}\nu'\right)f(\nu')}\,, \tag{3.2.30}$$

extends to a periodic function

$$h(\nu+2i)+h(\nu-2i)=0\,, \tag{3.2.31}$$

that is also entire and bounded in the strip as it does not have poles and decays at infinity; the only such function is a constant function and it has to be $h(\nu)=0$ as from $Q(0)=Q(\pm 2i)=0$ we deduce that $h(\pm 2i)=h(0)=0$. This completes the proof of the equivalence between the Baxter-TQ equation (3.2.29) and the integral equation determining the spectrum of mesons in the ν-space (3.2.6), and illustrates an interesting "integrable" structure underlining 't Hooft equation.

Decay of the eigenfunctions. As a simple application of the TQ-system presented above, let us derive a stronger[15] condition on the decay of the eigenfunctions of the 't

[12] An alternative and more direct proof of (3.2.28) and (3.2.29) is provided in [1, Appendix A]

[13] The reason for which we prefer this latter formulation in terms of $Q(\nu)$ rather than $\mathcal{Q}(\nu)$ will be clear only in section 3.2.3 where we extend the problem to an inhomogeneous one; at this level the two are completely equivalent.

[14] A similar argument is used in [152] to prove Lemma 2 and 3.

[15] Stronger then the polynomial decay.

Hooft equation. For any $q(\nu)$ periodic with period $2i$ and growing less than exponentially, $Q(\nu) \asymp e^{\pi k \nu} q(\nu)$ satisfies the $\nu \gg 1$ limit of (3.2.29):

$$Q(\nu+2i) + Q(\nu-2i) - 2Q(\nu) + \frac{4\pi\lambda}{\nu} Q(\nu) \asymp -4e^{\pi k\nu} q(\nu) \sin^2(k\pi) + \mathcal{O}(\nu^{-1}) \quad (3.2.32)$$

as long as $k \in \mathbb{Z}$. Now, given that $q(\nu)$ can be chosen arbitrarily, in order to guarantee that $Q(\nu)$ grows slower than an exponential, we must require $k \leq 0$. Henceforth, this already slightly more refined analysis demonstrates that requiring $Q(\nu)$ less than exponentially growing and $\Psi(\nu)$ decaying at infinity, automatically implies that the solutions $\Psi(\nu)$ decay exponentially at infinity.

Potential relation to W_∞-algebra. This connection to integrability opens up various promising directions for future exploration. Before proceeding further, let us remark that a hidden algebraic structure of the 't Hooft model was discussed long ago based on the *collective field approach* [153]. By reformulating the 't Hooft model in terms of bilocal fields, $M_{ij}(x,y) = \frac{1}{N} \operatorname{tr}\left[(\psi_i^a)^\dagger(x)\psi_j^a(y)\right]$, they found that mesons at large N_c transform under representations of the algebra[16] $W_\infty^L \otimes W_\infty^R \otimes U(N_f)$. This infinite-dimensional algebra acts as a spectrum-generating algebra of mesons since it does not commute with the Hamiltonian. In standard integrable systems, a similar role is played by Yangian or quantum group. It would be interesting to understand a connection between this W_∞-algebra and the integrable structure that we observed here.

3.2.3 Extending to an inhomogeneous problem

Solutions to the TQ-Baxter equation satisfying the quantization condition (3.2.24) (and the aforementioned asymptotic behavior) exist only for the discrete values of λ in the spectrum, and our task is solving simultaneously for $Q_n^{(\alpha)}(\nu)$ and λ_n. This, in general, is as difficult as the problem we started with in (3.1.16).

One way of making progress is to develop a systematic large λ expansion, which refines and improves the WKB expansion at large quantum number. For this purpose, it is important to first extend λ_n from discrete values to arbitrary values of $\lambda \in \mathbb{R}$. The situation is analogous to the large spin expansion in conformal field theory, for which a systematic analysis was made possible by the Lorentzian inversion formula [154] that enables the analytic continuation of the conformal data away from integer spins.

To achieve this, we pursue the strategy presented in [92], and simply introduce an appropriate inhomogeneous term $F(\nu)$ (which we specify later) to the 't Hooft equation (3.2.6). Then the solution $\phi(\nu|\lambda)$ (stressing now the dependence on the continuous parameter λ) satisfies the inhomogeneous Fredholm equation that extends (3.2.8),

$$\frac{F(\nu)}{\sqrt{f(\nu)}} = \phi(\nu|\lambda) - \lambda \int_{-\infty}^{\infty} \mathrm{d}\nu'\, \kappa(\nu,\nu')\phi(\nu'|\lambda), \quad (3.2.33)$$

[16] A W_∞ algebra in this context arises in the large N limit as a limit of W_N for any finite number of colors.

Solutions to this equation exist for arbitrary $\lambda \in \mathbb{R}$, and they admit the Liouville-Neumann (L-N) series representation, which can be obtained by successive iterations of the inhomogeneous term:

$$\phi(\nu;\lambda) = \sum_{n=0}^{\infty} \lambda^n \, \phi_n(\nu), \qquad \phi_n(\nu) = \int \mathrm{d}\mu \, K_n(\nu,\mu) \, \frac{F(\mu)}{\sqrt{f(\mu)}} \,, \tag{3.2.34a}$$

$$K_n(\nu,\mu) = \int \mathrm{d}\rho_1 \cdots \mathrm{d}\rho_{n-1} \, \kappa(\nu,\rho_1) \cdots \kappa(\rho_{n-1},\mu), \qquad K_0(\nu,\mu) := \delta(\nu-\mu) \,. \tag{3.2.34b}$$

To express the results more compactly, it is convenient to introduce the *resolvent* $R(\mu,\nu|\lambda)$ (see also relevant discussions in [148]), defined by $R := \frac{\kappa}{1-\lambda\kappa}$. By definition, it satisfies the related integral equation (independent of the inhomogeneous term F):

$$R(\mu,\nu|\lambda) - \lambda \int_{-\infty}^{+\infty} \mathrm{d}\rho \, R(\mu,\rho|\lambda) \, \kappa(\rho,\nu) = \kappa(\mu,\nu) \,, \qquad R(\mu,\nu|\lambda) = \sum_{n=0}^{\infty} \lambda^n K_n(\mu,\nu) \,. \tag{3.2.35}$$

In terms of the resolvent, the solution $\phi(\nu|\lambda)$ is simply $\phi(\nu|\lambda) = \int_{-\infty}^{+\infty} \mathrm{d}\mu \, R(\nu,\mu|\lambda) \, \frac{F(\mu)}{\sqrt{f(\mu)}}$.

Let us now specify the inhomogeneous term. As in [92], we choose the following basis of the inhomogeneous extensions, each of which has a definite parity under $\nu \to -\nu$:

$$F_+(\nu) = \frac{\nu}{\sinh\left(\frac{\pi}{2}\nu\right)}, \qquad F_-(\nu) = \frac{1}{\sinh\left(\frac{\pi}{2}\nu\right)} \,. \tag{3.2.36}$$

It is interesting to note that they correspond to a quadratic (even) and a linear (odd) potential in the $[0,1]$ box:

$$\mathcal{F}\left[F_+(\nu)\right] \propto x(1-2x), \qquad \mathcal{F}\left[F_-(\nu)\right] \propto (-1+2x) \,, \tag{3.2.37}$$

As already said, each of the two, through the L-N series, drives a unique solution of the extended eigenproblem $\Psi_\pm(\nu|\lambda)$ $(= \pm\Psi_\pm(-\nu|\lambda))$ (cf. (3.2.33)) :

$$F_\pm(\nu) = f(\nu) \, \Psi_\pm(\nu|\lambda) - \lambda \fint_{-\infty}^{+\infty} \mathrm{d}\nu' \, \frac{\pi(\nu-\nu')}{2\sinh\left(\frac{\pi}{2}(\nu-\nu')\right)} \, \Psi_\pm(\nu'|\lambda) \,. \tag{3.2.38}$$

The solutions to this inhomogeneous equation are (fast) decaying at $\nu \to \pm\infty$ as well. A direct way to see this is by noting that each of the $\phi_n(\nu)$ decays as infinity given that both the K_n and $F_\pm$ are exponentially suppressed.

At special values $\lambda = \lambda_n$, the inhomogeneous equation above has to reduce to the homogeneous one (3.2.6). This implies that the inhomogeneous eigenfunctions $\Psi_\pm(\nu|\lambda)$ are singular at $\lambda = \lambda_n$ with $\Psi_n(\nu|\lambda_n)$ being the residue at $\lambda = \lambda_n$. More precisely, because of the parity, we have[17]

$$\Psi_+(\nu|\lambda) \sim \sum_{k=0}^{\infty} \frac{c_{2n}\Psi_{2n}(\nu)}{\lambda-\lambda_{2n}} \,, \qquad \Psi_-(\nu|\lambda) \sim \sum_{k=0}^{\infty} \frac{c_{2n+1}\Psi_{2n+1}(\nu)}{\lambda-\lambda_{2n+1}} \,. \tag{3.2.39}$$

[17] As noted in [92], the coefficients c_k's are proportional to the matrix elements of $\bar\Psi\gamma^\mu\Psi$ and $\bar\Psi\Psi$. We plan to go back to studying correlation functions of this model somewhere else.

TQ-system. The inhomogeneous $Q_\pm(\nu|\lambda)$ defined as:

$$Q_\pm(\nu|\lambda) = \sinh\left(\frac{\pi\nu}{2}\right) f(\nu)\, \Psi_\pm(\nu|\lambda) = \mp Q_\pm(-\nu|\lambda) \tag{3.2.40}$$

satisfy the related inhomogeneous integral equation:

$$\sinh\left(\frac{\pi}{2}\nu\right) F_\pm(\nu) = Q_\pm(\nu) - \lambda \sinh\left(\frac{\pi}{2}\nu\right) \int_{-\infty}^{+\infty} \mathrm{d}\nu' \, \frac{\pi(\nu-\nu')}{2\sinh\left(\frac{\pi}{2}(\nu-\nu')\right)} \, \frac{Q_\pm(\nu')}{\sinh\left(\frac{\pi}{2}\nu'\right) f(\nu')} \tag{3.2.41}$$

From (3.2.41), it immediately follows that

$$Q_+(\pm 2i) = \pm 2i\,, \qquad Q_+(0) = 0\,, \qquad Q_-(\pm 2i) = Q_-(0) = 1\,. \tag{3.2.42}$$

As is clear from these, the quantization conditions (3.2.24) are not satisfied for the inhomogeneous extensions.

An argument analogous to the one presented below (3.2.23) implies that $Q_\pm(\nu)$ grow less than an exponential in the entire strip $[-2i, 2i]$. In addition, $Q_\pm(\nu)$ are analytic (without poles) in the strip. This is guaranteed by the $\sinh(\frac{\pi}{2}\nu)$ factor in the definition $Q(\nu) = \sinh(\frac{\pi}{2}\nu)\mathcal{Q}(\nu)$, which cancels the poles in $F_\pm$, and is ultimately the reason behind using $Q(\nu)$ rather than $\mathcal{Q}(\nu)$.

Now, since $F_\pm$ satisfies

$$\sinh\left(\frac{\pi(\nu+2i)}{2}\right) F_\pm(\nu+2i) + \sinh\left(\frac{\pi(\nu-2i)}{2}\right) F_\pm(\nu-2i) - 2\sinh\left(\frac{\pi}{2}\nu\right) F_\pm(\nu) = 0\,, \tag{3.2.43}$$

one can follow the derivation of the previous subsection to show that $Q_\pm(\nu|\lambda)$ satisfies the same TQ-Baxter equation[18] as in the homogeneous problem,

$$Q_\pm(\nu+2i|\lambda) + Q_\pm(\nu-2i|\lambda) - 2Q_\pm(\nu|\lambda) = \frac{-4\pi\lambda}{f(\nu)} Q_\pm(\nu|\lambda) \tag{3.2.44}$$

but this time for any value of $\lambda \in \mathbb{R}$.

Wronskian. The Wronskian constructed out of the two independent solutions $Q_\pm(\nu|\lambda)$:

$$W(\nu|\lambda) = Q_+(\nu+i|\lambda)Q_-(\nu-i|\lambda) - Q_+(\nu-i|\lambda)Q_-(\nu+i|\lambda), \tag{3.2.45}$$

results to be a periodic function as following from the straightforward computation:

$$\frac{W(\nu+i|\lambda)}{W(\nu-i|\lambda)} = \frac{Q_+(\nu+2i|\lambda)Q_-(\nu|\lambda) - Q_+(\nu|\lambda)Q_-(\nu+2i|\lambda)}{Q_+(\nu|\lambda)Q_-(\nu-2i|\lambda) - Q_+(\nu-2i|\lambda)Q_-(\nu|\lambda)} = 1\,. \tag{3.2.46}$$

[18] This TQ-system admits exponentially growing solutions at $\nu \gg 1$ as well (see also the discussions around (3.2.32)). However, they do not correspond to solutions of (3.2.41). The two problems are equivalent only under the asymptotic condition that Q grows less than an exponential.

Furthermore the asymptotic growth condition at $|\mathrm{Re}\,\nu| \gg 1$ and the analyticity of $Q_\pm$ in the strip guarantee that $W(\nu|\lambda)$ is a constant, depending only on the normalization of $Q_\pm(\nu|\lambda)$. With our normalization, fixed in (3.2.36) (see also (3.2.42)), we have:

$$W(\nu|\lambda) = W(i|\lambda) = Q_+(2i|\lambda)Q_-(0|\lambda) = 2i. \tag{3.2.47}$$

As mentioned before, at $\lambda = \lambda_n$, one of the solutions $Q_\pm$ develops a pole $\propto 1/(\lambda - \lambda_n)$. Owing to the identity $W(\nu|\lambda) = 2i$, this in turn means that the residue of (3.2.45) must be zero:

$$\begin{aligned} &Q_{2n}(\nu+i)Q_-(\nu-i|\lambda_{2n}) - Q_{2n}(\nu-i)Q_-(\nu+i|\lambda_{2n}) = 0\,, \\ &Q_+(\nu+i|\lambda_{2n+1})Q_{2n+1}(\nu-i) - Q_+(\nu-i|\lambda_{2n+1})Q_{2n+1}(\nu+i) = 0\,. \end{aligned} \tag{3.2.48}$$

Here Q_n is the homogeneous Q-function for $\lambda = \lambda_n$. These equations imply that Q_{2n} and Q_- (and similarly Q_{2n+1} and Q_+) coincide up to a multiplication of a periodic function when λ is part of the discrete spectrum. Therefore, at these values of λ, we only have a single non-degenerate solution to the TQ-system satisfying the required asymptotic behavior.

Spectral determinants. We have extended the problem (3.2.6) to homogeneous one (3.2.38) that can, in principle, be solved by means of the L-N series (3.2.34) resulting in two independent solutions for each $\lambda \in \mathbb{R}$. Yet, the solutions obtained in that way are only indirectly related to the solutions of the original problem that has a discrete spectrum. Fortunately, there is a way to relate the two explicitly making use of the crucial property of the kernel $\kappa(\nu,\nu')$; it belongs to the class of *"completely integrable kernels"* in the language of [155,156]. For this class of kernels, it is known that the resolvent is given in a closed form in terms of the two independent solutions. This is discussed in Appendix B of [92]. In our case, this translates into the following expression:

$$R(\mu,\nu|\lambda) = \frac{2\sinh\left(\frac{\pi}{2}\mu\right)\sinh\left(\frac{\pi}{2}\nu\right)}{\pi\sinh\left(\frac{\pi}{2}(\mu-\nu)\right)}\sqrt{f(\mu)\,f(\nu)}\,\left[\Psi_+(\nu|\lambda)\,\Psi_-(\mu|\lambda) - \Psi_-(\nu|\lambda)\,\Psi_+(\mu|\lambda)\right]. \tag{3.2.49}$$

In turn, this implies that the two spectral determinants

$$D_+(\lambda) = \left(\frac{8\pi}{e}\right)^\lambda \prod_{n=0}^{\infty}\left(1-\frac{\lambda}{\lambda_{2n}}\right)e^{\frac{\lambda}{n+1}}, \quad D_-(\lambda) = \left(\frac{8\pi}{e}\right)^\lambda \prod_{n=0}^{\infty}\left(1-\frac{\lambda}{\lambda_{2n+1}}\right)e^{\frac{\lambda}{n+1}}. \tag{3.2.50}$$

satisfy the following non-trivial integral identities :

$$\begin{aligned} \partial_\lambda \log(D_+(\lambda)D_-(\lambda)) &= 2 + \int_{-\infty}^{+\infty} \mathrm{d}\nu\,\frac{\pi}{2}\left[\frac{Q_+(\nu|\lambda)\,\partial_\nu Q_-(\nu|\lambda) - Q_-(\nu|\lambda)\,\partial_\nu Q_+(\nu|\lambda)}{f(\nu)} + \frac{\tanh\left(\frac{\pi}{2}\nu\right)}{\nu}\right], \\ \partial_\lambda \log\left(\frac{D_+(\lambda)}{D_-(\lambda)}\right) &= -\int_{-\infty}^{+\infty} \mathrm{d}\nu\,\frac{\pi^2}{2}\frac{Q_+(\nu|\lambda)\,Q_-(\nu|\lambda)}{\sinh(\pi\nu)f(\nu)}, \end{aligned} \tag{3.2.51}$$

This follows from the facts that the logarithm of the spectral determinants are given by

$$\log D_{\pm}(\lambda) = (\log(8\pi) - 1)\lambda - \sum_{s=1}^{+\infty} s^{-1}\, G_{\pm}^{(s)}\, \lambda^s \qquad G_{+}^{(s)} = \sum_{n=0}^{\infty} \frac{1}{\lambda_{2n}^s}, \qquad G_{-}^{(s)} = \sum_{n=0}^{\infty} \frac{1}{\lambda_{2n+1}^s}\,, \tag{3.2.52}$$

and that the spectral sums $G_{\pm}^{(s)}$ are encoded in to the traces of the resolvent as (cf. eq (8.9) and (8.10) of [92], and Appendix 3.5.2 for an analogous computation[19]):

$$\begin{aligned} \sum_{s=1}^{\infty} \lambda^{s-1} \left(G_{+}^{(s)} + G_{-}^{(s)}\right) &= C + \int_{-\infty}^{+\infty} \mathrm{d}\mu \left[R(\mu, -\mu|\lambda) + R^{(0)}(\mu)\right]\,, \\ \sum_{s=1}^{\infty} \lambda^{s-1} \left(G_{+}^{(s)} - G_{-}^{(s)}\right) &= \int_{-\infty}^{+\infty} \mathrm{d}\mu\, R(\mu, \mu|\lambda)\,. \end{aligned} \tag{3.2.53}$$

With the choice of $R^{(0)}(\mu)$ in (3.2.51), $\tanh(\pi\nu/2)/\nu$, one can check that the integrals are convergent using the asymptotic properties of the inhomogeneous Q-functions, and that the constant C is 2.

Using these expressions, we can extract the spectral data associated with the homogeneous problem from the inhomogeneous solutions $Q_{\pm}(\lambda)$. Specifically, we will illustrate in Section 3.4 how to extract analytical expressions for the meson masses λ_n as well as for spectral sums thereof (3.2.52).

3.3 Meson spectrum at complex quark mass and critical points

In this section we discuss the properties of the eigenvalues $\lambda(\alpha)$ as the masses of the quarks are analytically continued to the complex plane $\alpha \in \mathbb{C}$[20].

3.3.1 Poles of $\Psi(\nu)$ and boundary conditions

The key players in the following discussions are zeros of $f(\nu)$ and associated poles of $\Psi(\nu)$. We thus first explain their basic properties.

The starting point is the defining functional equation (3.2.6) that we report here for convenience:

$$f(\nu)\,\Psi(\nu) = \left(\frac{2\alpha}{\pi} + \nu \coth\frac{\pi}{2}\nu\right)\Psi(\nu) = \lambda(\alpha)\int_{-\infty}^{+\infty} \mathrm{d}\nu'\, \frac{\pi(\nu-\nu')}{2\sinh\frac{\pi}{2}(\nu-\nu')}\Psi(\nu') \tag{3.3.1}$$

For $\alpha > -1$, given that the kernel is continuous for any real value, the function $\Psi(\nu)$ has poles only in correspondence with the location of the zeros of $f(\nu)$:

$$f(\nu) = \frac{2\alpha}{\pi} + \nu \coth\left(\frac{\pi\nu}{2}\right) = 0\,, \tag{3.3.2}$$

[19] The specific form of the $F_{\pm}(\nu)$ is paramount to obtain these expressions (see discussion in Appendix B of [92], or the similar non-trivial trigonometric identities in (3.5.23))

[20] After the first version of this work appeared in arXiv, we learned that partial results on numerical investigation of the meson spectrum at complex quark mass and criticality was presented by Zamolodchikov in a talk [157]. See here.

and it is regular anywhere else in the strip Im $\nu \in [-2i, 2i]$. The zeros of $f(\nu)$ do not admit a closed form expression, but can be shown to lie for $\alpha > -1$ on the imaginary axis $\nu_k = \pm i u_k$, with $2ki < \nu_k < 2(k+1)i$, i.e. the first zero lies in $\nu_0 \in (0, 2i)$, the second $\nu_1 \in (2i, 4i)$, and so on. At each of these points $\pm\nu_k$, $\Psi(\nu)$ displays simple poles.

The closest poles of $\Psi(\nu)$ to the real axis regulate the exponential decay of the wavefunction in the Fourier dual space of ν, that is the space of rapidities $\theta = \frac{1}{2}\log\frac{x}{1-x}$ as:

$$\phi(\theta) \sim \mathcal{F}\left[\frac{1}{\nu + i u_0} \pm \frac{1}{\nu - i u_0}\right] = -i\left(\Theta(\theta) \pm \Theta(-\theta)\right) e^{-u_0|\theta|}, \qquad u_0 > 0\,, \tag{3.3.3}$$

where $\Theta(x)$ is the Heaviside step function. The farther poles are subleading contributions. This is consistent with the boundary conditions in x-space as $\exp(-u_0|\theta|) \sim x^{u_0/2}$ for $x \sim 0$ and $\exp(-u_0|\theta|) \sim (1-x)^{u_0/2}$ for $x \sim 1$; then the comparison between (3.3.2) and (3.1.19) (determining the allowed boundary conditions β_i) demonstrates that $\beta = \pm u_0/2$ (equal masses). Indeed we see that the $0 \leq |\beta| \leq 1$ is consistent with $0 \leq |u_0| \leq 2$. Thus, this argument provides an alternative derivation for the boundary conditions of the wavefunctions in position space, which we derived in (3.1.19). From this perspective the condition $0 \leq \beta \leq 1$ simply follows from the position of the closest (dominant) pole.

Instead, choosing non-regular boundary conditions for $\phi(x)$ corresponding to $\beta < 0$, produce exponentially divergent wavefunctions $e^{u_0|\theta|}$. These non-normalizable wavefunctions do not correspond to any solution of the spectral problem (3.2.6) (it is not possible to produce any such exponentially divergent solution by Fourier transform of any $\Psi(\nu)$). They correspond in ν-space to solutions of the problem outside of $\mathbb{L}^2$.

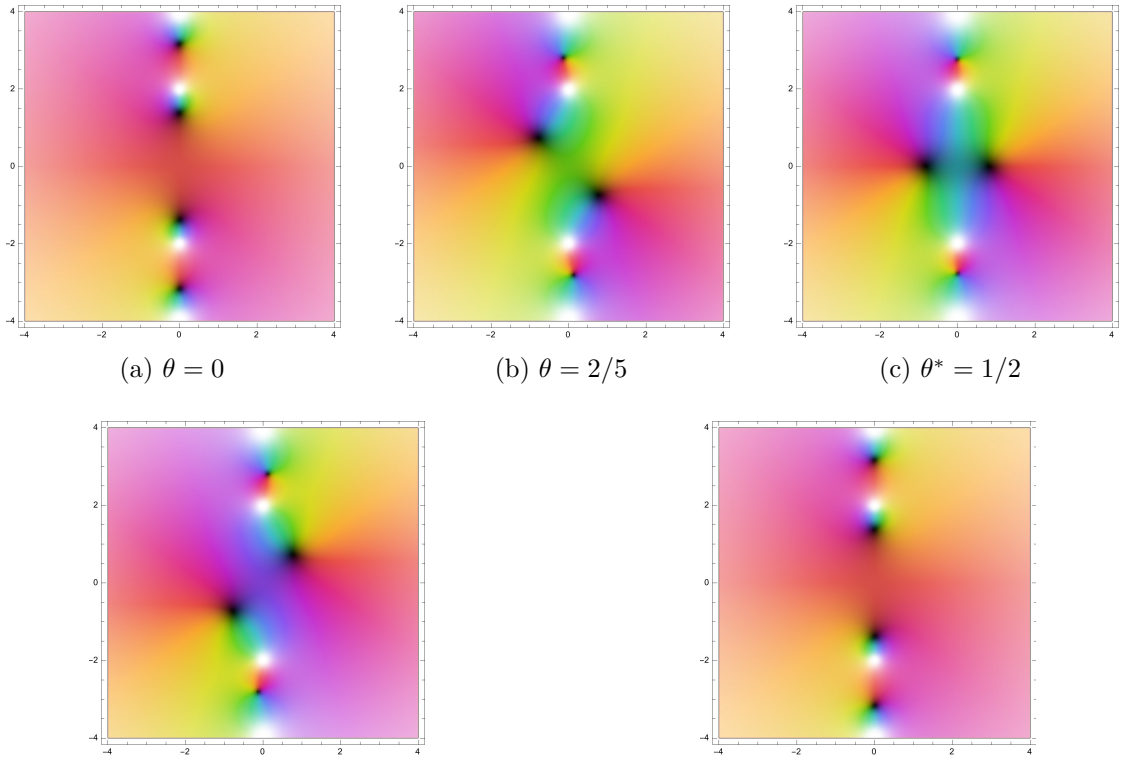
3.3.2 Criticality in the chiral limit

In the limit where the chiral symmetry becomes exact $\alpha \to -1$, the poles of $\Psi(\nu)$ surface to the real axes and degenerate into a double zero, $\nu_0(-1) = 0$:

$$\pm\nu_0(\alpha \to -1) = \pm\frac{2i}{\pi}\sqrt{\alpha}\,\sqrt{\alpha+1} \to 0\,. \tag{3.3.4}$$

Hence, $\Psi(\nu)$, that was regular on the real axis for any $\alpha > -1$, now becomes singular at the origin in the chiral limit. Indeed, we already saw in section 3.2.1 that the eigenfunction for the lowest eigenvalue is singular in the chiral limit being proportional to the $\delta(\nu)$ and is degenerate with $\delta'(\nu)$. We can also recover this results from the qualitative analysis of the previous subsection: the ground state $\Psi_0(\nu)$ must have no zeros on the real axis and parity even. So, taking the + sign in (3.3.3) and sending $u_0 \to 0$, we indeed recover $\Psi_0(\nu) = \delta(\nu)$. To obtain the other solution $\delta'(\nu)$, we use the fact that $f(\nu)$ now has a double zero at the origin and therefore $\Psi(\nu)$ can have a double pole. This leads to $\phi(\theta) \sim \mathcal{F}\left[\frac{1}{(\nu-i\epsilon)^2} + \frac{1}{(-\nu+i\epsilon)^2}\right] = \theta\, e^{-\epsilon|\theta|}$, corresponding to $\Psi(\nu) = \delta'(\nu)$, that is logarithmically divergent in x-space at the boundaries.

To further explore analytical properties of the eigenvalues close to this chiral point, it is useful to analytically continue the eigenproblem (3.2.6), which was initially defined



(a) $\theta = 0$ (b) $\theta = 2/5$ (c) $\theta^* = 1/2$

(d) $\theta = 3/5$ (e) $\theta = 1$

Figure 3.1: Positions of the zeros (black) and poles (white) of $f(\nu) = 1.5 + \nu \coth(\frac{\pi\nu}{2})$ in the ν-complex plane along the curve $\gamma_{1.5}(\theta) = 1.5\, e^{2i\pi\theta}$. The contour encloses the point $\alpha = -1$ and indeed the two zeros are exchanged upon analytical continuation. In Figure 3.1c the zeros cross the real axis in $\nu^* = \pm 0.819864$.

only for $\mathbb{R} \ni \alpha \geq -1$, to the complex plane of the masses α. For any real $\alpha > -1$, we consider the analytic continuation performed along a closed contour in the complex plane:

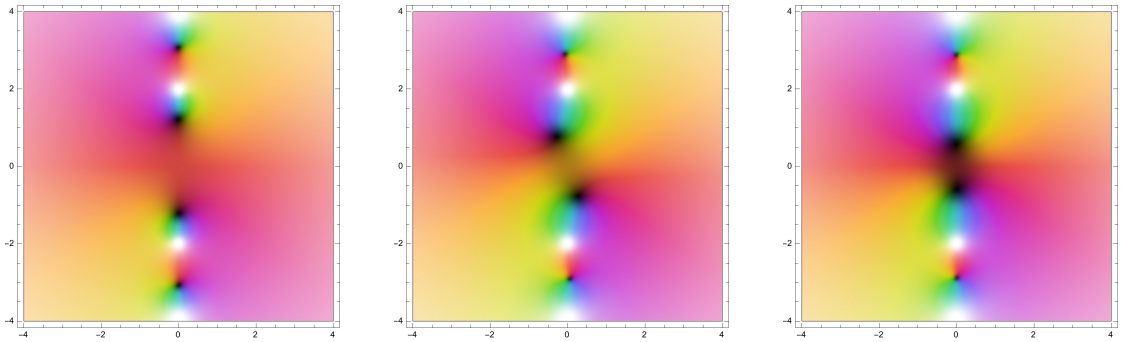
$$\gamma_\alpha(\theta) : [0, 2\pi] \to \mathbb{C}, \qquad \gamma_\alpha(2\pi) = \gamma_\alpha(0) = \alpha. \tag{3.3.5}$$

If $\gamma_\alpha(\theta)$ is such that it encloses the point $\alpha = -1$, the zeros of $f(\nu)$ in $\nu_0(\alpha) = \pm i u_0(\alpha)$ are exchanged along this contour

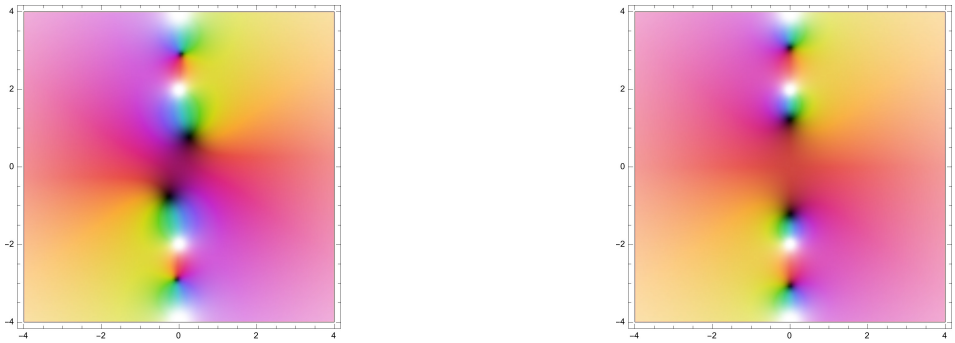
$$\widetilde{u_0}(\alpha) = u_0(\gamma_\alpha(2\pi)) = -u_0(\gamma_\alpha(0)) = -u_0(\gamma_\alpha(0)) = -u_0(\alpha), \tag{3.3.6}$$

where we have denoted by $\widetilde{g}$ the value of the function g after the analytic continuation. In particular, this means that, at some time θ^*, the leading zeros of $f(\nu)$, $\pm\nu_0 = \pm i u_0(\alpha(\theta))$, cross the real axis. As a result, at $\theta = \theta^*$, the eigenfunction $\Psi(\nu; \alpha(\theta^*))$ will display a pair of simple poles[21] on the real axis at $\nu = \pm\nu_0$. Instead, if the contour does not enclose $\alpha = -1$, $\widetilde{u_0}(\alpha) = u_0(\alpha)$. The two situations are exemplified in Figure 3.1 and Figure 3.2.

[21] One can see this also from the fact that zeros of $f(\nu)$ at generic complex values of α do not lie anymore on the imaginary axis, and for $\alpha < -1$, two of them are always reals, cf. Figure 3.1c.



(a) $\theta = 0$ (b) $\theta = 2/5$ (c) $\theta = 1/2$



(d) $\theta = 3/5$ (e) $\theta = 1$

Figure 3.2: Positions of the zeros (black) and poles (white) of $f(\nu) = 0.7 + \nu \coth(\frac{\pi\nu}{2})$ in the ν-complex plane along the curve $\gamma_{0.7}(\theta) = 0.7\, e^{2i\pi\theta}$. The contour does not enclose the point $\alpha = -1$ and the two zeros are not exchanged and do not cross the real axis.

Thus, as one analytically continue around the point $\alpha = -1$, the bound state equation is modified by picking up the pole contributions[22] coming from $\nu = \pm\nu_0$:

$$\begin{aligned}
&\left(\frac{2\alpha}{\pi} + \nu \coth\frac{\pi}{2}\nu\right)\widetilde{\Psi}(\nu;\alpha) = \widetilde{\lambda}(\alpha)\int_{-\infty}^{+\infty} \mathrm{d}\nu'\, \frac{\pi(\nu-\nu')}{2\sinh\frac{\pi}{2}(\nu-\nu')}\widetilde{\Psi}(\nu';\alpha) + \\
&+ \widetilde{\lambda}(\alpha)\mathrm{Res}\left(\frac{\pi(\nu-\nu')}{2\sinh\frac{\pi}{2}(\nu-\nu')}\Psi(\nu';\alpha), \nu' = -\nu_0\right) + \\
&- \widetilde{\lambda}(\alpha)\mathrm{Res}\left(\frac{\pi(\nu-\nu')}{2\sinh\frac{\pi}{2}(\nu-\nu')}\Psi(\nu';\alpha), \nu' = \nu_0\right)
\end{aligned} \tag{3.3.7}$$

The different sign depends on the opposite orientation with which two poles cross the real axis. Furthermore, we can readily see, that performing yet another analytic continuation around $\alpha = -1$, the two poles cross the real axis swap again, this time with opposite

[22] This is quite analogous to excited state Thermodynamic Bethe ansatz equation discussed in [158].

phases. Henceforth the two-folded analytically continued bound state equation:

$$\left(\frac{2\alpha}{\pi}+\nu\coth\frac{\pi}{2}\nu\right)\widetilde{\widetilde{\Psi}}(\nu;\alpha)=\widetilde{\widetilde{\lambda}}(\alpha)\int_{-\infty}^{+\infty}d\nu'\,\frac{\pi(\nu-\nu')}{2\sinh\frac{\pi}{2}(\nu-\nu')}\widetilde{\widetilde{\Psi}}(\nu'). \tag{3.3.8}$$

has exactly the same form of the original one, and therefore upon analytic continuation twice around the point $\alpha=-1$, the eigenvalue $\lambda(\alpha)=\widetilde{\widetilde{\lambda}}(\alpha)$. This means that as a function of complex α, the energy of the bound state has a non-trivial two-sheeted analytic structure. In the limit $\alpha\to-1$, the two poles $\pm\nu_0$ collide on the real axis and the two eigenvalues $\lambda(\alpha)$ and $\widetilde{\lambda}(\alpha)$ become degenerate (See Figure 3.3). This means that there is a square-root branch cut starting from $\alpha=-1$, and the lowest eigenvalue near $\alpha=-1$ behaves as

$$\lambda_0(\alpha)\sim\sqrt{\alpha+1}\,. \tag{3.3.9}$$

As already pointed out in [92], this behavior of the eigenvalue is reminiscent of critical points in phase transitions. In fact, as we see below, the infrared phase of the massless 't Hooft model ($\alpha=-1$) is described by conformal field theory, much like critical points in phase transitions.

3.3.3 Massless pion revisited

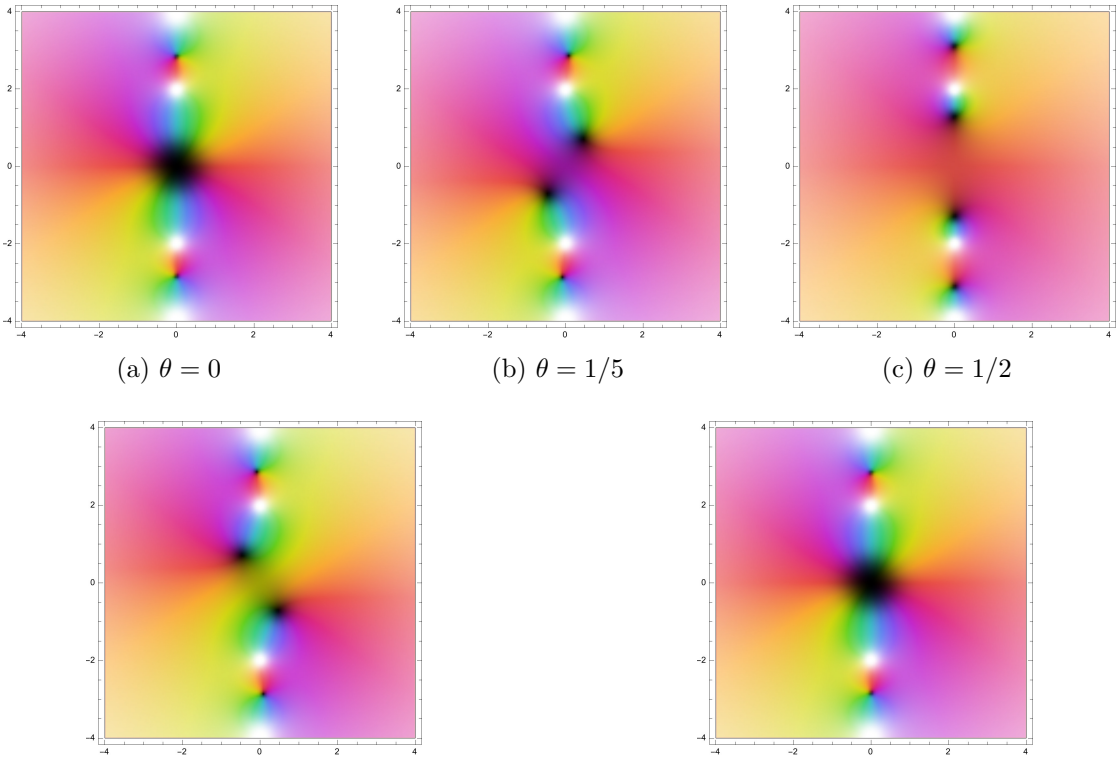
As we saw above, at $\alpha=-1$, the lowest meson has zero mass. In the literature, this is sometimes considered as a consequence of exact chiral symmetry and its spontaneous breaking. Strictly speaking, this is incorrect since the continuous global symmetry cannot be spontaneously broken in two dimensions [159,160]. However, there are large N examples [161] which exhibit the spontaneous continuous symmetry breaking in the strict $N\to\infty$ limit. In those examples, the "Goldstone bosons" at large N acquire mass at subleading orders in the $1/N$ expansion. Based on this fact, it was sometimes conjectured that the massless meson at $\alpha=-1$ will acquire mass because of the $1/N$ effects.

This conjecture is incorrect either. This follows from the recent analysis of the IR structure of 2d QCD [162,163]. As shown there, the IR phase of $SU(N)$ YM coupled to N_f flavor of fundamental quarks can be described as a gauged WZW model where one gauges the $SU(N)_{N_f}$ symmetry acting on the $SO(N\,N_f)_1$ WZW model describing the free fermion Lagrangian:

$$\mathcal{T}_{IR}\equiv\frac{SO(N\,N_f)_1}{SU(N)_{N_f}}=U(N_f)_N\,. \tag{3.3.10}$$

In particular, setting $N_f=1$, their analysis predicts the persistence of a free massless boson realizing a $U(1)_N$ current algebra[23] at level N.

[23]For $N_f>1$, a single $U(1)_N$ current corresponding to a massless boson decouples from the the remaining interacting $SU(N_f)_N$ WZW model. This is reminiscent of the "experimental" observations made in [164] (also in [132]) that 3-point (and higher) functions involving a massless meson and other massive mesons identically vanish. It would be interesting to provide a theoretical understanding for this observation.



(a) $\theta = 0$ (b) $\theta = 1/5$ (c) $\theta = 1/2$

(d) $\theta = 9/5$ (e) $\theta = 1$

Figure 3.3: Positions of the zeros (black) and poles (white) of $f(\nu) = -1 + \nu \coth(\frac{\pi\nu}{2})$ in the ν-complex plane along the curve $\gamma_{-1}(\theta) = (-1)\, e^{2i\pi\theta}$. The zero in $\nu = 0$ is double. The analytical continuation along a closed contour starting and ending at $\alpha = -1$ do not exchange the position of the zeros. While for any $\alpha = -1 + \epsilon$, $\epsilon \in \mathbb{C}$, we have either the situation in Figure 3.1 or Figure 3.2.

3.3.4 Critical points on the second sheet

Interestingly, the point at $\alpha = -1$ is not the only singularly of $\lambda(\alpha \in \mathbb{C})$ in the complex plane of the masses. Indeed, $f(\nu)$ develops double zeros whenever:

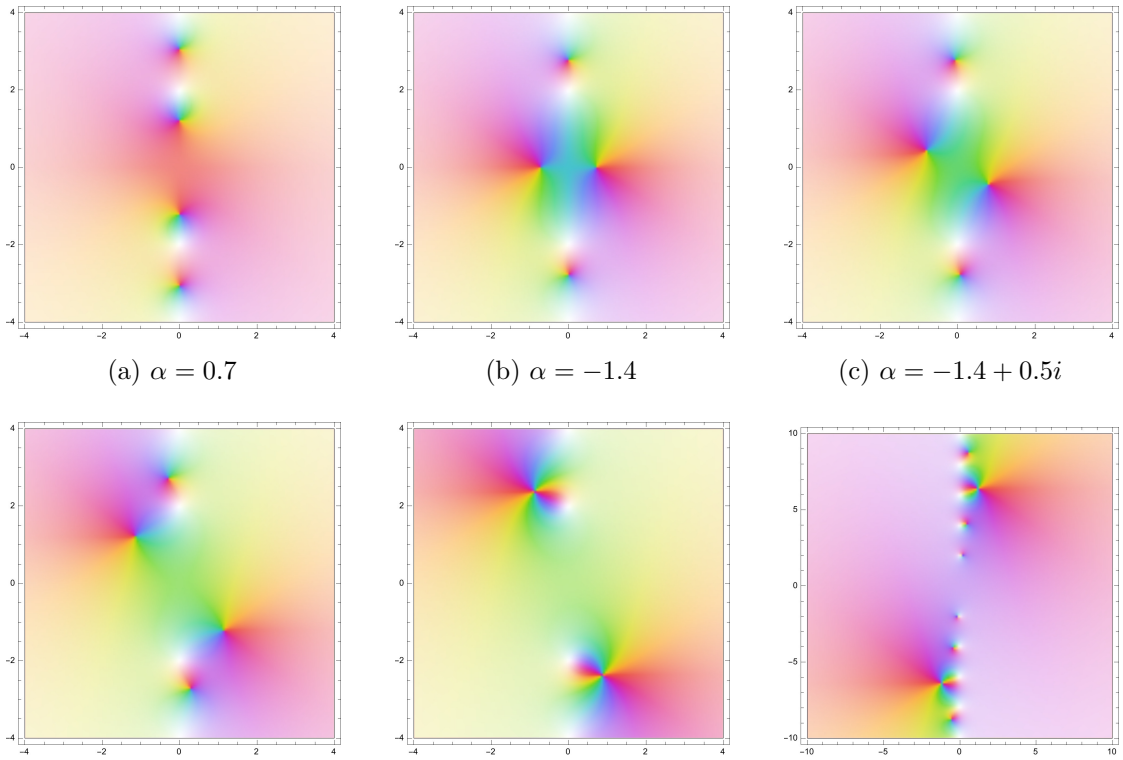
$$\begin{cases} \alpha_k = -\frac{\pi}{2}\nu_k \coth(\frac{\pi}{2}\nu_k) \\ \pi\nu_k = \sinh(\pi\nu_k) \end{cases} \quad \Longrightarrow \alpha_k = -\frac{1}{2}(1 + \cosh \pi\nu_k)\,. \tag{3.3.11}$$

Those are infinite values of α_k all located on the second sheet of the α-plane ($\arg\alpha > i\pi$), beyond the cut $(-\infty, -1)$, see Figure 3.6. At each of these α_k, there are two values[24] of $\nu_k = iu_k$

$$\frac{\pi}{2}\nu_k = \frac{i\pi}{2}u_k = \pm\sqrt{\alpha_k}\,\sqrt{\alpha_k + 1}\,, \tag{3.3.12}$$

[24]The equation (3.3.12) can be obtained by inverting the two equations on the left hand side of (3.3.11).

one in the upper half-plane and one in the lower half-plane, which degenerate to $\pm\nu_0$. See Figure 3.4. An argument analogous to the one used for $\alpha_0 = -1$ implies that all



(a) $\alpha = 0.7$ (b) $\alpha = -1.4$ (c) $\alpha = -1.4 + 0.5i$

(d) $\alpha = -1.67 + 1.9i$ (e) $\alpha = \alpha_1$ (f) $\alpha = \alpha_3$

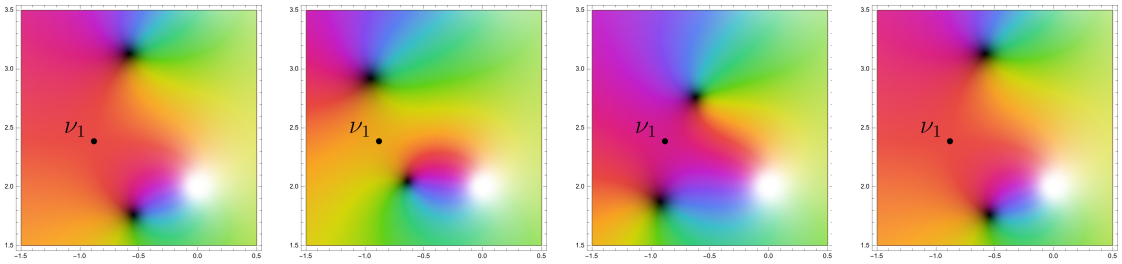
Figure 3.4: Positions of the zeros (black) and poles (white) of $f(\nu) = \alpha + \nu \coth(\frac{\pi\nu}{2})$ in the ν-complex plane for different values of α. As we vary α, the first zeros in the upper and lower half plane wander in the complex plane and at the specific values $\alpha = \alpha_k$, they degenerate into double zeros. In Figure 3.4e $\mp u_0$ degenerates with $\pm u_1$ at $\alpha = \alpha_1$ while in Figure 3.4f, at $\alpha = \alpha_3$, $\mp u_0$ degenerates with $\pm u_3$

those α_k are square-root branch cut singularities of the eigenvalues. Indeed, as before, one checks directly that upon analytically continuing around a closed curve, the zeros of the zeros u_0 and $u_{k\geq 1}$ are exchanged if and only if the curve circles around α_k an odd number of times. In Figure 3.5 we illustrate this for $\alpha = \alpha_1$.

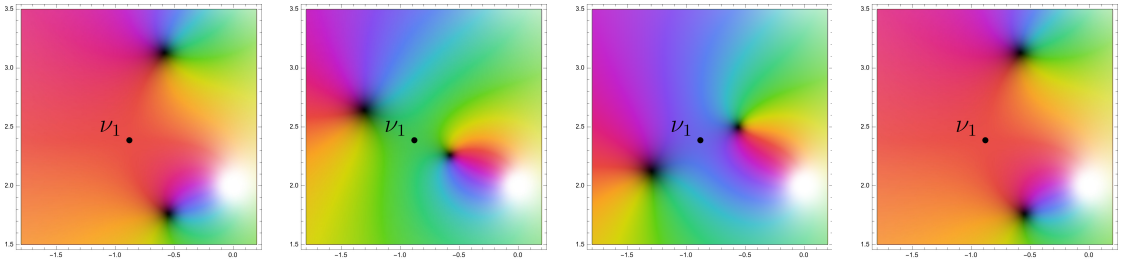
However, there is one point that needs to be taken into account: for odd n, $\Psi_n(\nu)$ is odd, and therefore its residues at $\nu \pm \nu_k$ have the same sign. Then, in this case, the residues produced by analytic continuation around α_k exactly cancel with each other. We thus conclude that as function of complex α they are single valued. By contrast, for even n, the eigenvalues will have square-root type singularities:

$$\lambda_{2k}(\alpha) \sim \sqrt{\alpha - \alpha_k} \tag{3.3.13}$$

These singularities are all in the second sheet and accumulate towards ∞. So, as a function of complex α, each of the even eigenvalues λ_{2n} have a square root branch point



(a) $\theta_1 = 0$ (b) $\theta_1 = 2/5$ (c) $\theta_1 = 3/5$ (d) $\theta_1 = 1$



(e) $\theta_2 = 0$ (f) $\theta_2 = 9/20$ (g) $\theta_2 = 11/20$ (h) $\theta_2 = 1$

Figure 3.5: Positions of the zeros (black) and poles (white) of $f(\nu) = a_i + \nu \coth(\frac{\pi\nu}{2})$ for $a_1 = \alpha_1 + 1$ and $a_2 = \alpha_1 + 0.7$ in the ν-complex plane along the curve respectively $\gamma_{a_1}(\theta_1) = a_1 + 0.7\, e^{2i\pi\theta_1}$ (Figures 5a - 5d) and $\gamma_{a_2}(\theta_2) = a_2 + \ e^{2i\pi\theta_2}$ (Figures 5e - 5h). The point marked with $\nu_1 = \frac{2}{\pi}\sqrt{\alpha_1}\,\sqrt{\alpha_1 + 1}$ is the position of the double zero (3.3.12) corresponding with the critical value $\alpha_1 \simeq -1.895 + 3.719\, i$. The analytical continuation along a closed contour starting and ending at a_i exchanges the position of the zeros if and only if the contour circulates around α_1 as clear from the figure.

in α_n. For example in Figure 3.6, the complex plane of λ is represented with a branch cut along $(-\infty, -1)$ in correspondence with the branch cut of λ_0. If we consider instead λ_{2n}, then there is branch cut on the second sheet at $\alpha = \alpha_k$. We conclude that, in the complex plane of the masses we find infinitely many critical points where (one of the) even eigenvalues vanish as a square root (i.e. with the same “critical exponent" of the point as $\alpha = -1$).

3.4 Extracting spectral data

In this section, we will discuss how to extract the spectrum of the eigenproblem (3.1.16), i.e. the energy levels of the mesons, from the reformulation of the latter in terms of the TQ-Baxter system (3.2.44). In Section 3.4.3 will construct an asymptotic expansion for the eigenvalues λ_n, while in 3.4.2, we will derive exact expressions for the spectral sums $G_{\pm}^{(s)}(\alpha)$ of (3.2.52).

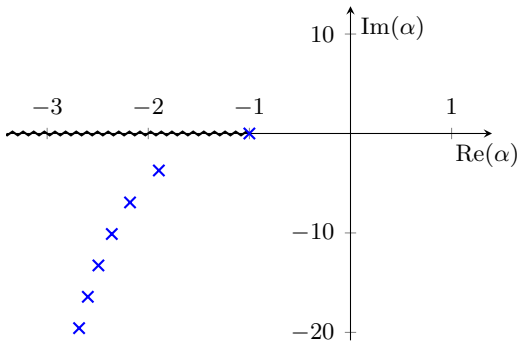


Figure 3.6: Square root branching points of λ in the second sheet of the α-plane in correspondence with the points α_k (in blue).

3.4.1 Solutions to TQ-system in terms of hypergeometric functions

As the first step, we generalize the discussion in [92] for $\alpha = 0$ and demonstrate that one can construct analytic expression for two independent solutions to the TQ-system (3.2.44)

$$Q_\pm(\nu+2i|\lambda) + Q_\pm(\nu+2i|\lambda) - 2Q_\pm(\nu|\lambda) = \frac{-4\pi\lambda}{\frac{2\alpha}{\pi} + \nu\coth(\frac{\pi\nu}{2})} Q_\pm(\nu|\lambda) \tag{3.4.1}$$

once we weaken the analyticity requirements.

The idea is to use the two standard solutions $\mathrm{U}(a,b,x)$, $\mathrm{M}(a,b,x)$ of the confluent hypergeometric differential equation ($\mathrm{M}(a,b,x)$ is sometimes referred to as ${}_1\mathrm{F}_1(a,b,x)$):

$$\left(\nu + \frac{2\alpha z}{\pi}\right) \mathrm{M}\left(1 + \frac{i}{2}\left(\nu + \frac{2\alpha z}{\pi}\right), 2, -2\pi i\lambda\, z\right) , \tag{3.4.2}$$

$$\Gamma\left(1 + \frac{i}{2}\left(\nu + \frac{2\alpha z}{\pi}\right)\right) \mathrm{U}\left(1 + \frac{i}{2}\left(\nu + \frac{2\alpha z}{\pi}\right), 2, -2\pi i\lambda\, z\right) . \tag{3.4.3}$$

Using the recurrence relations[25] for these functions, one can show that they satisfy the functional relation (3.2.44) if we set z to be

$$z := z(\nu) = z(\nu \pm 2i) = \tanh\left(\frac{\pi}{2}\nu\right) . \tag{3.4.5}$$

While the solution (3.4.2) is analytical everywhere on the real axis, (3.4.3) is not, having a logarithmic branch-cut singularity at $z = 0$, (formula (13.1.6) of [165]):

$$\mathrm{U}(a,2,z\sim 0) = \frac{(-1)^2}{2\Gamma(a-1)}\mathrm{M}(a,2,z)\log z + (\text{reg. }) . \tag{3.4.6}$$

[25] See formulas (13.4.1) and (13.4.15) of [165], which we report here, specialized to our case for convenience:

$$\begin{aligned} \frac{\Gamma(a)}{a-1}\Big[\mathrm{U}(a-1,2,z) + a(a-1)\mathrm{U}(a+1,2,z) - 2(a-1)\mathrm{U}(a,2,z)\Big] &= \frac{z}{a-1}\Gamma(a)\,\mathrm{U}(a,2,z) , \\ (a-2)\mathrm{M}(a-1,2,z) + a\mathrm{M}(a+1,2,z) - 2(a-1)\mathrm{M}(a,2,z) &= \frac{z}{a-1}(a-1)\mathrm{M}(a,2,z) . \end{aligned} \tag{3.4.4}$$

From the form of (3.4.6), it is evident that an appropriate linear combination of the two functions, (3.4.2) and (3.4.3), will give a single-valued and analytic solution on the real axis. Imposing further that the solutions to be parity eigenstates, the parity-odd one is given by

$$\begin{aligned}\mathrm{M}_+(\nu|\lambda) &= \left(\nu+\frac{2\alpha z}{\pi}\right) e^{i\pi\lambda z}\,\mathrm{M}\left(1+\frac{i}{2}\left(\nu+\frac{2\alpha z}{\pi}\right),2,-2\pi i\lambda\, z\right)\\ &= \left(\nu+\frac{2\alpha z}{\pi}\right) e^{i\pi\lambda z}\sum_{n=0}^{\infty}\frac{\left(1+\frac{i}{2}\left(\nu+\frac{2\alpha z}{\pi}\right)\right)_n}{n!(n+1)!}(-2\pi i\lambda\, z)^n\end{aligned} \tag{3.4.7}$$

while the parity-even one is ($\psi(x)$ is the Polygamma function)[26]

$$\begin{aligned}\mathrm{M}_-(\nu|\lambda) &= \frac{1}{2}\left(e^{i\pi\lambda z}\,\Sigma(\nu|\lambda)+e^{-i\pi\lambda z}\,\Sigma(-\nu|\lambda)\right)\\ \Sigma(\nu|\lambda) &= 1+\sum_{n=1}^{\infty}\frac{\left(\frac{i}{2}\left(\nu+\frac{2\alpha z}{\pi}\right)\right)_n}{n!(n-1)!}(-2\pi i\lambda\, z)^n\left[\psi\left(\frac{1}{2}\right)-\psi(n)-\psi(n+1)\right.\\ &\qquad\left.+\,\psi\left(n+\frac{i\nu}{2}+\frac{i\alpha z}{\pi}\right)+\log(16)\right]\end{aligned} \tag{3.4.8}$$

The notation $\mathrm{M}_\pm$ for the respectively odd/even function may seem misleading but it is chosen so that the resulting $\Psi_\pm(\nu)=\sinh^{-1}\left(\frac{\pi\nu}{2}\right)f^{-1}(\nu)\,Q_\pm(\nu)$ would then be even/odd.

Although the solutions $\mathrm{M}_\pm(\nu|\lambda)$ are regular on the real axis of ν, they do not satisfy the required analyticity; they have singularities in the strip $[-2i,2i]$ at $\nu=\pm i$ where $z(\nu)$ is singular. In particular, the last polygamma term in (3.4.8) introduces infinitely many singularities that accumulate at $z=\pm i$. Hence, as they stand, they do not provide a full solution of our TQ-system (3.2.44). Nevertheless, they provide a starting point for our analysis. Below we explain how to systematically correct the solutions and compute spectral sums by expanding in powers of α.

Constructing the analytical solutions. Because of the accumulation of singularities introduced by the term $\psi\left(n+\frac{i\nu}{2}+\frac{i\alpha z}{\pi}\right)$ in (3.4.8), at any order in λ, we treat this polygamma as its further power expansion in the mass parameter:

$$\psi\left(n+\frac{i\nu}{2}+\frac{i\alpha z}{\pi}\right)=\sum_{n=0}^{\infty}\psi^{(k)}\left(n+\frac{i\nu}{2}\right)\left(\frac{iz\alpha}{\pi}\right)^k. \tag{3.4.9}$$

[26]The log(16) is added to simplify the expressions below. It does not modify the analytical structure of the solution.

Then, at any order in this expansion in α and λ, (3.4.11) the function:

$$\begin{aligned}\mathrm{M}_{-}^{(k)}(\nu|\lambda) &= \frac{1}{2}\left(e^{i\pi\lambda z}\,\Sigma^{(k)}(\nu|\lambda) + e^{-i\pi\lambda z}\,\Sigma^{(k)}(-\nu|\lambda)\right)\\ \Sigma^{(k)}(\nu|\lambda) &= 1+\sum_{n=1}^{\infty}\frac{\left(\frac{i}{2}\left(\nu+\frac{2\alpha z}{\pi}\right)\right)_n}{n!(n-1)!}(-2\pi i\lambda\, z)^n\Big[\psi\left(\frac{1}{2}\right)-\psi(n)-\psi(n+1)\\ &\qquad +\log(16)+\sum_{k=0}\psi^{(k)}\left(n+\frac{i\nu}{2}\right)\left(\frac{z\alpha}{\pi}\right)^k\Big]\end{aligned} \tag{3.4.10}$$

exhibits only poles of increasing order in $\nu = \pm i$.

In order to construct solutions of the TQ-system with correct analyticity, we consider the following linear combination:

$$Q_{\pm}(\nu;\lambda) = A_{\pm}(\lambda,z)\,\mathrm{M}_{\pm}(\nu;\lambda) + 2\pi i\lambda^{\frac{1\mp1}{2}}\,z\,B_{\pm}(\lambda,z)\,\mathrm{M}_{\mp}(\nu;\lambda) \tag{3.4.11}$$

Although the coefficients depend on λ and z, this is still a solution to (3.2.44).

Then, we proceed by expanding both $\mathrm{M}_{\pm}$ and the coefficients in powers of λ and α. Since in the expansion in λ at order λ^n, $\mathrm{M}_{\pm}$ contains already powers of $\alpha^{n+\frac{1\pm1}{2}}$, we take the expansion in α to be at least of order n and $n+1$ respectively for M_{+} and M_{-}. At each other in this expansion, we fix the functions $A_{\pm}$ and $B_{\pm}$ such that the resulting expression is analytic in $[-2i, 2i]$ up to that order given order. This gives a well-defined problem at each order in λ and α that can be uniquely solved up to a trivial scaling, fixed by requiring $A_{\pm}(\lambda, 0) = 1$ for any order in α. Let us denote:

$$A_{\pm} = \sum_{l=0}^{\infty} A_{\pm}^{(l)}\lambda^l\,, \qquad B_{\pm} = \sum_{l=0}^{\infty} B_{\pm}^{(l)}\lambda^l\,, \tag{3.4.12}$$

then, each coefficient $A_{\pm}(l)$, $B_{\pm}(l)$ is itself given by an infinite series in α:

$$A_{\pm}^{(l)} = \sum_{k=0} A^{(l,k)}\alpha^k\,, \quad B_{\pm}^{(l)} = \sum_{k=0} B^{(l,k)}\alpha^k\,. \tag{3.4.13}$$

In the following we report the first few coefficients in the λ expansion up to order α^4.

Up to λ^2 and α^5 we have, and defining $\tau = \frac{\pi^2}{4}\tanh\frac{\pi\nu}{2}$:

$$
\begin{aligned}
A_{\pm}^{(0)} &= 1\,, \qquad A_{-}^{(1)} = \frac{8\alpha\tau}{\pi^2}\,,\\
A_{+}^{(1)} &= -\frac{8\alpha\tau}{\pi^2} + \frac{112\alpha^2\tau\zeta(3)}{\pi^4} + \alpha^3\left(\frac{224\tau^2\zeta(3)}{\pi^6} - \frac{1488\tau\zeta(5)}{\pi^6}\right)\\
&\qquad + \alpha^4\left(\left(-\frac{992\tau}{3\pi^6} - \frac{3968\tau^2}{\pi^8}\right)\zeta(5) + \frac{20320\tau\zeta(7)}{\pi^8}\right)\\
A_{-}^{(2)} &= -\frac{8\alpha\tau}{\pi^2} - \tau + \alpha^2\left(\frac{16\tau^2}{\pi^4} + \frac{56\tau\zeta(3)}{\pi^4}\right) + \alpha^3\left(\frac{112\tau\zeta(3)}{3\pi^4} - \frac{992\tau\zeta(5)}{\pi^6}\right) +\\
&\qquad + \alpha^4\left(\frac{15240\tau\zeta(7)}{\pi^8} - \frac{992\tau\zeta(5)}{\pi^6}\right)\\
A_{+}^{(2)} &= \tau + \alpha\left(-\frac{24\tau}{\pi^2} - \frac{28\tau\zeta(3)}{\pi^2}\right) + \alpha^2\left(-\frac{80\tau^2}{\pi^4} + \left(\frac{392\tau}{\pi^4} - \frac{56\tau^2}{\pi^4}\right)\zeta(3) + \frac{372\tau\zeta(5)}{\pi^4}\right) +\\
&\quad + \alpha^3\left[\left(\frac{112\tau}{\pi^4} + \frac{896\tau^2}{\pi^6}\right)\zeta(3) - \frac{1568\tau\zeta(3)^2}{\pi^6} + \left(-\frac{5952\tau}{\pi^6} + \frac{248\tau}{3\pi^4} + \frac{992\tau^2}{\pi^6}\right)\zeta(5) - \frac{5080\tau\zeta(7)}{\pi^6}\right]\\
&\quad + \alpha^4\left[\left(-\frac{3136\tau}{3\pi^6} - \frac{3136\tau^2}{\pi^8}\right)\zeta(3)^2 + \left(-\frac{10912\tau}{3\pi^6} - \frac{13888\tau^2}{\pi^8} + \frac{992\tau^3}{\pi^8}\right)\zeta(5) +\right.\\
&\quad \left. + \zeta(3)\left(\frac{896\tau^3}{\pi^8} + \frac{48608\tau\zeta(5)}{\pi^8}\right) + \left(\frac{86360\tau}{\pi^8} - \frac{2540\tau}{\pi^6} - \frac{15240\tau^2}{\pi^8}\right)\zeta(7) + \frac{71540\tau\zeta(9)}{\pi^8}\right]
\end{aligned}
\tag{3.4.14}
$$

$$
\begin{aligned}
B_+^{(0)} &= -\frac{\alpha}{\pi^2} \\
B_-^{(0)} &= -\frac{7\alpha\zeta(3)}{\pi^2} + \alpha^2\left(-\frac{14\tau\zeta(3)}{\pi^4} + \frac{93\zeta(5)}{\pi^4}\right) + \alpha^3\left(\left(\frac{62}{3\pi^4} + \frac{248\tau}{\pi^6}\right)\zeta(5) - \frac{1270\zeta(7)}{\pi^6}\right) + \\
&\quad + \alpha^4\left(\frac{248\tau^2\zeta(5)}{\pi^8} + \left(-\frac{635}{\pi^6} - \frac{3810\tau}{\pi^8}\right)\zeta(7) + \frac{17885\zeta(9)}{\pi^8}\right) \\
B_+^{(1)} &= \frac{1}{4} - \frac{2\alpha}{\pi^2} + \alpha^2\left(-\frac{4\tau}{\pi^4} + \frac{14\zeta(3)}{\pi^4}\right) + \alpha^3\left(\frac{28\zeta(3)}{3\pi^4} - \frac{248\zeta(5)}{\pi^6}\right) + \\
&\quad + \alpha^4\left(-\frac{248\zeta(5)}{\pi^6} + \frac{3810\zeta(7)}{\pi^8}\right) \\
B_-^{(1)} &= 2 + \alpha\left(\frac{8\tau}{\pi^2} - \frac{14\zeta(3)}{\pi^2}\right) + \alpha^2\left(\left(-\frac{28}{3\pi^2} - \frac{56\tau}{\pi^4}\right)\zeta(3) + \frac{248\zeta(5)}{\pi^4}\right) + \\
&\quad + \alpha^3\left(-\frac{112\tau^2\zeta(3)}{\pi^6} + \left(\frac{248}{\pi^4} + \frac{744\tau}{\pi^6}\right)\zeta(5) - \frac{3810\zeta(7)}{\pi^6}\right) + \\
&\quad + \alpha^4\left(\left(\frac{248}{5\pi^4} + \frac{496\tau}{3\pi^6} + \frac{1984\tau^2}{\pi^8}\right)\zeta(5) + \left(-\frac{5080}{\pi^6} - \frac{10160\tau}{\pi^8}\right)\zeta(7) + \frac{57232\zeta(9)}{\pi^8}\right) \\
B_+^{(2)} &= \frac{2}{3} + \alpha\left(-\frac{2}{\pi^2} + \frac{5\tau}{3\pi^2} - \frac{7\zeta(3)}{\pi^2}\right) + \alpha^2\left(-\frac{4}{3\pi^2} - \frac{8\tau}{\pi^4} + \left(\frac{56}{\pi^4} - \frac{14}{3\pi^2}\right)\zeta(3) + \frac{124\zeta(5)}{\pi^4}\right) + \\
&\quad + \alpha^3\left(-\frac{16\tau^2}{3\pi^6} + \left(\frac{56}{\pi^4} + \frac{56\tau}{\pi^6}\right)\zeta(3) - \frac{196\zeta(3)^2}{\pi^6} + \left(-\frac{1116}{\pi^6} + \frac{124}{\pi^4}\right)\zeta(5) - \frac{1905\zeta(7)}{\pi^6}\right) + \\
&\quad + \alpha^4\left[-\frac{784\zeta(3)^2}{3\pi^6} + \left(-\frac{1488}{\pi^6} + \frac{124}{5\pi^4} - \frac{992\tau}{\pi^8}\right)\zeta(5) + \zeta(3)\left(\frac{56}{5\pi^4} + \frac{112\tau}{3\pi^6} + \frac{6944\zeta(5)}{\pi^8}\right) + \right. \\
&\quad \left. + \left(\frac{18288}{\pi^8} - \frac{2540}{\pi^6}\right)\zeta(7) + \frac{28616\zeta(9)}{\pi^8}\right]
\end{aligned}
\tag{3.4.15}
$$

3.4.2 Spectral sums

Once we have an order-by-order expansion of (3.4.11), it is straightforward to apply at each order in λ the integral formulas (3.2.51) to compute the spectral sums $G_\pm^{(s)}(\lambda)$, $s \geq 2$ through eq. (3.2.50):

$$
\partial_\lambda \left(\log(D_+(\lambda)) \pm \log(D_+)(\lambda)\right) = (1 \pm 1)(\log(8\pi) - 1) - \sum_{s=1}^{\infty}\left(G_-^{(s)}(\alpha) \pm G_+^{(s)}(\alpha)\right)\lambda^s
\tag{3.4.16}
$$

that is, for $s > 1$:

$$G_{\pm}^{(s)}(\alpha) + G_{\pm}^{(s)}(\alpha) = \frac{1}{s-1}\left[\frac{\partial^{s-1}}{\partial\lambda^{s-1}}\int_{-\infty}^{+\infty} \mathrm{d}\nu\, \frac{\pi}{2}\frac{Q_+(\nu|\lambda)\,\partial_\nu Q_-(\nu|\lambda) - Q_-(\nu|\lambda)\,\partial_\nu Q_+(\nu|\lambda)}{f(\nu)}\right]_{\lambda=0}$$
$$G_{\pm}^{(s)}(\alpha) - G_{\pm}^{(s)}(\alpha) = \frac{-1}{s-1}\left[\frac{\partial^{s-1}}{\partial\lambda^{s-1}}\int_{-\infty}^{+\infty} \mathrm{d}\nu\, \frac{\pi^2}{2}\frac{Q_+(\nu|\lambda)\,Q_-(\nu|\lambda)}{\sinh(\pi\nu)f(\nu)}\right]_{\lambda=0} \tag{3.4.17}$$

For $s = 1$, using that:

$$Q_+(\nu) = 1 + \mathcal{O}(\lambda)\,, \qquad Q_-(\nu) = \nu + \mathcal{O}(\lambda) \tag{3.4.18}$$

one gets directly the formulas:

$$\begin{aligned}\partial_\lambda \log(D_+(\lambda)D_-(\lambda))|_{\lambda=0} &= 2 - \int_{-\infty}^{+\infty}\left[\frac{\tanh\left(\frac{\pi\nu}{2}\right)}{\nu} - \frac{1}{\frac{2\alpha}{\pi} + \nu\coth\left(\frac{\pi\nu}{2}\right)}\right]\mathrm{d}\nu \\ &= 2 - \int_{-\infty}^{+\infty}\frac{\alpha\tanh\left(\frac{\pi\nu}{2}\right)}{\frac{\pi\nu}{2}\left(\frac{2\alpha}{\pi} + \nu\coth\left(\frac{\pi\nu}{2}\right)\right)}\mathrm{d}\nu \\ &= 2 - \frac{\alpha}{2}\int_{-\infty}^{+\infty}\mathrm{d}\nu\,\frac{\pi}{2}\frac{\pi\alpha\sinh(\pi\nu)\sinh\left(\frac{\pi\nu}{2}\right)}{\frac{\pi\nu}{2}\cosh^2\left(\frac{\pi\nu}{2}\right)\left(\alpha\sinh\left(\frac{\pi\nu}{2}\right) + \frac{1}{2}\pi\nu\cosh\left(\frac{\pi\nu}{2}\right)\right)}\,.\end{aligned} \tag{3.4.19}$$

$$\begin{aligned}\partial_\lambda \log\left(\frac{D_+(\lambda)}{D_-(\lambda)}\right)\Big|_{\lambda=0} &= -\int_{-\infty}^{+\infty}\mathrm{d}\nu\,\frac{\pi\nu\,\mathrm{csch}(\pi\nu)}{\frac{2\alpha}{\pi} + \nu\coth\left(\frac{\pi\nu}{2}\right)} \\ &= \alpha\int_{-\infty}^{+\infty}\mathrm{d}\nu\,\frac{\pi}{2}\frac{\mathrm{sech}^2\left(\frac{\pi\nu}{2}\right)}{\left(\alpha + \frac{\pi\nu}{2}\coth\left(\frac{\pi\nu}{2}\right)\right)} - \int_{-\infty}^{+\infty}\mathrm{d}\nu\,\frac{\pi}{\cosh(\pi\nu)+1} \\ &= \alpha\int_{-\infty}^{+\infty}\mathrm{d}\nu\,\frac{\pi}{2}\frac{\mathrm{sech}^2\left(\frac{\pi\nu}{2}\right)}{\left(\alpha + \frac{\pi\nu}{2}\coth\left(\frac{\pi\nu}{2}\right)\right)} - 2\end{aligned} \tag{3.4.20}$$

Then, using the result above, and applying the relations (3.4.16) at lowest order in λ, one obtains directly:

$$G_{\pm}^{(1)}(\alpha) = \log(8\pi) - 2 \pm 1 - \frac{\alpha}{4}\int_{-\infty}^{\infty}\frac{\sinh(t)\big(\sinh(2t) \pm 2t\big)}{t\cosh^2(t)(\alpha\sinh(t) + t\cosh(t))}\,\mathrm{d}t \tag{3.4.21}$$

already reported in [92].

To obtain the spectral sums $G_{\pm}^{(2)}$, we need to consider the terms of $Q_\pm(\nu)$ up to the first order in λ. For this we only need $A_\pm$ up to order λ, B_+ at order λ, and B_- at order λ^0. These polynomials as well as $\mathrm{M}_\pm$ are only determined as power series in α, for any desired order thereof. Hence, in order to extract the spectral sums from the integral expressions (3.4.17), we expand the integrand in power of α, up to the desired order. We can then integrate them term by term in the α expansion.

Integrating numerically term-by-term we obtain:

$$G_+^{(2)}(\alpha) = 8.41439832 - 11.5719695\alpha + 13.7055746\alpha^2 - 15.2501917\alpha^3 + 16.4273895\alpha^4 + \mathcal{O}(\alpha^5)$$
$$G_-^{(2)}(\alpha) = 2.0000000 - 1.3333333\alpha + 0.95349463\alpha^2 - 0.71898694\alpha^3 + 0.56448932\alpha^4 + \mathcal{O}(\alpha^5) \tag{3.4.22}$$

that can be recognized[27] to coincide numerically with:

$$\begin{aligned}
G_+^{(2)}(\alpha) &= 7\zeta_3 + \alpha\left[\frac{8}{3} + \frac{14\zeta_3}{3} - \frac{56\zeta_3}{\pi^2} - \frac{124\zeta_5}{\pi^2}\right] + \alpha^2\left[-\frac{224\zeta_3}{3\pi^2} + \frac{196\zeta_3^2}{\pi^4} + \frac{1240\zeta_5}{\pi^4} - \frac{124\zeta_5}{\pi^2} + \frac{1905\zeta_7}{\pi^4}\right] + \\
&+ \alpha^3\left[-\frac{112\zeta_3}{5\pi^2} + \frac{784\zeta_3^2}{3\pi^4} + \frac{1984\zeta_5}{\pi^4} - \frac{124\zeta_5}{5\pi^2} - \frac{6944\zeta_3\zeta_5}{\pi^6} - \frac{21336\zeta_7}{\pi^6} + \frac{2540\zeta_7}{\pi^4} - \frac{28616\zeta_9}{\pi^6}\right] \\
&+ \alpha^3\left[\frac{784\zeta_3^2}{9\pi^4} + \frac{14384\zeta_5}{15\pi^4} - \frac{34720\zeta_3\zeta_5}{3\pi^6} + \frac{61504\zeta_5^2}{\pi^8} - \frac{40640\zeta_7}{\pi^6} + \frac{2921\zeta_7}{3\pi^4} + \frac{106680\zeta_3\zeta_7}{\pi^8} + \right. \\
&\left. + \frac{343392\zeta_9}{\pi^8} - \frac{143080\zeta_9}{3\pi^6} + \frac{429870\zeta_{11}}{\pi^8}\right] + \mathcal{O}(\alpha^5) \\
G_-^{(2)}(\alpha) &= 2 - \frac{4\alpha}{3} + \alpha^2\left[\frac{56\zeta_3}{3\pi^2} - \frac{124\zeta_5}{\pi^4}\right] + \alpha^3\left[\frac{56\zeta_3}{5\pi^2} - \frac{496\zeta_5}{\pi^4} + \frac{3048\zeta_7}{\pi^6}\right] \\
&+ \alpha^4\left[-\frac{5704\zeta_5}{15\pi^4} + \frac{10160\zeta_7}{\pi^6} - \frac{57232\zeta_9}{\pi^8}\right] + \mathcal{O}(\alpha^5)
\end{aligned} \tag{3.4.23}$$

that are the expansions of the formulas derived in [93] up to the same order.

For $s = 3$ we find:

$$G_+^{(3)}(\alpha) = 20.4981208 - 45.6613977\alpha + 72.1676608\alpha^2 - 98.7405496\alpha^3 + 124.869920\alpha^4 + \mathcal{O}(\alpha^5)$$
$$G_-^{(3)}(\alpha) = 1.71982418 - 2.03864075\alpha + 1.03864075\alpha^2 - 1.75397929\alpha^3 + 1.55184859\alpha^4 + \mathcal{O}(\alpha^5) \tag{3.4.24}$$

[27] With the help of numerical methods e.g. PSLQ algorithm implemented in Mathematica: see this URL.

These match perfectly with the respective expressions from [93] expanded up to α^4:

$$
\begin{aligned}
G_+^{(3)}(\alpha) = &-\frac{4\pi^2}{3} + 28\zeta_3 + \alpha\left[4 + \left(42 - \frac{84}{\pi^2}\right)\zeta_3 - \frac{147\zeta_3^2}{\pi^2} - \frac{651\zeta_5}{\pi^2}\right] + \\
&+ \alpha^2\left[\frac{12}{5} - \frac{196(-6+\pi^2)\zeta_3^2}{\pi^4} - \frac{1116(-2+\pi^2)\zeta_5}{\pi^4} + \zeta_3\left(14 - \frac{224}{\pi^2} + \frac{5208\zeta_5}{\pi^4}\right) + \frac{11430\zeta_7}{\pi^4}\right] + \\
&+ \alpha^3\Bigg[-\frac{196(-36+\pi^2)\zeta_3^2}{3\pi^4} - \frac{2744\zeta_3^3}{\pi^6} + \left(\frac{5952}{\pi^4} - \frac{8618}{15\pi^2}\right)\zeta_5 - \frac{46128\zeta_5^2}{\pi^6} + \frac{1524(-28+15\pi^2)\zeta_7}{\pi^6} + \\
&+ \zeta_3\left(-\frac{2212}{15\pi^2} + \frac{1736(-27+5\pi^2)\zeta_5}{\pi^6} - \frac{80010\zeta_7}{\pi^6}\right) - \frac{186004\zeta_9}{\pi^6}\Bigg] + \\
&+ \alpha^4\Bigg[-\frac{5488\zeta_3^3}{\pi^6} - \frac{92256(-5+\pi^2)\zeta_5^2}{\pi^8} + \zeta_3^2\left(\frac{22736}{15\pi^4} + \frac{145824\zeta_5}{\pi^8}\right) + \frac{508(-240+31\pi^2)\zeta_7}{\pi^6} + \\
&+ \zeta_5\left(-\frac{620(-56+\pi^2)}{7\pi^4} + \frac{1417320\zeta_7}{\pi^8}\right) - \frac{61320(-12+7\pi^2)\zeta_9}{\pi^8} + \\
&+ \zeta_3\left(-\frac{24}{\pi^2} + \frac{1736(-310+13\pi^2)\zeta_5}{5\pi^6} - \frac{32004(-24+5\pi^2)\zeta_7}{\pi^8} + \frac{1201872\zeta_9}{\pi^8}\right) + \frac{2947680\zeta_{11}}{\pi^8}\Bigg] \\
G_-^{(3)}(\alpha) = &\frac{4}{9}(-6+\pi^2) + \alpha\left[\frac{8}{3} - \frac{28\zeta_3}{3} + \frac{62\zeta_5}{\pi^2}\right] + \alpha^2\left[-\frac{8}{5} - \frac{28\zeta_3}{5} + \frac{248\zeta_5}{\pi^2} - \frac{1524\zeta_7}{\pi^4}\right] + \\
&+ \alpha^3\left[\frac{1288\zeta_3}{45\pi^2} + \frac{124(-40+23\pi^2)\zeta_5}{15\pi^4} - \frac{1016(-1+5\pi^2)\zeta_7}{\pi^6} + \frac{28616\zeta_9}{\pi^6}\right] + \\
&+ \alpha^3\left[\frac{16\zeta_3}{\pi^2} + \frac{248(-392+15\pi^2)\zeta_5}{105\pi^4} - \frac{2032(-15+7\pi^2)\zeta_7}{3\pi^6} + \frac{8176(-12+35\pi^2)\zeta_9}{3\pi^8} - \frac{491280\zeta_{11}}{\pi^8}\right]
\end{aligned}
\tag{3.4.25}
$$

3.4.3 Asymptotic expansion

We next study the spectrum at large λ. The most direct way to achieve this is constructing an asymptotic expansion in $|\lambda| \to \infty$ directly (rather than using the solutions (3.4.7) and (3.4.8) constructed above). To do that, we first observe that the expansion in $|\lambda| \to \infty$ of the two solutions, (3.4.7) and (3.4.8), contains a prefactor $(-\lambda)^{-\frac{i\nu}{2}-\frac{i\alpha z}{\pi}}$ times a further asymptotic series in powers of λ^{-1}[165]. Hence, it is natural to look for asymptotic solutions of (3.2.29) with the following structure around $\lambda \to -\infty$,

$$
S(\nu|\lambda) = (-\lambda)^{-\frac{i\nu}{2}-\frac{i\alpha z}{\pi}} \sum_{n=0}^{\infty} S_n(\nu)\,\lambda^{-n}\,, \tag{3.4.26}
$$

Note that $\lambda \to -\infty$ is not the physical region of the eigenvalues of 't Hooft equation and we will eventually analytically continue to the positive λ.

General strategy. By plugging the ansatz (3.4.26) into (3.2.29) we obtain:

$$
\sum_{k=0}^{\infty} S_k(\nu+2i)\,\lambda^{-k+1} + \sum_{k=0}^{\infty} S_k(\nu-2i)\,\lambda^{-k-1} + 2\sum_{k=0}^{\infty} S_k(\nu)\,\lambda^{-k} = \frac{4\pi\lambda}{\frac{\nu}{z}+\frac{2\alpha}{\pi}} \sum_{k=0}^{\infty} S_k(\nu)\,\lambda^{-k} \tag{3.4.27}
$$

that has to be satisfied at each order in λ. Remarkably, the order-n term is recursively fixed by the previous ones. So we just need to solve for the single function $S_0(\nu)$ to reconstruct the full series. Let us illustrates this in the simple case of $S_1(\nu)$ since the generalization is trivial. Assuming that the solution $S_0(\nu)$ at order $\mathcal{O}(\lambda^1)$ $(k=0)$ is known, we can plug the ansatz $S_1(\nu) = S_0(\nu)\, s_1(\nu)$ into the order $\mathcal{O}(\lambda^0)$ $(k=1)$ of (3.4.27):

$$S_1(\nu+2i) + 2S_0(\nu) = \frac{4\pi}{\frac{\nu}{z} + \frac{2\alpha}{\pi}} S_0(\nu) \quad \Rightarrow \quad s_1(\nu+2i) - s_1(\nu) = -\frac{1}{2\pi z}\left(\nu + \frac{2\alpha z}{\pi}\right), \tag{3.4.28}$$

that is solved uniquely by the function:

$$f_1(\nu) = \frac{1}{2\pi i z}\left(1 + \frac{i\nu}{2} + \frac{i\alpha z}{\pi}\right)\left(\frac{i\nu}{2} + \frac{i\alpha z}{\pi}\right). \tag{3.4.29}$$

up to an arbitrary constant that we can always set to zero. We can then generalise to any order k by using the ansatz $S_k(\nu) = s_k(\nu) S_0(\nu)$ leading to:

$$s_k(\nu) = \frac{1}{k!\,(2\pi i z)^k}\left(1 + \frac{i\nu}{2} + \frac{i\alpha z}{\pi}\right)_k \left(\frac{i\nu}{2} + \frac{i\alpha z}{\pi}\right)_k, \tag{3.4.30}$$

where we used the Pochhammer Symbol: $(a)_k = \Gamma(a+k)/\Gamma(a)$. Thus, as anticipated, the whole series (3.4.34) is determined just by the single function $S_0(\nu)$:

$$S(\nu|\lambda) \asymp (-\lambda)^{-\frac{i\nu}{2} - \frac{i\alpha z}{\pi}}\, S_0(\nu) \sum_{n=0}^{\infty} s_n(\nu)\, \lambda^{-n}. \tag{3.4.31}$$

As a preliminary remark, note that the series in (3.4.33) is divergent and it has to be understood only as an asymptotic expansion for the solutions of (3.2.29) (and therefore the symbol $\asymp$ has been used).

Solutions constructed in this way, in particular the coefficients $s_k(\nu)$, do not have the required analyticity in the strip. To remedy this, we build two independent solutions by taking appropriate linear combinations of $S(\pm\nu|\lambda)$ using the ν-dependent coefficients $P_\pm(z,\lambda)$:

$$\begin{aligned} Q_\pm(\nu|\lambda) &= P_\pm(\nu,\lambda)\, S(\nu|\lambda) \mp P_\pm(-\nu,\lambda)\, S(-\nu|\lambda); \\ P_\pm(\nu,\lambda) &= C_\pm(\lambda) \sum_k P_\pm^{(k)}\Big(z, z^{-1}, \log(-\lambda)\Big)\, \lambda^{-k} \end{aligned} \tag{3.4.32}$$

Here $P_\pm(z,\lambda)$ are functions of ν and λ, invariant under $\nu \to \nu \pm 2i$, which can be taken to have polynomial coefficients of the invariant variables z and $\frac{1}{z}$. We anticipate that this coefficients will contain a $\log(-\lambda)$ dependence. For convenience we factor out an overall normalization $C(\lambda)$, which is independent of ν.

The singularities at $\nu = i$ generated by the prefactor $(-\lambda)^{-\frac{i\alpha z}{2}}$ can be removed by a redefinition of the polynomial $P_\pm(z,\lambda) \to (-\lambda)^{\frac{i\alpha z}{2}} P_\pm(z,\lambda)$ given that $(-\lambda)^{\frac{i\alpha z}{2}}$ is invariant under $\nu \to \nu \pm 2i$. In fact, this could have been done already at the beginning by redefining the ansatz (3.4.31) to:

$$S(\nu|\lambda) = (-\lambda)^{-\frac{i\nu}{2}}\, S_0(\nu) \sum_{n=0}^{\infty} s_n(\nu)\, \lambda^{-n}. \tag{3.4.33}$$

Constructing $S_0(\nu)$. We now construct $S_0(\nu)$. This amounts to determining the solutions at order $\mathcal{O}(\lambda^1)$ of (3.4.27):

$$S_0(\nu+2i) = \frac{4\pi^2 z}{\pi\nu + 2\alpha z} S_0(\nu). \tag{3.4.34}$$

A solution of (3.4.34) with $\alpha = 0$ was already discussed in [92] and it is expressed in terms of Barnes G-functions:

$$S_0(\nu)\Big|_{\alpha=0} = (2\pi)^{-\frac{1}{2}-\frac{i\nu}{2}} \frac{G\left(2+\frac{i\nu}{2}\right) G\left(\frac{1}{2}-\frac{i\nu}{2}\right)}{G\left(1-\frac{i\nu}{2}\right) G\left(\frac{3}{2}+\frac{i\nu}{2}\right)}, \tag{3.4.35}$$

which is analytical everywhere inside the strip $(-2i, 2i)$. Having a solution of (3.4.34) with $\alpha = 0$, we can build a solution for $\alpha \neq 0$ by using again an ansatz of the form $S_0(\nu) = \left(S_0(\nu)\big|_{\alpha=0}\right) \sigma(\nu)$ with $\sigma(\nu)$ satisfying

$$\sigma(\nu+2i) = \left(1 + \frac{2\alpha}{\pi}\frac{z}{\nu}\right)^{-1} \sigma(\nu). \tag{3.4.36}$$

The recurrence equation (3.4.36) is solved exactly by:

$$\sigma(\nu) = \frac{\sqrt{\pi}}{\Gamma\left(\frac{1}{2}+\frac{i\alpha z}{\pi}\right)} \frac{\Gamma\left(1+\frac{i\nu}{2}+\frac{i\alpha z}{\pi}\right)}{\Gamma\left(1+\frac{i\nu}{2}\right)}, \qquad \sigma(i) = 1 \tag{3.4.37}$$

Yet, the resulting $S_0(\nu) = S_0(\nu; 0)\,\sigma(\nu)$ is not a solution of the TQ-System because of the poles at the zeros of $\left(\frac{1}{2}+\frac{i\alpha z}{\pi}\right)$ accumulating at $\nu = i$. In analogy to what done in the previous section, we proceed to expand $\sigma(\nu)$ in a formal power of α:

$$\sigma(\nu) = \sum_{k=0}^{\infty} \sigma_k(\nu, z)\, \alpha^k\,. \tag{3.4.38}$$

This function display unwanted poles of increasing order at $\nu = \pm i$, where z is singular. At any order in α, to remove then we can just multiply by polynomial in power of α fixed term by term by cancellation of poles:

$$S_0^{(k)}(\nu) = A^{(k)}(z)\, S_0(\nu)\,, \qquad A^{(k)}(\alpha, z) = \sum_{l=0}^{k} a^{(l)}\, \alpha^l \tag{3.4.39}$$

Let us introduce for simplicity: $\chi = i\pi \tanh \frac{\pi\nu}{2}$. $A^{(k)}(z)$ up to order α^4 is:

$$\begin{aligned}
A^{(4)}(z) = 1 &+ \alpha\chi\frac{(\gamma+\log 4)}{\pi^2} + \alpha^2\left(\chi^2 - \frac{(\pi^2 - 2(\gamma+\log 4)^2)}{4\pi^4} - \chi\frac{7\zeta_3}{\pi^4}\right) \\
&+ \alpha^3\Bigg[\chi^3\frac{\big((\gamma+\log 4)(-3\pi^2+8\log^2 2+\gamma(2\gamma+\log 256))+28\zeta_3\big)}{12\pi^6} \\
&\qquad + \chi^2\frac{(\pi^4 - 42(\gamma+\log 4)\zeta_3)}{6\pi^6} + \chi\frac{62\zeta_5}{\pi^6}\Bigg] \\
&+ \alpha^4\Bigg[\chi^4\Big(\frac{4\gamma^4 - \pi^4 + 32\gamma^3\log 2 - 48\pi^2\log^2 2 + 128\gamma\log^3 2 + 64\log^4 2 - 12\gamma^2(\pi^2 - 8\log^2 2)}{96\pi^8} \\
&\qquad + \frac{-16\gamma\pi^2\log 8 + 224(\gamma+\log 4)\zeta_3}{96\pi^8}\Big) \\
&\qquad - \chi^3\frac{\big(-2\gamma\pi^4 - 4\pi^4\log 2 + 21(-\pi^2 + 2(\gamma+\log 4)^2)\zeta_3 + 372\zeta_5\big)}{12\pi^8} \\
&\qquad - \chi^2\frac{(\pi^6 - 147\zeta_3^2 - 372(\gamma+\log 4)\zeta_5)}{6\pi^8} + \chi\left(\frac{31\zeta_5}{3\pi^6} - \frac{635\zeta_7}{\pi^8}\right)\Bigg]
\end{aligned} \tag{3.4.40}$$

Then, at any order k in α, the candidate for the two independent solutions of the the TQ-system in the asymptotic regime $\lambda \to -\infty$ are:

$$\begin{aligned}
S^{(k)}(\nu|\lambda) &= (-\lambda)^{-\frac{i\nu}{2}} S_0^{(k)}(\nu) \sum_{n=0}^{\infty} s_n(\nu)\, \lambda^{-n}\,, \\
Q_\pm^{(k)}(\nu|\lambda) &= P_\pm^{(k)}(\nu,\lambda)\, S^{(k)}(\nu|\lambda) \mp P_\pm^{(k)}(-\nu,\lambda)\, S^{(k)}(-\nu|\lambda)\,, \\
P_\pm^{(k)}(\nu,\lambda) &= C_\pm^{(k)}(\lambda) \sum_{n=0}^{\infty} P_\pm^{(k,n)}\Big(z, z^{-1}, \log(-\lambda)\Big)\, \lambda^{-n}
\end{aligned} \tag{3.4.41}$$

Removing the singularities. As mentioned before, the coefficient functions $s_n(\nu)$'s do not have a required analyticity in the strip $(-2i, 2i)$: they have poles of order $(n-1)$ at the point $\nu = 0$ and of order n at $\nu = \pm i$. To remove these singularities, we choose the polynomials $P_\pm^{(k)}\Big(z, z^{-1}, \log(-\lambda)\Big)$ so that they cancel all those singularities and any given order in λ and α. As we will see, this can be done uniquely. The contributions can be split as follows :

$$\begin{aligned}
P_\pm^{(k)}(z,\lambda) =& C_\pm^{(k)}(\lambda)\Big[\sum_{n=0} R_\pm^{(n,k)}(z^{-1};\alpha,\log(-\lambda))\,\lambda^{-n}\Big]\Big[\sum_{n=0} T^{(n)}(z;\alpha)\,\lambda^{-n}\Big] \\
:=& C_\pm(\lambda)\, R_\pm^{(k)}(z^{-1};\alpha,\lambda)\, T(z;\alpha,\lambda)\,.
\end{aligned} \tag{3.4.42}$$

The functions $R_\pm^{(k)}$ and T are polynomials in their first variable with α and λ appearing as parameters (also polynomially) in the coefficients thereof and they can be determined

independently from the other. In the function T we dropped the subscript (k) turns out to be exact in α (and indeed it matches perfectly with the one presented in [93]).

We proceed as follows:

- For any fixed k being the order of expansion in α, at every order in λ, we expand $Q_\pm(\nu|\lambda)$ in (3.4.32) around $\nu = 0$ and fix the coefficients $r_\pm^{(l)}(\alpha, \log(-\lambda))$ in the polynomials:

$$R_\pm^{(n,k)}\left(z^{-1}; \alpha, \log(-\lambda)\right) = \sum_{l=1}^{n-1} r_\pm^{(l,n,k)}(\alpha, \log(-\lambda))\, z^{-l} \tag{3.4.43}$$

so that they cancel all the poles of the form $1/\nu^k$ in $Q_\pm^{(k)}(\nu|\lambda)$. This fixes uniquely the function $R_\pm^{(n,k)}(z,\lambda)$ up to an overall λ-depending constant $C_-^{(k)}(\lambda)$ that we fix upon requiring the normalisation $Q_-(0;\lambda) = 1$ at all orders in λ. This automatically fixes also $C_+^{(k)}(\lambda)$ up to an overall scaling thanks to the relation presented in (4.12) of [92].

The resulting expression can be conveniently expressed through the combinations:

$$L = \log(-2\pi\lambda) + \gamma_E, \qquad c = i\pi z^{-1}, \qquad \beta = \alpha + 1\,, \tag{3.4.44}$$

and just to give a flavor of the resulting expressions, we report the result up to $\mathcal{O}\left(\frac{\log^2(\lambda)}{\lambda^4}\right)$ and α^3:

$$\begin{aligned} R_\pm^{(3)}(c,L) - 1 = \pm\frac{\beta c}{\lambda^2}\Bigg[\frac{1}{4\pi^4} + \frac{1}{24\pi^6\lambda}\Big(6c + \beta(6 \mp 1) - 12L + \\ + 12\alpha\,(1 + \log(4)) - \frac{84}{\pi^2}\alpha^2\zeta_3\Big) + 31\alpha^3\zeta_5/\pi^{10}\Bigg] + \mathcal{O}\left(\frac{\log^2(\lambda)\alpha^4}{\lambda^4}\right) \end{aligned} \tag{3.4.45}$$

that matches perfectly with what reported in [93] up to the order considered here.

- Analogously, as we expand the functions $Q_\pm(\nu;\lambda)$ near $\nu = i$ (only $\nu = i$ is enough given the parity of $Q_\pm(\nu|\lambda)$), we exhibit poles coming from $s_k(\nu)$ which cancellation determines uniquely the numbers $c_{m,l}$ that specify $T^{(k)}(z;\alpha)$:

$$T^{(k)}(z;\alpha) = \sum_{l=1}^{k}\sum_{m=k+1}^{2k} c_{m,l}\,\alpha^m\, z^l \tag{3.4.46}$$

In principle, one could have a different functions for $Q_\pm$, but it turns out that the same function works for both: $T_+^{(k)}(z;\alpha) = T_-^{(k)}(z;\alpha)$. We therefore suppressed the index. The determination of $T^{(k)}(z;\alpha)$ is completely independent from the one of $R_\pm(c,L)$. The overall scaling κ that is left unfixed is determined by imposing the Wronskian relation $Q_+(i;\lambda)\,Q_-(i;\lambda) = i$. In (3.4.45), we have already presented the $C_\pm(\lambda)$ with this normalization imposed.

Using the same variable as above $\chi = i\pi z$ for convenience, the first orders are:

$$T(\chi;\alpha,\lambda) = 1 - \frac{\alpha^2\chi}{2\pi^4\lambda} + \frac{\alpha^3\chi}{8\pi^8\lambda^2}\left(\alpha\chi - 2\pi^2\right) - \frac{\alpha^4\chi}{48\pi^{12}\lambda^3}\left(\alpha^2\chi^2 - 6\pi^2\alpha\chi + 10\pi^4\right) + \\ + \frac{\alpha^5\chi}{384\pi^{16}\lambda^4}\left(\alpha^3\chi^3 - 12\pi^2\alpha^2\chi^2 + 52\pi^4\alpha\chi - 84\pi^6\right) + \mathcal{O}\left(\lambda^{-5}\right) \tag{3.4.47}$$

3.5 Application to non-perturbative topological string

In recent years, an interesting relation has been established between partition functions associated to topological strings on a toric Calabi-Yau threefold X and the spectral problem following from the quantization of the curve encoding its local mirror Calabi-Yau $\widehat{X}$. This is sometimes referred to as the topological string/spectral theory (TS/ST) correspondence and was used to define a non-perturbative completion of the topological string partition function, which, in its original form, is defined only through perturbation theory. Reviewing this correspondence in full details goes beyond the scope of this work, and we refer to [134,135,137,149] and references therein for a comprehensive discussion. Instead, here we comment on connections and applications of the techniques employed in this work to that context.

3.5.1 Elements of TS/ST correspondence

The TQ-systems similar to the one considered in this thesis (3.2.29) arise from the quantization of a curve associated to a mirror dual of a toric Calabi-Yau threefold: $W_X\left(e^x, e^p\right) = 0$, that is a Riemann surface embedded in $\mathbb{C}^* \times \mathbb{C}^*$. Upon quantizing the curve $W_X\left(e^x, e^p\right)$ by promoting x, p to canonically conjugated variables $[\widehat{x}, \widehat{p}] = i\hbar$, it is promoted to the spectral problem[135]:

$$W_X\left(e^{\widehat{x}}, e^{\widehat{p}}\right)|\phi\rangle = \mathcal{O}(\widehat{x},\widehat{p})\,|\phi\rangle - \lambda\,|\phi\rangle = 0 \tag{3.5.1}$$

for the self-adjoint quantum operator $\mathcal{O}(\widehat{x},\widehat{p})$. When the mirror curve is elliptic (genus 1), the operator $\mathcal{O}(\widehat{x},\widehat{p})$ has a discrete and positive spectrum. Thus, the spectral problem above gives the well-defined eigenvalue problem :

$$\mathcal{O}(\widehat{x},\widehat{p})\,|\psi_n\rangle - e^{E_n}\,|\psi_n\rangle = 0\,. \tag{3.5.2}$$

Because of the positivity of the spectrum, the operator $\mathcal{O}(\widehat{x},\widehat{p})$ can be thought of as an exponential of an Hamiltonian $\mathcal{H}(\widehat{x},\widehat{p})$. In fact, it is more convenient to consider the spectral problem associated to its density matrix,

$$\rho(\widehat{x},\widehat{p}) = \mathcal{O}^{-1}(\widehat{x},\widehat{p}) = e^{-\mathcal{H}(\widehat{x},\widehat{p})} \tag{3.5.3}$$

since it is of the so called *trace-class*, i.e. such that all the spectral sums

$$Z_s = \sum_{n=0}^{\infty} e^{-sE_n} = \sum_{n=0}^{\infty} \frac{1}{\lambda_n^s}, \qquad s = 1, 2, \cdots \tag{3.5.4}$$

are convergent. Furthermore all the spectral data for the problem can be collected into the following spectral determinant (*Fredholm determinant*):

$$\begin{aligned}\Xi(\lambda,\hbar) &= \det(1+\lambda\rho) = \prod_{n=0}^{\infty}\left(1+\lambda e^{-E_n}\right) = \prod_{n=0}^{\infty}\left(1+\frac{\lambda}{\lambda_n}\right), \\ \log\Xi(\lambda,\hbar) &= -\sum_{s=1}^{\infty} Z_s \frac{(-\lambda)^s}{s},\end{aligned} \tag{3.5.5}$$

defined for any $\lambda\in\mathbb{R}$ and having zeros at the location of the eigenvalues of $\rho(\widehat{x},\widehat{p})$. It is clear that the quantities Z_s and $\Xi(\lambda,\hbar)$ are closely related (cfr. eq. (3.2.50), (3.2.52)) to the spectral sums $G_{\pm}^{(s)}$ and the spectral determinants $D_{\pm}(\lambda)$ defined in this work. The crucial content of the TS/ST correspondence is that $\log\Xi(\lambda,\hbar)$ is conjectured to be computed exactly by the non-perturbative topological string free energy that can in turn be computed using, among others, the tools from the enumerative geometry[135]. This allows, for instance, to determine exact non-perturbative quantization conditions determining the eigenvalues of $\rho(\widehat{x},\widehat{p})$ analogous to the ones we presented in our work.

3.5.2 Local $\mathbb{P}^1\times\mathbb{P}^1$: spectral determinants from inhomogeneous extension

Here we discuss the possibility of applying the methods developed in this work to this context, and present some preliminary results. Concretely, let us consider the case of the local $\mathbb{P}^1\times\mathbb{P}^1$ considered in [134]. In this case, the spectral problem associated with the density matrix is

$$\begin{aligned}\phi(x) &= \lambda\int_{-\infty}^{+\infty}\mathrm{d}y\,\rho(x,y)\phi(y), \qquad \lambda = \frac{e^E}{4\pi k}, \\ \rho(x,y) &= \frac{1}{\sqrt{2\cosh\left(\frac{x}{2}\right)}\sqrt{2\cosh\left(\frac{y}{2}\right)}}\frac{1}{\cosh\left(\frac{x-y}{2k}\right)}\end{aligned} \tag{3.5.6}$$

where $2\pi k=\hbar$. As expected, ρ gives an Hermitian Hilbert-Schmidt operator with discrete positive spectrum. It is convenient for the following to reformulate the integral problem as:

$$\begin{aligned}f(x)\Psi(x) &= \lambda\int_{-\infty}^{+\infty}\mathrm{d}y\,S(x-y)\,\Psi(y), \\ S(x) &= \frac{1}{2\cosh\left(\frac{x}{2k}\right)}, \qquad f(x) = 2\cosh\left(\frac{x}{2}\right), \qquad \phi(x) = \Psi(x)\sqrt{f(x)}.\end{aligned} \tag{3.5.7}$$

Now, following the analysis for the 't Hooft equation in ν-space (3.2.6) in Section 3.2.2, we define

$$Q(x) = \sinh\left(\frac{x}{k}\right) f(x)\Psi(x), \tag{3.5.8}$$

which satisfies the related integral equation

$$Q(x) = \lambda\sinh\left(\frac{x}{k}\right)\int_{-\infty}^{+\infty}\mathrm{d}y\,S(x-y)\,\frac{Q(y)}{\sinh\left(\frac{y}{k}\right)f(y)}. \tag{3.5.9}$$

Then the integral spectral problem becomes equivalent to the following TQ-system:

$$Q(x+i\pi k)+Q(x-i\pi k)=-2\pi k\lambda\frac{Q(x)}{f(x)} \tag{3.5.10}$$

Upon imposing that the $\mathcal{Q}(x) := Q(x)/\sinh(x/k)$ decays in the strip $[-i\pi,+i\pi]$, one finds that the solution to this equation exists only for discrete values of λ. Thus, the equation (3.5.10), together with the asymptotic decaying condition on $\mathcal{Q}(x)$, gives the quantization of the curve relative to the local $\mathbb{P}^1\times\mathbb{P}^1$, as already discussed in [134]. It also satisfies a "quantization" condition similar to (3.2.24):

$$Q(0)=Q(\pm i\pi k)=0\,. \tag{3.5.11}$$

Now, to study the equation (3.5.10) for any value of $\lambda\in\mathbb{C}$, we follow the analysis in the main text, and consider the following *inhomogeneous Fredholm equation*

$$f(x)\,\Psi(x|\lambda)-\lambda\int_{-\infty}^{+\infty}\mathrm{d}y\,S(x-y)\,\Psi(y|\lambda)=F(x|\lambda)\,. \tag{3.5.12}$$

The inhomogeneous term $F(x|\lambda)$ spans a two-dimensional space, and in accordance with the symmetry $x\to -x$ of the integral equation, we take the following function $F_\pm$ as a basis for this space:

$$F(x|\lambda)=q_+(\lambda)F_+(x)+q_-(\lambda)F_-(x),\qquad F_+(x)=\frac{1}{\cosh\left(\frac{x}{2k}\right)},\quad F_-(x)=\frac{1}{\sinh\left(\frac{x}{2k}\right)} \tag{3.5.13}$$

Then, the solutions $\Psi_\pm$ satisfy the following integral eigenproblems:

$$f(x)\,\Psi_+(x|\lambda)-\lambda\int_{-\infty}^{+\infty}\mathrm{d}y\,S(x-y)\,\Psi_+(y|\lambda)=F_+(x|\lambda) \tag{3.5.14}$$

$$f(x)\,\Psi_-(x|\lambda)-\lambda\fint_{-\infty}^{+\infty}\mathrm{d}y\,S(x-y)\,\Psi_-(y|\lambda)=F_-(x|\lambda) \tag{3.5.15}$$

Where the principal part is needed due to the inhomogeneous term in $x=0$. Then the $Q(x)$ satisfy the integral equation

$$\sinh\left(\frac{x}{k}\right)F_\pm(x)=Q_\pm(x)-\lambda\sinh\left(\frac{x}{k}\right)\fint_{-\infty}^{+\infty}\mathrm{d}y\,\frac{1}{\cosh\left(\frac{x-y}{2k}\right)}\,\frac{Q_\pm(y)}{\sinh\left(\frac{y}{k}\right)f(y)}\,, \tag{3.5.16}$$

for any $\lambda\in\mathbb{C}$. Thanks to the identity, $\sinh\left(\frac{x+ik\pi}{k}\right)F_\pm(\nu+ik\pi)+\sinh\left(\frac{x-ik\pi}{k}\right)F_\pm(\nu-ik\pi)=0$, $Q_\pm$ satisfy the same TQ-system:

$$Q_\pm(x+i\pi k)+Q_\pm(x-i\pi k)=-2\pi k\lambda\frac{Q_\pm(x)}{f(x)}\,. \tag{3.5.17}$$

As in the case of 't Hooft model, they do not satisfy the "quantization" condition:

$$Q_+(0)=0\,,\quad Q_+(i\pi k)=-Q_+(-i\pi k)=2i\,,\qquad Q_-(0)=2\,,\quad Q_-(\pm i\pi k)=0\,. \tag{3.5.18}$$

Now, consider the Liouville-Neumann series giving the exact solutions $\Psi_{\pm}(x|\lambda)$:

$$\begin{aligned} f(t)\Psi_{+}(t|\lambda) &= \sum_{n=0}^{\infty}\int_{-\infty}^{+\infty} F_{+}(x|\lambda)\prod_{j=1}^{n}\frac{\mathrm{d}t_j}{f(t_j)}S(t_j-t_{j-1}), \\ f(t)\Psi_{-}(t|\lambda) &= \sum_{n=0}^{\infty}\fint_{-\infty}^{+\infty} F_{-}(x|\lambda)\prod_{j=1}^{n}\frac{\mathrm{d}t_j}{f(t_j)}S(t_j-t_{j-1})\,, \end{aligned} \tag{3.5.19}$$

where $t_0 = t$. Then, upon considering the following combination, we obtain

$$\begin{aligned} &f(t)f(t')\Big[\Psi_{+}(t'|\lambda)\Psi_{-}(t|\lambda)-\Psi_{-}(t'|\lambda)\Psi_{+}(t|\lambda)\Big] = \\ &\sum_{l,m=0}^{\infty}\lambda^{l+m}\fint_{-\infty}^{+\infty}\cosh\Big(\frac{t'_l-t_m}{2k}\Big)\left(\frac{1}{\cosh\Big(\frac{t'_l}{2k}\Big)\sinh\big(\frac{t_m}{2k}\big)}-\frac{1}{\sinh\Big(\frac{t'_l}{2k}\Big)\cosh\big(\frac{t_m}{2k}\big)}\right) \\ &\times S(t'_l-t_m)\prod_{j=1}^{l}\frac{\mathrm{d}t'_j}{f(t'_j)}S(t'_j-t'_{j-1})\prod_{i=1}^{m}\frac{\mathrm{d}t_i}{f(t_i)}S(t_i-t_{i-1})\,, \end{aligned} \tag{3.5.20}$$

with $t_0 = t, t'_0 = t'$. Now, uniforming the notation for integration variables to:

$$(\tau_1,\cdots,\tau_m,\tau_{m+1},\cdots,\tau_{m+k}) = (t_1,\cdots,t_m,t'_k,\cdots,t'_1) \tag{3.5.21}$$

we get

$$\begin{aligned} &f(t)f(t')\Big[\Psi_{+}(t'|\lambda)\Psi_{-}(t|\lambda)-\Psi_{-}(t'|\lambda)\Psi_{+}(t|\lambda)\Big] = \\ &\sum_{l=1}^{\infty}\lambda^{l}\fint_{-\infty}^{+\infty}\left[\sum_{m=0}^{l}\cosh\Big(\frac{\tau_{m+1}-\tau_m}{2k}\Big)\left(\frac{1}{\cosh\big(\frac{\tau_{m+1}}{2k}\big)\sinh\big(\frac{\tau_m}{2k}\big)}-\frac{1}{\sinh\big(\frac{\tau_{m+1}}{2k}\big)\cosh\big(\frac{\tau_m}{2k}\big)}\right)\right] \\ &\quad\times\prod_{j=1}^{l}\frac{\mathrm{d}\tau_j}{f(\tau_j)}\prod_{j=1}^{l+1}S(\tau_j-\tau_{j-1}) \end{aligned} \tag{3.5.22}$$

The inhomogeneous function $F_{\pm}$ had been chosen such that sum over m could be performed analytically by means of the following identity:

$$\begin{aligned} &\sum_{m=0}^{l}\left(\frac{\cosh(t_{m+1}-t_m)}{\sinh(t_{m+1})\cosh(t_m)}-\frac{\cosh(t_{m+1}-t_m)}{\sinh(t_m)\cosh(t_{m+1})}\right) = \\ &=\left(\frac{\cosh(t_{l+1}-t_0)}{\sinh(t_{l+1})\cosh(t_0)}-\frac{\cosh(t_{l+1}-t_0)}{\sinh(t_0)\cosh(t_{l+1})}\right), \end{aligned} \tag{3.5.23}$$

which we can use, together with $\tau_{l+1} = t'_0 = t'$ and $\tau_0 = t_0 = t$, to rewrite our identity as:

$$\Xi(t,t')f(t)f(t')\Big[\Psi_{+}(t'|\lambda)\Psi_{-}(t|\lambda)-\Psi_{-}(t'|\lambda)\Psi_{+}(t|\lambda)\Big] = \sum_{l=1}^{\infty}\lambda^{l}\int_{-\infty}^{+\infty}\prod_{j=1}^{l}\frac{\mathrm{d}\tau_j}{f(\tau_j)}\prod_{j=1}^{l+1}S(\tau_j-\tau_{j-1})\,, \tag{3.5.24}$$

$$\frac{1}{\Xi(2kt,2kt')} = \frac{\cosh(t'-t)}{\sinh(t')\cosh(t)} - \frac{\cosh(t'-t)}{\sinh(t)\cosh(t')}\,. \tag{3.5.25}$$

Remarkably, the r.h.s. is proportional to the Liouville-Neumann series for the resolvent associated with our integral equation that, by definition, satisfies the following problem:

$$R(t,t'|\lambda) - \lambda\int_{-\infty}^{+\infty} \mathrm{d}\tau\, \frac{S(t-\tau)}{\sqrt{f(t)f(\tau)}}\, R(\tau,t'|\lambda) = \frac{S(t-t')}{\sqrt{f(t)f(t')}} \tag{3.5.26}$$

We thus arrive at the main formula:

$$R(t,t'|\lambda) = \Xi(t,t')\sqrt{f(t)f(t')}\left[\Psi_+(t'|\lambda)\Psi_-(t|\lambda) - \Psi_-(t'|\lambda)\Psi_+(t|\lambda)\right] \tag{3.5.27}$$

This shows that the kernel S for this problem is of the *completely integrable* type as well.

Using this identity, we can express the spectral determinants $D_\pm(\lambda)$ defined as in (3.2.50) in terms of Q-functions:

$$\begin{aligned}
\partial_\lambda \log\frac{D_+(\lambda)}{D_-(\lambda)} &= \int_{-\infty}^{+\infty} \mathrm{d}t\, R(t,-t|\lambda) = \int_{-\infty}^{+\infty} \mathrm{d}t\, \frac{1}{2f(t)\sinh\left(\frac{2t}{k}\right)} Q_+(t)Q_-(t)\,,\\
\partial_\lambda \log D_+(\lambda)D_-(\lambda) &= \int_{-\infty}^{+\infty} \mathrm{d}t\left[R(t,t|\lambda) - R^{(0)}(t)\right]\\
&= \int_{-\infty}^{+\infty} \mathrm{d}t\left[\frac{2k\left(Q_+(t)Q'_-(t) - Q_-(t)Q'_+(t)\right)}{2\pi f(t)} - R^{(0)}(t)\right]\,,
\end{aligned} \tag{3.5.28}$$

where $R^{(0)}(t)$ has to be chosen to guarantee convergence of this integral depending on the value of k. Those expressions are exactly the analogous to (3.2.51) and are the key consequence of the complete integrability of the kernel. Starting from these expressions, one can in principle proceed as in Section 3.4 to extract spectral sums and eigenvalues associated to this spectral problem. We hope to get back to study this in the future, as this could provide useful information on the convergence properties of the expansions compared with the exact one of [134].

Chapter 4

Generalized QCD

In this Chapter, based on [2] we study the generalized QCD theory. As in the 't Hooft model, at Large N_c the spectrum of mesons is encoded in a Bethe-Salpeter equation. The starting point of our analysis is the reformulation of this equation in terms of the TQ-Baxter equation and an associated inhomogeneous Fredholm equation. This allows us to explore detailed analytic structures of the meson spectrum as a function of parameters of the theory. A similar study for the 't Hooft model revealed an intricate structure of the spectrum in the complex quark-mass plane [1,92]: it has a multi-sheeted structure with infinitely many branch points, each of which signals a tachyonic instability of one of the mesons. The first of such branch points corresponds to a massless quark point where the chiral symmetry becomes exact. The IR phase of that point is described by a CFT with the $U(1)_N$ current algebra [162,166]. This suggests the correspondence between the branch points in the complex mass plane and actual *critical points* of the theory. In this work, we extend these results to the generalized QCD_2. A novelty in the present case is that we can also study the dependence on the coefficients of the potential $V(B)$. We found that the theory develops instability for a certain range of parameters and the onset of the instability is signaled by "critical points" at which one of the mesons becomes massless (and beyond which it becomes tachyonic). The connection to the inhomogeneous Fredholm equation provides a simple and systematic criterion for the stability, bypassing the case-by-case numerical analysis performed in [95]. In addition, we found that, when the coefficients of the potential are appropriately tuned, several mesons can become simultaneously massless, realizing "multi-critical points". As in the 't Hooft model, we conjecture that these "critical points" correspond to actual critical points of the theory. Unlike the standard QCD_2, the IR phases of the generalized QCD_2 have not been sufficiently explored in the literature and our results strongly motivate such analysis.

We also perform a similar analysis for the *large representation limit* of generalized Yang-Mills with the SU(2) gauge group coupled to quarks in the spin J representation of SU(2). This is the limit introduced recently for the 't Hooft model in [96], in which J is sent to infinity keeping $\lambda_J \equiv g_{\text{YM}}^2 J$ fixed. A similar double-scaling limit was studied extensively in the context of large charge limits of conformal field theory (see e.g [167–173] and references therein for the large charge double scaling limits and [174–180] for the

large representation limits of line defects) since it simplifies the dynamics of interacting conformal field theories and makes it accessible through analytic methods while still maintaining important qualitative features of the original theory. As in those examples, it was found in [96] that the dynamics of the 't Hooft model simplifies in the large representation limit and the meson spectrum can be determined by *exactly the same* integral equation as in the large N_c limit. We extend this result to the generalized QCD_2. Our result also provides evidence that the structures found in the large N_c limit (the connection to integrability and the analytic structure in the complex quark-mass plane) may persist even at finite N_c.

Outline. In Section 4.1, we review the generalized QCD_2 and the derivation of the integral equation determining the mass spectrum of the mesons. In Section 4.2, we rewrite the integral equation into the TQ-Baxter equation. In Section 4.3 we analyze the analytical structure of the spectrum of mesons as a function for generic $V(B)$ and complex quark masses, and we study in detail the example of a cubic potential $V(B)$ that demonstrates all the relevant features of the generic case. In Section 4.4, we generalize the analysis to the large representation limit of the generalized QCD_2 with gauge group $SU(2)$.

4.1 Generalized QCD in the large N limit

Generalized QCD_2 is described by the Lagrangian[95]:

$$\mathcal{L} = \frac{N}{8\pi}\mathrm{tr}\, B \wedge F - \mathrm{tr}\,\frac{N}{4\pi}g^2\, V(B) + \mathrm{tr}\,\overline{\Psi}\,(i\gamma^\mu D_\mu - m)\,\Psi\,, \tag{4.1.1}$$

where both the field strength $F = \mathrm{d}A$ and the B-field are in the adjoint representation of $SU(N)$, for simplicity we consider a single flavor of quarks Ψ in the fundamental representation[1]. Classical power counting implies that *any* potential for the scalar field B is allowed in two dimensions. In this work, we take the potential for the B-field to be given by the formal power series[2]:

$$V(B) = \sum_{n=2}^{\infty} v_n\, \mathrm{tr}\, B^n\,. \tag{4.1.2}$$

Integrating out the field B gives: $\mathrm{d}A = 2g^2\, V'(B)$, therefore, by fixing $V(B) = \frac{1}{8\pi}B^2$, the usual Yang-Mills Lagrangian is retrieved. While one could expect that the theory could admit a discrete and positive spectrum of mesons when the potential $V(B)$ is bounded from below, one of the results of this work is that this is neither a sufficient nor necessary condition. This is due to instabilities produced by the odd powers in (4.1.2). Instead, the more conservative choice $v_{2n+1} = 0, v_{2n} > 0$, guarantees positivity and discreteness of the spectrum. At the same time, one of the surprising facts we illustrate in this thesis is that also for unbounded-from below potentials, there exist regions of the parameter space where the theory admits a positive spectrum in the large N limit.

[1] The generalization to multi-flavors is analogous to the one for the 't Hooft model [91].

[2] This is not the most generic form of a self-interaction term: also power of traces would be allowed.

$$\Gamma(p,q) = \quad + \quad + \quad + \quad \cdots \quad = 2g^2 \sum_{n=2}^{\infty} (-i)^n n v_n \, I_n \,, \tag{4.1.5}$$

Figure 4.1: Planar diagram contributions to the quark self-energy. The *master integral* I_n is reported in (4.1.7)

Lightcone gauge. As for the standard 't Hooft model [91], upon going to lightcone coordinates[3] $x_\pm = \frac{1}{\sqrt{2}}(x_0 \pm x_1)$, and fixing lightcone gauge $A_- = 0, A_+ = A$, the lagrangian presentation (4.1.1) simplifies and reduces to:

$$\mathcal{L} = \frac{N}{8\pi} \mathrm{tr}\, B \partial_- A - \mathrm{tr}\, \frac{N}{4\pi} g^2 \sum_{n=2}^{\infty} v_n \mathrm{tr} B^n + \mathrm{tr}\, \overline{\Psi}_a (i\gamma_\mu \partial^\mu - m_a - \gamma_- A) \Psi_a \,. \tag{4.1.3}$$

Here, we can regard all the $v_n \mathrm{tr}\, B^n$ terms as interaction vertices, so the only Feynman rules are:

$$= \frac{p_-}{2p_+p_- - m^2 + i\epsilon} \,, \qquad = \frac{-8\pi}{k_-} \,, \qquad = \frac{i n v_n}{4\pi} \,. \tag{4.1.4}$$

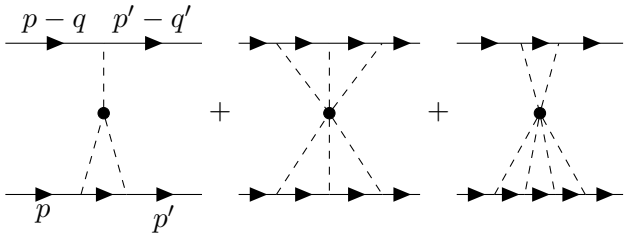
Henceforth in an arbitrary Feynman diagram, any propagator from a B^n vertex must be connected with a quark line. In the large N limit, the only Feynman diagrams that survive are the planar ones; an example of a planar contribution to the quark self energy is reported in Figure 4.1. For the case of the 't Hooft model [91] this revealed to be a crucial simplification and allowed us to obtain exact expression for the fermion propagators and for the equation determining the mesons' spectrum. Remarkably, as illustrated in [95] similar results are also available for its generalized version.

[3] The conventions on lightcone are the same of §2.1 of [1].

4.1.1 Bound state equation

The analog of 't Hooft equation for generalized QCD is obtained, as in the 't Hooft model, upon computing the 2PI kernel:

$$K(p,q,p',q') = \quad + \quad + \quad + \quad \cdots \tag{4.1.6}$$



$$= 4g^2 \sum_{n=2}^{\infty} (-i)^n n v_n \sum_{l=1}^{n} I_l(q,q') I_{n-l}(p'-q', p-q)\,,$$

that is expressed in terms of the following *master integrals* I_n:

$$I_n(p,q) = \int \mathrm{d}^{n-1}k \, \frac{1}{p_- - k_1} \, \mathrm{sgn} k_1 \, \frac{1}{k_1 - k_2} \, \mathrm{sgn} k_2 \cdots \frac{1}{k_{n-2} - k_{n-1}} \, \mathrm{sgn} k_{n-1} \, \frac{1}{k_{n-1} - q_-}\,, \tag{4.1.7}$$

whose computation is technically challenging because of their IR divergences. We refer to [95] for a thorough discussion. Following the same steps of [91] (also reviewed in [1]), from the homogeneous part of the 4-point Dyson equation we obtain the *Bethe-Salpeter* equation:

$$\Phi(p,r) = S(p)\, S(p-r) \int \mathrm{d}^2 k \, K(k,p,r)\, \Phi(p+k,r)\,, \tag{4.1.8}$$

as in (3.1.13), that in this model takes the form:

$$\left[2p_+ - m^2 \left(\frac{1}{p_-} + \frac{1}{p_- - q_-}\right)\right] \phi(p, p-q) = \left(\Gamma(q) + \Gamma(p-q)\right) \phi(q) + \\ + \int_0^{q_-} \mathrm{d}k_- \, K(k,p;q,q) \phi(k) \tag{4.1.9}$$

In this model, (4.1.9) can be expressed in the following contour-integral form [95]:

$$\left[2\pi^2 \lambda - (\alpha+1)\left(\frac{1}{x} + \frac{1}{1-x}\right)\right] \phi(x) = \\ = -2\pi \oint_{\gamma_\infty} \frac{\mathrm{d}z}{2\pi i} V'(z) \left[iz \frac{z^2+\pi^2}{(z^2-\pi^2)^2} \frac{2}{\pi} \arctan\left(\tfrac{\pi}{iz}\right) \left(\frac{1}{x} + \frac{1}{1-x}\right) \phi(x) + \right. \\ \left. + 2 \frac{z^2}{(z^2-\pi^2)^2} \fint_0^1 \mathrm{d}y \, \frac{1}{(x-y)^2} \exp\left(\frac{2}{\pi} \arctan\left(\tfrac{\pi}{iz}\right) \log\left(\tfrac{x(1-y)}{y(1-x)}\right)\right) \phi(y) \right], \tag{4.1.10}$$

where: $x = p_-/q_-$ is the momentum fraction, $\alpha = \pi m^2/g^2 - 1$, and $\phi(x)$ is the reduced meson wavefunction: $\phi(x) = \int \mathrm{d}p_+ \, \Phi(p,r)$ ($\Phi(p,r) = \langle \Omega | \, \overline{\psi}\psi \, | \Phi \rangle$). The contour integral

is along a curve γ_∞ enclosing all the singularities but the one at $z=\infty$. This, as 't Hooft equation, is an eigenproblem in $x\in[0,1]$ for the mesons wavefunctions $\phi(x)$ and masses μ^2.

Explicit form. We found closed-form expressions for the result of the contour integrations. The first term in the square bracket can be readily evaluated:

$$\begin{aligned}\alpha_n &= 2\pi\oint\frac{\mathrm{d}z}{2\pi i}\,in\,z^n\,\frac{z^2+\pi^2}{(z^2-\pi^2)^2}\,\frac{2}{\pi}\arctan(\tfrac{\pi}{iz}) = \\ &= \begin{cases}0 & n\,\text{odd}\\ 2\pi^{n-1}\,n^2\left(-1+\mathrm{H}(\frac{n-1}{2})+\log(4)\right) & n\,\text{even}\end{cases},\end{aligned} \tag{4.1.11}$$

where H(n) are the Harmonic numbers[4].

Denoting $m=n-2$ and employing the variable:

$$\Lambda := \log\left(\tfrac{x(1-y)}{y(1-x)}\right), \tag{4.1.12}$$

the second term is expressed as[5]:

$$\begin{aligned}p_n(\Lambda) &= 2\pi\oint\frac{\mathrm{d}z}{2\pi i}\,\frac{n\,z^{n+1}}{(z^2-\pi^2)^2}\exp\left(\Lambda\,\frac{2}{\pi}\arctan\left(\frac{\pi}{iz}\right)\right) = \\ &= 4\pi n\sum_{q=0}^{\lfloor\frac{m}{2}\rfloor}\sum_{p=0}^{\lceil\frac{m}{2}\rceil-1-q}\frac{(-2i)^{m-2p-2q}(q+1)\pi^{2q+2p}}{(m-2q-2p)!}\Lambda^{m-2q-2p}\kappa(p)\,, \\ \kappa(p) &= \sum_{k_0,\cdots,k_p=0}^{2p}\binom{2p}{k_0,\,\cdots,\,k_p}\prod_{t=2}^{p}\left(\frac{1}{2t+1}\right)^{k_t}\delta\left(\textstyle\sum_{l=0}^{p}k_l-2p\right)\,\delta\left(\textstyle\sum_{l=1}^{p}l\,k_l-p\right)\,.\end{aligned} \tag{4.1.13}$$

From this analytical expression[6], it is evident that for any n even (odd) $p_n(\Lambda)$ is a polynomial with real (imaginary) coefficients of degree $n-2$ in Λ containing only even (odd) powers thereof. The imaginary coefficients of the odd-terms guarantee simultaneously the hermitianity of the equation and the following parity of the eigenfunctions $\phi_n(x)=(-1)^n\phi_n(1-x)$.

Using the formulae above, the generalized 't Hooft equation is:

$$\mu^2\phi(x)=\left(\alpha+1-\sum_{n=1}^{\infty}v_{2n}\,\alpha_{2n}\right)\left(\frac{1}{x}+\frac{1}{1-x}\right)\phi(x)-\fint_0^1\mathrm{d}y\,\frac{\sum_{n=2}^{\infty}v_n\,p_n(\Lambda)}{(x-y)^2}\,\phi(y)\,. \tag{4.1.14}$$

[4]The combination $\left(\mathrm{H}(\frac{n-1}{2})+\log(4)\right)$ is a rational number for $n\in2\mathbb{Z}$.

[5]In practice, rather than using the explicit expression we exhibit in the text, it is more convenient to directly evaluate the integral below by taking the residue at infinity for any specific n.

[6]This was also observed empirically in [95].

We report here the first few terms as computed from the expressions above:

$$\sum_{n=1}^{\infty} v_{2n}\,\alpha_{2n} = 8\pi v_2 + \frac{160}{3}\pi^3 v_4 + \frac{744}{5}\pi^5 v_6 + \frac{31616}{105}\pi^7 v_8 + \frac{32440}{63}\pi^9 v_{10} + \cdots$$
$$\sum_{n=2}^{\infty} v_n\, p_n(\Lambda) = 8\pi v_2 - 24i\pi\, v_3\,\Lambda + 32\pi\, v_4\,\left(-\Lambda^2+\pi^2\right) - \frac{40i\pi}{3} v_5\,\left(-2\Lambda^3+7\pi^2\Lambda\right) + \cdots \tag{4.1.15}$$

As expected, by setting $v_n = \frac{1}{8\pi}\,\delta_{2,n}$ we recover the familiar 't Hooft equation of QCD_2:

$$\mu^2\phi(x) = \alpha\left(\frac{1}{x}+\frac{1}{1-x}\right)\phi(x) - \fint_0^1 \mathrm{d}y\;\frac{1}{(x-y)^2}\,\phi(y)\,. \tag{4.1.16}$$

A direct comparison between (4.1.14) and (4.1.16) illustrates that the self-interaction potential for the B-field at the level of the mesons effectively *renormalizes* the mass of the quarks α, to:

$$\alpha \to \tilde{\alpha} = \alpha + 1 - \sum v_{2n}\alpha_{2n}\,, \tag{4.1.17}$$

and modifies the kernel (that is an effective inter-quark potential) by adding logarithmic corrections.

4.2 Generalized 't Hooft equation as a TQ-system

4.2.1 ν-space representation

Following the approach initiated for the 't Hooft model [92], we perform a Fourier transform with respect to the rapidity variables $\theta = \frac{1}{2}\log\frac{x}{1-x}$:

$$\phi(y) = \int_{-\infty}^{+\infty}\frac{\mathrm{d}\nu}{2\pi}\left(\frac{x}{1-x}\right)^{-i\nu/2}\Psi(\nu)\,,\qquad \Psi(\nu) = \int_0^1\frac{\mathrm{d}x}{2x(1-x)}\left(\frac{x}{1-x}\right)^{i\nu/2}\phi(x)\,. \tag{4.2.1}$$

In ν-space, the generalized 't Hooft equation (4.1.14) takes the form ($2\pi^2\lambda = \mu^2$):

$$\lambda\int_{-\infty}^{+\infty}\mathrm{d}\nu'\,\frac{\pi(\nu-\nu')\,\Psi(\nu')}{2\sinh\left(\frac{\pi}{2}(\nu-\nu')\right)} = \underbrace{\left[\frac{2\tilde{\alpha}}{\pi}+\sum_{n=2}^{\infty} v_n\,p_n(\mathcal{I})\right]}_{=:f(\nu)}\Psi(\nu)\,, \tag{4.2.2}$$

where the polynomial $p_n(\mathcal{I})$ is obtained by replacing in $p_n(\Lambda)$ of (4.1.13) powers of Λ^n with $\mathcal{I}_{n+2}$:

$$\mathcal{I}_{n+2} = \left(\frac{\left(\frac{x}{1-x}\right)^{\frac{i\nu}{2}}}{\frac{2}{\pi}(x-1)x}\right)^{-1}\fint_0^1\mathrm{d}y\,\frac{\left(\frac{y}{1-y}\right)^{\frac{i\nu}{2}}\left(\log\left(\frac{y}{1-y}\right)-\log\left(\frac{x}{1-x}\right)\right)^n}{(x-y)^2}\,. \tag{4.2.3}$$

E.g. the first few terms are (cf. (4.1.15)):

$$\sum_{n=2}^{\infty} v_n\, p_n(\mathcal{I}) = 8\pi v_2\, \mathcal{I}_2 - 24\pi i\, v_3\, \mathcal{I}_3 + 32\pi\, v_4 \left(-\mathcal{I}_4 + \pi^2 \mathcal{I}_2\right) - \frac{40 i\pi}{3} v_5 \left(-2\mathcal{I}_5 + 7\pi^2 \mathcal{I}_3\right) + \cdots . \tag{4.2.4}$$

Computing the principal parts integrals in (4.2.3) is made straightforward by the following observation[7]:

$$\mathcal{I}_{n+2} = \left(\frac{2}{i}\right)^n \frac{\mathrm{d}^n}{\mathrm{d}\nu^n} \mathcal{I}_2 \,, \qquad \mathcal{I}_2 = \nu \coth\left(\frac{\pi\nu}{2}\right), \tag{4.2.6}$$

as $\mathcal{I}_2$ coincides with the integral computed in eq. (3.3) of [1] for the standard QCD_2. We list a few of them to give a flavor of the resulting expressions:

$$\mathcal{I}_3 = \frac{i(\pi\nu - \sinh(\pi\nu))}{\sinh^2\left(\frac{\pi\nu}{2}\right)}, \mathcal{I}_4 = 2\pi \frac{2 - \pi\nu \coth\left(\frac{\pi\nu}{2}\right)}{\sinh^2\left(\frac{\pi\nu}{2}\right)}, \mathcal{I}_5 = 2i\pi^2 \frac{3\sinh(\pi\nu) - \pi\nu(\cosh(\pi\nu) + 2)}{\sinh^4\left(\frac{\pi\nu}{2}\right)} \tag{4.2.7}$$

Henceforth, we can straightforwardly compute the function $f(\nu)$ given any potential $V(B)$ expressed via a polynomial form[8]:

$$f(\nu) = \alpha + 1 + \sum_{n=1}^{\infty} v_{2n}\alpha_{2n} + \sum_{n=2}^{\infty} v_n p_n\left(\mathcal{I}\right) . \tag{4.2.8}$$

As an example, taken $V(B)$ to be a quartic polynomial, the resulting expression for $f(\nu)$ is:

$$\begin{aligned} f(\nu) = \frac{2}{\pi}\left(\alpha + 1 - 8\pi v_2 - \frac{160\pi^3}{3} v_4\right) + \frac{8\pi}{\tanh\left(\frac{\pi\nu}{2}\right)}\left(v_2\nu + 4\pi^2 v_4 \nu - 6v_3\right) \\ + \frac{8\pi^2}{\sinh^2\left(\frac{\pi\nu}{2}\right)}\left(3v_3\nu + 8\pi v_4 \nu \coth\left(\frac{\pi\nu}{2}\right) - 16 v_4\right) \end{aligned} \tag{4.2.9}$$

4.2.2 Discreteness of the spectrum and instabilities

Although for any potential there is an associated bound state equation (4.2.2), arbitrary choices of $V(B)$ will not always lead to positive mass spectrum for the mesons[9]. This

[7] If one neglects the principal part integration, this follows by iteration from the definition of $\mathcal{I}_n$:

$$\frac{\mathrm{d}}{\mathrm{d}\nu}\mathcal{I}_{n+2} = \frac{i}{2}\left(\frac{\left(\frac{x}{1-x}\right)^{\frac{i\nu}{2}}}{\frac{2}{\pi}(x-1)x}\right)^{-1} \fint_0^1 \mathrm{d}y \left(\log\left(\frac{y}{(1-y)}\right) - \log\left(\frac{x}{(1-x)}\right)\right) \frac{\left(\frac{y}{1-y}\right)^{\frac{i\nu}{2}} \log^n\left(\frac{y(1-x)}{x(1-y)}\right)}{(x-y)^2} = \frac{i}{2}\mathcal{I}_{n+3} \,. \tag{4.2.5}$$

A more thorough proof is provided in Appendix A.1 where we compute them as Fourier transform of distributions.

[8] In ν-space the hermitianity of (4.2.2) for $v_i \in \mathbb{R}$ is evident from the fact that in the products $v_{2n+1}\mathcal{I}_{2m+1}$ are always real.

[9] This is a generalization of the condition $\alpha > -1$ in 't Hooft model that ensures a stable positive spectrum of mesons. In QCD_2 this condition corresponds to imposing reality of the quark masses: $\pi\frac{m^2}{g^2} - 1 = \alpha$.

was firstly empirically observed for the case of a cubic potential in [95], where, upon numerical direct solution of (4.1.14), it was found that for high values of v_3 the model exhibits tachyonic bound states. Below we use the reformulation of the eigenproblem (4.1.14) in ν-space in order to analyze the instablities of the generalized 't Hooft model and illustrates a rich and interesting analytical structure.

Exactly as discussed for the 't Hooft model [92], the generalized 't Hooft equation in ν-space takes the form of a homogeneous Fredholm equation of the second kind:

$$\phi(\nu) = \lambda \int_{-\infty}^{+\infty} \mathrm{d}\nu' \, \kappa(\nu,\nu') \, \phi(\nu'), \qquad \kappa(\nu,\nu') := \frac{\pi(\nu-\nu')}{2\sinh\left(\frac{\pi}{2}(\nu-\nu')\right)} \frac{1}{\sqrt{f(\nu)\, f(\nu')}} \,. \tag{4.2.10}$$

where $f(\nu)$ is defined in (4.2.2). The finiteness of the $L^2(\mathbb{R}^2)$ of $\kappa(\nu,\nu')$, guaranteed by $f(\nu \in \mathbb{R}) \neq 0$, ensures that this self-adjoint kernel defines a Hilbert-Schmidt integral operator with discrete and non-degenerate spectrum. Since from (4.2.2) follows that $\Psi(\nu)$ has poles at the location of zeros of $f(\nu)$, when the latter has zeros on the real axis, the eigenfunctions are not normalizable and do not correspond to physical bound states.

Henceforth, upon studying the zeros of $f(\nu)$ in the complex plane of the couplings, one determines the regions where the generalized QCD produces a physical confining theory. We defer to section 4.3 a detailed discussion of the rich analytical structure of generalized QCD as function of the (complexified) couplings.

We conclude this subsection by remarking that the region of coupling space where the meson spectrum is positive and real does not correspond to imposing that $V(B)$ is bounded from below as one could expect. Even potentials that are unbounded from below, such as polynomials with odd leading powers, surprisingly admit physical regions in the coupling space where the spectrum is real and discrete. A prototypical example of this feature, is the one of a cubic $V(B)$, analyzed thoroughly in section 4.3.3. Moreover, even for potentials that are bounded from below, for large values of any of the odd couplings v_{2n+1}, the spectrum develops instabilities, and becomes tachyonic at large values thereof. Indeed, already at the classical level, a potential with odd couplings does not have their minimum at $B \equiv 0$ and tachyonic modes are ultimately just a manifestation of the instability of the vacuum at the origin. Naturally, this classical analysis receives corrections from quantum effects: from the discussion in section 4.3, one can verify that even for a potential of the form $V(B) = v_2 B^2 + v_3 B^3 + v_4 B^4$, even though $B = 0$ is never the true minimum for $v_3 < 0$, there is a critical value $\overline{v_3}$ (depending on v_2 and v_4) such that for any $|v_3| < \overline{v_3}$ the model has a real and discrete spectrum of mesons.

Normalization and discrete symmetries. Having identified where the model admits a discrete meson spectrum, in this paragraph we restrict to such coupling range. The normalization of the eigenfunction in ν-space is fixed by (cf. eq. 3.11 of [1]):

$$\lambda_n \, \delta_{nm} = \lambda_n \int_0^1 \mathrm{d}x \, \phi_n(x) \, \phi_m^*(x) = \int_{-\infty}^{+\infty} \frac{\mathrm{d}\mu}{2\pi} \frac{f(\mu)}{2\pi} \, \Psi_n(\mu) \, \Psi_m^*(\mu) \,. \tag{4.2.11}$$

Convergence of this norm imposes that eigenfunctions decay at least polynomially fast on the real axis. Furthermore, since the function $f(\nu)$ enjoys the discrete symmetry:

$$f(\nu) = \check{f}(-\nu) \equiv f(-\nu)\Big|_{v_{2n+1}\to -v_{2n+1}}, \tag{4.2.12}$$

the solutions Ψ_n will be also eigenfunction thereof:

$$\Psi(\nu) = (-1)^n\, \check{\Psi}(-\nu)\,, \qquad \check{\Psi}(\nu) \equiv \Psi(\nu)\Big|_{v_{2n+1}\to -v_{2n+1}}. \tag{4.2.13}$$

This discrete symmetry is a direct generalization of the parity symmetry $f(\nu) \to f(-\nu)$ of 't Hooft model, and we consequently still refer to that as *parity*.

4.2.3 TQ-equation

In the following, we choose the generalized YM potential $V(B)$ such that $f(\nu \in \mathbb{R}) \neq 0$. According to the discussion of the previous subsection 4.2.2, this ensures that the model admits a physical discrete spectrum of mesons with real masses and normalizable eigenfunction. In particular, the right hand side $f(\nu)\Psi(\nu)$ of (4.2.2) does not have any singularities in the strip[10] $|\text{Im }\nu| < 2$ where we can analytically continue both sides of (4.2.2). Then, following [1,92], we introduce the *Q-functions*:

$$Q(\nu) = \sinh\left(\frac{\pi\nu}{2}\right)\left[\frac{2\tilde{\alpha}}{\pi} + \sum_{n=2}^{\infty} v_n\, p_n(\mathcal{I})\right]\Psi(\nu) = \sinh\left(\frac{\pi\nu}{2}\right) f(\nu)\,\Psi(\nu)\,, \tag{4.2.14}$$

that are defined to be regular in the strip, to decay less-than exponentially at $|\nu| \to \infty$. Moreover, these Q-functions satisfy the related integral equation:

$$Q(\nu) = \lambda \sinh\left(\frac{\pi}{2}\nu\right)\int_{-\infty}^{+\infty} \mathrm{d}\nu'\, \frac{\pi(\nu-\nu')}{2\sinh\left(\frac{\pi}{2}(\nu-\nu')\right)}\frac{Q(\nu')}{\sinh\left(\frac{\pi}{2}\nu'\right) f(\nu')}\,, \tag{4.2.15}$$

together with the *quantization* conditions

$$Q(0) = Q(\pm 2i) = 0\,. \tag{4.2.16}$$

This is completely analogous to the case of 't Hooft model [92]; in particular, one can show that $\Psi(\nu)$ is a solution of (4.2.2) decaying polynomially at infinity if and only if the associated $Q(\nu)$ (through (4.2.14)), analytical in $|\text{Im }\nu| < 2$, solves the following TQ-Baxter equation:

$$\boxed{Q(\nu+2i) + Q(\nu-2i) - 2Q(\nu) = \frac{-4\pi\lambda}{f(\nu)}\,Q(\nu) = \frac{-4\pi\lambda\, Q(\nu)}{\frac{2\tilde{\alpha}}{\pi} + \sum\limits_{n=2}^{\infty} v_n\, p_n(\mathcal{I})}}\,, \tag{4.2.17}$$

[10] The discussion of this subsection follows closely the approach of section 3.2 of [1], and we refer the reader to that paper for details concerning all the derivations.

subject to the quantization conditions (4.2.16), and decaying less-than-exponentially at infinity in the whole strip.

Thus, for any given generalized Yang-Mills potential, the only modification to the TQ-Baxter equation is contained inside the single function $f(\nu)$, computed in closed form (through equations (4.2.8), (4.1.13),(4.1.11)) for given any polynomial $V(B)$.

Asymptotic decay. The asymptotic decay of the eigenfunctions can be further refined upon studying the large-ν limit of (4.2.17). Assuming the asymptotic behavior $Q(\nu) \asymp e^{\pi k \nu} q(\nu)$, with $q(\nu)$ periodic by $2i$, and bounded by any exponential, (4.2.17) is:

$$0 = Q(\nu+2i)+Q(\nu-2i)-2Q(\nu)+\frac{4\pi\lambda}{8\pi\nu\sum\limits_{n=1}^{\infty} n^2 v_{2n}}Q(\nu) \asymp -4e^{\pi k\nu}\sin^2(\pi k)q(\nu)\,, \quad (4.2.18)$$

from which one deduces the stronger conditions of exponential decay of $\Psi(\nu)$ at $|\mathrm{Re}\,\nu| \to \infty$ in the strip $(-2i, 2i)$, that refines the polynomial decay guaranteed by square integrability[11].

4.2.4 Inhomogenous extension

The TQ-system (4.2.17) admits solutions with the given decay at infinity and quantization only at the discrete spectrum $\lambda = \lambda_n$ of the integral operator (4.2.10). The TQ-Baxter equation is a simultaneous problem for Q and λ and, as such, it is difficult to develop analytic approaches to the spectrum. However, in [92] a notable conceptual and practical simplification specific to this problem was obtained upon considering an auxiliary *inhomogeneous* problem, obtained by modifying (4.2.2) and (4.2.16), so that (4.2.17) admits solutions for *any* $\lambda \in \mathbb{R}$. This turned out to be extremely useful as it allowed one to study the TQ-equation in a two-step procedure: we first solve the simpler inhomogeneous problem, and then use this solutions to obtain the discrete spectrum of the homogeneous problem. This ultimately led to a fastly-convergent asymptotic analytic expansion for the spectral data [1,92,93]]. We refer the readers to those papers for a more thorough discussion.

The extension to the inhomogeneous problem is possible even in the generalized QCDs. We do so by:

$$\frac{F(\nu)}{\sqrt{f(\nu)}} = \phi(\nu|\lambda) - \lambda\int_{-\infty}^{\infty} \mathrm{d}\nu'\,\kappa(\nu,\nu')\phi(\nu'|\lambda), \quad (4.2.19)$$

$$F_+(\nu) = \frac{\nu}{\sinh\left(\frac{\pi}{2}\nu\right)}, \qquad F_-(\nu) = \frac{1}{\sinh\left(\frac{\pi}{2}\nu\right)}\,. \quad (4.2.20)$$

The inhomogeneous terms (4.2.20) are the same as in [1,92] and have definite parity under the discrete symmetry (4.2.13). Each of those drives a unique solution of the

[11] This result could have been imported directly from [1] given that in eq. (3.32) the r.h.s. does not depend on λ.

inhomogeneous integral equation depending on the continuous parameter λ:

$$F_\pm(\nu) = f(\nu)\,\Psi_\pm(\nu|\lambda) - \lambda \fint_{-\infty}^{+\infty} \mathrm{d}\nu' \,\frac{\pi(\nu-\nu')}{2\sinh\left(\frac{\pi}{2}(\nu-\nu')\right)}\,\Psi_\pm(\nu'|\lambda)\,, \tag{4.2.21}$$

whose solutions inherits definite parity:

$$\Psi_\pm(\pm\nu) = \pm\check{\Psi}_\pm(\nu)\,. \tag{4.2.22}$$

The *inhomogeneous* Q-function defined by (4.2.14):

$$Q_\pm(\nu|\lambda) = \sinh\left(\frac{\pi\nu}{2}\right) f(\nu)\,\Psi_\pm(\nu|\lambda) = \mp Q_\pm(-\nu|\lambda) \tag{4.2.23}$$

are also shown to satisfy the same TQ-equation of the homogeneous problem (4.2.17):

$$Q_\pm(\nu+2i|\lambda) + Q_\pm(\nu-2i|\lambda) - 2Q_\pm(\nu|\lambda) = \frac{-4\pi\lambda}{f(\nu)} Q_\pm(\nu|\lambda)\,, \tag{4.2.24}$$

but at any values of $\lambda \in \mathbb{R}$, upon assuming the same asymptotic, but subject to modified quantization conditions[12]:

$$Q_+(\pm 2i) = \pm 2i\,, \qquad Q_+(0) = 0\,, \qquad Q_-(\pm 2i) = Q_-(0) = 1\,. \tag{4.2.25}$$

The Wronskian constructed with the two solutions $Q_\pm(\nu|\lambda)$ results to be a constant:

$$W(\nu|\lambda) = Q_+(\nu+i|\lambda)Q_-(\nu-i|\lambda) - Q_+(\nu-i|\lambda)Q_-(\nu+i|\lambda) = W(i|\lambda) = 2i\,. \tag{4.2.26}$$

4.3 Analytical structure of the spectrum and critical points

The simple form of 't Hooft equation in ν-variables (4.2.2) allows for a straightforward qualitative analysis of the main features of the model in the complexified space of couplings. In particular, the analytical structure of the function $f(\nu)$ completely determines the analytical structure of the eignevalues $\lambda_n(\alpha, \boldsymbol{v})$ as functions of the complexified couplings. In what follows, in order to emphasize the dependence on the complexified couplings, we denote $f(\nu)$ by $f(\nu, \alpha, \boldsymbol{v})$.

As already observed in section 4.2.2, the zeros of $f(\nu, \alpha, \boldsymbol{v})$ coincide with the poles of the eigenfunction $\Psi_n(\nu)$, so that whenever they do not lie on the real line, the model will admit a discrete spectrum of mesons with normalizable eingenfunctions. Among the zeros of $f(\nu, \alpha, \boldsymbol{v})$ the higher order zeros, where also the derivatives thereof vanish are special and distinct points. Already in the case of the 't Hooft model [1], which can be recovered by setting all the v_k to zero, we found that the location of double zeros of $f(\nu, \alpha)$ in the complex plane on ν determines infinitely many square-root branch points at some specific values $\alpha_k \in \mathbb{C}$ where of one of the mesons becomes massless. At finite N_c these critical points are likely to become non-unitary interacting CFTs.

[12] Note that this changes the analytical properties of the solutions $\Psi(\nu|\lambda)$ compared to $\Psi_n(\nu)$, allowing for poles at the boundary of the strip.

This interesting structure extends and enriches greatly in the generalized Yang-Mills theory with polynomial potentials. In this section we describe the general features of the analytical structure, and of the type of criticality that we encounter in this very broad class of models by varying the polynomial potential $V(B)$. The reader can refer to the concrete example of a cubic self-interaction that we discuss thoroughly in section 4.3.3, that illustrates all the main features of the generic case.

$\mathcal{PT}$-symmetry and reality of the spectrum. It is important to note that physical choices of $V(B)$ shall not be limited to real values for the coefficients. Since the B-field is odd under $\mathcal{PT}$-symmetry (or equivalently, charge-conjugation), potentials with imaginary odd couplings, $v_{2n+1} \in i\mathbb{R}$, provide examples of $\mathcal{PT}$-symmetric quantum field theories. It is by now well-established that non-hermitian field theories enjoying unbroken $\mathcal{PT}$-symmetry, can have real spectra; we refer the reader to the classical papers [181–183] (and references therein) for a thorough discussion on the topic. However, $\mathcal{PT}$-symmetry can also be spontaneously broken, in which case the spectrum contains complex conjugate pairs, and in generalized QCD both cases happen (recently also observed in the context of non-unitary minimal models in [184–186]), see for instance ection 4.3.3.

4.3.1 Multicritical points from collision-of-roots

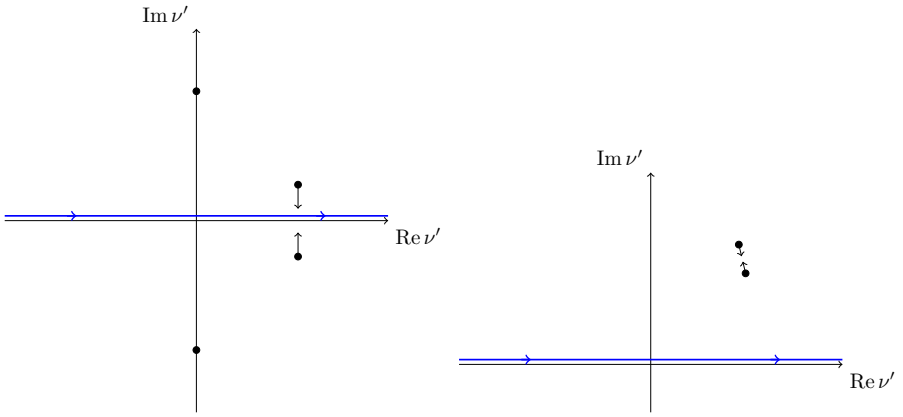
By tuning the parameters of the potential $V(B)$, one can make $f(\nu, \alpha, \boldsymbol{v})$ to have zeros of higher order[13]. As we explain below, a n-th order zero corresponds to a n-th root-branch point of the eigenvalues, if it is not possible to deform the contour of integration to avoid the pinching singularity. At each of these n-th branch-points the eigenvalues behave as $\lambda \sim (\alpha - \alpha^{(n)})^{1/n}$, (and similarly as functions of all the other couplings), and correspond to multicritical points where exactly $n-1$ mesons become simultaneously massless.

Collision-of-roots point and branch points. In general, roots of $f(\nu, \alpha, \boldsymbol{v})$, do not correspond to branch-point singularities of the spectrum, but only to poles of $\Psi(\nu)$. This is due to the fact that if the colliding roots are away from the integration contour, the integral eigenproblem (4.2.2) is still well-defined. On the other hand, if two roots collide in such a way that the contour of integration is trapped in between, the spectrum will develop a branch cut[14]. Only the collision-of-roots of type Figure 4.2a would lead to a singular point of λ, while the one of Figure 4.2b is not a singularity on this sheet of the complex plane since the contour is not trapped by the collision. However it will be a singularity on another sheet of the complex plane as we will shortly discuss.

Type of singular points. The precise type of singularity associated to this critical point is inferred by studying the monodromy of the zeros of the function f as we meromorphically continue the parameter α along a closed curve around any of the values

[13] For the physical potential, the order of the zeros is bounded from above by $\deg V(B)$.

[14] This is very well known in the context of scattering amplitudes where many singularities of these kind arise, cfr. e.g. [187].



(a) Trapped contour: singular point. (b) No singularity on this sheet.

Figure 4.2: Collision-of-roots points points may or may not lead to singularities.

of the critical values $\alpha^{(n)}$. If $\nu^{(n)}$ is the position of the n-th order zeros at $\alpha = \alpha^{(n)}$, as we move in the parameter space to $\alpha \neq \alpha^{(n)}$, the degeneracy of the roots will be generically split and we will be left with exactly n non degenerates roots $\nu_1 \cdots \nu_n$. Then it is easy to see that upon the analytical continuation of α along a closed curve winding around $\alpha^{(n)}$ a single time, $f(\nu, \alpha, \boldsymbol{v})$ encompass a monodromy that permutes the roots by: $\nu_i \to \nu_{i+1}$. Because of this non-trivial monodromy, each root of these root may or may not cross the integration contour, if this happens, then the integral eigenproblem will differ by the respective residue terms.

The simplest case is the one of a square-root cut, as in Figure 4.2: in this case after a 2π analytical continuation $\alpha \to \widetilde{\alpha}$, the eigenproblem will also undergo a non-trivial monodromy transformation, that act by adding two further residue terms:

$$\begin{aligned} f(\nu)\Psi(\nu) = \widetilde{\lambda}(\alpha) \int_{-\infty}^{+\infty} \mathrm{d}\nu' \, \frac{\pi(\nu-\nu')}{2\sinh\frac{\pi}{2}(\nu-\nu')}\Psi(\nu') \\ + \widetilde{\lambda}(\widetilde{\alpha})\mathrm{Res}\left(\frac{\pi(\nu-\nu')}{2\sinh\frac{\pi}{2}(\nu-\nu')}\Psi(\nu';\alpha_0,\boldsymbol{v_0}),\nu'=\nu_1\right) \\ - \widetilde{\lambda}(\widetilde{\alpha})\mathrm{Res}\left(\frac{\pi(\nu-\nu')}{2\sinh\frac{\pi}{2}(\nu-\nu')}\Psi(\nu';\alpha_0,\boldsymbol{v_0}),\nu'=\nu_2\right) . \end{aligned} \tag{4.3.1}$$

This indicates $\alpha^{(\mathrm{II})}$ is a square-root branch point of the eigenvalues. This point coincides with the boundary of the allowed region for having a positive spectrum of mesons, and indeed we find a corresponding critical point where one of the meson becomes massless upon direct solution (analytical or numerical) of the spectral problem. To illustrate a more complicated case, let us examine the case of a zero of order 3. As we thoroughly explain in section 4.3.3 the typical situation is the one of figure Figure 4.4a, where the contour cannot be continuously deformed to avoid a pinching-of-roots singularity at some special values of the couplings $\alpha^{(\mathrm{III})}, v_3^{(\mathrm{III})}$. Then, it is easy to see that the monodromy

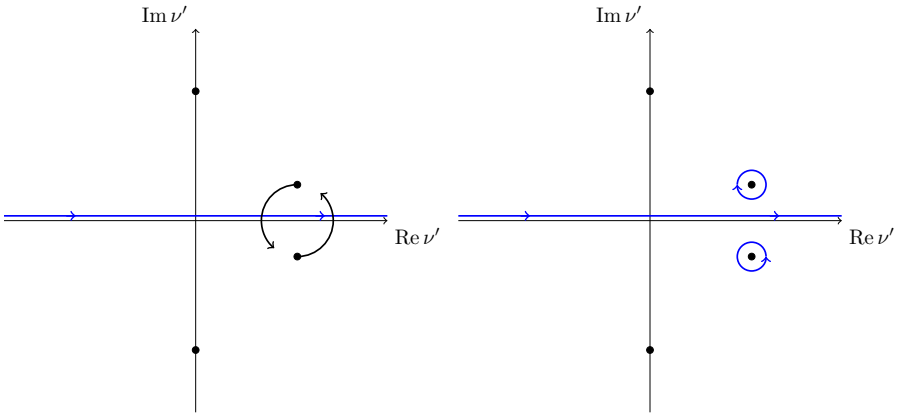
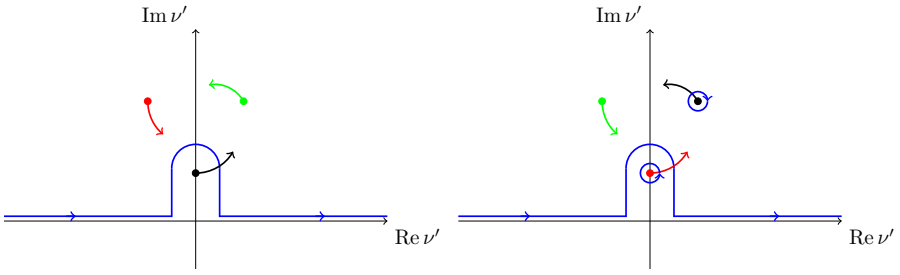
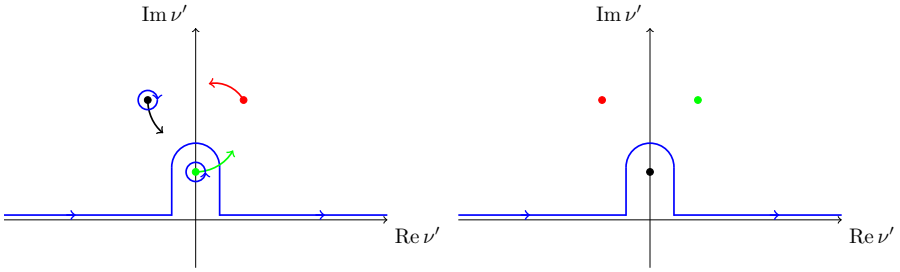


Figure 4.3: Complex plane before and after the a 2π analytical continuation with non-trivial monodromy.



(a) Roots in the first sheet.

(b) 2π monodromy.



(c) 4π monodromy.

(d) 6π monodromy.

Figure 4.4: Monodromy of the roots around a 3rd order zero in the complex plane.

of α under a 6π monodromy along a curve encircling the collision-of-root point $\alpha^{(\mathrm{III})}$ is the one described in Figure 4.4b, Figure 4.4c and Figure 4.4d, i.e. a third order zero leads to a cubic-root branch cut of the spectrum and a trictritical point where two of the meson masses turn simultaneously to zero (cfr. Figure 4.14). It is straightforward from the graphical representation in Figure 4.4 to write down, on each of the three sheets represented there, the corresponding bound state equation as we have done in (4.3.1). The generalization to arbitrary order of root is completely straightforward.

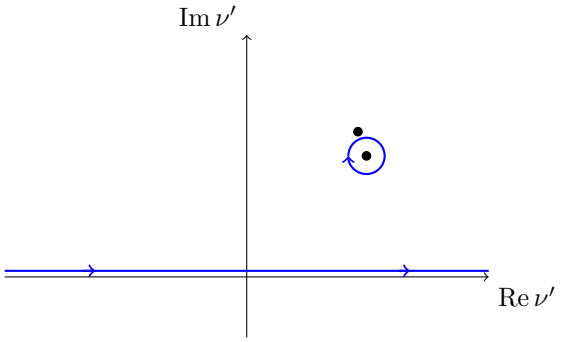


Figure 4.5: Collision-of-roots away from the contour are singularities in higher-sheet of the complex ν'-plane

Geometry of the phase space. For any given polynomial $V(B)$ of degree n, the singularities of type p-th root will form a codimension $n-p$ locus in the phase space of the theory given that they generically solve a system of p equations. In particular, n-th-root branch points form a set of infinitely many isolated points in the space of couplings, $(n-1)$-th-root branch points form set of lines that may intersect at n-th root branch points, and so on. The typical structure of the first sheet of the phase space is the one in Figure 4.12. Each of the several connected components of these loci, lives in a unique sheet of the complex plane. On a given sheet, only the collision-of-roots which pinches the contour leads to singularities, while the others are singular points on other sheets, as we discuss more later. These critical loci correspond to the boundary of regions where the spectrum of mesons is positive and discrete. At the special points in the space of couplings, several mesons become massless (as in Figure 4.7 and Figure 4.9).

4.3.2 Critical points beyond the first sheet

As anticipated already in the previous subsection, the singularities on the first sheet are only one of the many connected components forming the singular loci of the parameter space. Indeed, while collision-of-roots happening away from the integration contour are not singularity on the first sheet, they are singularities on other sheets of the complex plane: As we analytically continue beyond the cuts on the first sheet, the contour of integration for the integral equation picks up additional contributions from poles that crossed the contour (see (4.3.1) and Figure 4.4). After this happens, if these poles collide with other poles on the complex plane, they lead to singularities on the corresponding sheet. See e.g. Figure 4.5 (and the corresponding situation on the first sheet Figure 4.2b).

By comparing them with the analytical prediction or with the numerics, one can check that those singularities correspond to critical points where one of the higher mesons (instead of the lowest one) becomes tachyonic and triggers a critical phase transition.

4.3.3 A case study: cubic potential

In this section, we analyze the spectrum and phases of generalized QCD with a cubic potential: $V(B) = v_2\, B^2 + v_3\, B^3$ that is never bounded from below except for $v_3 = 0$. The latter is a purely quadratic potential and is the simplest example of a gYM potential $V(B) = v_2\, B^2$. In this case we have

$$f(\nu, \alpha, v_2) = \frac{2(\alpha + 1 - 8\pi v_2)}{\pi} + 8\pi v_2\, \nu \coth\left(\frac{\pi\nu}{2}\right) = 8\pi v_2 \left(\bar{\alpha} + \nu \coth\left(\frac{\pi\nu}{2}\right)\right) . \quad (4.3.2)$$

Clearly, the problem depends only on the single variable $\bar{\alpha} = \frac{\alpha - 8\pi v_2 + 1}{8\pi v_2}$ and the entire structure is equivalent to the usual QCD_2 analyzed in [1,92], upon the replacement $\bar{\alpha} \to \alpha$: the spectrum has a square root branch cut in $\bar{\alpha} = -1$ for any values of v_2, and the energy levels are real and positive for $v_2 > 0 (< 0)$ for $\bar{\alpha} > -1 (< -1)$.

For $v_3 \neq 0$, only two of the three couplings (α, v_2, v_3) are physically relevant and we can always canonically normalize $v_2 = \frac{1}{8\pi}$. From (4.2.8), we obtain

$$f(\nu, \alpha, v_3) = \frac{2\alpha}{\pi} + \nu \coth\left(\frac{\pi\nu}{2}\right) + 24\pi v_3 \frac{\pi\nu - \sinh(\pi\nu)}{\sinh^2\left(\frac{\pi\nu}{2}\right)} . \quad (4.3.3)$$

To identify regions in the parameter space where this model exhibits a real and positive spectrum of mesons, below we systematically study zeros of $f(\nu)$ in the complex space of the couplings (α, v_3).

Real couplings

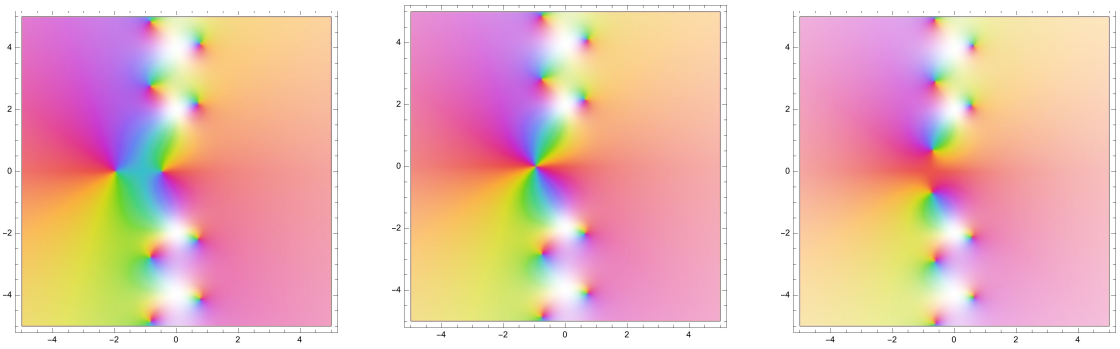
Let us start by considering real values of the quark masses corresponding to $\alpha \geq -1$. For arbitrary values of α and $v_3 \in \mathbb{R}$, zeros of $f(\nu)$ are all simple. Given any fixed value of α, there are two critical values $\pm v_3^{(\mathrm{II})}(\alpha)$, where the two zeros closest to the real axis degenerate to a double zero at $\nu = \pm\nu^{(\mathrm{II})}(\alpha) \in \mathbb{R}$:

$$f\left(\pm\nu^{(\mathrm{II})}(\alpha), \alpha, \pm v_3^{(\mathrm{II})}(\alpha)\right) = \partial_\nu f\left(\pm\nu^{(\mathrm{II})}(\alpha), \alpha, \pm v_3^{(\mathrm{II})}(\alpha)\right) = 0 . \quad (4.3.4)$$

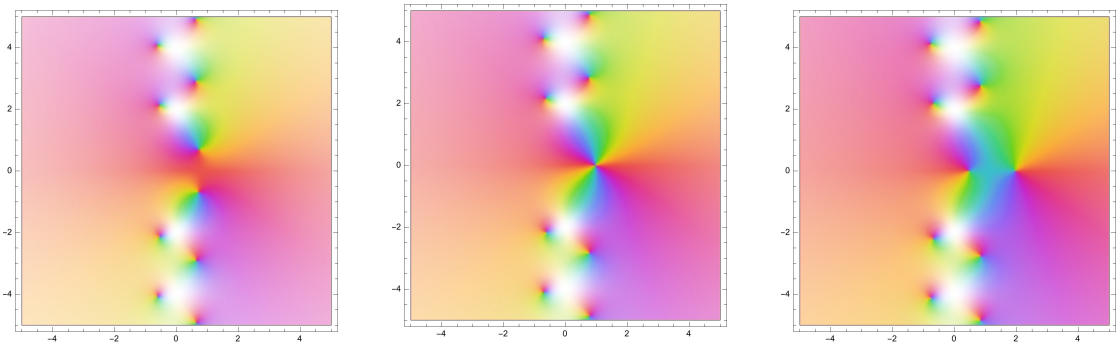
Solutions to this equation give a curve in Figure 4.7 in the plane (α, v_3). As shown in Figure 4.6, while for $|v_3| < v_3^{(\mathrm{II})}(\alpha)$ there are no real zeros of $f(\nu.\alpha, v_3)$, when $|v_3| > v_3^{(\mathrm{II})}(\alpha)$ exactly two of them lie on the real axis. Therefore, the analytical structure of the bound state equation (4.2.2) implies that the spectrum of mesons is positive in a shaded region of Figure 4.7 bounded by the curve [15] (4.3.4). For any $v_3 \neq 0$, $f(\nu, -1, v_3 \neq 0)$ has two real zeros, (one of which is always at $\nu = 0$), and therefore the eigenfunction are not-normalizable. So, for $m^2 = 0$ the massless meson becomes unstable at $v_3 \neq 0$. So that, for points laying outside of the region bounded by the curve, the eigenfunction are not normalizable and the spectrum becomes tachyonic.

It is worth stressing that, although the cubic potential is not bounded from below, in the large N_c approximation, the mesons can have a well-defined positive spectrum.

[15] Analytic solutions for the coupled equations (4.3.4) are not available. However near $\alpha = -1$, one can study the solution $v_3^* = v_3^*(\alpha)$ analytically by linearizing (4.3.4) in ν since we know that for small $\alpha \to -1$, both $v_3^{(\mathrm{II})}, \nu^{(\mathrm{II})} \to 0$. The result of the linear approximation, $v_3^*(\alpha) \simeq \pm\frac{\sqrt{\alpha+1}}{8\sqrt{6}\pi^2}, \nu^*(\alpha) \simeq \pm\frac{\sqrt{6}\sqrt{\alpha+1}}{\pi}$, exhibit many of the features we demonstrate in the text.



(a) $v_3 = -0.0156856$ (b) $v_3 = -v_3^{(\mathrm{II})}(0.5)$ (c) $v_3 = -0.00784281$



(d) $v_3 = 0.00784281$ (e) $v_3 = v_3^{(\mathrm{II})}(0.5)$ (f) $v_3 = 0.0156856$

Figure 4.6: Positions of the zeros (black) and poles (white) of $f(\nu, \alpha = 0.5, v_3)$ in the ν-complex plane for different values of v_3. For $|v_3| < v_3^{(\mathrm{II})}(0.5) \simeq 0.01176$ (Figure 4.6a, 4.6f)there are two distinct real zeros that degenerate for $v_3 = v_3^{(\mathrm{II})}(0.5)$ (Figure 4.6b, 4.6e) at $\nu^{(\mathrm{II})(0.5)} \simeq 0.974336$. In all the physical region $|v_3| < v_3^{(\mathrm{II})(0.5)}$, there are no real zeros of $f(\nu, 0.5, v_3)$.

Massless meson. The critical points $\left(v_3^{(\mathrm{II})}(\overline{\alpha}), \overline{\alpha}\right)$ solving (4.3.4) are square-root branch points of the eigenvalues $\lambda(\alpha, v_3)$, at which the lowest meson becomes massless. One can infer the branch-cut structure by studying the monodromy of the roots under analytical continuation of the quark mass α along a curve that encircles $\overline{\alpha}$ an odd number of times. As illustrated in Figure 4.8, it exchanges the two simple zeros $\overline{\nu}_\pm$ of $f(\nu, \alpha, v_3)$, which eventually degenerate into $\nu^{(\mathrm{II})}(\overline{\alpha})$.

This shows that, by tuning the strength of the potential v_3, for any real and positive value of the quark masses α, one can always produce a massless meson [16]. If we set $\alpha = -1$, where the quark are massless, the curve (4.3.4) degenerates into a point $v_3^{(\mathrm{II})} = 0$.

We tested these results against the numerical solutions of the ν-space eigenproblem (4.2.2), as explained in Appendix A.3. The numerical solutions in Figure 4.9 illustrate

[16] This agrees with some preliminary exploration of [95] for some specific values of the coupling. Note also that this meson is not associated with chiral symmetry as in [1].

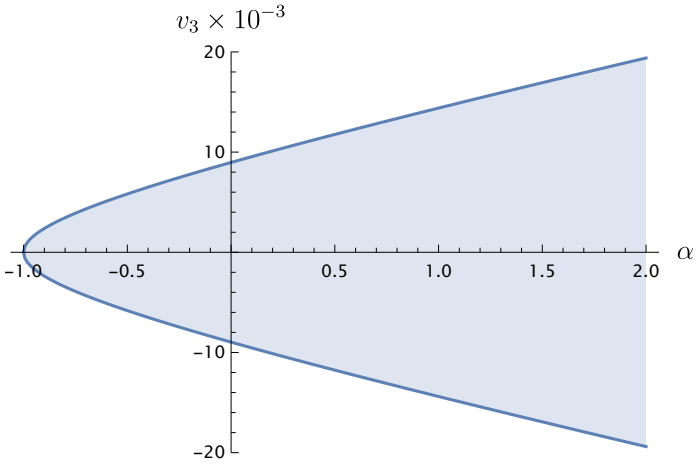
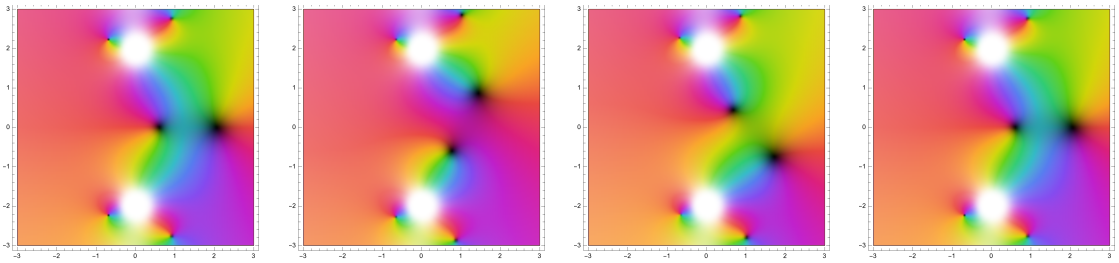


Figure 4.7: The shaded region correspond to the values of the couplings where the model has a positive spectrum of mesons, while the curve identifies the critical points where the theory has a massless mode.



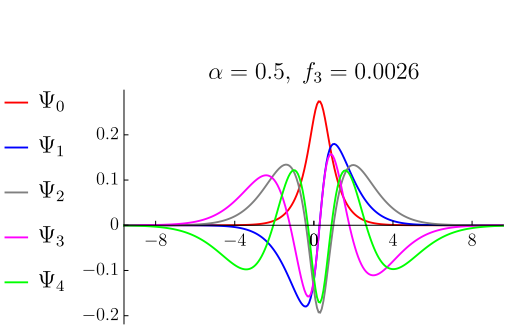
(a) $\theta = 0$ (b) $\theta = 1/3$ (c) $\theta = 3/5$ (d) $\theta = 1$

Figure 4.8: We fix $\overline{\alpha} \simeq 2.12$, its corresponding positive critical point is $v^{(\mathrm{II})}(\overline{\alpha}) \simeq 0.2$. The figure illustrates the positions of the zeros (black) of $f\left(\nu, \alpha(\theta), v^{(\mathrm{II})}(\overline{\alpha})\right)$, for values of $\alpha(\theta) = 2.4 - 0.4e^{i2\pi\theta}$ that encircle the point $\overline{\alpha}$. Along this analytical continuation in the complex plane the two zeros are exchanged.

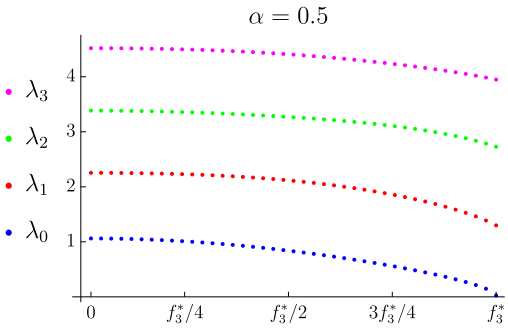
a typical confining spectrum of mesons with Regge-like trajectories. The ground state becomes massless in correspondance with the critical point identified by the collision of zero of $f(\nu, \alpha, v_3)$.

Analytical continuation and tricritical point

In the previous section, we analyzed the spectrum of mesons for real values of the quark masses ($\alpha \geq -1$) and cubic couplings. We showed that at any fixed $v_3 > 0$, there is a square root branch-cut in the α plane at $\alpha = \alpha^{(\mathrm{II})}(v_3)$, corresponding to a critical point in the first sheet, where the first meson becomes massless. In this section we are interested in the analytic continuation to negative values of α. Because of the branch cuts in the $\alpha, v_3 \in \mathbb{R}$ (see Figure 4.7), this requires an extra care. Below, we first analytically continue



(a) First five eigenfunctions with cubic potential for $v_3 = 0.0026$.



(b) First 4 energy levels for $v_3 \in [0, f_3^*]$ spanning the whole physical spectrum.

Figure 4.9: Energy levels and eigenfunctions for $\alpha = 0.5$, $v_3^{(\mathrm{II})}(0.5) = f_3^* \simeq 0.01176$.

v_3 to imaginary values keeping $\alpha > 1$, and we study the region $\alpha < -1$ aferwards.

Analytical continuation to imaginary couplings. At complex values of $v_3 \in \mathbb{C}$, the Hamiltonian is no longer hermitian, and the spectrum will be generically complex. Yet, if restrict to purely imaginary values of v_3, i.e. we take the self-interaction of the B-field to be:

$$V(B) = \frac{1}{8\pi} B^2 + i|v_3| B^3 \,, \tag{4.3.5}$$

the corresponding bound-state equation (4.2.2) enjoys $\mathcal{PT}$-symmetry[17], since the B field is odd under $\mathcal{PT}$ symmetry as discussed in general in section 4.3. At fixed $\alpha > -1$, for $v_3 \in i\mathbb{R}$, there are no collision-of-root singularities in the first sheet, and no zeros of $f(\nu, \alpha, v_3)$ on the real line. So we expect for this region of the parameter to have a positive spectrum of mesons. Indeed, by solving numerically the eigensystem at imaginary values of v_3 in a neighborhood of the real axis, we find that the spectrum remains real and positive as shown in Figure 4.10. This means that $\mathcal{PT}$-symmetry is not spontaneously broken for $\alpha > -1$ at least in the neighborhood of the real axis of v_3.

Critical points at $\alpha < -1$. The analytical continuation to imaginary values of v_3 allow us to also continue the spectrum to $\alpha < -1$ without crossing any of the branch cuts. More concretely, we first continue to[18] $v_3 = i\mathbb{R}^+$ at $\alpha > -1$, and only then we continue from $\alpha > -1$ to $\alpha < -1$. In doing that, exactly one of the roots crosses the real axis, (as $f(\nu, -1, v_3)$ has always a root at $\nu = 0$), yet, as long as one makes sure that there are no collision of roots on the contour, one can deform the ν' integration contour in (4.2.2), to avoid the singular point. This is illustrated in Figure 4.11.

Collision-of-roots singularities happens at $\alpha < -1$, whenever, upon varying v_3 the first two roots in Figure 4.11 pinch the contour. This happens, for any $\alpha < -1$, at

[17]The structure of the potential here considered can be regarded as a field theory analogous of the quantum mechanical system $\mathcal{H} = p^2 + m^2 x^2 + i x^3$ considered e.g. in [181].

[18]$|v_3|$ has to be large enough to guarantee any pinching of root singularity on the contour, as we will discuss below.

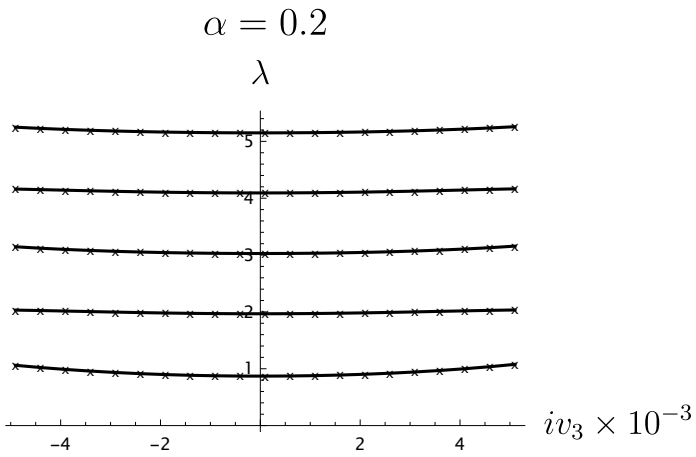
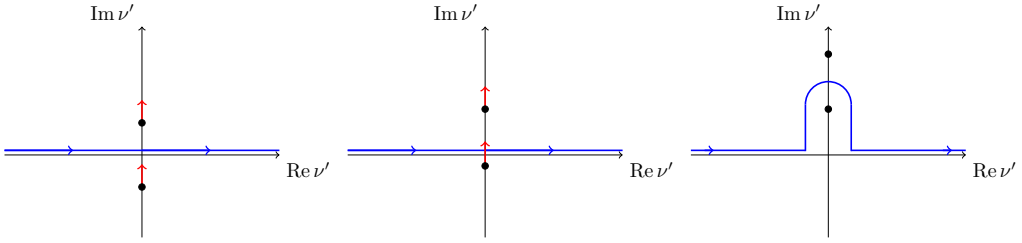


Figure 4.10: Numerical solutions for the first 5 levels.



(a) $\alpha > -1$ fixed, and $v_3 = 0$ (b) $\alpha > -1$ fixed, $iv_3 < 0$ (c) $\alpha < -1$, fixed $iv_3 < 0$

Figure 4.11: First two roots of $f(\nu', \alpha, v_3)$ upon analytical continuation. In (a) and (b), at fixed $\alpha > -1$, we analytically continue in v_3 to $v_3 \in i\mathbb{R}^+$. The red arrows illustrate the shift of the first two roots under this continuation. In (c), we then plot the result of the analytical continuation from $\alpha > -1$ to $\alpha < -1$ at fixed value $v_3 \in i\mathbb{R}$. The root crosses the real axis exactly at $\alpha = -1$. When the root crosses the real axis, the integration contour is deformed to avoid the singularity. For $iv_3 > 0$ it is analogous but with the root in the upper half plane moving in the lower half plane.

two isolated points on the imaginary axis $\pm v_3^{(\mathrm{II})}(\alpha)$, determined by the solutions of the equation $f(\nu, \alpha, v_3) = 0$ and $\partial_\nu f(\nu, \alpha, v_3) = 0$ at fixed $\alpha < -1$. Upon decreasing α, one finds solutions $v_3^{(\mathrm{II})}(\alpha) \in i\mathbb{R}$ only for $\alpha > \alpha^{(\mathrm{III})} \simeq -1.27649$, while for $\alpha > \alpha^{(\mathrm{III})}$ the corresponding solutions $v_3^{(\mathrm{II})}(\alpha)$ split in the complex plane (red curves in Figure 4.12). The collision-of-roots singularities are critical points in the spectrum where the first meson becomes massless. In Figure 4.12, we report the loci of critical points at $\alpha \in \mathbb{R}$ and v_3 in the upper half plane (the lower half plane of v_3 is symmetrical). The red curves correspond to the solutions for $\alpha > \alpha^{(\mathrm{III})}$ and are indeed located in a region of the parameter space where the 't Hooft equation is neither hermitian nor $\mathcal{PT}$-symmetric, and the masses of mesons are $\lambda_n \sim M_n^2$ are complex. The critical points in this region correspond to points where one of the complex eigenvalues turns to zero. Any analytical

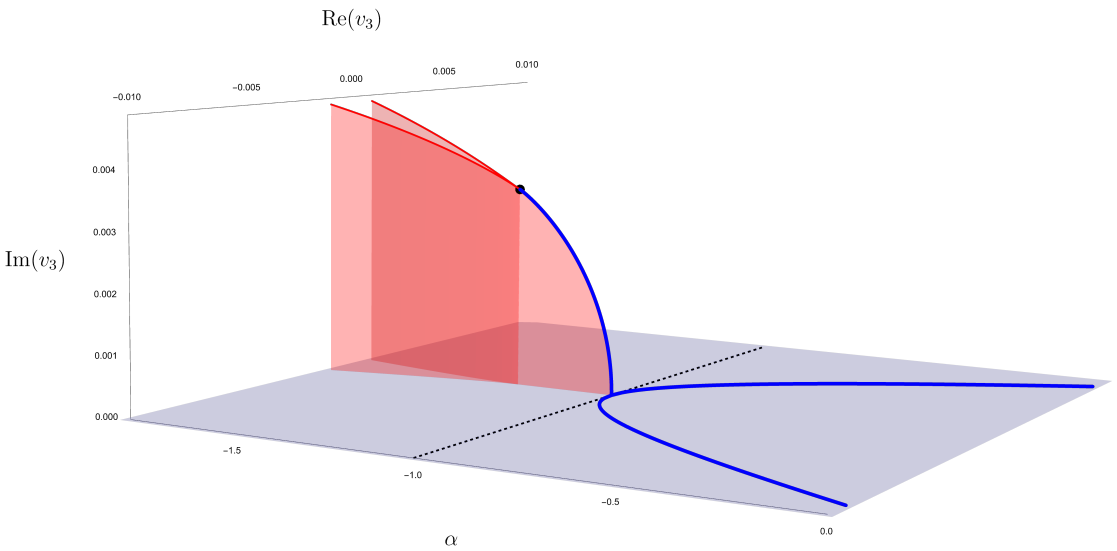


Figure 4.12: Critical points for $v_3 \in \mathbb{R}^+$ or $v_3 \in i\mathbb{R}^+$ and $\alpha \in \mathbb{R}$. For $\alpha > -1$, the blue curves are loci of critical points lying at $\mathrm{Im}(v_3) = 0$ and are exactly the one studied in Section 4.3.3 (cfr. Figure 4.7). The blue curve at $\alpha < -1$, is located at $\mathrm{Re}(v_3) = 0$ while the red ones correspond to critical points for the complex spectrum. The black dot corresponds to the tricritical point.

continuation performed along a path on the first sheet of v_3 and α that does not intersect any of the blue or red curves and does not ends in the region shaded in red, leads to a discrete and positive spectrum of mesons for $\alpha > \alpha^{(\mathrm{III})}$. Correspondingly, the $\mathcal{PT}$ symmetry is not spontaneously broken in this region of the parameter space. In Appendix A.4, we describe the spectrum also after analytically continuing it around the $\alpha^{(\mathrm{III})}$ in the region shaded in red. There, $\mathcal{PT}$-symmetry is spontaneously broken.

Tricritical point. As illustrated in the previous subsection, the line of critical points in the first sheet of the (α, v_3) plane for $\alpha < -1$, terminates at the special point:

$$\alpha^{(\mathrm{III})} \simeq -1.27649\,, \quad v_3^{(\mathrm{III})} \simeq \pm 0.00344328\, i\,, \tag{4.3.6}$$

where $f(\nu)$ has a triple zero. Here the contour has a singularity due to the collision of three roots simultaneously as shown in Figure 4.13. The monodromy of the roots under analytical continuation in α, is exactly the one illustrated in Figure 4.4. Henceforth, according to the general discussion of section 4.3, one expects that the theory admits a description in terms of a tricritical CFT where two of the energy levels turn to zero simultaneously as $\lambda \sim \sqrt[3]{\alpha - \alpha^{(\mathrm{III})}}$. In Figure 4.14 the result of the numerical spectrum after analytical continuation; we refer to Appendix A.3 for a detailed explanation of the method we employed to analytically continue to $\alpha < -1$.

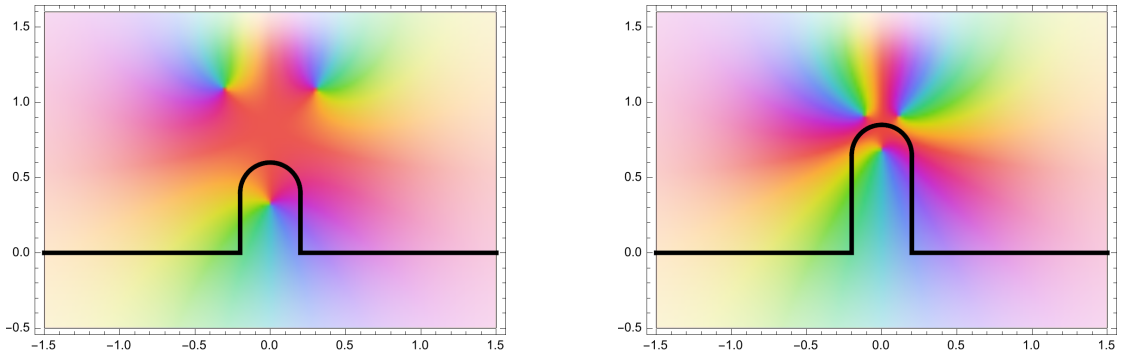


Figure 4.13: Integration contour in the ν' complex plane for $\alpha < \alpha^{(\mathrm{III})}$ at fixed $v_3 = v_3^{(\mathrm{III})}$. As α approaches the tricritical point, the contour is trapped between three singularities.

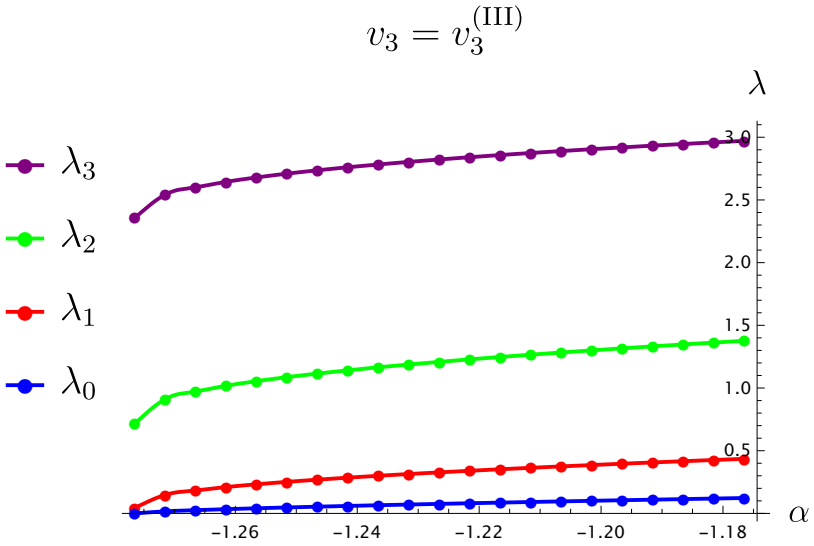
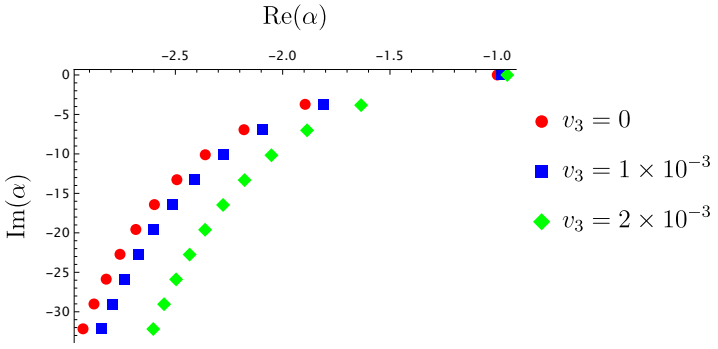
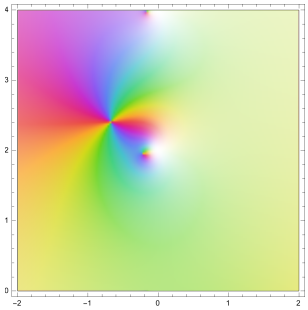


Figure 4.14: First 4 meson masses as a function of α at fixed $v_3 = v_3^{(\mathrm{III})}$. The first two levels turn to zero at $\alpha = \alpha^{(\mathrm{III})}$.



(a) Singularity in the second sheet of the α plane after analytical continuation through the cut along the real axis, for various values of v_3.



(b) Collision of the first singularity, after analytical continuation with one of the higher.

Figure 4.15: Singularities in the second sheet of the α plane continued through the cut at fixed $v_3 \in \mathbb{R}$.

Singularities beyond the cuts

Each of the critical point we discussed is associated to a branch cut in the complex plane of the coupling. As a generalization to what happens in the 't Hooft model [1], as we analytically continue the model to complex values of α and v_3, we probe a very rich and complicated multi-sheeted structure.

Critical points in the second sheet. For fixed $v_3 \in \mathbb{R}$, by analytically continuing in α through the square root cut, the two roots inevitably cross the integration contour, and the eigenproblem differs by a further contribution due to the contour integration around those singularities, as in Figure 4.3. In the second sheet of these cuts, we find infinitely many other critical points where, at complex values of α, one of the roots that took a monodromy after analytical continuation collides with one of the higher singularities (e.g. Figure 4.15b). On each of the corresponding sheets, the $k-$th meson becomes massless, rather than the first energy level λ_0. This is a generalization of what already discussed for the 't Hooft model [1], but at generic values of $v_3 \in \mathbb{R}$.

Tricritical points in higher sheets. A similar argument shows the existence of infinitely many tricitrical points after the analytic continuation in α through the cubic root branch cut at (4.3.6). On the second sheet relative to this cut, one finds two infinite towers of cubic branch points, each associated with distinct values of v_3 and located respectively in the second and third sheet of the α-plane. We report them in Figure 4.16, as determined by the points corresponding to triple zeros of $f(\nu, \alpha, v_3)$ in the complex plane.

The two infinite towers are distinguished by the sign of the imaginary part of the

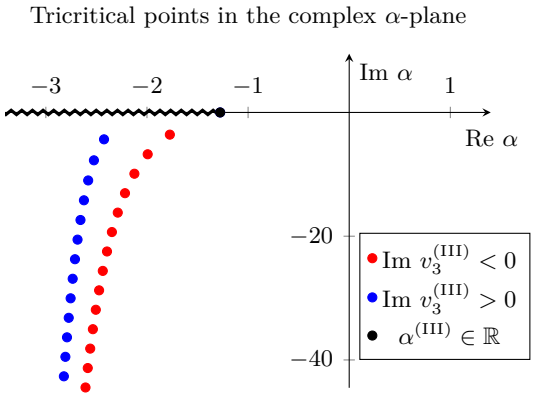


Figure 4.16: Position of the tricritical points in the complex α-plane. Each of them is associated with a distinct value of $v_3^{(\mathrm{III})}$.

corresponding $v_3^{(\mathrm{III})}$[19]. Each of those tricritical points is associated to a point where two of the higher meson masses, rather than the first and second, turn to zero simultaneously.

Second sheet critical points at imaginary v_3. As one consider the region $v_3 \in i\mathbb{R}$, a new type of critical points in the second sheet arise. Following the same strategy of the previous subsection, it is not difficult to show that for any value of $\alpha \in \mathbb{R}$, there are infinitely many double zeros $\pm v_3^{(\mathrm{II},k)}(\alpha) \in i\mathbb{R}$, $k \in \mathbb{N}$, strictly ordered as:

$$\left|v_3^{(\mathrm{II},0)}(\alpha)\right| \leq \left|v_3^{(\mathrm{II},1)}(\alpha)\right| \leq \left|v_3^{(\mathrm{II},2)}(\alpha)\right| \leq \cdots , \tag{4.3.7}$$

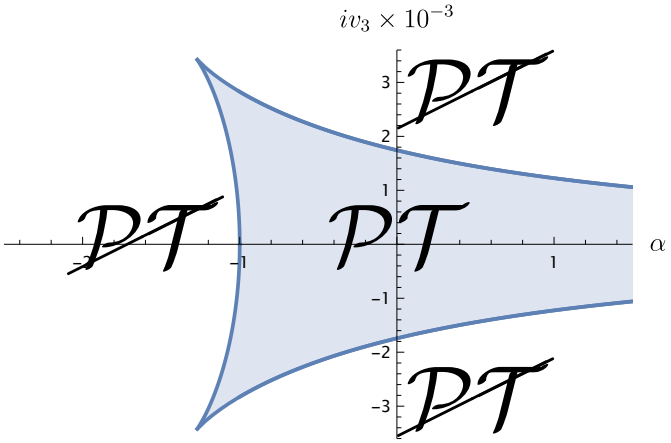
where $f(\nu, \alpha, v_3)$ has a double zero at $\nu^{(\mathrm{II},k)}(\alpha) \in i\mathbb{R}$:

$$f\left(\pm\nu^{(\mathrm{II},k)}(\alpha), \alpha, \pm v_3^{(\mathrm{II},k)}(\alpha)\right) = \partial_\nu f\left(\pm\nu^{(\mathrm{II},k)}(\alpha), \alpha, \pm v_3^{(\mathrm{II},k)}(\alpha)\right) = 0 , \tag{4.3.8}$$

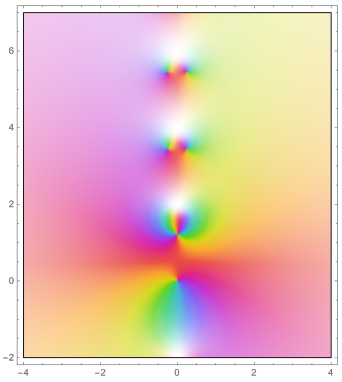
At the first of those critical points $\pm v_3^{(\mathrm{II},0)}$, the two closest roots of $f(\nu)$ in the upper-half plane (that are always in the strip $\nu \in [0, 2i]$) collide. At fixed α, none of these collision-of-root point is a singularity in the first sheet. But, if one first analytically continue in α along a closed curve enclosing a the square root branch point, then $v_3^{(\mathrm{II},k)}(\alpha)$ becomes a singular point where the first eigenvalues closes the gap and breaks spontaneously $\mathcal{PT}$-symmetry. This is exactly identical to what discussed in Section 6.3.1 of [1] (see Figure 16 there).

Note that the line of critical points at $\alpha < -1$ remains singular also in this second sheet, the resulting phase-space of the theory is illustrated in Figure 4.17a, where is is interesting to note that these new locus of critical point intersects the one discussed in the previous subsection exactly at the tricritical point.

[19] This can also be understood from the square root branch cut in the v_3-α plane, present for any value of α, in correspondence of which the value of v_3 changes sign.



(a) Phase space of the theory for $\alpha > -1$ in the second sheet of the α plane, and $v_3 \in i\mathbb{R}$. In the shaded region, the model present a physical and confining spectrum of mesons.



(b) First collision of roots of $f(\nu, \alpha, v_3)$ at $v_3^{(\mathrm{II},0)}$.

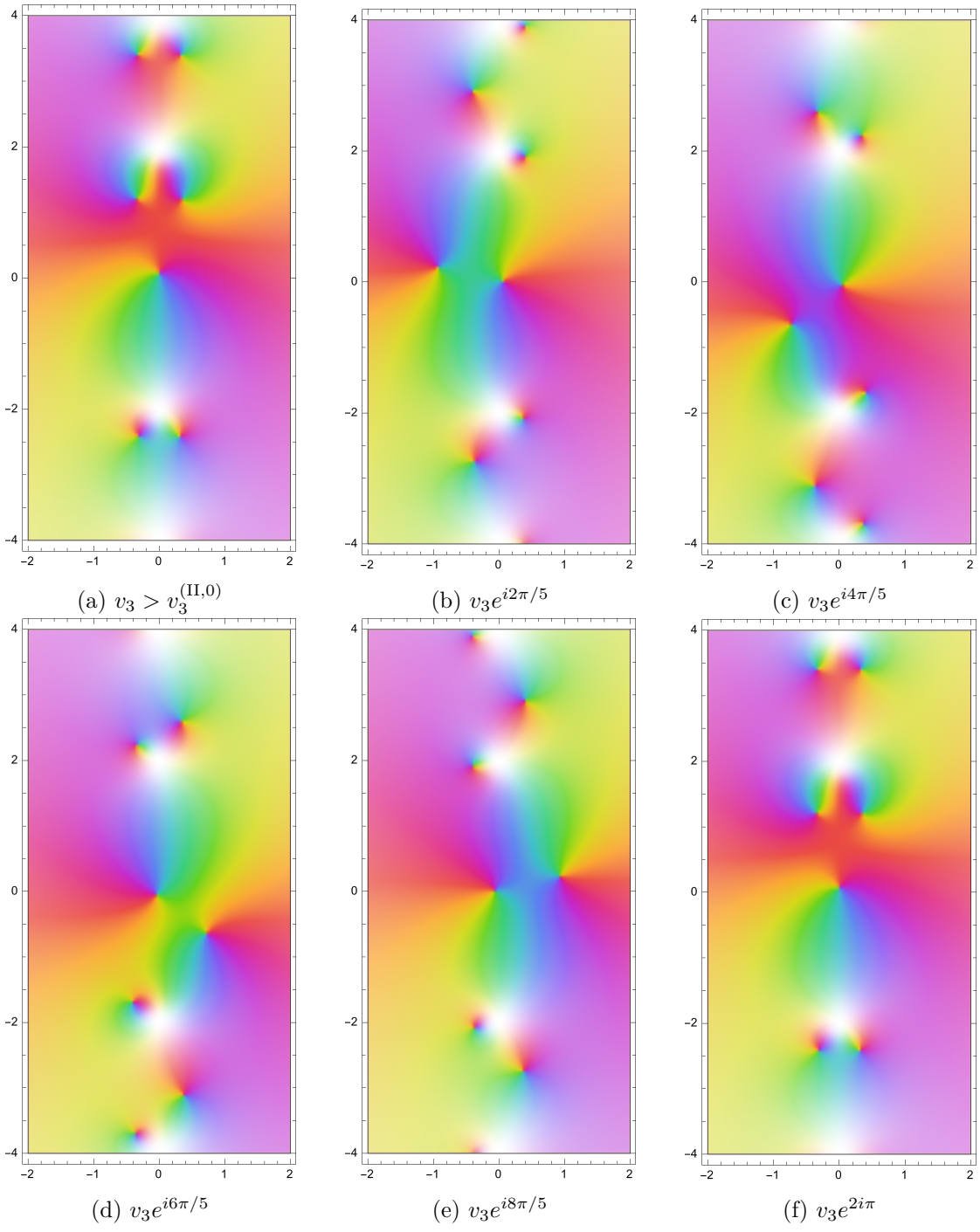
Figure 4.17: Collision of roots for imaginary v_3 and corresponding phase-space.

This can be generalized to any of the $\nu^{(\mathrm{II},k)}$. It turns out that, at any fixed α, $v_3^{(\mathrm{II},0)}(\alpha)$ is also a branch point of infinite degree in the v_3 plane. Indeed upon analytically continue in v_3 around any closed curve enclircling a single time $v_3^{(\mathrm{II},k)}(\alpha)$, one observes a monodromy of the roots of the form $\nu_i \to \nu_{i\pm1}$ where ν_i is the position of the roots of $f(\nu, \alpha, v_3)$ (with the exception of the one corresponding to $-v_3^{(\mathrm{II},0)}(\alpha)$) and $\pm$ depends on the sign of $\mathrm{Re}(\nu_i)$. This is illustrated in Figure 4.18. Then, it is easy to see that under this analytical continuation, one can always find a sheet where $\nu^{(\mathrm{II},k)}$ becomes a critical point and the corresponding k-th meson closes the gap and breaks spontaneously $\mathcal{PT}$-symmetry.

4.4 Mesons spectrum in the large representation limit

In this section we consider a theory with a finite number of colors N, but of fermions in a very large representation of the gauge group. This limit was also considered in [96] for the 't Hooft model. Here we illustrate that analogous results can be derived also for the generalized QCD case. Specifically, we consider an $SU(2)$ gauge theory coupled to a single flavor of quarks in the isospin J representation, and consider a scaling limit where $J \to \infty$.

Effective Hamiltonian for fermions. For our scopes, it is best to work with an Hamiltonian formulation of the theory. The starting point is the generalized YM Lagrangian in lightcone gauge, coupled to quarks in a generic representation of the gauge



(a) $v_3 > v_3^{(\mathrm{II},0)}$ (b) $v_3 e^{i2\pi/5}$ (c) $v_3 e^{i4\pi/5}$

(d) $v_3 e^{i6\pi/5}$ (e) $v_3 e^{i8\pi/5}$ (f) $v_3 e^{2i\pi}$

Figure 4.18: Monodromy of the roots under analytical continuation in v_3 around $v_3^{(\mathrm{II},0)}$.

group. Not not specifying yet $N = 2$ the Hamiltonian is:

$$\mathcal{L} = \frac{N}{4\pi}\mathrm{tr}\, B\,\partial_-\, A_+ - \frac{Ng^2}{4\pi}\sum_{n=2}^{\infty}\mathrm{tr}\, v_n B^n + \overline{\psi}_a\,(i\partial\!\!\!/ - m_a)\,\psi_a - \mathrm{tr}\, A_+^A\left(\overline{\psi}_a\,\gamma_-\,T^A\,\psi_a\right)\,, \quad (4.4.1)$$

and we take the generators $T^A\,, A = 1, \cdots N^2 - 1$ in a generic large dimensional representation of $SU(N)$. Integrating out the A_+ field in the path integral leads to the insertion of a delta function distribution setting

$$\frac{N}{4\pi}\partial_- B^A - \overline{\psi}_a\,\gamma_-\,T^A\,\psi_a = 0\,, \quad (4.4.2)$$

and leads to

$$\mathcal{L} = -\frac{Ng^2}{4\pi}\sum_{n=2}^{\infty}\mathrm{tr}_{\mathrm{adj}}\,\left(\frac{4\pi}{N}\right)^n v_n\left(\partial_-^{-1}\overline{\psi}_a\,\gamma_-\,T\,\psi_a\right)^n + \mathrm{tr}\,\overline{\psi}_a\,\left(i\partial\!\!\!/ - m_a\right)\,\psi_a\,, \quad (4.4.3)$$

where with $\mathrm{tr}_{\mathrm{adj}}$ we mean that the trace has to be taken in the adjoint representation:

$$\mathrm{tr}_{\mathrm{adj}}\left(\partial_-^{-1}\overline{\psi}_a\,\gamma_-\,T\,\psi_a\right)^n = \mathrm{tr}[F^{A_1}\cdots F^{A_N}]\prod_{i=1}^{n}\left(\partial_-^{-1}\overline{\psi}_a\,\gamma_-\,T^{A_i}\,\psi_a\right)\,, \qquad A_i = +, -, 3\,, \quad (4.4.4)$$

where F^A are the generators in the adjoint representation of $SU(N)$.

The component ψ_+ is non-dynamical because the field has no time derivatives in the lightcone gauge Lagrangian; it is fixed by the equations of motion to:

$$\psi_+ = \frac{im}{2}\partial_-^{-1}\,\psi_-\,. \quad (4.4.5)$$

Henceforth, one reduces the Lagrangian (4.1.1) to the following effective action for the only dynamical quark component ψ_-:

$$\mathcal{L}_{\mathrm{eff}} = -\frac{Ng^2}{4\pi}\sum_{n=2}^{\infty}\mathrm{tr}_{\mathrm{adj}}\,\left(\frac{4\pi}{N}\right)^n v_n\left(\partial_-^{-1}\overline{\psi}_a\,\gamma_-\,T\,\psi_a\right)^n + \mathrm{tr}\,\overline{\psi}_a\,\left(i\partial\!\!\!/ - m_a\right)\,\psi_a\,, \quad (4.4.6)$$

The standard quantization:

$$[\pi_-(x), \psi_-(y)] = \delta(x_- - y_-)\,, \qquad \pi(x) = \frac{\partial\mathcal{L}_{\mathrm{eff}}}{\partial\psi_-(x)} = i\sqrt{2}\,\psi_+^\dagger(x)\,, \quad (4.4.7)$$

leads to the effective Hamiltonian density:

$$\mathcal{H}_{\mathrm{eff}} = -\frac{Ng^2}{4\pi}\sum_{n=2}^{\infty}\left(\frac{4\pi}{N}\right)^n v_n\mathrm{tr}_{\mathrm{adj}}\left(\partial_-^{-1}\overline{\psi}_a\,\gamma_-\,T\,\psi_a\right)^n - i\frac{m^2}{4}\mathrm{tr}\,\psi_-^\dagger\partial_-^{-1}\psi_-\,, \quad (4.4.8)$$

The quarks depend on the two lightcone coordinates $\psi(y) = \psi(y_-, y_+)$, while in the potential only derivatives with respect to the y_- coordinate appear. To simplify the notation, we will momentarily drop the explicit "$-$" label of the coordinates, with the

understanding that inside the argument of the fermions $\psi(y) \equiv \psi(y_-, y_+)$, and everywhere else $y \equiv y_-$. Using the identities in Appendix A of [96], each of the quark bilinears that appears in (4.4.8) can readily expressed as[20]:

$$\partial_x^{-1}\psi_-^\dagger(x)\psi_-(x) = \int \mathrm{d}y\, \partial_y^{-1}\delta(x-y)\psi_-^\dagger(y)T^a\psi_-(y) = \frac{1}{2}\int \mathrm{d}y\, \mathrm{sgn}(x-y)\psi_-^\dagger(x)T^a\psi_-(y)\,. \tag{4.4.9}$$

Then, the effective Hamiltonian is ($y_1 := x, y_0 = y_n$):

$$\begin{aligned} H_{\text{eff}} = &-\frac{g^2}{4\pi}\sum_{n=2}^{\infty}\mathrm{tr}\,(2\pi)^n\, v_n \left(\prod_{k=1}^n \int \mathrm{d}y_k\, \mathrm{sgn}(y_k - y_{k-1})\psi_-^\dagger(y_k)T^{A_k}\psi_-(y_k)\right)\mathrm{tr}[F^{A_1}\cdots F^{A_n}] \\ &-\mathrm{tr}\, i\frac{m_a^2}{8}\int \mathrm{d}x\,\mathrm{d}y\,\psi_-^\dagger(x)\mathrm{sgn}(x-y)\psi_-(y) \end{aligned} \tag{4.4.10}$$

Large representation limit. Let us specialize to the group $SU(2)$. In the spin J representation, we have

$$\begin{aligned} \psi_-^\dagger T^+\psi_-(x) &= \sum_{m=-J}^{J}\sqrt{(J-m)(J+m+1)}\,\psi_{m+1,-}^*(x)\psi_-^m(x)\,, \\ \psi_-^\dagger T^-\psi_-(x) &= \sum_{m=-J}^{J}\sqrt{(J+m)(J-m+1)}\,\psi_{m,-}^*(x)\psi_-^{m+1}(x)\,, \\ \psi_-^\dagger T^3\psi_-(x) &= \sum_{m=-J}^{J} m\,\psi_{m-}^*(x)\psi_-^m(x)\,. \end{aligned} \tag{4.4.11}$$

Following the approach of [96], in the large J limit $\frac{m}{J}$ is approximated by a continuous variable $\frac{m}{J} = \cos\theta$. Rather than carrying a representation index m, in this limit, the quarks depend explicitly on the continuous variable θ:

$$\psi_-(\theta, x) := \sqrt{J}\,\psi_-^m(x)\,, \tag{4.4.12}$$

where, the additional factor $\sqrt{J}$ guarantees the correct scaling of the canonical quantization in the limit $J \to \infty$:

$$\{\psi_-^\dagger(\theta, x)\,,\, \psi_-(\theta', y)\} = J\left(\frac{1}{J\sin\theta}\delta(\theta-\theta')\right)\delta(x-y) \tag{4.4.13}$$

Accordingly, we must replace the trace over the representation by its continuous limit:

$$\sum_{m=-J}^{J} \to J\int_0^\pi \mathrm{d}\theta\,\sin\theta\,, \tag{4.4.14}$$

[20] A similar rewriting was also employed in this context in [188].

Using the continuous fields $\psi_-(\theta, x)$, one derives [96] the following large J scaling of (4.4.11):

$$\begin{aligned}\psi_-^\dagger(x)\, T^\pm\, \psi_-(x) &\to J \int_0^\pi \mathrm{d}\theta \sin^2\theta\, \psi_-^*(\theta, x)\psi_-(\theta, x)\,,\\ \psi_-^\dagger(x)\, T^3\, \psi_-(x) &\to J \int_0^\pi \mathrm{d}\theta \sin\theta\cos\theta\, \psi_-^*(\theta, x)\psi_-(\theta, x)\ .\end{aligned} \tag{4.4.15}$$

Now, let us assume that the potential truncates at a certain order $\bar{n} \in 2\mathbb{N}$ (the reason for fixing $\bar{n}$ even will be clear in a moment), and that the none of v_n scales with J. Then, because of the overall trace, the Hamiltonian is order J, and admits a double-scaling limit at $J \to \infty$ where the combination

$$4(2\pi)^{\bar{n}-1} g^2 J^{\bar{n}} = \lambda \tag{4.4.16}$$

is taken fixed. Taking $v_n = \mathcal{O}(J^0)$ suppresses any term $V(B)$ with $n < \bar{n}$[21]. Under this conditions, in the large spin limit, (4.4.10) is:

$$\begin{aligned}H_{\text{eff}} = -\frac{v_{\bar{n}}\lambda}{8}\mathrm{tr}\,&\left(\textstyle\prod_{k=1}^{\bar{n}} \int \mathrm{d}y_k\, \mathrm{sgn}(y_k - y_{k-1})\psi_{a,-}^\dagger(y_k)\, T^{A_k}\, \psi_{a,-}(y_k)\right) \mathrm{tr}\,[F^{A_1}\cdots F^{A_{\bar{n}}}]\\ &- \mathrm{tr}\, i\frac{m_a^2}{4}\int \mathrm{d}x\, \mathrm{d}y\, \psi_{a,-}^\dagger(x)\mathrm{sgn}(x-y)\psi_{a,-}(y)\,,\end{aligned} \tag{4.4.17}$$

where we intend that all the representation indexes are contracted through integrals over the respective θ variables and that we take the trace thereof ($\theta_1 = \theta_n$) to ensure gauge invariance. For the special case of $SU(2)$, only traces of an even number of adjoint generators are non-vanishing[22]. Henceforth, odd powers in the potential of $V(B)$ do not contribute (this is the reason for setting $\bar{n} \in 2\mathbb{N}$) to in an $SU(2)$ theory.

As in [96], we introduce the bi-local field:

$$\langle y, \phi|\, \boldsymbol{M}\, |x, \theta\rangle = M(x, y; \theta, \phi) = \psi_-(\theta, x)\psi_-^*(\phi, y)\,. \tag{4.4.18}$$

We will also use the notation $\boldsymbol{M}(x, y)$ whenever we want to specify the positions while keeping the short hand matrix notation. This notation is convenient for expressing contraction of bilinear fields in the continuum limit $\int \mathrm{d}\cos\theta\, A(x, y, \theta, \phi)B(z, t, \theta, \lambda)$ in the short-hand matrix multiplication notation $\boldsymbol{A}(x, y)\,\boldsymbol{B}(z, t)$. After we have substituted the adjoint representation traces, the interaction term of $\mathcal{H}_{\text{eff}}$, keeping only the symmetric terms in θ, and indicating the integration measure as $\mathrm{d}\boldsymbol{y}\,\mathrm{d}\boldsymbol{\theta} = \frac{1}{\bar{n}!}\prod_{i=1}^{\bar{n}} \mathrm{d}\theta_i \sin\theta_i\, \mathrm{d}y_i$, takes

[21] Any of them can be retained by imposing a scaling limit on the $v_n = \mathcal{O}\left(J^{\bar{n}-n}\right)$ at large J. Since the generalization to this case is straighforward, here we consider the simplest case where only the highest power contributes at large spin.

[22] We normalize the generators in the adjoint representation such that the killing form is $\kappa^{ab} = \left(\begin{smallmatrix} 0 & 1/2 & 0\\ 1/2 & 0 & 0\\ 0 & 0 & 1\end{smallmatrix}\right)$.

the form :

$$\int \mathrm{d}\boldsymbol{y}\,\mathrm{d}\boldsymbol{\theta}\prod_{i=1}^{\bar{n}}\mathrm{sgn}(y_k-y_{k-1})\Big[M(y_1,y_2;\theta_1,\theta_2)\widehat{M}(y_2,y_3,\theta_2,\theta_3)M(y_3,y_4,\theta_3,\theta_4)\widehat{M}(y_4,y_5;\theta_4,\theta_5)\cdots + \text{perm.}\Big], \tag{4.4.19}$$

where $\widehat{M}(y_i,y_j,\theta_i,\theta_j) := M(y_i,y_j,\theta_i,\theta_j)\cos(\theta_i-\theta_j)$. These quantities are conveniently expressed through the matrix notation introduced in (4.4.18):

$$\mathrm{tr}\int\prod_{i=1}^{\bar{n}}(\mathrm{d}y_i\,\mathrm{sgn}(y_k-y_{k-1}))\left(\boldsymbol{M}(y_1,y_2)\,\widehat{\boldsymbol{M}}(y_2,y_3)\boldsymbol{M}(y_3,y_4)\cdots\right). \tag{4.4.20}$$

Then, for an $SU(2)$ theory, at large spin, the Hamiltonian (4.4.8) is:

$$\begin{aligned}H_{\text{eff}} =&\frac{im^2}{8}\int \mathrm{d}x\,\mathrm{d}y\,\mathrm{sgn}(x-y)M(x,y;\theta,\theta)+\\ &+\frac{\lambda v_{\bar{n}}}{8}\int\prod_{i=1}^{\bar{n}}(\mathrm{d}y_i\,\mathrm{sgn}(y_k-y_{k-1}))\ \mathrm{tr}\left(\boldsymbol{M}(y_1,y_2)\widehat{\boldsymbol{M}}(y_2,y_3)\boldsymbol{M}(y_3,y_4)\cdots+\text{perm.}\right),\end{aligned} \tag{4.4.21}$$

Bound state equation. The fermions satisfy the same anti-commutation relation of [96], and therefore their same considerations apply here[23]: in particular the bilinear quantum operators $\boldsymbol{M}$ satisfy a W_∞^{2J+1} algebra (cf. §3.2, Appendix C,D of [96] and references therein). It has been shown in [96,153,189] that, in the case of 't Hooft model at large N or large J, the fluctuation along the co-adjoint orbit around a classical value of $\boldsymbol{M}$ can be identified with the meson wavefunction. The equation of motion for those fluctuations give the t' Hooft equation determining the spectrum of the mesons. At large spin, this is a very efficient way to obtain the bound state equation, as this method does not rely on planar perturbation theory. We illustrate this in Appendix A.2 where we compute the equation of motions for the fluctuation $\boldsymbol{W}$ around the classical solution:

$$\begin{aligned}&-i\partial_+ W(p,q;\theta,\phi)-\frac{m^2}{4}\left(\frac{1}{p}+\frac{1}{q}\right)W(p,q;\theta,\phi)\\ &-\frac{\lambda(-i)^n n v_n}{4\pi}\int_0^{p-q}\mathrm{d}k\,I_n(k,q)\left(W(k,q-k,\theta,\phi)\cos(\theta-\phi)-W(p,q;\theta,\phi)\right)=0\,.\end{aligned} \tag{4.4.22}$$

In order to get an equation for a gauge-invariant quantity, we take the trace over the representation indexes:

$$\phi(x)\equiv\phi(x,1-x):=\int\mathrm{d}\cos\theta\,W(x,1-x;\theta,\theta)\,,\qquad x:=\frac{p}{r}\,,\quad q:=p-r\,. \tag{4.4.23}$$

[23] Adding a potential for the gauge part of the action, does not modify the quantization of the fermions.

Recall the the functions $\phi(x)$ retain a residual dependence on the x_+ component. Going into its Fourier space $\phi(x;p_+) \equiv \phi(x)$, and restoring the $-$ label on the momenta, (A.2.11) takes the form:

$$4r_+r_-\phi(x) = m^2\left(\frac{1}{x}+\frac{1}{1-x}\right)\phi(x) - \frac{\lambda}{\pi}\int_0^1 \mathrm{d}y\, K(y,x;1-x,1-x)\,(\phi(y)-\phi(x)) \quad (4.4.24)$$

that, is exactly equivalent to the generalized Bethe-Salpeter equation (4.1.9) [95], with K and Γ computed using the potential $V(B) = B^{\bar{n}}$.

We can also obtain arbitrary potentials in the large representation limit (see also footnote 21), if we scale the coefficients v_n in the potential with appropriate powers of J. Specifically, once a double scaling limit of the YM coupling g^2 and J is fixed as in (4.4.16): $4(2\pi)^{\bar{n}-1}\, g^2 J^{\bar{n}} = \lambda$, imposing that of each of the other coefficients scales as $v_m = \mathcal{O}(J^{\bar{n}-m})$ at large J guarantees that all the combinations

$$4(2\pi)^{m-1}\, g^2 v_m J^m = \lambda_m \quad (4.4.25)$$

are finite and fixed in the limit $J \to \infty$. Henceforth, at large spin J, an arbitrary potential (that now depends also explicitly on J), $V(B,J)$ leads to a mass spectrum μ^2 of mesons determined by the same generalized 't Hooft equation (4.1.14):

$$2\pi\mu^2\phi(x) = \left(m^2 - \sum_{n=1}^{\infty}\lambda_{2n}\,\alpha_{2n}\right)\left(\frac{1}{x}+\frac{1}{1-x}\right)\phi(x) - \fint_0^1 \mathrm{d}y\, \frac{\sum_{n=1}^{\infty}\lambda_{2n}\,p_{2n}(\Lambda)}{(x-y)^2}\,\phi(y)\,, \quad (4.4.26)$$

where the summation is only over the even coefficients as a consequence of fixing the specific case of the $SU(2)$ algebra.

This implies that the all the results we have derived for the meson spectra at large N are equally valid in this large representation limit. This generalizes the result of [96], obtained for the specific case of standard QCD_2, corresponding to setting $v_n = \frac{1}{8\pi}\delta_{n,2}$. In particular, also in this limit, the theory exhibit the integrable structure.

Chapter 5

Outlook

In Part I, we studied the meson spectrum of 2D QCD and its generalizations. Building upon a framework proposed by [92], we illustrated a remarkable emergent integrability structure arising both in the large-N_c limit and in the regime where, at finite N_c, we couple to quarks in large isospin representations.

In these limits, the integral equation determining the meson spectrum can be recast as a TQ-Baxter equation. This turns out to be remarkably simple and universal: the dependence on the potential of the generalized Yang-Mills theory is entirely captured by the form of the transfer matrix, which can be computed explicitly for any given potential. From the analytic structure of the transfer matrix, we infer important properties of the IR fixed point of the theory; in particular, it provides a systematic diagnostic for gapless phases at low energies.

This structure appears to be highly universal. In a series of recent works, these results have been greatly extended, and the state-of-the-art is now full analytical expansions for the 't Hooft model and its multi-flavor case [93,94], as well as the Ising field theory (IFT) in a magnetic field [138], which—as discussed in Section 3—shares many features with the 't Hooft model in its Bethe-Salpeter limit [151]. This motivates us to explore several promising future directions. It would be interesting to see whether the discussion of [92–94] can be extended also to generalized QCD.

Scattering amplitudes. A natural continuation of this work is a detailed study of the implications of this emergent integrability at the level of form factors, meson scattering amplitudes, and correlation functions of conserved currents. The asymptotic expansions of wavefunctions developed in this work are expected to be particularly useful in evaluating such quantities. We will address this problem elsewhere.[1] Another complementary approach to scattering amplitudes is the S-matrix bootstrap. Using the integrability spectrum as input, one can attempt to bootstrap the $2 \to 2$ meson S-matrix–a meromorphic function of a single Mandelstam variable–by imposing unitarity and crossing symmetry. Due to its simplicity, this theory offers an ideal testing ground for applying S-matrix bootstrap techniques and understanding the structure of confining

[1] On this point, the author acknowledges numerous discussions and ongoing work with S. Komatsu and J. Donoghue.

S-matrices.[2] While the 't Hooft model exhibits particle production [164], an intriguing open question is whether the generalized QCD theory admits integrable points in the coupling space of $V(B)$. Can one tune[3] the couplings of the potential so that scattering becomes factorized?

Finite N_c corrections. It would be very interesting to systematically incorporate finite-N_c corrections to the 't Hooft equation and assess to what extent the integrable structure we have uncovered persists beyond the large-N_c limit. A preliminary study was initiated in [191], but the consequences for integrability have not yet been explored. We hope to revisit this topic. Systematically adding $1/N_c$ corrections would be essential for understanding the nature of the critical points on the second sheet of the complex mass plane and, in particular, for determining the fate of *critical exponents*, which may help identify the associated CFT in finite-N_c QCD_2.

IR phases. We showed that the spectrum of the generalized QCD_2 contains infinitely many branch points in the complex plane of quark masses. Evidence from the 't Hooft model [1,92] and the IFT case [138,151] suggests that these branch points correspond to genuine critical points of the theory, where the IR phase is described by a (multi-critical) CFT. It would be interesting to investigate whether these branch points persist at finite N_c and, if so, identify their precise CFT description by extending the analysis of [162,166]. Hints arise from the study of QED_2: after abelian bosonization, the generalized Schwinger model[4] becomes equivalent to a real scalar field interacting in a Landau-Ginzburg potential [95]:

$$\mathcal{L}_{\text{gen QED}} = \frac{1}{2\pi}\partial_\mu\phi\,\partial^\mu\phi - e^2V(\phi) + m^2\cos(2\phi)\,.$$

Famously, this flows to the unitary Virasoro minimal models $M(p,p+1)$ in the IR upon suitable tuning of the potential, exibiting multi-criticality in the IR, as well as ssb of $\mathcal{PT}$-symmetry [184–186].

In the non-abelian case, one might hope to generalize this construction. After non-Abelian bosonization of the (massless) case, one finds:

$$(\text{gen QCD}_2) \xrightarrow{\text{Bos}} \left[\frac{SO(N)_1}{SU(N)_1}\,\text{WZW}\right] \oplus \text{Tr}\left[\frac{N}{8\pi}B\wedge F - \frac{Ng_{\text{YM}}^2}{4\pi}V(B)\right].$$

Here, in contrast to the standard QCD case [162], the gluon kinetic term does not decouple in the $g_{\text{YM}}\to\infty$ limit. Therefore, it is conceivable that even at finite N_c, the theory may flow to interacting fixed points in the IR. We hope to investigate this further. On this front, many insights into RG flows and IR phases may be gained by imposing constraints from non-invertible symmetries. This will be the focus of Part II of this thesis, and we will not elaborate on it here. See also the recent work [192]. It would be interesting to apply these methods to generalized QCD as well.

[2] The author acknowledges ongoing work with P. Vieira and G. Lefundes.
[3] A procedure similar to the one used in [190] may prove useful.
[4] The author acknowledges discussions and ongoing work with B. Zan.

Adjoint QCD. Another direction we hope to pursue is the extension of our study to QCD_2 theories coupled to matter in other gauge representations and/or with different reality conditions (e.g., Majorana fermions). This topic has received considerable attention recently, especially regarding QCD with adjoint quarks [108–121,125–129,192–194]. It would be fascinating to determine whether an integrable structure similar to that of the 't Hooft model emerges in certain limits. Of particular interest are limits in which quark loops are suppressed (e.g., the large quark mass limit), where relevant diagrams reduce to "fishnet"-type graphs, for which integrability techniques are applicable [195–197].

The spectral problem of adjoint QCD is more intricate. Already at leading order in $1/N_c$, the lightcone Hamiltonian [198] couples adjoint strings of different lengths, complicating the spectral analysis. Nevertheless, variants of the separation of variables (SoV) method may enable crucial progress. This problem exhibits similarities with the spectral analysis of certain BPS operators in $\mathcal{N} = 4$ SYM [199] and the non-compact sl_2 spin chain [200]. Coupling generalized Yang-Mills theory to adjoint quarks may prove useful in this context. We hope to return to this question.[5]

Topological strings. Finally, regarding the connection to topological strings discussed in Section 3.5, it is important to clarify the relation between the techniques used in this work and those developed in the topological string literature. To this end, it would be helpful to complete the analysis started in Section 3.5 by computing the spectral sums and the asymptotic expansions of the spectrum and eigenfunctions. Another promising direction is to apply our methods to other toric Calabi–Yau backgrounds, particularly those whose mirror curve has higher genus. It has been shown [136,137] that open topological string wavefunctions satisfy the TQ-Baxter equation associated with the mirror curve. Understanding the precise relation between these wavefunctions and our $Q_{\pm}(x)$—which satisfy the TQ-system for the inhomogeneous problem—is an important task for future work.

[5]We acknowledge ongoing discussions with S. Komatsu.

Appendix A

Supplement to Part I

A.1 Recurrence relation for integrals

In this Appendix we provide a more in-depth proof for the formula (4.2.6). The starting point is the observation that the principal part integrals:

$$J_{n+2} = \fint_0^1 \frac{\left(\frac{y}{1-y}\right)^{\frac{i\nu}{2}} \left(\log\left(\frac{1-y}{y}\right)\right)^n}{(x-y)^2}\,, \tag{A.1.1}$$

can be computed as Fourier transforms of distributions, once represented through rapidity variables $\theta = \frac{1}{2}\log\left(\frac{y}{1-y}\right)$:

$$\begin{aligned} J_{n+2} &= \int_{-\infty}^{+\infty} \mathrm{d}\theta\, e^{i\theta\nu} \left(-2\frac{\cosh^2(\theta)}{\sinh^2(\theta-\varphi)}\right)(2\theta)^n = \left(\frac{2}{i}\right)^n \frac{\mathrm{d}^n}{\mathrm{d}\nu^n} J_2 \\ &= \left(\frac{2}{i}\right)^n \frac{\mathrm{d}^n}{\mathrm{d}\nu^n}\left[\left(\frac{\left(\frac{x}{1-x}\right)^{\frac{i\nu}{2}}}{\frac{2}{\pi}x(1-x)}\right)\mathcal{I}_2\right] \\ &= \left(\frac{2}{i}\right)^n \left(\frac{\left(\frac{x}{1-x}\right)^{\frac{i\nu}{2}}}{\frac{2}{\pi}x(1-x)}\right)\frac{\mathrm{d}^n}{\mathrm{d}\nu^n}\mathcal{I}_2 + \sum_{p=0}^{n-1}(-1)^{n-p+1}\binom{n}{p}\log^{n-p}\left(\frac{x}{1-x}\right) J_p \end{aligned} \tag{A.1.2}$$

where $\mathcal{I}_2$ is the one defined in (4.2.3). This can be equivalently expressed as:

$$\left(\frac{2}{i}\right)^n \frac{\mathrm{d}^n}{\mathrm{d}\nu^n}\mathcal{I}_2 = \left(\frac{\left(\frac{x}{1-x}\right)^{\frac{i\nu}{2}}}{\frac{2}{\pi}x(1-x)}\right)^{-1} \sum_{p=0}^{n}(-1)^{n-p}\binom{n}{p}\log^{n-p}\left(\frac{x}{1-x}\right) J_{p+2}\,, \tag{A.1.3}$$

but, using that:

$$\fint_0^1 \frac{\left(\frac{1-y}{y}\right)^{\frac{i\nu}{2}} \left(\log\left(\frac{1-y}{y}\right) - \log\left(\frac{1-x}{x}\right)\right)^n}{(x-y)^2} = \sum_{p=0}^{n}(-1)^{n-p}\binom{n}{p}\log^{n-p}\left(\frac{1-x}{x}\right) J_{p+2}\,, \tag{A.1.4}$$

from (A.1.3) we obtain (4.2.6):

$$\left(\frac{2}{i}\right)^n \frac{\mathrm{d}^n}{\mathrm{d}\nu^n}\mathcal{I}_2 = \mathcal{I}_{n+2}\,. \tag{A.1.5}$$

A.2 Derivation of the bound state equation in the large representation limit

In this appendix we follow closely [96,153,189]; we do not repeat many of the technical points that are carefully explained in Appendix D of [96] to which we refer the reader for more details.

The starting point is the action for a field for $\boldsymbol{M}$, that can be borrowed from the standard theory of quantization of the coadjoint orbits by adding a *kinetic term* $S_{\rm kin}(\boldsymbol{M})$[1] to the Hamiltonian $\mathcal{H}_{\rm eff}$:

$$\begin{aligned} S\left[\boldsymbol{M}\right] &= S_{\rm kin}(\boldsymbol{M}) - \frac{im^2}{8}\int \mathrm{d}x^+\,\mathrm{d}y_1^-\,\mathrm{tr}\,\boldsymbol{S}\boldsymbol{M} \\ &+ \frac{\lambda v_n}{8}\int \mathrm{d}x^+ \int \prod_{i=1}^{\bar{n}} \left(\mathrm{d}y_i\,\mathrm{sgn}(y_k - y_{k-1})\right)\,\mathrm{tr}\,\left(\boldsymbol{M}(y_1,y_2)\widehat{\boldsymbol{M}}(y_2,y_3)\boldsymbol{M}(y_3,y_4)\cdots + \text{perm.}\right)\,, \end{aligned} \tag{A.2.1}$$

where $S(x,y,\theta,\phi) = \mathrm{sgn}(x_- - y_-)\frac{1}{\sin(\theta)}\delta(\theta-\phi)$. This generalizes the action used in [96] only in the last term in (A.2.1).

We chose a coadjoint orbit with vanishing $U(1)$ charge, of whose a representative is $M_0(p,q,\theta,\phi) = 2\pi\Theta(p_-)\delta(p_- - q_-)\frac{1}{\sin\theta}\delta(\theta-\phi)$, where

$$M(p,q,\theta,\phi) = \int_{-\infty}^{+\infty} \mathrm{d}x_-\,\mathrm{d}y_-\,e^{ipx_-}e^{iqy_-}M(x,y,\theta,\phi)\,. \tag{A.2.2}$$

Fluctuation $\boldsymbol{W}$ around the coadjoint orbit are be parametrized as: (eq. 3.26 of [96]):

$$\boldsymbol{M} = \boldsymbol{M_0} + \frac{1}{\sqrt{J}}[\boldsymbol{W},\boldsymbol{M_0}] - \frac{1}{2J}[\boldsymbol{W},[\boldsymbol{W},\boldsymbol{M_0}]] + \mathcal{O}(J^{-3/2})\,. \tag{A.2.3}$$

The action (A.2.1) is order J , and therefore we must take the $\mathcal{O}(1/J)$ term under the variation (A.2.3) to get the finite leading order action for the fluctuations. The first two terms of (A.2.1), are directly borrowed the result from Appendix D of [96]:

$$\begin{aligned} \delta S_{\rm kin} &= i\frac{1}{J}\int \mathrm{d}x^+ \int_{p,q>0} \mathrm{d}p\,\mathrm{d}q\,\mathrm{tr}\,\boldsymbol{W}^{+-}(p,q)\partial_+\boldsymbol{W}^{-+}(q,p)\,, \\ \delta S_{\rm mass} &= -\frac{m^2}{4J}\int_{k,q>0}\mathrm{d}p\,\mathrm{d}q\left(\frac{1}{k}+\frac{1}{p}\right)\mathrm{tr}\,\boldsymbol{W}^{+-}(k,p)\boldsymbol{W}^{-+}(p,k)\,, \end{aligned} \tag{A.2.4}$$

[1] The details of this are not important for our discussion, we refer the interested reader to [96].

where, for clarity of comparison, we use the notation[2] : $W^{\pm\pm}(p,q) = W(\pm p, \pm q)$. The interaction term of H_{eff} receives three contributions (up to permutations of θ_i) at order $\mathcal{O}(1/J)$. Schematically:

$$\text{I}: \boldsymbol{M_0}\frac{1}{2J}\widehat{\boldsymbol{W}\boldsymbol{W}}\left(\underbrace{\boldsymbol{M_0}\,\widehat{\boldsymbol{M_0}}\cdots}_{(\bar{n}-2)\,\text{terms}}\right), \quad \text{II}: \widehat{\boldsymbol{M_0}}\frac{1}{2J}\boldsymbol{W}\boldsymbol{W}\left(\underbrace{\boldsymbol{M_0}\,\widehat{\boldsymbol{M_0}}\cdots}_{(\bar{n}-2)\,\text{terms}}\right) \simeq \text{I}\,, \tag{A.2.5}$$

the II and the I are equal contributions up to permutations of the θ_is; a third, inequivalent contribution is:

$$\text{III}: \frac{1}{\sqrt{J}}\boldsymbol{W}\frac{1}{\sqrt{J}}\widehat{\boldsymbol{W}}\left(\underbrace{\boldsymbol{M_0}\,\widehat{\boldsymbol{M_0}}\cdots}_{(\bar{n}-2)\,\text{terms}}\right) \tag{A.2.6}$$

All this contribution to the variation of (A.2.1) can be computed as a generalization of Appendix D of [96]. The contributions I, II are evaluated to[3]:

$$-i\int_{p,q>0}\mathrm{d}p\,\mathrm{d}q\int_0^{p-q}\mathrm{d}k\int\mathrm{d}^{\bar{n}-1}\boldsymbol{k}\,\frac{-i\mathrm{sgn}(k_1)}{2\pi(k-k_1)}\,\frac{-i\mathrm{sgn}(k_2)}{2\pi(k_1-k_2)}\cdots\frac{-i\mathrm{sgn}(k_{\bar{n}-1})}{2\pi(k_{\bar{n}-1}-k_1)}\mathrm{tr}\,\boldsymbol{W}^{-+}(p,q)\boldsymbol{W}^{+-}(q,p) \tag{A.2.7}$$

all the $\bar{n}+1$ integrations over $\mathrm{d}p\,\mathrm{d}q$ but the two remaining above over $\mathrm{d}p\,\mathrm{d}q$ are removed by the $\bar{n}-3$ $\delta(\theta_i-\theta_{i+1})$ inside each of the $\boldsymbol{M_0}$, this also cancel all the $\cos(\theta_i-\theta_{i+1})$ trigonometric factors. the integral over the k_i is eactly the *master integral* (4.1.7) introduced in section 4.1:

$$\int_{p,q>0}\mathrm{d}p\,\mathrm{d}q\int_0^{p-q}\mathrm{d}k\,I_n(k,q)\mathrm{tr}\,\boldsymbol{W}^{-+}(p,p)\boldsymbol{W}^{+-}(q,p)\,. \tag{A.2.8}$$

Analogously, the third contribution is evaluated as:

$$\int_{p,q>0}\mathrm{d}p\,\mathrm{d}q\int_0^{p-q}\mathrm{d}k\,I_n(k,q)\mathrm{tr}\,\left[\boldsymbol{W}^{+-}(q-k,q)\widehat{\boldsymbol{W}}^{-+}(p,q)+\boldsymbol{W}^{-+}(k,q-k)\widehat{\boldsymbol{W}}^{+-}(q,p)\right]. \tag{A.2.9}$$

Once we sum over all the permutations of I, II and III, taking into account the combinatorial factor $\frac{1}{n!}$, we obtain the following expression for the interaction term of $\mathcal{H}_{\text{eff}}$ at order $\mathcal{O}(1/J)$:

$$\frac{-\lambda}{4J}v_n(-i)^{\bar{n}}\bar{n}\int_{q,p>0}\mathrm{d}p\,\mathrm{d}q\int_0^{p-q}\mathrm{d}k\,I_n(k,q)\,\mathrm{tr}\,\Big[\left(\widehat{\boldsymbol{W}}^{+-}(q-k,k)-\boldsymbol{W}^{+-}(q,p)\right)\boldsymbol{W}^{-+}(p,q)+\left(\widehat{\boldsymbol{W}}^{-+}(k,q-k)-\boldsymbol{W}^{-+}(p,q)\right)\boldsymbol{W}^{+-}(q,p)\Big] \tag{A.2.10}$$

[2]The same of [96] up to $+(-)\leftrightarrow p(n)$.

[3]The form of the integral over the k_i can be readily obtained (for instance) from a direct generalizing eq. D.17 of [96]: in each of the two integral the sign can be recognized to be $\mathrm{sgn}(k)$, and $1/k^2$ (Fourier transform of $|x|$) is replaced for each term of our problem with $\frac{i}{(k_{i-1}-k_i)}\frac{i}{(k_i-k_{i+1})}$ (Fourier transform of $\mathrm{sgn}(x)$), with $k_0=k$, $k_{\bar{n}}=q$

Varying the action w.r.t. $W^{+-}(p,q;\theta,\phi)$ we obtain the following equation of motions:

$$-i\partial_+ W^{-+}(p,q;\theta,\phi) - \frac{m^2}{4}\left(\frac{1}{p}+\frac{1}{q}\right) W^{-+}(p,q;\theta,\phi)$$
$$-\frac{\lambda(-i)^n n v_n}{4\pi}\int_0^{p-q} \mathrm{d}k\, I_n(k,q)\left(W^{-+}(k,q-k,\theta,\phi)\cos(\theta-\phi) - W^{-+}(p,q;\theta,\phi)\right) = 0\,. \tag{A.2.11}$$

In the main text we report (A.2.11) by replacing $W^{-+} \mapsto W$ in (4.4.22) to simplify the notation.

A.3 Numerical methods for analytical continuation

In this appendix we illustrate the numerical method we employ to solve numerically the 't Hooft equation in ν-space (4.2.2) in the complex space of the couplings. As discussed in the main text (cfr. Section 4.3), the integral eigenvalue problem exhibits a multi-sheeted sctructure in the complex plane, arising from collision-of-roots singularities inside the kernel of (4.2.2) due to the poles of $\Psi(\nu)$. Compared to the same integral equation in x-space, the problem in Fourier space, is particularly convenient to solve numerically even in the complex space of the couplings. To solve this eigenproblem numerically, we employ an orthonormal basis of Hermite polynomials:

$$\langle n|x\rangle = H_n(x) = \frac{(-1)^n e^{\frac{x^2}{2}}}{\sqrt{2^n \pi^{1/2} n!}} \frac{\mathrm{d}^n}{\mathrm{d}x^n} e^{-x^2}\,, \qquad \langle m|n\rangle = \delta_{nm}\,, \tag{A.3.1}$$

that share many properties with the eingefunction $\Psi_n(x)$ having exactly n zeros and definite parity in $x \in (-\infty, +\infty)$.

In this basis the generalized 't Hooft equation (4.2.2)reduces to the eingeproblem for the following "Hamiltonian":

$$\langle m|\,\mathcal{H}\,|n\rangle = \mathcal{H}_{mn} = \int_{-\infty}^{+\infty} \mathrm{d}x \int_{-\infty}^{+\infty} \mathrm{d}y\, \frac{H_m(x) H_n(y)}{f(x)} \frac{\pi(x-y)}{2\sinh(\frac{\pi}{2}(x-y))}\,, \tag{A.3.2}$$

that can be straightforwardly solved upon truncation of the basis. The eigenvalues e_k of $\mathcal{H}_{nm}$ are related to the masses of the mesons λ_k by inversion: $\lambda_k = e_k^{-1}$.

This numerical method is particularly akin to analytical continuation. Indeed, whenever upon analytically continuation of the couplings $\alpha, \boldsymbol{v}$, one (or more) of the zeros of $f(\nu)$ crosses the integration contour, one can just modify the Hamiltonian $\mathcal{H}_{mn}$ simply by including the corresponding residue terms.

To exemplify, consider the case of $V(B) = \frac{1}{8\pi}B^2 + i|v_3|B^3$. Fixed any $v_3 > 0$, for $\alpha > -1$ no zeros of $f(\nu)$ lie on the integration contour, while upon analytically continue in α to values $\alpha < -1$, exactly one of the zero crosses the real axis, and therefore the contour has to be deformed to avoid this singular point as in Figure A.1. Then, the $\mathrm{d}x$

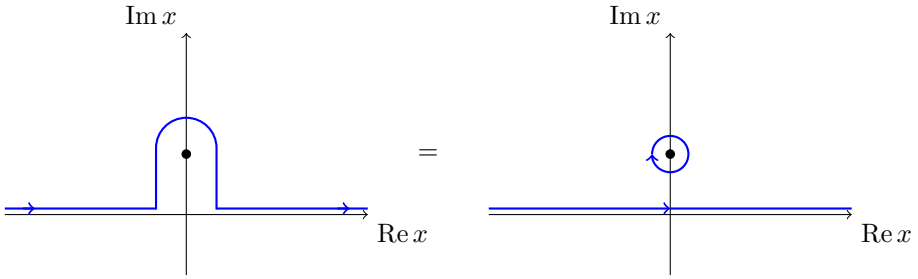


Figure A.1: The integration contour in the x-plane of (A.3.2) is deformed under analytical continuation from $\alpha > -1$ to $\alpha < -1$ at fixed $-iv_3 > 0$.

integral in (A.3.2) will pick a further contribution due a residue term[4]:

$$\mathcal{H}_{mn} \to \mathcal{H}_{mn} - 2\pi i H_m(x_0)\,\mathrm{Res}\left[f^{-1}(x,\alpha,v_3), x = x_0\right]\int_{-\infty}^{+\infty} \mathrm{d}y\, H_n(y)\frac{\pi(x_0-y)}{2\sinh\left(\frac{\pi}{2}(x_0-y)\right)}\,, \tag{A.3.3}$$

where $x_0 = x_0(\alpha, v_3)$ is the position of the zero of $f(x,\alpha,v_3)$ that has crossed the integration contour.

Analogous manipulations make straightforward the numerical analysis of (4.2.2) among the various sheets in the couplings-space. In practice, already truncating the basis at $n_{max} \sim 30$, reproduces the first 4 eigenvalues of [92] up to an accuracy of 10^{-5}, that used a basis of 400 elements to diagonalize the x-space for teh simplest case of $\boldsymbol{v} = \mathbf{0}$ and $\alpha = 0$. This is yet another illustration of the efficiency of solving the ν-space problem, rather than the original one in x-space, also at the level of numerical methods.

A.4 Non-critical spontaneous symmetry breaking of $\mathcal{PT}$-symmetry

In this appendix, we study the meson spectrum associated with a cubic generalized QCD potential, $V(B) = \frac{1}{8\pi}B^2 + v_3 B^3$, in the region of the parameter space obtained by analytically continuing around the cubic-root branch cut located at $\alpha = \alpha^{(\mathrm{III})}$. We perform this analytical continuation along a path lying at imaginary values of v_3. This guarantees that the $\mathcal{PT}$ symmetry is preserved all along the path. As already stated in the main text, whenever $\mathcal{PT}$ symmetry is not spontaneously broken by the eigenfunctions, the spectrum is real. This is the case for values of $\alpha > \alpha^{(\mathrm{III})}$ and $i\mathbb{R} \ni v_3 > v_3^{(\mathrm{II})}$, i.e. in the entire region bounded from below by the critical line in Figure 4.12. Another possibility is that $\mathcal{PT}$ symmetry could be broken *spontaneously* by the eigenfunctions, i.e. *some* of the eigenfunctions and eigenvalues become complex conjugate pairs. As we have already explained in Section 4.3.3 (cfr. Figure 4.17a) in our model this happens in correspondence with the critical points at $v_3^{(\mathrm{II})}$. Crossing the branch cut associated to any of the critical points leads into a spontaneously broken phase of $\mathcal{PT}$-symmetry. At this special point the massless state become doubly degenerated with a non-normalizable

[4]Note that the sign of the residue comes from the contour orientation in Figure A.1

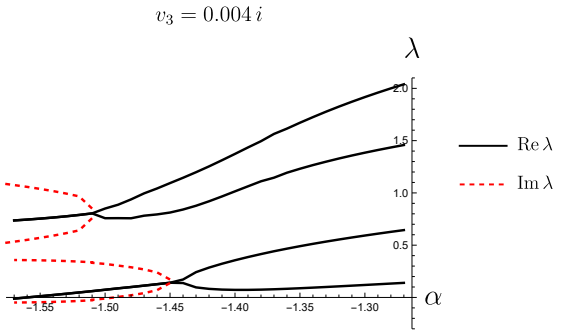


Figure A.2: First four eigenvalues for $v_3 = 0.004i$ varying α. The non-critical $\mathcal{PT}$ symmetry is associated to the first two eigenvalues becoming complex-conjugated pairs without turning to zero. To facilitate reading this plot, the imaginary parts of the eigenvalues are displayed shifted by the corresponding real values at the degenerated point.

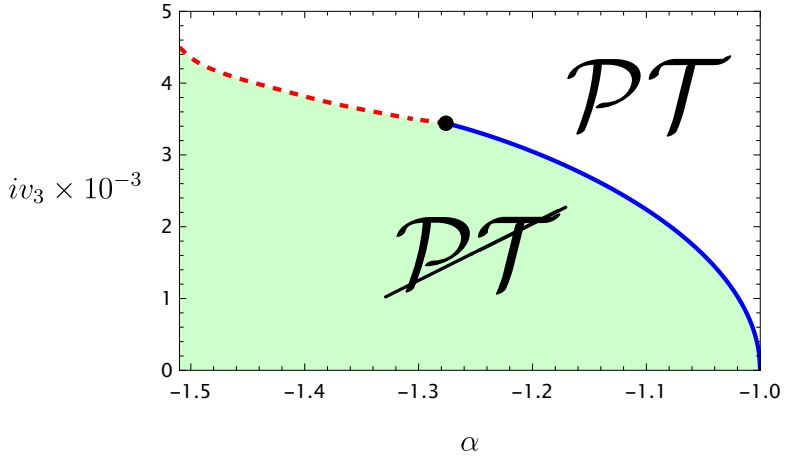


Figure A.3: Critical and non-critical $\mathcal{PT}$ symmetry breaking in the $(\alpha, v_3 \in i\mathbb{R})$ plane. In the region shaded in green $\mathcal{PT}$ symmetry is spontaneously broken by the eigenfunctions and the spectrum is populated by complex-conjugate eigenvalues. The blue line is the line of critical points where the first meson mass turns to zero, as computed analytically from the singularities of $f(\nu)$. The dashed red line is the line of spontaneous non-critical $\mathcal{PT}$ breaking determined numerically. The dot is located at the tricritical transition.

eigenstate[5]. At fixed α, the pair becomes complex conjugated as we cross the branch cut beyond $v_3 < v_3^{(\mathrm{II})}(\alpha)$.

These critical points shall be regarded as associated to the spontaneous symmetry breaking of $\mathcal{PT}$ symmetry, so that the *critical* $\mathcal{PT}$ breaking is nothing but a usual incarnation of the Landau paradigm. More subtle is what happens beyond the tricritical

[5]The argument follows from the analogous discussion in section 6.3.1 of [1].

point $(\alpha^{(\mathrm{III})}, v_3^{(\mathrm{III})})$, where the line of critical points is split to complex values of v_3 and does not lie anymore at $\mathcal{PT}$-symmetric values of the parameters. Henceforth, $\mathcal{PT}$ symmetry cannot be broken spontaneously at a critical points: it is rather broken[6] *non-critically* [185,186]. Non-critical $\mathcal{PT}$-breaking happens when two of the meson masses degenerate and become complex conjugate. In this case the transition to a spontaneously broken phase of $\mathcal{PT}$-symmetry is not associated with a critical point as there are no massless modes in the spectrum[7]. The typical situation is reported in Figure A.2. At the non-critical breaking point, the lowest two eigenvalues (and eigenfunctions) degenerate and become complex conjugate. Upon delving deepen in the ssb broken phase, more and more states become degenerate and and turn into complex conjugate pairs, exhibiting non-critical $\mathcal{PT}$-breaking.

These non-critical transitions cannot be diagnosed by the singularities of the (inverse of) tranfer matrix $f(\nu)$. Yet one can compute numerically the eigenvalues for a large range of α and v_3 to scan[8] where the first two levels undergo a non-critical phase transition. This results in the phase diagram reported in Figure A.3. This completes the phase space of Figure 4.12.

[6] Yet, one should expect that ssb breaking of $\mathcal{PT}$-symmetry must happen at some point in the parameter space: as if this would not be the case, one could find a continuous path, from the $\mathcal{PT}$-symmetric phase at $(\alpha > \alpha^{(\mathrm{II})}, v_3 > v_3^{(\mathrm{II})})$ to the ssb one at values $v_3 < v_3^{(\mathrm{II})}$ without crossing any branch cut.

[7] Interestingly, the same phenomenon was also recently illustrated for the non-unitary version of tricritical Ising model (the minimal model M(2,7)) in [185,186]. Generalized YM shares many features with the the multicritical minimal models of the Ising or YL series.

[8] In practice, one fixes v_3 and scans over all the α's until the first two level become complex conjugate. Repating this over v_3 leads to the figure.

Part II

Symmetries and flows of deformed 2d CFTs

Chapter 6

Introduction

Symmetries play a fundamental role in quantum field theory (QFT), constraining both the spectrum of states and the structure of operators. While gauge symmetries represent redundancies in our description, global symmetries correspond to intrinsic physical properties. Crucially, even when a QFT admits multiple equivalent formulations—perhaps in terms of different microscopic variables—its global symmetries must remain unambiguously identical. This requirement provides a powerful non-perturbative check for proposed dualities. Moreover, global symmetries are robust across energy scales, including in theories without a known Lagrangian description.

Generalized Symmetries

Recent developments in QFT have firmly established that topological defect operators of arbitrary codimension implement global symmetries. This modern viewpoint, first articulated in the seminal work [66], has led to a profound rethinking of symmetries and anomalies (see [67,68] for recent reviews).

In this framework, traditional notions of global symmetries have been extended to include *higher-form*, *non-invertible*, and more generally *higher-categorical* symmetries. These generalizations replace group-like structures with richer algebraic ones, such as fusion higher-categories, allowing for intricate interactions among extended operators of different dimensions. Central to these advances is the study of topological defects: the more control we gain over this subset of operators, the more powerful the constraints we can derive.

A paradigmatic example is the one-form symmetry $U(1)_e^{(1)} \times U(1)_m^{(1)}$ of four-dimensional Maxwell theory, associated with the topological surface operators:

$$U_g^{(e)} = \exp\left(g \int_{\mathcal{M}^{(2)}} F\right), \qquad U_g^{(m)} = \exp\left(g \int_{\mathcal{M}^{(2)}} \star F\right),$$

under which dyonic line operators are charged. Here, topological defects obey an abelian fusion structure.

While symmetries in quantum mechanics (i.e., QFTs in 0+1D) are implemented by (anti-)unitary, invertible operators, in higher dimensions the equal-time fusion of

topological operators typically does not yield a group but rather a (higher-)fusion category. In particular, there can exist defects $\mathcal{D}$ without an inverse $\mathcal{D}'$ such that $\mathcal{D} \circ \mathcal{D}' = \mathbb{1}$. This leads to the notion of *non-invertible symmetries*. The fact that QFT symmetries are not always unitary operators is a feature—not a bug. A hallmark of non-invertible symmetry defects is their ability to map order to disorder states in the Hilbert space or mix operators of different codimensions.

A prototypical example is provided by the topological defect lines (TDLs) of the 2D Ising CFT (Virasoro minimal model $M(3,4)$), which has three such lines: the identity $\mathbb{1}$, an invertible $\mathbb{Z}_2$ symmetry line η with $\eta^2 = \mathbb{1}$, and the Kramers-Wannier duality defect $\mathcal{D}$ satisfying

$$\mathcal{D} \times \mathcal{D} = \mathbb{1} + \eta, \qquad \mathcal{D} \times \eta = \eta \times \mathcal{D} = \mathcal{D}.$$

The non-invertible line $\mathcal{D}$ encodes the $\mathbb{Z}_2$ Tambara–Yamagami category (TY_2), the simplest fusion category built from a finite group. This structure underpins many features of the theory at the KW duality-invariant point $T \leftrightarrow 1/T$. We will encounter further instances of this structure in Part II.

In Part II, we focus on two-dimensional CFTs and their deformations. In 2D, the only extended operators are line defects. Non-invertible symmetries are ubiquitous in this setting [201–204]: topological line operators generating 0-form symmetries typically form a fusion category rather than a group.

Generalized symmetries are now recognized as powerful tools to probe dynamics and constrain phases of quantum theories. However, their implications for scattering amplitudes and massive flows remain underexplored. In two dimensions, non-invertible topological line defects have recently been shown to induce rich dynamical phenomena. These include modifications of the crossing equation [205,206], new degeneracies [207], predictions of novel RG flows [98,208,209], and new bootstrap constraints [205].

RG Flows Between Rational CFTs

Consider an RG flow triggered by deforming a CFT with a relevant bulk operator:

$$\mathcal{H}(\lambda_I) = \mathcal{H}_{\mathrm{CFT}} + \lambda_I \int dx\, \phi_I, \qquad \Delta_{\phi_I} < 2.$$

Some topological line defects may remain topological along the flow. If so, the corresponding symmetry is preserved, and strong constraints on the IR fixed point follow [98,118,201,210–213]. In particular, for a massless IR fixed point, the category of preserved TDLs must match the UV anomaly.

Chapter 7 is devoted to studying RG flows originating from rational CFTs. While we focus on gapless flows ending in IR minimal models, our methods may extend to gapped phases as well. Recently, Tanaka and Nakayama [98] conjectured a new class of flows between Virasoro minimal models:

$$M(kq + I, q) \xrightarrow{\phi_{(1,2k+1)}} M(kq - I, q), \tag{6.0.1}$$

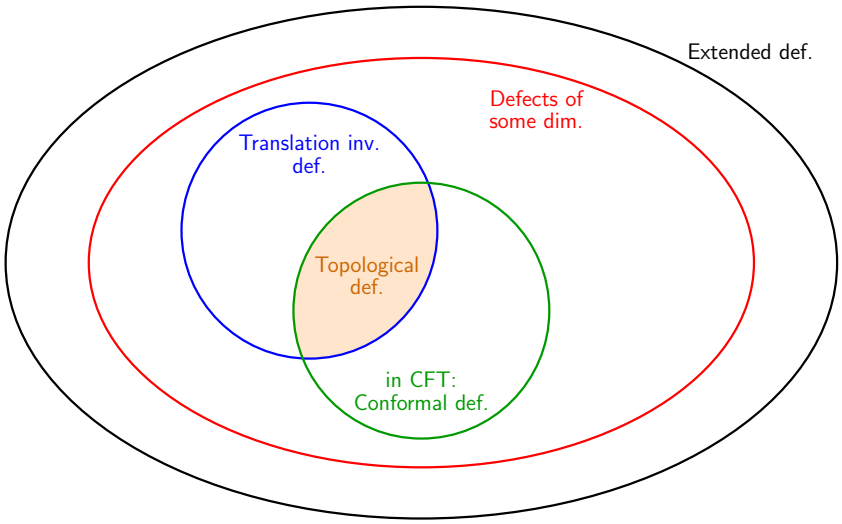


Figure 6.1: Space of defects.

based on anomaly matching for a preserved $SU(2)_{q-1}$ subcategory of the UV's non-invertible symmetries.

In this thesis, we propose a conjectural description of these flows via nonlinear integral equations of the TBA type, encoding the finite-size spectrum. Prior to this work, such a description existed only for the integrable deformations $\phi_{(1,2)}$, $\phi_{(1,3)}$, and $\phi_{(1,5)}$, corresponding to $k = \frac{1}{2}, 1, 2$. Our findings for general k are new and suggest the possibility of underlying integrability, warranting further investigation. In the outlook (Chapter 9), we comment on extensions to minimal models of the $\mathcal{W}_N$ algebras [**?**].

Translational Invariant Defects

In Chapter 8, we explore a broader notion of symmetry defects that includes non-topological ones, motivated by our findings in Chapter 7 and [4]. Counting arguments (see Section 8.3) suggest that no extra local conserved charges exist beyond those associated with known integrable deformations.

However, our results indicate a richer structure. We construct *translational invariant defects*: line operators that commute with the full deformed Hamiltonian $\mathcal{H}(\mu)$, but not necessarily with the undeformed Hamiltonian or the stress tensor individually. These are preserved under rigid translations but not under general local deformations.

These defects form a category larger than that of topological defects, as represented in Figure 6.1. They have a non singularl fusion and impose nontrivial constraints on the dynamics. Although still largely unexplored, our preliminary results suggest these may reveal new layers of structure in perturbed 2D CFTs.

We formulate sufficient conditions for translational invariance using only CFT data. This is best expressed using a version of the 3D symmetry topological field theory (SymTFT), adapted to the study of 2D CFTs, which we review in detail.

Applying these ideas to Virasoro minimal models, we find that the conserved charges preserved along $\phi_{(1,2k+1)}$ deformations extend beyond the known set of TDLs $\mathcal{L}$ commuting with the deformation. Notably, we construct infinite families of commuting conserved charges even when the perturbing operator is not one of $\phi_{(1,2)}$, $\phi_{(1,3)}$, or $\phi_{(1,5)}$. The existence of such charges is often a hallmark of integrability, suggesting a new direction in the study of minimal models.

Contents of Part II

7 Non-invertible symmetries and flows between minimal models **121**
7.1 Primer on Virasoro minimal models. 122
7.2 RG flows between Virasoro Minimal Models 123
7.3 Description via NLIE 126

8 Conserved Defects in 2D CFTs **135**
8.1 SymTFT and non-local conserved charges 139
8.2 Non-local commuting charges in minimal models 154
8.3 Local conserved charges 166

9 Outlook **175**

B Supplement to Part II **181**
B.1 Detailed description of some RG flows 181
B.2 F-matrix in the case $\boldsymbol{x} \otimes \boldsymbol{x} \cong \mathbf{1}$ 184
B.3 Bulk commutation condition and mutual commutativity for $\mathcal{D} = \mathbf{1} \oplus x$ . . 185
B.4 Details of the calculation of a local conserved current 189

Chapter 7

Non-invertible symmetries and flows between minimal models

In the special case of Rational 2d CFTs with diagonal modular invariance, i.e. the Virasoro Minimal Models $\mathcal{M}(p,q)$, the set of topological line operators is known to coincides with the finitely many Verlinde line defect, forming a *fusion modular category* [84,201]. From this perspective, the study of RG flows from a minimal model provides a unique arena where we have a complete understanding of the full set of *categorical* symmetries of the UV theory, and it has indeed recently received considerable attention [208,214–220]. This approach was first undertaken in [201,204] and, more recently, in [98], where the authors predict infinitely many new RG flows between minimal models: $\mathcal{M}(kq+I,q) \to \mathcal{M}(kq-I,q)$, preserving a special A_{q-1} fusion category containing the standard $\mathbb{Z}_2$ symmetry.
Moreover, ome specific deformations of minimal models are *integrable*, meaning the scattering events of the deformed theory are factorized and the 2-body S-Matrix satisfies the Yang-Baxter equation along the entire flow [221–223]. Integrable flows allow for an exact, non-perturbative description through the Thermodynamic Bethe Ansatz (TBA) equations [224] – equivalently, a Non-Linear Integral Equation (NLIE) [225,226] – encoding their exact, finite-size energy spectrum along the whole flow.
In this Chapter, we extend the investigation of RG flows between minimal models predicted by anomaly-matching conditions associated with non-invertible symmetries. We also present evidence that the ground-state energy of all these RG flows – not just the integrable ones – admits an explicit NLIE description. We base this statement on the observation that a three-parameter family of NLIE encodes non-trivial features of the RG flows predicted by anomaly-matching conditions. In particular, for multi-operator deformations – which is the case for most of the RG flows we looked at – the scaling function obtained from the NLIEs shows clear signs of multi-scale behaviour in the UV, with exponents agreeing with the operators predicted by the anomaly-matching conditions. Additionally, for the deformations triggered by the $\phi_{(1,3)}$, $\phi_{(1,5)}$, $\phi_{(2,1)}$ and $\phi_{(1,2)}$ operators, the kernels of the NLIEs reduce to the known ones [227–234]. This is substantial evidence supporting the interpretation of the NLIEs as a universal description for RG flows between minimal models. Definitive evidence will come from

accurate numerical investigation and by comparison against Conformal Perturbation Theory [224] or Hamiltonian Truncation [235]. We will embark on this project in the near future. The NLIEs are a potential non-perturbative description for all the flows $\mathcal{M}(kq+I,q) \xrightarrow{\phi_{(1,2k+1)}} \mathcal{M}(kq-I,q)$ conjectured in [98], providing an explicit proof of their existence. They greatly expand the class of flows that can be studied non-perturbatively, even in the absence of a known integrable structure.

7.1 Primer on Virasoro minimal models.

In this section we collect some basic notions on minimal models and we fix the conventions used in this letter. Virasoro Minimal Models $M(p,q)$, with p,q being coprime integers (we take with $p>q$), are 2d rational CFTs enjoying diagonal Modular Invariance. Their central charge is:

$$c(p,q) = 1 - 6\frac{(p-q)^2}{pq}\,, \tag{7.1.1}$$

they consist of $(p-1)(q-1)/2$ primaries $\phi_{(r,s)}$ in a fundamental domain $r=1,\cdots,q-1\,, s=1,\cdots,p-1$ with $sq+rp<pq$, having conformal weights:

$$h_{(r,s)} = h_{(q-r,p-s)} = \frac{(pr-qs)^2-(p-q)^2}{4pq}\,. \tag{7.1.2}$$

For simplicity, we will often denote the primaries just by ϕ_ρ, with $\phi_0 = \phi_{(1,1)} = \mathbb{1}$.

The primary fields form the fusion ring:

$$[\phi_\rho]\times[\phi_\sigma] = \sum_\kappa N^\kappa_{\rho\sigma}\,[\phi_\kappa] \tag{7.1.3}$$

where the fusion coefficients $N^\kappa_{\rho\sigma}$ are given in terms of the modular S-matrix $S_{\rho\sigma}$ as:

$$N^\kappa_{\rho\sigma} = \sum_\lambda \frac{S_{\rho\lambda}\,S_{\sigma\lambda}S_{\kappa\lambda}}{S_{0\lambda}} \tag{7.1.4}$$

$$S_{(r,s),(\rho,\sigma)} = (-1)^{1+s\rho+r\sigma}\sqrt{\frac{8}{pq}}\sin\left(\pi\frac{p}{q}r\rho\right)\,\sin\left(\pi\frac{q}{p}s\sigma\right) \tag{7.1.5}$$

The topological Verlinde line operators, are in one-to-one correspondence with the primary fields $\mathcal{L}_{(r,s)}$ (that we will also equivalently denote as $\mathcal{L}_\rho$). They satisfy the same fusion ring as the primary fields:

$$\mathcal{L}_\rho\times\mathcal{L}_\sigma = \sum_\lambda N^\lambda_{\rho\sigma}\,\mathcal{L}_\lambda\,. \tag{7.1.6}$$

We denote the fusion modular category generated by the Verlinde lines by $\mathcal{V}_{(p,q)}$.

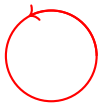
Let us denote by $\phi_\rho\,|0\rangle = |\phi_\rho\rangle$ a state on the cylinder. Then, the action of a Verlinde line on a primary field is given by:

$$\mathcal{L}_\rho\,|\phi_\sigma\rangle = \quad \mathcal{L}_\rho \quad \phi_\sigma \quad = \frac{S_{\rho\sigma}}{S_{0\sigma}}\,|\phi_\sigma\rangle\,. \tag{7.1.7}$$



The action of a Verlinde line on a field, should be thought as generating the Ward Identity for the discrete symmetries associated to the topological line. The vacuum expectation value of a Verlinde line on the cylinder is known as *Quantum dimension*:

$$\langle \mathcal{L}_\rho \rangle = \langle 0 | \, \mathcal{L}_\rho \, | 0 \rangle = \quad \mathcal{L}_\rho \quad = d_\rho \, . \tag{7.1.8}$$



Whenever the symmetry generated by $\mathcal{L}_\rho$ is an invertible and non-anomalous group-like element, then $d_\rho = 1$, but it is an irrational number for a non-invertible element of the fusion category, and it can be dressed by a phase whenever the symmetry has a 't Hooft anomaly.

The torus partition function with the insertion of a Verlinde line operator $\mathcal{L}$ along the spatial cycle is after a modular transformation, the partition function over the defect Hilbert space $\mathcal{H}_\mathcal{L}$ of local operators living at the endpoint of $\mathcal{L}$. It is given explicitly by a twisted trace over the Virasoro characters:

$$Z_{\mathcal{L}_\lambda}(\tau, \overline{\tau}) = \sum_{\rho,\sigma} N^\lambda_{\rho\sigma} \, \chi_\rho(\tau) \, \overline{\chi}_\sigma(\overline{\tau}) \, . \tag{7.1.9}$$

From (7.1.9) we read off the spin content of the defect Hilbert space by evaluating

$$s_\lambda = (h_\rho - h_\sigma) \mod \mathbb{Z} \tag{7.1.10}$$

over non-zero fusion coefficients. Spins being non-semi integers signal the presence of a 't Hooft anomaly of the global symmetry generated by $\mathcal{L}_\lambda$

7.2 RG flows between Virasoro Minimal Models

Consider a UV fixed point described by a Virasoro minimal model $\mathcal{T}_{\rm UV} = M(p,q)$.

Here, we are interested in studying deformations of the UV theory by one of its relevant ($h_{(r,s)} < 1$) primary fields:

$$\mathcal{H}_{M(p,q)} + g_{(r,s)} \int \mathrm{d}x \, \phi_{(r,s)} \, , \tag{7.2.1}$$

where $\mathcal{H}_{M(p,q)}$ is the Hamiltonian of the minimal model $M(p,q)$. The IR fixed point at the end of this RG flow may be either *gapped* or *gapless*. The former case is typical for generic deformations, having an IR described by a Topological Quantum Field Theory (TQFT). We will not consider these in our analysis, albeit they can be studied with similar techniques to those discussed here [98,192,201,204–206,236]. We refer the reader to the discussion at the end of this letter for comments on this matter. In the latter case, when the IR theory is gapless, we assume here it may be described by another minimal model itself :

$$\mathcal{T}_{\rm UV} \quad = \quad M(p,q) \xrightarrow{\phi_{(r,s)}} M(p',q') \quad = \quad \mathcal{T}_{\rm IR} \, . \tag{7.2.2}$$

An important constraint on $\mathcal{T}_{\rm IR}$ is given by the $c_{\rm eff}$-theorem: along RG flows between $\mathcal{PT}$-symmetric non-unitary CFT, the effective central charge:

$$c_{\rm eff}(p,q) = 1 - \frac{6}{pq} \tag{7.2.3}$$

is monotonically decreasing [237], and reduces to the usual Zamolodchikov c-theorem [238] for the case of unitary CFT. We will assume that $\mathcal{PT}$-symmetry is always preserved along our flows, as tested by now in all the examples considered in the literature [184,185,215–217], where it has been observed that CFT transition happens precisely at the spontaneous $\mathcal{PT}$ breaking locus. Furthermore, $\mathcal{PT}$-symmetry guarantees the reality of the energy spectrum at finite volume (and therefore of conformal dimensions) along the entire flow down to the IR CFT, as is the case for the non-unitary minimal models. Stringent constraints follow from the non-invertible symmetry lines of the minimal models. We will describe a very general strategy we plan to employ also for more general UV fixed points in future work.

Whenever, for any state on the cylinder $|\Phi\rangle$, the line $\mathcal{L}_\sigma$ commutes with the deformation triggering the RG flow:

$$\Big[\mathcal{L}_\sigma, \phi_{(r,s)}\Big]\,|\Phi\rangle = 0\,, \tag{7.2.4}$$

then the line operator $\mathcal{L}_\sigma$ is unbroken by the deformation. The maximal subcategory $\{\mathcal{L}_\sigma\}^{(r,s)}_{\rm UV} \subset \mathcal{V}_{(p,q)}$ of Verlinde lines commuting with the deformation is closed under fusion and generates the symmetry that is preserved along the RG flow. Using the fusion rules and Verlinde line action on the primary fields:

$$\mathcal{L}_\sigma\,|\phi_\rho\rangle = \quad \mathcal{L}_\sigma \quad \phi_\rho \quad = \frac{S_{\sigma\rho}}{S_{0\rho}}\,|\phi_\rho\rangle\ , \tag{7.2.5}$$

(7.2.4) is turned into a trigonometric equation for the label σ, at fixed (r,s). In particular, it implies that the quantum dimension of the preserved lines is an RG flow invariant:

$$\mathcal{L}_\sigma \quad \phi_\rho \quad |\Phi\rangle \quad = \quad \mathcal{L}_\sigma \quad \phi_\rho \quad |\Phi\rangle \tag{7.2.6}$$

as well as the spin content of the defect Hilbert spaces associated with the preserved lines $\mathcal{H}_{\mathcal{L}_\sigma}$[1]. These two pieces of RG-invariant categorical data are to be considered as 't Hooft anomaly matching conditions in the realm of fusion categories. To explore the possible $\mathcal{T}_{\rm IR}$ we proceed as follows:

1. Given $\mathcal{T}_{\rm UV}$, for any relevant primary field $\phi_{(r,s)}$ of $\mathcal{T}_{\rm UV}$, we compute the fusion subcategory[2] of Verlinde lines $\{\mathcal{L}_\sigma\}^{(r,s)}_{\rm UV}$ commuting with the perturbation via eq. (7.2.4).

[1] More precisely, the defect spin content in the IR is a subset of the UV one due to possible massive decouplings.

[2] Note that this implies the closure of this category under fusion.

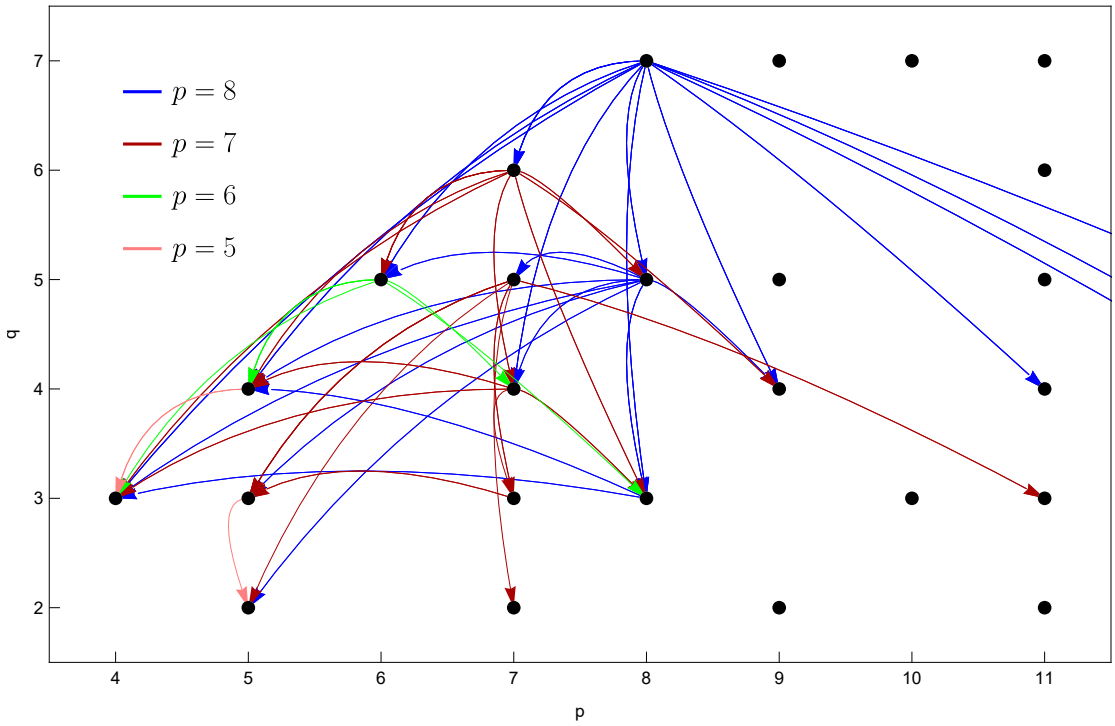


Figure 7.1: Flows between minimal models determined by our algorithm$\mathcal{T}_{\text{UV}} = M(p \leq 8, q)$.

2. We generate a list of the possible minimal models $\mathcal{T}_{\text{IR}}$ that satisfy $c_{\text{eff}}(\mathcal{T}_{\text{UV}}) > c_{\text{eff}}(\mathcal{T}_{\text{IR}})$. This list is always finite.

3. We select among the $\mathcal{T}_{\text{IR}}$ determined above, only the minimal models containing a fusion subcategory $\{\mathcal{L}_\rho\}_{\text{IR}}$ of Verlinde lines coinciding with $\{\mathcal{L}_\sigma\}_{\text{UV}}^{(r,s)}$. This means that all the quantum dimensions, fusion rules, and spins in the defect Hilbert spaces in these two subcategories coincide with $\{\mathcal{L}_\sigma\}_{\text{UV}}^{(r,s)}$.

This, for any given (p, q) produces a list of candidate flows of the form (7.2.2) fulfilling all the anomaly-matching conditions by construction. This procedure shall be regarded as exclusive rather than inclusive, meaning that anomaly-matching does not guarantee that the flow will dynamically exist. Generically more than a single relevant operator may trigger the same flow. If the set of operators triggeri ng the flow also preserves the same fusion subcategory of lines, then along the flow all such operators (and all the Virasoro descendants thereof) may be dynamically generated. The critical point in the IR will be hit by fine-tuning a combination of the UV deformations, we refer to the appendix for a more detailed illustration. Lastly, the existence of a gapless flow triggered by a given relevant operator does not exclude the existence of gapped phases for other critical couplings. For example, the $\phi_{(1,3)}$ perturbation of the tricritical Ising model $M(5, 4)$ flows to either a gapped phase or to $M(4, 3)$ depending on the sign of the

perturbation. One can also determine which fields, govern the approachentering direction of the flow to the IR. Indeed, given that the topological lines are preserved along the flow, one can analogously determine which are the most relevant irrelevant operators of $\mathcal{T}_{\rm IR}$, commuting with the same subcategory of the UV theory

Note that those may also be Virasoro descendants of relevant primaries. Often the most relevant irrelevant among the operators is $T\overline{T}$, that is is always a viable direction given that it commutes with all the topological lines. In this case, the flow either enters along the $T\overline{T}$ direction[3] or along the least irrelevant descendant of a (relevant) primary that has commutations relations with the preserved topological lines and RG invariants consistent with the UV data. From this perspective, the non-invertible symmetries also provide a strong organizing principle for the effective field theory (or conformal perturbation theory) expansion around both the UV and IR. The procedure is easily automatized and implemented in `Mathematica`. In Figure 7.1 we report the outcome up to $p = 8$, but it can be readily extended to any value of p [4] . Among others, we reproduce all the $\mathbb{Z}_2$ symmetric flows conjectured in [98], as well as the $\phi_{(1,2)}$, and $\phi_{(2,1)}$ flows known to be integrable [234,239], but not belonging to that family. In addition, we find new flows that are not part of the known families but are allowed by anomaly matching. An example is $M(7,5) \xrightarrow{\phi_{(2,3)}} M(11,3)$ discussed in the Appendix (together with a detailed discussion up to $p = 7$). An interesting case is the integrable flows with $\phi_{(1,5)}$, while $\phi_{(1,3)}$ could a priory be dynamically generated along the flow, the solutions of the NLIEs suggest that this is not the case. We plan to study in detail the relation between integrability and non-invertible symmetries somewhere else.

7.3 Description via NLIE

Since the seminal article [240], it was shown that certain special perturbations of minimal models could be described as *quantum reductions* of integrable quantum field theories. Specifically, perturbations controlled by the relevant field $\phi_{(1,3)}$ are obtained as quantum reductions of the sine-Gordon (sG) model [227,228,241–243], while perturbations by the fields $\phi_{(1,5)}$, $\phi_{(2,1)}$ and $\phi_{(1,2)}$ arise from the quantum reduction of the "Zhiber-Mikhailov-Shabat" (ZMS) model [239,244–246]. Thanks to their integrability, it has been possible to derive a Non-Linear Integral Equation (NLIE) that *non-perturbatively* encodes the energies $E_{\rm s}(R)$ of any state s on a cylinder of radius R, which acts as an RG parameter. As functions of $r = Rm$, with m being the mass scale of the system, the energies interpolate between the UV regime

$$E_{\rm s}(R) \xrightarrow{r\to 0} -\frac{\pi(c_{\rm UV} - 24h_{\rm s})}{6R}\,,$$

the usual Casimir behaviour [247], and the IR one

$$E_{\rm s}(R) \xrightarrow{r\to\infty} {\rm N}_{\rm s} \in \mathbb{Z}_{\geq 0}\,.$$

[3] E.g. $M(3,4) \to M(2,5)$, or $M(4,5) \to M(3,4)$. See Appendix B for more examples.

[4] The known flows[184,185] $M(2k+1,2) \to M(2k+1,2)$ are not displayed in the figure given that these degenerate cases where all the topological lines are broken are not determined by our method.

In [229,232,233] it was shown that the integrable structure of sG could be equally well employed to encode *massless flows* interpolating between successive unitary minimal models $M(p+1,p) \xrightarrow{\phi_{(1,3)}} M(p,p-1)$. Soon it became clear that this description could also address flows $M(p,q) \xrightarrow{\phi_{(1,3)}} M(2p-q,q)$ [230,231] and, using the integrable structure of ZMS, massless flows $M(2p+I,p) \xrightarrow{\phi_{(1,5)}} M(2p-I,p)$ and lastly in [234] the flows $M(2p-I,p) \xrightarrow{\phi_{(2,1)}} M(2p-I,p-I)$.

One of the main results of this letter is that the NLIEs encoding the finite size spectrum of massless flows between minimal models can be extended – at the very least on a qualitative level – beyond the $\phi_{(1,3)}$, $\phi_{(1,5)}$, $\phi_{(2,1)}$ and $\phi_{(1,2)}$ cases, to the whole family of flows predicted by anomaly matching conditions associated to non-invertible symmetries.

The structure of the "massless NLIEs" is the same as for the known cases [229,234]: one first computes the solutions $f_{\mathrm{R}}(\theta)$ and $f_{\mathrm{L}}(\theta)$ to the following coupled NLIE system

$$\begin{aligned} f_{\mathrm{R}}(\theta) &= i\alpha' - i\frac{r}{2}e^{\theta} - \sum_{\sigma=\pm}\sigma\int_{\mathcal{C}_{\mathrm{s}}^{\sigma}} d\theta' \left[\phi(\theta-\theta')L_{\mathrm{R}}^{-\sigma}(\theta') + \chi(\theta-\theta')L_{\mathrm{L}}^{\sigma}(\theta')\right], \\ f_{\mathrm{L}}(\theta) &= -i\alpha' - i\frac{r}{2}e^{-\theta} + \sum_{\sigma=\pm}\sigma\int_{\mathcal{C}_{\mathrm{s}}^{\sigma}} d\theta' \left[\phi(\theta-\theta')L_{\mathrm{L}}^{\sigma}(\theta') + \chi(\theta-\theta')L_{\mathrm{R}}^{-\sigma}(\theta')\right], \end{aligned} \tag{7.3.1}$$

where $L^{\pm}_{\substack{\mathrm{R}\\\mathrm{L}}}(\theta) = \log\left[1+\exp\left(\pm f_{\substack{\mathrm{R}\\\mathrm{L}}}(\theta)\right)\right]$. Then, the *scaling function* $f_s(r) = 6RE_{\mathrm{s}}(R)/\pi$ is determined as

$$f_s(r) = \sum_{\sigma=\pm}\frac{3ir\sigma}{2\pi^2}\int_{\mathcal{C}_{\mathrm{s}}^{\sigma}} d\theta \left[e^{-\theta}L_{\mathrm{L}}^{\sigma}(\theta) - e^{\theta}L_{\mathrm{R}}^{-\sigma}(\theta)\right]. \tag{7.3.2}$$

In these equations, the parameter α' is known as *twist*. The kernels $\phi(\theta)$ and $\chi(\theta)$ identify the specific theory, while the contours $\mathcal{C}_{\mathrm{s}}^{\pm}$ determine the state. In particular, the ground state is obtained with the choice $\mathcal{C}_{\mathrm{s}}^{\pm} = \mathbb{R} \pm i\eta$, with $\eta \gtrsim 0$.

The flows described in this letter correspond to the following choice of kernels[5]

$$\begin{aligned} \phi(\theta) &= -\int_{\mathbb{R}}\frac{d\omega}{2\pi}e^{i\theta\omega}\frac{\sinh\left(\frac{1}{\kappa}\pi\omega\right)\cosh\left(\frac{2\xi-\kappa}{2\kappa}\pi\omega\right)}{\sinh\left(\frac{\xi-1}{\kappa}\pi\omega\right)\cosh\left(\frac{1}{2}\pi\omega\right)}, \\ \chi(\theta) &= -\int_{\mathbb{R}}\frac{d\omega}{2\pi}e^{i\theta\omega}\frac{\sinh\left(\frac{1}{\kappa}\pi\omega\right)\cosh\left(\frac{\kappa-2}{2\kappa}\pi\omega\right)}{\sinh\left(\frac{\xi-1}{\kappa}\pi\omega\right)\cosh\left(\frac{1}{2}\pi\omega\right)}, \end{aligned} \tag{7.3.3}$$

[5]We find it worth mentioning that these kernels were derived from an educated guess. We asked their Fourier transform to have the following properties: 1) be a ratio of trigonometric functions; 2) be non-vanishing at $\omega = 0$ (as this value enters the expressions of $c_{\mathrm{eff}}^{\mathrm{UV/IR}}$ and $h_{(r,s)}$); 3/ be decaying as $\omega \to \pm\infty$; 4/ present poles at $\omega = \pm i$ (which produce the bulk term in the UV expansion of $f(r)$); 5/ present two free parameters (that, along with the twist α, allow to tune the UV and IR central charges and the UV conformal dimension at will). Asking additionally for a minimal number of trigonometric functions, we arrived at the expressions (7.3.3).

where $\kappa > 2$ and $\xi > 1$, making the Fourier image integrable[6] on $\mathbb{R}$. The physical parameters of the UV and IR CFTs are determined as follows

$$\begin{aligned} c_{\text{eff}}^{\text{UV}}(p,q) &\equiv 1 - \frac{6}{pq} = 1 - 3\left(\frac{\alpha'}{\pi}\right)^2 \frac{(\xi-1)^2}{\xi(\xi+1)}\,, \\ c_{\text{eff}}^{\text{IR}}(p',q') &\equiv 1 - \frac{6}{p'q'} = 1 - 3\left(\frac{\alpha'}{\pi}\right)^2 \frac{\xi-1}{\xi}\,, \\ h_{(r,s)} &\equiv \frac{(pr-qs)^2-(p-q)^2}{4pq} = 1 - \frac{1}{z_{(r,s)}}\frac{\kappa}{\xi+1}\,. \end{aligned} \tag{7.3.4}$$

with $h_{(r,s)}$ being the conformal dimension of the perturbing field $\phi_{(r,s)}$ in the UV and $z_{(r,s)} = 1, 2$ depending on whether the field $\phi_{(r,s)}$ is even or odd under the natural $\mathbb{Z}_2$ symmetry in the UV[7]. Fixing these three physical parameters, i.e. choosing a UV starting CFT, together with an outgoing direction, and a target IR CFT uniquely fixes the form of the NLIEs (7.3.1). Consequently, any additional information extracted from (7.3.2) can be considered a non-trivial prediction. One quantity that can be analytically computed is the conformal dimension of the operator that attracts the flow in the IR CFT:

$$h_{(r',s')} = 1 + \frac{1}{z_{(r',s')}}\frac{\kappa}{\xi-1}\,. \tag{7.3.5}$$

The request that this conformal dimension appears, as it should, in the Kač table of the IR minimal model $\mathcal{M}(p',q')$ enforces a constraint on the allowed values of the integers p, q, p', q', r, s, r', and s'.

$$\frac{p(r+1)-q(s-1)}{p'(r'+1)-q'(s'-1)} = -\frac{z_{(r',s')}}{z_{(r,s)}}\frac{p'(r'-1)-q'(s'+1)}{p(r-1)-q(s+1)}\,, \tag{7.3.6}$$

While we could not find the most general solution to the above Diophantine equation, we can verify that the special family of solutions that corresponds to the flows discovered in [98]

$$\{M_{(\mu p+I,p)} \xrightarrow{\phi_{(1,2\mu+1)}} M_{(\mu p-I,p)}\}\,, \tag{7.3.7}$$

solve all the constraints with 2μ and $\mu p - I$ being positive integers. This family includes the familiar $\phi_{(1,3)}$, $\phi_{(1,5)}$, $\phi_{(2,1)}$ and $\phi_{(1,2)}$ flows[8]. In the Appendix, we show how the NLIEs (7.3.1) reduce the known integrable cases for $\mu = 1/2, 1, 2$[9]. where $p'/2 \leq p \leq p' - 2$. Further restrictions can be imposed on the solutions using the non-invertible symmetry matching.

[6] The limit case $\kappa = 2$ yields the $\phi_{(1,3)}$ massless flows [229–231]. This limit is non-trivial and is discussed in details in the supplementary material.

[7] Specifically, $z_{(r,s)} = 1 + \big[\big(p(r-1) - q(s-1)\big) \pmod 2\big]$.

[8] The case $\phi_{(2,1)}$ in eq. (3.9) in [234] is recovered from (7.3.7) by setting $\mu = 1/2$, re-defining $p = 2P - J$ and $I = J/2$ and swapping the indices of the minimal models and of the primary fields.

[9] It is perhaps worth to remark that we did not ask for the known integrable cases to be included in the educated guess that yielded (7.3.3). This is a post-hoc result that reveals our kernels to be a 1-parameter deformation of the known integrable ones.

7.3.1 Recovering the known, integrable cases

The NLIEs in eq. (7) of the main text with kernels given in eq. (9) there, are conjectured to encode the spectrum of a very wide class of massless flows. Amongst these – in particular, in the class of Tanaka-Nakayama's flows (eq. (13) of the main text) – are the more familiar $\phi_{(1,3)}$, $\phi_{(1,5)}$, and $\phi_{(1,2)}$ flows, studied since the '90s in the literature [229–234]. It is straightforward to check that the choice $\kappa = 3$ yields the same kernels considered in [234]. Indeed it is not difficult to see that the parameter μ in eq. (13) of the main text is related to κ as $\mu = \kappa/z_{(1,2\mu+1)} - 1$. Since $z_{(1,2\mu+1)}$ can be either 1 or 2 for $\mathbb{Z}_2$ even or odd operators, respectively, we have the two options $\mu = 2$ or $\mu = 1/2$, corresponding, respectively, to $\phi_{(1,5)}$ and $\phi_{(1,2)}$ deformations.

Recovering $\phi_{(1,3)}$ is slightly more subtle[10]. In fact, one would need to set $\kappa = 2$ in the expressions of the kernels in eq. (9) of the main text, which is not immediately possible, since for $\kappa = 2$ the Fourier image of $\phi(\theta)$ is not integrable on $\mathbb{R}$. We need to proceed more carefully. We notice that

$$\lim_{\kappa\to 2}\hat{\phi}(\omega) = 2\hat{\phi}_{\rm Z}(\omega) - 1\ , \qquad \lim_{\kappa\to 2}\hat{\chi}(\omega) = 2\hat{\chi}_{\rm Z}(\omega)\ , \tag{7.3.8}$$

where $\hat{\phi}(\omega)$ and $\hat{\chi}(\omega)$ are the Fourier images of the kernels in eq. (9) of the main text. The Fourier images $\hat{\phi}_{\rm Z}(\omega)$ and $\hat{\chi}_{\rm Z}(\omega)$ are those used in [230,231,248] to describe the $\phi_{(1,3)}$ massless flows. Then we find

$$\lim_{\kappa\to 2}\phi(\theta) = 2\phi_{\rm Z}(\theta) - \delta(\theta)\ , \qquad \lim_{\kappa\to 2}\chi(\theta) = 2\chi_{\rm Z}(\theta)\ . \tag{7.3.9}$$

At the level of the NLIEs in eq. (7) of the main text, we take the limit $\kappa \to 2$ and find

$$\begin{aligned}
f_{\rm R,Z}(\theta) &= i\alpha' - i\frac{r}{2}e^{\theta} - 2\sum_{\sigma=\pm}\sigma\int_{\mathcal{C}_{\rm s}^{\sigma}} d\theta'\,\Big[\phi_{\rm Z}(\theta-\theta')L^{-\sigma}_{\rm R,Z}(\theta') + \chi_{\rm Z}(\theta-\theta')L^{\sigma}_{\rm L,Z}(\theta')\Big] + \\
&\quad + \sum_{\sigma=\pm}\sigma\int_{\mathcal{C}_{\rm s}^{\sigma}} d\theta'\,\delta(\theta-\theta')L^{-\sigma}_{\rm R,Z}(\theta')\ , \\
f_{\rm L,Z}(\theta) &= -i\alpha' - i\frac{r}{2}e^{-\theta} + 2\sum_{\sigma=\pm}\sigma\int_{\mathcal{C}_{\rm s}^{\sigma}} d\theta'\,\Big[\phi(\theta-\theta')L^{\sigma}_{\rm L,Z}(\theta') + \chi(\theta-\theta')L^{-\sigma}_{\rm R,Z}(\theta')\Big] + \\
&\quad - \sum_{\sigma=\pm}\sigma\int_{\mathcal{C}_{\rm s}^{\sigma}} d\theta'\,\delta(\theta-\theta')L^{\sigma}_{\rm L,Z}(\theta')\ .
\end{aligned} \tag{7.3.10}$$

Now, from the definition of the functions $L^{\pm}$ we have the identity

$$\sum_{\sigma=\pm}\sigma\int_{\mathcal{C}_{\rm s}^{\sigma}} d\theta'\,\delta(\theta-\theta')L^{-\sigma}_{\rm R,Z}(\theta') = -\int_{-\infty}^{\infty} d\theta'\,\delta(\theta-\theta')f_{\rm R,Z}(\theta') = -f_{\rm R,Z}(\theta)\ , \tag{7.3.11}$$

[10] We thank Roberto Tateo for suggesting this calculation.

where we used the Cauchy theorem. A similar manipulation can be performed for the term with subscript L. Now, a slight shuffling of the furniture in (7.3.10), yields

$$f_{\mathrm{R,Z}}(\theta) = i\frac{\alpha'}{2} - i\frac{r}{4}e^{\theta} - \sum_{\sigma=\pm}\sigma\int_{\mathcal{C}_{\mathrm{s}}^{\sigma}} d\theta' \left[\phi_{\mathrm{Z}}(\theta-\theta')L_{\mathrm{R,Z}}^{-\sigma}(\theta') + \chi_{\mathrm{Z}}(\theta-\theta')L_{\mathrm{L,Z}}^{\sigma}(\theta')\right],$$
$$f_{\mathrm{L,Z}}(\theta) = -i\frac{\alpha'}{2} - i\frac{r}{4}e^{-\theta} + \sum_{\sigma=\pm}\sigma\int_{\mathcal{C}_{\mathrm{s}}^{\sigma}} d\theta' \left[\phi(\theta-\theta')L_{\mathrm{L,Z}}^{\sigma}(\theta') + \chi(\theta-\theta')L_{\mathrm{R,Z}}^{-\sigma}(\theta')\right], \tag{7.3.12}$$

which coincides precisely with the equations in [230,231,248], provided that we rescale α' and r by a factor 2.

7.3.2 Numerical analysis and conformal perturbation theory.

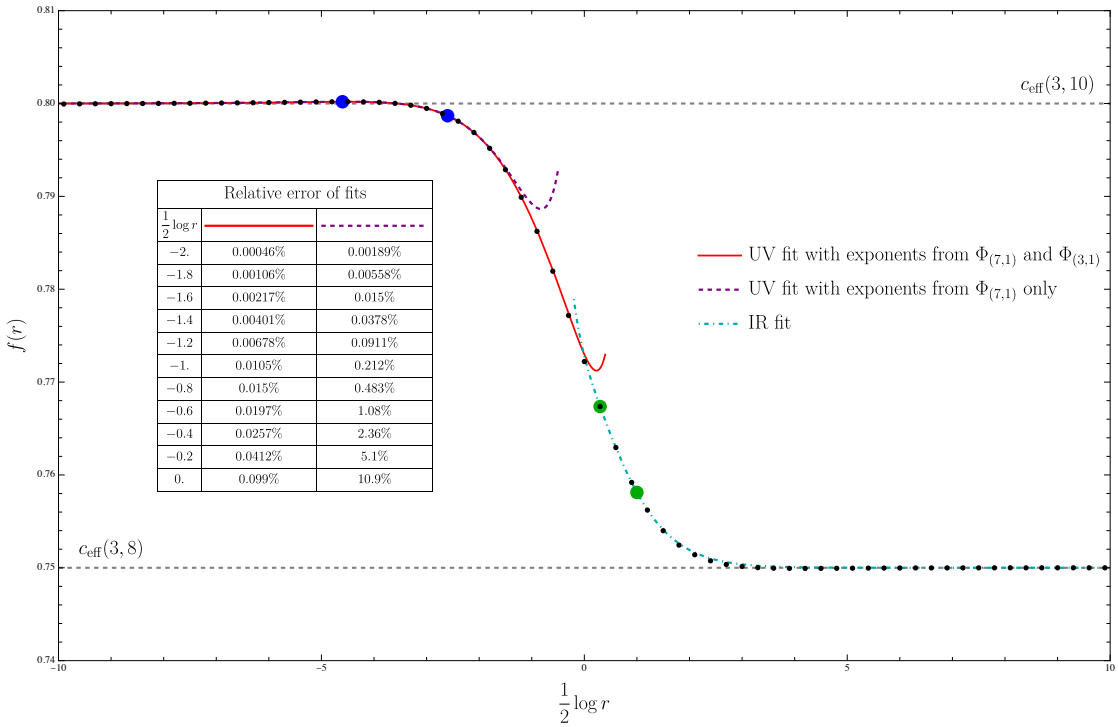
Extracting analytically any further non-trivial prediction from NLIEs of the form (7.3.1, 7.3.2) is a notoriously arduous task. We can make some headway by studying them numerically. In particular, we can compare the behavior of the scaling function for large and small values of r to the predicted behaviour of the ground-state energy along the flow (7.2.2). Contrary to the well-known integrable cases, we expect the general flow to be a *multi-field deformation* of the UV CFT, with the IR theory only arising upon fine-tuning of the critical coupling of the various deforming fields, e.g. in the flow $\mathcal{M}(7,2) \to \mathcal{M}(5,2)$, where both UV fields $\phi_{(1,2)}$ and $\phi_{(1,3)}$ were seen to contribute by using a Hamiltonian truncation method [184,185]. Indeed, all relevant operators allowed by the preserved generalized symmetries will contribute to the flow, in agreement with the standard Wilsonian RG lore. For a flow triggered by a number M of relevant UV fields $\{\phi_{(r_i,s_i)}\}_{i=1}^{M}$, the expected small r behaviour of the scaling function (7.3.2) is

$$\begin{aligned} f(r) \overset{r\to 0}{=} & \frac{3r^2/(4\pi)}{\sin\left(\frac{\pi\kappa}{\xi+1}\right)} + \sum_{\{l_i\}=0}^{\infty} a_{l_1,\dots,l_M} r^{\sum_{i=1}^{M} l_i y_{(r_i,s_i)}}, \\ y_{(r,s)} = & 2z_{(r,s)}(1-h_{(r,s)}), \\ a_{0,0,\dots,0} = & c_{\mathrm{eff}}(p,q) = 1 - \frac{6}{pq}. \end{aligned} \tag{7.3.13}$$

Here the coefficients $a_{l_1,\dots,l_M}$ are proportional to the correlation functions of the perturbing fields on the vacuum (see [249] for more details). While the expansion (7.3.13) is expected to have a finite radius of convergence [224,249], the situation in the IR is much less under control. There, the Conformal Perturbation Theory (CPT) expansion

$$f(r) \overset{r\to\infty}{=} f(p',q') + \sum_{l=1}^{\infty}\left(a'_l r^{l y_{(r',s')}} + b'_l r^{-2l}\right) + \cdots \tag{7.3.14}$$

is asymptotic, and there is little [250] control over the omitted further contributions. We performed a numerical analysis of the NLIEs (7.3.1) for several cases and found that, in



Relative error of fits

$\frac{1}{2}\log r$	—	- - -
−2.	0.00046%	0.00189%
−1.8	0.00106%	0.00558%
−1.6	0.00217%	0.015%
−1.4	0.00401%	0.0378%
−1.2	0.00678%	0.0911%
−1.	0.0105%	0.212%
−0.8	0.015%	0.483%
−0.6	0.0197%	1.08%
−0.4	0.0257%	2.36%
−0.2	0.0412%	5.1%
0.	0.099%	10.9%

Figure 7.2: Ground state scaling function (7.3.2) for the flow $\mathcal{M}(10,3) \to \mathcal{M}(8,3)$, triggered by $\phi_{(1,7)}$. We fitted the points between the pairs of larger blue and green dots against UV and IR CPT predictions, respectively. The fit performed including the contributions of all perturbing fields (red full line) – here $y_{(1,5)} = 3y_{(1,7)}$ – performs much better than the fit for a single field (purple dashed line). The table collects the relative errors on points that were not used .

all of them, the scaling function (7.3.2) agrees perfectly with the expected behaviours (7.3.13, 7.3.14). While the parameters (7.3.4), are built in the kernel by construction, the agreement with the multiple sum for small r shall be regarded as a highly non-trivial check that our data passes with flying colours. In principle, further support can come from comparing the first few coefficients of the expansions with the estimates coming from CPT. We will report on this in a future publication. Figure 7.2 reports the numerical results for the flow $\mathcal{M}(10,3) \to \mathcal{M}(8,3)$, triggered by $\phi_{(1,7)}$, first proposed in [251], which has recently received a lot of attention [215,217,252]. The fit that includes contributions from all the perturbing fields, is numerically favoured, independently agreeing with the results obtained in [215] by employing Hamiltonian truncation and CPT methods.

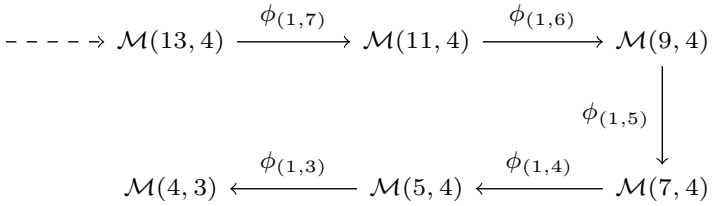


Figure 7.3: Chain of flows from $M(13,4)$ to Ising. We only report in the figure the most relevant deformation triggering the flow.

7.3.3 Chain of flows from $M(13,4)$

We analyse here the NLIE solutions for the chain of flows[11] reported in Figure 7.3, starting with $M(13,4)$ and landing ultimately on the Ising model $M(4,3)$. Using the procedure discussed in the main text we can split this flow in

- $M(13,4) \to M(11,4)$. The most relevant operator triggering the flow is $\phi_{(1,7)}$ preserving the TY_2 fusion category generated by the identity line, the invertible non-anomalous $\mathbb{Z}_2$ line $\mathcal{L}_{(3,1)}$ and $\mathcal{L}_{(2,1)}$ with $d_{(2,1)} = \sqrt{2}$. The spin content of the defect Hilbert space is:

$$s_{(2,1)} = \mathbb{Z} \pm \left\{ \frac{1}{16}, \frac{7}{16} \right\}, \qquad s_{(3,1)} = \mathbb{Z} \pm \left\{ 0, \frac{1}{2} \right\} \tag{7.3.15}$$

  In the IR the flow enters in the $\phi_{(1,7)}$ direction in $M(11,4)$. Furthermore the same category of lines is preserved by the entire tower $\{\phi_{(1,3)}, \phi_{(1,5)}, \phi_{(1,7)}\}$, that are therefore dynamically generated along the $\phi_{(1,7)}$ flow. The operators $\phi_{(1,2)}, \phi_{(1,4)}, \phi_{(1,6)}$ commute only with the $\mathcal{L}_{(1,3)}$, so they cannot be generated by $\phi_{(1,7)}$ flow.

- $M(11,4) \to M(9,4)$. This flow is interesting because it explicitly break the Kramers-Wannier duality defect (this was also observed in [98]). The perturbations are $\phi_{(1,2)}, \phi_{(1,4)}, \phi_{(1,6)}$, in the IR $\phi_{(1,6)}$ arrives on $\phi_{(1,6)}$.

- $M(9,4) \to M(7,4)$. Both UV and IR have anomalous TY_2 category having quantum dimensions $(1, -\sqrt{2}, 1)$. This subalgebra is preserved by $\phi_{(1,5)}, \phi_{(1,3)}$ in the UV, with the former being the most relevant. They enter the IR in the $\phi_{(1,5)}, \phi_{(1,3)}$ directions. The flow is integrable, and single field with $\phi_{(1,5)}$.

- $M(7,4) \to M(5,4)$. Same feature as before: they break KW duality. As in $M(7,4)$ is anomalous, and in $M(5,4)$ is not. The most relevant operator in the UV is $\phi_{(1,4)}$, while $\phi_{(1,2)}$ also preserves $\mathbb{Z}_2$. They enter the IR along the $\phi_{(1,2)}$ direction.

[11] This is a fragment of a semi-infinitely long sequence comprising $M(4k+1,4) \xrightarrow{\phi_{1,2k+1}} M(4k-1,4)$ and $M(4k-1,4) \xrightarrow{\phi_{1,2k}} M(4k-3,4)$. Here, for concreteness, we chose to truncate it at $M(13,4)$.

Flow	UV χ^2_{red}	UV d.o.f.	IR χ^2_{red}	IR d.o.f.
$\mathcal{M}(13,4) \to \mathcal{M}(11,4)$	0.935364	39	1.69241	59
$\mathcal{M}(11,4) \to \mathcal{M}(9,4)$	1.47083	59	0.988184	58
$\mathcal{M}(9,4) \to \mathcal{M}(7,4)$	1.02055	58	1.02304	58
$\mathcal{M}(7,4) \to \mathcal{M}(5,4)$	5.21225	51	56439.4	38
$\mathcal{M}(5,4) \to \mathcal{M}(4,3)$	1.16287	30	0.842416	48

Table 7.1: Quantitative, goodness-of-fit data of the behaviours (eqs. (14) and (15) of the main text) for the numerical data obtained by standard iteration of the NLIEs for the chain of flows in Figure 7.3.

- $M(5,4) \to M(4,3)$. This is the famous Zamolodchikov tri-critical Ising to Ising flow. The only allowed perturbing operator in the UV is $\phi_{(1,3)}$, and the flows enters the IR along the $T\bar{T}$ direction.

We numerically analysed the flows belonging to the chain in Figure 7.3. We fitted the numerical data against the expected UV and IR behaviours in eqs. (14) and (15) of the main text. We found excellent agreement with the predicted behaviour in all cases except the IR of $M(7,4) \to M(5,4)$, in which the numerical data was too unstable to be reliable. More quantitatively, the goodness-of-fit data is collected in Table 7.1. Note that all fits were performed with a CPT series truncated at 10 terms (bulk energy coefficient excluded).

The results are represented graphically in Figure 7.4.

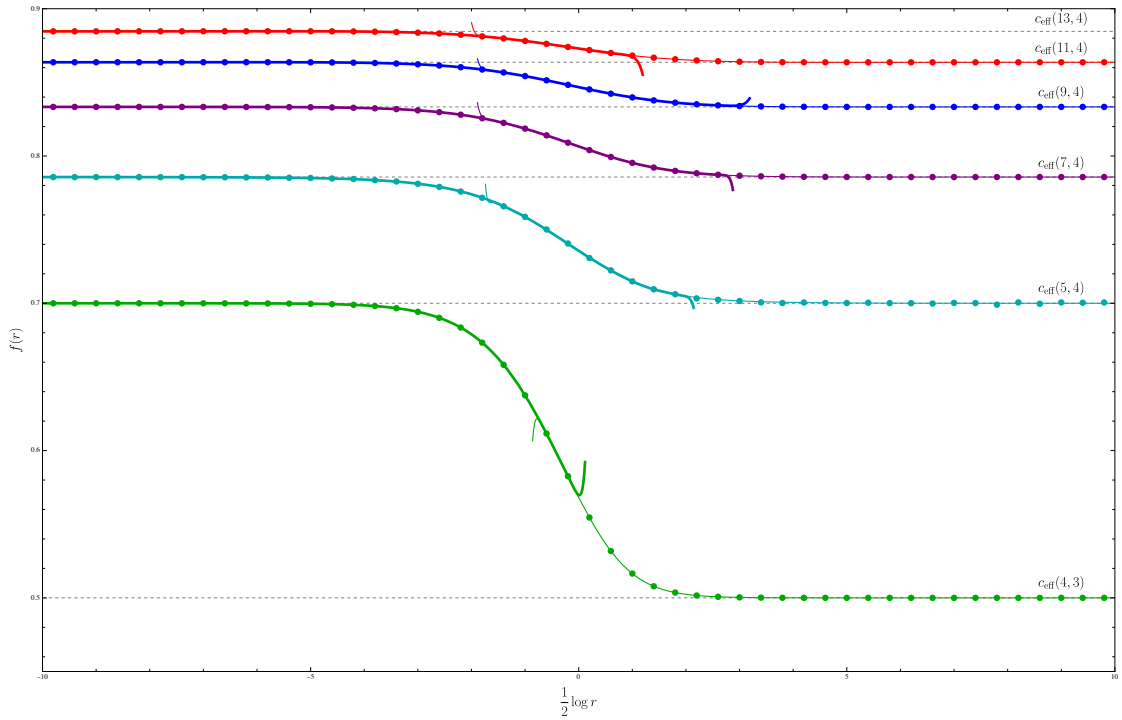


Figure 7.4: Plot of the scaling functions $f(r)$ for the chain of flows in Figure 7.3. The dots represent numerical data obtained by standard iteration of the NLIEs in eq. (7) of the main text. The thick and thin lines were obtained by fitting the numerical data against, respectively, the expected UV and IR behaviours (eqs. (14) and (15) of the main text).

Chapter 8

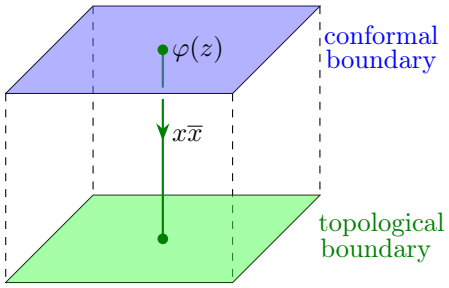
Conserved Defects in 2D CFTs

In this Chapter we construct and study a new set of conserved charges in deformed 2d CFT. Those are non-local charges commuting with the deformed bulk Hamiltonian but not with the Stress-Energy tensor. Our construction builds on the works [99,100,253–257]. Here, we make no direct relation to early work on non-local charges in quantum field theories [258–260] which lie behind Yangian and affine quantum group symmetry of many models.

Below we give a quick summary of our construction using the 3d SymTFT of a 2d CFT and we present our findings in the example of Virasoro minimal models.

We start from a 2d CFT $\mathcal{C}$ which we describe via the SymTFT picture (see [67,261–268]) as a 3d TFT with a conformal and a topological boundary condition. Concretely we will use the 3d TFT obtained by folding from the original TFT description of CFT correlators developed in [65,269,270], see Section 8.1.1. The relation between these two points of view is briefly explained e.g. in [268,271].

The CFT $\mathcal{C}$ is perturbed by a relevant primary field φ, which in the SymTFT is represented by a line defect stretching between the conformal and the topological boundary of the 3d TFT, together with a choice of topological junction on the topological boundary,



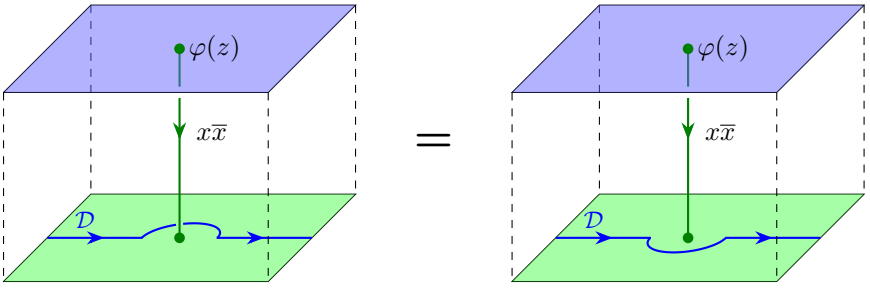
(8.0.1)

The label of the line defect is the product $x\overline{x}$ of line defects x and $\overline{x}$, where x ends on a holomorphic field on the conformal boundary and $\overline{x}$ on an antiholomorphic field.[1] We

[1] In more detail, elementary line defects in this SymTFT are labelled by pairs $u \boxtimes v$, where $u = u \boxtimes \mathbf{1}$ labels a line that ends on a holomorphic field on the conformal boundary, and $v = \mathbf{1} \boxtimes v$ ends on an antiholomorphic field. Using this notation, the product of u and v is $uv = u \boxtimes v$, cf. [268, Fig. 3.4].

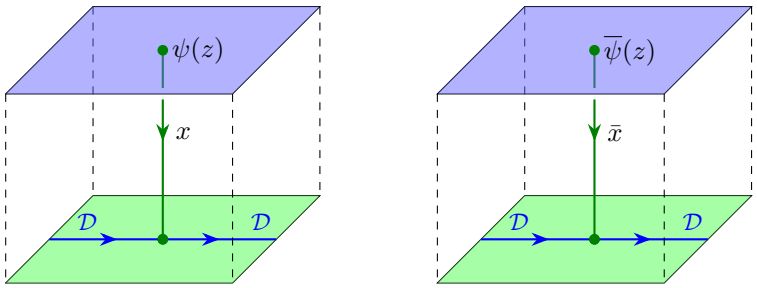
write $\mathcal{C}(\mu\varphi)$ for $\mathcal{C}$ perturbed by $2i\mu\varphi$, $\mu \in \mathbb{C}$. The factor of $2i$ is a convention which reduces the factors of i in our main application, alternatively we could have worked with $\mu' := 2i\mu$ everywhere.

A topological line defect $\mathcal{D}$ in the 2d CFT is represented by a line $\mathcal{D}$ in the topological boundary. If the defect $\mathcal{D}$ commutes with the perturbing field φ, it remains topological in $\mathcal{C}(\mu\varphi)$ for all $\mu \in \mathbb{C}$. In the SymTFT, this condition takes the form



(8.0.2)

Apart from topological defects, the CFT $\mathcal{C}$ contains another important class of defects, namely those which are invariant under rigid translations, i.e. commute with the Hamiltonian of $\mathcal{C}$. Such defects still allow for a non-singular fusion operation and have interesting algebraic properties [99,272]. One can now ask if such translation invariant operators also exist in the perturbed theory $\mathcal{C}(\mu\varphi)$. To this end, denote by ψ and $\overline{\psi}$ the holomorphic and antiholomorphic defect fields on the topological defect $\mathcal{D}$ described in SymTFT as



(8.0.3)

Here, $\mathcal{D}$ can be an elementary defect or a superposition of elementary defects, and ψ can be a linear combination of fields that live on elementary defects and fields that interpolate them.

A simple condition for the existence of translation invariant operators is the *bulk commutation condition* [100], which in the SymTFT picture is given in Figure 8.1. Note that (8.0.2) is a special case of this condition when one chooses $\psi = \overline{\psi} = 0$.

If the bulk commutation condition is satisfied, we obtain a translation invariant operator in $C(\mu\varphi)$ as follows. Denote by $\mathcal{D}(\lambda\psi + \widetilde{\lambda}\,\overline{\psi})$ the topological defect $\mathcal{D}$ perturbed by the defect field $\lambda\psi + \widetilde{\lambda}\,\overline{\psi}$, then for $\lambda\widetilde{\lambda} = \mu$ the perturbed defect $\mathcal{D}(\lambda\psi + \widetilde{\lambda}\,\overline{\psi})$ commutes with the Hamiltonian of the perturbed theory $\mathcal{C}(\mu\varphi)$ (see Section 8.1.2). We refer to $\mathcal{D}(\lambda\psi + \widetilde{\lambda}\,\overline{\psi})$ as a *non-local conserved charge* – "non-local" because it is obtained by integrating (anti)holomorphic fields which only exist on the defect $\mathcal{D}$ and are not local currents in the bulk of the CFT.

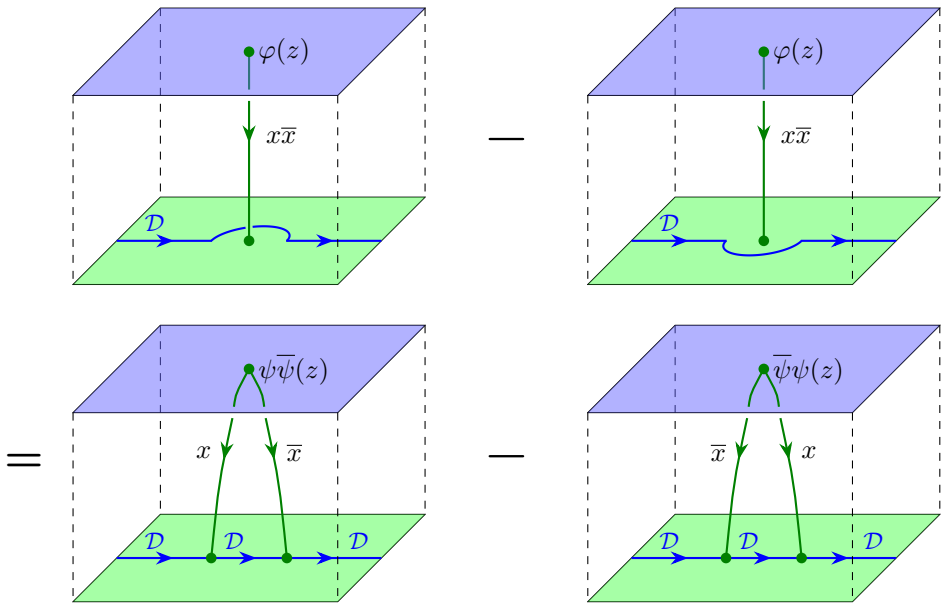


Figure 8.1: Bulk commutation condition in the SymTFT picture

Altogether, we obtain a one-parameter family $\mathcal{D}(\lambda\psi + \mu/\lambda\,\overline{\psi})$ for $\lambda \in \mathbb{C}^\times$ of non-local conserved charges for $\mathcal{C}(\mu\varphi)$. In all the examples we consider in detail, we can moreover show that the defect operators commute for different values of λ,

$$\big[\,\mathcal{D}(\lambda\psi + \mu/\lambda\,\overline{\psi})\,,\,\mathcal{D}(\lambda'\psi + \mu/\lambda'\,\overline{\psi})\,\big] \;=\; 0\;. \tag{8.0.4}$$

In other words, we obtain a one-parameter family of non-local conserved charges in involution in the perturbed CFT $\mathcal{C}(\mu\varphi)$, which is an indication that $\mathcal{C}(\mu\varphi)$ describes an integrable deformation of $\mathcal{C}$.

Such non-local conserved charges were first considered in the chiral free boson theory in [253,255,256] and for chiral minimal models in [254]. The formulation in terms of perturbed defects in full minimal models was given in [99,100] using the TFT formulation of CFT correlators.

If we apply the above to the unperturbed theory, i.e. to $\mathcal{C}(\mu\varphi)$ with $\mu = 0$, we are lead to considering $\mathcal{D}(\lambda\psi + \widetilde{\lambda}\,\overline{\psi})$ with either $\lambda = 0$ or $\widetilde{\lambda} = 0$. Indeed, the defect D perturbed by only ψ or by only $\overline{\psi}$ commutes with the conformal Hamiltonian and provides families of non-local conserved charges in the CFT $\mathcal{C}$ [99].

To summarise the discussion so far, in addition to the topological line defects $\mathcal{T}(\mu)_{\text{top}}$ of $\mathcal{C}(\mu\varphi)$, one should consider all rigidly translation invariant defects $\mathcal{T}(\mu)$ in $\mathcal{C}(\mu\varphi)$. These share some of the good properties with $\mathcal{T}(\mu)_{\text{top}}$, in particular their fusion is non-singular so that $\mathcal{T}(\mu)$ is a monoidal category (see Section 8.1.5). The bulk commutation condition gives access to perturbatively defined rigidly translation invariant defects

$\mathcal{T}(\mu)_{\text{pert}}$, and it turns out that these again close under fusion. We obtain inclusions of monoidal subcategories,

$$\mathcal{T}(\mu)_{\text{top}} \ \subset \ \mathcal{T}(\mu)_{\text{pert}} \ \subset \ \mathcal{T}(\mu) \ . \tag{8.0.5}$$

This contains the case $\mu = 0$ of the unperturbed theory. We propose that considering $\mathcal{T}(\mu)$, rather than just $\mathcal{T}(\mu)_{\text{top}}$, gives important additional information about the family of perturbed CFTs $C(\mu\varphi)$. For example, a rigidly translation invariant defect is expected to flow to a topological defect in the infrared theory as the requirement of conformal invariance combined with translation invariance is sufficient to prove a defect is topological, as we show in Section 8.1.5.

In this thesis we restrict our attention to two-dimensional QFTs, but rigidly translation invariant defects can be considered in d-dimensional QFTs as well. They would again have well-defined fusion and would form a d-categorical structure extending that of topological defects.

Let us now turn to examples of the above construction. We focus on A-type minimal models $M(p,q)$. Here $p, q \geq 2$ are coprime integers.

Denote by $\mathcal{I}$ the set of Kac-labels for $M(p,q)$, that is all (r,s) with $1 \leq r < p$ and $1 \leq s < q$ modulo the identification $(r,s) \sim (p-r, q-s)$. We write $h_{r,s}$ for the conformal weight of the primary state in the irreducible Virasoro representation corresponding to (r,s). The primary bulk fields of $M(p,q)$ are labelled by $x = (r,s) \in \mathcal{I}$ and have conformal weights $(h_{r,s}, h_{r,s})$. The elementary topological line defects are equally labelled by $a = (r,s) \in \mathcal{I}$ [270,273], and the (anti)holomorphic defect fields which live on the topological defect a are precisely those of weight $(h_y, 0)$ or $(0, h_y)$ for y occurring in the fusion $a \otimes a$, i.e. those for which $N_{aa}^{\ y} \neq 0$.

In Table 8.1 we list the cases of primary bulk fields φ and topological defect D that we investigate in some detail in Section 8.2. Each produces a solution to the bulk commutation condition in Figure 8.1 and – at least in the cases where the perturbation does not require regularisation – a one-parameter family of translation invariant defect operators $\mathcal{D}(\lambda\psi + \mu/\lambda\ \overline{\psi})$ in the minimal model $M(p,q)$ perturbed by $\mu\varphi$. We also verify that the corresponding defect operators commute for different value of λ as in (8.0.4), indicating that the corresponding perturbations are integrable. We only list cases $(1,s)$, the cases $(s,1)$ can be obtained by exchanging $p \leftrightarrow q$.

The solutions include the perturbations by $(1,2)$, $(1,3)$ and $(1,5)$, which are the standard integrable deformations of minimal models. The perturbed defects do not require regularisation for $t < \frac{4}{3}$, $t < \frac{3}{4}$, and $t < \frac{2}{5}$, respectively. We note that the $(1,7)$-perturbations require regularisation in all cases listed in Table 8.1 (except $M(2,9)$). Still, the $(1,7)$-perturbation of the minimal model $M(3,10)$ has recently received considerable attention and is a new candidate for an integrable flow [3,98,217,252], and it is interesting to observe that the bulk-commutation relation is satisfied in this case.

There are many more solutions to the bulk commutation condition than those listed in Table 8.1; we collect some of these in Section 8.2.8.

An indicator of integrability which has been extensively studied is the existence of higher spin conserved currents in the perturbed CFT (see e.g. [223]). A necessary

Minimal model $M(p,q)$	perturbing bulk field φ	weights $h=\overline{h}$ of φ	topological defect $\mathcal{D}$ in Figure 8.1
$q\geq 3$	$(1,2)$	$h_{1,2}=\frac{3}{4}t-\frac{1}{2}$	$(1,1)\oplus(1,2)$
$q\geq 4$	$(1,3)$	$h_{1,3}=2t-1$	$(1,2)$
$q\geq 6$	$(1,5)$	$h_{1,5}=6t-2$	$(1,3)$
$q=9,10,18$	$(1,7)$	$h_{1,7}=12t-3$	$(1,5)$

Table 8.1: Examples of minimal models in which we solve the bulk commutation condition (Figure 8.1) and verify that the corresponding perturbed defects mutually commute. As is usual, $t=p/q$. For the (1,7)-perturbation on the (1,5)-defect, the bulk commutation condition can only be solved for the given values of q. (But other solutions exist for different choices of topological defect.)

condition for a holomorphic field $W(z)$ in the CFT to survive as a conserved current when the CFT is perturbed by $\varphi(w)$ is that the first order pole in the OPE $W(z)\varphi(w)$ is a total derivative [274]. We analyse this condition in Section 8.3.1. The standard integrable perturbations $(1,2)$, $(1,3)$, $(1,5)$ are known to possess higher conserved charges related to exponents of affine Lie algebras. For the $(1,7)$-perturbation we find such higher conserved charges only in a few models, and in particular not in all the models that solve the bulk commutation condition.

Outline. This Chapter is organized as follows. In Section 8.1 we state the bulk commutation condition and give two criteria which imply that the corresponding perturbed defects mutually commute. We introduce the monoidal category of rigidly translation invariant defects. In Section 8.2 we investigate the bulk commutation condition and mutual commutativity of the perturbed defects in perturbed Virasoro minimal models. In Section 8.3 we systematically look for local conserved charges in the models studied in Section 8.2.

8.1 SymTFT and non-local conserved charges

To understand properties of a quantum field theory in d dimensions, such as its locality properties and topological symmetries, it is useful to represent the theory as a $(d+1)$-dimensional topological field theory together with a non-topological boundary and a topological boundary, see e.g. [67,261–268]). We will apply this picture in the specific situation that the QFT in question is a two-dimensional conformal field theory, so that the SymTFT is three-dimensional.

Below we will first describe bulk and defect fields in the SymTFT picture, in particular making the relation to the original "unfolded" or "chiral" TFT description of CFT correlators in [65,269,270]. Then we formulate the bulk commutation condition from

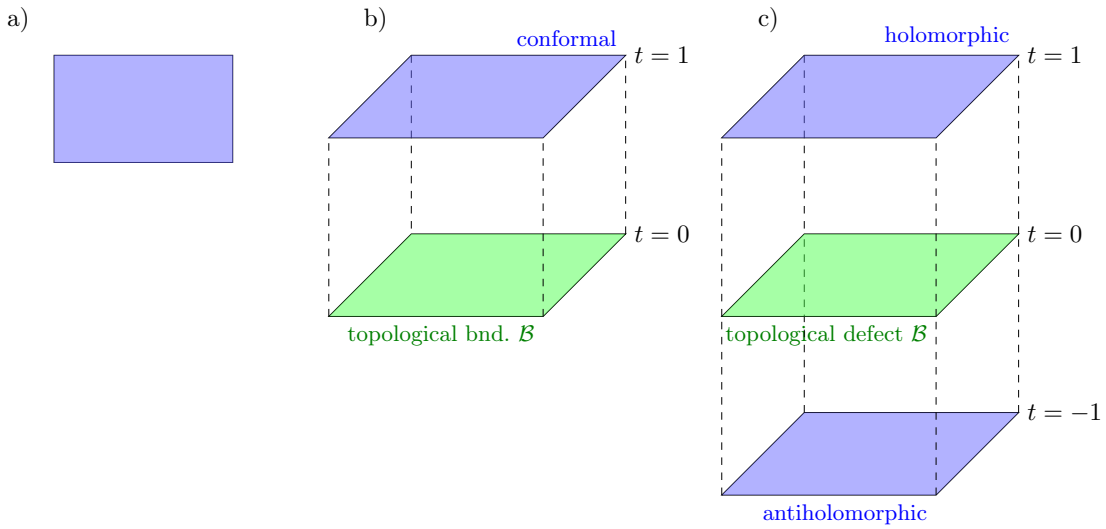


Figure 8.2: a) A patch of the surface Σ on which the 2d CFT is defined. b) The SymTFT presentation on $\Sigma \times [0,1]$ with topological boundary condition $\mathcal{B}$. c) The chiral TFT presentation on $\Sigma \times [-1,1]$ with a topological surface defect with defect condition $\mathcal{B}$ at $\Sigma \times \{0\}$.

[100] in SymTFT and chiral TFT language. We explain how it leads to non-local conserved charges in the perturbed theory and state two criteria which ensure that the defect operators mutually commute. Finally, we briefly discuss the extension from topological line defects to rigidly translation invariant defects.

8.1.1 CFT with defects via SymTFT

We present the fields and defects that we will we need in three ways: on the world sheet, in SymTFT, and in chiral TFT where holomorphic and antiholomorphic fields are on separate boundaries of the 3d TFT.

Let us start with the **geometric setup**, cf. Figure 8.2. Let Σ be a surface with complex structure on which we can evaluate correlators of the 2d CFT. Then in SymTFT, this becomes $\Sigma \times [0,1]$, where $\Sigma \times \{1\}$ is a copy of Σ with its complex structure, and $\Sigma \times \{0\}$ is a topological boundary and carries a boundary condition $\mathcal{B}$. Different choices of $\mathcal{B}$ give different choices of full (or absolute) 2d CFT upon collapsing the interval $[0,1]$. In the chiral TFT description, we consider $\Sigma \times [-1,1]$. The boundaries $\Sigma \times \{1\}$ and $\Sigma \times \{-1\}$ are both non-topological and carry a complex structure, with the former supporting the holomorphic and the latter the antiholomorphic local degrees of freedom. The holomorphic and antiholomorphic boundaries are separated by a topological surface defect placed at $\Sigma \times \{0\}$ and which we also label by $\mathcal{B}$ for a reason that will become clear momentarily. The interpretation of the construction in [270] in terms of surface defects is due to [275,276]. For more on surface defects in these types of 3d TFTs see [277,278].

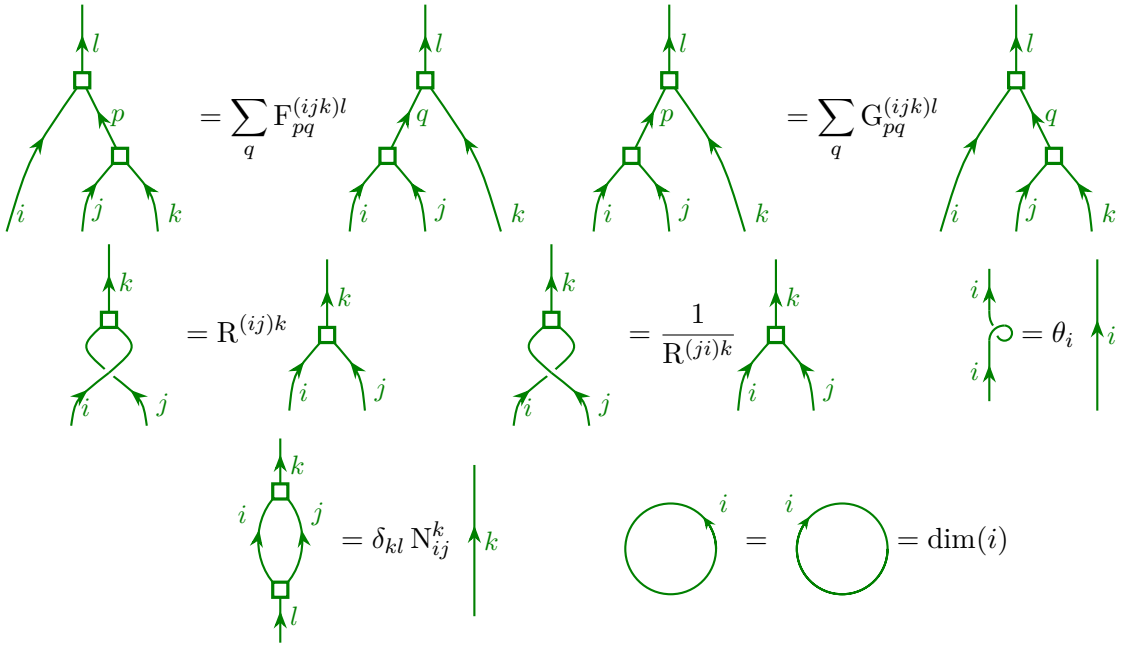


Figure 8.3: Local identities for line defects in the chiral TFT for the modular fusion category $\mathcal{F}$. Here, $i, j, k, \dots \in \mathrm{Irr}(\mathcal{F})$ denote simple objects, and the small boxes denote the basis element $\lambda^k_{ij} : i \otimes j \to k$ and its dual $k \to i \otimes j$.

To obtain the SymTFT picture from the chiral TFT picture, we fold the chiral TFT picture at $\Sigma \times \{0\}$, i.e. we identify $t \sim -t$ in the interval $[-1, 1]$. This creates a topological boundary at the fixed point $t = 0$ and a non-topological boundary with both holomorphic and antiholomorphic fields at $t = 1$. The topological boundary condition at $t = 0$ is obtained from the topological defect condition $\mathcal{B}$.

For our explicit computations, the chiral TFT picture will be the most convenient. Technically, the chiral TFT is obtained as the Reshetikhin-Turaev TFT for the modular fusion category $\mathcal{F} := \mathrm{Rep}\mathcal{V}$, the category of representations of the chiral algebra (a rational vertex operator algebra) $\mathcal{V}$. Line defects in the chiral TFT are labelled by objects of $\mathcal{F}$, i.e. by representations of the chiral algebra. Write $\mathrm{Irr}(\mathcal{F})$ for a choice of simple objects (irreducible representations) in $\mathcal{F}$. We denote by $\mathbf{1} \in \mathrm{Irr}(\mathcal{F})$ the unit object (vacuum representation). For $i, j, k \in \mathrm{Irr}(\mathcal{F})$, the fusion coefficients $N_{ij}{}^k$ give the multiplicity of k in the product $i \otimes j$. For simplicity we will make the

Assumption: $N_{ij}{}^k \in \{0, 1\}$ for all $i, j, k \in \mathrm{Irr}(\mathcal{F})$.

This avoids multiplicity labels and is satisfied in Virasoro minimal models, which are the explicit examples we consider later on. If $N_{ij}{}^k = 1$, we fix once and for all a non-zero vector $\lambda^k_{ij} \in \mathrm{Hom}_{\mathcal{F}}(i \otimes j, k)$, which is hence a basis of that one-dimensional space. The

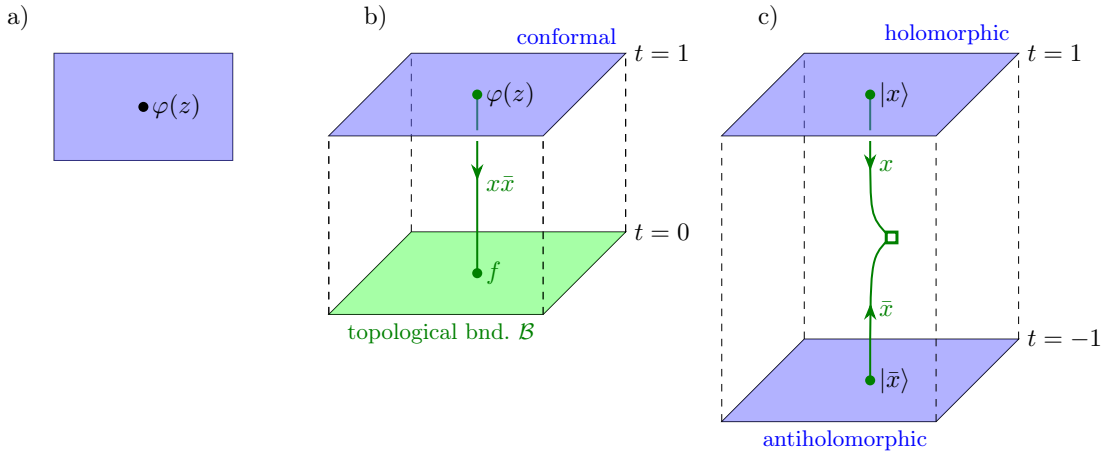


Figure 8.4: a) CFT: A patch of the surface Σ with an insertion of the bulk field $\varphi(z)$ of the 2d CFT. b) SymTFT presentation. c) Chiral TFT presentation. Note that we are now assuming the surface defect in Figure 8.2 c) to be trivial.

local rules to manipulate networks of line defects in the chiral TFT are collected in Figure 8.3 – these agree with the conventions used in [270].

For the rest of this Chapter, on the side of the chiral TFT we will only consider the trivial surface defect, as this is the situation we will use later on. In SymTFT we keep the picture general.

Let us now describe **bulk fields** $\varphi(z)$ in the 2d CFT,[2] cf. Figure 8.4. On the SymTFT side, the bulk field is described by a non-topological point insertion φ on the conformal boundary and a topological point insertion f on the topological boundary. In the chiral TFT, the bulk field consists of two line defects pointing away from the boundary which meet at a topological junction which we label by our standard basis $\lambda^{\mathbf{1}}_{x\overline{x}}$, and which we represent by a small box. The endpoints of the line defect on the holomorphic and antiholomorphic boundary and are labelled by states (primary in our application) $|x\rangle \in x$ and $|\overline{x}\rangle \in \overline{x}$, so that $\varphi = |x\rangle \otimes_{\mathbb{C}} |\overline{x}\rangle$ with conformal weights $(h, \overline{h}) = (h_x, h_{\overline{x}})$.

Topological line defects in the 2d CFT are given by line defects $\mathcal{D}$ on the topological boundary of the SymTFT, and simply by line defects $\mathcal{D}$ in the chiral TFT (as we assume the surface defect to be trivial). We will only need holomorphic and antiholomorphic **defect fields**, not general defect fields. Their description is as for bulk fields, but now the TFT line defects which are along the interval direction need to end on the line defect, see Figure 8.5. On the side of the chiral TFT, the defect is labelled by a not necessarily simple object $\mathcal{D} \in \mathcal{F}$, and $f : x \otimes \mathcal{D} \to \mathcal{D}$, $g : \mathcal{D} \otimes \overline{x} \to \mathcal{D}$ are morphisms in $\mathcal{F}$. The chiral TFT has the advantage of clearly showing which fields are holomorphic, and which fields are antiholomorphic (and which are neither, as the bulk field shown in Figure 8.4 c).

[2] We take the notation $\varphi(z)$ to mean the field φ inserted at point z, and that there is no implicit statement about $\varphi(z)$ being holomorphic or not. We will mostly avoid the notation $\varphi(z, \bar{z})$ which is often used in 2d CFT in this context.

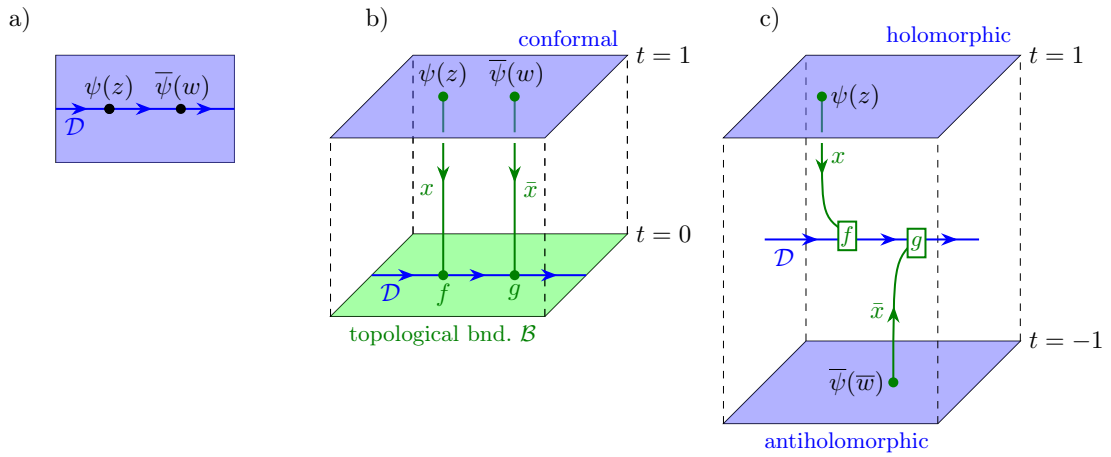


Figure 8.5: a) CFT: A patch of the surface Σ with an insertion of a topological line defect D, a holomorphic defect field ψ and an antiholomorphic defect field $\overline{\psi}$. b) SymTFT presentation. Here we assume that the endpoints of x and $\overline{x}$ on the conformal boundary depend holomorphically (resp. antiholomorphically) on the insertion point. c) Chiral TFT presentation.

8.1.2 The bulk commutation condition

Consider the perturbation of the CFT $\mathcal{C}$ by a a spin-less bulk field φ, that is, a bulk field with conformal dimensions $h = \overline{h}$. We take φ to transform in the representations x and $\overline{x}$ of the holomorphic and antiholomorphic copy of the chiral algebra $\mathcal{V}$, respectively. Its representation in SymTFT and chiral TFT is as in Figure 8.4.

Denote by $\mathcal{C}(\mu\varphi)$ the CFT $\mathcal{C}$ perturbed by $2i\mu\varphi$, $\mu \in \mathbb{C}$ (the normalisation factor of $2i$ will be convenient later). This includes the case $\mu = 0$, which is just the unperturbed theory. We consider $\mathcal{C}(\mu\varphi)$ on cylinder of circumference L. The Hamiltonian of $\mathcal{C}(\mu\varphi)$ is

$$H(\mu) = H_0 + H_{\text{pert}}(\mu) \quad , \quad H_0 = \frac{2\pi}{L}\Big(L_0 + \overline{L}_0 - \frac{c}{12}\Big) \quad , \quad H_{\text{pert}}(\mu) = 2i\mu \int_0^L \varphi(s)\, ds \ . \tag{8.1.1}$$

Next we choose a topological defect $\mathcal{D}$ of the unperturbed CFT $\mathcal{C}$, as well as two defect fields ψ and $\overline{\psi}$, where ψ is holomorphic and transforms in representation x, while $\overline{\psi}$ is antiholomorphic and transforms in representation $\overline{x}$. Their TFT representation is as in Figure 8.5. We write $\mathcal{D}(\lambda\psi + \widetilde{\lambda}\,\overline{\psi})$ for the defect $\mathcal{D}$ perturbed by the field $\Psi = \lambda\psi + \widetilde{\lambda}\,\overline{\psi}$. Explicitly,

$$\mathcal{D}(\lambda\psi + \widetilde{\lambda}\,\overline{\psi}; t) = \exp\Big(\int_0^L (\lambda\psi(s+it) + \widetilde{\lambda}\,\overline{\psi}(s+it))\, ds \Big) \ , \tag{8.1.2}$$

where we include the position t of the defect loop along the cylinder, and s is the position on the defect. See Figure 8.6 for one term in the perturbative expansion. If we would like the integrals to converge without further regularisation, we should impose

$$2h - h_{\text{min}} \ < \ 1 \ , \tag{8.1.3}$$

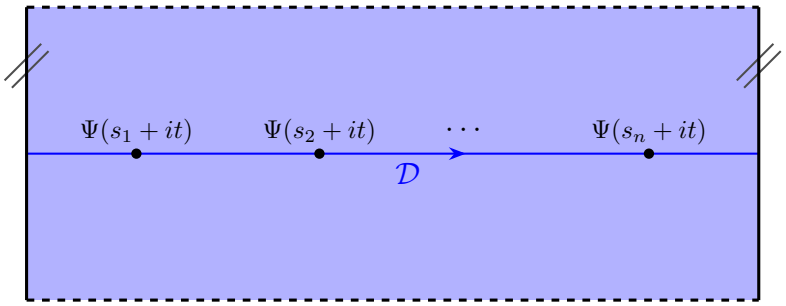


Figure 8.6: A contribution to the perturbative expansion of $\mathcal{D}(\lambda\psi+\widetilde{\lambda}\,\overline{\psi})$ placed around a cylinder of circumference L. Here $\Psi=\lambda\psi+\widetilde{\lambda}\,\overline{\psi}$ and the positions $0<s_1<\cdots<s_n<L$ of the fields are being integrated over.

where $h_{\min}$ is the smallest weight of primary fields that occur on the OPE $\psi(x)\psi(y)=(x-y)^{h_{\min}-2ph}\phi(y)+\dots$ (and so in particular has to be a holomorphic defect field on $\mathcal{D}$). As the CFT can be non-unitary, $h_{\min}<0$ is possible.

This is a stronger condition than that of ψ being relevant, which would be $h<1$. Note also that more stringent constraints than (8.1.3) can arise by considering iterated OPEs.

We would like $\mathcal{D}(\lambda\psi+\widetilde{\lambda}\,\overline{\psi})$ to be rigidly translation invariant in the perturbed CFT $C(\mu\varphi)$. In other words, we would like it to commute with the perturbed Hamiltonian:

$$\big[\,H(\mu)\,,\,\mathcal{D}(\lambda\psi+\widetilde{\lambda}\,\overline{\psi})\,\big]\;=\;0\;. \tag{8.1.4}$$

There is a simple condition which implies (8.1.4) order by order in perturbation theory, and which is formulated in the CFT $\mathcal{C}$, not in the perturbed theory:

$$\mu\,[\mathcal{D},\varphi(p)]\;=\;\lambda\widetilde{\lambda}\,[\psi(p),\,\overline{\psi}(p)]\;. \tag{8.1.5}$$

Here, the first commutator is understood as being taken along the cylinder, and the second along the defect; the commutators are taken in the CFT, not in the perturbed theory, and $\mathcal{D}$ is the unperturbed topological defect.

If $\mu=0$, this says that chiral defects (i.e. only one of λ and $\widetilde{\lambda}$ is non-zero) are translationally invariant in the undeformed CFT [99] (see also [253,279,280]) as are defects for which the defect fields commute (as happens for example in the fusion product of deformed defects). If neither of the commutators in (8.1.5) vanishes, then we can rescale the fields such that (8.1.5) is equivalent to the two conditions

$$[\mathcal{D},\varphi(p)]=[\psi(p),\,\overline{\psi}(p)]\;, \tag{8.1.6}$$

$$\lambda\widetilde{\lambda}=\mu\;. \tag{8.1.7}$$

We call the condition (8.1.6) the *bulk commutation condition*. In terms of SymTFT, the bulk commutation condition is given in Figure 8.1. The chiral TFT formulation is shown in Figure 8.7 (with the surface defect in Figure 8.2 taken to be trivial).

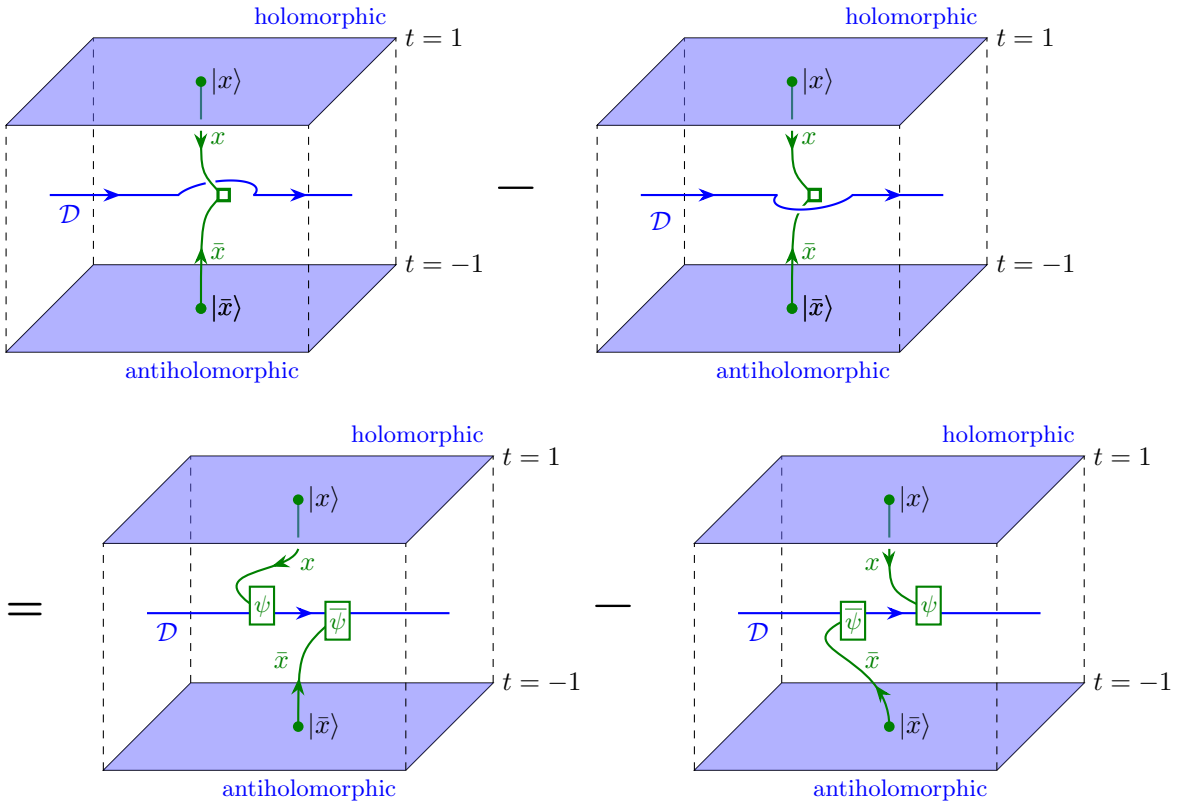


Figure 8.7: The bulk commutation condition expressed in terms of chiral TFT with trivial surface defect – the SymTFT formulation was already given in Figure 8.1.

It is shown in [100] (and in more generality in [101, App. A.2]) that (8.1.6) and (8.1.7) imply (8.1.4). We will briefly review the argument below. Implicit in this argument is the assumption that the integrals in $\mathcal{D}(\lambda\psi + \widetilde{\lambda}\,\overline{\psi})$ are well-defined at each order in $\lambda, \widetilde{\lambda}$, cf. (8.1.3). Otherwise one would need a regularisation procedure which is compatible between bulk and defect and we will not investigate this here.

The case $\mu = 0$ was already discussed above, so we now take $\mu \neq 0$ and restate (8.1.6) in this case:

$$[\mathcal{D}, \varphi(p)] \;=\; [\psi(p),\, \overline{\psi}(p)] \quad \Rightarrow \quad [H(\mu), \mathcal{D}(\lambda\psi + \mu/\lambda\,\overline{\psi})] \;=\; 0\;. \tag{8.1.8}$$

Since $\lambda \in \mathbb{C}^\times$ is still arbitrary, the bulk commutation condition always provides a one-parameter family of rigidly translation invariant defects in $\mathcal{C}(\mu\varphi)$. We will address the question if the defect operators mutually commute for different values of λ in Section 8.1.4.

Let us now quickly recap the argument leading to (8.1.8) as given in [100,101]. Define

$\Theta = \lambda\psi - \widetilde{\lambda}\,\overline{\psi}$ and $\Psi = \lambda\psi + \widetilde{\lambda}\,\overline{\psi}$ (as in Figure 8.6). Observe that

$$\begin{aligned}\frac{\partial}{\partial t}\Psi(s+it) &= \frac{\partial}{\partial t}\Big(\psi(s+it) + \overline{\psi}(s+it)\Big)\\ &= -i\frac{\partial}{\partial s}\Big(\psi(s+it) - \overline{\psi}(s+it)\Big) = -i\frac{\partial}{\partial s}\Theta(s+it)\ ,\end{aligned} \tag{8.1.9}$$

because ψ is holomorphic and $\overline{\psi}$ antiholomorphic. While the OPE of Ψ and Θ may be singular, for the difference of the two orders to take the OPE in we have

$$\Theta(p+\varepsilon)\Psi(p) - \Psi(p+\varepsilon)\Theta(p) \xrightarrow{\varepsilon\to 0} 2\lambda\widetilde{\lambda}\big(\,\psi(p)\,\overline{\psi}(p) - \overline{\psi}(p)\psi(p)\,\big)\ . \tag{8.1.10}$$

Using this, we compute

$$\begin{aligned}&\Big[H_0\,,\int_{0\le s_1<\cdots<s_n\le L}\Psi(s_1)\cdots\Psi(s_n)\,d^n s\Big]\\ &\overset{(1)}{=}\frac{\partial}{\partial t}\int_{0\le s_1<\cdots<s_n\le L}\Psi(s_1+it)\cdots\Psi(s_n+it)\,d^n s\Big|_{t=0}\\ &\overset{(2)}{=}-i\sum_{k=1}^{n}\int_{0\le s_1<\cdots<s_n\le L}\Psi(s_1)\cdots\frac{\partial}{\partial s_k}\Theta(s_k)\cdots\Psi(s_n)\,d^n s\\ &\overset{(3)}{=}-i\sum_{k=1}^{n-1}\int_{0\le s_1<\cdots<s_{n-1}\le L}\Psi(s_1)\cdots\big(-\Psi(s_k)\Theta(s_k)+\Theta(s_k)\Psi(s_k)\big)\cdots\Psi(s_{n-1})\,d^{n-1}s\\ &\overset{(4)}{=}-2i\lambda\widetilde{\lambda}\sum_{k=1}^{n-1}\int_{0\le s_1<\cdots<s_{n-1}\le L}\Psi(s_1)\cdots\big(\psi(s_k)\,\overline{\psi}(s_k)-\overline{\psi}(s_k)\psi(s_k)\big)\cdots\Psi(s_{n-1})\,d^{n-1}s\\ &\overset{(5)}{=}2i\lambda\widetilde{\lambda}\sum_{k=1}^{n-1}\int_{0\le s_1<\cdots<s_{n-1}\le L}\big[\,\varphi(s_k)\,,\,\Psi(s_1)\cdots\widehat{\Psi(s_k)}\cdots\Psi(s_{n-1})\,\big]\,d^{n-1}s\\ &=2i\lambda\widetilde{\lambda}\Big[\int_0^L\varphi(r)\,dr\,,\int_{0\le s_1<\cdots<s_{n-2}\le L}\Psi(s_1)\cdots\Psi(s_{n-2})\,d^{n-2}s\Big]\ .\end{aligned} \tag{8.1.11}$$

Step (1) follows as all expressions above are in the unperturbed theory $\mathcal{C}$ and H_0 generates translations along the cylinder. Step (2) is (8.1.9). In step (3) the integration over s_k is carried out and we reorganise the sum to arrive at the non-singular combination (8.1.10). Here one should really work with a cut-off regularisation and take the cut-off to zero at the end. This has been done in [101, App A.2] to which we refer for details. Step (4) is (8.1.10) and step (5) finally makes use of the bulk commutation condition (8.1.6). The hat indicates that $\Psi(s_k)$ is omitted.

Altogether, this establishes (8.1.8) order by order in $\mu = \lambda\widetilde{\lambda}$.

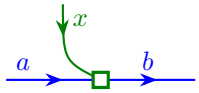
8.1.3 The bulk commutation condition in a basis

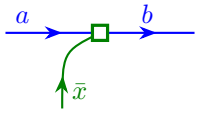
Here we give an explicit expression for the bulk commutation condition using the chiral TFT presentation in Figure 8.7 and the relations listed in Figure 8.3. Let

$$\mathcal{D} = \bigoplus_{a\in\mathcal{D}} a \tag{8.1.12}$$

be an object in $\mathcal{F}$, with $a \in \mathrm{Irr}(\mathcal{F})$. Recall that via the chiral TFT description in Figure 8.5, $\mathcal{D}$ represents a topological defect of the CFT $\mathcal{C}$ which is a superposition of the elementary defects $a \in \mathcal{D}$.

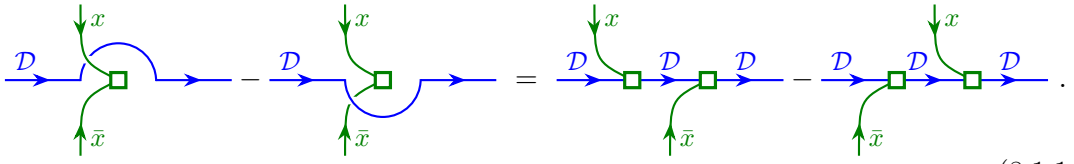
We expand the holomorphic and antiholomorphic defect fields in representation x and $\overline{x}$ in a basis as

$$\psi = \sum_{a,b\in\mathcal{D}} \kappa_{ab}$$ 

$$, \qquad \overline{\psi} = \sum_{a,b\in\mathcal{D}} \widetilde{\kappa}_{ab}$$ 

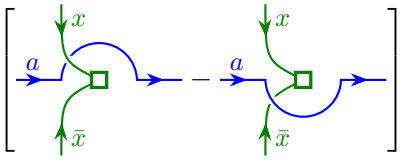
$$, \tag{8.1.13}$$

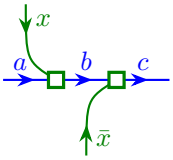
with $\kappa_{ab}, \widetilde{\kappa}_{ab} \in \mathbb{C}$. The bulk field φ is represented as in Figure 8.4 c). The bulk commutation condition in Figure 8.7 reads

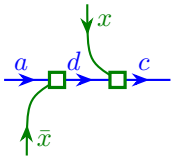


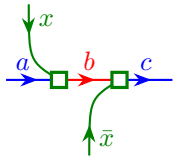
(8.1.14)

Expanding this into its simple components gives that for all $a, c \in \mathcal{D}$,

$$\delta_{a,c}$$ 

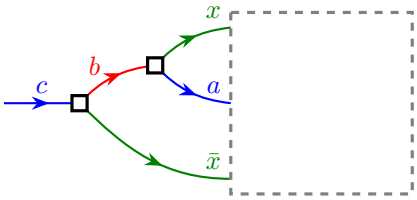
$$= \sum_{b\in\mathcal{D}} \kappa_{ab}\widetilde{\kappa}_{bc}$$ 

$$- \sum_{d\in\mathcal{D}} \widetilde{\kappa}_{ad}\kappa_{dc}$$ 

$$= \sum_{b\in\mathrm{Irr}(\mathcal{F})} \left[\delta_{b\in\mathcal{D}}\, \kappa_{ab}\widetilde{\kappa}_{bc} - \sum_{d\in\mathcal{D}} \mathrm{F}_{db}^{(xa\overline{x})c}\, \widetilde{\kappa}_{ad}\kappa_{dc} \right]$$ 

(8.1.15)

where the last equality follows from applying an F-move (Figure 8.3). Composing (8.1.15) with



(8.1.16)

for $b \in \mathrm{Irr}(\mathcal{F})$ one obtains the following equivalent formulation of the bulk commutation condition: For all $a, c \in \mathcal{D}$ and all $b \in \mathrm{Irr}(\mathcal{F})$ with $b \in a \otimes x$ and $b \in c \otimes x$ (so that the diagram in (8.1.16) is non-zero) we must have

$$\boxed{\delta_{ac} \left(\mathrm{R}^{(xa)b} - \frac{1}{\mathrm{R}^{(ax)b}} \right) \mathrm{F}_{1b}^{(ax\overline{x})a} = \delta_{b\in\mathcal{D}}\, \kappa_{ab}\widetilde{\kappa}_{bc} - \sum_{d\in\mathcal{D}} \mathrm{F}_{db}^{(xa\overline{x})c}\, \widetilde{\kappa}_{ad}\kappa_{dc}} \tag{8.1.17}$$

This is the most important equation of this section, and we will study some of its solutions in the case of minimal models in Section 8.2.

8.1.4 Fusion of defects and commutativity

Consider a topological defect $\mathcal{D} = \bigoplus_{a\in\mathcal{D}} a$ in $\mathcal{C}$ and suppose we can find a solution to the bulk commutation condition for $\mathcal{D}$ for a given bulk perturbation $\mathcal{C}(\mu\varphi)$. In this section we give two (sufficient but not necessary) criteria for the one-parameter family of perturbed defects to be mutually commuting. More generally, one can consider two different perturbed defects, say $\mathcal{D}(\lambda\psi + \mu/\lambda\,\overline{\psi})$ and $\mathcal{D}'(\lambda'\psi' + \mu/\lambda'\,\overline{\psi}')$. The parameter μ has to stay the same so that both defects are rigidly translation invariant in the same theory $\mathcal{C}(\mu\varphi)$. We then ask if, for $\lambda, \lambda' \in \mathbb{C}^\times$,

$$\big[\,\mathcal{D}(\lambda\psi + \mu/\lambda\,\overline{\psi})\,,\,\mathcal{D}'(\lambda'\psi' + \mu/\lambda'\,\overline{\psi}')\,\big] \;=\; 0\;. \tag{8.1.18}$$

Both criteria we discuss use the fusion of the two perturbed defects. This is given by taking the fusion $\mathcal{D}\otimes\mathcal{D}'$ of the corresponding topological defects and perturbing by

$$\lambda\psi + \lambda'\psi' + \mu/\lambda\,\overline{\psi} + \mu/\lambda'\,\overline{\psi}'\;, \tag{8.1.19}$$

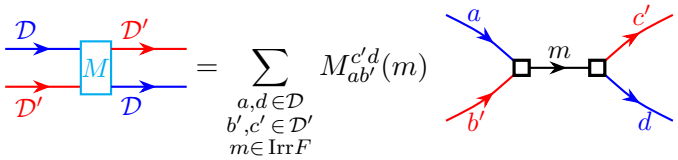
where it is understood that ψ, $\overline{\psi}$ are inserted on $\mathcal{D}$, and ψ', $\overline{\psi}'$ on $\mathcal{D}'$.

Commuting defects via a topological junction

The first criterion is a version of the standard construction used in integrable lattice models to commute two transfer matrices past each other. In the present setting we are looking for a topological junction $M = M(\lambda,\lambda') : \mathcal{D}\otimes\mathcal{D}' \to \mathcal{D}'\otimes\mathcal{D}$ which commutes with (8.1.19). This leads to two conditions, one for the holomorphic fields and one for the antiholomorphic fields, whose chiral TFT presentation is shown in Figure 8.8. If they are satisfied, the junction $M(\lambda,\lambda')$ remains topological in the perturbed theory. If the junction $M(\lambda,\lambda')$ has an inverse, one can insert a pair $\mathrm{id} = MM^{-1}$ next to each other and move M around the defect circle to arrive at $M^{-1}M = \mathrm{id}$ and with the two defects $\mathcal{D}(\lambda\psi + \mu/\lambda\,\overline{\psi})$ and $\mathcal{D}'(\lambda'\psi' + \mu/\lambda'\,\overline{\psi}')$ exchanged.

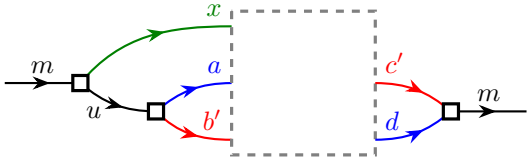
In summary, the first criterion states that if we can find an $M(\lambda,\lambda')$ which commutes with the perturbation as in Figure 8.8 and which is invertible, then (8.1.18) holds.

For explicit computations it is useful to express the above condition in a basis. For simplicity we assume that the elementary defects contained in $\mathcal{D}$ and $\mathcal{D}'$ have no multiplicities. Then the most general ansatz for M is



. (8.1.20)

Next substitute this ansatz into the first condition in Figure 8.8, together with the expansions of ψ and $\overline{\psi}$ in (8.1.13), and compose with



(8.1.21)

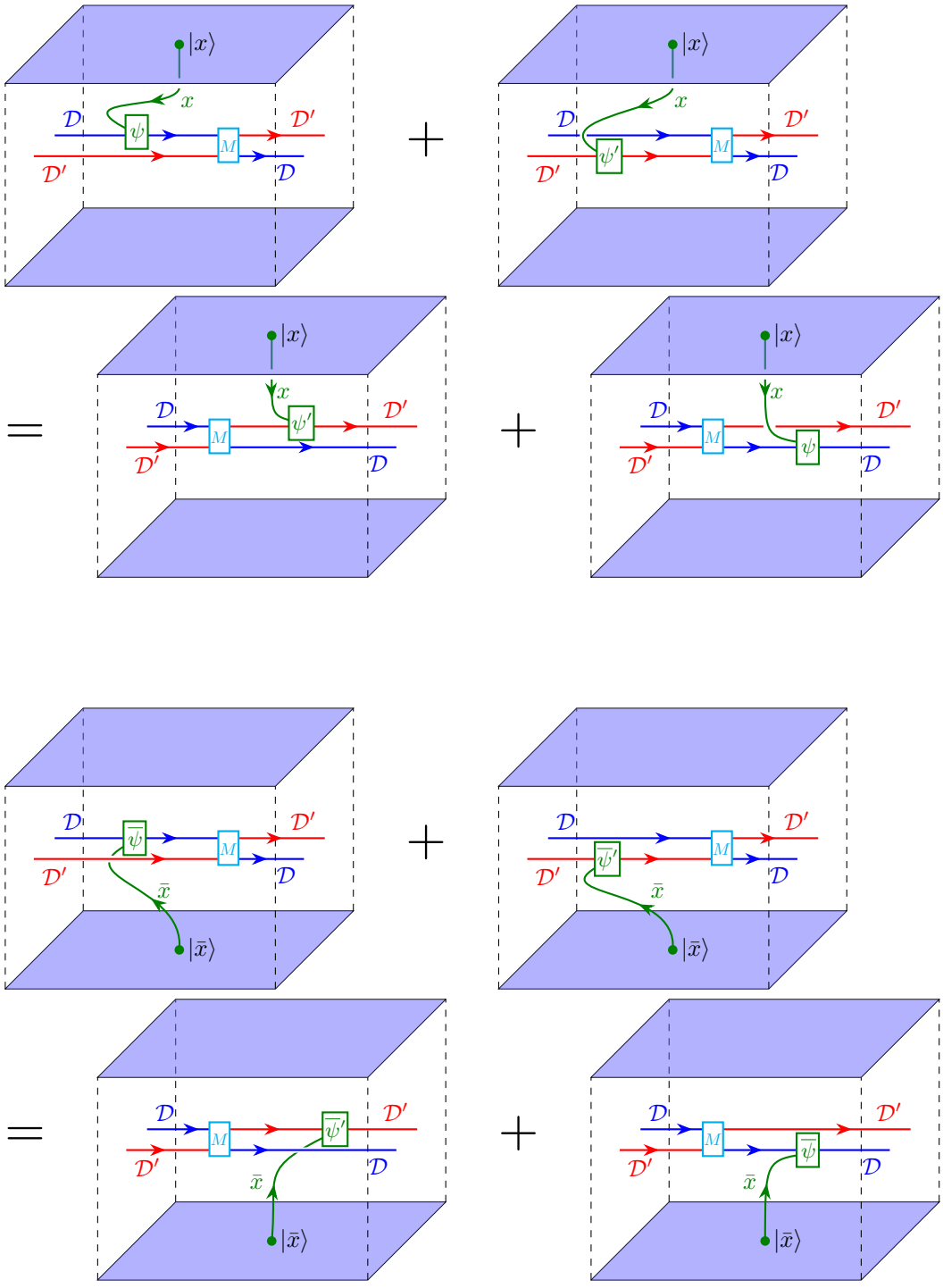


Figure 8.8: The two conditions for a topological junction $M : \mathcal{D} \otimes \mathcal{D}' \to \mathcal{D}' \otimes \mathcal{D}$ to commute with the defect perturbation.

from the left and right, respectively. The resulting condition is that for all $a, d \in \mathcal{D}$, $b', c' \in \mathcal{D}'$, $u \in \mathrm{Irr}(\mathcal{F})$, $m \in \mathcal{D} \otimes \mathcal{D}'$,

$$\begin{aligned}&\sum_{e\in\mathcal{D}} \kappa_{ae}\, M_{eb}^{c'd}(m)\, \mathrm{G}_{eu}^{(xab')m} + \sum_{f'\in\mathcal{D}'} \kappa'_{b'f'}\, M_{af'}^{c'd}(m)\, \frac{\mathrm{R}^{(f'a)m}}{\mathrm{R}^{(b'a)u}}\, \mathrm{G}_{f'u}^{(xb'a)m} \\ &= \sum_{f'\in\mathcal{D}'} \kappa'_{f'c'}\, M_{ab'}^{f'd}(u)\, \mathrm{G}_{c'u}^{(xf'd)m} + \sum_{e\in\mathcal{D}} \kappa_{ed}\, M_{ab'}^{c'e}(u)\, \frac{\mathrm{R}^{(dc')m}}{\mathrm{R}^{(ec')u}}\, \mathrm{G}_{du}^{(xec')m} \ .\end{aligned} \tag{8.1.22}$$

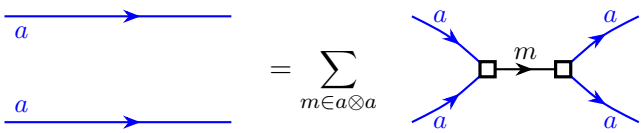
An analogous computation for the second condition gives

$$\begin{aligned}&\sum_{e\in\mathcal{D}} \widetilde{\kappa}_{ae}\, M_{eb'}^{c'd}(m)\, \frac{\mathrm{R}^{(b'e)m}}{\mathrm{R}^{(b'a)u}}\, \mathrm{F}_{eu}^{(b'ax)m} + \sum_{f'\in\mathcal{D}'} \widetilde{\kappa}'_{b'f'}\, M_{af'}^{c'd}(m)\, \mathrm{F}_{f'u}^{(ab'x)m} \\ &= \sum_{f'\in\mathcal{D}'} \widetilde{\kappa}'_{f'c'}\, M_{ab'}^{f'd}(u)\, \frac{\mathrm{R}^{(dc')m}}{\mathrm{R}^{(df')u}}\, \mathrm{F}_{c'u}^{(df'x)m} + \sum_{e\in\mathcal{D}} \widetilde{\kappa}_{ed}\, M_{ab'}^{c'e}(u)\, \mathrm{F}_{du}^{(c'ex)m} \ .\end{aligned} \tag{8.1.23}$$

A special case of these conditions was already given in [100].

Mutually commuting defects via a fusion graph

For the second criterion we specialise to the case $\mathcal{D} = \mathcal{D}' = a$, i.e. both defects are equal and given by the elementary defect a. We can now decompose the identity on $\mathcal{E} := \mathcal{D} \otimes \mathcal{D} = a \otimes a$ as



(8.1.24)

Write ϕ and $\overline{\phi}$ for the perturbing fields on $\mathcal{E}$. Inserting the above decomposition of the identity between defect fields on $\mathcal{D} \otimes \mathcal{D}$, we obtain

$$\phi = \sum_{m,n\in a\otimes a} \phi_{m\to n} \quad , \quad \overline{\phi} = \sum_{m,n\in a\otimes a} \overline{\phi}_{m\to n} \ , \tag{8.1.25}$$

where, with $\widetilde{\lambda} = \mu/\lambda$ and $\widetilde{\lambda}' = \mu/\lambda'$,

$$\begin{aligned}
\phi_{m\to n} &= \lambda \quad + \lambda' \\
&= \mathrm{G}^{(xaa)n}_{am}\left(\lambda + \lambda'\frac{\mathrm{R}^{(aa)n}}{\mathrm{R}^{(aa)m}}\right) \quad , \\
\overline{\phi}_{m\to n} &= \frac{\mu}{\lambda} \quad + \frac{\mu}{\lambda'} \\
&= \mathrm{F}^{(aax)n}_{am}\left(\frac{\mu}{\lambda'} + \frac{\mu}{\lambda}\frac{\mathrm{R}^{(aa)n}}{\mathrm{R}^{(aa)m}}\right) \quad .
\end{aligned} \tag{8.1.26}$$

The prefactors of $\phi_{m\to n}$ and $\overline{\phi}_{m\to n}$ can be split into a part invariant under $\lambda \leftrightarrow \lambda'$ and a common factor that is not manifestly so,

$$\phi_{m\to n} \;:\; \frac{\mathrm{G}^{(xaa)n}_{am}}{\mathrm{R}^{(aa)m}}\Delta_{m\to n} \quad , \qquad \overline{\phi}_{m\to n} \;:\; \frac{\mu}{\lambda\lambda'}\frac{\mathrm{F}^{(aax)n}_{am}}{\mathrm{R}^{(aa)m}}\Delta_{m\to n} \; , \tag{8.1.27}$$

where

$$\Delta_{m\to n} = \lambda \mathrm{R}^{(aa)m} + \lambda' \mathrm{R}^{(aa)n} \; . \tag{8.1.28}$$

Now define a graph Γ whose vertices are the labels $m \in a \otimes a$, and where there is an (undirected) edges between m and n if the prefactor of $\phi_{m\to n}$ is non-zero (which is equivalent to either of the prefactors of $\overline{\phi}_{m\to n}$, $\phi_{n\to m}$, or $\overline{\phi}_{n\to m}$ being non-zero by properties of the F-symbols).

Consider a term in the perturbative expansion of $\mathcal{E}(\phi + \overline{\phi})$ on a cylinder as in Figure 8.6 (with $\mathcal{E}$ in place of $\mathcal{D}$). Expand this expression further into a sum over elementary defects in $\mathcal{E}$, and expand the sum $\phi + \overline{\phi}$ at each insertion into $\phi_{m\to n}$ and $\overline{\phi}_{m\to n}$. Each non-zero term in this sum defines a closed path γ on Γ which is obtained by following the elementary defect labels $m \in \mathcal{E}$ as one passes along the defect from $s = 0$ to $s = L$ on the cylinder. We also obtain a function δ from the edges of γ to ± 1 where $+1$ corresponds to an insertion of $\phi_{m\to n}$ and -1 to one of $\overline{\phi}_{m\to n}$.

Let $F_{\gamma,\delta}(\lambda, \lambda')$ be the product of the prefactors in (8.1.27), where we take the prefactor of $\phi_{m\to n}$ if δ for that edge is $+1$ and of $\overline{\phi}_{m\to n}$ if it is -1. This now depends on the direction of γ as e.g. the prefactors of $\phi_{m\to n}$ and $\phi_{n\to m}$ differ. Then (8.1.18) holds if for all closed paths γ on Γ and all maps δ from the edges of Γ to $\{\pm 1\}$ we have $F_{\gamma,\delta}(\lambda, \lambda') = F_{\gamma,\delta}(\lambda', \lambda)$. But in order to verify this, we can drop the manifestly symmetric part in (8.1.27) and only consider the product of the common factor $\Delta_{m\to n}$ in (8.1.28). This means we do not need the function δ and we define $F_\gamma(\lambda, \lambda')$ be the product of the factors $\Delta_{m\to n}$ as dictated by the path γ.

Altogether, the second criterion is that (8.1.18) holds if for all closed paths γ on Γ we have

$$F_\gamma(\lambda, \lambda') = F_\gamma(\lambda', \lambda) \ . \tag{8.1.29}$$

We will see explicit examples of how to use this condition in Section 8.2. Here we just make three general remarks which will be useful later:

- For $m = n$ the factor $\Delta_{m\to m}$ is invariant under $\lambda \leftrightarrow \lambda'$. Hence in the graph Γ and in the path γ one may disregard edges from a vertex m to itself.

- If γ passes from m to n along an edge and later from n to m, then $F_\gamma(\lambda, \lambda')$ will involve the product $\Delta_{m\to n}\Delta_{n\to m}$ which is invariant under $\lambda \leftrightarrow \lambda'$. Thus, if the are no non-trivial closed looks, i.e. if every path has to eventually retrace itself, then (8.1.29) holds.

- If Γ does contain loops, one needs to check for a choice of generating loops that the corresponding product of $\Delta_{m\to n}$'s is invariant under $\lambda \leftrightarrow \lambda'$. Combining this with the previous point, we again obtain that (8.1.29) holds.

8.1.5 The category of rigidly translation invariant defects

We briefly collect some properties of the category $\mathcal{T}(\mu)$ formed by rigidly translation invariant defects, and in particular of those obtained form joint perturbation of bulk and defect as above. Note that the CFT itself occurs as a special case for zero perturbation parameter.

The objects in $\mathcal{T}(\mu)$ are rigidly translation invariant defects $\mathcal{X}$ in the CFT $\mathcal{C}(\mu\varphi)$ (or in any 2d QFT for that matter). Morphisms $\mathcal{X} \to \mathcal{X}'$ in $\mathcal{T}(\mu)$ are defect changing fields which are topological in the sense that they can be moved freely on the defect line. Note that the topological defects which still exist in $\mathcal{C}(\mu\varphi)$ form a full subcategory $\mathcal{T}_{\text{top}}(\mu) \subset \mathcal{T}(\mu)$.

Most importantly, $\mathcal{T}(\mu)$ has a tensor product, given by fusion of defects in $\mathcal{T}(\mu)$. This is well-defined as by translation invariance no singularity arises in the fusion of parallel line defects.

The rigidly translation invariant defects $\mathcal{D}(\lambda\psi + \mu/\lambda\,\overline{\psi})$ in $\mathcal{C}(\mu\varphi)$ obtained from solutions to the bulk commutation condition also form a full monoidal subcategory $\mathcal{T}_{\text{pert}}(\mu) \subset \mathcal{T}(\mu)$. The category $\mathcal{T}_{\text{pert}}(\mu)$ has a representation theoretic reformulation. Namely, let $x \in \mathcal{F}$ label the perturbing field, and denote by $T(x) = 1 \oplus x \oplus x^{\otimes 2} \oplus x^{\otimes 3} \oplus \cdots$ the tensor algebra of x in (a completion of) $\mathcal{F}$. Then $T(x)$ is a Hopf algebra in $\mathcal{F}$, and the bulk commutation condition for a line defect $\mathcal{D}$ with defect fields ψ, $\overline{\psi}$ can be rephrased as the condition that $\mathcal{D}$ carries the structure of a $T(x)$-$T(\overline{x})$-Yetter-Drinfeld module (where the perturbing bulk field provides the Hopf-pairing), see [101, Sec. 4]. The fusion of perturbed line defects amounts to the tensor product of Yetter-Drinfeld modules. Thus

$$\mathcal{T}_{\text{pert}}(\mu) \text{ is monoidally equivalent to } T(x)\text{-}T(\overline{x})\text{-Yetter-Drinfeld modules in } \mathcal{F}.$$

From this observation we see that $\mathcal{T}(\mu)_{\text{pert}}$ is an abelian category (in particular it has kernels and quotients), and that it is rigid (has left and right duals).[3] However, it is in general neither semisimple, nor spherical or pivotal (see [272, Sec. 4.3] for an example). It typically has continua of simple objects, and the fusion of two simple objects is generically again simple. In this sense, $\mathcal{T}_{\text{pert}}(\mu)$ behaves a lot like evaluation representations of quantum affine algebras. This relation has been made precise in the perturbed free boson example treated in [101].

While the parameter $\mu \in \mathbb{C}$ enters the definition of $\mathcal{T}_{\text{pert}}(\mu)$, it depends on μ only weakly in the sense that $\mathcal{T}_{\text{pert}}(\mu)$ is monoidally equivalent (but not equal) to $\mathcal{T}_{\text{pert}}(1)$ for all $\mu \in \mathbb{C}^\times$. However, in general $\mathcal{T}_{\text{pert}}(0) \ncong \mathcal{T}_{\text{pert}}(1)$.

We propose that the monoidal categories

$$\mathcal{T}(\mu)_{\text{top}} \;\subset\; \mathcal{T}(\mu)_{\text{pert}} \;\subset\; \mathcal{T}(\mu) \tag{8.1.30}$$

contain important information about the family $\mathcal{C}(\mu\varphi)$ of deformed CFTs, and should all be considered together, instead of just $\mathcal{T}(\mu)_{\text{top}}$.

As a point in case, we expect that under the renormalisation group, defects in $\mathcal{T}(\mu)$ flow to topological defects in the infrared conformal field theory. Indeed, a defect $\mathcal{D}$ in a conformal field theory, which is both rigidly translation invariant and conformal, is necessarily topological. This is easy to see from the conditions on the defect operator $\widehat{\mathcal{D}}$ on a circle. The conditions of conformality and translation invariance are, respectively,

$$[\, L_m - \overline{L}_{-m}, \widehat{\mathcal{D}}\,] = 0\,, \qquad (\text{all } m)\,, \tag{8.1.31}$$

$$[\, L_0 + \overline{L}_0, \widehat{\mathcal{D}}\,] = 0\,. \tag{8.1.32}$$

Taking 8.1.31 in the case $m = 0$ and (8.1.32), we then get

$$[\, L_0, \widehat{\mathcal{D}}\,] = [\, \overline{L}_0, \widehat{\mathcal{D}}\,] = 0\,. \tag{8.1.33}$$

Now we consider the commutators

$$[\, L_0, L_m - \overline{L}_{-m}\,] = -m\, L_m \quad \Rightarrow\; [\, m\, L_m, \widehat{\mathcal{D}}\,] = 0 \quad \Rightarrow\; [\, L_m, \widehat{\mathcal{D}}\,] = 0\,, \qquad (m \neq 0) \tag{8.1.34}$$

$$[\, \overline{L}_0, L_m - \overline{L}_{-m}\,] = m\, \overline{L}_m \quad \Rightarrow\; [\, m\, \overline{L}_{-m}, \widehat{\mathcal{D}}\,] = 0 \quad \Rightarrow\; [\, \overline{L}_{-m}, \widehat{\mathcal{D}}\,] = 0\,, \qquad (m \neq 0) \tag{8.1.35}$$

and taking (8.1.33) with (8.1.34) and (8.1.35), we see that $\widehat{\mathcal{D}}$ satisfies the conditions of topological invariance:

$$[\, L_m, \widehat{\mathcal{D}}\,] = [\, \overline{L}_m, \widehat{\mathcal{D}}\,] = 0\,, \qquad (\text{all } m)\,. \tag{8.1.36}$$

[3] Note that while $T(x)$ only lives in a completion of $\mathcal{F}$ and does not have a dual, the object $\mathcal{D}$ which carries the $T(x)$-$T(\overline{x})$-Yetter-Drinfeld module structure is taken to be in $\mathcal{F}$, not in its completion. In particular, $\mathcal{D}$ has a dual $\mathcal{D}^*$ in $\mathcal{F}$, and indeed $\mathcal{D}^*$ carries the structure of the dual Yetter-Drinfeld module. This situation is reminiscent of finite-dimensional representations of the universal enveloping algebra of a Lie algebra.

As a second application, consider two perturbed CFTs $\mathcal{C}(\mu\varphi)$ and $\mathcal{C}'(\mu'\varphi')$. Then the category of *all* interfaces between $\mathcal{C}(\mu\varphi)$ and $\mathcal{C}'(\mu'\varphi')$ (not necessarily topological, or rigidly translation invariant, or conformal) is a bimodule category over $\mathcal{T}(\mu)$ and $\mathcal{T}'(\mu')$. For example, if $\mathcal{C}'$ is trivial, these interfaces are just boundaries for $\mathcal{C}(\mu\varphi)$, and fusing with defects in $\mathcal{T}(\mu)$ can be used to find boundary flows from defect flows and vice versa, see [100,280–282].

8.2 Non-local commuting charges in minimal models

Here we investigate the bulk commutation condition and the question of mutual commutativity of perturbed defects in the case of A-type minimal models $M(p,q)$. We first specialise the results in the previous section and review our conventions for minimal models. Then we treat the perturbations by $(1,2)$, $(1,3)$, $(1,5)$ and $(1,7)$ in $M(p,q)$ some detail, as well as all perturbations of $M(3,10)$. This section concludes with some further observations for which we do not provide a systematic treatment.

8.2.1 Properties of elementary defects $\mathcal{D}$ and of $\mathcal{D} = \mathbf{1} \oplus x$

Elementary defect $\mathcal{D}$

We start by restating the bulk commutation condition (8.1.17) in the case that $\mathcal{D} = a$ is an elementary defect: for all $b \in x \otimes a$ we must have

$$\begin{aligned} b = a: &\quad \left(\mathrm{R}^{(xa)a} - \frac{1}{\mathrm{R}^{(ax)a}}\right) \mathrm{F}_{1a}^{(ax\overline{x})a} = (1 - \mathrm{F}_{aa}^{(xa\overline{x})a})\, \kappa\widetilde{\kappa}\ , \\ b \neq a: &\quad \left(\mathrm{R}^{(xa)b} - \frac{1}{\mathrm{R}^{(ax)b}}\right) \mathrm{F}_{1b}^{(ax\overline{x})a} = -\mathrm{F}_{ab}^{(xa\overline{x})a}\, \kappa\widetilde{\kappa}\ . \end{aligned} \tag{8.2.1}$$

Note that by construction $a \in x \otimes a$, so that $b = a$ is indeed one of the values we need to consider. If $\mathrm{F}_{aa}^{(xa\overline{x})a} \neq 1$, if there is a solution at all, it must be given by

$$\kappa\widetilde{\kappa} = \left(\mathrm{R}^{(xa)a} - \frac{1}{\mathrm{R}^{(ax)a}}\right) \frac{\mathrm{F}_{1a}^{(ax\overline{x})a}}{1 - \mathrm{F}_{aa}^{(xa\overline{x})a}}\ . \tag{8.2.2}$$

If $\mathrm{F}_{aa}^{(xa\overline{x})a} = 1$ there can only be a solution if the left hand side of the $b = a$ condition is also zero.

Elementary defect $\mathcal{D}$ and $x \otimes x \cong \mathbf{1}$

To avoid having to treat the case $x \otimes x \cong \mathbf{1}$ separately in the examples below, we cover it here. Note that this condition implies that x is invertible under fusion with the inverse being the dual, so that also $\overline{x} = x$. For x to live on the defect a we furthermore need $x \otimes a = a$.

In (8.2.1) only the case $b = a$ remains. In Appendix B.2 we explain that

$$\mathrm{F}_{aa}^{(xax)a} = \mathrm{R}^{(xx)1} \in \{\pm 1\}\ . \tag{8.2.3}$$

The other two possibilities $\mathrm{R}^{(xx)1} \in \{\pm i\}$ are excluded by the existence of a fixed point (see again the appendix). Let us discuss the two cases in turn:

- $\mathrm{F}_{aa}^{(xax)a} = -1$: In this case, (8.2.1) is uniquely solved by (8.2.2)
- $\mathrm{F}_{aa}^{(xax)a} = +1$: Here (8.2.1) has a solution if and only if $\mathrm{R}^{(xa)a}\,\mathrm{R}^{(ax)a} = 1$. If this equality holds, (8.2.1) becomes $0 = 0$ and there are no constraints on $\kappa\widetilde{\kappa}$.

For minimal models we list R-matrices in the next section, and one finds that the condition $\mathrm{F}_{aa}^{(xax)a} = \mathrm{R}^{(xx)1} = -1$ is equivalent to the conformal weight satisfying $h_x \in \mathbb{Z} + \frac{1}{2}$, and $\mathrm{F}_{aa}^{(xax)a} = +1$ is equivalent to $h_x \in \mathbb{Z}$. In the latter case, $\mathrm{R}^{(xa)a}\mathrm{R}^{(ax)a} = 1$ holds automatically.

Defect $\mathcal{D}$ of the form $\mathbf{1} \oplus x$

Next we turn to the case that $\mathcal{D} = \mathbf{1} \oplus x$, where x is the label of the perturbing field. We assume that $x = \overline{x}$ and that $\mathrm{F}_{11}^{(xxx)x} \neq 1$. For the application below we are interested in the case that ψ and $\overline{\psi}$ do not have a component $x \to x$, that is, we make the additional assumption that

$$\kappa_{xx} = 0 = \widetilde{\kappa}_{xx} \ . \tag{8.2.4}$$

In this case one quickly checks that (8.1.17) is equivalent to the equalities

$$\kappa_{1x}\widetilde{\kappa}_{x1} = \kappa_{x1}\widetilde{\kappa}_{1x} = \frac{\mathrm{R}^{(xx)1} - (\mathrm{R}^{(xx)1})^{-1}}{(\mathrm{F}_{11}^{(xxx)x})^{-1} - 1} = \frac{1}{\mathrm{R}^{(xx)b}} - \mathrm{R}^{(xx)b} \ , \tag{8.2.5}$$

where the last equality has to hold for all $b \in x \otimes x$, $b \neq \mathbf{1}$. Here we used that necessarily[4] $\mathrm{F}_{1b}^{(xxx)x} \neq 0$ for all $b \in x \otimes x$. The F-matrix element in the above formula is given by

$$\mathrm{F}_{11}^{(xxx)x} = \frac{\nu_x}{\dim x} \ , \tag{8.2.6}$$

where $\nu_x \in \{\pm 1\}$ is the Frobenius-Schur indicator of $x = \overline{x}$, see [270, Eqns. (2.20), (2.47)]. Thus our assumption $\mathrm{F}_{11}^{(xxx)x} \neq 1$ is equivalent to $\dim x \neq \nu_x$.

We show in Appendix B.3 that if $x \otimes x \cong 1 \oplus y$, i.e. if the decomposition of $x \otimes x$ contains precisely two simple objects, then (8.2.5) automatically also holds for $b = y$. We also show there that (8.1.22) and (8.1.23) have a solution. Altogether:

> Suppose that $x \in \mathrm{Irr}(\mathcal{F})$ satisfies $x = \overline{x}$ and $x \otimes x \cong 1 \oplus y$ for some simple object $y \in \mathrm{Irr}(\mathcal{F})$. Then the bulk commutation condition can be solved for $\mathcal{D} = 1 \oplus x$ with perturbation x, and the resulting perturbed defects mutually commute for different values of λ.

[4] This is a special case of the general observation that $\mathrm{G}_{1i}^{(k\bar{k}j)j} \neq 0$ if $j \in k \otimes i$, see e.g. [270, Eqn. (2.60)] and observe that the left hand side there must be non-zero. By (2.61) in that paper, also $\mathrm{F}_{1i}^{(j\bar{k}k)j} \neq 0$.

8.2.2 Chiral data for minimal models

For $p, q \geq 2$ and coprime, we denote by $M(p,q)$ the A-type minimal model of central charge

$$c = 1 - \frac{6(p-q)^2}{pq} \,. \tag{8.2.7}$$

We write

$$t = \frac{p}{q} \,. \tag{8.2.8}$$

The irreducible representations of the Virasoro algebra that make up the model are indexed by Kac-labels

$$\mathcal{I}_{p,q} := \big\{\, (r,s) \,\big|\, 1 \leq r < p \;,\; 1 \leq s < q \,\big\} / \sim \quad , \quad \text{where} \;\; (r,s) \sim (p-r, q-s) \,. \tag{8.2.9}$$

The conformal weight of the primary state in the representation (r,s) is

$$h_{r,s} = \frac{(r-st)^2 - (1-t)^2}{4t} \,. \tag{8.2.10}$$

The vacuum representation is labelled by $\mathbf{1} = (1,1) = (p-1, q-1)$. We will only need the fusion rules for representations of the form $(1,s)$, and these are

$$(1,r) \otimes (1,s) \;\cong\; \bigoplus_{\substack{u=|r-s|+1 \\ \text{step } 2}}^{\min(r+s-1, 2q-r-s-1)} (1,u) \,. \tag{8.2.11}$$

The R-matrix and twist are expressed in terms of the conformal weights as, for $a, b, c \in \mathcal{I}_{p,q}$,

$$\theta_a = e^{2\pi i h_a} \quad , \quad \mathrm{R}^{(ab)c} = e^{\pi i (h_c - h_a - h_b)} \,. \tag{8.2.12}$$

The quantum dimension of $a = (r,s) \in \mathcal{I}_{p,q}$ is given in terms of the modular S-matrix by $\dim(a) = S_{a1}/S_{11}$. Explicitly,

$$\dim(r,s) = (-1)^{r-1} \frac{\sin(\pi r/t)}{\sin(\pi/t)} \cdot (-1)^{s-1} \frac{\sin(\pi s t)}{\sin(\pi t)} \,. \tag{8.2.13}$$

The F-matrix entries can be determined via a closed form expression [283,284] (summarised in [285, App. A.1.1]), or recursively [286]. Here we will use the expressions from [285,286], the relation to the notation used there is

$$\mathrm{F}_{pq}^{(jkl)i} \;=\; \mathrm{F}_{pq}\big[\begin{smallmatrix} j & k \\ i & l \end{smallmatrix}\big] \,. \tag{8.2.14}$$

The inverse G of the F-matrix is given by (combine [270, Eqn. (2.61)] with (8.2.12))

$$\mathrm{G}_{pq}^{(abc)d} = \mathrm{F}_{pq}^{(cba)d} \,. \tag{8.2.15}$$

The F-matrix has the symmetries

$$\mathrm{F}_{pq}^{(abc)d} = \mathrm{F}_{pq}^{(bad)c} = \mathrm{F}_{pq}^{(cda)b} = \mathrm{F}_{pq}^{(dcb)a} \,, \tag{8.2.16}$$

and obeys (for $d \in b \otimes c$)

$$\mathrm{F}_{db}^{(1bc)d} = \mathrm{F}_{db}^{(b1d)c} = \mathrm{F}_{db}^{(cd1)b} = \mathrm{F}_{db}^{(dcb)1} = 1 \qquad \text{and} \qquad \mathrm{F}_{11}^{(aaa)a} = \frac{1}{\dim(a)} \ . \tag{8.2.17}$$

Comparing to (8.2.6) we see that the Frobenius-Schur indicators are $\nu_a = 1$ for all $a \in \mathcal{I}_{p,q}$.

8.2.3 (1,2)-perturbation of the defect (1,1)⊕(1,2)

That the bulk commutation condition can be solved for the $(1,2)$-perturbation and $\mathcal{D} = (1,1) \oplus (1,2)$ was already shown in Section 8.2.1, as was the fact that the resulting defect operators mutually commute. These solutions exist for all $M(p,q)$ with $q \geq 4$.

For concreteness, let us also solve (8.2.5) explicitly. The conditions are

$$\begin{aligned} \kappa_{1x}\widetilde{\kappa}_{x1} = \kappa_{x1}\widetilde{\kappa}_{1x} &= -2i\,\frac{\sin\left(\frac{\pi}{2}t(x^2-1)\right)}{\frac{\sin(\pi t x)}{\sin(\pi t)} + (-1)^x} \\ &\overset{(*)}{=} -2i(-1)^x \sin\Big(\tfrac{\pi}{4}\big(t(1+b^2-2x^2) - 2(b+1)\big)\Big) \ , \end{aligned} \tag{8.2.18}$$

where $(*)$ is the consistency condition to check, and it has to hold for all $b \in x \otimes x$, $b \neq (1,1)$. For $x = (1,2)$ this is solved with

$$\kappa_{1x}\widetilde{\kappa}_{x1} = \kappa_{x1}\widetilde{\kappa}_{1x} = -2i\sin\left(\tfrac{\pi t}{4}\right) \ . \tag{8.2.19}$$

We note in passing that also $x = (1,3)$ solves the above condition, in that case one has to check $b = (1,3)$ and $b = (1,5)$. Thus the bulk commutation condition can be solved on $(1,1) \oplus (1,3)$ for the $(1,3)$-perturbation in such a way that ψ and $\overline{\psi}$ do not involve a component $(1,3) \to (1,3)$.

8.2.4 (1,3)-perturbation of the defect (1,2)

Next we investigate the case where bulk and defect are perturbed by $(1,3)$ fields in $M(p,q)$ with $q \geq 4$. For the topological defect $\mathcal{D}$ we choose $\mathcal{D} = (1,2)$. This case was already treated in [100], and we review this result in our current notations. We need to solve (8.2.1) for $x = (1,3)$, $a = (1,2)$, and $b \in (1,2) \otimes (1,3) \cong (1,2) \oplus (1,4)$. The case $b = (1,4)$ only occurs for $q \geq 5$.

For $q = 4$ we have $x \otimes x \cong \mathbf{1}$ which was treated in Section 8.2.1. Since $h_{1,3} = 2t - 1 = \frac{1}{2}p - 1$, and since p has to be odd, we always have $h_{1,3} \in \frac{1}{2} + \mathbb{Z}$. Hence the bulk commutation condition can be solved for all $M(p,4)$.

Now suppose $q \geq 5$. The F-matrix entries occurring in (8.2.1) are

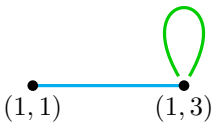
$$\begin{aligned} \mathrm{F}_{12}^{(233)2} &= \frac{\Gamma(2-2t)\Gamma(-1+3t)}{\Gamma(1-t)\Gamma(2t)} \ , & \mathrm{F}_{14}^{(233)2} &= -\frac{\sin(4\pi t)}{\sin(3\pi t)}\,\frac{\Gamma(2-2t)\Gamma(-1+4t)}{\Gamma(1-t)\Gamma(3t)} \ , \\ \mathrm{F}_{22}^{(323)2} &= -\frac{\sin(\pi t)}{\sin(3\pi t)} \ , & \mathrm{F}_{24}^{(323)2} &= -\frac{\sin(4\pi t)}{\sin(3\pi t)}\,\frac{\Gamma(2-3t)\Gamma(-1+4t)}{\Gamma(1-2t)\Gamma(3t)} \ . \end{aligned} \tag{8.2.20}$$

Using these, one can verify that (8.2.1) is uniquely solved by the value for $\kappa\widetilde{\kappa}$ given in (8.2.2):

$$\kappa\widetilde{\kappa} = i\,\frac{\sin(3\pi t)}{\cos(\pi t)}\,\frac{\Gamma(2-2t)\Gamma(-1+3t)}{\Gamma(1-t)\Gamma(2t)}\ . \tag{8.2.21}$$

For the further examples discussed in Section 8.2 we will no longer list the explicit F-matrices or the explicit solution for $\kappa\widetilde{\kappa}$ – one just obtains longer expressions of a similar form as above. Will will, however, discuss in detail when such solutions exist.

That the defect operators obtained by perturbing the $(1,2)$ defect by $(1,3)$-fields mutually commute can be checked with the condition in Section 8.1.4. Since $\mathcal{D}\otimes\mathcal{D}\cong(1,1)\oplus(1,3)$, the graph Γ takes the simple form:

$\Gamma =$ 

(8.2.22)

This graph has no non-trivial closed loops, and so by the observations at the end of Section 8.1.4, the perturbed defect operators mutually commute for different values of λ.

8.2.5 (1,5)-perturbation of the defect (1,3)

Consider $M(p,q)$ for $q\geq 6$ perturbed by $x=(1,5)$, and the elementary topological defect $\mathcal{D}=a=(1,3)$.

The case $q=6$ is the one treated in Section 8.2.1. We have $h_{1,5}=6t-2=p-2$. Thus for the present x and a, in $M(p,6)$ the commutation relation is satisfied for any choice of $\kappa\widetilde{\kappa}$.

Assume now that $q\geq 7$. We first check the value of $\mathrm{F}_{aa}^{(xa\overline{x})a}$ in the case $b=a$ in (8.2.1) to see if it can be 1. Explicitly,

$$\mathrm{F}_{33}^{(535)3} = \frac{\sin(2\pi t)}{4\sin(5\pi t)\cos(\pi t)\cos(2\pi t)} =: f(t)\ . \tag{8.2.23}$$

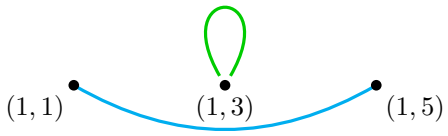
The only solutions to the trigonometric equation $f(t)=1$ are of the form $t\in\frac{s}{6}+2\mathbb{Z}$ for certain values of s. But for us $t=\frac{p}{q}$ with p,q coprime and $q\geq 7$, so that we can conclude

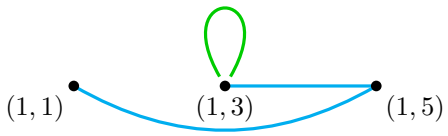
$$\mathrm{F}_{33}^{(535)3}\neq 1 \quad \text{for } q\geq 7\ . \tag{8.2.24}$$

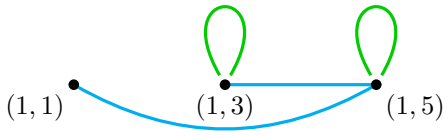
The case $b=a$ in (8.2.1) thus dictates the value for $\kappa\widetilde{\kappa}$ as given in (8.2.2). Since $x\otimes a=(1,5)\otimes(1,3)\cong(1,3)\oplus(1,5)\oplus(1,7)$ (where $(1,7)$ is only present for $q\geq 8$), the cases $b\neq a$ in (8.2.1) have to be checked for $b=(1,3)$ and $b=(1,7)$ (for $q\geq 8$), and we did verify that they indeed hold for the value of $\kappa\widetilde{\kappa}$ in (8.2.2)

The perturbed defect operators mutually commute by the criterion in Section 8.1.4. Namely, the fusion of $\mathcal{D}$ with itself is $\mathcal{D}\otimes\mathcal{D}\cong(1,1)\oplus(1,3)\oplus(1,5)$. The graph Γ depends

on the value of q:

$q = 6 \ : \ \Gamma =$ 

$q = 7 \ : \ \Gamma =$ 

$q \geq 8 \ : \ \Gamma =$ 

(8.2.25)

In all these cases, the graph has no non-trivial closed loops, and so by Section 8.1.4, the perturbed defect operators mutually commute for different values of λ.

In summary, the bulk commutation condition for the $(1,5)$-perturbation on the $(1,3)$-defect can be solved for all $M(p,q)$ with $q \geq 6$, and in all cases the perturbed defect operators mutually commute for different values of λ.

8.2.6 (1,7)-perturbation of the defect (1,5)

Consider now $M(p,q)$ perturbed by $x = (1,7)$, and the elementary defect $\mathcal{D} = a = (1,5)$. The perturbation x is supported on the defect a only for $q \geq 9$, so that we restrict to those values in the following.

Bulk commutation relation. One may verify that

$$\mathrm{F}_{55}^{(757)5} - 1 = -\frac{4\cos(4\pi t) + 4\cos(8\pi t) + (\cos(4\pi t))^{-1}}{4\cos(2\pi t) + 4\cos(4\pi t) + 4\cos(8\pi t) + 2} \neq 0 \quad \text{for all } t \in \mathbb{R}\ , \tag{8.2.26}$$

so that, if a solution to the equation with $b = a$ in (8.2.1) exist, then $\kappa\widetilde{\kappa}$ is given by (8.2.2). To see if such a solution exist we must check that all the equations in (8.2.1) with $a \otimes x \ni b \neq a$ are also satisfied. The content of $a \otimes x$ depends on q via (8.2.11). For $q \geq 9$ we have $(1,3), (1,5) \in a \otimes x$, and therefore (8.2.1) with $b = (1,3)$ must be satisfied for all choices of $q \geq 9$.

We first check that the F-matrix element multiplying $\kappa\widetilde{\kappa}$ in the second line of (8.2.1) is not zero. Explicitly,

$$\mathrm{F}_{53}^{(757)5} = \frac{4^{1-8t}\sin(2\pi t)\tan(3\pi t)\,\Gamma\left(\frac{3}{2} - 4t\right)\Gamma(1-3t)\Gamma(1-t)\Gamma(4t)}{\sin(5\pi t)\sin(7\pi t)\Gamma(2-5t)\Gamma(2-4t)\Gamma(t)\Gamma\left(4t - \frac{1}{2}\right)}\ . \tag{8.2.27}$$

For $t = \frac{p}{q}$ with p, q coprime and $q \geq 9$, none of the Γ-function arguments is in $\mathbb{Z}_{\leq 0}$, none of the sin-arguments is in $\pi\mathbb{Z}$, and the tan-argument is not in $\frac{\pi}{2}\mathbb{Z}$. So $\mathrm{F}_{53}^{(757)5}$ is well-defined and non-zero.

Next we substitute the value of $\kappa\widetilde{\kappa}$ in (8.2.2) into the second line in (8.2.1) with $b = (1,3)$.

$$\left(\mathrm{R}^{(75)3} - \frac{1}{\mathrm{R}^{(75)3}}\right) \mathrm{F}_{13}^{(577)5} \;=\; -\mathrm{F}_{53}^{(757)5} \left(\mathrm{R}^{(75)5} - \frac{1}{\mathrm{R}^{(75)5}}\right) \frac{\mathrm{F}_{15}^{(577)5}}{1 - \mathrm{F}_{55}^{(757)5}} \,. \tag{8.2.28}$$

The F-matrix elements are all non-zero (see also Footnote 4), and $\mathrm{R}^{(75)3} - 1/\mathrm{R}^{(75)3} = -2i\sin(16\pi t)$.

We first treat the case that $t \notin \frac{1}{16}\mathbb{Z}$. Then the left hand side is non-zero, and we can divide by it. Substituting the explicit values gives

$$\frac{2 + (\cos(8\pi t))^{-1}}{4\cos(4\pi t) + 4\cos(8\pi t) + 4\cos(12\pi t) + 6} = 1 \,, \tag{8.2.29}$$

whose solutions are $t \in f + \frac{1}{2}\mathbb{Z}$, $f = \pm\frac{1}{5}, \pm\frac{1}{9}, \pm\frac{2}{9}, \pm\frac{1}{10}, \pm\frac{1}{18}$. From this one can read off that the solutions with $q \geq 9$ are precisely

$$t = \frac{p}{q} \,, \qquad q = 9, 10, 18 \,, \qquad \text{any } p \text{ coprime with } q \,. \tag{8.2.30}$$

The further equations depend on the values of q:

$$\begin{aligned} q = 9 : &\qquad a \otimes x = (1,3) \oplus a \\ q = 10 : &\qquad a \otimes x = (1,3) \oplus a \oplus (1,7) \\ q = 18 : &\qquad a \otimes x = (1,3) \oplus a \oplus (1,7) \oplus (1,9) \end{aligned} \tag{8.2.31}$$

We have verified that in each respective case the corresponding equations in (8.2.1) are satisfied by $\kappa\widetilde{\kappa}$ in (8.2.2).

Next we turn to the case $t \in \frac{1}{16}\mathbb{Z}$. In order to solve (8.2.28), also the right hand side must be zero, that is, we need $\mathrm{R}^{(75)3} - 1/\mathrm{R}^{(75)3} = 2i\sin(12\pi t) = 0$. This is the case for $t \in \frac{1}{48}\mathbb{Z}$. However, one can verify that then (8.2.1) does not hold for the choice $b = (1,7)$.

Altogether, we find that the bulk commutation relation for the $(1,7)$-perturbation on the $(1,5)$-defect is satisfied only in the minimal models

$$M(p,9) \,, \qquad M(p,10) \,, \qquad M(p,18) \,. \tag{8.2.32}$$

Mutual commutation. Let us now discuss the mutual commutation. The fusion graphs Γ for the three cases are listed in Figure 8.9. Note that in writing the fusion graph for $q = 10$ we omitted the edge $(1,3)-(1,7)$. While this edge would be allowed by the fusion rules, the corresponding F-symbol

$$\mathrm{F}_{a7}^{(aax)3}\Big|_{q=10} = \frac{\left(\sin\left(\frac{\pi p}{5}\right) - \sin\left(\frac{2\pi p}{5}\right) + \sin\left(\frac{3\pi p}{5}\right) - \sin\left(\frac{4\pi p}{5}\right)\right) \Gamma\left(2 - \frac{3p}{5}\right) \Gamma\left(\frac{4p}{5} - 1\right) \Gamma\left(\frac{2p}{5}\right)}{\pi \left(2\cos\left(\frac{\pi p}{5}\right) - 1\right) \Gamma\left(\frac{3p}{5}\right)} \tag{8.2.33}$$

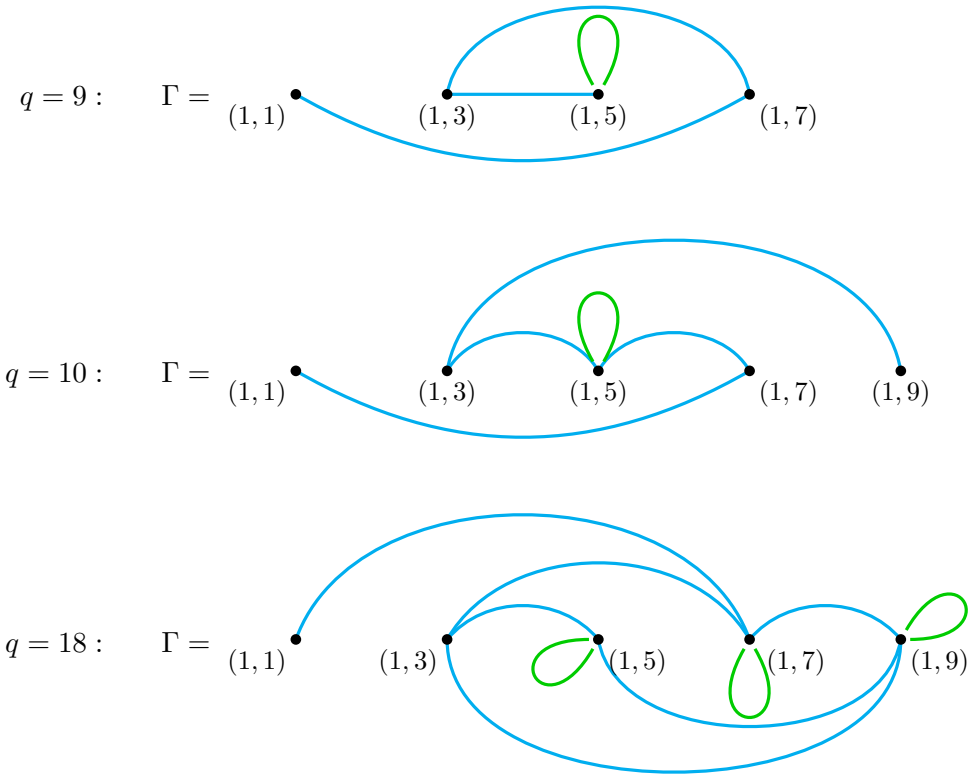


Figure 8.9: The fusion graphs for the $(1,7)$-perturbation on of $(1,5)$-defect in $M(p,q)$.

vanishes for any odd p at $q = 10$ (but not for $q = 9, 18$). Analogously, in the $q = 18$ diagram, we did not draw the edge $(1,5)-(1,7)$ as for $q = 18$ (but not for $q = 9, 10$)

$$\mathrm{F}_{a7}^{(aax)5}\Big|_{q=18} = 0 \tag{8.2.34}$$

for any p coprime to $q = 18$.

The argument in Section 8.1.4 implies that the perturbed defects mutually commute for $q = 9$ and $q = 10$ since there are no non-trivial loops.

For $q = 18$ one needs to check that (8.1.29) holds for a selection of generating loops γ. We choose

$$\gamma_{359} = 3 \to 5 \to 9 \to 3\,, \qquad \gamma_{379} = 3 \to 7 \to 9 \to 3\,. \tag{8.2.35}$$

Since the two differ only by $5 \leftrightarrow 7$, we write generically γ_{3k9}, with $k = 5, 7$. We need to check (8.1.29) for these two path:

$$F_{\gamma_{3k9}}(\lambda, \lambda') = F_{\gamma_{3k9}}(\lambda', \lambda) \quad \text{for} \quad k = 5, 7\,. \tag{8.2.36}$$

a	$x \in a \otimes a$
$(1,1)$	$(1,1)$
$(1,2)$	$(1,1)\,,\ (1,3)$
$(1,3)$	$(1,1)\,,\ (1,3)\,,\ (1,5)$
$(1,4)$	$(1,1)\,,\ (1,3)\,,\ (1,5)\,,\ (1,7)$
$(1,5)$	$(1,1)\,,\ (1,3)\,,\ (1,5)\,,\ (1,7)\,,\ (1,9)$
$(1,6)$	$(1,1)\,,\ (1,3)\,,\ (1,5)\,,\ (1,7)$
$(1,7)$	$(1,1)\,,\ (1,3)\,,\ (1,5)$
$(1,8)$	$(1,1)\,,\ (1,3)$
$(1,9)$	$(1,1)$

Table 8.2: The (anti)holomorphic defect fields on the elementary defect a are indexed by those x that appear in the fusion $a \otimes a$.

One readily computes that

$$\begin{aligned} &F_{\gamma_{3k9}}(\lambda,\lambda') - F_{\gamma_{3k9}}(\lambda',\lambda) \\ &\quad = \lambda\,\lambda'(\lambda-\lambda')(\mathrm{R}^{(55)3} - \mathrm{R}^{(55)k})(\mathrm{R}^{(55)3} - \mathrm{R}^{(55)9})(\mathrm{R}^{(55)k} - \mathrm{R}^{(55)9})\ . \end{aligned} \tag{8.2.37}$$

For $q = 18$ one has

$$\mathrm{R}^{(55)3} - \mathrm{R}^{(55)9} = -e^{-i5\pi p/9}\left(1 + e^{i\pi p}\right) = 0\,. \tag{8.2.38}$$

Altogether we see that (8.1.29) holds for the two generating loops, and hence for all loops. By the criterion in Section 8.1.4 we can conclude that also for $q = 18$ the perturbed defect operators mutually commute.

8.2.7 The minimal model $M(3,10)$ in detail

Up to now we have looked at a fixed combination of perturbation and defect and asked in which models the bulk commutation condition is satisfied, and whether the perturbed defects mutually commute. Here we want to instead consider one example, namely the minimal model $M(3,10)$, and look at two situations: perturbing an elementary defect $\mathcal{D} = a$ by some x, and perturbing $\mathcal{D} = \mathbf{1} \oplus x$ by x. In both cases it is understood that the bulk CFT is perturbed by the bulk field labelled x.

We note that the $M(3,10)$ minimal model is one of the three cases where a product of two minimal models is again a minimal model. Here, the D-invariant of $M(3,10)$ is the product of two copies of the Lee-Yang model $M(2,5)$. This and the other two cases are treated in more detail e.g. in [287, App. C].

Non-local charges in $M(3,10)$ from $\mathcal{D} = a$

As unique representatives of the Kac-labels in $M(3,10)$ we can take $(1,s)$ with $1 \le s \le 9$. The primary holomorphic and antiholomorphic defect fields on the elementary topological defect $\mathcal{D} = a$ are indexed by those x that are contained in the fusion $a \otimes a$, see Table 8.2.

For each a, and for each $x \in a \otimes a$ we ask if a solution to the bulk commutation condition exists, and if the criteria in Section 8.1.4 can be used to show that the perturbed defects mutually commute. The results are collected in Table 8.3.

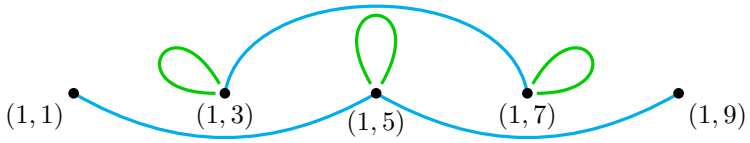
Checking whether the bulk commutation condition holds for a given a and x in the table simply amounts to verifying whether (8.1.17) has a solution in that case or not. We have checked this condition, with the results in the table.

Mutual commutativity of the perturbed defects can be seen using the criterion in Section 8.1.4. Let us go through this criterion for the columns one by one:

- $x = (1,3)$: In this case the fusion graph Γ cannot have non-trivial closed loops.
- $x = (1,5)$: The case $a = (1,3)$ was treated in Section 8.2.5, and the case $a = (1,7)$ works analogously. For $a = (1,5)$ the fusion graph Γ turns out to have no loops due to the vanishing of F-matrix elements:

$$\mathrm{F}_{53}^{(555)5} = 0 \quad \text{and} \quad \mathrm{F}_{57}^{(555)5} = 0 \ . \tag{8.2.39}$$

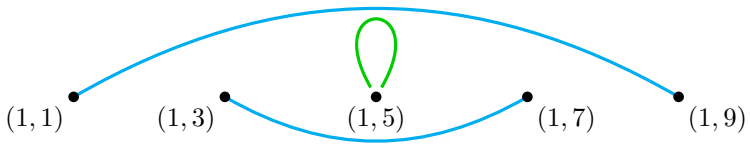
  Thus the edges $(1,3)-(1,5)$ and $(1,5)-(1,7)$ which would by allowed by the fusion rules are not present (see (8.1.26)) and there are indeed no loops:

$\Gamma =$ 

(8.2.40)

  Note that in this example, the composition of perturbed defect operators decomposes into a sum of a $(1,5)$-perturbation on $(1,1) \oplus (1,5) \oplus (1,9)$ and on $(1,3) \oplus (1,7)$, both of which therefore satisfy the bulk commutation condition.

- $x = (1,7)$: This case was treated in Section 8.2.6.
- $x = (1,9)$: Note that $x \otimes x \cong \mathbf{1}$ and we are in the situation discussed in Section 8.2.1. The conformal weight of the primary state in the representation x is $h_x = 2$, and so (8.2.1) just becomes $0 = 0$, i.e. the bulk commutation condition is solved for any choice of κ and $\widetilde{\kappa}$. The fusion graph Γ again has no loops:

$\Gamma =$ 

(8.2.41)

Recall that the D-invariant of $M(3,10)$ is equivalent to two copies of $M(2,5)$. Denote the representations of $M(2,5)$ by $\mathbf{1}$ and ϕ. Then in terms of $M(3,10)$-representations, the representations in the product decompose as

$$\mathbf{1} \times \mathbf{1} = (1,1) \oplus (1,9) \quad , \quad \mathbf{1} \times \phi = \phi \times \mathbf{1} = (1,5) \quad , \quad \phi \times \phi = (1,3) \oplus (1,7) \ . \tag{8.2.42}$$

Defect, a	Perturbation, x			
	$(1,3)$	$(1,5)$	$(1,7)$	$(1,9)$
$(1,2)$	✓✓	–	–	–
$(1,3)$	✓✓	✓✓	–	–
$(1,4)$	✓✓	×	×*	–
$(1,5)$	✓✓	✓✓	✓✓*	✓✓*
$(1,6)$	✓✓	×	×*	–
$(1,7)$	✓✓	✓✓	–	–
$(1,8)$	✓✓	–	–	–

Table 8.3: Perturbation by x on the topological defect a. The entries are as follows: $-$, the perturbation does not exist; $\times$, the perturbed defect does not commute with the Hamiltonian; ✓✓, the non-local charges commute with the Hamiltonian and we can also prove that they mutually commute; * indicates that the non-local charges require regularisation and so the arguments are only formal.

In $M(2,5)$, the ϕ-perturbation on the ϕ-defect satisfies the bulk commutation condition and mutual commutativity, and so it is maybe not too surprising to find the same in $M(3,10)$. But it would still be interesting to understand in more detail how these conditions behave under gauging of topological symmetries (a $\mathbb{Z}_2$ in this case).

Non-local charges in $M(3,10)$ based on two defects $\mathbf{1} \oplus x$

The perturbations that are supported on a superposition of defects $\mathbf{1} \oplus a$ are those that are supported by the defect a alone, and those which interpolate the defects $\mathbf{1}$ and a, which is forced to be of type a. In Table 8.4 we give the results for the defects of type $\mathbf{1} \oplus x$ perturbed by x. This includes cases in which the defect x supports the field x and cases in which it does not.

Let us explain the entries for mutual commutativity in more detail. The case $x = (1,2)$ is treated in Section 8.2.3, relying on the criterion in Section 8.2.1. The $(1,3)$-perturbation of $(1,1) \oplus (1,3)$ can be obtained by taking the product of two $(1,2)$-defects perturbed by $(1,3)$. Since by Table 8.3, these do mutually commute, the same holds for their products. For $x = (1,8)$ we have $x \otimes x = (1,1) \oplus (1,3)$ and so the criterion in Section 8.2.1 applies: both, the bulk commutation condition and mutual commutativity are satisfied.

The representations $(1,s)$ of $M(3,10)$ with s even do not occur in the product of two $M(2,5)$-models and whether or not they solve the bulk commutation condition can not be predicted from there. For these, we only find solutions on $(1,1) \oplus (1,s)$ for $s = 2,8$. The $(1,2)$-perturbation is generically integrable and the $(1,8)$-perturbation is only formal as it would need regularisation.

Defect, $1 \oplus x$	Perturbation, x
$(1,1) \oplus (1,2)$	✓✓
$(1,1) \oplus (1,3)$	✓✓
$(1,1) \oplus (1,4)$	×
$(1,1) \oplus (1,5)$	✓
$(1,1) \oplus (1,6)$	×
$(1,1) \oplus (1,7)$	✓*
$(1,1) \oplus (1,8)$	✓✓*
$(1,1) \oplus (1,9)$	✓*

Table 8.4: The x-perturbation on the defect $\mathcal{D} = 1 \oplus x$. The entries in the right column are as in Table 8.3, and in addition a single tick ✓ means that the perturbed defect commutes with the Hamiltonian, but we are unsure if the charges mutually commute.

8.2.8 Further observations

After the systematic treatment in the previous sections, here we collect some additional observations which indicate that we are still quite far from a complete picture of solutions to the commutation condition in minimal models:

- In Section 8.2.6 we saw that for the $(1,7)$-perturbation on the $(1,5)$-defect allows for a solution of the bulk commutation condition iff $q = 9, 10, 18$. If we instead take the defect $(1,1) \oplus (1,7)$, there are solutions for $M(p,11)$ and $M(p,18)$.

- We found solutions to the $(1,4)$-perturbation on $(1,1) \oplus (1,4)$ in $M(p,5)$, $M(p,6)$ for all p, in $M(p,7)$ for all even p, and exceptionally in $M(2,9)$, $M(2,11)$. For the $(1,6)$-perturbation on $(1,1) \oplus (1,6)$ we found solutions for $q = 7,8,9$ (and exceptionally in $M(2,11)$).

- In addition to the perturbations already mentioned, we looked at the bulk commutation relation for $(1,2k+1)$-perturbations of elementary defects for $k = 4,5,6$. Again, we do not have a complete picture for these perturbations, but have found the following.

  i) The $(1,9)$-deformation of $(1,5)$ defect satisfies bulk commutation in the minimal models $M(p,10)$, $M(p,11)$, $M(p,12)$. The same deformation on the $(1,6)$ defect is supported on $M(p,11)$, $M(p,12)$, on the $(1,7)$ defects commutes in $M(p,12)$, $M(p,14)$. We have not found any solutions for the $(1,9)$ deformation of the elementary defects $(1,n)$, for $8 \leq n \leq 19$.

  ii) The $(1,11)$-deformation of the $(1,6)$-defect satisfies the bulk commutation in $M(p,12)$ and $M(p,13)$, and of the $(1,7)$-defect in $M(p,13)$ and $M(p,14)$. We did not find any other solution to the bulk commutation relation for the $(1,11)$-deformation of the $(1,n)$-defect for $8 \leq n \leq 19$.

iii) The $(1,13)$-deformation of the $(1,7)$-defect satisfies the bulk commutation in $M(p,14)$, $M(p,15)$ and $M(p,16)$, of the $(1,8)$-defect in $M(p,15)$ and $M(p,16)$, and of the $(1,9)$-defect in $M(p,16)$, $M(p,18)$. We have not found any solutions for the $(1,13)$ deformation of the elementary defects $(1,n)$, for $10 \leq n \leq 19$.

- In all solutions to the bulk commutation condition that we found, the perturbing field is of the form (r,s) with either $r=1$ or $s=1$.

We did not try to check mutual commutativity in these cases.

8.3 Local conserved charges

It has long been recognised that the presence of non-trivial local conserved quantities can lead to the integrability of quantum field theories – see e.g. [223] for a discussion. Up to now, these have only been found in cases related to some classically integrable system (e.g. generalised affine Toda theories/Drinfeld-Sokolov hierarchies) or where there is a relation to extended chiral symmetry.

For the Virasoro minimal models, the three standard integrable perturbations, $(1,2)/(5,1)$, $(1,3)/(3,1)$ and $(1,5)/(2,1)$, can be identified with quantisations of the affine Toda theories related to $a_2^{(2)}$, $a_1^{(1)}$ and $a_2^{(2)}$ respectively. It is known [288] that there are generically (i.e. for irrational central charge c) local conserved quantities with spins equal to the exponents of the corresponding affine algebra, that is all odd spins for $(1,3)/(1,3)$ perturbations, and all spins congruent to 1 or 5 mod 6 for the other perturbations. However, we do not know of a statement or proof of the general number of conserved quantities of each spin for each perturbation in the case of minimal models. A conserved charge predicted in the classical theory may vanish in the quantum model (as happens for the spin 5 charge for the $(1,2)$ perturbation of the Ising model), and the number of charges may also be increased if there is a relation to an extended symmetry (as happens for the $(1,3)$ perturbation of the Ising model where the perturbing field has weight $h=\frac{1}{2}$ and there are extra conserved charges due to its relation to a free fermion).

It is also possible that a perturbation can be identified with a different integrable system, which can lead to further particular perturbations being integrable in specific models, or a change in the number of conserved quantities. As an example of the last case, the $(1,2)$ perturbation of the Ising model can also be identified with a quantised $e_8^{(1)}$ affine Toda theory, which "explains" why the spin 5 charge vanishes as 5 is not an exponent of $e_8^{(1)}$.

In the series of papers [253,255,256], it was shown that there is a quantum version of the classical result that the monodromy matrices have an asymptotic expansions in the local conserved charges. These papers defined "quantum transfer matrices" (which can be identified as perturbed defects) which have an asymptotic expansion over the set of local conserved charges – i.e. there is an intrinsic relation between the non-local perturbed defects and the local charges.

We have consequently two questions we can try to answer – are there local conserved quantities for the new perturbations that we have found that are not related to known

classical integrable hierarchies? – if not, is there a reason why the perturbed defects we have defined do not have an asymptotic expansions over local charges? We consider these two questions in Sections 8.3.1 and 8.3.2 respectively.

8.3.1 Search for local conserved quantities

The consideration of quantum local conserved charges in perturbed conformal field theories defined entirely through the properties of the quantum field theory (rather than derived from some underlying construction, such as the non-local charges that can be shown to exist through a free-field construction related to Toda theory) dates back to [274]. This states that the expression for the antiholomorphic derivative in the perturbed theory, $\overline{\partial}W$ of a field W which is holomorphic in the unperturbed theory, can be expanded out order by order in μ,

$$\overline{\partial}W = \sum_{n=1}(2i\mu)^n V_n = (2i\mu)V_1 + \sum_{n=2}(2i\mu)^n V_n \ . \tag{8.3.1}$$

Using $[\cdot]$ to denote (mass) scaling dimension as usual, $[\overline{\partial}W] = h_W + 1$ and $[\mu] = 2 - 2h_\varphi$ so $[V_n] = 2nh_\varphi - 2n + h_W + 1$. Since $[\varphi] = 2h_\varphi$, V_1 is always an allowed term, as a level $h_W - 1$ descendant of φ. Whether other V_n are allowed or not depends in detail on the model and perturbation under consideration.

For a rational model, since the dimension of μ is rational, there will always be some power N for which μ^N has integer dimensions, and so higher contributions V_{1+rN} will always be possible for h_W large enough).

It is a necessary condition for the conservation of W that V_1 is a total ∂-derivative. In the lucky circumstance that the expansion (8.3.1) terminates at the first term, this constitutes a proof of the existence of a conserved charge in the perturbed model. In general, if V_1 is a total derivative, the conservation condition may be obstructed by higher terms V_n, but if V_1 is *not* a total derivative, then this cannot be improved by higher order terms and this proves that there is no associated conserved current. So, from now, on, we focus entirely on the condition on V_1.

The condition on V_1 is given in Equation (B.4.8) in [4, Appendix C] and can be checked explicitly (using `Mathematica`) in any particular cases. Note that the existence of solutions to (B.4.8) has no bearing on the mutual commutativity, or otherwise, of the corresponding charges.

The general expectation is that we will find solutions to (B.4.8) with spins equal to those in the corresponding classical system whenever the perturbation can be identified as the quantisation of classical integrable system, although some of the charges may vanish through singular vector conditions in particular models, and extra solutions can also arise – but up to now nobody has identified any perturbed models outside the classically integrable class which have local conserved charges.

This is what we also find (in all but one case in which the classical system is so far unidentified). We have performed checks in a large number of models for a large number of perturbations and we have found solutions to (B.4.8) in the following cases.

$M(p,q)$	$\mathrm{pert}^{n.}$	h	4	5	6	7	8	9	10	11	12	13	14	15	16	17	18	19	20
$(2,5)$	$(1,2)$	$-\frac{1}{5}$	–	–	1	–	1	–	–	–	1	–	1	–	–	–	1	–	1
	$(1,3)$	$-\frac{1}{5}$	$-^1$	–	1	–	1	–	$-^1$	–	1	–	1	–	$-^1$	–	1	–	1
$(2,11)$	$(1,2)$	$-\frac{4}{11}$	–	–	1	–	1	–	–	–	–	–	1	–	–	–	1	–	1
	$(1,3)$	$-\frac{7}{11}$	1	–	1	–	1	–	1	–	1	–	1	–	1	–	1	–	1
	$(1,4)$	$-\frac{9}{11}$	–	–	–	–	1	–	–	–	1	–	1	–	–	–	1	–	1
	$(1,5)$	$-\frac{10}{11}$	–	–	1	–	1	–	–	–	1	–	1	–	–	–	1	–	1
$(3,4)$	$(1,2)$	$\frac{1}{16}$	–	–	$-^1$	–	1	–	–	–	1	–	1	–	–	–	1	–	1
	$(1,3)^2$	$\frac{1}{2}$	1	–	1	–	1	–	1	–	2	–	2	1	3	1	4	2	5
$(4,5)$	$(1,2)$	$\frac{1}{10}$	–	–	1	–	1	–	–	–	1	–	1	–	–	–	1	–	1
	$(1,3)$	$\frac{3}{5}$	1	–	1	–	1	–	1	–	1	–	1	–	1	–	1	–	1
	$(3,1)^2$	$\frac{3}{2}$	1	–	1	–	2	–	2	1	3	1	5	2	6	4	9	6	13
	$(2,1)$	$\frac{7}{16}$	–	–	1	–	1	–	–	–	1	–	1	–	–	–	1	–	1
	$(2,2)$	$\frac{3}{80}$	–	–	–	–	–	–	–	–	–	–	–	–	–	–	–	–	–

Table 8.5: Spins of conserved currents in selected models. In some cases, currents which are expected by relation to classical integrable systems vanish (marked ^{1}); in some cases there are extra currents (marked ^{2}). See the text for details.

(1,2), (1,3) and (1,5) perturbations

These perturbations are are related to the $a_1^{(1)}$ (for (1,3)) and $a_2^{(2)}$ (for (1,2) and (1,5)) algebras and classically one has conserved charges of all odd spins in the first case and all spins congruent to 1 or 5 mod 6 in the second case. This is not exactly the case for the quantum systems since, as mentioned already, some charges may vanish unexpectedly and extra charges can occur, as with the examples in Table 8.5.

(1,4) perturbations

These are not typically identifiable with a classical integrable model, and in all the cases we have checked there are no local conserved charges, apart from one exception, the $(1,4)$ perturbation in $M(2,11)$. In this particular case the chiral algebra can be identified with the degeneration of the WG_2 chiral algebra to at $c=-232/11$ to the Virasoro algebra [289], and the $(1,4)$ perturbation can be identified as related to $d_4^{(3)}$ affine Toda theory. Again, see Table 8.5.

(1,7) perturbations

We have searched for solutions to the first-order conservation condition (B.4.8) for $(1,7)$ perturbations of the models $M(p,q)$ with $p,q\leq 20$, which includes the specific cases $q\in\{9,10,18\}$ discussed in Section 8.2.6. The results are in Table 8.6. In almost all cases we found no conserved charges with spins ≤ 16, with only the following exceptions:

- $M(2,9)$ - the perturbation can be identified with $(1,2)$

$M(p,q)$	c	h	4	5	6	7	8	9	10	11	12	13	14	15	16
$(2,9)$	$-\frac{46}{3}$	$-\frac{1}{5}$	–	–	1	–	1	–	–	–	1	–	1	–	–
$(2,11)$	$-\frac{232}{11}$	$-\frac{9}{11}$	–	–	–	–	1	–	–	–	1	–	1	–	–
$(3,8)$	$-\frac{21}{4}$	$\frac{3}{2}$	–	–	1	–	2	–	2	1	3	1	5	3	6
$(5,8)$	$-\frac{7}{20}$	$\frac{9}{2}$	–	–	–	–	1	–	–	–	–	–	–	–	–
$(7,8)$	$\frac{25}{28}$	$\frac{15}{2}$	–	–	–	–	–	–	–	–	–	–	1	–	–
$(13,18)$	$\frac{14}{39}$	$\frac{17}{3}$	–	–	–	–	–	–	–	–	–	–	1	–	1

Table 8.6: Models $M(p,q)$ with $p,q \leq 20$ for which there are currents with spins ≤ 16 for $\psi_{1,7}$ perturbations which solve the first-order conservation condition (B.4.8), together with the number of independent currents for each spin.

- $M(2,11)$ - the perturbation can be identified with $(1,4)$ and so, as above, the chiral algebra can be identified with WG_2 and the perturbation can be identified with $d_4^{(3)}$ affine Toda theory.
- $M(3,8)$ - the perturbation can be identified with $(2,1)$, and has extra conserved charges as $h = 3/2$.
- $M(p,8)$ - the perturbation is a simple current of half-integer weight and is related to an extended chiral algebra. We conjecture that in each case there is a solution of (B.4.8) of spin $(3p-7)$ and have checked that there is a conserved current of spin 20 for $p = 9$. The cases with $p > 7$ do not appear in Table 8.6 because this is greater than 16. These are all irrelevant perturbation and so there are an infinite number of extra terms which can arise in the the conservation condition (8.3.1).
- $M(13,18)$ at $c = 14/39$ - we do not have an identification, as yet, of this with the quantisation of a classical integrable system. This is, again, an irrelevant perturbation and so there are an infinite number of extra terms which can arise in the conservation condition (8.3.1).

This is not a proof of the existence of these conserved quantities since in all cases there are potential extra terms coming from $\lambda^3 V_3$ with V_3 in the $(1,5)$ representation, as well as possibly higher terms, and we do not know a way to calculate these potential corrections.

8.3.2 Local charges from perturbed defects

As we have said, quantum non-local operators were shown to be related to local charges in [253,255,256]. The first two papers considered critical bulk theories and chiral perturbations and the third paper considered the addition of bulk perturbations. In the first case, they showed that the "quantum transfer matrices" they considered had an

expansion for small perturbation parameter λ as non-local charges, and for large λ an asymptotic expansion in terms of local charges. In our language, the quantum transfer matrix corresponds to a chirally perturbed topological defect $\mathcal{D}(\lambda\psi)$ in the CFT which in the UV has an expansion in λ of integrals along the defect, but for large λ, the same perturbed defect has an expansion in local charges. For this to be valid, the IR limit of the perturbed defect must be the identity defect.

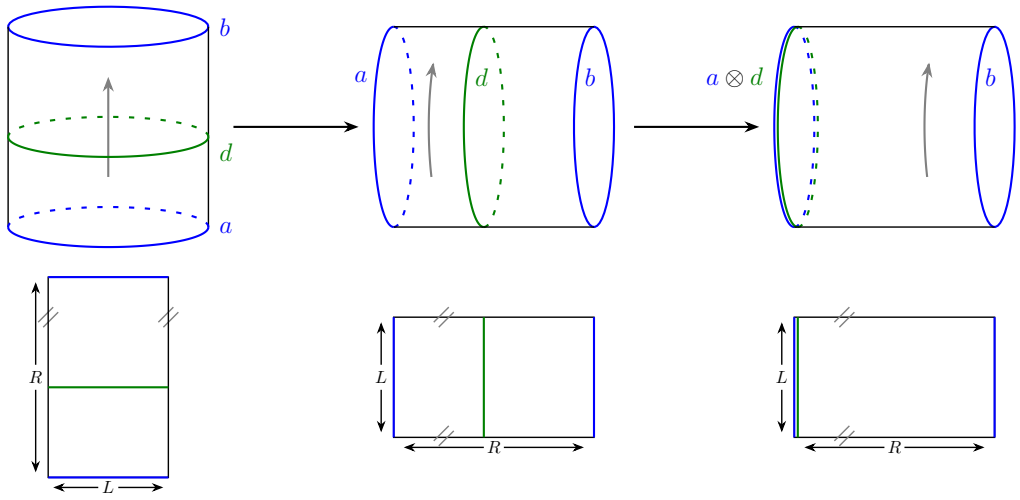
We have found models in which we propose the existence of non-local conserved charges as perturbed defects but for which we have not (as yet) found any local conserved currents. While we have paid most attention to bulk-perturbed theories, we can choose to turn off the bulk perturbation and then consider the resulting chirally perturbed defects in the unperturbed CFT. Any flow in the IR to an expansion over local conserved charges in the bulk-perturbed model ought then imply a flow of the chirally perturbed defects to an expansion over corresponding local conserved charges in the unperturbed CFT. Such a relation will only be possible if the ultimate IR endpoint of the chirally perturbed defect is the identity defect.

All our calculations so far in this thesis have been perturbative, but there is a non-perturbative technique which can be used to investigate the IR endpoint of perturbed defect, which is the truncated conformal space approach (TCSA). This is a numerical approximation to a perturbed theory in finite-dimensional spaces which has already been applied to defect models, in particular it was used to investigate the joint bulk- and defect-perturbations of the Lee-Yang model in [290]. In this section we apply this technique to study chiral defect perturbations in CFT and investigate their IR endpoints. For technical reasons, it is simplest to consider the original system on a cylinder with boundary conditions on the two ends so that in the crossed channel the system is propagating along a strip with boundary conditions on the two sides.

The principal idea is that the nature of an IR fixed point can be constrained or even identified by the spectrum of the corresponding Hamiltonian. While we have, up to now, thought of defects as operators which may or may not commute with a bulk Hamiltonian, we can also look at a crossed channel in which the defect runs along the "timelike" direction at a fixed spatial position x and the Hamiltonian for the system with such a defect is the conformal Hamiltonian perturbed by a defect operator $\hat{D}(x)$ located on the defect, as in Figure 8.10.

Since the chirally-perturbed defect is translationally invariant, it can be moved to the boundary so that spectrum of the Hamiltonian H' on the strip with boundary conditions a and b and a defect d is equal to the spectrum of the Hamiltonian H'' of the system on the strip without a defect but with boundary conditions $a \otimes d$ and b perturbed by a boundary field $\hat{B}_L$. For the Lee-Yang model, boundary perturbations were studied extensively in [291] (see e.g. Figures 1a and 1b there).

We have now investigated several models with commuting non-local charges. In each case, we chose the boundary conditions a and b to be the identity representation. With no perturbation turned on, the spectrum of the strip with identity boundary conditions on the two edge and a defect of type d is given by the d representation. If the defect flows to the identity in the IR, the IR end point will simply be the system on a strip



$H = \frac{2\pi}{L}\left(L_0 + \overline{L}_0 - \frac{c}{12}\right)$ $H' = \frac{2\pi}{L}\left(L_0 + \overline{L}_0 - \frac{c}{12}\right) + \hat{D}(x)$ $H'' = \frac{2\pi}{L}\left(L_0 + \overline{L}_0 - \frac{c}{12}\right) + \hat{B}_L$

Figure 8.10: The Hamiltonian H' in the crossed channel corresponding to propagation along the defect d on a system on a cylinder of length R with boundary conditions a and b on the ends of the cylinder, and H'' for the same system where the defect has been fused to the left boundary.

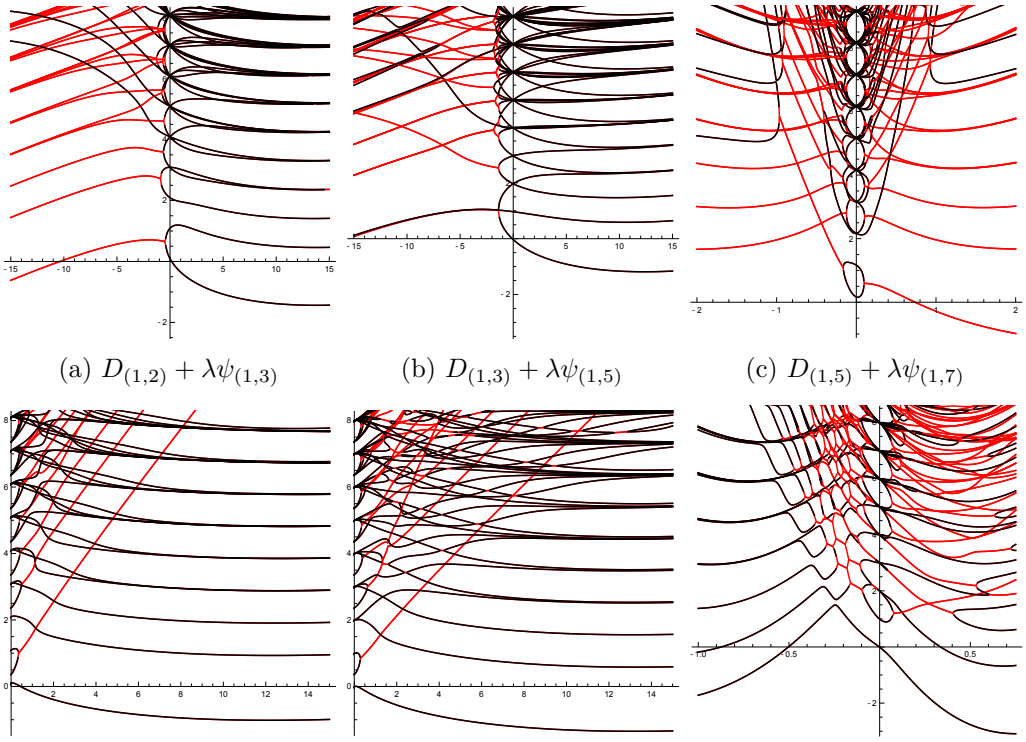
with identity boundary conditions and its spectrum will be the identity representation; if the spectrum is not given by that of the identity representation, the perturbed defect does not flow to the identity defect in the IR.

In each case we looked at where there are associated local charges, the spectrum of the perturbed defect flows in the IR to the identity, and in each case where there are no associated local charges, the defect does not flow to the identity defect in the IR.

We illustrate this in the case of the model $M(3, 10)$ in Figure 8.11.

We show plots of the spectrum of the purely chiral defect Hamiltonian against the perturbation parameter, calculated using the TCSA method used in [291], for three classes of models. In these plots, black lines indicate real energies, red lines indicate energies with non-zero imaginary part. In each case there is a non-trivial ground state energy which we have adjusted for clarity - the difference in behaviour between the perturbations by $(1, 2), (1, 3), (1, 4), (1, 5)$ on the one hand and $(1, 7)$ on the other is that the first four perturbations have $h < 1/2$ and a finite ground state energy while the $(1, 7)$ perturbation has $h > 1/2$ and so the ground state energy diverges as the truncation level increases.

It is also often the case that one can see strong indications of integrability, or lack of integrability, of the perturbed Hamiltonian from the presence, or absence, of line-crossings. It is common folklore that the spectrum can only have degeneracies if there is some conserved quantity which distinguishes states of the same energy. In TCSA, the only exact symmetries are discrete symmetries; those from local conserved currents being



(a) $D_{(1,2)} + \lambda\psi_{(1,3)}$ (b) $D_{(1,3)} + \lambda\psi_{(1,5)}$ (c) $D_{(1,5)} + \lambda\psi_{(1,7)}$

(d) $D_{(1,1)} \oplus D_{(1,2)} + \lambda\psi_{(1,2)}$ (e) $D_{(1,1)} \oplus D_{(1,4)} + \lambda\psi_{(1,4)}$ (f) $D_{(1,4)} + \lambda\psi_{(1,7)}$

Figure 8.11: The lowest 77 levels in the spectrum of the perturbed defect Hamiltonian on a strip in the model $M(3, 10)$ for various perturbations as calculated in TCSA with truncation up to level 18. The black lines correspond to real eigenvalues, the red lines to eigenvalues with non-zero imaginary part. In all cases a function of the perturbation parameter has been added to the eigenvalues for reasons of clarity. Plots (a), (b) and (d) have clear line crossing of black lines (an indication of integrability), while in (e) and (f) there are clear line avoidances; plot (c) is more ambiguous. Note that in cases (d) and (e) we only show the graphs for positive values since the perturbation is $\mathbb{Z}_2$ symmetric.

broken explicitly by the truncation, so one can only have an indication of integrability, not a proof.

We identified each perturbed defect flow as falling into one of the following three classes:

i) The massive perturbation has local conserved charges and we find the commuting non-local charges as a perturbed defect.

   This is the case for the perturbations $D_{(1,1)} \oplus D_{(1,2)} + \lambda\psi_{(1,2)}$ (Figure 8.11d), $D_{(1,2)} + \lambda\psi_{(1,3)}$ (Figure 8.11a) and $D_{(1,3)} + \lambda\psi_{(1,5)}$ (Figure 8.11b). In each case there is a flow in which the IR spectrum is that of the identity representation (indicating the IR endpoint is the identity defect).

The plots also exhibit multiple line crossings (an indication that the perturbation is integrable)

ii) The massive perturbation has no local conserved charges and have not found any non-local charges as a perturbed defect.

This is the case for the perturbations $D_{(1,1)} \oplus D_{(1,4)} + \lambda\psi_{(1,4)}$ (Figure 8.11e), $D_{(1,4)} + \lambda\psi_{(1,7)}$ (Figure 8.11f). In each case there is a flow in which the IR spectrum is that of the identity representation (indicating the IR endpoint is the identity defect).

There are also multiple line avoidances, suggesting that the perturbation is not integrable.

iii) The massive perturbation has no local conserved charges, but there are a family of commuting non-local charges.

This is the case for $D_{(1,5)} + \lambda\psi_{(1,7)}$ (Figure 8.11c). In this case, in neither direction of the flow does the spectrum flow to that of the vacuum representation - in both directions, the ground states are a pair with complex conjugate energies, so in neither direction does the defect flow to the identity defect.

The evidence on line crossings is more ambiguous - there are multiple possible line crossings indicating that the perturbation may well be integrable, but there are also large renormalisation effects due to the divergence of the perturbation which would require much more work to reduce.

To summarise, for the known integrable perturbations, (1,2), (1,3) and (1,5), in each case we find that there is a flow to the identity defect. These all exhibit the "typical" characteristic of integrable theories of line-crossings from the UV to the IR, and the flow to the IR to a single identity defect implies that in this limit the system can be described by a perturbation by local conserved currents.

For the perturbations by (1,4) and (1,7) we considered, we find that only the case $D(1,5) + \lambda\psi_{1,7}$ exhibits possible line-crossings, but that there is no IR limit in which the system flows to a single identity defect. The presence of line-crossings suggests the flow may be integrable, but we cannot deduce the existence of local conserved quantities since there is no flow to the identity defect. This is consistent with the results of our search in section 8.3.1 which did not reveal any local currents with spins less than 20.

Chapter 9

Outlook

In Part II, we studied symmetries and RG flows in perturbed two-dimensional CFTs. Due to their large symmetry algebras, 2D CFTs are highly constrained. Here, we addressed the question of how much of this structure is preserved under deformations by primary fields:

$$\mathcal{H}(\mu) = \mathcal{H}_{\text{CFT}} + \mu \int dx\, \varphi.$$

We found that studying line operators provides invaluable physical insight. Based on the constraints from preserved non-invertible symmetries [98], infinitely many new RG flows have been conjectured. For these, we propose a novel non-perturbative description that generalizes the known systems of nonlinear integral equations (NLIEs) for integrable minimal model flows [224,234].

Generalization to gapped phases. This analysis extends naturally to flows ending in gapped phases. In this context, the constraints from non-invertible symmetries [201,213] can be employed to determine vacuum structure and particle-soliton degeneracies. We leave a complete treatment of these flows for future work. Moreover, our NLIE system admits natural deformations to describe massive flows. While massless flows require fine-tuning, massive flows are generic. Therefore, analyzing the massive NLIE may facilitate robust numerical checks of our conjectures—for example, via Hamiltonian truncation.[1]

Minimal Models of $\mathcal{W}_N$ Algebras Another promising direction involves extending our non-invertible symmetry analysis to $\mathcal{W}_N$ minimal models, as will be presented in [97]. $\mathcal{W}_N$ algebras are extensions of the Virasoro algebra, arising naturally in 2D CFTs with higher-spin symmetry. While the Virasoro algebra is generated by the modes of a spin-2 current (the stress-energy tensor), $\mathcal{W}_N$ algebras include additional holomorphic currents of integer spin $s = 3, \ldots, N$. Each current $W^{(s)}(z)$ is a primary field with conformal weight s, and satisfies:

$$T(z)W^{(s)}(w) \sim \frac{sW^{(s)}(w)}{(z-w)^2} + \frac{\partial W^{(s)}(w)}{z-w} + \cdots .$$

[1] We acknowledge ongoing discussions with M. Lencsés and S. Negro on this point.

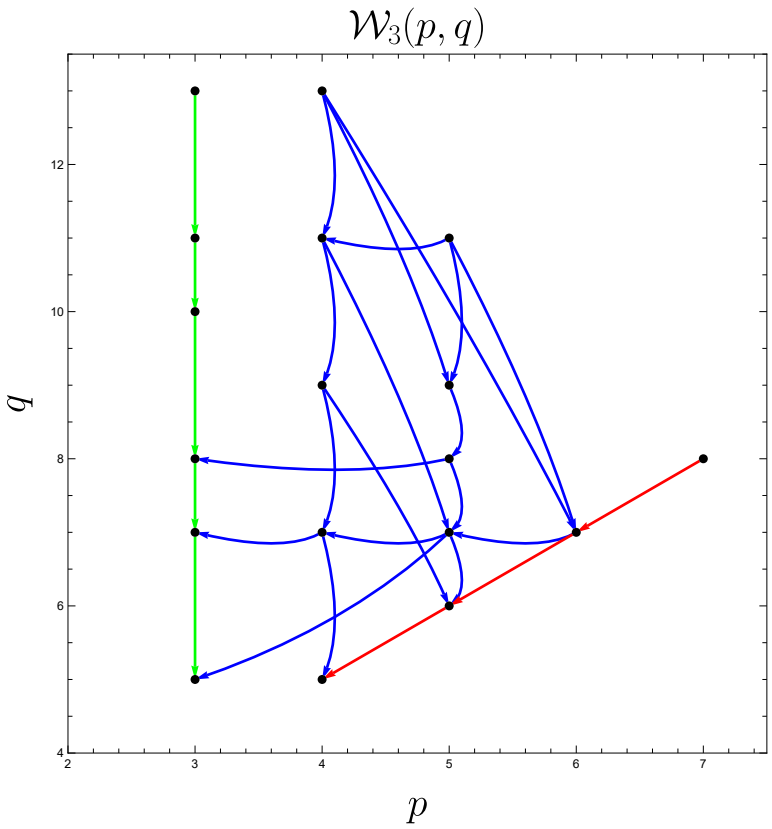


Figure 9.1: Flows between $\mathcal{W}_3$ minimal models from UV points with $pq \leq 56$, derived from anomaly constraints of non-invertible symmetries. Flows in red are integrable flows between unitary models also studied in [292]; green ones are of the Yang-Lee type.

The $\mathcal{W}_3$ algebra is the simplest nontrivial case, with a spin-3 current $W(z) \equiv W^{(3)}(z)$ satisfying:

$$\begin{aligned} T(z)W(w) &\sim \frac{3W(w)}{(z-w)^2} + \frac{\partial W(w)}{z-w} + \cdots, \\ W(z)W(w) &\sim \frac{c/3}{(z-w)^6} + \frac{2T(w)}{(z-w)^4} + \frac{\partial T(w)}{(z-w)^3} + \cdots \\ &\quad + \frac{1}{(z-w)^2}\left(\frac{3}{10}\partial^2 T(w) + \frac{32}{22+5c}\Lambda(w)\right) + \cdots, \end{aligned}$$

where $\Lambda(w) =: TT : (w) - \frac{3}{10}\partial^2 T(w)$ is a normal-ordered composite field of spin 4.

Minimal models of $\mathcal{W}_N$ are labeled by coprime pairs (p, q) and have central charge

$$c_{p,q}^{(N)} = (N-1)\left[1 - \frac{N(N+1)(p-q)^2}{pq}\right].$$

For $N = 2$, these reduce to Virasoro minimal models. In [**?**], we generalize the symmetry and RG analysis to these $\mathcal{W}_N$ models, deriving many new flows—see Figure 9.1 for $\mathcal{W}_3$.

All flows beyond the known unitary ones, as far as we know, are new. These results generalize the Virasoro structure $M(pk+I,p) \to M(pk-I,p)$. We plan to report on these in [97].

From SCFT to Minimal Models. To any four-dimensional $\mathcal{N}=2$ SCFT one canonically associates a vertex operator algebra (VOA) (a.k.a. chiral algebra) via the construction of [103]. This sector of (*Schur*) operator arises as the cohomological reduction with respect to a certain nilpotent supercharge $\mathbb{Q}$, and exactly correspond to the operators that contribute to the Schur index (cfr. for a more in depth discussion 12.2 on the Schur index) . In order to be in the cohomology of $\mathbb{Q}$, the local operators must lie in a fixed plane $\mathbb{R}^2 \subset \mathbb{R}^4$, and their correlators can be shown to be non-trivial meromorphic functions of their positions on the plane.

The central charge of the 2d chiral algebra c_{2d} is determined by the 4d Weyl anomaly (c-type) $c_{2d} = -12\, c_{4d}$, and the vacuum character of the VOA is exactly the Schur index. In certain non-Lagrangian SCFTs—most notably Argyres–Douglas theories—this chiral algebra is precisely identified with a non-unitary Minimal Model[104], such as a Virasoro or $\mathcal{W}_N$ algebra at rational central charge. For example, the simplest (A_1, A_2) Argyres–Douglas theory (that we also discuss in Chapter 12) corresponds to the non-unitary $M(2,5)$ Virasoro minimal model with central charge $c = -\frac{22}{5}$. This remarkable connection between the non-unitary $\mathcal{W}_N$ Minimal Models of the algebra of BPS operators of certain non-Lagrangian theories is an interesting linking point of this thesis. An important question that we leave for further investigation is what we can learn about this class of 4d $\mathcal{N}=2$ theories, from the corresponding flows between the Minimal Models we have studied here.

From great defects come great responsibility

In Chapter 8, we characterized [4,99–101] the class of defects commuting with the deformed Hamiltonian of a perturbed CFT. These are perturbed line operators:

$$\mathcal{D}(\lambda\psi + \widetilde{\lambda}\overline{\psi}; t) = \exp\left(\int_0^L \left(\lambda\psi(s+it) + \widetilde{\lambda}\overline{\psi}(s+it)\right) ds\right),$$

which are translationally invariant in the QFT if they satisfy:

$$[\mathcal{D}, \varphi(p)] = [\psi(p), \overline{\psi}(p)], \qquad \lambda\widetilde{\lambda} = \mu.$$

They are conserved in the perturbed CFT, but are generically only rigidly translational invariant, rather than topological. This large class of defects is very natural. They form a category[101] that is larger than the one of topological defects of the UV theory. In the IR fixed point, they are topological as conformal translational invariant defects are automatically topological. Furthermore, they represent a very natural *adiabatic* extension of a symmetry defects in a perturbed QFT. Preserved Verlinde lines satisfy the rigid constraints

$$[\mathcal{H}_{\text{CFT}}, \mathcal{D}] = 0 = [\mathcal{D}, \varphi]$$

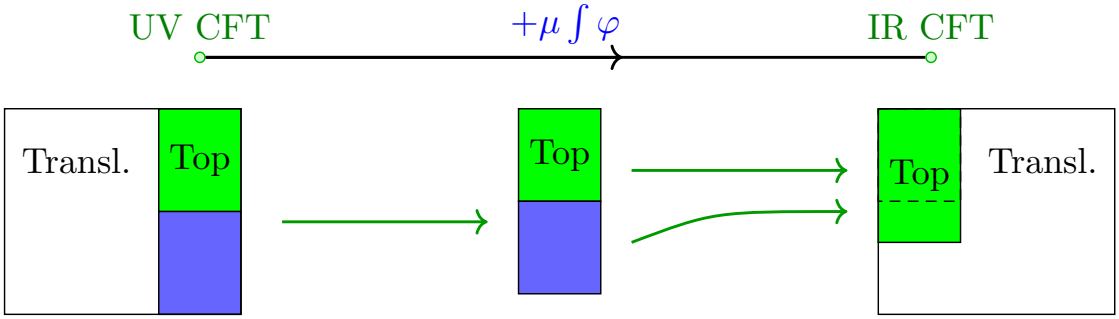


Figure 9.2: Schematic diagram of defects along the RG flow. Green: topological defects. Blue: translational invariant but non-topological defects. The dashed line represents the presence of extra topological defects in the IR in addition to the preserved subcategory of the UV.

Instead, translational invariant defects are allowed to also receive correction along the flow in such a way that at any point of the flow (i.e. for any μ) the resulting defect stays conserved. Therefore, along an RG flow the defects evolves schematically as in Figure 9.2.

There are many interesting question to address. Let us mention some of them, while more can be found in [4, Section 5]

Symmetry enhancement. It is known that in the IR one may have emergent symmetries. It is natural to ask whether our new defects may be responsible for IR symmetry enhancement. In Figure 9.2 we schematically represent how this can arise. As we perturb the UV fixed point, the subcategory of Verlinde lines commuting with the deformation, will remain topological. The set of (perturbatively) translationally invariant defects of the perturbed CFT corresponds with the class of defects we characterized here: they are the ones satisfying the bulk commutation condition. In the IR, at the end of the bulk+defect flow, all the translational invariant defects are topological; if the do not flow to any of the other IR defects in the image of the preserved subgateory of the UV, then they might be responsible for new symmetries of the IR.[2] To this aim, it would be important to compute linking rules of these defects with local operators as well as the fusion algebra thereof. These would be a natural generalization of the usual Ward Identities and topological invariants $\mathcal{L}_\sigma |\Omega\rangle$ associated to the preserved Verlinde lines. See also the recent related work [293]. We hope to come back to this in future works.

Regularization. The only perturbation not of the form $(1,2)$, $(1,3)$, or $(1,5)$ that we found which does not require regularization is the $(1,4) = (1,7)$ perturbation of $M(2,11)$. An important question is therefore to understand if there is a regularization procedure which is compatible with the bulk commutation condition in the sense that the perturbed defect continues to commute with the perturbed Hamiltonian. This would be particularly

[2] We note some points of contact with the works [175,176].

interesting for the $(1,7)$-perturbations in $M(3,10)$ and $M(5,18)$ in order to compare them to the flows investigated in [3,98,215–217,252]. [3]

T-systems and integrability. The existence of mutually commuting families of conserved charges is not, however, in itself sufficient to prove integrability. There is further work to be done to show that standard quantities such as the spectrum can be found using these new defects.
The formalism we present also makes it possible to find the functional relations between different non-local conserved charges. For the $(1,3)$-perturbation this has been analysed in [100]. In terms of the formulation as Yetter-Drinfeld modules briefly mentioned in Section 8.1.5, this amounts to finding instances where the tensor product of two modules forms a (possibly non-split) exact sequence. One should verify that also in the case of $(1,2)$ and $(1,5)$ one recovers the expected T-system functional relations [254,257,294]. Much more interesting of course is what happens in the new examples, such as $(1,7)$. This again relies on a regularization procedure, but the hope would be that one can pass through the integrable tool chain from T-system to Y-system to non-linear integral equations. These could then be compared to the proposed non-linear integral equations in [3]. If that indeed works, this would be an indication that the approach via non-local conserved charges is a more fundamental criterion for integrability than the existence of local conserved charges as the latter are absent for example in the $(1,7)$-perturbation of $M(5,18)$.

Strip algebra The rigidly translation invariant defects do not only exist on cylinders with periodic boundary conditions, but one can also investigate them on a strip (possibly with suitably perturbed boundary conditions), or on a cylinder with twisted boundary conditions. For the latter case it is for example possible to twist by another rigidly translation invariant defect, and to use a solution for the exchange matrix M (Section 8.1.4) at the crossing point with the defect wrapping the cylinder. This indicates that there are interesting generalizations of the strip and tube algebras, whose purely topological variants have for example been used to analyze the field content of various models, see e.g. [201,212,213,295–297].

Higher dimensions. One might speculate whether analogous construction works in higher dimensions. For example, one could try perturb a q-dimensional topological defect by suitable p-dimensional operators for $p < q$ in a d-dimensional QFT.

[3] In [3,98] an infinite number of flows is considered, namely $M(p, pk+I) \to M(p, pk-I)$ induced by a $(1, 2k+1)$-perturbation. Apart from $k = 1, 2$, we have (so far) only found a solution to the bulk commutation condition in the case $k = 3$ with $(p, I) = (2, 3)$, $(2, 5)$, $(3, 1)$, $(5, 3)$; for $k = 4$ with $(p, I) = (2, 3)$, $(3, 2)$; and for $k = 5$ and $k = 6$ with $(p, I) = (2, 3)$.

Appendix B

Supplement to Part II

B.1 Detailed description of some RG flows

In this appendix we provide a detailed discussion of all the flows that can be predicted based on generalized symmetries constraints from a UV fixed point $M(p,q)$ with $pq \leq 42$, corresponding to all minimal models having effective central charge less or equal than the one of $M(7,6)$.[1].

We remind that in order to determine putative RG flows, we proceed as explained in the main text below eq. (6). Specifically, fixed the UV CFT $M(p,q)$:

1) for any of its relevant deformations, we compute the fusion subcategory (if there is any) that is left unbroken by the deformation;

2) we determine all the minimal models having effective central charge less than the one of the UV theory;

3) we select only the IR models having a fusion subcategory whose RG invariants match the UV one.

Let us remark that the case of $M(2k+1,2)$ is quite degenerate as any relevant deformation breaks all the non-invertible lines[98]. For this reason, flows from $M(2k+1,2)$ are hard to identify using this method. Of course flows between these multicritical YL models are well known in the literature[184,185], but we will not discuss them here.

We organize the flows by increasing value of pq of the UV theory, or equivalently or increasing UV effective central charge. Unless explicitly indicated, we do find a choice of parameters α', ξ and κ in the NLIE kernels for all these flows. We do not report a detailed analysis for all of them here, except for the $M(10,3) \to M(8,3)$ discussed in the main text and chain of flows presented in Appendix D. In the following, we denote $\mathcal{L}_{(1,1)} := \mathbb{1}$.

- $\boldsymbol{M(5,3) \xrightarrow{\phi_{(2,1)}} M(5,2)}$. The relevant $\left(h_{(1,2)} = \frac{3}{4}\right)$ deformation preserves the non-unitary Fibonacci category[2] generated by the non-invertible element $\mathcal{L}_{(1,3)}$,

[1] We thank the anonymous referee of the paper [3]for the valuable suggestion of organizing these flows by their effective central charge.

[2] There are two Fibonacci categories with fusion rules $W^2 = 1 + W$, distinguished by their anomalies (F-symbols), or equivalently, by the defect Hilbert Space spins [201]

with

$$d_{(1,3)} = \frac{1}{2}\left(1-\sqrt{5}\right)\,, \qquad s_{(1,3)} = \mathbb{Z} \pm \left\{0, \frac{1}{5}\right\}\,, \qquad \mathcal{L}_{(1,3)} \times \mathcal{L}_{(1,3)} = \mathbb{1} + \mathcal{L}_{(1,3)}\,. \tag{B.1.1}$$

$\mathcal{L}_{(1,3)}$ of $M_{3,5}$ flows to the unique non-trivial line $\mathcal{L}_{(1,2)}$ of the Lee-Yang model $M(5,2)$ that famously satisfies the anomalous fusion category above. More interesting is the fate of the $\phi_{(2,1)}$ primary field that enters in the IR in the $T\overline{T}$-direction[3] This deformation was known to be integrable from [234].

- $\boldsymbol{M(5,4) \xrightarrow{\phi_{(1,3)}} M(4,3)}$. This is gives the famous integrable Zamolodchikov flow preserving the entire Ising fusion category (Tambara-Yamagami TY_2 category) generated by the Kramers-Wannier duality defect $\mathcal{L}_{(3,1)} := \mathcal{N}$ and the invertible $\mathbb{Z}_2$-line $\mathcal{L}_{(2,1)} := \eta$. This flow is studied in [201], and we will not repeat the discussion here, apart from mentioning that the $\phi_{(1,3)}$ flow enters purely along the $T\overline{T}$ direction. We emphasize, that, in principle, there could be a putative flow $M(5,4) \xrightarrow{\phi_{(1,2)}} M(4,3)$ only preserving the invertible $\mathbb{Z}_2$-line η but not the Kramers-Wannier duality defect $\mathcal{N}$. Such a flow could only happen if the Kramers-Wannier duality is restored by symmetry enhancement in the IR.

- $\boldsymbol{M(7,3) \xrightarrow{\phi_{(1,5)}} M(5,3)}$. This flow is triggered by the most relevant field $\phi_{(1,5)}$ preserving the anomalous $\mathbb{Z}_2$ line $\mathcal{L}_{(2,1)}$ [298]:

$$\mathcal{L}_{(2,1)} \times \mathcal{L}_{(2,1)} = \mathbb{1}\,, \quad d_{(2,1)} = -1\,, \quad s_{(2,1)} = \mathbb{Z} \pm \frac{1}{4} \tag{B.1.2}$$

  Along the flow also $\phi_{(1,3)}$ could be dynamically generated given that it commutes with $\mathcal{L}_{(2,1)}$ as well. In the IR, the flow enters along the $T\bar{T}$ direction, with contribution also from the descendants of $\phi_{(1,2)}$ of the IR model. Yet, it has been observed that $\phi_{(1,3)}$ does not contribute, and $\phi_{(1,5)}$ is a single-field integrable deformation. Indeed, integrability protects further the flow, by generating this operator. We plan to go back to this point somewhere else.

- $\boldsymbol{M(8,3) \xrightarrow{\phi_{(1,5)}} M(4,3)}$. This flow is triggered by the most relevant deformation $\phi_{(1,5)}$. It is a known integrable flow preserving a non-anomalous $\mathbb{Z}_2$ symmetry generated by $\{\mathbb{1}, \mathcal{L}_{(2,1)}\}$ in the UV and entering in the IR along the irrelevant $\phi_{(3,1)}$ direction. Also the operator $\phi_{(1,3)}$ is generated along the flow. We find that the same deformation but flowing to $M(5,4)$ would be also possible based on $\mathbb{Z}_2$ symmetry preservation. Yet, we only find values of the NLIE parameters that can reproduce the flow to $M(4,3)$ and not the one to $M(5,4)$.

[3] We thank Roberto Tateo for clarifications on this point.

- $\boldsymbol{M(7,4) \xrightarrow{\phi_{(2,1)}} M(7,3)}$. It preserves the category generated by $\left\{\mathbb{1}, \mathcal{L}_{(1,3)}, \mathcal{L}_{(1,5)}\right\}$ that is an $SU(2)_4$ fusion ring:

$$\begin{gathered}\mathcal{L}_{(1,3)} \times \mathcal{L}_{(1,3)} = \mathbb{1} + \mathcal{L}_{(1,3)} + \mathcal{L}_{(1,5)}\,, \qquad \mathcal{L}_{(1,5)} \times \mathcal{L}_{(1,5)} = \mathbb{1} + \mathcal{L}_{(1,3)} \\ \mathcal{L}_{(1,3)} \times \mathcal{L}_{(1,5)} = \mathcal{L}_{(1,5)} \times \mathcal{L}_{(1,3)} = \mathcal{L}_{(1,3)} + \mathcal{L}_{(1,5)}\,,\end{gathered} \tag{B.1.3}$$

and anomalies:

$$\begin{aligned} d_{(1,3)} &= -\frac{1}{2}\csc\left(\frac{3\pi}{14}\right)\,, & s_{(1,3)} &= \mathbb{Z} \pm \left\{0\,, \frac{1}{7}\,, \frac{2}{7}\right\}\,, \\ d_{(1,5)} &= 2\sin\left(\frac{\pi}{14}\right)\,, & s_{(1,5)} &= \mathbb{Z} \pm \left\{0\,, \frac{2}{7}\,, \frac{5}{7}\right\}\,. \end{aligned} \tag{B.1.4}$$

This flow is known to be integrable from [234]. No other operators commute with this fusion category, and no other operator (apart from its descendants) may be generated along the flow. The flow enters in $M(3,7)$ along the $\phi_{(2,1)}$. The line operators $\mathcal{L}_{(1,3)}, \mathcal{L}_{(1,5)}$ flow to the same line operators of $M(7,3)$.

- $\boldsymbol{M(7,4) \xrightarrow{\phi_{(1,4)}} M(5,4)}$. The flow is generated by $\phi_{(1,4)}$ and preserves only the invertible non-anomalous $\mathbb{Z}_2$ line $\mathcal{L}_{(3,1)}$, but breaks the KW duality defect. In this flow also the relevant operator $\phi_{(1,2)}$ may be generated, that is also dynamically generated. The flow enters along the $\phi_{(1,4)}$ direction. It naturally implies all the flows from $M(5,4)$.

- $\boldsymbol{M(7,4) \xrightarrow{\phi_{(1,4)}} M(8,3)}$. This flow is generated by $\phi_{(1,4)}$ and $\phi_{(1,2)}$ with the former being the most relevant. It enters along the $\phi_{(2,1)}$ direction. We do not find any values of the NLIE parameters that agree with this flow.

- $\boldsymbol{M(10,3) \xrightarrow{\phi_{(1,7)}} M(8,3)}$. This flow is triggered by the most relevant deformation $\phi_{(1,7)}$. $\phi_{(1,3)}$ and $\phi_{(1,5)}$ are also generated along the flow [215,252] and it preserves a non-anomalous $\mathbb{Z}_2$ symmetry generated by $\{\mathbb{1}, \mathcal{L}_{(2,1)}\}$ in the UV and entering in the IR along the irrelevant $\phi_{(2,1)}$ direction. We note that the same deformation would allow for a flow to $M(7,4)$ with the same choice of deformation. We also mention that there are clearly also chained flows from $M(10,3) \to M(8,3) \to M(5,4) \to M(4,3)$ consistent with the flows already presented.

- $\boldsymbol{M(6,5) \xrightarrow{\phi_{(1,3)}} M(5,4)}$. This is the integrable flow between tetracritical Ising and tricritical Ising, this is discussed in details in [201]. The flow preserves the non-invertible lines of $\{\mathcal{L}_{2,1}, \mathcal{L}_{3,1}, \mathcal{L}_{4,1}\}$ flowing to the $\{\mathcal{L}_{1,2}, \mathcal{L}_{1,3}, \mathcal{L}_{3,1}\}$ lines in $M(5,4)$ respectively, having spin content:

$$s_{(2,1)} = \mathbb{Z} \pm \left\{0\,, \frac{1}{10}\,, \frac{2}{5}\,, \frac{1}{2}\right\}\,, \quad s_{(3,1)} = \mathbb{Z} \pm \left\{0\,, \frac{2}{5}\right\}\,, \quad s_{(4,1)} = \mathbb{Z} \pm \left\{0\,, \frac{1}{2}\right\}\,. \tag{B.1.5}$$

The flow enters along the $\phi_{3,1}$ direction in the IR. We also see the corresponding flow to $M(4,3)$.

- $\boldsymbol{M(6,5) \xrightarrow{\phi_{(2,3)}} M(7,4)}$. The flow is allowed by the effective central charge theorem as $c_{\text{eff}}\,(7,4) = \frac{11}{14}$, $c_{\text{eff}}\,(6,5) = \frac{5}{6}$. The $\phi_{(2,3)}$ deformation preserves the non-anomalous $\mathbb{Z}_2$ generated by the $\mathcal{L}_{(4,1)}$ line, but breaks the KW duality defects. In the IR, the flow enters along the $T\overline{T}$ direction.

- $\boldsymbol{M(6,5) \xrightarrow{\phi_{(2,3)}} M(8,3)}$. With the same field, there could also be a flow to this minimal model preserving the same symmetry line. It could enter along the first descendent of $\phi_{(1,5)}$. This is also consistent with the flow $M(7,4) \to M(8,3)$ also predicted above. We do not find any values of the NLIE parameters that can agree with this flow.

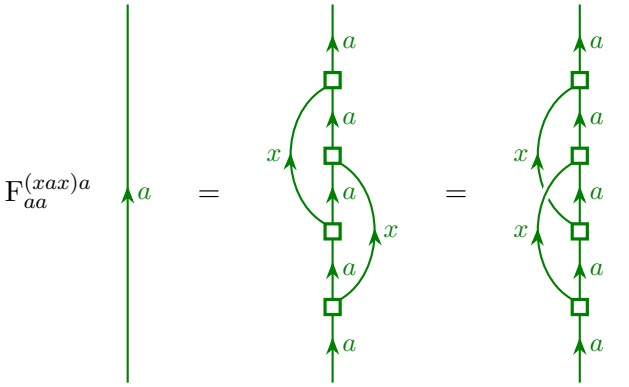
- $\boldsymbol{M(11,3) \xrightarrow{\phi_{(1,7)}} M(7,3)}$. This is a flow generating also $\phi_{(1,5)}$ and $\phi_{(1,3)}$ and preserving an anomalous $\mathbb{Z}_2$ symmetry with $d_{(2,1)} = -1, s_{(2,1)} = \mathbb{Z} \pm \frac{1}{4}$. It enters along the direction of descendants of $\phi_{(2,2)}$. Clearly the same deformations also allow a flow to $M(5,3)$ by tuning of the critical couplings as consistent with the $M(7,3) \to M(5,3)$ flow discussed above.

  For more worked out cases cfr. [3, Appendix B]

B.2 F-matrix in the case $x \otimes x \cong \mathbf{1}$

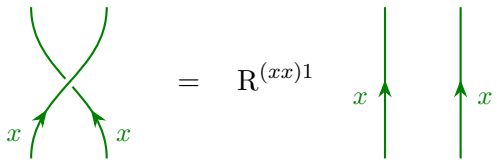
Let $x \in \text{Irr}(\mathcal{F})$ satisfy $x \otimes x \cong \mathbf{1}$, and let $a \in \text{Irr}(\mathcal{F})$ be a fixed point for x, that is, $x \otimes a \cong a$. Note that $x \otimes x \cong \mathbf{1}$ implies $x = \overline{x}$. We are interested in the F-matrix element $\mathrm{F}_{aa}^{(xax)a}$. It is given by evaluating

$\mathrm{F}_{aa}^{(xax)a}$



(B.2.1)

where in the second step we used the R-matrix (Figure 8.3) to rotate the x-loop from the right to the left. Now substitute



(B.2.2)

which follows from the assumption $x \otimes x \cong \mathbf{1}$ by composing with the preferred basis element $x \otimes x \to \mathbf{1}$ from the top.

After the substitution, the rightmost diagram in (B.2.1) turns into two basis / dual basis pairs, and we arrive at

$$\mathrm{F}_{aa}^{(xax)a} = \mathrm{R}^{(xx)1} \ . \tag{B.2.3}$$

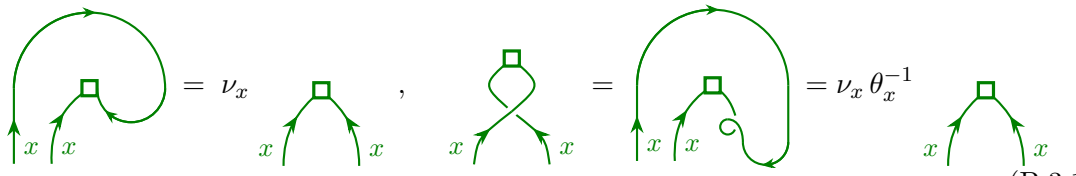
The possible values of $\mathrm{R}^{(xx)1}$ for a simple object of order 2 are $\{\pm 1, \pm i\}$. But we could have chosen to rotate the loop above the other way, in which case we would have obtained $\mathrm{F}_{aa}^{(xax)a} = 1/\mathrm{R}^{(xx)1}$. This is only in agreement with the first computation if $\mathrm{R}^{(xx)1} \in \{\pm 1\}$.

B.3 Bulk commutation condition and mutual commutativity for $\mathcal{D} = \mathbf{1} \oplus x$

Here we consider the bulk commutation condition and mutually commutativity in the case $\mathcal{D} = \mathbf{1} \oplus x$, where x is the perturbing field. We assume that $\mathcal{F}$ is a ribbon fusion category, and that $x \in \mathcal{F}$ is simple and satisfies $x \otimes x \cong \mathbf{1} \oplus y$, where $y \ncong \mathbf{1}$ and y is simple (hence in particular non-zero).

B.3.1 F- and R-matrices

Since $\mathbf{1}$ appears in the tensor product, x is self-dual, $x = \overline{x}$. For later use we note



(B.3.1)

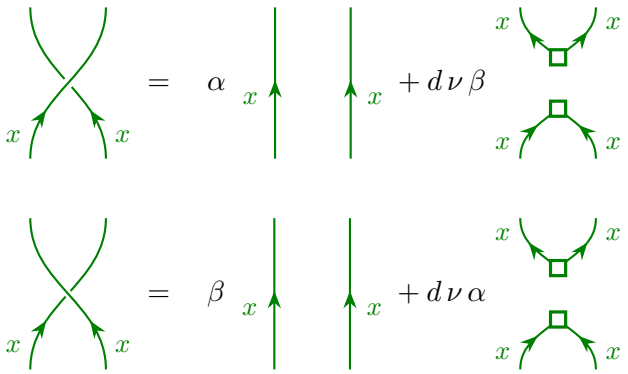
where ν_x is the Frobenius-Schur indicator of the self-dual object x as already encountered in (8.2.6). This implies

$$\mathrm{R}^{(xx)1} = \nu_x \theta_x^{-1} \ . \tag{B.3.2}$$

We abbreviate

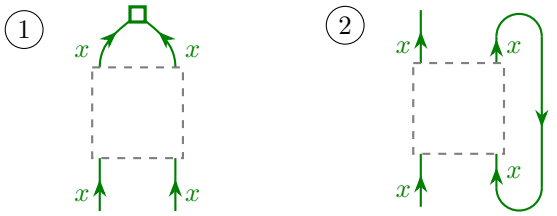
$$d = \dim(x) \ , \quad \theta = \theta_x \ , \quad \nu = \nu_x \ , \quad \alpha = \frac{d\theta - \nu\theta^{-1}}{d^2 - 1} \ , \quad \beta = \frac{d\theta^{-1} - \nu\theta}{d^2 - 1} \ . \tag{B.3.3}$$

By assumption, $\mathrm{Hom}(x \otimes x, x \otimes x)$ is two-dimensional and therefore any three morphisms $x \otimes x \to x \otimes x$ must satisfy a linear relation. We claim:



(B.3.4)

To check this, insert both sides of each equation into the following diagrams:



(B.3.5)

For example, the first equation in (B.3.4) produces

$$\textcircled{1}\ :\ \nu\theta^{-1} = \alpha + d\nu\beta \quad , \qquad \textcircled{2}\ :\ \theta = \alpha\, d + \nu\, \beta \ , \tag{B.3.6}$$

where in (1) we used (B.3.2). It is easy to check that these indeed hold for the values of α and β as above. We also note that composing both equations in (B.3.4) with the chosen basis element in $x \otimes x \to y$ yields

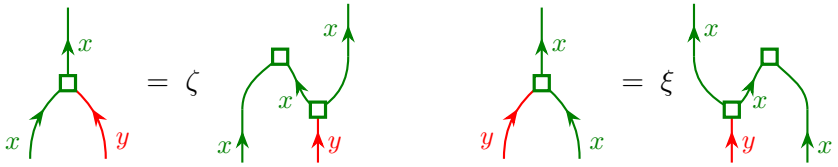
$$\mathrm{R}^{(xx)y} = \alpha = \beta^{-1} \ . \tag{B.3.7}$$

The equality $\alpha = \beta^{-1}$ can be equivalently written as

$$(d\theta - \nu\theta^{-1})(d\theta^{-1} - \nu\theta) = (d^2-1)^2 \quad \overset{d\neq 0}{\Leftrightarrow} \quad d^3 - 3d + \nu(\theta^{-2} + \theta^2) = 0 \tag{B.3.8}$$

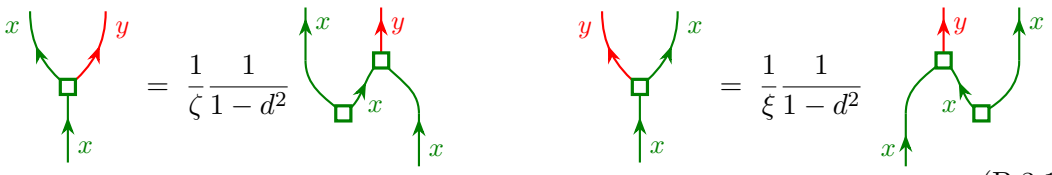
This relation between quantum dimension, Frobenius-Schur indicator, and ribbon twist (all of x) is implied by the fusion rule $x \otimes x \cong \mathbf{1} \oplus y$ that we assumed at the outset.

We will also need the F-matrix $\mathrm{F}_{ab}^{(xxx)x}$ with $a, b \in \{\mathbf{1}, y\}$, as well as $\mathrm{R}^{(xy)x}$ and $\mathrm{R}^{(yx)x}$. To this end, fix basis elements in $x \otimes y \to x$ and $y \otimes x \to x$ as follows (these Hom-spaces are one-dimensional as $x \otimes x \cong 1 \oplus y$):



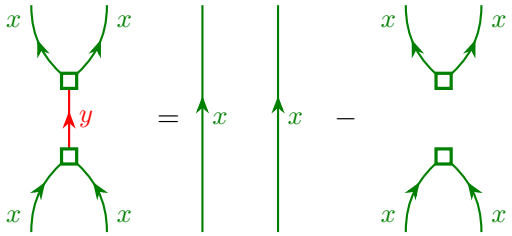
(B.3.9)

Here $\zeta, \xi \in \mathbb{C}^\times$ are constants which parametrise different choices of basis – the final results have to be independent of these. The dual basis is (in the sense that they compose to id_x with the corresponding element above)



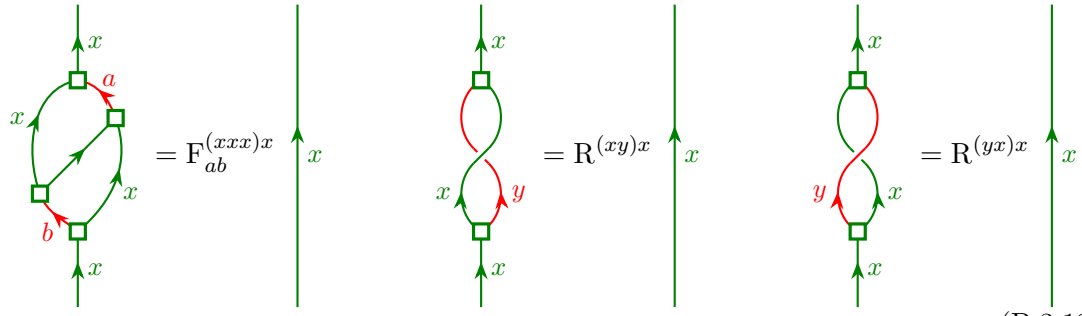
(B.3.10)

The projector onto the summand y in $x \otimes x \cong \mathbf{1} \oplus y$ can be expressed as



(B.3.11)

Combining these ingredients, it is now straightforward to compute the R- and F-matrix by evaluating the three diagrams



(B.3.12)

We find (here $\mathrm{F}_{ab} = \mathrm{F}^{(xxx)x}_{ab}$, $\mathrm{G}_{ab} = \mathrm{G}^{(xxx)x}_{ab}$)

$$\begin{pmatrix} \mathrm{F}_{11} & \mathrm{F}_{1y} \\ \mathrm{F}_{y1} & \mathrm{F}_{yy} \end{pmatrix} = \begin{pmatrix} \frac{\nu}{d} & \zeta\,(1-d^{-2}) \\ \xi^{-1} & -\frac{\zeta}{\xi}\,\frac{\nu}{d} \end{pmatrix} \quad , \quad \begin{pmatrix} \mathrm{G}_{11} & \mathrm{G}_{1y} \\ \mathrm{G}_{y1} & \mathrm{G}_{yy} \end{pmatrix} = \begin{pmatrix} \frac{\nu}{d} & \xi\,(1-d^{-2}) \\ \zeta^{-1} & -\frac{\xi}{\zeta}\,\frac{\nu}{d} \end{pmatrix} \tag{B.3.13}$$

and

$$\mathrm{R}^{(xy)x} = \frac{\xi}{\zeta}\,\beta\,\nu\,\theta^{-1} \quad , \quad \mathrm{R}^{(yx)x} = \frac{\zeta}{\xi}\,\beta\,\nu\,\theta^{-1} \ . \tag{B.3.14}$$

We conclude this preparatory section by giving the values for $d, \nu, \theta, \zeta, \xi$ in the example of the minimal model $M(p,q)$ with $x = (1,2)$, $y = (1,3)$ (recall that $t = p/q$):

$$\begin{aligned} d &= \frac{S_{1x}}{S_{11}} = -\frac{\sin(2\pi t)}{\sin(\pi t)} \ , \quad \nu = +1 \ , \quad \theta = e^{2\pi i h_x} = e^{\pi i (3t-2)/2} \ , \\ \zeta &= \xi = -2\cos(\pi t)\,\frac{\Gamma(2-2t)\Gamma(-1+3t)}{\Gamma(1-t)\Gamma(2t)} \ . \end{aligned} \tag{B.3.15}$$

The solution we present here also applies to $x = (1, q-2)$, $y = (1,3)$, with appropriately adapted constants.

B.3.2 Solving the bulk commutation condition

We can now complete the verification of the bulk commutation condition from Section 8.2.1. The second identity in (8.2.5) becomes

$$\frac{\mathrm{R}^{(xx)1} - (\mathrm{R}^{(xx)1})^{-1}}{(\mathrm{F}^{(xxx)x}_{11})^{-1} - 1} = \frac{1}{\mathrm{R}^{(xx)y}} - \mathrm{R}^{(xx)y} \quad \Leftrightarrow \quad \frac{\theta^{-1} - \theta}{d - \nu} = \beta - \alpha \ . \tag{B.3.16}$$

It is easy to check that the second equality does indeed hold for the values of α and β given in (B.3.3).

B.3.3 Perturbed defects mutually commute

Next we check that the perturbed defects mutually commute, as claimed in Section 8.2.1. Namely, we solve the condition in Section 8.1.4 under the assumptions made in the beginning of Appendix B.3. We take $\mathcal{D} = \mathcal{D}' = \mathbf{1} \oplus x$, but we keep different choices of defect field coefficients (see (8.1.13)) κ_{ab}, κ'_{ab}, $\widetilde{\kappa}_{ab}$, $\widetilde{\kappa}'_{ab}$ on the two defects. Recall from (8.2.4) that we take $\kappa_{xx} = \widetilde{\kappa}_{xx} = \kappa'_{xx} = \widetilde{\kappa}'_{xx} = 0$ and so the non-zero defect field coefficients are

$$\kappa_{1x} \quad , \quad \kappa_{x1} \quad , \quad \kappa'_{1x} \quad , \quad \kappa'_{x1} \ , \tag{B.3.17}$$

and analogously for $\widetilde{\kappa}_{ab}$. The coefficients κ_{ab} and $\widetilde{\kappa}_{ab}$ are related by (8.2.5),

$$\widetilde{\kappa}_{x1} = \frac{\Lambda}{\kappa_{1x}} \ , \quad \widetilde{\kappa}_{1x} = \frac{\Lambda}{\kappa_{x1}} \quad \text{where} \quad \Lambda = \frac{1}{\mathrm{R}^{(xx)y}} - \mathrm{R}^{(xx)y} = \beta - \alpha \ , \tag{B.3.18}$$

The same relations hold for κ'_{ab} and $\widetilde{\kappa}'_{ab}$.

There are nine entries in $M_{ab}^{cd}(m)$ in (8.1.20) which can be non-zero, and we arrange them into matrices according to the label m of the summand on the fused defect:

$$\begin{pmatrix} M_{11}^{11}(1) & M_{xx}^{11}(1) \\ M_{11}^{xx}(1) & M_{xx}^{xx}(1) \end{pmatrix} \ , \quad \begin{pmatrix} M_{1x}^{1x}(x) & M_{x1}^{1x}(x) \\ M_{1x}^{x1}(x) & M_{x1}^{x1}(x) \end{pmatrix} \ , \quad M_{xx}^{xx}(y) \ . \tag{B.3.19}$$

We can now write the conditions in (8.1.22) and (8.1.23) for these variables, where $a, b, c, d \in \{\mathbf{1}, x\}$, $m, u \in \{\mathbf{1}, x, y\}$. For example, for $a = b = c = u = 1$ and $d = m = x$ we get the conditions

$$\begin{aligned} \kappa_{1x}\, M_{x1}^{1x}(x) + \kappa'_{1x}\, M_{1x}^{1x}(x) &= \kappa'_{x1}\, M_{11}^{xx}(1)\, \mathrm{G}_{11}^{(xxx)x} + \kappa_{1x}\, M_{11}^{11}(1) \ , \\ \frac{\Lambda}{\kappa_{x1}}\, M_{x1}^{1x}(x) + \frac{\Lambda}{\kappa'_{x1}}\, M_{1x}^{1x}(x) &= \frac{\Lambda}{\kappa'_{1x}}\, M_{11}^{xx}(1)\, \frac{1}{\mathrm{R}^{(xx)1}}\, \mathrm{F}_{11}^{(xxx)x} + \frac{\Lambda}{\kappa_{x1}}\, M_{11}^{11}(1) \ . \end{aligned} \tag{B.3.20}$$

Altogether, these conditions form a homogeneous system of 24 linear equations for 9 variables. It turns out that there is a one-dimensional space of solutions, which is spanned by:

$$\begin{aligned} M_{11}^{11}(1) &= \frac{(d-\nu)\theta^2(\kappa_{1x}\kappa_{x1})^2 + \big(\nu - d\nu\theta + \theta^2(-d+\theta)\big)\kappa_{1x}\kappa_{x1}\kappa'_{1x}\kappa'_{x1} + (d\nu - 1)\theta(\kappa'_{1x}\kappa'_{x1})^2}{(\theta^2-1)(\theta\kappa_{1x}\kappa_{x1} - \nu\kappa'_{1x}\kappa'_{x1})} \\ M_{xx}^{11}(1) &= \frac{d\kappa_{1x}\kappa'_{1x}(\kappa_{1x}\kappa_{x1} - \kappa'_{1x}\kappa'_{x1})}{\theta\kappa_{1x}\kappa_{x1} - \nu\kappa'_{1x}\kappa'_{x1}} \\ M_{11}^{xx}(1) &= \frac{\theta\kappa_{x1}\kappa'_{x1}(\kappa_{1x}\kappa_{x1} - \kappa'_{1x}\kappa'_{x1})}{\theta\kappa_{1x}\kappa_{x1} - \nu\kappa'_{1x}\kappa'_{x1}} \\ M_{xx}^{xx}(1) &= \frac{(d\nu-1)\theta(\kappa_{1x}\kappa_{x1})^2 + \big(\nu - d\nu\theta + \theta^2(-d+\theta)\big)\kappa_{1x}\kappa_{x1}\kappa'_{1x}\kappa'_{x1} + (d-\nu)\theta^2(\kappa'_{1x}\kappa'_{x1})^2}{(\theta^2-1)(\theta\kappa_{1x}\kappa_{x1} - \nu\kappa'_{1x}\kappa'_{x1})} \end{aligned}$$

$$
\begin{aligned}
M^{1x}_{1x}(x) &= \kappa_{1x}\kappa'_{x1} \ , \\
M^{1x}_{x1}(x) &= M^{x1}_{1x}(x) = \frac{(d-\nu)\,\theta\,(\kappa_{1x}\kappa_{x1} - \kappa'_{1x}\kappa'_{x1})}{\theta^2-1} \ , \\
M^{x1}_{x1}(x) &= \kappa_{x1}\kappa'_{1x} \ , \\
M^{xx}_{xx}(y) &= \frac{(1+d^2\theta^2 - d\nu(1+\theta^2))\,\kappa_{1x}\kappa_{x1} - (d^2+\theta^2-d\nu(1+\theta^2))\,\kappa'_{1x}\kappa'_{x1}}{(d^2-1)(\theta^2-1)} \ .
\end{aligned}
\tag{B.3.21}
$$

In order to verify that the above coefficients indeed solve (8.1.22) and (8.1.23) one needs to make use of the relation in (B.3.8).

For special values of $\kappa_{1x}\kappa_{x1}/\kappa'_{1x}\kappa'_{x1}$, the resulting M in (8.1.20) is not invertible or not well-defined, but generically it is. Invertibility amounts to all three matrices in (B.3.19) being simultaneously invertible. At the special values, we expect the defect operators to obey T-system type functional relations. Related functional equations were investigated in [99–101,272].

Altogether, away from values of $\zeta := \kappa_{1x}\kappa_{x1}/\kappa'_{1x}\kappa'_{x1}$ where the matrices (B.3.19) are not well-defined or not invertible, the coefficients above make the topological junction M in (8.1.20) solve (8.1.22) and (8.1.23), and thus the perturbed defects mutually commute away from the singular values of ζ. The singular values are isolated points in the complex ζ-plane, and since all matrix elements of the commutator vanish away from these points, by holomorphicity in ζ they will also vanish at these points.

B.4 Details of the calculation of a local conserved current

Let us consider a holomorphic field $W(z)$ in the CFT of weight h_W. According to [274], the first order term V_1 in (8.3.1) can be calculated using[4]

$$
V_1 = \oint_z \varphi(\zeta,\overline{\zeta})\,W(z)\,\frac{d\zeta}{2\pi i} \ ,
\tag{B.4.1}
$$

where the contour is a small circle around z.

At first sight, the dependence of the integrand on $\overline{\zeta}$ suggests that the integral is not a complex integral, but simply a line integral and dependent on the contour. However, the operator product can be replaced by its expansion,

$$
\varphi(\zeta,\overline{\zeta})\,W(z) = \sum_{n=0}^{h_W-1} \frac{1}{(\zeta-z)^{h_W-n}}\varphi^{(n)}(z,\overline{z}) + O(1) \ ,
\tag{B.4.2}
$$

(where $\varphi^{(n)}$ is a level n descendant of φ) and hence the dependence of the integrand on $\overline{\zeta}$ vanishes in the limit that the contour shrinks to a small circle around z. Now applying the residue theorem, we see that the condition that V_1 is a total ∂-derivative is that the

[4]Note that in this appendix we revert to more standard CFT conventions and denote the field φ inserted at the point z by $\varphi(z,\overline{z})$ to show clearly that it is not a chiral field.

coefficient of the first order pole, $\varphi^{(h_W-1)}$, is a total derivative. By expanding the OPE (B.4.2) about ζ, instead of z, we have

$$\varphi(\zeta,\bar{\zeta})\,W(z) = \sum_{n=0}^{h_W-1} \frac{1}{(z-\zeta)^{h_W-n}} \hat{W}_{-n}\varphi(\zeta,\bar{\zeta}) + O(1)\ , \tag{B.4.3}$$

and so the state corresponding to the field $\varphi^{(h_W-1)}$ can be written

$$\left|\varphi^{(h_W-1)}\right\rangle = (-1)^{h_W-1} W_{-h_W+1}\,|\varphi\rangle + L_{-1}\,[...]\ . \tag{B.4.4}$$

It is perfectly possible to calculate explicitly $W_{-h_W+1}\,|\varphi\rangle$ for arbitrary choices of W and test if they are total L_{-1} derivatives, but it is much simpler to follow [274] and define (in a similar way)

$$D_n = \oint \varphi(z,\bar{z}) z^n \frac{dz}{2\pi i}\ . \tag{B.4.5}$$

Then

$$\left|\varphi^{(h_W-1)}\right\rangle = D_0\,|W\rangle\ , \tag{B.4.6}$$

and the action of D_0 can be calculated using

$$[L_m, D_n] = ((\Delta_\varphi - 1)(m+1) - n)D_{n+m}\ ,\quad D_{-n-1}\,|0\rangle = \frac{1}{n!}L_{-1}^n\,|\varphi\rangle\ . \tag{B.4.7}$$

If we can show that

$$D_0 W_{-h_w}\,|0\rangle \neq L_{-1} N_{-h_w+1}\,|\varphi\rangle\ , \tag{B.4.8}$$

for any N_{-h_W+1}, then there is no conserved quantity associated with W; if we can show that for every field W of weight h_W, the corresponding state $|V_1\rangle$ is not a total derivative, then we have shown there is no local conserved charge of spin $h_W - 1$.

Part III

The Analytic Langland Correspondance and Schur Quantization of 4d $\mathcal{N} = 2$ QFTs

Chapter 10

Introduction

There is a remarkable interplay between the analytic Langlands correspondence, complex Chern-Simons (CS) theory, integrability, and four-dimensional $\mathcal{N} = 2$ supersymmetric quantum field theories (SQFTs). A brief overview of these deep and beautiful relations is given in Section 1.2.3.

Schur Quantization

Given a collection of $\frac{1}{2}$-BPS line defects $\{L_{a_i}\}$ in a 4d $\mathcal{N} = 2$ SQFT, one can define a class of protected quantities known as *Schur correlation functions* $I_{a_1,\ldots,a_n}(\mathfrak{q})$. These functions, which generalize the Schur index, are graded Witten indices that count local operators at the junctions between line defects, with $0 < \mathfrak{q}^2 < 1$ a fugacity for transverse spin.[1] One of the key proposal of [22,83] is that these correlation functions define a Hilbert space of states $|a\rangle$ equipped with a Schur pairing

$$I_{a,b}(\mathfrak{q}) = \langle a|b\rangle,$$

describing a quantum mechanical system of protected quantities. This crucially uses positivity of the Schur pairing as an input. This has been extensively tested both using the UV [83] and IR formulas [5]. This quantum mechanical system carries a unitary representation of the algebra of $\frac{1}{2}$-BPS line operators on the Coulomb branch, as unbounded normal operators acting on the Schur Hilbert space. This construction, known as *Schur quantization*, may be thought as a quantization of the (K-theoretic) Coulomb branch moduli space (compactified on S^1).

This protected quantum mechanical sector encodes highly nontrivial information about the full theory. Chapter 12 is devoted to developing a comprehensive framework for Schur quantization in the IR of 4d $\mathcal{N} = 2$ theories. In particular, we study supersymmetric RG flows preserving the $SU(2)$ R-symmetry. These induce a corresponding RG map between the algebra of $\frac{1}{2}$-BPS line operators of the UV and IR. Yet, since the Schur index is not invariant under generic RG flows, e.g. the ones where massive degrees of freedom

[1] Equivalently, these are partition functions on $S^3 \times_{\mathfrak{q}} S^1$ with line defects inserted along a great circle in S^3 and wrapping S^1.

decouple, the Schur quantization in the UV is not directly lifted to a quantization in the IR. To study how RG flows and Schur indeces are intertwined [5] employs the known IR formulas[90] for the Schur indices (the analogous analysis using the UV localization formulas was performed in [83]), originally formulated only for conformal SQFTs, but also applicable to the non-conformal case via the holomorphic-topological twist perspective (as reviewed in Section 12.2). Upon, investigating the evolution of Schur indices and fusion algebras of BPS line defects under RG flow, [5] illustrates that one can associated to generic RG flows a spectrum generator S intertwining RG and Schur:

$$I^{(2)}_{\mathrm{RG}(a)\cdot S,\mathrm{RG}(b)\cdot S} = I^{(1)}_{a,b}$$

allowing to lift the RG map to a isometry of the Schur Hilbert spaces in the UV and IR. Furthermore, a new computational tool to extract the spectrum generator S, based on exploiting multi-step RG flows, is developed[5]. This simplifies the computation of S, once this is known for simple (unflavored) gauge theories.

We also present a quantization of the complex Teichmüller space in the regime of Schur quantization, following from the Schur quantization of Class $\mathcal{S}$ theories. This adapts the construction for $|\mathfrak{q}| = 1$ of [299–306] to the Schur quantization regime, and employs a version of the Faddeev quantum dilogarithm [307], first presented by Woronowicz [308,309]. The same special function governs the solutions of the diagonalization problem for the Wilson Line on the annulus, corresponding to the spectral problem:

$$F[w_1]\, g_n(\zeta) = g_{n+1}(\mathfrak{q}\,\zeta) + g_{n-1}(\mathfrak{q}^{-1}\,\zeta) + \mathfrak{q}^{-n}\zeta\, g_n(\zeta)$$

providing the building block to relate UV and IR Schur quantization. This spectral problem is the Schur analogous of the one discussed in [310].

Schur quantization has far-reaching consequences. Through a sequence of dualities in Class $\mathcal{S}$ theories [21,83], the states of the Schur Hilbert space can be identified with states in complex Chern-Simons theory at imaginary level $\kappa = ik \in i\mathbb{R}$:

$$S = \frac{ik}{2} S_{\mathrm{CS}}(\mathcal{A}) - \frac{ik}{2} S_{\mathrm{CS}}(\bar{\mathcal{A}}), \qquad \mathfrak{q} = e^{-\pi/k}.$$

This offers a novel quantization of CS theory in the regime relevant to 3D pure gravity in de Sitter space.

Furthermore, the work by Gaiotto and Verlinde [311] proposes a striking triality among the double-scaled SYK model (DSSYK), Schur half-indices of 4d $SU(2)\,\mathcal{N} = 2$ SW theory with Neumann boundary conditions, and holomorphic Wilson line correlators in SL(2) CS theory. These frameworks exhibit matching partition functions, operator algebras (skein algebras), and Hilbert spaces.

Analytic Langlands

(Quantum) analytic Langlands correspondence[22] arises as a special instance of Schur quantization[83]. The latter may be employed to provide an alternative description of

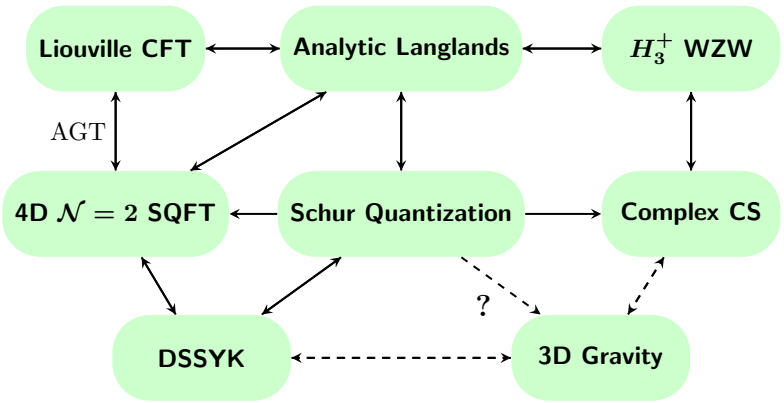


Figure 10.1: Web of dualities and relations between SUSY theories, complex Chern–Simons theory, the Langlands correspondence, and 3d gravity.

the same Schur Hilbert space [22]. In an extension of the usual CS construction [312], states $|\Lambda\rangle$ in CS theory correspond to wavefunctions

$$|\Lambda\rangle = \Psi_\Lambda(\boldsymbol{x}, \boldsymbol{z}),$$

which are normalizable, single-valued solutions to the Knizhnik–Zamolodchikov (KZ) equations arising in CFTs with affine Lie algebra symmetry.

The quantum analytic Langlands correspondence, combined with the SoV method[22, 82,83] constructs precisely these single-valued wavefunctions [19,22], thus providing the Hilbert space of CS theory [83]. Chapter 11 is devoted to the analytic version, which can be summarized schematically as:

$$\boxed{\begin{array}{c}\Lambda\\ \text{Real } {}^L G \text{ opers}\end{array}} \quad \longleftrightarrow \quad \boxed{\begin{array}{c}\Psi_\Lambda\\ L^2 \text{ and single-valued}\\ \text{Hitchin eigenstates}\end{array}}$$

Analytic Langlands

It conjectures a precise correspondance between singled-valued normalizable eigenfunctions of the Hitchin integrable system:

$$\mathsf{H}_r \Psi_\Lambda(\boldsymbol{x}, \bar{\boldsymbol{x}}) = E_r \Psi_\Lambda(\boldsymbol{x}, \bar{\boldsymbol{x}}), \qquad \bar{\mathsf{H}}_r \Psi_\Lambda(\boldsymbol{x}, \bar{\boldsymbol{x}}) = \bar{E}_r \Psi_\Lambda(\boldsymbol{x}, \bar{\boldsymbol{x}})$$

on Bun_G, and real ${}^L G$ opers Λ:

$$\left(\partial_u^2 + t_\Lambda(u)\right) \chi(u, \bar{u}) = 0, \qquad \left(\partial_{\bar{u}}^2 + t_\Lambda(\bar{u})\right) \chi(u, \bar{u}) = 0.$$

with real monodromy. In Chapter 11, we propose a proof of the correspondence in genus zero and rank one, based on the Separation of Variables (SoV) transformation [6,22] between the Gaudin and Whittaker models.

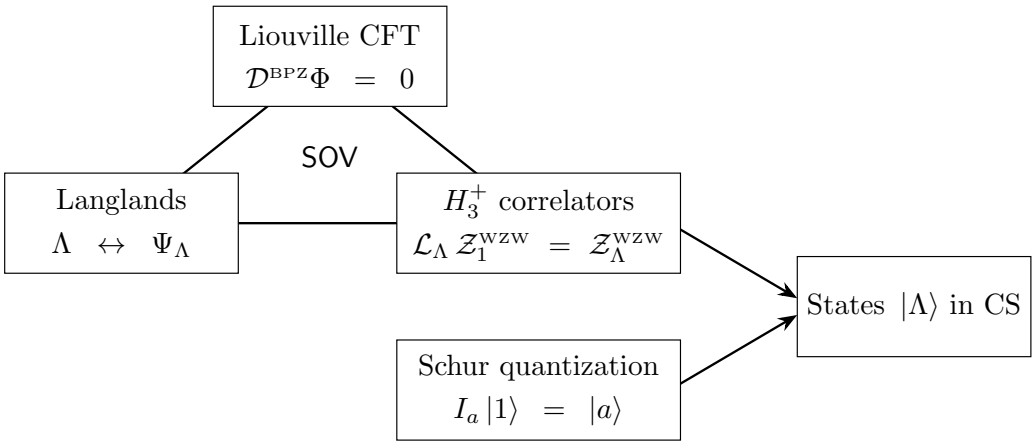


Figure 10.2: Relations between analytic Langlands, Schur quantization, and complex Chern–Simons theory.

Quantum deformation. Let us end this introduction by discussing some aspects of (quantum) analytic Langlands, to make contact with Schur quantization again. In the rank-one case, the analytic Langlands correspondence arises as the critical level limit $k \to -2$ of the SoV transform between two 2D CFTs: the non-compact $H_3^+ = \mathrm{SL}(2,\mathbb{C})/\mathrm{SU}(2)$ WZW model and Liouville CFT. Correlation functions of the H_3^+ model $\mathcal{Z}^{\text{WZW}}$, modified by inserting special Verlinde line operators $\mathcal{L}_\Lambda$, that are associated with half-integer laminations Λ [22], generate the space of single-valued KZ solutions:

$$\mathcal{L}_\Lambda \mathcal{Z}_1^{\text{WZW}}(\boldsymbol{x}, \boldsymbol{z}; \boldsymbol{j}) \simeq \mathcal{Z}_\Lambda^{\text{WZW}}(\boldsymbol{x}, \boldsymbol{z}; \boldsymbol{j}),$$

upon acting on a reference wavefunction. These line operators are obtained via parallel transport of degenerate fields satisfying BPZ [313] equations—second-order differential equations that correspond to quantum deformations of the oper equations. In the critical level limit

$$\mathcal{Z}_\Lambda^{\text{WZW}}(\boldsymbol{x}, \boldsymbol{z}; \boldsymbol{j}) \xrightarrow{k\to -2} e^{\frac{1}{k+2}S(\boldsymbol{z})} \Psi_\Lambda(\boldsymbol{x}, \boldsymbol{z}),$$

insertion of Verlinde lines corresponds geometrically to the operation of *grafting* [22,81], which is known to span the space of real opers by acting on a distinguished reference oper (the *uniformizing oper*). This rounds off a picture schematically as in Figure 10.2 relating Schur, Langlands and Complex CS.

Let us also mention a beautiful consequence of this set of relation for class $\mathcal{S}$ theories coming from the interplay with the AGT correspondance. In rank 1, H_3^+ correlators are dual in AGT [78] to supersymmetric partition functions for class $\mathcal{S}$ theories on the full 4-Ellipsoid $\mathbb{E}^4_{\epsilon_1,\epsilon_2}$ background modified by the insertion of codimension 2 BPS Gukov-Witten operators (cfr. [62] and references therein). Those are characterized by prescribed singularities for the singular behavior of the gauge fields on their locus [314], parametrized by a coordinate $\boldsymbol{s} = (s_1, \cdots, s_{3g+n-3})$: $\mathcal{Z}^{\mathbb{E}^4_{\epsilon_1,\epsilon_2}}(\boldsymbol{s}, \boldsymbol{\tau}, \boldsymbol{m})$, where $\boldsymbol{\tau}$ and $\boldsymbol{m}$ are the complexified couplings and the mass parameter of the class $\mathcal{S}$ theory. Via the AGT dictionary the parameters in gauge theory and CFT are schematically related as

$(\boldsymbol{s}, \boldsymbol{\tau}, \boldsymbol{m}) \leftrightarrow (\boldsymbol{x}, \boldsymbol{z}, \boldsymbol{j})$. Then, it is natural to conjecture[2] that Verlinde-line modifications of H_3^+ correlators, are partition functions on the full 4-ellipsoid of class $\mathcal{S}$-theory with surface defects, further refined by line operators insertions (dual to Verlinde lines via AGT[314]):

$$\mathcal{Z}_{\Lambda}^{\mathbb{E}^4_{\epsilon_1,\epsilon_2}}(\boldsymbol{s}, \boldsymbol{\tau}, \boldsymbol{m}) \equiv \mathcal{Z}_{\Lambda}^{\mathrm{WZW}}(\boldsymbol{x}, \boldsymbol{z}; \boldsymbol{j})\,.$$

Indeed, as one takes the Nekrasov-Shatashvili limit [106,315], where one of the two deformation parameters $\epsilon_2 \to 0$ vanishes (this corresponds to the critical level limit in CFT), one recovers the quantum integrable structure of the Hitchin system with the further refinement given by the laminations (grafting):

$$\lim_{\epsilon_2 \to 0} \mathcal{Z}_{\Lambda}^{\mathbb{E}^4_{\epsilon_1,\epsilon_2}}(\boldsymbol{x}, \boldsymbol{\tau}, \boldsymbol{m}) = e^{\frac{1}{\epsilon_2} S(\boldsymbol{z})} \Psi_{\Lambda}(\boldsymbol{x}, \boldsymbol{z})\,.$$

This illustrates the beautiful interplay between defects, integrability, Langlands correspondance, 2d CFTs, and susy QFTs.

Contents of Part III

11 The Langlands Correspondance **199**
11.1 The many faces of the Langlands Correspondence . . . 199
11.2 Quantum Analytic Langlands: a tale of two CFTs . . . 211
11.3 Analytic Langlands correspondence from SoV . . . 216

12 RG flows in Schur Quantization **233**
12.1 Schur meets RG . . . 234
12.2 Schur pairing and the Schur index . . . 241
12.3 Schur Quantization . . . 248
12.4 A minimal sequence of examples: rank 2 lattice . . . 255
12.5 Adding Flavor: the $\mathcal{N} = 2^*$ $SU(2)$ example . . . 265
12.6 The Spectrum Generator for RG flows triggered by large masses. . . . 271
12.7 Towards higher ranks: examples with $SU(3)$ gauge group . . . 285
12.8 Applications to the theory of quantum groups . . . 289
12.9 Partial RG flows and $SL(2)$ character varieties . . . 294
12.10 Quantization of the Teichmüller space . . . 296

13 Outlook **303**

C Supplement to Part III **307**
C.1 A primer on H_3^+ and Liouville CFT . . . 307
C.2 Spectral problem on the annulus . . . 310

[2] We thank J. Teschner for having shared the slides from the talk [105] where some of this content was presented.

Chapter 11

The Langlands Correspondance

In this chapter we aim to: first provide an introduction to the rich landscape of the Langlands Correspondence, and ultimately describe the results of upcoming work with Jörg Teschner [6] that is the subject of section 11.3 and represents the original contribution of the author to this chapter.

11.1 The many faces of the Langlands Correspondence

In this section we introduce the relevant background on the geometric and (quantum) Analytic Langlands Correspondence, being a variant of the former formulated by imposing further restrictions. Giving a thorough account of all the subtle definition and caveats that appear at any of the steps is beyond the scope of this section. Rather, the goal will be the one of introducing all the data needed to understand the scope and relevance of our work that is subsequently presented in section 11.3.

11.1.1 Geometric Langlands

The Geometric Langlands Correspondence, may be formulated as an correspondence of two - in principle completely distinct - categories associated to Riemann Surfaces $\mathcal{C} := \mathcal{C}_{g,n}$, of genus g and n-punctures, (that we also refer to as *curves*) given the data a complex (split and reductive) Lie Group G:

$$\boxed{{}^{\mathrm{L}}G - \text{local systems on } \mathcal{C}} \qquad \Longleftrightarrow \qquad \boxed{\mathcal{D} - \text{modules on } \mathrm{Bun_G}(\mathcal{C})}$$

Let us unpack this:

- $\mathrm{Bun}_G(\mathcal{C})$ is the moduli stack of principal G-bundles[1] over the curve $\mathcal{C}$.
- A $\mathcal{D}$-module on $\mathrm{Bun}_G(\mathcal{C})$ is a (quasi-coherent) sheaf[2] on the $\mathrm{Bun}_G(\mathcal{C})$ carrying an action of the sheaf of differential operators. Intuitively, section of $D_{\mathrm{Bun}_G(\mathcal{C})}$ are

[1] Recall that a principal G-bundle on $\mathcal{C}$ is a fiber bundle locally isomorphic to $G \times \mathcal{C}$

[2] Recall that, intuitively, a sheaf over a topological space assigns sets to each open set in an open cover of the base space, such that the restriction agree on overlaps of patches of the base space. A quasi-coherent sheaf is a generalization of a vector bundle. Instead of requiring that it looks like a free

G	${}^{L}G$
GL_n	GL_n
SL_n	PGL_n
Sp_{2n}	SO_{2n+1}
SO_{2n}	SO_{2n}

Table 11.1: Selected reductive groups and their Langlands duals. We omit the reductive group associated to the exeptional lie algebras as they are self-Langlands dual: ${}^{L}\mathrm{F}_4 = \mathrm{F}_4\,, {}^{L}\mathrm{G}_2 = \mathrm{G}_2\,, {}^{L}\mathrm{E}_{6,7,8} = \mathrm{E}_{6,7,8}$. Whenever not specified and when it is not misleading, we will always refer to the denote by G the complex group, e.g. $\mathrm{SL}_2 \equiv \mathrm{SL}_2(\mathbb{C})$. Whenever we consider the real form thereof, we will explicit write it.

G-valued differential operators acting locally on $\mathrm{Bun}_G(\mathcal{C})$, and admitting a global gluing.

- a ${}^{\mathrm{L}}G$-local systems on $\mathcal{C}$ may be described as a pair $(\mathcal{E}, \nabla)$ of a locally ${}^{\mathrm{L}}G$ bundle[3] equipped with a flat ${}^{\mathrm{L}}G$ connection, where we have indicated by ${}^{\mathrm{L}}G$ the Langlands-dual group to G (${}^{\mathrm{L}}\mathfrak{g}$ is the Langlands dual of $\mathfrak{g}$); for some examples of Langlands dual groups see 11.1.

11.1.2 The Beilinson-Drinfeld approach

A very explicit approach to geometric Langlands is due to Beilinson-Drinfeld [16], and entails the correspondence between local systems in oper-form and the $\mathcal{D}$-module represented by the quantum Hitchin Hamiltonians, being the quantization of the Hitchin integrable system. This is a special case of the Geometric Langlands, that may be understood as a quantization of the Hitchin Integrable system. We will mostly discuss the rank one case, where $\mathfrak{g} = \mathfrak{sl}_2$. More specifically, we take the group G to be the Projective Linear Group[4] $G = \mathrm{PGL}_2(\mathbb{C}) \simeq \mathrm{PSL}_2(\mathbb{C}) \simeq \mathrm{SL}_2(\mathbb{C})/\mathbb{Z}_2$. From now on, unless specified, we will always intend to work with the complex version of G, e.g. $\mathrm{SL}_2 \equiv \mathrm{SL}_2(\mathbb{C})$. The reason is a mere convenience of describing the moduli stack on bundles Bun_G over a group G being centerless. Indeed those bundles have trivial automorphism in their open stratum, rather than $\mathrm{Aut}(\mathrm{Bun}_G) \supset Z(G)$ ($Z(G)$ is the center of G). We will go back in Section 11.1.3 to discuss this subtle point thoroughly. For now, the reader may take the choice $G = \mathrm{PGL}_2$ as a definition, that simplifies some points.

module locally (as in vector bundles), we allow it to look like any module. In particular, this more general notion allows for singularities on patches.

[3] Recall that the Langland dual group ${}^{\mathrm{L}}G$ is obtained from G by swapping the weight and co-weight lattice.

[4] Note that $\mathrm{PGL}_2(\mathbb{C}) \simeq \mathrm{PSL}_2(\mathbb{C})$ is only true over the complex Field, while it would not hold over the $\mathbb{R}$.

Opers

One considers pairs of local systems of *oper*-connection type. In this case, the local system is described by the pair $(\mathcal{E}, \nabla_\eta)$, where:

- The oper bundle $\mathcal{E}_{\rm op}$ is defned by the extension, unique up to isomporphism:

$$0 \to K^{1/2} \to \mathcal{E}_{\rm op} \to K^{-1/2} \to 0 \tag{11.1.1}$$

  where $K^{1/2}$ is a square root of the Canonical line bundle[5] K, i.e. is the bundle of holomorphic 1/2-forms $\sqrt{z}\,\mathrm{d}z$ (holomorphic half-densities)

- The oper connection ∇_η in oper form, is a class of holomorphic connections:

$$\nabla = \mathrm{d}z\,(\partial_z + A_\eta(z)) \tag{11.1.2}$$

  locally gauge equivalent to:

$$\nabla_\eta = \mathrm{d}z\left(\partial_z + \begin{pmatrix} 0 & -t_\eta \\ 1 & 0 \end{pmatrix}\right) \tag{11.1.3}$$

  For the case of $\mathrm{SL}_2 = {}^L\mathrm{PGL}_2$, t_η transform as a projective connection defined on a trivialized determinand line bundle(as the stress-energy tensor) under local change of coordinates $z = \phi(z)$:

$$t(z) = (\phi'(z))^2\,\widetilde{t}(\phi(z)) + \frac{1}{2}\{\phi, z\}_{\rm Shw}\,, \qquad \{\phi, z\}_{\rm Shw} := \frac{\phi'''}{\phi'} - \frac{3}{2}\left(\frac{\phi''}{\phi'}\right)^2 \tag{11.1.4}$$

A connection in oper form defines a Schrödinger operator:

$$\nabla_\eta \cdot \begin{pmatrix} \psi \\ \widetilde{\psi} \end{pmatrix} = 0 \qquad \Longleftrightarrow \qquad \left(\partial_u^2 + t_\eta(u)\right)\psi = 0 \tag{11.1.5}$$

we call this differential equation: *oper equation*. The space of opers $Op_G(\mathcal{C})$ is an affine space modeled on $H^0(\mathcal{C}, K^2)$, the space of quadratic differential. $Op_G(\mathcal{C})$ forms a Lagrangian subspace in the space of all local systems. For the sake of notation, whenever we omit the group G, we indicate:

$$Op_{\mathrm{SL}_2}(\mathcal{C}) \equiv Op(\mathcal{C})\,.$$

One can give coordinates in this affine space by fixing a reference point t_0 and considering the difference:

$$q_\eta = t_\eta - t_0 \tag{11.1.6}$$

[5] The canonical line bundle is the bundle of holomorphic 1-forms on $\mathcal{C}$. So the $K^{1/2}$ is defined to be the Line bundle cL such that $\mathcal{L}^{\otimes 2} = K$

that, since each of them transform as a projective connection, is coordinate independent, and transforms as a quadratic differential. Hence, we can introduce local coordinates for opers by:

$$q_\eta = \sum_{r=1}^{3g+n-3} E_r(\eta)\theta_r \tag{11.1.7}$$

where θ_r is a basis for the $3g+n-3$-dimensional space of the quadratic differentials on $\mathcal{C}$. For convenience let us denote:

$$|H^0(\mathcal{C}, K^2)| = d = 3g + n - 3 \tag{11.1.8}$$

$\mathcal{D}$-modules

In the case of Beilinson and Drinfeld[16], the $\mathcal{D}$-module on $\mathrm{Bun}_G(\mathcal{C})$ is represented concretely by system of partial differential equations, taking the form of eigenvalues equations for the quantum Hitchin Hamiltonians. The Hitchin integrable system plays a prominent role in theoretical and mathematical physics as well as in pure mathematics. Let us recall some facts about the Hitchin Integrable system, for more details the reader may refer to [19,22].

The quantum Hitchin Hamiltonians correspond to the quantization of the classical Hitchin integrable system. To introduce the Quantum Hitchin Hamiltonians, one has first to describe the integrable structure on Hitchin Moduli space. Let us describe it momentarily for the rank 1 case, as this is the main case considered by us. The discussion may be readily extended to any reductive Lie Group. For $G = \mathrm{SL}_2$ the Hitchin Moduli space is the moduli stack of pair $(\mathcal{E}, \varphi)$, with $\mathcal{E}$ being an holomorphic SL-bundle on $\mathcal{C}$, and and Higgs field $\varphi \in H^0(\mathcal{C}, \mathrm{End}(\mathcal{E}) \otimes K)$. For $n \neq 0$ φ has only simple poles at the punctures. The integrable structure is given by the following quadratic differential $\theta = \frac{1}{2}\,\mathrm{tr}\,\varphi^2 \in H^0(\mathcal{C}, K^2)$, whose expansion determines the Poisson[6] commuting (classical) Hitchin Hamiltonians H_r:

$$\theta = \sum_{r=1}^{3g+n-3} H_r Q_r(z)\,, \qquad \{H_r, H_s\} = 0 \tag{11.1.9}$$

So that the Hitchin Hamiltonians define an integrable structure on the Hitchin moduli space. Beilinson and Drinfeld [16]proved the existence of a quantization of the Hitchin Hamiltonians, given by $|H^0(\mathcal{C}, K^2)| = d$ commuting (partial) differential operators $\mathrm{H_r}$ acting on half densities $K^{1/2}$ on $\mathrm{Bun}_G(\mathcal{C})$ whose symbols[7] reduce to the (classical) Hitchin Hamiltonians. Their construction illustrates the existence of a quantization of the classical Hitchin Hamiltonians as a very explicit $\mathcal{D}$-module on $\mathrm{Bun}_G(\mathcal{D})$. $\mathrm{Bun}_G(\mathcal{C})$ admits special loci of given codimensions, called *wobbly loci*, where the Higgs field is nihilpotent, and the Hitchin Hamiltonian are singular. The complement of the wobbly loci define the *very stable* bundles which are not wobbly, once restricted to those the Higgs Field is

[6]The Poisson structure on the Hicthin moduli space is canonically defined, cfr. [19,22] for details

[7]Recall that a symbol of a differential operator is schematically defined as $\sum \alpha_A D^A \to \alpha_A \xi^A$, for a multi-index A, differential operator D^A, and cotangent vectors ξ^A.

diagonalizable with distinct eingevalues. Outside of the very stable bundles, one has to be more careful in dealing with possible singularities. We will come back to this point later.

Hitchin Hamiltonians in genus zero and rank 1. In the case of $\mathcal{C} = \mathcal{C}_{0,n} = \mathbb{P}^1/\{z_1, \cdots, z_n\}$ and $\mathfrak{g} = \mathfrak{sl}_2$ the Higgs field is meromorphic $\varphi \in H^0(\mathcal{C}, \mathrm{End}(\mathcal{E}) \otimes K)$ with simple poles at the punctures:

$$\varphi = \sum_{r=1}^{n} \frac{\phi_r}{z - z_r}\,, \qquad \phi_r = \begin{pmatrix} \mathcal{D}_r^0 & \mathcal{D}_r^- \\ \mathcal{D}_r^+ & -\mathcal{D}_0 \end{pmatrix} \in \mathfrak{sl}_2 \tag{11.1.10}$$

where $\mathcal{D}_r^a$ are the three standard generators of $\mathfrak{sl}_2$ in differential representation:

$$\mathcal{D}_r^0 = x_r \partial_{x_r} + j_r\,, \qquad \mathcal{D}_r^+ = \partial_{x_r}\,, \qquad \mathcal{D}_r^- = x_r^2 \partial_{x_r} - 2 x_r j_r\,. \tag{11.1.11}$$

Upon taking the trace of the Higgs φ^2, one extract the quantized Hitchin Hamiltonian given by:

$$\mathrm{H}_r = \sum_{r \neq s=1}^{n} \frac{\eta_{ab} \mathcal{D}_s^a \mathcal{D}_s^b}{z_r - z_s} \tag{11.1.12}$$

where, η_{ab} is the standard $\mathfrak{sl}_2$ Killing form. Global $\mathfrak{sl}_2$ invariance implies that the Hitchin Hamiltonian are subjected to the 3 Hamiltonian constraints $\sum_i \mathrm{H}_i = 0$. They then indeed give a set of $n - 3 = |H^0(\mathcal{C}_{0,n}, K^2)|$ commuting partial differential operators acting on half densities.

The correspondence

Specifically, the $\mathcal{D}$-module introduced above is presented by the set of eigenvalues equations:

$$\mathrm{H}_r \Psi = E_r \Psi\,, \qquad r = 1, \cdots, d = 3g + n - 3 \tag{11.1.13}$$

for the commuting Hitchin Hamiltonians:

$$[\mathrm{H}_r, \mathrm{H}_s] = 0\,, \qquad r, s = 1, \cdots, d\,. \tag{11.1.14}$$

acting on half-densities of the canonical line bundle in $\mathrm{Bun}_G(\mathcal{C})$. This is a system of coupled partial differential equations valued in G.

In the approach of Beilinson and Drinfeld[16], Geometric Langlands becomes particularly explicit via the set of equations (11.1.13) that provide a one-to-one correspondence between the quantum Hitchin eigen $\mathcal{D}$-moduli and Opers (11.1.7), that result to be labeled by the same identical data. From this perspective, Geometric Langlands encode the relation between the quantization of the Hitchin system and the space of Opers on $\mathcal{C}$.

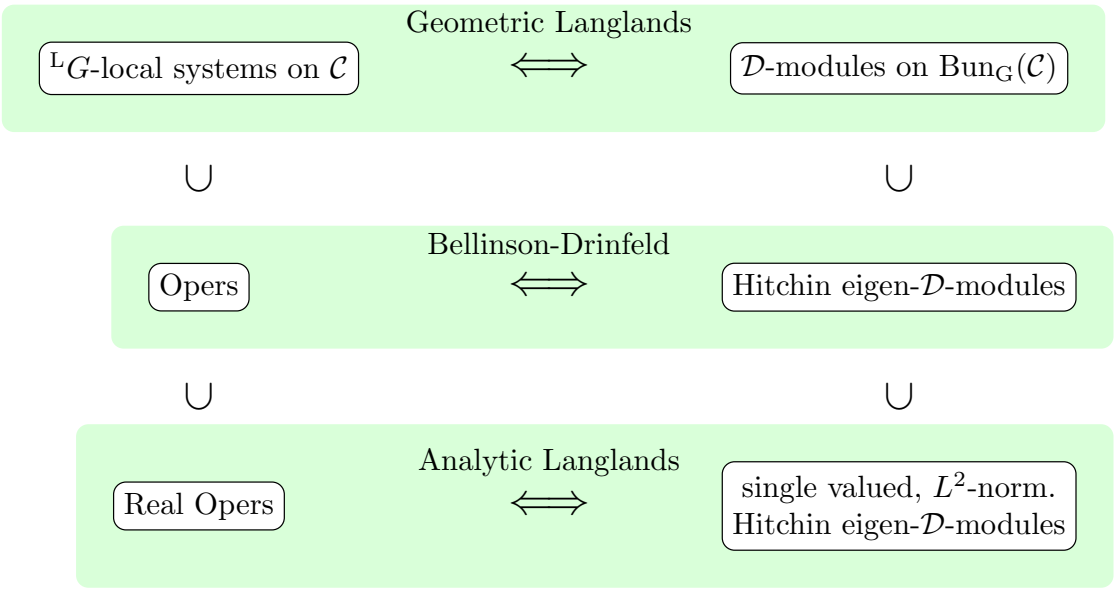


Figure 11.1: Summary of the three version of Langlands discussed so far.

11.1.3 Analytic Langlands Correspondance

The Analytic Langlands Correspondance is a further restriction of the case above, obtained by imposing single-valuedness and square-normalizability of the solutions to the eigenproblem (11.1.13) [20,79,80,316] on the $\mathcal{D}$-module side of the correspondence. It is an important conjecture of [79–81,316], that the corresponding local systems are *real* opers, being opers in $\mathrm{Op}(\mathcal{C})$ with real monodromy. The picture drawn so far is summarized in Figure 11.1. The Analytic version of Langlands, is a more than a mere specialization of the more broad Geometric version. Indeed, the works of Teschner and Etingof, Frenkel and Kazhdan have truly deepened the story introducing a crucial interplay between geometry, harmonic analysis, CFTs and the theory of Integrable models.

A precise formulation of the analytic Langlands correspondence is encoded in Theorem 1 below. In section 11.3 we propose a pathway to prove this result for the case of genus 0, $\mathcal{C} = \mathbb{P}^1/\{z_1, \cdots, z_n\}$ and rank 1. This proof is made possible thanks to the connection with CFTs, and specifically the SOV tranform relating Liouville CFT and the H_3^+ WZW model. We refer to section 11.3 for a thorough discussion of the result, while in this section we will maintain a less formal tone to guide the reader towards all the necessary ingredients entering the proof.

Single-valuedness

The requirement of single-valuedness in a very natural quantization condition for the Hitchin system from the perspective of integrable models and CFT. One consider two

independent pairs of holomorphic H_r and anti-holomorphic $\overline{\mathrm{H}}_r$ Hitchin Hamiltonians:

$$\begin{array}{l} \mathrm{H}_r\Psi = E_r\Psi \\ \overline{\mathrm{H}}_r\Psi = \overline{E}_r\Psi \end{array} , \qquad r = 1, \cdots, d = 3g + n - 3 \tag{11.1.15}$$

By anti-holomorphic Hitchin Hamiltonians we refer to the same construction as in the previous section but now based on the moduli stack of pairs $\left(\bar{\mathcal{E}}, \bar{\varphi}\right)$ of anti-holomorphic bundles $\mathcal{E}$ and Higgs fields being anti-holompmrhic sections in $H^0(\bar{\mathcal{E}}, \mathrm{End}(\bar{\mathcal{E}}) \otimes \bar{K})$. Let us not straight away that for this Eigenvalue problem to be well defined, we must have that: the Hitchin Hamiltonians H_r are normal and adjoint operators to their conjugate $\bar{H}_r$.

Locally we can introduce coordinates $\boldsymbol{x} = (x_1, \cdots, x_d)$ on $\mathrm{Bun}_G\mathcal{C}$, and analogously $\bar{\boldsymbol{x}}$ on its anti-holomorphic copy. Then, given that the Hitchin Hamiltonians are purely holomorphic or anti-holomorphic, solutions to the system of equations (11.1.15) may be locally represented as some linear combination of factorized solutions:

$$\Psi(\boldsymbol{x}, \bar{\boldsymbol{x}}) = \sum_{r,s} c_{rs}\psi_r(\boldsymbol{x})\overline{\psi}_s(\bar{\boldsymbol{x}}) \tag{11.1.16}$$

where the sum runs over all the independent solutions[8] $\psi_r(\boldsymbol{x})$ and $\overline{\psi}_s(\bar{\boldsymbol{x}})$ to $\mathrm{H}_r\psi(\boldsymbol{x}) = E_r\psi(\boldsymbol{x})$ and $\overline{\mathrm{H}}_r\bar{\psi}(\boldsymbol{x}) = \overline{E}_r\bar{\psi}(\boldsymbol{x})$. Generic solutions ψ and $\bar{\psi}$ will have generically non-trivial monodromies. The further single-valuedness condition imposes that the $\Psi(\boldsymbol{x}, \bar{\boldsymbol{x}})$ must be globally single-valued.

The Hilbert Space framework

The works [20,79,80] established important aspects of harmonic analysis to the Langlands correspondence, introducing an Hilbert space framework to the setting. To do that, the first step is to consider a restriction of the (stable) bundles $\mathrm{Bun}_G(\mathcal{C})$ such that the resulting space is a smooth algebraic variety that is suitable to perform analysis. Indeed, the (stable) bundles $\mathrm{Bun}_G(\mathcal{C})$ carrying an action of the automorphisms of G, are not smooth spaces, rather they may be singular at various loci. Yet, there are also other sources of singularities. Indeed an algebraic space carrying the action of an automorphism Γ is inherently not smooth[9].

The regular-semisimple moduli space To obtain a smooth algebraic space from the moduli stack of bundle $\mathrm{Bun}_G(\mathcal{C})$, we shall restrict to the so called *regular-semisimple moduli space of bundles* $\mathrm{Bun}_G^{\mathrm{rs}}(\mathcal{C})$. This is obtained from $\mathrm{Bun}_G(\mathcal{C})$ by:

1) First restricting to the open substack $\mathrm{Bun}_G^{\circ}(\mathcal{C})$ having minimal automorphism group, this is called the *stable bundles*. This minimal stratum has the center of G $Z(G)$ as its automorphism group acting at every point in $\mathrm{Bun}_G^{\circ}(\mathcal{C})$.

[8] The dimension of the Hilbert space of solutions to the Hitchin Hamitonian Eigenvalue equation is given by the Verlinde Formula.

[9] Just to clarify, consider a stack $\mathcal{E}$ carrying a $\mathbb{Z}_N$ automorphism, in a local chart this stack may be $\mathcal{E} \sim \mathbb{C}^n/\mathbb{Z}_N$ that is not a smooth algebraic space.

2) Forgetting the minimal automorphsim group. The automorphism group $Z(G)$ acts freely on the stable bundles $\mathrm{Bun}_G^\circ(\mathcal{C})$. Forgetting the automorphism corresponds to quotient it at the level of the moduli stack $\mathrm{Bun}_G^\circ(\mathcal{C})/Z(G) = \mathrm{Bun}_G^{\mathrm{rs}}(\mathcal{C})$. The resulting object is a (disconnected piecewise) smooth variety.

The regular-semisimple moduli space $\mathrm{Bun}_G^{\mathrm{rs}}(\mathcal{C})$ is a space with disconnected components:

$$\mathrm{Bun}_G^{\mathrm{rs}}(\mathcal{C}) = \bigsqcup_{\gamma\in\pi_1(G)} \mathrm{Bun}_{G,\gamma}^{\mathrm{rs}}(\mathcal{C})\,. \tag{11.1.17}$$

where $\pi_1(G)$ is the fundamental group of G.

For $G = \mathrm{SL}_2$ one has $Z(G) = \mathbb{Z}_2 = \{\pm I\}$ acting freely at each point in $\mathrm{Bun}_{\mathrm{SL}_2}^\circ(\mathcal{C})$. The associated regular-semisimple moduli space is a space with a single connected component, given that $\pi_1(\mathrm{SL}_2) = 0$.

This is one of the main reason to vouch for the choice $G = \mathrm{PGL}_2(\mathbb{C})$. Indeed, in this case the stable bundles $\mathrm{Bun}_{\mathrm{PGL}_2}^\circ(\mathcal{C})$ are open and dense in $\mathrm{Bun}_{\mathrm{PGL}_2}(\mathcal{C})$, and furthermore the automorphism group of the stable bundles is trivial given that PGL_2 is centerless. In this case the dense stable bundles are already regular-semisimple. Since $\pi_1(\mathrm{PGL}_2) = \mathbb{Z}_2$ we have

$$\mathrm{Bun}_{\mathrm{PGL}_2}^\circ(\mathcal{C}) = \mathrm{Bun}_0 \sqcup \mathrm{Bun}_1\,,$$

(dropping the superscripts $rs, \circ$ for sake of notation), corresponding to the two topologically disconnected components having distinct second Stiefel-Whitney $w_2(\mathrm{Bun}_i) = i/\mathbb{Z}_2$.

Before proceeding, we want to stress that, interestingly, most of the rich structure that we are neglecting here by restricting to this smooth section, albeit making the introducing of an Hilbert Space framework simpler, does play a crucial and important role in the quantum Separation of Variables for Hitchin systems. This is subject of ongoing work with J. Teschner, and we will not say much about it in this thesis.

The Hilbert space. Having restricted ourselves to the smooth space $\mathrm{Bun}_G^{\mathrm{rs}}(\mathcal{C}) = \bigsqcup_{\gamma\in\pi_1(G)} \mathrm{Bun}_{G,\gamma}^{\mathrm{rs}}(\mathcal{C})$, one can introduce an associated Hilbert spaces $\mathcal{H}_{G,\gamma}$, for $\gamma \in \pi_1(G)$ on each of the disconnected smooth spaces components as follows. Consider the space $\mathcal{S}_{\Omega_{G,\gamma}^{1/2}}$ of compactly supported smooth section of the line bundle of half-densities:

$$\Omega_{G,\gamma}^{1/2} := |K^{1/2}_{\mathrm{Bun}^{\mathrm{rs}}_{G,\gamma}}| = K^{1/2}_{\mathrm{Bun}^{\mathrm{rs}}_{G,\gamma}} \otimes \overline{K}^{1/2}_{\mathrm{Bun}^{\mathrm{rs}}_{G,\gamma}}\,.$$

Then, the Hilbert spaces $\mathcal{H}_{G,\gamma}$ are defined to be the completion of $\Omega_{G,\gamma}^{1/2}$ with respect to the Hermitian inner product:

$$\langle v, w\rangle := \int_{\mathrm{Bun}^{\mathrm{rs}}_{G,\gamma}} v\,\overline{w}\,, \qquad v, w \in \Omega_{G,\gamma}^{1/2}\,.$$

This is modeled after the usual construction of L^2 space of functions. The outcome is a space of square integrable half-density on Bun_i, that we schematically indicate as $\mathcal{H}_{G,\gamma} = L^2(\mathrm{Bun}_{G,\gamma}^{\mathrm{rs}}(\mathcal{C}))$.

In the case of $G = \mathrm{PGL}_2$, this produces two Hilbert spaces $\mathcal{H}_0, \mathcal{H}_1$ of L^2 normalizable half-densities respectively on Bun_0 and Bun_1, simplifying the notations for the following discussion. We will consider mainly 2 classes of operators acting on this Hilbert spaces: pairs of holomorphic/antiholomorphic differential operators, and Hecke integral operators.

Coordinates on Bun. Coordinates on Bun_i are naturally inherited by upgrading the bundle with a parabolic structure[20]. Giving a parabolic structure to a PGL_2 rank 2 bundle $\mathcal{E}$ on $\mathbb{P}^1$ accounts for specifying a 1-dimensional subline bundle $\ell_i \subset \mathcal{E}\big|_{z_i}$ in the fiber of the bundle at each puncture z_i (a flag). This turns punctures into structured projective lines. The parabolic structure gives bi-rational charts $x_i \in \mathbb{P}^1$ parameterizing the projective line at each of the flags, and after trivialization (gauge fixing) gives the isomorphism:

$$\mathcal{H}_i \simeq \mathbb{P}^n$$

for a $(n+3)$-punctured sphere $\mathbb{P}^1 \setminus \{z_{-1} = 0, z_0 = 1, z_1, \cdots, z_n, z_{n+1} = \infty\}$. Henceforth, we employ the local coordinates $(x_1, \cdots, x_n)$ on the n-dimensional moduli space to parametrized half-densities in $\mathcal{H}_i$. To be more precise parabolic structures give two distinct but isomorphic parametrizations for $\mathcal{H}_0$ and $\mathcal{H}_1$, (identified by Hecke modifications as we will discuss in section 11.1.4).

Real Opers

At this stage, we introduce real opers. For more details the reader can consult [22,81] where the theory their classification in terms of Grafting operations, and explicit Fenchel-Nielsen coordinates for the space of real opers are discussed in great details. The classification and characterization of real opers heavily uses the one-to-one correspondence between opers and projective structures on $\mathcal{C}$. We will eclipse on this beautiful piece of mathematics, introducing real opers in a more minimalistic way. We will focus on the case of rank 1.

Let us consider again the locally defined oper equation $\left(\partial_u^2 + t_\eta(u)\right)\psi(u) = 0$. Monodromies of such differential equations for generic choices of SL_2 opers η naturally[10] lie in $\mathrm{PSL}_2(\mathbb{C})$.

Real opers $Op_G(\mathcal{C})_{\mathbb{R}}$ are defined to be set set of $Op_G(\mathcal{C})$ opers such that, their monodromy representation is isomorphic to its complex conjugate.

For the case of ${}^L G = SL_2$, real opers $Op_{\mathrm{SL}_2}(\mathcal{C})_{\mathbb{R}}$ are therefore characterized to have monodromy in $\mathrm{PSL}_2(\mathbb{R}) \subset \mathrm{PSL}_2(\mathbb{C})$.

Consider a pair of a holomorphic oper equation $\eta \in Op(\mathcal{C})$, and its anti-holomorphic complex conjugate copy $\overline{\eta} \in \overline{Op}(\mathcal{C})$. Associated to them, we locally defined pair of oper equations:

$$\left(\partial_u^2 + t_\eta(u)\right)\chi(u) = 0\,, \qquad \left(\partial_{\bar{u}}^2 + t_{\bar{\eta}}(\bar{u})\right)\overline{\chi}(\bar{u}) = 0\,. \tag{11.1.18}$$

[10] Monodromy of a linear combination of the two independent solutions would be naively lie in PGL_2 (An overall minus sign may be always reabsorbed into a normalization). Yet since the Wronskian $W(\psi_1, \psi_2)$ between two solutions is constant, the monodromies must actually lie only in $\mathrm{SL}_2(\mathbb{C}) \subset \mathrm{PGL}_2$

It is argued in [81] that, given the four independent solutions $\chi_1(u), \chi_2(u), \overline{\chi}_1(\bar{u}), \overline{\chi}_2(\bar{u})$ to (11.1.18) a unique single-valued section χ:

$$\chi(u,\bar{u}) = \sum_{i,j=1}^{2} c_{ij}\chi_i(u)\,\overline{\chi}_j(\bar{u}) \tag{11.1.19}$$

exists if and only if η is a real oper. This implies that real opers η are completely characterized by single valued solutions $\chi(u,\bar{u})$ to (11.1.18).

The space of opers, and analogously of real ones, is a disjoint union of connected components:

$$Op_G(\mathcal{C}) = \bigsqcup_{\gamma\in\theta(\mathcal{C})} Op_G^{\gamma}(\mathcal{C})\,,$$

where $\theta(\mathcal{C})$ is the set of isomorphism classes of square roots of the canonical line bundle (choices of spin structure). Furthermore, each connected component is isomorphic to the opers over the adjoint group $G_{\rm ad} = \widetilde{G}/Z(\widetilde{G})$, where $\widetilde{G}$ is the simply connected global form of the group. In the rank 1 case one has:

$$Op_{\mathrm{SL}_2}(\mathcal{C}) = \bigsqcup_{\gamma\in H^1(\mathcal{C},\mathbb{Z}_2)} Op_{\mathrm{SL}_2}^{\gamma}(\mathcal{C})\,, \qquad Op_{\mathrm{SL}_2}^{\gamma}(\mathcal{C}) \simeq Op_{\mathrm{PGL}_2}(\mathcal{C})$$

where $H^1(\mathcal{C},\mathbb{Z}_2) \simeq \mathbb{Z}_2^{2g+n-1}$. The monodromy of an oper $\chi \in Op_{\mathrm{SL}_2}^{\gamma}(\mathcal{C})_{\mathbb{R}}$ lie in $\mathrm{PSL}_2(\mathbb{R})$. Opers in $Op_{\mathrm{SL}_2}(\mathcal{C})$ are a larger set, refined by the data given by a spin structure, labeling the choice of spin structure.

The correspondence

The Analytic Langlands Correspondence is formulated as a precise statement in terms of the eigenspaces of the Hitchin Hamiltonians:

Theorem 1: Analytic Langland Correspondance

The single-valued eigestates of the Hitchin Hamiltonians form a complete set in $\mathcal{H}_{G,i\in\pi_1(G)}$:

$$\mathcal{H}_i = \bigoplus_{\chi\in\mathcal{S}_i} \mathcal{H}_\chi\,.$$

The Eigenspaces $\mathcal{H}_\chi$ are one-dimensional and coincide with the eigenspaces of the Hecke Operators. Furthermore the set $\mathcal{S}_i$ is the set of Real Opers $Op_{\mathrm{SL}}^{\gamma}(\mathcal{C})_{\mathbb{R}}$ independently of i.

This theorem is proved in section 11.3 for the case $\mathcal{C} = \mathbb{P}^1/\{z_1,\cdots,z_n\}$ and $G = \mathrm{PGL}_2$.

There are many non-trivial elements of this theorem. Foremost, we have not introduced yet one of the key players: the Hecke operators, this will be the subject of 11.1.4.

The crucial result of the theorem is a one-to-one correspondence between single valued and L^2 normalizable eigenfunction $\Psi(\boldsymbol{x},\bar{\boldsymbol{x}})$ of the Hitchin Hamiltonians:

$$\begin{array}{l} \mathrm{H}_r\Psi(\boldsymbol{x},\bar{\boldsymbol{x}}) = E_r\Psi(\boldsymbol{x},\bar{\boldsymbol{x}}) \\ \overline{\mathrm{H}}_r\Psi(\boldsymbol{x},\bar{\boldsymbol{x}}) = \overline{E}_r\Psi(\boldsymbol{x},\bar{\boldsymbol{x}}) \end{array}\,, \qquad r = 1,\cdots,d \tag{11.1.20}$$

and the set of real Opers, characterized by the single valued solution $\chi(u,\bar{u})$ of:

$$\left(\partial_u^2 + t_\eta(u)\right)\chi(u,\bar{u}) = 0\,, \qquad \left(\partial_{\bar{u}}^2 + t_{\bar{\eta}}(\bar{u})\right)\chi(u,\bar{u}) = 0\,.$$

Hence, we see how Analytic Langlands encodes the one-to-one correspondance between single values solutions to Hitchin eigensystems and opers with real monodromy.

11.1.4 Hecke Operators

Hecke operators play a crucial role: they implement the bijection between real opers and single-valued Hitchin eigenstates. Hecke and Hitchin Hamiltonians share the same Eigenspace by Theorem 1 and one has:

$$\mathsf{H}_u\Psi(\boldsymbol{x},\bar{\boldsymbol{x}}) = \chi(u,\bar{u})\,\Psi(\boldsymbol{x},\bar{\boldsymbol{x}}) \tag{11.1.21}$$

This is the most important relation of the Analytic Langlands Correspondance, and it is known as *Hecke eigenvalue property*.

λ-Hecke operators $\mathsf{H}_\lambda[u]$ (the slightly more general notation compared to the one above will be clear shortly) are defined as integral transforms acting on half-densities on $\mathcal{E} = \mathrm{Bun}_G(\mathcal{C})$, and take the schematic form

$$(\mathsf{H}_\lambda[u,\bar{u}]\,f)(\mathcal{E}) := \int_{Z_\lambda(\mathcal{E},u)} q_1^*(f),$$

where: $u \in \mathcal{C}$ is a fixed point, $Z_\lambda(\mathcal{E},u)$ is the moduli space of λ-Hecke modifications of $\mathcal{E}$ at u, λ is a coweight of G indexing the Hecke modification, and $q_1^*(f)$ is the pullback of the half-density f along the Hecke correspondence. In other words, Hecke Operators are defined as averages of Hecke Modification at a fixed point.

Hecke Modifications

Having defined the Hecke Operators as an average over the moduli space of Hecke modifications, we now give more details on those geometric modifications.

A Hecke modification of a G-bundle $\mathcal{E}$ at a point $u \in \mathcal{C}$ of type λ is a new G-bundle $\mathcal{E}'$ over $\mathcal{C}$, together with an isomorphism

$$\varphi : \mathcal{E}|_{\mathcal{C}\setminus\{u\}} \xrightarrow{\sim} \mathcal{E}'|_{\mathcal{C}\setminus\{u\}},$$

such that the singularity of this isomorphism at u is classifies by the doninant coweigth $\lambda \in \Lambda^+$. At the formal disc around a point $u \in X$ $\mathcal{D}_u$ the two G-bundles $\mathcal{E}$ and $\mathcal{E}'$ become trivial, but their difference is measured by a transition function over the punctured disc $\mathcal{D}_u^\times = \mathrm{Spec}(\mathbb{C}((t)))$. That is, the difference between $\mathcal{E}$ and $\mathcal{E}'$ is encoded by an element of the affine Grassmannian:

$$\mathrm{Gr}_G = G(\mathbb{C}((t)))/G(\mathbb{C}[[t]]).$$

parameterizing exactly G-bundles on a formal disc, trivialized away from the origin. The affine Grassmannian is stratified into Schubert cells:

$$\mathrm{Gr}_G = \bigsqcup_{\lambda\in\Lambda^+} \mathrm{Gr}_\lambda\,.$$

So specifying an Hecke modification, accounts for specifying a particular transitions function between local trivializations of punctured disks, i.e. by a particular Schubert cell (or more precisely closure thereof).

This definition is very technical for an arbitrary bundle modification λ. Yet, for our scopes it is enough to discuss the case of elementary Hecke modifications, denoted as H_u in the following (this is what was used above in (11.1.21)), or somewhat improperly as $\mathsf{H}_{\frac{1}{2}}[u]$ making reference to their counterpart in 2d CFT. Coweights of both PGL_2 and SL_2 are $\Lambda \simeq \mathbb{Z}(1,-1)$, and dominant coweights are of the form $(n,-n)$ $n\geq 0$, so we can indicate a dominant coweight by $\Lambda^+ \simeq \mathbb{N}^+$. The connected components of the affine Grassmanians are indexed by $\Lambda/Q^\vee$, where $Q^\vee$ is the coroot lattice. For PGL_2 $\Lambda/Q^\vee \simeq \mathbb{Z}(1,-1)/2\mathbb{Z}$ and coweights lie in even and odd classes devending on the parity. Instead, for SL_2 there is only a single connected component of the affine Grassmanian. Only the even dominant coweights of PGL_2 admit a lift to dominant coweights of SL_2. Hence, elementary Hecke of SL_2 are not elementary thought as PGL_2 modifications.

General Hecke modifications, may be obtained as $\mathsf{H}_{\frac{n}{2}} \sim \mathrm{Sym}_n \mathsf{H}_{\frac{1}{2}}$. For $G=\mathrm{PGL}_2$, Gr_0 is just a point (the trivial modification), while the elementary Hecke is associated with the Schubert Cell $\mathrm{Gr}_1 \simeq \mathbb{P}^1$. In our situation of Hecke modification of a rank 2 bundle, this elementary Hecke corresponds to a bundle modification such that the new bundle $\mathcal{E}'$ is obtained by $\mathcal{E}$ by allowing sections to have simple poles at a subline bundle $\mathcal{L} = \mathcal{E}\big|_u$. More precisely, let us consider the rank 2 bundle $\mathcal{E}$ defined by the extension

$$0 \longrightarrow \mathcal{L}_1 \longrightarrow \mathcal{E} \longrightarrow \mathcal{L}_2 \longrightarrow 0\,, \tag{11.1.22}$$

then the Hecke modified bundle at u is the extension

$$0 \longrightarrow \mathcal{L}_1 \longrightarrow \mathcal{E} \longrightarrow \mathcal{L}_2 \otimes \mathcal{O}(u) \longrightarrow 0, \tag{11.1.23}$$

Hecke shifts the degree of the bundle exactly by one and gives an isomorphism[20]:

$$\mathsf{H}_u : \mathrm{Bun}_0 \xrightarrow{\sim} \mathrm{Bun}_1$$

between the two disconnected components of $\mathrm{Bun}_{\mathrm{PGL}_2}$.

For simplicity, let us give an example for split bundles on $\mathbb{P}^1$, having the form:

$$\mathcal{E} \simeq \mathcal{O}(D_1)\oplus\mathcal{O}(D_2) \simeq \mathcal{O}(D_1)\,(\mathcal{O}\oplus\mathcal{O}(D_2-D_1)) \equiv \mathcal{O}\oplus\mathcal{O}(D)$$

where D_i are divisors on $\mathbb{P}^1$, and $D = D_2 - D_1$. The degree $d=\deg(D)$ of the bundle, is only defined up to line bundle twists, and therefore only modulo 2 for PGL_2, and we have indeed the decomposition $\mathrm{Bun}_0 \sqcup \mathrm{Bun}_1$ depending on the parity of d. We can then consider the two representatives: $\mathcal{E}_0 = \mathcal{O}\oplus\mathcal{O}$ and $\mathcal{E}_1 = \mathcal{O}\oplus\mathcal{O}(1)$ in Bun_0 and Bun_1 respectively.

Employing a parametrization $\ell_i = \mathbb{C}(1, x_i)$ for the flags in Bun_1, the Hecke modification $\mathbb{H}_{z,x} : \mathrm{Bun}_0 \to \mathrm{Bun}_1$ acts geometrically by the change of coordinate[20]:

$$y_i = -\frac{z_i - z}{x_i - x}, \qquad i = 1, \cdots n \tag{11.1.24}$$

parameterizing the Hecke modified flags in Bun_1 $\ell'_i = \mathbb{C}(1, y_i)$. This changes of coordinates realizes explicitly the isomorphism between $\mathrm{Bun}_0 \simeq \mathrm{Bun}_1$. To be more precise, on $\mathrm{Bun}_{\mathrm{PGL}_2} = \mathrm{Bun}_0 \oplus \mathrm{Bun}_1$, Hecke operators take the form $\left(\begin{smallmatrix} 0 & \mathsf{H}_z \\ \mathsf{H}_z & 0 \end{smallmatrix}\right)$, so that there are pairs of opposite eigenvalues of Hecke over the full bundle.

Hecke modifications act on half-densities over the moduli of $\mathrm{Bun}_{\mathrm{PGL}_2}(\mathbb{P}^1 \backslash \{z_1, \cdots, z_{n-1}, \infty\})$ as:

$$\mathbb{H}_{z,x}\Psi(x_1, \cdots, x_{n-1}) = \prod_{i=1}^{n-1} \frac{|z_i - z|^{\frac{1}{2}}}{|x_i - x|} \Psi\left(-\frac{z_1 - z}{x_1 - x}, \cdots, -\frac{z_{n-1} - z}{x_{n-1} - x}\right). \tag{11.1.25}$$

Where we have already included an extra factors in front accounting for the integration measure for half-densities and an important normalization factor. Its average over the moduli $x \in \mathbb{P}^1 \simeq Z_1(\mathrm{Bun}_0, z)$ is the Hecke operator:

$$H_z = \int \mathrm{d}^2 x \, \mathbb{H}_{z,x}\Psi(x_1, \cdots, x_n) = \int \mathrm{d}^2 x \prod_{i=1}^{n-1} \frac{|z_i - z|^{\frac{1}{2}}}{|x_i - x|} \Psi\left(-\frac{z_1 - z}{x_1 - x}, \cdots, -\frac{z_{n-1} - z}{x_{n-1} - x}\right). \tag{11.1.26}$$

One of the non trivial result needed for Analytic Langlands is compactness and normality of these operators over $\mathcal{H}_i$. This is discussed in [20]. In section 11.3 we will prove the Hecke eigenvalue property (11.1.21): normalizable singled valued eigenstates of the Hitchin Hamiltonians are simultaneous eigenstates of Hecke of eigenspace dimension 1, furthermore eigenvalues of Hecke coincide with the set of real opers $Op^{\gamma}_{\mathrm{SL}_2}(\mathcal{C})_{\mathbb{R}}$. The Hecke eigenvalue properties is crucial as, given the data of the Hitchin system, returns the unique solution χ with real monodromy determining uniquely the oper η corresponding to single valued solutions of the Hitchin system.

Let us conclude by discussing the case of $G = \mathrm{SL}_2$. Since the determinant line bundle is trivial for such bundles, elementary Hecke cannot change the degree of the determinant line bundle and must be of the form:

$$0 \longrightarrow \mathcal{L}_1 \otimes \mathcal{O}(-u) \longrightarrow \mathcal{E}' \longrightarrow \mathcal{L}_2 \otimes \mathcal{O}(u) \longrightarrow 0.$$

where again $d = \deg(D)$. This is indeed an even modification of type of type $(2, -2)$ from the point of view of a PGL_2 as already mentioned above.

11.2 Quantum Analytic Langlands: a tale of two CFTs

In this section we will describe a generalization of Analytic Langland correspondence for the case of[11] $G = \mathrm{PGL}_2$. This is motivated by the physical observation that the

[11] For the generic case of a group G, one may replace the H_3^+ by the corresponding G/G_c WZW model (G_c is the compact Lie Group), and the corresponding SOV dual CFT.

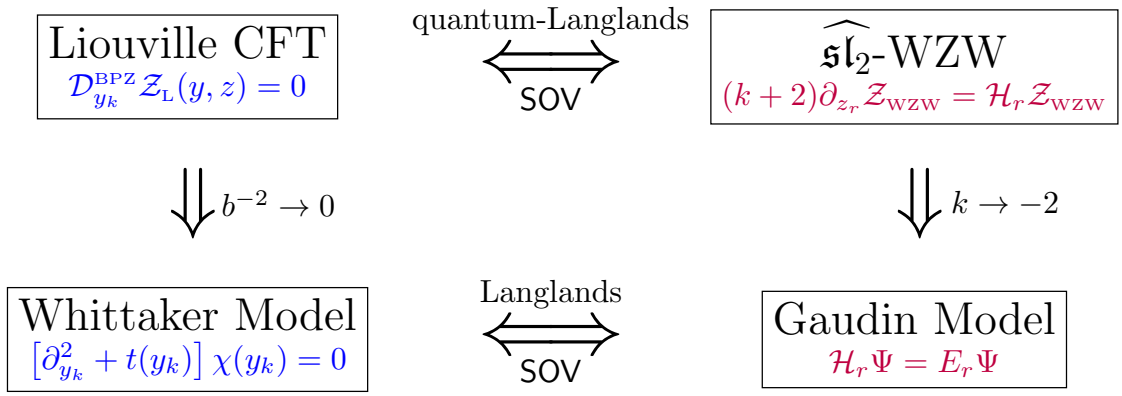


Figure 11.2: Schematic summary of the quantum deformation of Analytic Langlands based on the quantum SoV transform between Liouville CFT and the H_3^+ WZW model.

correspondence between the Hitchin (Gaudin) integrable model and opers, arises as the critical level limit of the far richer correspondence between two 2 dimensional CFTs: the $\widehat{\mathfrak{sl}_2}$ WZW model and Liouville CFT. This crucial observation is the physical motivation behind the proposal of a *quantum version* of Analytic Langlands[22,102] schematically summarized in Figure 11.2.

This correspondance is based over the SoV transform between the Liouville CFT and the H_3^+ WZW model based on the affine $\widehat{\mathfrak{sl}_2}$ symmetry proposed in [82]. We will come to a precise description of the correspondence in a moment, but the crucial result is a precise correspondence between correlation functions of Liouville theory with some particular degenerated insertions $\mathcal{Z}_{\text{L}}(\boldsymbol{y}|\boldsymbol{z})$ and correlation functions in the H_3^+ model $\mathcal{Z}_{\text{WZW}}(\boldsymbol{x};\boldsymbol{z})$. This is formulated as an integral transform schematically as:

$$\mathcal{Z}_{\text{WZW}}(\boldsymbol{x};\boldsymbol{z})=\int \mathrm{d}\boldsymbol{y}\,\mathcal{K}_{\text{SoV}}(\boldsymbol{x},\boldsymbol{y},\boldsymbol{z})\,\mathcal{Z}_{\text{L}}(\boldsymbol{y}|\boldsymbol{z})$$

for an SoV that we know explicitly. Such a correspondence is possible thanks to the equivalence of the Knizhnik–Zamolodchikov (KZ) equations:

$$(k+2)\partial_{z_r}\mathcal{Z}_{\text{WZW}}=\mathrm{H}_r\,\mathcal{Z}_{\text{WZW}}$$

encoding the $\widehat{\mathfrak{sl}_2}$ invariance of H_3^+ correlation functions and the Belavin–Polyakov–-Zamolodchikov (BPZ) equations:

$$\mathcal{D}^{\text{BPZ}}_{y_k}\mathcal{Z}_{\text{L}}=0$$

that are second order differential operators associated to each degenerated representation of the Virasoro algebra at y_k of Liouville momentum $-1/2b$. Remarkably, it turns out that the critical level limit of KZ equations $k\to -2$ (k is the level of the WZW model) reduces them exactly to the eigenvalue problem for the Hitchin (Gaudin) system, and in parallel, the corresponding classical limit $b^{-2}\to 0$ in Liuoville theory reduces the BPZ equations to the oper equation in the Whittaker model.

This produces then the diagram in Figure 11.2 where the uplift of the Analytic Langlands to the full CFT, predicts a far richer quantum deformed version. Furthermore, this richer version of Langlands, in many regards, accommodates for a very interesting ground play where many quantities, that become singular in the critical level, have a smooth and analytical and geometrical lift.

This deformation admits an interpretation as a quantum theory obtained by quantising the Hitchin moduli space in a holomorphic symplectic structure that differs from the one considered in relation to the analytic Langlands correspondence. Single-valued solutions to KZ-equations lie on the moduli space of PGL_2 bundles and represent states in this quantum theory. This quantum theory may be interpreted as a (Schur) quantization [83] of complex Chern-Simons theory with the H_3^+ replacing the rational WZW model as in conventional Chern-Simons theory. In [22] this remarkable story is even enriched by a beautiful discussion on how WZW correlators modified by Verlinde line insertion generate a basis for the space of states of this quantum theory, i.e. for single valued solutions of KZ-equations . Furthermore these operators are shown there to be dual in the critical level limit to a geometric operation called grafting, constructing a new real oper from a given reference one. This provides a beautiful and rich geometrical, analytical and CFT coherent story with endless ramifications. We will not discuss here many of those aspects.

In the following, after having introduced a lightning review of necessary background we will describe the SOV tranform between H_3^+ model and Liouville. Finally, in section 11.3 we will employ those ideas to prove analytic Langlands by strictly staying at the critical level.

11.2.1 Ribault-Teschner SoV

Let us now briefly discuss the SoV transform between H_3^+ model and Liouville CFT[62,82]. Let us consider correlation functions on a partially gauge fixed minimal bundle $\mathcal{O}\oplus\mathcal{O}(1)$ over $\mathbb{P}^1\setminus\{z_1,\cdots,z_{n-1},\infty\}$ with $x_n\to\infty$.

Separation of Variables

n-point correlation functions in the H_3^+ model are uniquely determined by Liouville conformal n-point blocks with additional $(n-3)$ degenerated insertion via:

$$\mathcal{Z}_{\rm WZW}(\boldsymbol{k},\boldsymbol{z};\boldsymbol{j})=\Theta_n(\boldsymbol{z},\boldsymbol{y})\mathcal{Z}_{\rm L}(\boldsymbol{y},\boldsymbol{z};\boldsymbol{\alpha})$$

where $\boldsymbol{y}=(y_1,\cdots,y_{n-3})$ is the separated variable basis determined by the $n-1$ momenta $\boldsymbol{k}$ (subjected to the remaining 2 $\mathfrak{sl}_2$ automorphisms) via the Skylianin SoV:

$$k_r(\boldsymbol{y})=y\frac{\prod_{j=1}^{n-3}(z_r-y_j)}{\prod_{s\neq r}^{n-1}(z_r-z_s)}\,,\qquad y=\sum_{r=1}^{n-1}z_rk_r\,,\qquad r=1,\cdots,n-1\,,$$

the central charges and representations are related by:

$$(k+2)=-b^{-2}\,,\qquad \alpha_r=b(j_r+1)+\frac{1}{2b}$$

and Θ is the twist factor:

$$\Theta(\boldsymbol{y},\boldsymbol{z})=\prod_{r<s\leq n-1}(z_r-z_s)^{\frac{1}{2b^2}}\prod_{k<l\leq n-3}(y_k-y_l)^{\frac{1}{2b^2}}\prod_{r=1}^{n-1}\prod_{k=1}^{n-3}(z_r-y_k)^{-\frac{1}{2b^2}}.$$

The SoV can be also recasted into x space as map given by the composition:

$$\mathsf{FT}^{-1}\circ\mathsf{SoV}:\quad \mathcal{Z}_{\rm L}(\boldsymbol{y},\boldsymbol{z};\boldsymbol{\alpha})\mapsto\mathcal{Z}_{\rm WZW}(\boldsymbol{x},\boldsymbol{z};\boldsymbol{j})$$

where FT^{-1} is the inverse Fourier transform from $\boldsymbol{k}$ to $\boldsymbol{x}$ space. The H_3^+-Liouville correspondence can formulated as the integral transform:

$$\boxed{\mathcal{Z}_{\rm WZW}(\boldsymbol{x},\boldsymbol{z};\boldsymbol{j})=\int_{(\mathbb{P}^1)^{n-3}}\mathrm{d}^2y_1\cdots\mathrm{d}^2y_{n-3}\,\mathcal{K}_{\mathsf{SoV}}(\boldsymbol{y},\boldsymbol{z})\,\mathcal{Z}_{\rm WZW}(\boldsymbol{y},\boldsymbol{z};\boldsymbol{\alpha})}\tag{11.2.1}$$

where the SoV kernel $\mathcal{K}^{\mathsf{SoV}}$ is given by:

$$\mathcal{K}_{\mathsf{SoV}}(\boldsymbol{y},\boldsymbol{z})=N_J\prod_{k<l}|y_k-y_l|^{1/b^2}\,\mathrm{d}\mu_{\rm Skl}\left|\sum_{r=1}^{n-1}x_r\frac{\prod_j(z_r-y_j)}{\prod_{s\neq r}(z_r-z_s)}\right|^{2J}\prod_{r=1}^{n-1}\left[\frac{\prod_{s\neq r}|z_r-z_s|^2}{\prod_j|z_r-y_j|^2}\right]^{\alpha_r/b}$$

where $J=\sum_{r=1}^{n-1}j_r-j_n$, N_J is an unimportant normalization and

$$\mathrm{d}\mu_{\rm Skl}=\frac{\prod_{k=1}^{n-3}\prod_{l=k+1}^{n-3}|y_k-y_l|^2}{\prod_{r=1}^{n-1}\prod_{s=r+1}^{n-1}|z_r-z_s|^2}\tag{11.2.2}$$

is the Skylianin measure associated with the change of variables $\boldsymbol{k} \to \boldsymbol{y}$.

11.2.2 Quantum Analytic Langlands

The separation of variables induces a very non trivial identification of correlation functions in two, in principle completely distinct 2d conformal field theories. Its proof [82] relies on the observation of the equivalence of the two distinct set of partial differential equations acting on the two correlation functions. The proof of the equivalence between the KZ equations and the BPZ differential operators together with the global $\mathfrak{sl}_2$ Ward Identities. This produces exactly the quantum deformation on Analytical Langlands we have announced: to each single valued solution to the system of holomorphic/antiholomorphic KZ equations $\mathcal{Z}_{\text{WZW}}$:

$$\begin{aligned} (k+2)\tfrac{\partial}{\partial z_r}\mathcal{Z}_{\text{WZW}}(\boldsymbol{x},\boldsymbol{z};\boldsymbol{j}) &= \mathrm{H}_r\,\mathcal{Z}_{\text{WZW}}(\boldsymbol{x},\boldsymbol{z};\boldsymbol{j}) \\ (k+2)\tfrac{\partial}{\partial \bar{z}_r}\mathcal{Z}_{\text{WZW}}(\boldsymbol{x},\boldsymbol{z};\boldsymbol{j}) &= \overline{\mathrm{H}}_r\,\mathcal{Z}_{\text{WZW}}(\boldsymbol{x},\boldsymbol{z};\boldsymbol{j}) \end{aligned} \qquad r = 1,\cdots,n \tag{11.2.3}$$

correspond a unique solutions to the system of BPZ differential equations:

$$\begin{aligned} \mathcal{D}_i^{\text{BPZ}}\,\mathcal{Z}_{\text{L}}(\boldsymbol{y},\boldsymbol{z};\boldsymbol{\alpha}) &= 0 \\ \overline{\mathcal{D}}_i^{\text{BPZ}}\,\mathcal{Z}_{\text{L}}(\boldsymbol{y},\boldsymbol{z};\boldsymbol{\alpha}) &= 0 \end{aligned} \qquad r = 1,\cdots,n \tag{11.2.4}$$

where we have omitted the dependence on $\overline{\boldsymbol{x}}$ etc... for sake of notation. This therefore represent a 1 parameter (k or b) deformation of Analytic Langlands where the $\mathcal{D}$ module side is upgraded from Hitchin integrable system to the full H_3^+ WZW model, and the local systems side is upgraded to Liouville theory decorated by degenerate representations satisfying the second order BPZ differential operators, that are of oper type. This realizes the picture presented in Figure 11.2.

11.2.3 Critical level limit

Let us now discuss how one recovers the Analytic Langlands correspondence from the classical limit of this correspondence. The classical/critical level limit corresponds to:

$$k \to -2 \Longleftrightarrow b^2 \to \infty$$

The asymptotic of KZ equations is studied in [82,317], solutions are formal power series of the WKB type:

$$\mathcal{Z}_{\text{WZW}}(\boldsymbol{k},\boldsymbol{z};\boldsymbol{j}) = e^{\frac{1}{k+2}S(\boldsymbol{z})}\widetilde{\Psi}(\boldsymbol{k})(1+\mathcal{O}(k+2))$$

where we take the limit at fixed j_r. This provides a solution of KZ at leading order in $k+2$ if Ψ and S satisfy:

$$\begin{aligned} \mathrm{H}_r\widetilde{\Psi}(\boldsymbol{k},\boldsymbol{z}) &= E_r\widetilde{\Psi}(\boldsymbol{k},\boldsymbol{z}) \\ \overline{\mathrm{H}}_r\widetilde{\Psi}(\boldsymbol{k},\boldsymbol{z}) &= \overline{E}_r\widetilde{\Psi}(\boldsymbol{k},\boldsymbol{z}) \end{aligned} \quad , \qquad \begin{aligned} \tfrac{\partial S}{\partial z_r} &= -E_r \\ \tfrac{\partial S}{\partial \bar{z}_r} &= -\overline{E}_r \end{aligned}$$

that is the Gaudin spectral problem, in the Fourier basis $\boldsymbol{k}$.

Let us now consider the semiclassical limit of the Liouville conformal block: $\mathcal{Z}_{\rm L}(\boldsymbol{y},\boldsymbol{z})$. The n fields with generic Liouville momentum α_i are *heavy* in the $b\to\infty$ limit as their scaling dimension, at fixed j_r is $\Delta_{\alpha_r}\sim b(j_r+1)$. These provide a classical background geometry given by the classical solution ϕ_{cl} of the Liouville e.o.m. corresponding to the heavy field at z_i. This classical geometry is unperturbed by the additional insertion of the *light* degenerate fields $V_{-1/2b}(y_i,\bar y_i)\to\chi(y_i,\bar y_i)$ (this follows from the OPE), that hsve subleading dimension in the classical limit. Then, also in this case, one has a WKB-like expansion:

$$\mathcal{Z}_{\rm L}(\boldsymbol{y},\boldsymbol{z})=e^{b^2S^{\rm L}[\phi_{cl}](z_1,\cdots)}\prod_{i=1}^{n-3}\chi(y_i,\bar y_i)$$

It turns out that because of the SoV that $S^{\rm L}[\phi_{cl}](z_1,\cdots)$ is exactly the generating function for the Gaudin eigenvalues. The OPE prescribes the singular behavior

$$\chi(y,\bar y)=\ |y-z_r|^{2j_n+2}C_+(j_n)(1+\mathcal{O}(|y-z_n|)+|y-z_n|^{-2j_n}C_-(j_n)(1+\mathcal{O}(|y-z_r|)$$

as one of the y variables approaches a puncture. To round off the picture, one recognizes that note in order to satisfy the BPZ equation, the WKB ansatz must satisfy:

$$\left(\partial^2_{y_i}+t(y_i)\right)\chi(y_i,\bar y_i)=0\,,\quad \left(\partial^2_{\bar y_i}+t(\bar y_i)\right)\chi(y_i,\bar y_i)=0\,,\quad i=1,\cdots n-3$$

that is the separated variable system satisfying the oper equation.
Furthermore, since $\Theta_n\xrightarrow{b^2\to\infty}1$, one has the simple relation between Hitchin Eigenstates and opers:

$$\widetilde\Psi(\boldsymbol{k})=\Phi(\boldsymbol{y})=\prod_{i=1}^{n-3}\chi(y_i,\bar y_i)$$

Hence, we see that SoV paves an explicit pathway to analytic Langlands, providing a direct integral transform between single valued solution of Hitchin Ψ and real opers χ. This is simply given by taking the critical level limit of the kernel (11.2.1)

$$\Psi(\boldsymbol{x})=\int_{\mathbb{C}^{n-3}}d\mu_{\rm Skl}(\boldsymbol{y})\,\mathcal{S}_{\boldsymbol{j}}(\boldsymbol{x},\boldsymbol{y})\Phi(\boldsymbol{y})\,,\tag{11.2.5}$$

One of our main result[6] is the proof of unitarity of the this map on Bun_i. This together with the Hecke eigenvalue property will be the crucial result needed to prove Theorem 1. A detailed account of this is the subject of section 11.3.

11.3 Analytic Langlands correspondence from SoV

Quantisation of the Hitchin system

We shall consider quantised Hitchin systems on $C=\mathbb{P}^1\setminus\{z_1,\dots,z_{n-1},\infty\}$. The relevant geometrical background is described in [20].

We shall define two Hilbert spaces $\mathcal{H}_i$, $i = 0, 1$, of homogeneous and translation invariant functions. The elements of $\mathcal{H}_i$ are represented by functions Ψ_i of $n-1$ complex variables $\boldsymbol{x} = (x_1, \dots, x_{n-1})$ satisfying

$$\begin{aligned} &\Psi_i(x_1 + \delta, \dots, x_{n-1} + \delta) = \Psi_i(x_1, \dots, x_{n-1}), \\ &\Psi_i(\rho x_1, \dots, \rho x_{n-1}) = |\rho|^{2J_i} \Psi_i(x_1, \dots, x_{n-1}), \end{aligned} \qquad i = 0, 1, \tag{11.3.1}$$

where

$$J_i = \sum_{r=1}^{n-1} j_r - \begin{cases} j_n & \text{for } i = 0, \\ -j_n - 1 & \text{for } i = 1. \end{cases}$$

Translation invariance allows one to represent the functions Ψ_i by the homogenous functions mapping $(z_2, \dots, z_{n-1}) \in \mathbb{C}^{n-2}$ to $\Psi_i(0, z_2, \dots, z_{n-1})$. Such functions can be represented as

$$\Psi_i(0, x_2, \dots, x_{n-1}) = |x_{n-1}|^{2J_i} \psi_i(x_2/x_{n-1}, \dots, x_{n-2}/x_{n-1}), \tag{11.3.2}$$

The functions ψ_i on the right side of (11.3.2) represents a section of line bundles $\mathcal{L}_{J_i}$ of densities on the complex projective space $\mathbb{P}^d$ in a particular chart.

We may observe that the Hilbert space structure on $L^2(\mathbb{C}^d)$ defines a natural norm of regular homogenous functions. With the help of (11.3.2) we may represent this norm as

$$\|\Psi\|^2 = \int_{\mathbb{C}^d} d^{2d}\boldsymbol{z}\ |\psi(\boldsymbol{z})|^2, \qquad \boldsymbol{z} = (z_2, \dots, z_{n-2}). \tag{11.3.3}$$

Representatives for the scaling equivalence class can, of course, be represented in other ways than (11.3.2). It can be checked that $\|\Psi\|^2$ does not depend on the representation, explaining why (11.3.3) defines a norm on the Hilbert space $\mathcal{H}_J$ of square-integrable sections of $\mathcal{L}_J$ on $\mathbb{P}^d$.

We furthermore note that the Hilbert spaces $\mathcal{H}_i$, $i = 0, 1$, are canonically isomorphic, with unitary isomorphisms $\mathsf{H}_\infty : \mathcal{H}_i \to \mathcal{H}_{i+1}$ being defined by sending ψ_i to ψ_{i+1}, for $i \in \mathbb{Z}/2$, but the representation in terms of homogenous functions differs.

The quantum integrable structure of the Hitchin system is defined by the Hamiltonians. In order to define the Hamiltonians, we shall first introduce the differential operators

$$\mathcal{D}_r^+ = \partial_{x_r}, \qquad \mathcal{D}_r^0 = x_r \partial_{x_r}, \qquad \mathcal{D}_r^- = 2j_r x_r - x_r^2 \partial_{x_r}, \tag{11.3.4}$$

allowing us to define

$$\mathsf{H}_r = \sum_{s \neq r} \frac{\eta_{ab} \mathcal{D}_r^a \mathcal{D}_r^b}{z_r - z_s}.$$

Such differential operators will be unbounded, as usual. In order to control the functional-analytic aspects it will be advantageous to introduce the Baxter operators.

Baxter operators

We shall define the Baxter operators Q_y as the composition $\mathsf{Q}_y = \mathbf{H}_\infty \cdot \mathbf{H}_y$, with the Hecke-operators $\mathbf{H}_y : \mathcal{H}_i \to \mathcal{H}_{i+1}$, being defined as

$$(\mathbb{H}_{y,x}\Psi)(x_1,\dots,x_{n-1}) = \prod_{r=1}^{n-1} \frac{|x_r - x|^{4j_r}}{|z_r - z|^{2j_r}} \Psi(y_1(x_1,x,y),\dots,y_{n-1}(x_{n-1},x,y)),$$
$$\mathbf{H}_y\Psi = \int_{\mathbb{C}} d^2x\, \mathbb{H}_{y,x}\Psi, \qquad y_r(x_r,x,y) := -\frac{z_r - y}{x_r - x}.$$

The Baxter operators are compact, hence bounded, for all $y \in \mathbb{C} \setminus \{z_1,\dots,z_{n-1}\}$ [20]. They are furthermore self-adjoint and mutually commuting [20],

$$[\,\mathsf{Q}_y\,,\mathsf{Q}_{y'}\,] = 0, \qquad \forall\, y,y' \in \mathbb{C} \setminus \{z_1,\dots,z_{n-1}\}.$$

The spectral problem for the family of Baxter operators is therefore well-posed, and the abstract spectral theorem of [20, Theorem 3.17] asserts existence of a discrete set $\mathcal{S}$ such that

$$\mathcal{H}_i \simeq \bigoplus_{\chi \in \mathcal{S}_i} \mathcal{H}_\chi, \tag{11.3.5}$$

where $\mathcal{H}_\chi$ are the eigenspaces for fixed eigenvalues χ, represented by functions $\chi(y,\bar{y})$ on C such that $\mathsf{Q}_y\Psi_\chi = \chi(y,\bar{y})\Psi_\chi$. The spaces $\mathcal{H}_\chi$ are finite-dimensional for all $\chi \in \mathcal{S}$.

[20, Proposition 4.3] clarifies the relation between Baxter operators and Hamiltonians, which can be concisely formulated as the operator differential equation

$$(\partial_y^2 + \mathsf{T}(y))\mathsf{Q}_w = 0, \qquad \mathsf{T}(y) = \sum_{r=1}^{n} \left(\frac{\delta_r}{(y-z_r)^2} + \frac{\mathsf{H}_r}{y - z_r} \right), \tag{11.3.6}$$

where $\delta_r = j_r(j_r+1)$. We refer to [20] for the precise statement. This will imply that eigenstates of the Baxter operators are eigenstates of H_r, $r = 1,\dots,d$.

Formulation of the analytic Langlands correspondence

The analytic Langlands correspondence describes the spectrum of Hitchin systems in geometric terms. as a one-to-one correspondence between eigenstates and real opers.

Definition 1. *An oper on $C_{0,n} = \mathbb{P}^1 \setminus \{z_1,\dots,z_n\}$ is a differential operator having the form $\partial_y^2 + t(y)$ on $\mathbb{C} \setminus \{z_1,\dots,z_n\}$, with $t(y)$ of the form*

$$t(y) = \sum_{r=1}^{n} \left(\frac{\delta_r}{(y-z_r)^2} + \frac{E_r}{y - z_r} \right), \tag{11.3.7}$$

having a finite limit $\lim_{y\to\infty} y^4 t(y)$. An oper on $C_{0,n}$ is a real oper if it has real monodromy.

An important role will be played by the solutions to the system of differential equations

$$(\partial_y^2 + t(y))\chi(y,\bar{y}) = 0, \qquad (\partial_{\bar{y}}^2 + \bar{t}(\bar{y}))\chi(y,\bar{y}) = 0. \tag{11.3.8}$$

An oper admits solutions χ that are single-valued on $C_{0,n}$ if and only if it is real. The solution χ is uniquely determined by the oper $\partial_y^2 + t(y)$, and vice-versa.

The analytic Langlands correspondence is the content of the following theorem.

Theorem 1. *The eigenspaces $\mathcal{H}_\chi$ are one-dimensional, and the set $\mathcal{S}$ is in bijection to the set $\mathrm{Op}_{\mathbb{R}}(C)$ of all real opers on C.*

11.3.1 Construction of the SoV transformation

The main tool for the proof of Theorem 1 will be an integral transformation referred to as Separation of Variables (SoV) transformation that will be defined in this section. It serves to simplify the eigenvalue problems for Hitchin's Hamiltonians.

Let us define $\mathcal{H}_{\mathrm{Skl}} = L^2(\mathbb{C}^{n-3}, d\mu_{\mathrm{Skl}})$, with

$$d\mu_{\mathrm{Skl}}(\boldsymbol{y}) = d^{2(n-3)}\boldsymbol{y} \prod_{\substack{r,s=1\\ r<s}}^{n-1} |z_r - z_s|^2 \prod_{\substack{k,l=1\\ k<l}}^{n-3} |y_k - y_l|^2 \prod_{r=1}^{n-1} \frac{1}{|\kappa_r(\boldsymbol{y})|^2}, \tag{11.3.9}$$

where

$$\kappa_r(\boldsymbol{y}) := \frac{\prod_{k=1}^{n-3}(z_r - y_k)}{\prod_{s\neq r}(z_r - z_s)}, \qquad r = 1, \dots, n-1. \tag{11.3.10}$$

We will construct the SoV transformations $\mathsf{S}_{\boldsymbol{j},i} : \mathcal{H}_i \to \mathcal{H}_{\mathrm{Skl}}$, $\boldsymbol{j} = (j_1, \dots, j_n)$, $i = 0, 1$, as the composition

$$\mathsf{S}_{\boldsymbol{j},i} = \mathsf{SoV} \circ \mathsf{F}_{\boldsymbol{j},i},$$

where $\mathsf{F}_{\boldsymbol{j},i}$ is a twisted version of the Fourier transformation of homogeneous translation-invariant functions defined below, and SoV is defined by a change of variables.

Fourier-transformation

We note that homogenous functions Ψ define homogenous regular distribution D_Ψ on the Schwartz space $\mathcal{S}(\mathbb{C}^{d+1})$ by means of

$$\langle D_\Psi, f\rangle = \int_{\mathbb{C}^{d+1}} d^{2(d+1)}\boldsymbol{x}\ \Psi(\boldsymbol{x}) f(\boldsymbol{x}), \qquad f \in \mathcal{S}(\mathbb{C}^{d+1}). \tag{11.3.11}$$

The Fourier-transformation of D_Ψ can be defined in the distributional sense, yielding a homogenous distribution $\widetilde{D}_\Psi$. It turns out that the homogenous distribution $\widetilde{D}_\Psi$ is regular, meaning that there exists a a homogenous function $\widetilde{\Psi}$ such that $\widetilde{D}_\Psi = D_{\widetilde{\Psi}}$. Let $\eta_\chi : \mathbb{R}_+ \rangle \mathbb{R}$ be a family of smooth functions satisfying $\eta(x) = 1$ for $x < \rho$ and $\eta(x) = 0$ for $x > 2\rho$.

Lemma 1. *$\widetilde{\Psi}$ can be represented for smooth homogenous functions Ψ as the limit*

$$\widetilde{\Psi}(\boldsymbol{k}) = \lim_{\rho\rangle\infty} \int_{\mathbb{C}^{d+1}} d^{2(d+1)}\boldsymbol{x}\ \Psi(\boldsymbol{x})\,\eta_\chi(\|\boldsymbol{x}\|) \prod_{r=2}^{n-1} e^{-2\mathrm{i}\,\mathrm{Im}(k_r x_r)}, \tag{11.3.12}$$

where $\boldsymbol{k} = (k_2, \ldots, k_{n-1})$. In this case, (11.3.12) defines a smooth function $\widetilde{\Psi}(\boldsymbol{k})$.

The proof of [318, Lemma 1] can be adapted to our case. We note that

$$\widetilde{\Psi}(\lambda\boldsymbol{k}) = |\lambda|^{2\bar{J}}\,\widetilde{\Psi}(\boldsymbol{k}), \qquad \bar{J} := -J - d - 1 = -\frac{d+1}{2} - iS. \tag{11.3.13}$$

The function $\widetilde{\Psi}(\boldsymbol{k})$ therefore defines a homogenous regular distribution on $\mathbb{C}^{d+1}$, represented by functions $\widetilde{\Psi}(k_2, \ldots, k_{n-1})$ of the form

$$\widetilde{\Psi}(k_2, \ldots, k_{n-1}) = |k_{n-1}|^{2\bar{J}}\,\widetilde{\psi}(k_2/k_{n-1}, \ldots, k_{n-2}/k_{n-1}). \tag{11.3.14}$$

It follows from Lemma (1) that the Fourier-transformation maps the space $\mathcal{S}_J$ of smooth sections of $\mathcal{L}_J$ to the space $\mathcal{S}_{-J-d-1}$. The definition of the norm given in (11.3.3) can be applied to $\widetilde{\Psi}$.

Theorem 2. *The Fourier transformation sending $\psi \in \mathcal{S}_J$ to $\widetilde{\psi} \in \mathcal{S}_{-J-d-1}$ is unitary.*

The argument used in [318, Section 3] can be adapted to our case. This implies, in particular, that the map F has a natural extension from $\mathcal{S}_J$ to the space $\mathcal{H}_J$ of square-integrable sections of $\mathcal{L}_J$.

Separation of Variables

It will be convenient to use a "twisted" version of the Fourier-transformation, sending ψ to

$$(\mathsf{F}_{\boldsymbol{j}}\Psi)(\boldsymbol{k}) := |\rho(\boldsymbol{k})|^{-2(j_n+1)} \prod_{r=1}^{n-1} |k_r|^{2j_r+2}\,\widetilde{\Psi}(\boldsymbol{k}), \qquad \rho(\boldsymbol{k}) := \sum_{r=1}^{n-1} z_r k_r. \tag{11.3.15}$$

The change of variables defined by

$$k_r(\boldsymbol{y}, \rho) := \rho\kappa_r(\boldsymbol{y}), \qquad \kappa_r(\boldsymbol{y}) := \frac{\prod_{k=1}^{n-3}(z_r - y_k)}{\prod_{s\neq r}(z_r - z_s)}, \qquad r = 1, \ldots, n-1, \tag{11.3.16}$$

allows us to define

$$\Phi(\boldsymbol{y}, \rho) := (\mathsf{F}_{\boldsymbol{j}}\Psi)(\boldsymbol{k}(\boldsymbol{y}, \rho)), \tag{11.3.17}$$

It follows easily from (11.3.13) that $\Phi(\boldsymbol{y}, \lambda\rho) = \Phi(\boldsymbol{y}, \rho)$, implying that $\Phi(\boldsymbol{y}, \rho) = \phi(\boldsymbol{y})$. We then have

Proposition 1. *The map $\widetilde{\mathcal{H}}_{-J-d-1}\rangle\mathcal{H}_{\mathrm{Skl}}$ sending $\widetilde{\psi}$ to the function ϕ defined above is unitary.*

Proof. We note that the change of variables defined by

$$\langle_r(\boldsymbol{y}) := \frac{\kappa_r(\boldsymbol{y})}{\kappa_{n-1}(\boldsymbol{y})}, \quad r = 2, \dots, n-2, \tag{11.3.18}$$

induces the following change of measures

$$d^{2(n-3)}\boldsymbol{\lambda} = \frac{d^{2(n-3)}\boldsymbol{y}}{|\kappa_{n-1}(\boldsymbol{y})|^{2(n-2)}} \prod_{\substack{r,s=1 \\ r<s}}^{n-1} |z_r - z_s|^2 \prod_{\substack{k,l=1 \\ k<l}}^{n-3} |y_k - y_l|^2. \tag{11.3.19}$$

It furthermore follows from (11.3.17) that

$$\left|\psi(\boldsymbol{\lambda}(\boldsymbol{y}))\right|^2 = |\phi(\boldsymbol{y})|^2 \, |\kappa_{n-1}(\boldsymbol{y})|^{2(n-2)} \prod_{r=1}^{n-1} \frac{1}{|\kappa_r(\boldsymbol{y})|^2}. \tag{11.3.20}$$

By combining (11.3.19) and (11.3.20) it follows that

$$\int_{\mathbb{C}^{n-3}} d^{2(n-3)}\boldsymbol{\lambda} \, |\psi(\boldsymbol{\lambda})|^2 = \int_{\mathbb{C}^{n-3}} d\mu_{\mathrm{Skl}}(\boldsymbol{y}) \, |\phi(\boldsymbol{y})|^2, \tag{11.3.21}$$

which is what we wanted to prove. □

Unitarity of the map SoV follows by combining Theorem 2 and Proposition 1.

For any given differential operator D of the form

$$\mathsf{D}(z) = \sum_{\alpha \in \mathcal{I}} f_\alpha(z) \mathsf{D}_\alpha,$$

with $\{\mathsf{D}_\alpha; \alpha \in \mathcal{I}\}$ being a finite set of differential operators in the variables k_r, and f_α, $\alpha \in \mathcal{I}$ being holomorphic functions on C, we may define a differential operator $\mathsf{D}(y_k)$ by substituting z by y_k "from the left", more precisely defined by

$$\mathsf{D}(y_k) := \sum_{\alpha \in \mathcal{I}} f_\alpha(y_k) \mathsf{D}_\alpha. \tag{11.3.22}$$

A crucial property of the composition $\mathsf{S}_{\boldsymbol{j},i} = \mathsf{SoV} \circ \mathsf{F}_{\boldsymbol{j},i}$ can now be formulated as follows.

Proposition 2.

$$\mathsf{S}_{\boldsymbol{j},i} \cdot \mathsf{T}(y_k) = -\partial_{y_k}^2 \cdot \mathsf{S}_{\boldsymbol{j},i}, \tag{11.3.23}$$

implying that $\mathsf{S}_{\boldsymbol{j},i}$ *intertwines the system of eigenvalue equations for the Hamiltonians* H_r *with the system of decoupled equations*

$$(\partial_{y_k}^2 + t(y_k))\Phi(\boldsymbol{y}) = 0, \qquad k = 1, \dots, d. \tag{11.3.24}$$

Identity has (11.3.23) has been discovered in a closely related context in [319]. A self-contained proof of (11.3.23) is given below.

Proof. As a preparation, let us note that $\widetilde{\mathsf{T}}(z) := \mathsf{F} \cdot \mathsf{T}(z) \cdot \mathsf{F}^{-1}$ can be represented as

$$\widetilde{\mathsf{T}}(z) = -(\mathsf{a}(z))^2 + \mathsf{a}'(z) - \mathsf{c}(z)\mathsf{b}(z), \tag{11.3.25}$$

where

$$\mathsf{c}(z) = \sum_{r=1}^{n-1} \frac{k_r}{z - z_r}, \quad \mathsf{a}(z) = \sum_{r=1}^{n-1} \frac{-k_r}{z - z_r} \frac{\partial}{\partial k_r}, \quad \mathsf{b}(z) = \sum_{r=1}^{n-1} \frac{1}{z - z_r} \left(\frac{\delta_r}{k_r} - k_r \frac{\partial^2}{\partial k_r^2} \right). \tag{11.3.26}$$

The equations (11.3.16) imply the key identity

$$\begin{aligned} \mathsf{a}(y_k) F(\boldsymbol{k}(\boldsymbol{y}, \rho)) &= -\sum_{r=1}^{n-1} \frac{k_r}{y_k - z_r} \frac{\partial}{\partial k_r} F(\boldsymbol{k}(\boldsymbol{y}, \rho)) \\ &= -\sum_{r=1}^{n-1} \frac{\partial k_r}{\partial y_k} \frac{\partial}{\partial k_r} F(\boldsymbol{k}(\boldsymbol{y}, \rho)) = -\frac{\partial}{\partial y_k} F(\boldsymbol{k}(\boldsymbol{y}, \rho)), \end{aligned} \tag{11.3.27}$$

for $k = 1, \ldots, n-3$. Equation (11.3.27) furthermore implies that the identity

$$\mathsf{a}^2(y_k) = \frac{\partial}{\partial y_k} \mathsf{a}(y_k) = \mathsf{a}(y_k) \frac{\partial}{\partial y_k} + \mathsf{a}'(y_k) = \frac{\partial^2}{\partial y_k^2} + \mathsf{a}'(y_k) \tag{11.3.28}$$

is valid when acting on functions of the form $F(\boldsymbol{k}(\boldsymbol{y}, \rho))$. With the help of equations (11.3.25) and (11.3.28) it is now easy to see that

$$\widetilde{\mathsf{T}}(y_k) = -\frac{\partial^2}{\partial y_k^2}, \qquad k = 1, \ldots, n-3. \tag{11.3.29}$$

This is equivalent to (11.3.23). □

The inverse transformation

Unitarity of the SoV-transformation ensures existence of an inverse transformation. It can be realised explicitly by inverting the relation (11.3.17), taking advantage of the fact that equations (11.3.16) can be used to define functions $y_k = y_k(\boldsymbol{k})$ up to permutations $y_k \mapsto y_l$, $y_l \mapsto y_k$. The resulting map SoV^{-1} takes elements ϕ of $\mathcal{H}_{\mathrm{Skl}}$ to functions $\widetilde{\Psi}(\boldsymbol{k})$ of $n-2$ variables $\boldsymbol{k} = (k_2, \ldots, k_{n-1})$ satisfying (11.3.13).

It follows from (11.3.23) that $\mathsf{S}^{-1}_{\boldsymbol{j},i}$ maps elements ϕ_χ of $\mathcal{H}_{\mathrm{Skl}}$ having the form

$$\phi_\chi(\boldsymbol{y}) = \prod_{k=1}^{n-3} \chi(y_k, \bar{y}_k), \qquad \begin{aligned} (\partial_y^2 + t(y))\chi(y, \bar{y}) &= 0, \\ (\partial_{\bar{y}}^2 + \bar{t}(\bar{y}))\chi(y, \bar{y}) &= 0, \end{aligned} \tag{11.3.30}$$

to eigenfunctions $\Psi_{\boldsymbol{E},i}$ of the differential operators H_r, with eigenvalues E_r determined by $t(y)$ using (11.3.7). One may furthermore easily check that $\phi_\chi(\boldsymbol{y})$ is normalizable, representing an element of $\mathcal{H}_{\mathrm{Skl}}$. This can be verified using (11.3.9), and taking into account that χ is analytic on C, having singular behaviour of the form

$$\chi(y, \bar{y}) = \sum_{\epsilon = \pm 1} |y - z_r|^{1 + \epsilon(2j_r + 1)} C_{r,\epsilon}(\boldsymbol{j})(1 + \mathcal{O}(|y - z_r|), \tag{11.3.31}$$

near the punctures z_r, $r = 1, \dots, n$. Unitarity of the SoV-transformation allows us to conclude that the eigenfunctions $\Psi_{\boldsymbol{E},i} = \mathsf{S}^{-1}_{\boldsymbol{j},i}(\phi_\chi)$ are normalisable.

One should note that $\mathsf{S}^{-1}_{\boldsymbol{j},i}(\phi_\chi)$ is not necessarily point-wise defined, being defined using the Fourier-transformation of homogenous distributions. However, it represents a distributional solution of the eigenvalue equations of the differential operators H_r. Elliptic regularity implies that $\Psi_{\boldsymbol{E},i}$ can be represented by functions $\Psi_{\boldsymbol{E},i}(\boldsymbol{x})$ which are smooth away from singularities of the differential operators H_r. Such singularities are associated to the so-called wobbly bundles.

However, one should note that the type of singular behaviour that can occur at the wobbly locus is constrained by the unitarity of the SoV transformation. As $\Psi_{\boldsymbol{E},i}$ are in the image of $\mathcal{H}_{\mathrm{Skl}}$ under the unitary operators $\mathsf{S}^{-1}_{\boldsymbol{j},i}$, it is ensured that the singularities of $\Psi_{\boldsymbol{E},i}$ can not spoil square-integrability. The unitarity of the SoV-transformation will allow us to avoid a detailed analysis of the singularities that may occur at the wobbly loci.

Let us finally note another property of the inverse transformation $\mathsf{S}^{-1}_{\boldsymbol{j},i}(\phi_\chi)$ that will become important below. Considering the dependence of the wave-functions $\Psi_{\boldsymbol{E},i}$ with respect to the parameters $j_1, \dots, j_n$, one may note that this dependence is meromorphic. In order to see this, one may first note that the dependence of χ on $j_1, \dots, j_n$ is analytic, as χ is the solution to a system of differential equations having coefficients depending analytically on $j_1, \dots, j_n$. The regular distribution associated to the function $\widetilde{\Psi}_{\boldsymbol{E}}(\boldsymbol{k})$ defined by inverting the relation (11.3.17) then depends meromorphically on $j_1, \dots, j_n$. These features are preserved by the inverse Fourier-transformation. We may therefore consider the analytic continuation of wave-functions $\Psi_{\boldsymbol{E},i}$ away from the range $j_r \in -\frac{1}{2}+\mathrm{i}\mathbb{R}$ in which the unitarity of the SoV-transformation holds.

11.3.2 Proof of the analytic Langlands correspondence

Outline of the proof

Theorem 1 will follow from the following two results.

i) (*Separation of variables*) Any eigenstate $\Psi_\chi \in \mathcal{H}_i$ of H_w defines an element $\Phi_\chi = \mathsf{S}_{\boldsymbol{j},i}\Psi_\chi$ of $\mathcal{H}_{\mathsf{SoV}}$. The wave-function $\Phi_\chi(\boldsymbol{y})$ representing Φ_χ has the form

$$\Phi_\chi(\boldsymbol{y}) = \prod_{k=1}^{n-3} \chi(y_k, \bar{y}_k), \tag{11.3.32}$$

where $\chi(y, \bar{y})$ satisfies

$$(\partial_y^2 + t_\chi(y))\chi(y, \bar{y}) = 0, \qquad (\bar{\partial}_{\bar{y}}^2 + \bar{t}_\chi(\bar{y}))\chi(y, \bar{y}) = 0.$$

Single-valuedness of χ implies that $\partial_y^2 + t_\chi(y)$ must be a real oper.

ii) (*Hecke eigenvalue property*) To each real oper $\partial_w^2 + t(w)$ we may associate the unique solution χ of the pair of differential equations

$$(\partial_w^2 + t(w))\chi(y, \bar{y}) = 0, \qquad (\bar{\partial}_{\bar{w}}^2 + \bar{t}(\bar{w}))\chi(y, \bar{y}) = 0. \tag{11.3.33}$$

The functions $\mathsf{S}^{-1}_{\boldsymbol{j},i}\Phi_\chi$ associated to χ, with Φ_χ defined in (11.3.32), are eigenstates of H_w with eigenvalue $\chi(w,\bar w)$.

In order to prove these two results, we shall consider the SoV transformations $\mathsf{S}^{(n+1)}_{\boldsymbol{j}',i}$, associated to $C_{0,n+1}=\mathbb{P}^1\setminus\{z_0,\dots,z_n\}$, $\boldsymbol{j}'=(j_0,j_1,\dots,j_n)$. The definition of $\mathsf{S}^{(n+1)}_{\boldsymbol{j}',i}$ is completely analogous to the definition of $\mathsf{S}^{(n)}_{\boldsymbol{j},i}:=\mathsf{S}_{\boldsymbol{j},i}$ given in the previous section, assigning index 0 to all variables associated to the additional puncture z_0, and admitting the factorisation $\mathsf{S}^{(n+1)}_{\boldsymbol{j}',i}=\mathsf{SoV}^{(n+1)}\circ\mathsf{F}^{(n+1)}_{\boldsymbol{j},i}$. In the special case $j_0=-1$, we will exhibit relations between $\mathsf{S}^{(n+1)}_{\boldsymbol{j}',i}$ and composition of $\mathsf{S}^{(n)}_{\boldsymbol{j},i}$ with the Hecke operators, implying the results i), ii) formulated above.

SoV-transform of eigenstates

The interplay between SoV-transform and Hecke operators will prove one direction of the analytic Langlands correspondence rather easily.

Proposition 3. *The SoV-transform $\Phi_\chi=\mathsf{S}^{(n)}_{\boldsymbol{j},i}\Psi_\chi$ of an eigenstate Ψ_χ can be represented in terms of the eigenvalue $\chi(z_0,\bar z_0)$ of the Baxter operators H_{z_0} as*

$$\Phi_\chi(\boldsymbol{y})=\prod_{k=1}^{n-3}\chi(y_k,\bar y_k).$$

Proof. Let us note that

$$(\mathsf{F}^{(n)}_{\boldsymbol{j},i}\mathsf{H}_{z_0}\Psi)(\boldsymbol{k})=\lim_{k_0\to 0}(\mathsf{F}^{(n+1)}_{\boldsymbol{j}',i}\Psi')(\boldsymbol{k}'),\qquad \Psi'(\boldsymbol{x}'):=\mathbb{H}_{z_0,x_0}\Psi(\boldsymbol{x}),\tag{11.3.34}$$

using the notations $\boldsymbol{x}'=(x_0,\dots,x_{n-1})$ and $\boldsymbol{k}'=(k_0,\dots,k_{n-1})$. When $\Psi\equiv\Psi_\chi$ is an eigenstate of H_{z_0} with eigenvalue $\chi(z_0,\bar z_0)$, we may conclude from (11.3.34) that

$$\chi(z_0,\bar z_0)(\mathsf{F}^{(n)}_{\boldsymbol{j},i}\Psi_\chi)(\boldsymbol{k})=\lim_{k_0\to 0}(\mathsf{FT}^{(n+1)}_{\boldsymbol{j}',i}\Psi'_\chi)(\boldsymbol{k}').\tag{11.3.35}$$

The change of variables $\mathsf{SoV}^{(n+1)}$, explicitly given by

$$k'_0(\boldsymbol{y}')=y\,(z_0-y_0)\frac{\prod_{k=1}^{n-3}(z_0-y_k)}{\prod_{r=1}^{n-1}(z_0-z_s)},\quad k'_r(\boldsymbol{y}')=y\,\frac{z_r-y_0}{z_r-z_0}k_r(\boldsymbol{y}),\quad r=1,\dots,n.\tag{11.3.36}$$

can be used to define the SoV transform $\phi'=\mathsf{S}^{(n+1)}_{\boldsymbol{j}',i}\Psi'_\chi$ of the function Ψ'_χ as before. The function $\phi'(y_0,\dots,y_{n-3})$. is manifestly symmetric in $y_0,\dots,y_{n-3}$.

Noting that $y_0\to z_0$ implies that $k'_0(\boldsymbol{y}')\to 0$ and $k'_r(\boldsymbol{y}')\to k_r(\boldsymbol{y})$, it follows from (11.3.35) that

$$\lim_{y_0\to z_0}(\mathsf{S}^{(n+1)}_{\boldsymbol{j}',i}\Psi'_\chi)(\boldsymbol{y}')=\chi(z_0,\bar z_0)(\mathsf{S}^{(n)}_{\boldsymbol{j},i}\Psi_\chi)(\boldsymbol{y}).\tag{11.3.37}$$

As the function on the left side of (11.3.37) is symmetric under permutations of the arguments exchanging z_0 with y_k for any $k = 1, \dots, n-3$, it follows that

$$\lim_{y_0 \to z_0} (\mathsf{S}^{(n+1)}_{\boldsymbol{j}',i} \Psi'_\chi)(\boldsymbol{y}') = \chi(z_0, \bar{z}_0) \prod_{k=1}^{n-3} \chi(y_k, \bar{y}_k).$$

The claim follows immediately. □

As the SoV-transform can be inverted, we see that eigenstates are uniquely determined by their eigenvalues, which means that the spectrum is simple.

Hecke eigenvalue property

We have seen that eigenstates define real opers as their Hecke eigenvalues. It remains to prove that all real opers define eigenstates. To this aim, we shall consider inverse SoV transformations of the form $(\mathsf{S}^{(n+1)}_{\boldsymbol{j}',i})^{-1} \phi'_\chi$, where

$$\phi'_\chi(\boldsymbol{y}') = \chi(y_0, \bar{y}_0) \phi_\chi(\boldsymbol{y}), \quad \phi_\chi(\boldsymbol{y}) = \prod_{k=1}^{n-3} \chi(y_k, \bar{y}_k), \quad \begin{matrix} \boldsymbol{y} = (y_1, \dots, y_{n-3}), \\ \boldsymbol{y}' = (y_0, y_1 \dots, y_{n-3}), \end{matrix} \tag{11.3.38}$$

where $\chi(y, \bar{y})$ is the solution to the differential equation associated to a real oper on $C_{0,n}$ rather than $C_{0,n+1}$. Opers on $C_{0,n+1}$ are differential operators of the form $\partial_y^2 + t^{(n+1)}(y)$, with

$$t^{(n+1)}(y) = \sum_{r=0}^{n} \left(\frac{j_r(j_r+1)}{(y-z_r)^2} + \frac{E_r}{y-z_r} \right). \tag{11.3.39}$$

We see that opers on $C_{0,n+1}$ represent opers on $C_{0,n}$ if $j_0 = -1$ and $E_0 = 0$.

The following theorem expresses a crucial link between the inverse Separation of Variables transformation and the Hecke modifications.

Theorem 3. *The Hecke modification of the states $(\mathsf{S}^{(n)}_{\boldsymbol{j},i})^{-1} \phi_\chi \in \mathcal{H}_i$ can be represented as*

$$\mathbb{H}_{z_0,x_0} (\mathsf{S}^{(n)}_{\boldsymbol{j},i})^{-1} \phi_\chi = (\mathsf{S}^{(n+1)}_{\boldsymbol{j}',i})^{-1} \phi'_\chi. \tag{11.3.40}$$

This theorem is proven in Subsection 11.3.3. It will be the key to one of our main results:

Theorem 4. *The states $\psi_\chi = (\mathsf{S}^{(n)}_{\boldsymbol{j},i})^{-1} \phi_\chi \in \mathcal{H}_i$ are eigenstates of the Hecke operators,*

$$\mathsf{H}_{z_0} \psi_\chi = \chi(z_0, \bar{z}_0) \psi_\chi. \tag{11.3.41}$$

In order to prove (4) using (3) it will help to note that the Hecke operator H_{z_0} can be represented as the limit $j_0 \to -1$, $x_0 \to 0$ of the reflection operator

$$(\mathsf{R}_{j_0} \Psi')(\boldsymbol{x}') = -\frac{2j_0+1}{\pi} \int_{\mathbb{C}} d^2 x_0 \, |x_0 - x'_0|^{-4j_0-4} \Psi'(\boldsymbol{x}').$$

Proposition 4. *The inverse* SoV*-transformation* $(\mathsf{S}^{(n+1)}_{\boldsymbol{j}',i})^{-1}$ *satisfies the reflection property*

$$\mathsf{R}_{j_0}(\mathsf{S}^{(n+1)}_{\boldsymbol{j}',i})^{-1} = \frac{\Gamma(-2j_0)}{\Gamma(2j_0+2)}(\mathsf{S}^{(n+1)}_{\boldsymbol{j}'',i})^{-1}, \tag{11.3.42}$$

where $\boldsymbol{j}'' = (-j_0-1, j_1, \dots)$ *if* $\boldsymbol{j}' = (j_0, j_1, \dots)$.

Proof. (Proposition 4) The identity (e.g. equation (7) of Appendix B1.7 in [320])

$$\frac{2j+1}{\pi}\int_{\mathbb{C}} d^2x' \, |x-x'|^{-4j-4} e^{kx'-\bar{k}\bar{x}'} = e^{kx-\bar{k}\bar{x}}|k|^{2(2j+1)}\frac{\Gamma(-2j-1)}{\Gamma(2j+1)}\,. \tag{11.3.43}$$

implies that $\mathsf{R}_{j_0}(\mathsf{F}^{(n+1)}_{\boldsymbol{j}',i})^{-1} = \frac{\Gamma(-2j)}{\Gamma(2j+2)}(\mathsf{F}^{(n+1)}_{\boldsymbol{j}'',i})^{-1}$, implying our claim. □

Proof. (Theorem 4) It remains to observe that the identity

$$\lim_{j\to -1}\frac{\Gamma(-2j)}{\Gamma(2j+2)}|y|^{2j} = 2\pi\delta^2(y),$$

implies that

$$\lim_{j_0\to -1}\frac{\Gamma(-2j_0)}{\Gamma(2j_0+2)}(\mathsf{S}^{(n+1)}_{\boldsymbol{j}'',i})^{-1}\phi'_\chi = \chi(z_0,\bar{z}_0)(\mathsf{S}^{(n)}_{\boldsymbol{j},i})^{-1}\phi_\chi. \tag{11.3.44}$$

By combining equations (11.3.42) and (11.3.44), one gets

$$\mathsf{H}_{z_0}\psi_\chi = \lim_{j_0\to -1}\mathsf{R}_{j_0}(\mathsf{S}^{(n+1)}_{\boldsymbol{j}',i})^{-1}\phi'_\chi = \lim_{j_0\to -1}\frac{\Gamma(-2j_0)}{\Gamma(2j_0+2)}(\mathsf{S}^{(n+1)}_{\boldsymbol{j}'',i})^{-1}\phi'_\chi = \chi(z_0,\bar{z}_0)(\mathsf{S}^{(n)}_{\boldsymbol{j},i})^{-1}\phi_\chi,$$

implying the Hecke eigenvalue property. □

11.3.3 Hecke modification of the inverse SOV transformation

We shall here prove the crucial Theorem 3.

An alternative representation

It will be useful to note that the inverse SoV-transformation can be represented as a certain limit of the inverse Fourier-transformation

$$\Sigma^{(n)}_\chi\left(\begin{smallmatrix} j_1 & \dots & j_n \\ x_1 & \dots & x_n\end{smallmatrix}\right) = \tag{11.3.45}$$
$$= \int d^{2(n-2)}\boldsymbol{k}\;\delta^{(2)}(\textstyle\sum_{r=1}^n k_r)|\kappa(\boldsymbol{k})|^2\left(\prod_{r=1}^n \frac{e^{2\mathrm{i}\,\mathrm{Im}(k_r x_r)}}{|k_r|^{2j_r+2}}\right)\prod_{k=1}^{n-2}\chi(y_k(\boldsymbol{k}),\bar{y}_k(\boldsymbol{k})),$$

with $y_k(\boldsymbol{k})$, $k=1,\dots,n-2$, and $\kappa(\boldsymbol{k})$ defined by the equations

$$k_r = \kappa(\boldsymbol{k})\frac{\prod_{k=1}^{n-2}(z_r - y_k(\boldsymbol{k}))}{\prod_{s\neq r}(z_r - z_s)}, \qquad r=1,\dots,n, \qquad \kappa(\boldsymbol{k}) = \sum_{r=1}^n z_r k_r. \tag{11.3.46}$$

We are going to show that there exists a function $D(j_n)$ such that

$$\lim_{x_n,z_n\to\infty}|z_n|^{4j_n}|x_n|^{-4j_n}\Sigma_\chi^{(n)}\left(\begin{smallmatrix} j_1 & \dots & j_n \\ x_1 & \dots & x_n\end{smallmatrix}\right)=D(j_n)(\mathsf{S}^{(n)-1}_{\boldsymbol{j},i}\phi_\chi)(\boldsymbol{x}). \tag{11.3.47}$$

The leading contributions to the limit $x_n\to\infty$ are coming from the region where $k_n\to 0$. It follows from (11.3.46) that there must exist an index k such that $y_k\to z_n$. The permutation symmetry of the integrand allows us to assume without loss of generality that $y_{n-2}\to z_n$. We may next note that

$$k_r=\kappa\frac{(z_r-y_{n-2})}{(z_r-z_n)}\frac{\prod_{k=1}^{n-3}(z_r-y_j)}{\prod_{r\neq s}^{n-1}(z_r-z_s)}=\kappa\frac{\prod_{k=1}^{n-3}(z_r-y_k)}{\prod_{r\neq s}^{n-1}(z_r-z_s)}+\mathcal{O}(x_n^{-1}). \tag{11.3.48}$$

It follows that the functions $y_k(\boldsymbol{k})$, $k=1,\dots,n-3$, and $\kappa(\boldsymbol{k})$ become independent of k_n in the limit of our interest. In the limit $y\to z_n$ we may furthermore use

$$\begin{aligned}\chi(y,\bar y)=&|y-z_n|^{2j_n+2}C_+(j_n)(1+\mathcal{O}(|y-z_n|)\\&+|y-z_n|^{-2j_n}C_-(j_n)(1+\mathcal{O}(|y-z_n|).\end{aligned} \tag{11.3.49}$$

As k_n is proportional to $y_{n-2}-z_n$, it follows that the integration over k_n can be carried out explicitly using (11.3.43). One of the terms is a distribution supported at $x_n=0$ which can not contribute to the limit $x_n\to\infty$. The other term leads to a result of the following form

$$D(j_n)\int d^{2(n-3)}\boldsymbol{k}\;\delta^{(2)}(\textstyle\sum_{r=1}^{n-1}k_r)|\kappa|^2\left(\prod_{r=1}^{n-1}\frac{e^{2\mathrm{i}\,\mathrm{Im}(k_rx_r)}}{|k_r|^{2j_r+2}}\right)\prod_{k=1}^{n-3}\chi(y_k(\boldsymbol{k}),\bar y_k(\boldsymbol{k})),$$

which yields (11.3.47).

Differential equations

We will now consider even more general inverse Fourier-transformations of the form

$$\Sigma_\chi^{(n+1)}\left(\begin{smallmatrix} j_0 & \dots & j_n \\ x_0 & \dots & x_n\end{smallmatrix}\right)=\int\prod_{r=0}^{n}\frac{d^2k_r}{|k_r|^{2j_r+2}}e^{2\mathrm{i}\,\mathrm{Im}(k_rx_r)}|\kappa|^2\delta^2(k_0+\dots+k_n)\prod_{k=0}^{n-2}\chi(y_k,\bar y_k), \tag{11.3.50}$$

with $\boldsymbol{k}=(k_0,\dots,k_n)$ related to $\boldsymbol{y}=(y_0,\dots,y_{n-2})$ and κ by the relations

$$k_r=\kappa\frac{\prod_{k=0}^{n-2}(z_r-y_k)}{\prod_{s\neq r}(z_r-z_s)},\qquad r=0,\dots,n,\qquad \kappa=\sum_{r=0}^{n}z_rk_r, \tag{11.3.51}$$

and with $\chi(y,\bar y)$ satisfying

$$\begin{aligned}&(\partial_y^2+t_{n+1}(y))\chi(y,\bar y)=0,\\&(\partial_{\bar y}^2+\bar t_{n+1}(\bar y))\chi(y,\bar y)=0,\end{aligned}\qquad t_{n+1}(y)=\sum_{r=0}^{n}\left(\frac{\delta_r}{(y-z_r)^2}+\frac{E_r}{y-z_r}\right). \tag{11.3.52}$$

By using the appropriately modified version of (11.3.47) one finds that $\mathsf{S}^{(n+1)-1}_{\boldsymbol{j}',i}\phi'_\chi$ can be represented as a limit of $\Sigma_\chi^{(n+1)}$.

When j_0 is generic, one finds that $\Sigma_\chi^{(n+1)}$ satisfies a holonomic system of differential equations:

Proposition 5. *The distribution* $\Sigma_\chi^{(n+1)}$ *satisfies* $\mathcal{D}_a\Sigma_\chi^{(n+1)}=0$, $a\in\{-,0,+\}$,

$$\mathcal{D}_+=\sum_{r=0}^n\frac{\partial}{\partial x_r}\,,\qquad \mathcal{D}_0=\sum_{r=0}^n\Big(x_r\frac{\partial}{\partial x_r}-j_r\Big)\,,\qquad \mathcal{D}_-=\sum_{r=0}^n\Big(x_r^2\frac{\partial}{\partial x_r}-2j_rx_r\Big),$$

together with the eigenvalue equations for the Hitchin system on $C_{0,n+1}$.

It will be crucial to observe that the system of differential equations satisfied by $\Sigma_\chi^{(n+1)}$ simplifies somewhat when $j_0=-1$ and $E_0=0$.

Proposition 6. *When* $j_0=-1$ *and* $E_0=0$, *the distribution* $\Sigma_\chi^{(n+1)}$ *satisfies the differential equations* $\mathcal{D}_a\Sigma_\chi^{(n+1)}=0$, $a\in\{-,0,+\}$, *and furthermore*

$$\mathcal{N}\Sigma_\chi^{(n+1)}=0,\qquad \mathcal{N}=\sum_{r=1}^n\frac{1}{z_0-z_r}\Big((x_r-x_0)^2\frac{\partial}{\partial x_r}-2j_r(x_r-x_0)\Big).\tag{11.3.53}$$

Proof. The condition $E_0=0$ implies that

$$0=\Big(\operatorname*{Res}_{z=z_0}\widetilde{\mathsf{T}}(z)\Big)\,\widetilde{\Sigma}_\chi^{(n+1)}=-k_0\,\widetilde{\mathcal{N}}\,\widetilde{\Sigma}_\chi^{(n+1)},$$

where $\widetilde{\mathsf{T}}(z)$ was defined in (11.3.25), and

$$\widetilde{\mathcal{N}}:=\sum_{r=1}^{n-1}\frac{k_r}{z_0-z_r}\Big(\frac{\partial^2}{\partial k_r^2}-\frac{\delta_r}{k_r^2}-2\frac{\partial^2}{\partial k_r\partial k_0}+\frac{\partial^2}{\partial k_0^2}\Big).$$

It follows that $\widetilde{\mathcal{N}}\widetilde{\Sigma}_\chi^{(n+1)}=0$, implying (11.3.53) by Fourier-transformation. □

Remark 1. The equation (11.3.53) has a geometric meaning. In the classical limit of the Hitchin system one may relate (11.3.53) to the fact that a Higgs field φ having an additional pole at $y=z_0$ such that $\mathrm{tr}(\varphi(y)^2)$ is holomorphic at this point can be considered as a Higgs field on $E=\mathcal{O}\oplus\mathcal{O}(z_0)$. The pair (E,φ) is gauge-equivalent to a pair (E',φ'), with $E'=\mathcal{O}\oplus\mathcal{O}(-1)$ and Higgs field φ' which is holomorphic at $y=z_0$.

Form of the solutions to the differential equations

It follows, in particular, that there exists a function $\widetilde{\Psi}_\chi$ such that

$$\Sigma^{(n+1)}\Big(\begin{smallmatrix}-1 & j_1 & \dots & j_n\\ x_0 & x_1 & \dots & x_n\end{smallmatrix}\Big)=\prod_{r=1}^n\frac{|x_r-x_0|^{4j_r}}{|z_r-z_0|^{2j_r}}\,\widetilde{\Psi}_\chi\Big(-\frac{z_1-z_0}{x_1-x_0},\dots,-\frac{z_n-z_0}{x_n-x_0}\Big),\tag{11.3.54}$$

with $\widetilde{\Psi}_\chi(x_1,\dots,x_n)$ being annihilated by $\sum_{r=1}^n\frac{\partial}{\partial x_r}$ and

$$\widetilde{\mathcal{T}}=\sum_{r=1}^n z_r\frac{\partial}{\partial x_r}\,,\quad \widetilde{\mathcal{D}}=x_n\frac{\partial}{\partial x_n}+1+j_n+\sum_{r=1}^{n-1}\Big(x_r\frac{\partial}{\partial x_r}-j_r\Big).\tag{11.3.55}$$

This implies, in particular, that $\widetilde{\Psi}_\chi$ is constant along the flows of $\sum_{r=1}^n (z_r - z_0)\frac{\partial}{\partial x_r}$,

$$\widetilde{\Psi}_\chi(x_1 + \delta(z_1 - z_0), \dots, x_n + \delta(z_n - z_0)) = \widetilde{\Psi}_\chi(x_1, \dots, x_n). \tag{11.3.56}$$

We may note, on the one hand, that

$$\lim_{x_0 \to x_n} \Big[\prod_{r=1}^n \frac{|x_r - x_0|^{4j_r}}{|z_r - z_0|^{2j_r}} \widetilde{\Psi}_\chi\Big(- \frac{z_1 - z_0}{x_1 - x_0}, \dots, -\frac{z_n - z_0}{x_n - x_0}\Big) \Big]_{z_0 - z_n = (x_0 - x_n)^2} =$$
$$= \prod_{r=1}^{n-1} \frac{|x_r - x_n|^{4j_r}}{|z_r - z_n|^{2j_r}} \widetilde{\Psi}_\chi\Big(- \frac{z_1 - z_n}{x_1 - x_n}, \dots, -\frac{z_{n-1} - z_n}{x_{n-1} - x_n}, 0\Big).$$

The function

$$\psi_\chi(x_1, \dots, x_{n-1}) := \widetilde{\Psi}_\chi(x_1, \dots, x_{n-1}, 0)$$

determines $\widetilde{\Psi}_\chi$ uniquely, and satisfies

$$\psi_\chi(x_1 + \delta(z_1 - z_n), \dots, x_{n-1} + \delta(z_{n-1} - z_n)) = \psi_\chi(x_1, \dots, x_{n-1}). \tag{11.3.57}$$

We may next consider the limit $x_n \to \infty$, $z_n \to \infty$ such that $z_n = -x_n^2$, using the observation

$$-\frac{z_r - z_n}{x_r - x_n}\Big|_{z_n = -x_n^2} = \frac{z_r - z_n}{x_n} - \frac{z_n}{x_n^2} x_r + \mathcal{O}(x_n^{-1}).$$

It follows that

$$\lim_{x_n \to \infty} \prod_{r=1}^{n-1} \frac{|x_r - x_n|^{4j_r}}{|z_r - z_n|^{2j_r}} \widetilde{\Psi}_\chi\Big(- \frac{z_1 - z_n}{x_1 - x_n}, \dots, -\frac{z_{n-1} - z_n}{x_{n-1} - x_n}, 0\Big)\Big|_{z_n = -x_n^2} = \psi_\chi(x_1, \dots, x_{n-1}). \tag{11.3.58}$$

We conclude that the differential equations satisfied by $\Sigma_\chi^{(n+1)}\left(\begin{smallmatrix} -1 & \dots \\ x_0 & \dots \end{smallmatrix}\right)$ have a unique solution that can be expressed in terms of the function ψ_χ obtained from $\Sigma_\chi^{(n+1)}\left(\begin{smallmatrix} -1 & \dots \\ x_0 & \dots \end{smallmatrix}\right)$ by performing the double limit considered above.

We will next compute the same limit using the integral representation defining $\Sigma_\chi^{(n+1)}\left(\begin{smallmatrix} -1 & \dots \\ x_0 & \dots \end{smallmatrix}\right)$.

Factorization of the integrand

Concerning the limit $z_0 \to z_n$ may then observe that

$$\begin{aligned} k_0 &= \rho \frac{z_0 - y_0}{z_0 - z_n} \frac{\prod_{k=1}^{n-2}(z_r - y_k)}{\prod_{s \neq r,n}(z_r - z_s)}, \quad k_n = \rho \frac{z_n - y_0}{z_n - z_0} \frac{\prod_{k=1}^{n-2}(z_n - y_k)}{\prod_{s \neq r,0}(z_n - z_s)}, \\ k_r &= \rho \frac{z_r - y_0}{z_r - z_0} \frac{\prod_{k=1}^{n-2}(z_r - y_k)}{\prod_{s \neq r}(z_r - z_s)}, \qquad r = 1, \dots, n-1, \end{aligned} \tag{11.3.59}$$

implying, in particular that

$$k_{0n} := k_0 + k_n = \rho \frac{\prod_{k=1}^{n-2}(z_n - y_k)}{\prod_{s \neq r}(z_n - z_s)} + \mathcal{O}(z_0 - z_n). \tag{11.3.60}$$

It should be observed that $k_1, \dots, k_{n-1}$ and k_{0n} become independent of y_0 in the limit $z_0 \to z_n$. This implies that $y_1, \dots, y_{n-2}$ will only depend on $k_1, \dots, k_{n-1}$ in this limit.

We may also note that the relation between y_0 and k_0, k_n simplifies in the limit $z_0 \to z_n$ to

$$\begin{aligned} y_0 - z_0 &= (z_n - z_0)\frac{k_0}{k_0 + k_n} + \mathcal{O}((z_0 - z_n)^2), \\ y_0 - z_n &= (z_0 - z_n)\frac{k_n}{k_0 + k_n} + \mathcal{O}((z_0 - z_n)^2). \end{aligned} \tag{11.3.61}$$

This means that a part of the integrand in (11.3.50) factorises as a product of a function depending only on $k_1, \dots, k_{n-1}$, and a function only depending on k_0 and k_n. It should be kept in mind, however, that $k_1, \dots, k_{n-1}$ and k_0, k_n are related on the support of the integrand of (11.3.50) by the distribution $\delta^2(k_0 + \cdots + k_n)$.

Factorisation of the measure

We next note that the measure of integration in (11.3.50) can be represented as a convolution by means of

$$\begin{aligned} &\int \prod_{r=0}^{n} d^2k_r \; e^{2\mathrm{i}\,\mathrm{Im}(k_r x_r)} \delta^2(k_0 + \cdots + k_n) = \\ &\quad = \frac{1}{\pi^2} \int d^2x \left(\int \prod_{r=1}^{n-1} d^2k_r e^{2\mathrm{i}\,\mathrm{Im}(k_r x_r)} d^2k_{0n} e^{2\mathrm{i}\,\mathrm{Im}(k_{0n} x)} \delta^2(k_1 + \cdots + k_{n-1} + k_{0n}) \right) \\ &\qquad\qquad \times \left(\int \prod_{r=0,n} d^2k_r e^{2\mathrm{i}\,\mathrm{Im}(k_r x_r)} d^2k'_{0n} e^{2\mathrm{i}\,\mathrm{Im}(k'_{0n} x)} \delta^2(k_0 + k_n + k'_{0n}) \right) \end{aligned} \tag{11.3.62}$$

It follows that the integral (11.3.50) can be represented as a convolution of the following form

$$\Sigma_\chi^{(n+1)} \left(\begin{smallmatrix} j_0 & \cdots & j_n \\ x_0 & \cdots & x_n \end{smallmatrix} \right) = \frac{1}{\pi^2} \int d^2x \; \Sigma_\chi^{(n)} \left(\begin{smallmatrix} j_1 & \cdots & j_{n-1} & -j_{0n}-1 \\ x_1 & \cdots & x_{n-1} & x \end{smallmatrix} \right) \Sigma_\chi^{(3)} \left(\begin{smallmatrix} j_{0n} & j_n & j_0 \\ x & x_n & x_0 \end{smallmatrix} \right), \tag{11.3.63}$$

where $j_0 = -1$, and

$$\begin{aligned} \Sigma_\chi^{(n)} \left(\begin{smallmatrix} j_1 & \cdots & j_{n-1} & -j_{0n}-1 \\ x_1 & \cdots & x_{n-1} & x_n \end{smallmatrix} \right) &= \int \prod_{r=1}^{n-1} \frac{d^2k_r}{|k_r|^{2j_r+2}} e^{2\mathrm{i}\,\mathrm{Im}(k_r x_r)} \int \frac{d^2k_{0n}}{|k_{0n}|^{-2j_{0n}}} e^{2\mathrm{i}\,\mathrm{Im}(k_{0n} x)} \\ &\quad \times |\rho|^2 \delta^2(k_1 + \cdots + k_{n-1} + k_{0n}) \prod_{k=1}^{n-2} \chi(y_k, \bar{y_k}), \end{aligned} \tag{11.3.64}$$

$$\begin{aligned} \Sigma_\chi^{(3)} \left(\begin{smallmatrix} j_{0n} & j_n & j_0 \\ x & x_n & x_0 \end{smallmatrix} \right) &= \int \prod_{r=0,n} \frac{d^2k_r}{|k_r|^{2j_r+2}} e^{2\mathrm{i}\,\mathrm{Im}(k_r x_r)} \int \frac{d^2k'_{0n}}{|k'_{0n}|^{2j_{0n}+2}} e^{2\mathrm{i}\,\mathrm{Im}(k'_{0n} x)} \\ &\quad \times |\rho_\infty|^2 \, \delta^2(k_0 + k_n + k_{0n}) \, \chi(y_0, \bar{y}_0) \end{aligned} \tag{11.3.65}$$

using the notation $\rho_\infty := k_{0n}$. For later use we have introduced factors $|k_{0n}|^{2j_{0n}}$ and $|k'_{0n}|^{-2j_{0n}}$ that will cancel each other in the convolution integral. We will later see that

the convolution (11.3.63) becomes proportional to $\Sigma_\chi^{(n)}\left(\begin{smallmatrix} j_1 & \dots & j_{n-1} & j_{0n} \\ x_1 & \dots & x_{n-1} & x_n \end{smallmatrix}\right)$ for a specific choice of j_{0n}.

We also have to recall the behavior of $\chi(y,\bar{y})$ in the limit $y \to z_n$. It takes the form

$$\begin{aligned}\chi(y,\bar{y}) = |y-z_n|^{2j_n+2} C_+(j_n)(1+\mathcal{O}(|y-z_n|) \\ + |y-z_n|^{-2j_n} C_-(j_n)(1+\mathcal{O}(|y-z_n|).\end{aligned} \tag{11.3.66}$$

As convenient notation we shall introduce

$$\chi_n^{\pm}(y,\bar{y}) = |y-z_n|^{1\pm(2j_n+1)} C_\pm(j_n). \tag{11.3.67}$$

We will see later that the first term in (11.3.66) does not contribute to the limit of our interest.

Evaluation of $\Sigma^{(3)}$

By using (11.3.66),(11.3.67) and (11.3.61) one may express the integrand in (11.3.65) in terms of

$$|\rho_\infty|^2\, \delta^2(k_0+k_n+k_{0n})\, \chi_n^{\pm}(y_0,\bar{y}_0) = |z_0-z_n|^{-1\mp(2j_n+1)}\, C_\pm(j_n) d_\pm(j_n),$$

with $d^{\pm}(j_n)$ being the distributions

$$d^{\pm}(j_n) = \delta^2(k_0+k_n+k_{0n})\, |k_n|^{1\pm(2j_n+1)} |k_{0n}|^{1\mp(2j_n+1)}. \tag{11.3.68}$$

At this stage it is useful to note that $d_\pm(j_n)$ are proportional to special cases of a three-parameter family of distributions defined by the Fourier-transformation

$$D\left(\begin{smallmatrix} j_1 & j_2 & j_3 \\ k_1 & k_2 & k_3 \end{smallmatrix}\right) = \frac{1}{\pi^3} \prod_{i=1}^3 |k_i|^{2j_i+2} \int \prod_{i=1}^3 d^2k_r\, e^{2\mathrm{i}\,\mathrm{Im}(k_r x_r)} C\left(\begin{smallmatrix} j_1 & j_2 & j_3 \\ x_1 & x_2 & x_3 \end{smallmatrix}\right), \tag{11.3.69}$$

in terms of the functions

$$C\left(\begin{smallmatrix} j_1 & j_2 & j_3 \\ x_1 & x_2 & x_3 \end{smallmatrix}\right) = |x_1-x_2|^{2(j_1+j_2-j_3)} |x_2-x_3|^{2(j_2+j_3-j_1)} |x_3-x_1|^{2(j_3+j_1-j_2)}, \tag{11.3.70}$$

defining invariants in three-fold tensor products of principal series representations of $\mathrm{SL}(2,\mathbb{C})$. An explicit expression for $D\left(\begin{smallmatrix} j_3 & j_2 & j_1 \\ k_3 & k_2 & k_1 \end{smallmatrix}\right)$ can be computed using [321, Equation (3.64)],

$$\begin{aligned} D\left(\begin{smallmatrix} j_3 & j_2 & j_1 \\ k_3 & k_2 & k_1 \end{smallmatrix}\right) &= \pi\, \delta^2(k_1+k_2+k_3)\, |k_2|^{-2j_1-2j_3-2} |k_1|^{2j_1+2} |k_3|^{2j_3+2} \\ &\times \left(\frac{\gamma(j_{23}^1+1)\gamma(j_{13}^2+1)}{\gamma(-j_{123}-1)\gamma(2j_3+2)} {}_2\mathcal{F}_1(j_{123}+2, j_{13}^2+1, 2j_3+2; k_3/k_2) \right. \\ &\left. + \frac{\gamma(j_{12}^3+1)}{\gamma(-2j_3)} \left|\frac{k_2}{k_3}\right|^{2(2j_3+1)} {}_2\mathcal{F}_1(-j_{23}^1, j_{12}^3+1, -2j_3; k_3/k_2) \right), \end{aligned} \tag{11.3.71}$$

where $j_{ijk} = j_i + j_j + j_k$ and $j_{ij}^k = j_i + j_j - j_k$, and $\gamma(x) = \Gamma(x)/\Gamma(1-x)$, and

$$ {}_2\mathcal{F}_1(a,b,c;x) = {}_2F_1(a,b,c;x)\,{}_2F_1(a,b,c;\bar{x}),$$

${}_2F_1(a,b,c;x)$ being the standard hypergeometric function.

By using formula (11.3.71) one can verify that $D\left(\begin{smallmatrix} j_{0n} & j_n & j_0 \\ k_{0n} & k_n & k_0 \end{smallmatrix}\right)$ has a pole at $j_{0n} = j_n$ with residue proportional to $d_+(j_n)$. The Fourier-inversion of (11.3.69) yields a distribution supported at $x_0 = x_n$ in this limit. The limit of our interest is defined by considering functions depending on x_0 and x_n, as well as z_0 and z_n, which are well-defined away from $z_0 = z_n$, with limit taken such that $z_0 - z_n = (x_0 - x_n)^2$. As the definition of this limit requires that $x_0 \neq x_n$ before taking the limit, we conclude that the distribution $d_+(j_n)$ does not contribute to such a limit.

We may, on the other hand, verify that

$$ D\left(\begin{smallmatrix} -j_n-1 & j_n & j_0 \\ k_{0n} & k_n & k_0 \end{smallmatrix}\right) = (2j_n+1)^{-2} d_-(j_n). \tag{11.3.72}$$

Taken together we find that there exists a function $C(j_n)$ such that

$$ \Sigma_\chi^{(3)}\left(\begin{smallmatrix} j_{0n} & j_n & j_0 \\ x_n & x_0 & x \end{smallmatrix}\right) = |z_0 - z_n|^{-2j_n}\, C(j_n) C\left(\begin{smallmatrix} j_{0n} & j_n & j_0 \\ x & x_n & x_0 \end{smallmatrix}\right). \tag{11.3.73}$$

Taking the limit

It remains to notice that due to $j_{0n} = j_0 - j_n$ we have

$$ C\left(\begin{smallmatrix} j_0 & j_n & j_{0n} \\ x_0 & x_2 & x \end{smallmatrix}\right) = |x_0 - x_n|^{4j_n} |x - x_n|^{4j_{0n}} (1 + \mathcal{O}(x_0 - x_n)), \tag{11.3.74}$$

implying that the convolution in (11.3.63) reduces to the application of the reflection operator on $\Sigma^{(n)}$ in the limit $x_0 \to x_n$. This implies that there exists a function $D(j_n)$ such that

$$ \lim_{x_0 \to x_n} \Sigma_\chi^{(n+1)}\left(\begin{smallmatrix} j_0 & \dots & j_n \\ x_0 & \dots & x_n \end{smallmatrix}\right)_{z_0 - z_n = (x_0 - x_n)^2} = D(j_n) \Sigma_\chi^{(n)}\left(\begin{smallmatrix} j_1 & \dots & j_{n-1} & -j_n-1 \\ x_1 & \dots & x_{n-1} & x_n \end{smallmatrix}\right), \tag{11.3.75}$$

which implies Theorem 3 with the help of (11.3.47).

Chapter 12

RG flows in Schur Quantization

Four-dimensional $\mathcal{N} = 2$ Supersymmetric Quantum Field Theories are associated to a rich collection of physical and mathematical results [32,76–78,322–325], many of which were developed to understand the Seiberg-Witten solution of $SU(2)$ supersymmetric Yang-Mills theory and its generalizations. The Seiberg-Witten solution provides a description of the space of vacua of the gauge theory, as well as a large amount of information about the low-energy effective field theory in each of these vacua and about the RG flow itself, in the form of a complete spectrum of supersymmetry-preserving (BPS) massive particles.

From the very beginning, the formalism included sequential RG flows passing through one or more intermediate (mesoscopic) effective description, due to hierarchical spectra of massive particles. A classical example was the low effective description of pure $SU(2)$ gauge theory as an $U(1)$ gauge theory coupled to a light hypermultiplet, which provided an interpretation of confinement as a monopole condensation [32]. This feature was soon employed to define novel SQFTs as intermediate steps of known RG flows [323].

Another notion which was present from the very beginning is "wall-crossing": discrete features of the RG flow such as the BPS spectrum are locally constant as we vary the choice of vacua or couplings of the theory, but may jump across special "walls" in the space of parameters. The mathematical work of Kontsevich and Soibelman [86], which arose in the context of wall-crossing in String Theory, provided a conjectural universal description of such wall-crossing phenomena and motivated much work to understand the physical and mathematical aspects of the formula [60,326–332].

One of the tools developed in this context is the fusion algebra $\mathcal{A}$ of half-BPS loop operators [60,313,314,327,333–335]. This is an algebra over $\mathbb{Z}[\mathfrak{q}, \mathfrak{q}^{-1}]$ which inherits additional properties from its physical definition. For example, $\mathcal{A}$ is equipped with an automorphism ρ mapping a loop operator to its (right) dual as well as a "Schur index" pairing

$$I_{a,b}(\mathfrak{q}) = I_{1,\rho(a)b}(\mathfrak{q}) = I_{1,b\rho^{-1}(a)}(\mathfrak{q}) \in \mathbb{C}((\mathfrak{q})) \tag{12.0.1}$$

which is expected to converge for $|\mathfrak{q}| < 1$. From now on, we specialize $\mathfrak{q}$ to be a real number in the range $-1 < \mathfrak{q} < 1$.

Recently, a conjectural positivity constraint

$$I_{a,a} > 0 \qquad a \neq 0 \qquad -1 < \mathfrak{q} < 1 \tag{12.0.2}$$

was employed [83] to introduce a representation-theoretic framework called Schur quantization. The output of Schur quantization is an Hilbert space $\mathcal{H}$ which carries an action of $\mathcal{A}$ as unbounded normal operators W_a. The Hilbert space includes a *spherical vector*, a normalizable vector $|1\rangle \in \mathcal{H}$ satisfying

$$|a\rangle \equiv W_a|1\rangle = W^\dagger_{\rho(a)}|1\rangle \tag{12.0.3}$$

such that the expectation values

$$\mathrm{Tr}(a) := \langle 1|a|1\rangle \tag{12.0.4}$$

are finite for all $a \in \mathcal{A}$ and coincide with Schur indices:

$$I_{a,b} = \langle a|b\rangle = \mathrm{Tr}\,\rho(a)b\,. \tag{12.0.5}$$

The vectors $|a\rangle$ give a natural domain for the action of $\mathcal{A}$:

$$W_a\, W^\dagger_{\rho(c)}|b\rangle = |abc\rangle\,. \tag{12.0.6}$$

Concrete representations for the output of Schur quantization exist when explicit results for $\mathcal{A}$ and I_{ab} are available. A general class of examples are $\mathcal{N} = 2$ gauge theories, defined by a UV Lagrangian whose form is determined by a choice of gauge group G and symplectic matter representation[1] M. We will denote such a theory as $T[G, M]$ when necessary.

The algebra $\mathcal{A}[G, M]$ for $T[G, M]$ is linearly generated by "'t Hooft-Wilson" loop operators $D_{m,e}$, labelled by a magnetic weight m and an electric weight e for G defined up to the Weyl group action on the pair. The algebra structure can be computed via localization [336], though that may require advanced algebraic-geometric tools [335,337]. It is known mathematically as the K-theoretic Coulomb branch algebra. The Schur index is also computed via localization by a relatively simple integral formula [87].

12.1 Schur meets RG

It is natural to ask how Schur quantization interacts with RG flow. We expect an RG flow from a theory T_1 to a theory T_2 to induce an algebra map

$$\mathrm{RG} : \mathcal{A}_1 \to \mathcal{A}_2\,, \tag{12.1.1}$$

with multi-step flows $T_1 \to T_2 \to T_3$ giving compatible maps:

$$\mathrm{RG}_{31} = \mathrm{RG}_{32} \circ \mathrm{RG}_{21}\,. \tag{12.1.2}$$

There are two obstructions to lifting the RG maps to Schur quantization:

[1] Subject to a discrete anomaly cancellation condition which is automatically satisfied if M is of cotangent type when restricted to all simple factors of G.

- The RG flow and dualization maps do not commute:

$$\rho_2 \circ \mathrm{RG} \neq \mathrm{RG} \circ \rho_1 \,. \tag{12.1.3}$$

- The Schur indices do not match under the naive RG flow:

$$I^{(2)}_{\mathrm{RG}(a),\mathrm{RG}(b)} \neq I^{(1)}_{a,b} \,. \tag{12.1.4}$$

For the special case of T_2 being an $U(1)^r$ SYM gauge theory and the RG flow being the Seiberg-Witten solution of the theory T_1, it is known that both obstructions [60,89,90] are removed by the same object: the quantum spectrum generator S, also known as (the inverse of) the generating function of Donaldson-Thomas invariants [338].

We will generalize this result and associate to any RG flow as above a quantum spectrum generator S defined as an invertible element in a formal completion of $\mathcal{A}_2((\mathfrak{q}))$ such that

- Conjugation by S intertwines the ρ_1 and ρ_2 dualization maps:

$$\mathrm{RG}(a) \cdot S = S \cdot \rho_2^{-1}(\mathrm{RG}(\rho_1(a))) \,. \tag{12.1.5}$$

- Right multiplication by S intertwines the Schur indices:

$$I^{(2)}_{\mathrm{RG}(a)\cdot S,\mathrm{RG}(b)\cdot S} = I^{(1)}_{a,b} \,. \tag{12.1.6}$$

Furthermore, if we have multi-step flow $T_1 \to T_2 \to T_3$,

$$S_{31} = \mathrm{RG}_{32}(S_{21}) \cdot S_{32} \tag{12.1.7}$$

Accordingly, we find a relation between the Schur quantization for T_1 and T_2: the map

$$|1\rangle \to |S\rangle \equiv W_S|1\rangle \tag{12.1.8}$$

extends to an isometry $\mathcal{H}_1 \to \mathcal{H}_2$ which intertwines the standard action of $\mathcal{A}_1$ on $\mathcal{H}_1$ and the action by $W_{\mathrm{RG}(a)}$ on $\mathcal{H}_2$. This composes nicely for multi-step flows. We will also formulate a set of conjectures which implies that $\mathcal{H}_1 \to \mathcal{H}_2$ is an unitary transformation.

This formalism has a variety of algebraic and representation-theoretic consequences:

1. It simplifies the derivation of spectrum generators. First of all, standard strategies to build S can be simplified by considering multi-step flows. Furthermore, we find an explicit formula for the spectrum generator associated to the flow $T[G, T^*N] \to T[G, 0]$, so the conventional spectrum generator for any such gauge theory can be derived from that of a SYM theory.

2. It allows access to Schur quantization for non-Lagrangian theories for which the spectrum generator is otherwise available and gives new strategies to derive it.

3. Specialized to theories of class $\mathcal{S}$, it gives tools to quantize Chern-Simons theory with complex gauge group in a manner analogous to the well-known quantization of (higher) Teichmüller space [316,339–344].

4. Specialized to four-dimensional lifts of $T_\rho[G]$ theories [345], it gives a rich collection of unitary representations of "complex" quantum groups and provides acces to their spectral analysis.

12.1.1 Seiberg-Witten RG flows, Donaldson-Thomas invariants and tropical labels

An Abelian SYM $T[U(1)^r, 0]$ of rank r is equipped with a charge lattice Γ of rank $2r$ and an anti-symmetric, integral Dirac pairing $\langle \bullet, \bullet \rangle$ which we take to be non-degenerate and unimodular. The corresponding fusion algebra $\mathcal{A}[U(1)^r, 0]$ of 't Hooft-Wilson loop operators is the *quantum torus* algebra $\mathcal{Q}_\Gamma$: it has generators X_γ for $\gamma \in \Gamma$, relations $X_\gamma X_{\gamma'} = \mathfrak{q}^{\langle \gamma, \gamma' \rangle} X_{\gamma+\gamma'}$, and a canonical automorphism $\rho_{\mathcal{Q}}(X_\gamma) = X_{-\gamma}$. The Schur indices are

$$I_{X_\gamma, X_{\gamma'}} = (\mathfrak{q}^2)^{2r}_\infty \delta_{\gamma,\gamma'} \tag{12.1.9}$$

and Schur quantization is implemented on the Hilbert space $\ell^2(\Gamma)$. Concretely, $|X_\gamma\rangle$ can be identified with the function $(\mathfrak{q}^2)^r_\infty$ supported at γ and

$$W_{X_\gamma} |X_{\gamma'}\rangle = |X_\gamma X_{\gamma'}\rangle = \mathfrak{q}^{\langle \gamma, \gamma' \rangle} |X_{\gamma+\gamma'}\rangle \,. \tag{12.1.10}$$

Any known $\mathcal{N} = 2$ SQFT T is endowed with a moduli space of "Coulomb" vacua, which do not spontaneously break the $SU(2)_R$ symmetry of the theory. As generic Coulomb vacua, we expect an RG flow $T \to T[U(1)^r, 0]$ to an Abelian SYM. In particular, we have an RG flow map $\mathrm{RG} : \mathcal{A} \to \mathcal{Q}_\Gamma$ from the UV fusion algebra $\mathcal{A}$ to the appropriate quantum torus algebra $\mathcal{Q}_\Gamma$:

$$F_a := \mathrm{RG}(a) = \sum_{\gamma \in \Gamma} \Omega_a^\gamma(\mathfrak{q}) X_\gamma \,. \tag{12.1.11}$$

These Laurent polynomials are generating functions for "framed BPS degeneracies" $\Omega_a^\gamma(\mathfrak{q})$, which count the low energy ground states of a loop operator a which carry gauge charge γ. The $\mathfrak{q}$ variable plays the role of a spin fugacity.[2]

The choice of Coulomb vacuum which triggers the RG flow provides some extra data which constrains the form of the F_a's and of the spectrum generator S. For the purpose of this work, the data takes the form of a generic real linear functional on Γ, which splits non-zero charges into a positive cone and and its opposite and thus gives an ordering $\gamma \prec \gamma'$ of charges. The spectrum generator is supported on positive charges:

$$S = 1 + \sum_{\gamma \succ 0} \Sigma_\gamma(\mathfrak{q}) X_\gamma \,, \tag{12.1.12}$$

[2] Conjecturally, $\Omega_a^\gamma(\mathfrak{q})$ are positive linear combinations of $SU(2)$ characters $[n]_\mathfrak{q}$.

and conjecturally there is a linear "tropical basis" ℓ_γ in $\mathcal{A}$ such that

$$F_{\ell_\gamma} = X_\gamma + \sum_{\gamma' \succ \gamma} \Omega_a^{\gamma'}(\mathfrak{q}) X_{\gamma'} \tag{12.1.13}$$

The physical origin of this particular conjecture is unclear to us, but it holds in all known examples and we will assume it in this thesis. We will also observe other remarkable properties of the tropical basis. For example, $\rho(\ell_\gamma)$ appears to belong to the tropical basis as well.

These support conditions guarantee that $F_{\ell_\gamma} S - X_\gamma$ is also supported on charges $\gamma' \succ \gamma$. We will employ them to argue that the above-defined isometry from the Schur quantization Hilbert space $\mathcal{H}$ to $\ell^2(\Gamma)$ is an unitary transformation.

We should observe that given any collection of Laurent polynomials F_{ℓ_γ} which form a closed algebra and a formal power series S which satisfies the intertwining conditions

$$F_{\ell_\gamma} \cdot S = S \cdot \rho_{\mathcal{Q}}(F_{\rho(\ell_\gamma)}) \,, \tag{12.1.14}$$

one may formally attempt to run the Schur quantization procedure to build a representation on $\ell^2(\Gamma)$. The existence of Schur indices, i.e.

$$I_{a,b} = \langle F_a S | F_b S \rangle < \infty \,, \tag{12.1.15}$$

thought, is far from obvious. Indeed, we will see examples of tentative spectrum generators which fail this condition and thus presumably are not associated to an actual 4d $\mathcal{A}N = 2$ SQFT.

Finally, we can compare the Seiberg-Witten solution of two theories related by RG flow, via a multi-step process $T_1 \to T_2 \to T[U(1)^r, 0]$. Then the RG flow map and the framed BPS degeneracies will be related as

$$F_a^{(1)} = F^{(2)}_{\mathrm{RG}_{21}(a)} \tag{12.1.16}$$

If we assume that both algebras admit a tropical basis, we learn that

$$\mathrm{RG}_{21}(\ell_\gamma^{(1)}) = \ell_\gamma^{(2)} + \sum_{\gamma' \succ \gamma} \Omega^{\gamma'}_{\ell_\gamma^{(1)}}(21; \mathfrak{q}) \ell^{(2)}_{\gamma'} \tag{12.1.17}$$

If we "forget" about the last step of the RG flow and only preserve the tropical bases and ordering $\ell_\gamma^{(2)} \prec \ell_{\gamma'}^{(2)}$ iff $\gamma \prec \gamma'$, we see that RG flows $T_1 \to T_2$ must also be associated to a tropical basis for $\mathcal{A}_2$, with support conditions both for RG and for S and novel partial BPS degeneracies $\Omega_a^{\gamma'}(21; \mathfrak{q})$. This will provide an argument for $\mathcal{H}_1 \to \mathcal{H}_2$ also being an unitary transformation.

12.1.2 Schur quantization and complex cluster quantization

In the $\mathfrak{q} \to \pm 1$ limit, the fusion algebra $\mathcal{A}$ becomes commutative and is identified with the algebra of holomorphic functions on a complex symplectic manifold $\mathcal{M}$, the space

of vacua for a circle compactification of the 4d SQFT. In the same limit, the full $*$-double $\mathfrak{A}$ can be identified with a Poisson algebra combining both holomorphic and anti-holomorphic functions on $\mathcal{M}$, using the imaginary part of the complex symplectic form bracket. Accordingly, Schur quantization gives a quantization of $\mathcal{M}$ as a real phase space[3], say with $\mathfrak{q} = \pm e^{-\hbar}$.

An RG flow $T_1 \to T_2$ gives a Poisson map $\mathcal{M}_2 \to \mathcal{M}_1$: the low energy description T_2 only covers a patch of the full space of vacua $\mathcal{M}_1$. In particular, the Seiberg-Witten RG flow gives a $(\mathbb{C}^*)^{2r}$ log-Darboux coordinate patch on the space of vacua of the UV theory. The RG flow description of Schur quantization can thus be interpreted as a procedure where we first quantize the coordinate patch to $\ell^2(\Gamma)$ and then express quantized (anti)holomorphic functions on $\mathcal{M}$ as unbounded normal operators acting on an appropriate domain in $\ell^2(\Gamma)$.

As one moves on the space of 4d vacua for a theory T, the resulting RG flows will give a collection of coordinate patches which cover the whole $\mathcal{M}$. Usually, there is no guarantee that a "patch-by-patch" quantization of a phase space should be possible or consistent, with compatible unitary lifts of the classical coordinate transformations. Here, the unitary equivalences with the underlying UV definition guarantee the procedure success. In particular, the inner products

$$I_{a,b} = \langle F_a S | F_b S \rangle \,, \tag{12.1.18}$$

must be well defined and coincide in all RG coordinate charts.

In all known examples, the coordinate patches defined by the Seiberg-Witten RG flows equip $\mathcal{M}$ with the structure of a cluster variety [346–348]: each chart is related to nearby charts by wall-crossing transformations which take the form of "cluster transformations" labelled by a finite collection of charges γ_i. Turning on $\mathfrak{q}$, cluster transformations act on all the RG flow ingredients:

- $F_a \to E_{\mathfrak{q}}(X_{\gamma_i})^{-1} F_a E_{\mathfrak{q}}(X_{\gamma_i})$.
- $S \to E_{\mathfrak{q}}(X_{\gamma_i})^{-1} S E_{\mathfrak{q}}(X_{-\gamma_i})$.
- $|a\rangle \to E_{\mathfrak{q}}(X_{\gamma_i})^{-1} E_{\mathfrak{q}}(X_{\gamma_i})^{\dagger}$.

The collection of charges γ_i and the tropical labeling of $\mathcal{A}$ also mutates in a specific manner we review below.[4] Accordingly, Schur quantization becomes a form of "cluster" quantization, analogous to the better known quantization of the positive part of $\mathcal{M}$.

An important visualization tool for the collection of γ_i charges in Γ is the "BPS quiver", with nodes labelled by γ_i and

$$|i \to j| \equiv \max(0, \langle \gamma_i, \gamma_j \rangle) \tag{12.1.19}$$

[3] Both $\mathfrak{q} \to 1$ and $\mathfrak{q} \to -1$ limit to the Poisson algebra of function on two versions of $\mathcal{M}$, see [60].

[4] A confusing aspect of the relation between cluster technology and SQFTs is that certain cluster transformations may not correspond to allowed wall-crossing transformations in the theory. We will investigate in examples if the full Schur quantization structure may detect these discrepancies.

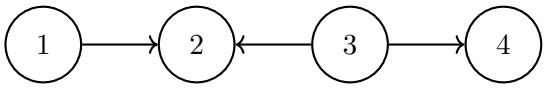


Figure 12.1: The BPS quiver for the $[A_1, A_4]$ Argyres-Douglas theory. It describes a collection of charges $\gamma_1, \cdots \gamma_4$ with non-trivial pairings $\langle \gamma_1, \gamma_2 \rangle = \langle \gamma_3, \gamma_2 \rangle = \langle \gamma_3, \gamma_4 \rangle = 1$.

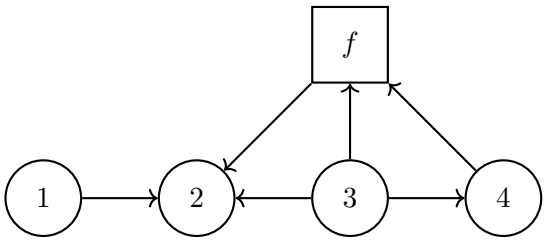


Figure 12.2: The A_4 BPS quiver for the $[A_1, A_4]$ AD theory with an extra framing node. It describes a tropical charge γ with non-trivial pairings $\langle \gamma_2, \gamma \rangle = \langle \gamma, \gamma_3 \rangle = \langle \gamma, \gamma_4 \rangle = 1$.

arrows from the i-th to the j-th nodes. See Figure 12.1. A tropical charge γ can be represented by an extra "framing" node with label γ. See Figure 12.2. Cluster transformations 'mutate" the BPS quiver at one node by a simple rule.

12.1.3 Class $\mathcal{S}$ Schur quantization and complex Chern-Simons theory

Class S theories are defined by the data of an ADE Lie algebra $\mathfrak{g}$ and a decorated Riemann surface C [77,349]. They have the property that the associated algebra $\mathcal{A}$ coincides with the "skein algebra" $\mathrm{Sk}(\mathfrak{g}, C)$ and the manifold $\mathcal{M}$ of vacua coincides with a "character variety" of $\mathfrak{g}$ local systems on C with appropriate singularities. The Schur indices have an interpretation in terms of an $\mathfrak{q}$-deformation of 2d YM theory [87].

These properties, reinforced by an appropriate duality chain, leads to the identification between Schur quantization and the quantization of "complex" Chern-Simons theory on C [83].

There is also a well-developed geometric approach [60,350–352] to the study of RG flows, F_a's and quantum spectrum generators, etc. We expect the theory of multi-step RG flows we set up to help simplify this geometric approach.

12.1.4 Computational strategies

The Schur quantization and RG flow machinery we discuss in this Chapter is most useful if the data of F_{ℓ_γ} and S can be explicitly derived or at least proven to exist in a mathematically rigorous manner. Multiple strategies have been developed in the past for this purpose:

1. The original work by Kontsevich and Soibelman on Cohomological Hall Algebras (CoHA) takes as an input a BPS quiver equipped with a "superpotential" W. It outputs a graded algebra whose equivariant character is expected to coincide with S^{-1}. The addition of a framing node conjecturally allows the computation of

$S^{-1}F_{\ell_\gamma}$ [353–355]. We are not aware of a physical prescription for W, unless the SQFT has an embedding into String Theory, but the choice of a "generic" W seems consistent with available data. The superpotential makes computations difficult. A recently conjectured alternative construction of the relevant CoHAs tentatively allows for a fully automated computation of $S^{-1}F_{\ell_\gamma}$ for any BPS quiver (See [356] for a further wrinkle in the story). We will verify that "unphysical" BPS quivers fail to give convergent Schur indices.

2. The theory of "scattering diagrams" [338,357] appears to offer an alternative combinatorial route to the computation of the F_{ℓ_γ}'s from a BPS quiver, from which one can reconstruct ρ and then S.

3. Our conjectural partial RG flow $T[G, T^*N] \to T[G, 0]$ allows for the computation of S for all gauge theories for which G for which the quantum spectrum generator of $T[G, 0]$ is known. The ρ map is known from the gauge theory description and one can then recover the F_a's from that information. Partial RG flows allow one to "transport" this information to a larger class of theories.

4. Above-mentioned geometric computational tools ("spectral networks") are available for theories of class S.

As the whole structure is very constrained, it is often possible to reconstruct it from partial information. We will review a variety of computational strategies in examples.

12.1.5 Outline.

This Chapter is organized as follows. Section 12.2 reviews some physical background for our constructions. Section 12.3 is devoted to the illustration of the Schur quantization and its application to Coulomb branch IR description of $4d\mathcal{N} = 2$ theories. In Section 12.4 we focus on the minimal example of Schur quantization applied to 4d $\mathcal{N} = 2$ theories with rank 2 lattice. In Section 12.5 and 12.6, building on the example of $SU(2)$ $\mathcal{N} = 2^*$ and the partial RG flow technique, we illustrate a powerful conjecture how to compute the spectrum generator of theories with flavor. One of the outcome is the computation of the Spectrum generator for $SU(2)$ $N_f = 4$, which was not known by other means. In Section 12.7 we test our technology further on $SU(3)$ gauge theories. In Section 12.8 we discuss some applications to the theory of quantum groups. In Section 12.9 we briefly discuss how to define RG flows geometrically in theories of class S labelled by $\mathfrak{sl}_2$. In Section 12.10 we discuss complex quantization of $\mathfrak{sl}_2$ character varieties in a manner parallel to the conventional quantization of Teichmüller space. Appendix C.2 discusses in detail the spectral problem relating UV and IR Schur quantization in $SU(2)$ gauge theories.

In Section 12.9 we briefly discuss how to define RG flows geometrically in theories of class S labelled by $\mathfrak{sl}_2$. In Section 12.10 we discuss complex quantization of $\mathfrak{sl}_2$ character varieties in a manner parallel to the conventional quantization of Teichmüller space. Appendix C.2 discusses in detail the spectral problem relating UV and IR Schur quantization in $SU(2)$ gauge theories.

12.2 Schur pairing and the Schur index

In this section we will briefly review the physical origin of the fusion algebra of loop operators and of the Schur pairing on the algebra. Recall the four-dimensional $\mathcal{N} = 2$ super-algebra:

$$\begin{aligned} \{Q^A_\alpha, Q^B_\beta\} &= 0 \\ \{Q^A_\alpha, \bar{Q}^B_{\dot\beta}\} &= \epsilon^{AB} P_{\alpha\dot\beta} \\ \{\bar{Q}^A_{\dot\alpha}, \bar{Q}^B_{\dot\beta}\} &= 0 \end{aligned} \tag{12.2.1}$$

Here α, β and $\dot\alpha$, $\dot\beta$ are spinor indices of the two chiralities, A, B are doublet indices for the $SU(2)_R$ R-symmetry.

We will always assume the existence of $SU(2)_R$. All 4d $\mathcal{N} = 2$ gauge theories have that property, with the exception of Abelian gauge theories deformed by FI parameters. Theories of class $\mathcal{S}$ also have $SU(2)_R$ symmetry. Furthermore, we will essentially define a Coulomb vacuum or RG flow as being $SU(2)_R$-preserving.

SCFTs are also equipped with an $U(1)_r$ symmetry giving charge ± 1 to super-charges depending on their chirality. The theories, vacua and RG flows we consider typically break $U(1)_r$.

In a Coulomb vacuum, with the exception of the conformal vacuum of an SCFT, the SUSY algebra is typically deformed by central charges:

$$\begin{aligned} \{Q^A_\alpha, Q^B_\beta\} &= \epsilon^{AB}\epsilon_{\alpha\beta} Z \\ \{Q^A_\alpha, \bar{Q}^B_{\dot\beta}\} &= \epsilon^{AB} P_{\alpha\dot\beta} \\ \{\bar{Q}^A_{\dot\alpha}, \bar{Q}^B_{\dot\beta}\} &= \epsilon^{AB}\epsilon_{\dot\alpha\dot\beta} \bar{Z} \end{aligned} \tag{12.2.2}$$

The central charge is a complex linear combination of flavour symmetries of the theory and in particular it vanishes in the vacuum itself, but is carried by massive excitations. Indeed, it sets a lower "BPS" bound on the mass of particles which carry it: $M \geq |Z|$.

Particles which saturate this bound are called BPS. Their spectrum (in the sense of an appropriate supersymmetric index) is robust and only jumps across certain walls of marginal stability in parameter space, which we will discuss below. The quantum spectrum generator S captures the spectrum in a particularly convenient way and is invariant across walls of marginal stability for BPS particles.

In superconformal or free field theories one can neatly organize local operators into supersymmetry multiplets and define superconformal indices which count special "short" supersymmetry multiplets in a robust manner. The Schur index we employ through this work was originally defined in a similar manner, but it is believed to make sense for non-conformal theories as well. This is done by selecting a specific nilpotent supercharge

$$Q \equiv Q^-_- + Q^{\dot-}_{\dot-} \tag{12.2.3}$$

and expressing the Schur index as a graded Euler character/Witten index of the cohomology of that supercharge in the space of local operators.

The super-charge Q is called Holomorphic-Topological [358] because most translations are Q-exact except $P_{++} = \partial_z$, where z is an holomorphic coordinate in a plane $\mathbb{C} \subset \mathbb{R}^4$ in spacetime. Accordingly, if an operator O contributes to the cohomology only the $\partial_z^n O$ derivatives will also contribute. The supercharge Q commutes with the combination $\hat{J} = J_3 - I_3$ of the rotation generator J_3 of $\mathbb{C}$ and R-symmetry generator I_3. The ∂_z derivatives increase $\hat{J}$ by 2. We will assume that the cohomology $H(Q)$ of local operators has finite-dimensional $\hat{J}$ eigenspaces and thus the Schur index

$$I(\mathfrak{q}) \equiv \mathrm{Tr}_{H(Q)}(-1)^{2I_3}\mathfrak{q}^{2J_3-2I_3} \tag{12.2.4}$$

is well-defined. We can also insert fugacities μ for flavor symmetries.

The Schur index is expected to be invariant under continuous deformations of the SQFT. In gauge theories with an explicit Lagrangian description, a standard strategy to compute the Schur index is to make the couplings arbitrarily weak and count gauge-invariant polynomials in cohomology representatives of the space of fields. Concretely, each half-hypermultiplet of matter fields contributes a single bosonic field and its ∂_z derivatives, and each vectormultiplet of gauge fields contributes two fermionic fields and their ∂_z derivatives. The outcome are the UV formulae for the Schur index we employ in this thesis.

The behavior of the Schur index under RG flow has important subtleties. Superconformal indices are often RG flow invariant, but not always. A typical proof strategy is to define a generalization of the indices which can be defined away from conformality and which remains constant along the flow. As RG flows may involve the decoupling of very massive degrees of freedom, this only works if such degrees of freedom do not contribute to the final answer. The Schur index is already defined away from conformality, but it can manifestly receive contributions from massive degrees of freedom: an hypermultiplet can be given a mass which preserves Q and $\hat{J}$ and has non-trivial Schur index. Accordingly, the RG flow from a massive free hypermultiplet to a trivial theory cannot preserve the Schur index.

The IR formulae for the Schur index were initially proposed for SCFTs, where the state-operator map can be used to replace local operators with states on a three-sphere S^3. Assuming that the $S^3 \times \mathbb{R}$ setup could be deformed to allow the theory to move to a non-trivial Coulomb vacuum, it was conjectured that only massive BPS particles would contribute to the Q-cohomology, and only if placed at specific central charge-dependent locations on the S^3. The spectrum generator S would then collect the contribution of half of the possible locations, leading to the $I(\mathfrak{q}) = \langle S|S\rangle$ formula.

The extension of this perspective to a general SQFT is challenging but possible in the language of Holomorphic-Topological twists, which we review below. Alternatively, one could take a perspective analogue to [359], where local operators are characterized in terms of the "fans" of BPS particles they can create out of the vacuum.

For SCFTs, convergence of the Schur index for $|\mathfrak{q}| < 1$ is roughly guaranteed by the state-operator map to a partition function on a certain $S^1 \times S^3$ geometry. For a general SQFT the statement is less obvious. The Holomorphic-Topological twist interpretation below provides a possible argument.

The main actors in our story are line defects which preserve

- Half of the supercharges, of the general form

$$q^A_\alpha \equiv Q^A_\alpha + e^{i\vartheta} n^{\dot\beta}_\alpha \bar{Q}^A_{\dot\beta} \tag{12.2.5}$$

  where n is the (time-like) unit vector pointing in the direction of the line defect in space-time and ϑ an angle we will specify momentarily. These anti-commute to

$$\{q^A_\alpha, q^B_\beta\} = 2\epsilon^{AB} e^{i\vartheta} n \cdot P \tag{12.2.6}$$

  i.e. to the translations along the defect. We set our conventions so that a standard line defect extending along the time direction has $n^{\dot\beta}_\alpha = \delta^{\dot\beta}_\alpha$ and thus $q^- = Q$ if $\vartheta = 0$.

- The $SO(3)$ rotation symmetry in the directions perpendicular to the defect and the full $SU(2)_R$ R-symmetry.

- The flavour symmetries of the theory.

These constraints are not as restrictive as it may appear. In particular, they hold for natural 't Hooft-Wilson line defects defined in gauge theory as well as in theories of class S. They are also preserved by the RG flows we are interested in. Furthermore, they can be defined uniformly for any choice of ϑ, though one finds that a continuous evolution $\vartheta \to \vartheta + 2\pi$ may not bring a defect back to the original. For example, in non-conformal gauge theories it will shift the electric charge of a 't Hooft-Wilson line by a multiple of the magnetic charge, via an analogue of Witten's effect. Ultimately, this will give rise to the ρ^2 map on line defects.

Any such line defect L will be associated to some space of local operators supported on the defect. This space is acted upon by the symmetries preserved by the line defect. Assuming that we have tuned the choice of n and ϑ so that $Q = q^-$, e.g. as described above, we can define a Schur index $I_{L,L}(\mathfrak{q})$ counting such local operators. If we have two line defects L_1 and L_2 with the same orientation in space-time, we can count defect-changing local operators between them by a Schur index $I_{L_1;L_2}(\mathfrak{q})$ [89,90,334].

One can arrange $Q = q^-$ for line defects with a generic orientation in the plane transverse to the z direction by adjusting ϑ to equal the angle off the (euclidean time) vertical in the plane. A collection of line defects L_i with a cyclic sequence of slopes in the plane can then end at the origin and support some space of junctions. The corresponding Schur index will be denoted as

$$I_{L_1,\cdots L_k}(\mathfrak{q}) \tag{12.2.7}$$

We do not need to specify the slopes in detail, as the index is a deformation invariant.

Here we defined the setup with all line defects "outgoing" from the junction point and labeled the line defects as if they had been brought back to the vertical. Accordingly, if we bring a line all around the cyclic order we need to pay a ρ^2 map:

$$I_{L_1;\cdots L_k}(\mathfrak{q}) = I_{\rho^2(L_k);L_1;\cdots L_{k-1}}(\mathfrak{q})\,, \tag{12.2.8}$$

etc.

We can compare this definition with the original $I_{L_1,L_2}(\mathfrak{q})$ by defining a map ρ which rotates the slope of a line defect by π and then re-interprets it as defect along the original direction. Then

$$I_{L_1,L_2}(\mathfrak{q}) = I_{\rho(L_1);L_2}(\mathfrak{q}) = I_{L_2;\rho^{-1}(L_1)}(\mathfrak{q}) \tag{12.2.9}$$

As the Schur indices are deformation-invariant, they can be thought of as depending on some kind of deformation classes of line defects. A general expectation is that there will be some collection of "elementary" line defects L_i such that all other ones line defects with the same amount of symmetry sit in deformation classes which include a direct sum of L_i defects dressed by auxiliary "Chan-Paton" vector spaces with the same action of symmetries. The Schur indices would then be expressed in terms of the Schur indices for elementary line defects and of the the characters $\mathrm{Tr}(-1)^{2I_3}\mathfrak{q}^{2J_3-2I_3}$ of these auxiliary vector spaces, which are linear combinations of $\mathfrak{q}$-integers coming from $SU(2)$ irreps.

The notion of fusion of half-BPS line defects involves the same kind of assumption: two parallel line defects, say both placed at the origin of the z plane and preserving the same SUSY, can be interpreted as a single defect breaking $SO(3)$ rotation symmetry to the $SO(2)$ subgroup generated by $\hat{J}$. The general expectation is that such a defect would also belong to the same deformation class as some linear combination of L_i's, though the CP factors will only carry an action of $SO(2)$ rotations. This leads to the notion of fusion algebra $\mathcal{A}$ of line defects we employ in the main text, with coefficients which are integral Laurent polynomials in $\mathfrak{q}$ [60,333,335,345,355,358].

With a bit of help from the HT twist setup described below, one can then argue that

$$I_{L_1;\cdots L_k}(\mathfrak{q}) = I_{L_1\cdots L_k}(\mathfrak{q}) \tag{12.2.10}$$

i.e. consecutive line defects can be fused without changing the Schur indices.

There is an important subtlety concerning the $I_{L_1,L_2}(\mathfrak{q})$ indices and the map ρ. If we dress L_2 by an auxiliary CP space V, the Schur index will be multiplied by the character of V. If we dress L_1, though, the index will be multiplied by the character of $V^\vee$. The same discrepancy occurs for ρ: if L is dressed by V then $\rho(L)$ should be dressed by $V^\vee$.

The character of $V^\vee$ is obtained from the character of V by flipping all fugacities. We already accounted for the effect on flavor fugacities when we set $\rho(\mu) = \mu^{-1}$. But we also need to invert the $\mathfrak{q}$ fugacity. At the same time, it is easy to see graphically that ρ acting on the fusion of two lines should give the fusion of their ρ images in the opposite order. The correct definition of ρ is thus that of a map

$$\rho : \mathcal{A}_{\mathfrak{q}} \to \mathcal{A}^{\mathrm{op}}_{\mathfrak{q}^{-1}} \tag{12.2.11}$$

Because of the $SO(3)$ rotation symmetry of the physical line defects we employ, we get for free an identification $A^{\mathrm{op}}_{\mathfrak{q}^{-1}} \simeq A_{\mathfrak{q}}$ mapping the L_i to themselves and mapping $\mathfrak{q} \to \mathfrak{q}^{-1}$. This map is implicitly included in the definitions we use in the main text, where ρ is defined as an algebra map $\mathcal{A} \to \mathcal{A}$ and the pairing $I_{a,b}$ as a pairing on $\mathcal{A}$. In other word, we start from $\rho(L_i)$ and I_{L_i,L_j} and extend them linearly to the whole $\mathcal{A}$.

We do not have a solid physical argument for $I_{a,b}$ being positive-definite. In a sense, the IR formulae for the Schur index are the best evidence available for that statement.

12.2.1 RG flow of line defects

If we consider RG flows triggered by vacua or mass deformations which preserve $SU(2)_R$ symmetry, a line defect which preserves the symmetries we discussed above will be described in a low-energy effective field theory as a line detect preserving the same symmetries. At the level of deformation classes, we assume that each $L_i^{\rm UV}$ line defect will be described as a direct sum of $L_i^{\rm IR}$ reference defects for the effective field theory, with Chan-Paton coefficients which can carry representations of the symmetries. This is the origin of the RG map from $\mathcal{A}^{\rm UV}$ to $\mathcal{A}^{\rm IR}$. It is an algebra map if we assume that the RG flow and fusion operations commute within a given deformation class.

A surprising observation is that the same argument will fail when comparing RG flow and rotations. Namely, if we denote as RG_ϑ the RG flow map for line defects of slope ϑ we will find that the map jumps at special values of ϑ. The reason for that is that a massive BPS particle of central charge Z can preserve the same SUSY as a line defect whose slope agrees with the argument of Z. Accordingly, the low energy effective description of a line defect of that slope becomes ambiguous/dependent on the scheme we use to distinguish a line defect from a line defect superimposed to a BPS particle. The definition of a deformation class of line defects as we vary their slope will break down. In particular, ρ and RG do not commute.

This problem is intimately connected to the corrections to the Schur index due to BPS particles. We can already see it in the presence of a single line defect of slope ϑ, say $0 < \vartheta < \pi$. Then the IR formula for the Schur index would involve the schematic combination

$$S_{0,\vartheta}\mathrm{RG}_\vartheta(L)S_{\vartheta,\pi} \tag{12.2.12}$$

where $S = S_{0,\vartheta}S_{\vartheta,\pi}$ has been factored into contributions of BPS particles of central charge phase supported in the two intervals. As we change ϑ, $\mathrm{RG}_\vartheta(L)$ passes across the phase of BPS particles and jumps in such a manner that the overall contribution remains constant and equal to $\mathrm{RG}(a)S = S\rho_{\rm IR}^{-1}(\mathrm{RG}(\rho_{\rm UV}(a)))$.

12.2.2 The HT twist perspective

The Holomorphic Topological twist of a physical theory is defined by treating Q as a BRST charge. The result is a new QFT which is holomorphic in the z plane and topological in the two transverse directions. Essentially by definition, the Schur index counts local operators in the new theory.

The line defects we studied become topological line defects in the twisted theory. The twisted theory may have many other topological line defects, thought, which do not arise in this manner. Topological line defects in the HT theory, say placed at the origin of the $\mathbb{C}$ z plane, automatically form a category Lines with specific properties. Namely,

- The spaces of morphism $\mathrm{Hom}(L_1, L_2)$ coincide with the space of defect-changing local operators and have an action of $\mathbb{C}^*$ rotations of z and of flavor symmetries. Their graded character is $I_{L_1,L_2}(\mathfrak{q})$.

- Fusion of line defects equip Lines with a monoidal structure.

- Rotations of the topological plane equip Lines with the notion of left- and right-duals, leading to the categorical version of ρ. In particular,

$$\mathrm{Hom}(L_1, L_2) \simeq \mathrm{Hom}(1, \rho(L_1) \otimes L_2) \simeq \mathrm{Hom}(1, L_2 \otimes \rho^{-1}(L_1) \tag{12.2.13}$$

  are the categorical versions of the relation between indices and ρ.

The RG flow of line defects should map to a functor between corresponding categories $\mathrm{Lines}_{\mathrm{UV}}$ and $\mathrm{Lines}_{\mathrm{IR}}$, which we do not expect to preserve Hom's or ρ. Fixing this issue is an important open problem, see [355] for a recent proposal.

The HT twist of gauge theories is reasonably well understood, and so is the corresponding category Lines, see [360,361]. It would be interesting to study the categorical analogue of our RG flow to the pure gauge theory.

12.2.3 Vacua, central charges and walls of marginal stability.

A typical 4d $\mathcal{N} = 2$ SQFT T is endowed with an $SU(2)_R$ R-symmetry, as well as space of vacua $\mathcal{B}$ with the property that $SU(2)_R$ is not spontaneously broken. The vacua are parameterized by the expectation values of certain "Coulomb branch" BPS local operators and have a complex structure such that these expectation values are holomorphic. We refer to "u" as the collection of such expectation values.

For generic values of u, outside a co-dimension 1 discriminant locus $\mathcal{D}$, the low-energy effective description of T is expected to be a pure Abelian gauge theory. The lattice Γ is the lattice of charges for that effective theory. This is only defined locally on $\mathcal{B}_0 \equiv \mathcal{B}/\mathcal{D}$ and undergoes monodromies around the discriminant locus, which fix the sub-lattice of flavour charges Γ_f.

The low-energy effective action is built from a certain central charge function Z, a locally holomorphic function $\mathcal{B}_0 \times \Gamma \to \mathbb{C}$ linear in the second factor. We write it as $Z_\gamma(u)$ for a charge γ and vacuum u. The central charge restricted to Γ_f is u-independent and coincides with the "mass parameters" m of T. An important property of the central charge is that it maps $\mathcal{B}_0$ into a Lagrangian submanifold of $\mathbb{C}^{\mathrm{rk}(\Gamma_g)}$, i.e.

$$\langle dZ, dZ \rangle = 0 \tag{12.2.14}$$

where we used the fact that dZ vanishes on Γ_f and inverted the inner product on Γ_g.

The central charge function controls the BPS bound

$$M \geq |Z_\gamma| \tag{12.2.15}$$

on particles in the low-energy theory and insures that massive BPS particles can enter/exit the spectrum only at walls of marginal stability, where the phases of central charges of two particles align.

It also controls the BPS bound

$$E \geq -\mathrm{Re}\, e^{-i\vartheta} Z_\gamma \tag{12.2.16}$$

for BPS states in the presence of an half-BPS line defect, aka "framed BPS states", which insures that framed BPS states enter/exit the spectrum only at "$\mathcal{K}^{\vartheta}_{\gamma}$-walls" of framed marginal stability, where

$$\begin{aligned} &\mathrm{Im}\, e^{-i\vartheta} Z_\gamma = 0 \\ &\mathrm{Re}\, e^{-i\vartheta} Z_\gamma < 0\,. \end{aligned} \tag{12.2.17}$$

The phase ϑ controls which supersymmetries are preserved by the line defect and BPS states. We will set $\vartheta = 0$ unless otherwise specified, and refer to $\mathcal{K}_\gamma$-walls accordingly.

An important idea is that the jumps across $\mathcal{K}_\gamma$-walls in the spectrum of framed BPS states are controlled by the spectrum of BPS particles of charge multiple of γ via a framed wall-crossing formula. In turn, self-consistency of the framed wall-crossing formula implies a wall-crossing formula for the BPS particles themselves.

12.2.4 Framed degeneracies and the quantum torus algebra

As for the definition of T, the definition and classification of supersymmetric line defects in T is also a difficult problem. For our purposes, the only information we are interested in are the graded Witten indices $F(L)_\gamma$ of the space of framed BPS states of charge γ in the presence of the line defect L. The indices are graded by a combination of spin and $SU(2)_R$ charge, with fugacity $\mathfrak{q}$ and we collect them in the generating function

$$F(L) \equiv \sum_{\gamma\in\Gamma} F(L)_\gamma X_\gamma\,. \tag{12.2.18}$$

This generating function is expected to have a finite number of non-zero terms. As a Witten index, it is expected to be invariant under deformations unless we cross a wall of marginal stability.

It is convenient to take the X_γ formal variables to be generators of the quantum torus algebra. Then the product $F(L)F(L')$ counts the BPS states in the presence of both L and L', placed in a specific order along the axis fixed by the rotation generator used to grade the Witten index. With some work, it is possible to define the notion of fusion $L \circ L'$ of parallel BPS line defects, so that

$$F(L)F(L') = F(L\circ L') \tag{12.2.19}$$

The fusion operation is an UV notion independent of a choice of vacuum.

We can formalize this idea by defining an "algebra of line defects" A over $\mathbb{Z}[\mathfrak{q},\mathfrak{q}^{-1}]$ [5] which is a property of T only, such that $L \to F(L)$ is an algebra morphism $A \to Q_\Gamma$ for every choice of u and ϑ.

The definition of Witten indices Ω_γ which count BPS particles of charge γ is a bit more subtle due to the position zeromodes and their super-partners. In our story, they will exclusively enter through a multi-particle index

$$\mathcal{K}_\gamma \equiv \prod_{n=1}^{\infty}\prod_{s} E_{\mathfrak{q}}((-\mathfrak{q})^s X_{n\gamma})^{a_{n\gamma,s}} \tag{12.2.20}$$

[5] Really, the equivariant K-theory of a monoidal category.

where

$$\Omega_{n\gamma} = \sum_s a_{n\gamma,s}(-\mathfrak{q})^s \tag{12.2.21}$$

The framed wall-crossing formula is the statement that

$$F^+(L)\mathcal{K}_\gamma = \mathcal{K}_\gamma F^-(L) \tag{12.2.22}$$

where $F^\pm(L)$ are the framed BPS degeneracies on the two sides of a $\mathcal{K}_\gamma$ wall, with $\pm$ being the sign of $\mathrm{Im}\, Z_\gamma$.

Away from a wall of framed marginal stability, define Γ_+ as the cone of charges such that $\mathrm{Im}, Z_\gamma > 0$. Then the spectrum generator is defined as

$$S \equiv \prod_{\gamma\in\Gamma_+}^{\rightarrow} \mathcal{K}_\gamma \tag{12.2.23}$$

where the product is taken in order of $\arg Z_\gamma$, with larger phases to the left. This quantity is invariant across walls of marginal stability, away from walls of framed marginal stability.

12.3 Schur Quantization

The typical algebraic structure we encounter in Schur quantization (and in sphere quantization for 3d theories [362,363]) is a quadruple $(\mathcal{A}, \rho, \mathcal{H}, |1\rangle)$, where[6]

1. $\mathcal{A}$ is an algebra over the complex numbers.
2. ρ is an anti-linear automorphism of $\mathcal{A}$.
3. $\mathcal{H}$ is an Hilbert space equipped with a representation of $\mathcal{A}$ by unbounded operators such that $[a, b^\dagger] = 0$ for all $a, b \in \mathcal{A}$.[7]
4. $|1\rangle$ is a cyclic vector in the domain of $\mathcal{A}$ which satisfies a "spherical" condition:

$$|a\rangle \equiv a|1\rangle = \rho(a)^\dagger|1\rangle\,. \tag{12.3.1}$$

   Here $|a\rangle$ are normalizable states also in the domain of $\mathcal{A}$.

We will refer to this structure as a ρ-spherical unitary representation of $\mathcal{A}$.

Observe that the vectors of the form $|a\rangle$ give a dense common domain for the action of $\mathcal{A}$:

$$a\rho(c)^\dagger|b\rangle = ab\rho(c)^\dagger|1\rangle = |abc\rangle \tag{12.3.2}$$

Furthermore,

$$\mathrm{Tr}\; a \equiv \langle 1|a|1\rangle \tag{12.3.3}$$

[6] The condition (c) can be better stated in the language of $*$-algebras by defining a $*$-algebra double $\mathfrak{A} \equiv \mathcal{A} \otimes \mathcal{A}^{\mathrm{op}}$ with $*$-structure $(a \otimes b)^* = \rho(b) \otimes \rho^{-1}(a)$. Then $\mathcal{H}$ is an unitary representation of $\mathfrak{A}$. The condition (d) is that $(a \otimes 1)|1\rangle = (1 \otimes a)|1\rangle$.

[7] In principle we should distinguish elements a of $\mathcal{A}$ from the operators W_a which represent them. To lighten the notation, we will denote both with the same symbol.

is a ρ^2-twisted trace on $\mathcal{A}$:

$$\langle a|b\rangle = \mathrm{Tr}\ \rho(a)b = \mathrm{Tr}\ b\rho^{-1}(a)\,. \tag{12.3.4}$$

In several physical contexts, $\mathcal{A}$, ρ and Tr are given as protected quantities in some SQFT and are computable via localization. Then $\mathcal{H}$ can be abstractly recovered as the closure of $\mathcal{A}$ with respect to the inner product $\mathrm{Tr}\,\rho(a)b$.

Suppose now that we are given such a quadruple $(\mathcal{A}_{\mathrm{IR}}, \rho_{\mathrm{IR}}, \mathcal{H}_{\mathrm{IR}}, |1\rangle_{\mathrm{IR}})$ and an embedding

$$\mathrm{RG} : \mathcal{A}_{\mathrm{UV}} \to \mathcal{A}_{\mathrm{IR}} \tag{12.3.5}$$

of a second algebra $\mathcal{A}_{\mathrm{UV}}$ into $\mathcal{A}_{\mathrm{IR}}$, as well as a choice of ρ_{UV} which does *not* agree with ρ_{IR}, i.e.

$$\mathrm{RG} \neq \rho_{\mathrm{IR}}^{-1} \circ \mathrm{RG} \circ \rho_{\mathrm{UV}} \tag{12.3.6}$$

Then $\mathcal{A}_{\mathrm{UV}}$ acts on $\mathcal{H}$, but $|1\rangle_{\mathrm{IR}}$ is not spherical.

In order to define a spherical vector, we may seek a formal linear combination S of elements in $\mathcal{A}_{\mathrm{IR}}$ such that

$$\mathrm{RG}(a) \cdot S = S \cdot \rho_{\mathrm{IR}}^{-1}(\mathrm{RG}(\rho_{\mathrm{UV}}(a))) \tag{12.3.7}$$

If we can find such an element, then

$$S|1\rangle_{\mathrm{IR}} = |S\rangle_{\mathrm{IR}} \tag{12.3.8}$$

formally satisfies the spherical condition for the $\mathcal{A}_{\mathrm{UV}}$ action:

$$\mathrm{RG}(a)|S\rangle_{\mathrm{IR}} \equiv S\,\mathrm{RG}(\rho_{\mathrm{UV}}(a))^\dagger|1\rangle_{\mathrm{IR}} = \mathrm{RG}(\rho_{\mathrm{UV}}(a))^\dagger|S\rangle_{\mathrm{IR}} \tag{12.3.9}$$

If the $\mathrm{RG}(a)|S\rangle_{\mathrm{IR}}$ vectors are in addition normalizable and dense in $\mathcal{H}_{\mathrm{IR}}$, then we can define a quadruple $(\mathcal{A}_{\mathrm{UV}}, \rho_{\mathrm{UV}}, \mathcal{H}_{\mathrm{IR}}, |S\rangle_{\mathrm{IR}})$.

We will apply these constructions to the situation where $\mathcal{A}$ is the fusion algebra of supersymmetric loop operators in a four-dimensional $\mathcal{N} = 2$ SQFT. The relevant algebras are defined over $\mathbb{Z}[\mathfrak{q}, \mathfrak{q}^{-1}]$ and we represent them after specializing $\mathfrak{q}$ to be a real number in the interval $-1 < \mathfrak{q} < 1$.

A typical example of $\mathcal{A}_{\mathrm{IR}}$ is the quantum torus algebra $\mathcal{Q}_\Gamma$ associated to a lattice Γ equipped with an anti-symmetric unital integral pairing $\langle \bullet, \bullet \rangle$: it has linear generators X_γ with $\gamma \in \Gamma$ and relations

$$X_\gamma X_{\gamma'} = \mathfrak{q}^{\langle \gamma, \gamma' \rangle} X_{\gamma+\gamma'} \tag{12.3.10}$$

This algebra has an automorphism $\rho_{\mathcal{Q}}(X_\gamma) = X_{-\gamma}$ and a trace[8]

$$\mathrm{Tr}_Q\, X_\gamma = (\mathfrak{q}^2)_\infty^{\mathrm{rk}\,\Gamma} \delta_{\gamma,0}\,. \tag{12.3.11}$$

We can build a quadruple $(\mathcal{Q}_\Gamma, \rho_Q, \ell^2(\Gamma), |0\rangle)$ with an action

$$X_\gamma|\gamma'\rangle = \mathfrak{q}^{\langle \gamma, \gamma' \rangle}|\gamma + \gamma'\rangle\,. \tag{12.3.12}$$

[8]The overall normalization is chosen for future convenience.

Indeed,

$$X_\gamma^\dagger|\gamma'\rangle = \mathfrak{q}^{\langle\gamma,\gamma'\rangle}|-\gamma+\gamma'\rangle\,. \tag{12.3.13}$$

We denoted as $|\gamma\rangle$ a basis of $\ell^2(\Gamma)$, normalized as

$$\langle\gamma|\gamma'\rangle = (\mathfrak{q}^2)_\infty^{\mathrm{rk}\,\Gamma}\delta_{\gamma,\gamma'} \tag{12.3.14}$$

As discussed in the Introduction, there are well understood physical and mathematical constructions of algebra embeddings $\mathcal{A}\to\mathcal{Q}_\Gamma$

$$\mathrm{RG}(a) = F_a \tag{12.3.15}$$

and of a "quantum spectrum generator" S such that

$$F_a\cdot S = S\cdot\rho_Q(F_{\rho(a)})\,, \tag{12.3.16}$$

for a specific automorphism ρ. This is precisely the data required to identify a formal spherical vector $|1\rangle\equiv S|0\rangle$ in $\ell^2(\Gamma)$ as discussed above.

The conjectural IR formulae for Schur indices [89,90] claim that

- The inner products
$$I_{a,b} = \langle a|b\rangle \tag{12.3.17}$$
for $|a\rangle\equiv F_aS|0\rangle$ are convergent power series in $\mathfrak{q}$.
- $I_{a,b}$ computes specific protected quantities (Schur indices) in the underlying SQFT.

In particular, these conjectures imply that $|1\rangle\in\ell^2(\Gamma)$ is an actual spherical vector, but do not imply that it is cyclic.

There is an additional mathematical result whose physical meaning is somewhat unclear: the existence of a *tropical basis* for $\mathcal{A}$. This is a linear basis ℓ_γ of $\mathcal{A}$ in bijection with elements in Γ, such that

$$F_{\ell_\gamma} = X_\gamma + \sum_{\delta\in\Gamma_+}\Omega_{\ell_\gamma}^{\gamma+\delta}(\mathfrak{q})X_{\gamma+\delta}, \tag{12.3.18}$$

where Γ_+ is a positive cone in Γ and

$$S = 1+\sum_{\delta\in\Gamma_+}\Sigma_\delta(\mathfrak{q})X_\delta \tag{12.3.19}$$

with $\Sigma_\delta(\mathfrak{q})\in\mathbb{Z}[[\mathfrak{q}]]$.[9] We will denote interchangeably $\gamma'-\gamma\in\Gamma_+$ as $\gamma'\succ\gamma$. The latter notation generalizes better.

The vectors

$$|\ell_\gamma\rangle = |\gamma\rangle + \sum_{\delta\in\Gamma_+}\Omega_{\ell_\gamma}^{\gamma+\delta}(\mathfrak{q})|\gamma+\delta\rangle \tag{12.3.20}$$

[9] In actual examples, $\Sigma_\delta(\mathfrak{q})$ resum to rational functions of $\mathfrak{q}$ with poles at rational points on the unit circle only. Furthermore, $\mathfrak{q}\to\mathfrak{q}^{-1}$ maps S to S^{-1}. It would be nice to understand this structure in greater detail.

has a triangular form and span $\ell^2(\Gamma)$. We conclude that $(\mathcal{A}, \rho, \ell^2(\Gamma), S|0\rangle)$ is a quadruple in the above sense.

We typically have many distinct choices of physically-motivated RG maps, e.g. different cluster coordinate charts of a quantum cluster variety. As the $I_{a,b}$ should not depend on the choice of RG map, we learn that the corresponding representations of $\mathcal{A}$ must be unitarily equivalent, with matching spherical vectors. They must also agree with "Schur quantization", which defines $\mathcal{H}$ directly in terms of the abstract Schur indices $I_{a,b}$ [83].

12.3.1 On the domains of definition

One should note that the operators W_a implementing the a action on $\mathcal{H}$ are unbounded, in general. This means that they can be defined only on a dense subset of $\mathcal{H}$. This is a standard feature that needs to be treated with some care. We'd like to point that there is a canonical domain of definition, which can be regarded as an analog of the Schwarz space in our context. To this aim, let us introduce a family of semi-norms

$$\nu_a(\psi) := \big\| W_a|\psi\rangle \big\|_{\mathcal{H}}, \qquad a \in A. \tag{12.3.21}$$

Note that the vectors $|b\rangle = W_b|1\rangle$ in a spherical unitary representation have finite semi-norms ν_a, as we assumed that $\langle 1|W_a^\dagger W_a|1\rangle$ is finite in a spherical representation. We can therefore introduce the generalised Schwartz space $\mathcal{S}$ as the completion of the dense subspace spanned by the vectors $|b\rangle \in \mathcal{H}$ with respect to the topology defined by the family of semi-norms ν_a. The space $\mathcal{S}$ is, essentially by definition, a common domain for all W_a and $\widetilde{W}_a \equiv W^\dagger_{\rho(a)}$.

12.3.2 An extended tropical conjecture

A consequence of the intertwining relations (12.3.16) is that

$$F_{\rho(\ell_\gamma)} = X_{-\gamma} + \sum_{\delta \in \Gamma_+} \Omega^{-\gamma-\delta}_{\rho(\ell_\gamma)}(\mathfrak{q}) X_{-\gamma-\delta}, \tag{12.3.22}$$

gives a tropical basis with respect to the cone $-\Gamma_+$. In examples, we find that the two tropical bases coincide, so that $\rho(\ell_\gamma) = \ell_{\sigma(\gamma)}$ for some "tropical spectrum generator" map $\sigma : \Gamma \to \Gamma$. This relation allows one to read off ρ in situations where only the tropical basis is given.

Combining the two restrictions, we learn that

$$F_{\ell_\gamma} = X_\gamma + \left[\sum_{-\sigma^{-1}(\gamma) \succ \delta \succ \gamma} \Omega^{\delta}_{\ell_\gamma}(\mathfrak{q}) X_\delta \right] + X_{-\sigma^{-1}(\gamma)}, \tag{12.3.23}$$

is supported on a finite collection of charges bounded by γ and $-\sigma^{-1}(\gamma)$.

This support condition implies that such a "doubly-tropical" basis F_{ℓ_γ} is only ambiguous up to shifts by $F_{\ell_{\gamma'}}$ such that both γ' and $-\sigma^{-1}(\gamma')$ sit in the $\gamma + \Gamma_+ \cap -\sigma^{-1}(\gamma) - \Gamma_+$ intersection. We will encounter both examples of F_{ℓ_γ} where the definition is unambiguous

and ambiguous examples, such as situations where 0 belongs to the intersection and thus X_0 can be freely added.

A final experimental observation which we will discuss at length in later Sections is that there is a canonical and physically reasonable choice of a basis ℓ_i in $\mathcal{A}$ such that for all physical definitions of RG map F we can find a labelling $i(\gamma)$ such that $\ell_\gamma = \ell_{i(\gamma)}$ is a doubly-tropical basis. This observation strongly suggests the existence of a physical definition of the ℓ_i. It would be interesting to find it.

12.3.3 Restoring flavour

A slightly more general situation involves a lattice extension

$$0 \to \Gamma_f \to \Gamma \to \Gamma_g \to 0 \tag{12.3.24}$$

and the pairing $\langle \bullet, \bullet \rangle$ is defined on Γ_g and pulled back to Γ.

The quantum torus algebra Q_Γ now has central elements X_{γ_f} for $\gamma_f \in \Gamma_f$. The IR formulae for the Schur index employ an auxiliary vector space which we will denote as $\ell^2(\Gamma_g)$, with a small subtlety: the basis vectors $|\gamma\rangle$ are labelled by elements of Γ with identification

$$|\gamma + \gamma_f\rangle = \mu_{\gamma_f} |\gamma\rangle \tag{12.3.25}$$

where μ is an unitary character for Γ_f. The action of $\mathcal{Q}_\Gamma$ is as before and the inner products/Schur indices $I_{a,b}(\mathfrak{q}, \mu)$ are now functions of $\mathfrak{q}$ and μ.

The output of the construction is thus a family of ρ-spherical representations of $\mathcal{A}$ parameterized by the unitary character μ.

12.3.4 Partial RG flow

Another situation where our construction can be made explicit involves a chain of algebra morphisms

$$\mathcal{A}_{\rm UV} \to \mathcal{A}_{\rm IR} \to \mathcal{Q}_\Gamma \,. \tag{12.3.26}$$

We denote the image of $\mathcal{A}_{\rm UV}$ elements in $\mathcal{Q}_\Gamma$ as $F_a^{\rm UV}$ and the image of $\mathcal{A}_{\rm IR}$ elements as $F_a^{\rm IR}$, so that

$$F_a^{\rm UV} = F^{\rm IR}_{{\rm RG}(a)} \tag{12.3.27}$$

Suppose that we have quantum spectrum generators $S_{\rm UV}$ and $S_{\rm IR}$ such that

$$\begin{aligned} F_a^{\rm UV} \cdot S_{\rm UV} &= S_{\rm UV} \cdot \rho_Q(F^{\rm UV}_{\rho_{\rm UV}(a)}) \\ F_a^{\rm IR} \cdot S_{\rm IR} &= S_{\rm IR} \cdot \rho_Q(F^{\rm IR}_{\rho_{\rm IR}(a)}) \end{aligned} \tag{12.3.28}$$

which we combine into

$$F^{\rm IR}_{{\rm RG}(a)} \cdot S_{\rm UV} S_{\rm IR}^{-1} = S_{\rm UV} S_{\rm IR}^{-1} \cdot F^{\rm IR}_{\rho_{\rm IR}^{-1}({\rm RG}(\rho_{\rm UV}(a)))} \tag{12.3.29}$$

We can then find a candidate S for the $\mathcal{A}_{\rm UV} \to \mathcal{A}_{\rm IR}$ map by solving the equation

$$F_S^{\rm IR} = S_{\rm UV} S_{\rm IR}^{-1} \,, \tag{12.3.30}$$

Conversely, the relation

$$S_{\rm UV} = F_S^{\rm IR} S_{\rm IR} \tag{12.3.31}$$

can be sometimes used to compute the spectrum generator $S_{\rm UV}$ of a complicated system by first computing $S_{\rm IR}$ and $F^{\rm IR}$ for a simpler subsystem and then finding S.

This setup arises in specific physical situations we describe below. It leads to a generalization of the IR formulae for Schur indices and to a broad collection of interesting algebraic identities.

As discussed in the Introduction, RG and S inherit some tropical properties from this multi-step flow, where we define $\ell_\gamma^{\rm IR} \succ \ell_{\gamma'}^{\rm IR}$ if $\gamma \succ \gamma'$ and then abstract the tropical bases of $\mathcal{A}_{\rm UV}$ and $\mathcal{A}_{\rm IR}$ from the Γ labelling.

12.3.5 Cluster Structure

A general phenomenon frequently occurs: each $\mathcal{A} \to \mathcal{Q}_\Gamma$ "quantum chart" can undergo mutations μ_{γ_i} (and $\mu_{-\gamma_i}^{-1}$) for some specific finite collection of charges γ_i, which have the property that the condition $\gamma \succ \gamma'$ can be refined in all tropical formulae to $\gamma - \gamma'$ being a non-negative linear combination of the γ_i's.

The resulting quantum charts have the same property with new set of charges

$$\mu_i^t : \qquad \gamma_i \to -\gamma_i \qquad\qquad \gamma_j \to \gamma_j + \max(\langle \gamma_j, \gamma_i \rangle, 0)\gamma_i \tag{12.3.32}$$

Such situations have a close relationship to the theory of cluster algebras, cluster varieties and their quantization. The relation between Schur quantization and IR formulae for the Schur index for such theories can be encoded as a general strategy to quantize cluster varieties as complex phase spaces. We will see an importance instance of this in section when we discuss the Quantization of Teichmüller space in Section 12.10.

In a cluster algebra perspective, one focuses on the $x_i \equiv X_{\gamma_i(u)}$ generators and the integers $\langle \gamma_i(u), \gamma_j(u) \rangle$. Define

$$|i \to j| = \max(\langle \gamma_i, \gamma_j \rangle, 0) \tag{12.3.33}$$

which can be conveniently interpreted as the number of arrows in an auxiliary "BPS quiver" [332,364–371].

The actual embedding of the charges in an overall lattice Γ is forgotten. This allows one to disregard the difference between $\mu_{\gamma_i(u)}$ and $\mu_{-\gamma_i(u)}^{-1}$, which are unified into the notion of mutation of the BPS quiver:

1. Add arrows between nodes connected to the i-th node:

$$|j \to k| \to |j \to k| + |j \to i||i \to k| \,. \tag{12.3.34}$$

2. Remove pairs of edges with opposite orientation until $|j \to k||k \to j| = 0$.

3. Flip the edges connected to the i-th node: $|i \to j| \leftrightarrow |j \to i|$.

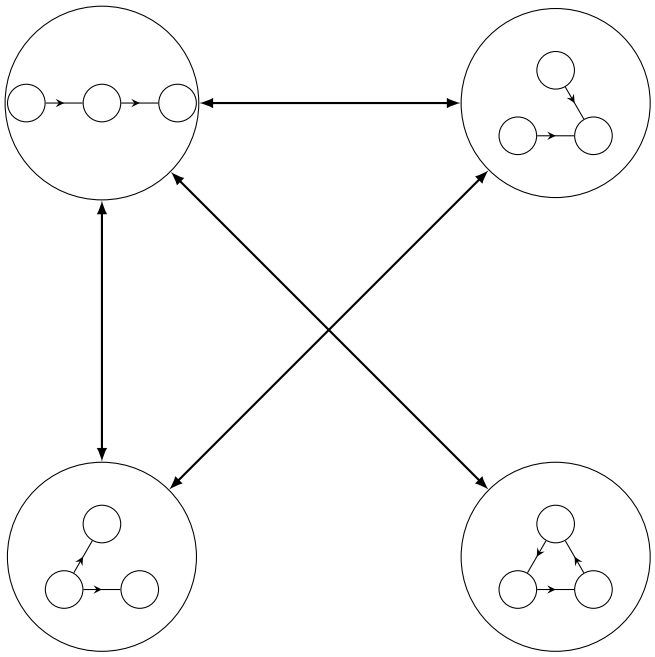


Figure 12.3: The mutation orbit of the A_3 BPS quiver. Figure from [355].

Some BPS quivers generate finite orbits under mutations, see e.g. Figure 12.3, but most have infinite orbits. Sometimes, the γ_i do not generate Γ and we need to keep track of some extra generators. These are usually denoted as "frozen" nodes. We will denote them as dashed in figures.

The spectrum generator and functions F_a are not included in the cluster data, but there are multiple strategies to recover them which we review in the next Section.

For now, we describe a simple strategy which requires a certain amount of guesswork [372]. One can simply restore the Γ lattice (as the span of the γ_i) and apply mutations (but not inverse mutations) while keeping track of the charges. If we can find a sequence of mutations $\mu_{\gamma(k)}$ after which $\gamma_i \to -\gamma_i$, then we can postulate

$$S = E_{\mathfrak{q}}(X_{\gamma(1)})E_{\mathfrak{q}}(X_{\gamma(2)})\cdots \tag{12.3.35}$$

so that the sequence of mutations transforms it into

$$S = E_{\mathfrak{q}}(X_{-\gamma(1)})E_{\mathfrak{q}}(X_{-\gamma(2)})\cdots . \tag{12.3.36}$$

We can then recover the F_a from S. This is facilitated by knowing the action of mutation on tropical labels. In particular, knowing both the "smallest" and the "largest" monomial in F_{ℓ_γ} leaves a finite collection of unknown coefficients in each.

Another important expected property is that the coefficients in F_{ℓ_γ} are positive integral linear combinations of $\mathfrak{q}$-integers

$$[n]_{\mathfrak{q}} = \mathfrak{q}^{n-1} + \mathfrak{q}^{n-3} + \cdots + \mathfrak{q}^{1-n} . \tag{12.3.37}$$

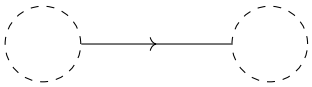


Figure 12.4: A BPS quiver diagram for a pure $U(1)$ gauge theory has no nodes, as the RG flow is trivial, $S = 1$ and there are no mutations available. We thus include frozen nodes (dashed) with generators $(1, 0)$ and $(0, 1)$.

In many physically relevant examples, the BPS quiver is available but it does not allow for a definition of S as a finite sequence of mutations. Nevertheless, it is believe that the data of the BPS quiver determines uniquely the whole structure of S and F's. We will come back to this in later Sections.

12.4 A minimal sequence of examples: rank 2 lattice

We now discuss a few examples based on the rank 2 lattice $\Gamma = \mathbb{Z}^2$, with inner product

$$\langle (a, b), (c, d) \rangle = ad - bc \tag{12.4.1}$$

12.4.1 The minimal quantum torus algebra

The first example is the quantum torus algebra $\mathcal{Q}_\Gamma$ itself, the algebra associated to pure $U(1)$ gauge theory. A minimal presentation has generators u, u^{-1}, v, v^{-1} and relation

$$uv = \mathfrak{q}^2 vu\,. \tag{12.4.2}$$

The

$$X_{a,b} \equiv \mathfrak{q}^{-ab} u^a v^b \tag{12.4.3}$$

linear basis makes manifest the $SL(2, \mathbb{Z})$ automorphisms inherited from Γ. Also, $\rho_Q(X_{a,b}) = X_{-a,-b}$.

A standard way to represent $\mathcal{Q}_\Gamma$ is to give v as a multiplication operator and u as a shift operator. E.g. we can act on $L^2(S^1) \otimes \ell^2(\mathbb{Z})$ by

$$\begin{aligned} v \cdot \psi_m(\zeta) &= \mathfrak{q}^{-m} \zeta \psi_m(\zeta) \\ u \cdot \psi_m(\zeta) &= \psi_{m-1}(\mathfrak{q}\zeta)\,. \end{aligned} \tag{12.4.4}$$

so that $[u, v^\dagger] = 0$, etc. This is the representation which naturally arises in localization calculations of Schur indices.

It is convenient to Fourier-transform along S^1 to recover the ρ_Q-spherical representation on $\ell^2(\mathbb{Z}^2)$. Introducing orthogonal basis elements $|a, b\rangle$ supported on (a, b) with norm $(\mathfrak{q}^2)^2_\infty$, we have

$$\begin{aligned} u|a, b\rangle &= \mathfrak{q}^b |a + 1, b\rangle \\ v|a, b\rangle &= \mathfrak{q}^{-a} |a, b + 1\rangle \end{aligned} \tag{12.4.5}$$

Essentially by definition,

$$|a, b\rangle = X_{a,b}|0, 0\rangle = X^\dagger_{-a,-b}|0, 0\rangle \tag{12.4.6}$$

and $|0, 0\rangle$ is the spherical vector.

The $\mathfrak{q}$-Weyl algebra

The next example is (one of the possible definition of) the $\mathfrak{q}$-deformed Weyl algebra $\mathcal{W}$, the algebra associated to the theory SQED_1, aka $T[U(1), T^*\mathbb{C}]$. It has generators $u_\pm$, v and v^{-1}, with

$$\begin{aligned} u_+ v &= \mathfrak{q}^2 v u_+ \\ u_- v &= \mathfrak{q}^{-2} v u_- \\ u_+ u_- &= 1 + \mathfrak{q} v \\ u_- u_+ &= 1 + \mathfrak{q}^{-1} v \end{aligned} \tag{12.4.7}$$

The analogy with the Weyl algebra arises from the relation

$$\mathfrak{q}^{-1} u_+ u_- - \mathfrak{q} u_- u_+ = \mathfrak{q}^{-1} - \mathfrak{q}\,. \tag{12.4.8}$$

The algebra has a linear basis consisting of

$$D_{a,b} \equiv \mathfrak{q}^{-ab} u_+^a v^b \qquad\qquad D_{-a,b} \equiv \mathfrak{q}^{ab} u_-^a v^b\,, \tag{12.4.9}$$

with $a \geq 0$, and Serre automorphism

$$\rho(D_{a,b}) = D_{-a,-a-b} \qquad\qquad \rho(D_{-a,b}) = D_{a,-b}\,, \tag{12.4.10}$$

with $a \geq 0$.

Localization calculations naturally lead to multiplication-and-shift representations on $L^2(S^1) \otimes \ell^2(\mathbb{Z})$. Either

$$\begin{aligned} v \cdot \psi_m(\zeta) &= \mathfrak{q}^{-m} \zeta \psi_m(\zeta) \\ u_+ \cdot \psi_m(\zeta) &= \psi_{m-1}(\mathfrak{q}\zeta)\,. \\ u_- \cdot \psi_m(\zeta) &= (1 + \mathfrak{q}^{-m-1}\zeta)\psi_{m+1}(\mathfrak{q}^{-1}\zeta)\,, \end{aligned} \tag{12.4.11}$$

or

$$\begin{aligned} v \cdot \psi_m(\zeta) &= \mathfrak{q}^{-m} \zeta \psi_m(\zeta) \\ u_+ \cdot \psi_m(\zeta) &= (1 + \mathfrak{q}^{-m+1}\zeta)\psi_{m-1}(\mathfrak{q}\zeta)\,. \\ u_- \cdot \psi_m(\zeta) &= \psi_{m+1}(\mathfrak{q}^{-1}\zeta)\,, \end{aligned} \tag{12.4.12}$$

These two representations are related by an unitary map

$$\psi_m(\zeta) \to \left[\prod_{k=0}^{\infty} \frac{1 + \mathfrak{q}^{2k+m+1}\zeta^{-1}}{1 + \mathfrak{q}^{2k+m+1}\zeta}\right] \zeta^{-m} \psi_m(\zeta)\,. \tag{12.4.13}$$

These representations have a spherical vector. In the first representation, it can be taken to be the wavefunction

$$\psi[1]_m(\zeta) \equiv \frac{(\mathfrak{q}^2)_\infty \delta_{m,0}}{\prod_{k=0}^{\infty}(1 + \mathfrak{q}^{2k+1}\zeta)}\,, \tag{12.4.14}$$

We can then compute

$$\begin{aligned}\psi[D_{a,b}]_m(\zeta) &= \frac{(\mathfrak{q}^2)_\infty \zeta^b \delta_{m,a}}{\prod_{k=0}^{\infty}(1+\mathfrak{q}^{2k+1+a}\zeta)} \\ \psi[D_{-a,b}]_m(\zeta) &= \frac{(\mathfrak{q}^2)_\infty \zeta^b \delta_{m,-a}}{\prod_{k=0}^{\infty}(1+\mathfrak{q}^{2k+1+a}\zeta)}\,,\end{aligned} \tag{12.4.15}$$

with $a \geq 0$. These are examples of vectors in $\mathcal{U}(\mathcal{W})$. In the second representation,

$$\psi[1]_m(\zeta) \equiv \frac{(\mathfrak{q}^2)_\infty \delta_{m,0}}{\prod_{k=0}^{\infty}(1+\mathfrak{q}^{2k+1}\zeta^{-1})}\,. \tag{12.4.16}$$

As mentioned, these representations are already essentially presented as special cases of the general formalism. In the first case, we write

$$F_v = X_{0,1} \qquad F_{u_+} = X_{1,0} \qquad F_{u_-} = X_{-1,0} + X_{-1,1} \tag{12.4.17}$$

and

$$S = E_{\mathfrak{q}}(X_{0,1}) \tag{12.4.18}$$

with the"bosonic" quantum dilogarithm defined as

$$E_{\mathfrak{q}}(x) \equiv (-\mathfrak{q}x;\mathfrak{q}^2)_\infty^{-1} = \frac{1}{\prod_{n=0}^{\infty}(1+\mathfrak{q}^{2n+1}x)} = \sum_{n\geq 0}\frac{(-\mathfrak{q})^n}{(\mathfrak{q}^2)_n}x^n \tag{12.4.19}$$

In the second we write

$$F_v = X_{0,1} \qquad F_{u_+} = X_{1,1} + X_{1,0} \qquad F_{u_-} = X_{-1,0} \tag{12.4.20}$$

and

$$S = E_{\mathfrak{q}}(X_{0,-1}) \tag{12.4.21}$$



Figure 12.5: In this example we have two possible RG flows, exchanged by mutations. A BPS quiver for the first RG flow (left) has a normal node for the mutable charge $\gamma_1 = (0,1)$ and a frozen node to keep track of the second generator $(1,0)$ in Γ. An mutation at γ_1 produces the second quiver, associated to the mutable charge $(0,-1)$. This is a way to derive S in this example.

The Pentagon algebra

We are ready for the third example, associated to the $[A_1, A_2]$ Argyres-Douglas theory. We will denote it as the Pentagon algebra $\mathbb{CP}$. This algebra has five generators, which we denote as L_i with $L_i = L_{i+5}$ to make a $\mathbb{Z}_5$ symmetry manifest:

$$\begin{aligned} L_{i+1}L_i &= \mathfrak{q}^2 L_i L_{i+1} \\ L_{i+1}L_{i-1} &= 1 + \mathfrak{q} L_i \\ L_{i-1}L_{i+1} &= 1 + \mathfrak{q}^{-1} L_i \end{aligned} \tag{12.4.22}$$

The full linear basis for $\mathbb{CP}$ is given by

$$D_{i;a,b} \equiv \mathfrak{q}^{ab} L_i^a L_{i+1}^b \tag{12.4.23}$$

with an obvious $\mathbb{Z}_5$ action. Finally, $\rho(L_i) = L_{i+2}$.

In this example, localization formulae for Schur indices are not available and we do not have a ready-made ρ-spherical representation for $\mathbb{CP}$. We can instead apply our formalism to the five known cluster parameterizations $\mathbb{CP} \to \mathcal{Q}_{\mathbb{Z}^2}$, intertwined by the $\mathbb{Z}_5$ action. Later on, we will recover this from a partial RG flow of the theory $T[SU(2), T^*\mathbb{C}^2]$. We have

$$\begin{aligned} F_{L_0} &= X_{1,0} \\ F_{L_1} &= X_{0,-1} \\ F_{L_2} &= X_{-1,-1} + X_{-1,0} \\ F_{L_3} &= X_{-1,0} + X_{-1,1} + X_{0,1} \\ F_{L_4} &= X_{0,1} + X_{1,1} \end{aligned} \tag{12.4.24}$$

We already ordered the monomials in a manner which anticipates the tropical labeling appropriate for this parameterization: $\gamma_1 = (1,0) \succ 0$ and $\gamma_2 = (0,1) \succ 0$. Note that in this example we do not need to specify a full choice of positive cone Γ_+: terms in a sum will always have charges which differ by a non-negative integral combination of "mutable" charges such as γ_1 and γ_2. This is a hallmark of systems with a cluster description.

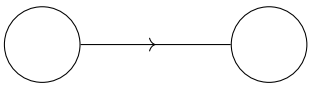


Figure 12.6: The BPS quiver diagram now has two standard nodes of charges $\gamma_1 = (1,0)$ and $\gamma_2 = (0,1)$. A mutation at the first node gives charges $(-1,0)$ and $(0,1)$, which can be mutated further at the second node to get $(-1,0)$ and $(0,-1)$. This is one way to compute S. If we start with a mutation at the second node we get $(1,1)$ and $(0,-1)$, then $(-1,-1)$ and $(1,0)$ and then $(0,-1)$ and $(-1,0)$, explaining the alternative form for S.

We read off the tropical labels:

$$\begin{aligned} L_0 &= \ell_{1,0} = \rho(\ell_{-1,0}) \\ L_1 &= \ell_{0,-1} = \rho(\ell_{0,1}) \\ L_2 &= \ell_{-1,-1} = \rho(\ell_{1,0}) \\ L_3 &= \ell_{-1,0} = \rho(\ell_{0,-1}) \\ L_4 &= \ell_{0,1} = \rho(\ell_{-1,-1}) \end{aligned} \tag{12.4.25}$$

It is not hard to verify that the $D_{i;a,b}$ form the tropical basis, decomposing $\mathbb{Z}^2$ into five conical sectors.

The spectrum generator takes a simple form:

$$S = E_{\mathfrak{q}}(X_{\gamma_1})E_{\mathfrak{q}}(X_{\gamma_2}) \tag{12.4.26}$$

Famously, the spectrum generator can also be written as

$$S = E_{\mathfrak{q}}(X_{\gamma_2})E_{\mathfrak{q}}(X_{\gamma_1+\gamma_2})E_{\mathfrak{q}}(X_{\gamma_1}) \tag{12.4.27}$$

thanks to the pentagon identity for quantum dilogarithms.

We can verify the intertwining relations $L_i S = S\rho_{\mathcal{Q}}(L_{i+2})$ step-by-step, using the basic properties of the quantum dilogarithm:

$$\begin{aligned} E_{\mathfrak{q}}(X_\gamma)X_{\gamma'} &= \sum_{k=0}^{\langle\gamma,\gamma'\rangle} \binom{\langle\gamma,\gamma'\rangle}{k}_{\mathfrak{q}} X_{\gamma'+k\gamma}E_{\mathfrak{q}}(X_\gamma) \qquad \langle\gamma,\gamma'\rangle \geq 0 \\ X_{\gamma'}E_{\mathfrak{q}}(X_\gamma) &= \sum_{k=0}^{\langle\gamma',\gamma\rangle} \binom{\langle\gamma',\gamma\rangle}{k}_{\mathfrak{q}} E_{\mathfrak{q}}(X_\gamma)X_{\gamma'+k\gamma} \qquad \langle\gamma,\gamma'\rangle \leq 0 \end{aligned} \tag{12.4.28}$$

We leave this as an exercise for the reader.

We are now in position to describe the ρ-spherical representation of $\mathbb{CP}$ on $\ell^2(\mathbb{Z}^2)$. The spherical vector is

$$|1\rangle \equiv S|0\rangle = (\mathfrak{q}^2)_\infty \sum_{n,m\geq 0} \frac{(-1)^{n+m}\mathfrak{q}^{n+m+nm}}{(\mathfrak{q}^2)_n(\mathfrak{q}^2)_m}|n,m\rangle \tag{12.4.29}$$

It has finite norm in the desired range $-1 < \mathfrak{q} < 1$:

$$I(\mathfrak{q}) \equiv \langle 1|1\rangle = (\mathfrak{q}^2)_\infty^2 \sum_{n,m\geq 0} \frac{\mathfrak{q}^{2n+2m+2nm}}{(\mathfrak{q}^2)_n^2(\mathfrak{q}^2)_m^2} \tag{12.4.30}$$

The same is true of the other states $D_{i;a,b}|1\rangle$, but we should stress that this statement is not immediately obvious. It is clearly true for

$$|D_{0;a,b}\rangle = (\mathfrak{q}^2)_\infty \sum_{n,m\geq 0} \frac{(-1)^{n+m}\mathfrak{q}^{n+m+nm}}{(\mathfrak{q}^2)_n(\mathfrak{q}^2)_m}\mathfrak{q}^{am+bn}|a+n,-b+m\rangle \tag{12.4.31}$$

but it would not be the case for a generic $X_{a,b}|1\rangle$ if $a > 0$ or $b < 0$.

Normalizability of all the $|a\rangle$ states can be reduced to finiteness of the expectation value

$$|\langle 1|a|1\rangle| < \infty \tag{12.4.32}$$

which is invariant under the action of ρ thanks to the intertwining property. Hence finiteness of $\langle 1|D_{0;a,b}\rangle$ is thus sufficient to prove finiteness of all inner products $\langle a|b\rangle$.

Notice that ρ also intertwines the five different choices of cluster map $\mathbb{CP} \to \mathcal{Q}_{\mathbb{Z}^2}$. We immediately learn that these give equivalent ρ-spherical unitary representations of $\mathbb{CP}$, matched by identifying the $|a\rangle$ vectors in each of them. The unitary equivalence can be reduced to the action of transformations of the form (12.4.13).

Each of the $D_{i;a,b}$ can be mapped to $D_{0;a,b}$ by some power of ρ and then diagonalized by a Fourier transform, with a spectrum of the form $e^{i\phi}\mathfrak{q}^k$ for integer k.

We are now ready to discuss our first example of multi-step RG flow: $\mathbb{CP} \to \mathcal{W} \to \mathcal{Q}_{\mathbb{Z}^2}$. We can identify

$$\begin{aligned} S_{\text{UV}} &= E_{\mathfrak{q}}(X_{\gamma_1})E_{\mathfrak{q}}(X_{\gamma_2}) \\ S_{\text{IR}} &= E_{\mathfrak{q}}(X_{\gamma_2}) \\ S &= E_{\mathfrak{q}}(u_+) \end{aligned} \tag{12.4.33}$$

Comparing the F's for the two theories gives the RG map:

$$\begin{aligned} \text{RG}(L_0) &= u_+ \\ \text{RG}(L_1) &= v^{-1} \\ \text{RG}(L_2) &= \mathfrak{q}v^{-1}u_- \\ \text{RG}(L_3) &= u_- + v \\ \text{RG}(L_4) &= v + \mathfrak{q}vu_+ \end{aligned} \tag{12.4.34}$$

We also get a tropical structure on $\mathcal{W}$ adapted to this: $v \succ 0$, $u_+ \succ 0$, $v \succ u_-$, etc. For every $D_{a,b}$ in $\mathcal{A}_{\text{IR}}$, we can find a $D_{i;c,d}$ such that $\text{RG}(D_{i;c,d}) = D_{a,b} + \cdots$ where the ellipsis is "larger" than $D_{a,b}$.

12.4.2 The last rank 2 example: $\mathfrak{su}(2)$ Seiberg-Witten theory

This example has a small subtlety: there really are two closely related theories, $T[SU(2), 0]$ and $T[SO(3), 0]$, and two corresponding algebras $\mathcal{A}_{SU(2)}$ and $\mathcal{A}_{SO(3)}$. These share a large sub-algebra and are themselves sub-algebras of a larger algebra $\mathcal{A}$ defined over $\mathbb{Z}[\mathfrak{q}^{\frac{1}{2}}, \mathfrak{q}^{-\frac{1}{2}}]$. We will employ $\mathcal{A}$ through the Section and restrict to the sub-algebras $\mathcal{A}_{SU(2)}$ and $\mathcal{A}_{SO(3)}$ only if strictly necessary, at the price of restricting $\mathfrak{q} > 0$.

A crucial role in the story is played by a special element of the quantum torus algebra, the Wilson line

$$F_{w_1} \equiv X_{0,-1} + X_{-1,1} + X_{0,1} \tag{12.4.35}$$

which is fixed by ρ. Together with

$$F_{H_0} \equiv X_{\frac{1}{2},0} \tag{12.4.36}$$

it generates the image of $\mathcal{A}$ in an extended quantum torus algebra $\mathcal{Q}_{\frac{1}{2}\mathbb{Z}\oplus\mathbb{Z}}$. In particular, one finds (the image of) a sequence of increasingly complicated operators H_i which satisfy

$$w_1 H_i = \mathfrak{q}^{\frac{1}{2}} H_{i-1} + \mathfrak{q}^{-\frac{1}{2}} H_{i+1} \qquad\qquad H_i w_1 = \mathfrak{q}^{-\frac{1}{2}} H_{i-1} + \mathfrak{q}^{\frac{1}{2}} H_{i+1} \tag{12.4.37}$$

and thus can be obtained from repeated $\mathfrak{q}^{\frac{1}{2}}$-commutators with w_1:

$$\begin{aligned}
\cdots &= \cdots \\
F_{H_{-3}} &= X_{\frac{1}{2},-3} + (\mathfrak{q}+\mathfrak{q}^{-1}) X_{-\frac{1}{2},-1} + X_{-\frac{3}{2},1} + X_{-\frac{1}{2},1} \\
F_{H_{-2}} &= X_{\frac{1}{2},-2} + X_{-\frac{1}{2},0} \\
F_{H_{-1}} &= X_{\frac{1}{2},-1} \\
F_{H_0} &= X_{\frac{1}{2},0} \\
F_{H_1} &= X_{-\frac{1}{2},1} + X_{\frac{1}{2},1} \\
F_{H_2} &= X_{-\frac{1}{2},0} + X_{-\frac{3}{2},2} + (\mathfrak{q}+\mathfrak{q}^{-1}) X_{-\frac{1}{2},2} + X_{\frac{1}{2},2} \\
\cdots &= \cdots
\end{aligned} \tag{12.4.38}$$

These are part of a tropical basis with $(1,0) \succ 0$ and $(-1,2) \succ 0$. The first monomial is the "smallest", giving the tropical charge. Looking at the "largest" monomials, we recognize $\rho(H_a) = H_{a-2}$. The transformation $H_a \to H_{a+1}$ generates a $\mathbb{Z}$ symmetry of the algebra.

The H_a themselves satisfy quadratic relationships:

$$\begin{aligned}
H_{i-1}H_i &= \mathfrak{q} H_i H_{i-1} \\
H_{i-1}H_{i+1} &= 1 + \mathfrak{q} H_i^2 \\
H_{i+1}H_{i-1} &= 1 + \mathfrak{q}^{-1} H_i^2 \\
H_{i-2}H_{i+1} &= \mathfrak{q}^{-\frac{1}{2}} w_1 + \mathfrak{q} H_{i-1} H_i \\
H_{i+1}H_{i-2} &= \mathfrak{q}^{\frac{1}{2}} w_1 + \mathfrak{q}^{-1} H_i H_{i-1}
\end{aligned} \tag{12.4.39}$$

etcetera. More generally, a linear basis for the whole algebra consists of w_a polynomials in w_1 defined by

$$w_1 w_a = w_{a+1} + w_{a-1} \tag{12.4.40}$$

together with

$$D_{i;a,b} \equiv \mathfrak{q}^{-\frac{ab}{2}} H_{i-1}^a H_i^b \tag{12.4.41}$$

It is not hard to verify that the tropical charges of these basis elements cover Γ exactly once.

The spectrum generator is known explicitly:

$$S = E_{\mathfrak{q}}(X_{1,0}) E_{\mathfrak{q}}(X_{-1,2}) \tag{12.4.42}$$

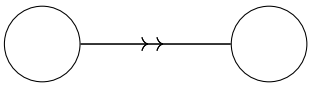


Figure 12.7: The BPS quiver diagram has two standard nodes of charges $\gamma_1 = (1,0)$ and $\gamma_2 = (-1,2)$, with two arrows between them. Either mutation flips the direction of the arrow, leading to an isomorphic quiver. A mutation at the first node followed by the second node flips the charges and explains the form of S in the text.

notice that the charges $\gamma_1 = (1,0)$ and $\gamma_2 = (-1,2)$ have pairing 2. These will be the mutable charges. It is easy to check that the intertwining relations hold for w_1 and H_0, and thus for all elements in the algebra.

The corresponding state in $\ell^2(\Gamma)$ becomes

$$|1\rangle = (\mathfrak{q}^2)_\infty \sum_{n,m\geq 0} \frac{(-1)^{n+m}\mathfrak{q}^{n+m+2nm}}{(\mathfrak{q}^2)_n(\mathfrak{q}^2)_m}|n,m\rangle \tag{12.4.43}$$

The Schur index is thus given by the convergent power series

$$I(\mathfrak{q}) = (\mathfrak{q}^2)_\infty^2 \sum_{n,m\geq 0} \frac{\mathfrak{q}^{2n+2m+4nm}}{(\mathfrak{q}^2)_n^2(\mathfrak{q}^2)_m^2} \tag{12.4.44}$$

which experimentally coincides with the UV gauge theory answer

$$I(\mathfrak{q}) = 1 + \mathfrak{q}^4 + \mathfrak{q}^{12} + \mathfrak{q}^{24} + \mathfrak{q}^{40} + \cdots = \sum_{k=0}^{\infty} \mathfrak{q}^{2k(k+1)} \tag{12.4.45}$$

Finiteness of $\langle 1|D_{i;a,b}|1\rangle$ is not immediately obvious, but finiteness of $\langle 1|D_{0;a,b}|1\rangle$ is. An argument based on ρ-invariance then buys finiteness of $\langle 1|D_{2i;a,b}|1\rangle$. Odd labels require a bit more brute-force work. Also, the presence of factors of $\mathfrak{q}^{\frac{1}{2}}$ when working with $\mathcal{A}$ means that we can only work in the $0 < \mathfrak{q} < 1$ range until we restrict to

- $\mathcal{A}_{\mathrm{SU}(2)}$ consisting of all w_a and $D_{i;2a,b}$, with tropical charges of the form (n,m) defining the integral lattice $\Gamma_{\mathrm{SU}(2)}$.
- $\mathcal{A}_{\mathrm{SO}(3)}$ consisting of w_{2a} and $D_{i;a,2b}$, with tropical charges of the form $(n/2, 2m)$ defining the integral lattice $\Gamma_{\mathrm{SO}(3)}$.

In any case, we obtain a ρ-spherical unitary representation of these algebras on $\ell^2(\Gamma_{\mathrm{SU}(2)})$ or $\ell^2(\Gamma_{\mathrm{SO}(3)})$ respectively.

Differently from the case of $\mathbb{CP}$, where all basis elements could be mapped to a monomial by one of the cluster maps and then diagonalized by a Fourier transform, the w_1 operator is special here and its spectrum is more interesting. We will now argue that the spectrum takes the form

$$\lambda + \lambda^{-1} \qquad\qquad \lambda = e^{i\phi}\mathfrak{q}^k\,. \tag{12.4.46}$$

for $SU(2)$ gauge theory. For $SO(3)$, w_2 has spectrum of the form

$$\lambda + 1 + \lambda^{-1} \qquad \lambda = e^{i\phi}\mathfrak{q}^k \,. \tag{12.4.47}$$

It is not difficult to find some formal eigenfunctions. Observe that

$$F[w_1] - \lambda - \lambda^{-1} = X_{-1,1} + X_{0,1}(1 - \lambda X_{0,-1})(1 - \lambda^{-1} X_{0,-1}) \,. \tag{12.4.48}$$

In the Fourier-transformed presentation with diagonalized $X_{1,0}$ we can write a test wave-function

$$\psi_m(\zeta;\lambda) = (-\zeta)^{m-1} \frac{(\mathfrak{q}^{2+m}\lambda^\dagger\zeta;\mathfrak{q}^2)_\infty(\mathfrak{q}^{2+m}(\lambda^\dagger)^{-1}\zeta;\mathfrak{q}^2)_\infty}{(\mathfrak{q}^m\lambda\zeta^{-1};\mathfrak{q}^2)_\infty(\mathfrak{q}^m\lambda^{-1}\zeta^{-1};\mathfrak{q}^2)_\infty} \tag{12.4.49}$$

Formally, this is annihilated by both $F[w_1] - \lambda - \lambda^{-1}$ and its Hermitean conjugate. We really have two such solution, one supported at integral m, the other at half-integral m. in the representation over $\mathbb{L}^2(\mathbb{Z} \times S^1)$ $F[w_1]$ acts as the difference operator

$$F[w_1]\, g_n(\zeta) = g_{n+1}(\mathfrak{q}\zeta) + g_{n-1}(\mathfrak{q}^{-1}\zeta) + \mathfrak{q}^{-n}\zeta g_n(\zeta) \,, \tag{12.4.50}$$

To prove that this distributional wave function solves the spectral problem we note that (12.4.50) coincides with the difference operator associated to the trace of the Lax Operator of (discrete) Quantum Liouville theory. In Appendix C.2, we exploit this connection to the Liouville spectral problem to provide a proof for the spectrum (12.4.46) and for the formal solution (12.4.49).

Strictly speaking, one should test the distributional eigenfunction ψ against the $|a\rangle$ vectors. This is in general challenging, but it follows from the basic test against the spherical vector:

$$\langle \psi(\mathfrak{q}^n e^{i\theta})|1\rangle = \cdots \delta_{n,0}(\mathfrak{q}^2 e^{2i\theta};\mathfrak{q}^2)_\infty(\mathfrak{q}^2 e^{-2i\theta};\mathfrak{q}^2)_\infty \,, \tag{12.4.51}$$

as the intertwining relations for the 't Hooft operators allow one to compute more general $\langle \psi(\mathfrak{q}^n e^{i\theta})|a\rangle$ inner products. Conversely one can express:

$$|1\rangle = \frac{1}{4\pi}\int_0^{2\pi} d\theta\, (\mathfrak{q}^2;\mathfrak{q}^2)_\infty(e^{2i\theta};\mathfrak{q}^2)_\infty(e^{-2i\theta};\mathfrak{q}^2)_\infty \psi_m(\zeta;e^{i\theta}) \,. \tag{12.4.52}$$

Covariance of the ψ kernel under mutations is a remarkable identity which can be reduced to the unitary pentagon identity. See [373] for a discussion and a geometric construction for many useful kernels associated to full or partial RG flows in class S theories labelled by $\mathfrak{sl}_2$. The reference defines 3d $\mathcal{N} = 2$ theories whose superconformal indices [374] give the desired kernels [334].[10]

[10] Ellipsoid partition functions [375] give kernels for Teichmüller quantization [376].

Weak coupling factorization

In later examples, we will need a remarkable alternative factorization of S:

$$E_{\mathfrak{q}}(X_{-1,2})E_{\mathfrak{q}}(X_{-1,4})\cdots E_{\mathfrak{q}}^{-1}(-\mathfrak{q}^{-1}X_{0,2})E_{\mathfrak{q}}^{-1}(-\mathfrak{q}X_{0,2})\cdots E_{\mathfrak{q}}(X_{1,4})E_{\mathfrak{q}}(X_{1,2})E_{\mathfrak{q}}(X_{1,0}) \tag{12.4.53}$$

which employs two semi-infinite sequences of quantum dilogs sandwiching an extra contribution

$$(X_{0,2};\mathfrak{q}^2)_\infty(\mathfrak{q}^2X_{0,2};\mathfrak{q}^2)_\infty \tag{12.4.54}$$

which is formally identical to (twice!) the integration measure in the UV definition of the Schur index. This pattern persists for other $SU(2)$ gauge theories. We will come back to this in later Sections.

This factorized expression for S is rather "dangerous", in the sense that it involves heavy concellations between terms with arbitrarily negative powers of $\mathfrak{q}$. The same factorization for S^{-1} is safer, as it only involve positive terms and no cancellations.

Some extra formulae

In later Sections, we will need to express charges as linear combinations of γ_1 and γ_2:

$$\begin{aligned}
\cdots &= \cdots \\
F_{H_{-3}} &= X_{-\gamma_1-\frac{3}{2}\gamma_2} + (\mathfrak{q}+\mathfrak{q}^{-1})X_{-\gamma_1-\frac{1}{2}\gamma_2} + X_{-\gamma_1+\frac{1}{2}\gamma_2} + X_{+\frac{1}{2}\gamma_2} \\
F_{H_{-2}} &= X_{-\frac{1}{2}\gamma_1-\gamma_2} + X_{-\frac{1}{2}\gamma_1} \\
F_{H_{-1}} &= X_{-\frac{1}{2}\gamma_2} \\
F_{H_0} &= X_{\frac{1}{2}\gamma_1} \\
F_{H_1} &= X_{\frac{1}{2}\gamma_2} + X_{\gamma_1+\frac{1}{2}\gamma_2} \\
F_{H_2} &= X_{-\frac{1}{2}\gamma_1} + X_{-\frac{1}{2}\gamma_1+\gamma_2} + (\mathfrak{q}+\mathfrak{q}^{-1})X_{\frac{1}{2}\gamma_1+\gamma_2} + X_{\frac{3}{2}\gamma_1+\gamma_2} \\
\cdots &= \cdots \\
F_{w_1} &= X_{-\frac{1}{2}\gamma_1-\frac{1}{2}\gamma_2} + X_{-\frac{1}{2}\gamma_1+\frac{1}{2}\gamma_2} + X_{\frac{1}{2}\gamma_1+\frac{1}{2}\gamma_2}
\end{aligned} \tag{12.4.55}$$

Notice that all terms in a given sum have charges which differ by integral multiples of γ_1 and γ_2. This is also the hallmark of a cluster RG map.

12.4.3 Fake examples

We should caution the reader that not all cluster seeds/BPS quivers are expected to occur in a physical context, and our general construction is thus not expected to apply to generic seeds.

For example, consider $S = E_{\mathfrak{q}}(\gamma_1)E_{\mathfrak{q}}(\gamma_2)$ with $\langle\gamma_1,\gamma_2\rangle = 3$. This can be analyzed in the same manner as our previous examples, generating a sequence of candidate F_{L_i} from mutations of $F_{L_0} = X_{\gamma_1/3}$. But we find experimentally that $F_{L_i}F_{L_j}|1\rangle$ is not normalizable for $|i-j|$ sufficiently large.

12.5 Adding Flavor: the $\mathcal{N} = 2^*$ $SU(2)$ example

We now consider a rich example based on a $\Gamma = \mathbb{Z}^3$ lattice, associated to $\mathcal{N} = 2^*$ $SU(2)$ gauge theory, aka $T[SU(2), T^*\mathbb{C}^3]$. The inner product on the lattice is

$$\langle (c_1, c_2, c_3), (d_1, d_2, d_3) \rangle = 2c_1d_2 + 2c_2d_3 + 2c_3d_1 - 2c_2d_1 - 2c_3d_2 - 2c_1d_3 \tag{12.5.1}$$

The element $\mu = X_{\frac{1}{2},\frac{1}{2},\frac{1}{2}}$ is central.

As for the pure $SU(2)$ case, it is convenient to enlarge the associated algebra at the pice of having half-integral powers of $\mathfrak{q}$ at intermediate steps. We now have three analogues of the Wilson line operator:

$$\begin{aligned} F_{D_{1,0}} &= X_{0,-\frac{1}{2},-\frac{1}{2}} + X_{0,-\frac{1}{2},\frac{1}{2}} + X_{0,\frac{1}{2},\frac{1}{2}} \\ F_{D_{0,1}} &= X_{-\frac{1}{2},0,-\frac{1}{2}} + X_{\frac{1}{2},0,-\frac{1}{2}} + X_{\frac{1}{2},0,\frac{1}{2}} \\ F_{D_{1,1}} &= X_{-\frac{1}{2},-\frac{1}{2},0} + X_{-\frac{1}{2},\frac{1}{2},0} + X_{\frac{1}{2},\frac{1}{2},0} \end{aligned} \tag{12.5.2}$$

Here the linear basis for the algebra $\mathcal{A}$ consists of $D_{a,b} = D_{-a,-b}$ with integer a and b, all invariant under ρ, with an overall $SL(2,\mathbb{Z})$ symmetry. It is a special case of Double-Affine Hecke Algebra.

The product of two operators $D_{p,q}$ and $D_{p',q'}$ is simple if $|pq' - p'q| = 1$:

$$D_{p,q}D_{p',q'} = \mathfrak{q}^{-\frac{1}{2}} D_{p+p',q+q'} + \mathfrak{q}^{\frac{1}{2}} D_{p-p',q-q'} \qquad\qquad pq' - p'q = 1\,, \tag{12.5.3}$$

but becomes more complicated as $pq' - p'q$ increases. Each of the $D_{p,q}$ with p and q coprime behaves as a fundamental Wilson line, i.e.

$$D_{p,q}D_{ap,aq} = D_{ap,aq}D_{p,q} = D_{(a+1)p,(a+1)q} + D_{(a-1)p,(a-1)q} \tag{12.5.4}$$

and $D_{ap,aq}$ from a sub-algebra isomorphic to the representation ring of $SU(2)$, which can be identified with Wilson lines in a specific Lagrangian description of the theory.

We can compute more F's from these relations. For example, from $F_{D_{1,0}}F_{D_{0,1}}$ we compute

$$F_{D_{1,-1}} = X_{-\frac{1}{2},-\frac{1}{2},-1} + X_{\frac{1}{2},-\frac{1}{2},-1} + (\mathfrak{q}^{-1} + \mathfrak{q})X_{\frac{1}{2},-\frac{1}{2},0} + X_{\frac{1}{2},-\frac{1}{2},1} + X_{\frac{1}{2},\frac{1}{2},1} \tag{12.5.5}$$

and cyclic rotations

$$F_{D_{1,2}} = X_{-1,-\frac{1}{2},-\frac{1}{2}} + X_{-1,\frac{1}{2},-\frac{1}{2}} + (\mathfrak{q}^{-1} + \mathfrak{q})X_{0,\frac{1}{2},-\frac{1}{2}} + X_{1,\frac{1}{2},-\frac{1}{2}} + X_{1,\frac{1}{2},\frac{1}{2}} \tag{12.5.6}$$

and

$$F_{D_{2,1}} = X_{-\frac{1}{2},-1,-\frac{1}{2}} + X_{-\frac{1}{2},-1,\frac{1}{2}} + (\mathfrak{q}^{-1} + \mathfrak{q})X_{-\frac{1}{2},0,\frac{1}{2}} + X_{-\frac{1}{2},1,\frac{1}{2}} + X_{\frac{1}{2},1,\frac{1}{2}} \tag{12.5.7}$$

We can recover $F_{D_{p,q}}$ in this manner.

The three mutations available in this chamber involve charges $\gamma_1 = (1,0,0)$, $\gamma_2 = (0,1,0)$ and $\gamma_3 = (0,0,1)$.

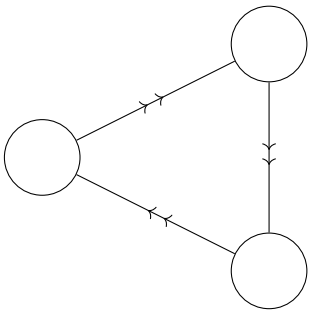


Figure 12.8: The BPS quiver in this example. Mutation at any node gives an isomorphic quiver. Note the pure $SU(2)$ sub-quiver, associated to the RG flow described below.

For example the mutation by $X_{0,0,1}$ gives new degeneracies:

$$\begin{aligned} F'_{D_{1,0}} &= X_{0,-\frac{1}{2},-\frac{1}{2}} + X_{0,\frac{1}{2},\frac{3}{2}} + X_{0,\frac{1}{2},\frac{1}{2}} \\ F'_{D_{0,1}} &= X_{-\frac{1}{2},0,\frac{1}{2}} + X_{-\frac{1}{2},0,-\frac{1}{2}} + X_{\frac{1}{2},0,-\frac{1}{2}} \\ F'_{D_{1,-1}} &= X_{-\frac{1}{2},-\frac{1}{2},-1} + X_{\frac{1}{2},-\frac{1}{2},-1} + X_{\frac{1}{2},\frac{1}{2},1} \end{aligned} \tag{12.5.8}$$

which can be related to the original F by a combination of an automorphism of $\mathcal{A}$ and a charge redefinition $(c_1, c_2, c_3) \to (c_2, c_1, 2c_2 - c_3)$, so that the next available set of mutations would involve charges $(1, 0, 0)$, $(0, 1, 2)$, $(0, 0, -1)$.

This is an example where the spectrum generator is not expected to be expressible as a sequence of mutations! Instead, a "weak coupling" infinite product is available in the literature. Observe that the intertwining relation with the F's only determines S up to a function of μ. This ambiguity can be fixed in two ways: we can compare it to the UV localization formulae for the Schur index or we can modify the theory to enlarge the algebra of loop operators without changing the BPS spectrum. We will explore all of these strategies in the following.

12.5.1 Intertwining recursion

First, we can explore the intertwining relations for the available F's. Starting from

$$S = \sum_{p=0}^{\infty} \sum_{q=0}^{\infty} \sum_{r=0}^{\infty} \Sigma_{p,q,r}(\mathfrak{q}) X_{p,q,r} \tag{12.5.9}$$

with $\Sigma_{0,0,0}(\mathfrak{q}) = 1$ and $\Sigma_{p,q,r}(\mathfrak{q}) = 0$ outside that summation range, we have

$$\Sigma_{p,q,r}(\mathfrak{q}) = \frac{\mathfrak{q}^{2p-r-q+1}}{\mathfrak{q}^{q-r} - \mathfrak{q}^{r-q}} (\Sigma_{p,q-1,r}(\mathfrak{q}) - \Sigma_{p,q,r-1}(\mathfrak{q})) + \Sigma_{p,q-1,r-1}(\mathfrak{q}) \tag{12.5.10}$$

and cyclic rotations. Curiously, the equation is symmetric in q and r. Also, if $q = r$ we should replace it with $\Sigma_{p,q-1,q}(\mathfrak{q}) = \Sigma_{p,q,q-1}(\mathfrak{q})$, which is also compatible with S_3 invariance. As expected, $\Sigma_{p,p,p}(\mathfrak{q})$ is not fixed by the equations.

We thus find

$$\begin{aligned}
\Sigma_{1,0,0}(\mathfrak{q}) &= \Sigma_{0,1,0}(\mathfrak{q}) = \Sigma_{0,0,1}(\mathfrak{q}) = -\frac{\mathfrak{q}}{1-\mathfrak{q}^2} \\
\Sigma_{1,1,0}(\mathfrak{q}) &= \Sigma_{0,1,1}(\mathfrak{q}) = \Sigma_{1,0,1}(\mathfrak{q}) = \frac{\mathfrak{q}^4}{(1-\mathfrak{q}^2)^2} \\
\Sigma_{2,0,0}(\mathfrak{q}) &= \Sigma_{0,2,0}(\mathfrak{q}) = \Sigma_{0,0,2}(\mathfrak{q}) = \frac{\mathfrak{q}^2}{(1-\mathfrak{q}^2)(1-\mathfrak{q}^4)} \\
\Sigma_{3,0,0}(\mathfrak{q}) &= \Sigma_{0,3,0}(\mathfrak{q}) = \Sigma_{0,0,3}(\mathfrak{q}) = -\frac{\mathfrak{q}^3}{(1-\mathfrak{q}^2)(1-\mathfrak{q}^4)(1-\mathfrak{q}^6)} \\
\Sigma_{2,1,0}(\mathfrak{q}) &= \cdots = -\frac{\mathfrak{q}^7}{(1-\mathfrak{q}^2)^2(1-\mathfrak{q}^4)} \\
\Sigma_{4,0,0}(\mathfrak{q}) &= \Sigma_{0,4,0}(\mathfrak{q}) = \Sigma_{0,0,4}(\mathfrak{q}) = -\frac{\mathfrak{q}^4}{(1-\mathfrak{q}^2)(1-\mathfrak{q}^4)(1-\mathfrak{q}^6)(1-\mathfrak{q}^8)} \\
\Sigma_{3,1,0}(\mathfrak{q}) &= \cdots = \frac{\mathfrak{q}^{10}}{(1-\mathfrak{q}^2)^2(1-\mathfrak{q}^4)(1-\mathfrak{q}^6)} \\
\Sigma_{2,2,0}(\mathfrak{q}) &= \cdots = \frac{\mathfrak{q}^{12}}{(1-\mathfrak{q}^2)^2(1-\mathfrak{q}^4)^2} \\
\Sigma_{2,1,1}(\mathfrak{q}) &= \cdots = -\frac{\mathfrak{q}}{1-\mathfrak{q}^2}\left(\Sigma_{1,1,1}(\mathfrak{q}) + \frac{\mathfrak{q}^7}{(1-\mathfrak{q}^2)^2(1-\mathfrak{q}^4)}\right) + \frac{\mathfrak{q}^4}{(1-\mathfrak{q}^2)^2}
\end{aligned} \tag{12.5.11}$$

As expected, $\Sigma_{p,p,p}(\mathfrak{q})$ are undetermined. We can potentially compare $||S\rangle|^2$ and the UV formula for the Schur index:

$$I(\mathfrak{q};\mu) = \oint \frac{d\zeta}{4\pi i\zeta} \frac{(\mathfrak{q}^2;\mathfrak{q}^2)_\infty^2 (\zeta^2;\mathfrak{q}^2)_\infty (\mathfrak{q}^2\zeta^2;\mathfrak{q}^2)_\infty (\zeta^{-2};\mathfrak{q}^2)_\infty (\mathfrak{q}^2\zeta^{-2};\mathfrak{q}^2)_\infty}{(\mathfrak{q}\mu;\mathfrak{q}^2)_\infty (\mathfrak{q}\mu^{-1};\mathfrak{q}^2)_\infty (\mathfrak{q}\mu\zeta^2;\mathfrak{q}^2)_\infty (\mathfrak{q}\mu^{-1}\zeta^2;\mathfrak{q}^2)_\infty (\mathfrak{q}\mu\zeta^{-2};\mathfrak{q}^2)_\infty (\mathfrak{q}\mu^{-1}\zeta^{-2};\mathfrak{q}^2)_\infty}, \tag{12.5.12}$$

to fix them recursively, by making some reasonable assumptions about the power of $\mathfrak{q}$. This is un-illuminating, so we will move to a more conceptual approach. We note a curious observation: a simple choice such as $\Sigma_{p,p,p} = 0$ for $p > 0$ leads to a candidate spherical vector which does not even appear to be normalizable. Finding the correct μ dependence is thus necessary in order to complete the quantization program.

12.5.2 Improved intertwining recursion

A physical way to address the problem is to weakly gauge the Cartan subgroup of the flavour symmetry group in the physical theory, resulting in an $U(1) \times SU(2)$ gauge theory with matter in $T^*\mathbb{C}^3$. Effectively, this enlarges the charge lattice to $\mathbb{Z}^4$ and makes the pairing non-degenerate, without changing the BPS spectrum of the theory and thus S itself.

A general feature of gauge theories is that the algebra of loop operators contains sub-algebras generated by the 't Hooft-Wilson operators charged under a single factor of the gauge group. Here that means the extended $\mathcal{A}$ will contain both the $SU(2)$ $\mathcal{N} = 2^*$

algebra and the algebra of SQED_3 (aka $T[U(1), T^*\mathbb{C}^3]$) as sub-algebras. Wilson lines charged under one factor of the gauge group commute with 't Hooft-Wilson lines in other factors, but 't Hooft lines for different factors do not typically commute.

We build a candidate IR charge lattice by adding an extra charge γ_m which pairs with one of the elementary ones. If we denote the charges which appear in mutations as

$$\begin{aligned}\gamma_1 &= (0;1,0,0)\\ \gamma_2 &= (0;0,1,0)\\ \gamma_3 &= (0;0,0,1)\end{aligned} \tag{12.5.13}$$

we can add an extra "frozen" charge

$$\gamma_m = (1;0,0,0) \tag{12.5.14}$$

with $\langle \gamma_m, \gamma_i \rangle = \delta_{i1}$. This definition naively breaks the $\mathbb{Z}_3$ symmetry of the problem, but that can be restored by a charge re-definition. We will see this choice is compatible with the identification of $D_{1,0}$ as the Wilson line for the $SU(2)$ gauge group.

We conjecture that $F_{u_+} = X_{1;0,0,0}$ is a valid (and tropical) choice of F, associated to an "Abelian 't Hooft loop" operator. It obviously behave well under the three possible mutations: two leave it unchanged and the third maps it to $X_{1;0,0,0} + X_{1;1,0,0}$. Rather than testing the behaviour under further mutations, we can look at the interplay with known F's:

$$\begin{aligned}F_{u_+} \cdot F_{D_{1,0}} &= X_{1;0,-\frac{1}{2},-\frac{1}{2}} + X_{1;0,-\frac{1}{2},\frac{1}{2}} + X_{1;0,\frac{1}{2},\frac{1}{2}} = F_{D_{1,0}} \cdot F_{u_+}\\ F_{u_+} \cdot F_{D_{0,1}} &= \mathfrak{q}^{-\frac{1}{2}} X_{1;-\frac{1}{2},0,-\frac{1}{2}} + \mathfrak{q}^{\frac{1}{2}} (X_{1;\frac{1}{2},0,-\frac{1}{2}} + X_{1;\frac{1}{2},0,\frac{1}{2}})\\ F_{u_+} \cdot F_{D_{1,1}} &= \mathfrak{q}^{-\frac{1}{2}} (X_{1;-\frac{1}{2},-\frac{1}{2},0} + X_{1;-\frac{1}{2},\frac{1}{2},0}) + \mathfrak{q}^{\frac{1}{2}} X_{1;\frac{1}{2},\frac{1}{2},0}\end{aligned} \tag{12.5.15}$$

The new F_{u_+} commutes with $F_{D_{1,0}}$. We identify the latter with the w_1 Wilson line of the $SU(2)$ gauge theory, which commutes with the $U(1)$ 't Hooft operators. The remaining summands on the last two lines provide new candidate F's for 't Hooft operators of mixed charges. It can be easily verified that they behave well under all three mutations, supporting our conjecture. Decomposing further products we can generate many more candidate F's and provide further support for our conjecture.

With some patience we could identify each of these F's with 't Hooft-Wilson operators $D_{m_1,e_1;m_2,e_2}$ for the extended theory. We leave this as an exercise for the enthusiastic reader.

Identifying F's with opposite tropical charge is a bit more challenging. We can try to build a candidate tropical F of the form

$$X_{-1;0,0,0} + \cdots \tag{12.5.16}$$

In order to survive all three mutations, it must include an extra term

$$X_{-1;0,0,0} + X_{-1;1,0,0} + \cdots \tag{12.5.17}$$

Good behavior under the $(0,0,1)$ mutation then requires some extra terms

$$X_{-1;0,0,0} + X_{-1;1,0,0} + (\mathfrak{q} + \mathfrak{q}^{-1})X_{-1;1,0,1} + X_{-1;1,0,2} + \cdots \tag{12.5.18}$$

The last term requires an extra correction to survive a $(0,1,0)$ mutation:

$$X_{-1;0,0,0} + X_{-1;1,0,0} + (\mathfrak{q} + \mathfrak{q}^{-1})X_{-1;1,0,1} + X_{-1;1,0,2} + (\mathfrak{q} + \mathfrak{q}^{-1})X_{-1;1,1,2} + X_{-1;1,2,2} + \cdots . \tag{12.5.19}$$

Then the $(1,0,0)$ mutation requires

$$\begin{aligned} X_{-1;0,0,0} + X_{-1;1,0,0} + (\mathfrak{q} + \mathfrak{q}^{-1})X_{-1;1,0,1} + X_{-1;1,0,2} + (\mathfrak{q} + \mathfrak{q}^{-1})X_{-1;1,1,2} + \\ + X_{-1;1,2,2} + X_{-1;2,2,2} . \end{aligned} \tag{12.5.20}$$

at which point we are fortunately done! We record the effect of the three mutations:

$$\begin{aligned} (1,0,0) : & X_{-1;0,0,0} + (\mathfrak{q} + \mathfrak{q}^{-1})X_{-1;1,0,1} + (\mathfrak{q} + \mathfrak{q}^{-1})X_{-1;2,0,1} + X_{-1;1,0,2} + \\ & + [3]_{\mathfrak{q}} X_{-1;2,0,2} + [3]_{\mathfrak{q}} X_{-1;3,0,2} + X_{-1;4,0,2} + (\mathfrak{q} + \mathfrak{q}^{-1})X_{-1;1,1,2} + \\ & + (\mathfrak{q} + \mathfrak{q}^{-1})X_{-1;2,1,2} + X_{-1;1,2,2} \\ (0,1,0) : & X_{-1;0,0,0} + X_{-1;1,0,0} + (\mathfrak{q} + \mathfrak{q}^{-1})X_{-1;1,1,0} + X_{-1;1,2,0} + \\ & + (\mathfrak{q} + \mathfrak{q}^{-1})X_{-1;1,0,1} + X_{-1;1,0,2} + X_{-1;2,2,2} \\ (0,0,1) : & X_{-1;0,0,0} + X_{-1;1,0,0} + (\mathfrak{q} + \mathfrak{q}^{-1})X_{-1;1,1,2} + \\ & + X_{-1;1,2,2} + (\mathfrak{q} + \mathfrak{q}^{-1})X_{-1;1,2,2} + X_{-1;1,2,3} + X_{-1;2,2,2} . \end{aligned} \tag{12.5.21}$$

As an extra test of our conjecture, note that

$$F_{u_+} \cdot (X_{-1;0,0,0} + X_{-1;1,0,0} + [2]_{\mathfrak{q}} X_{-1;1,0,1} + X_{-1;1,0,2} + [2]_{\mathfrak{q}} X_{-1;1,1,2} + X_{-1;1,2,2} + X_{-1;2,2,2}) \tag{12.5.22}$$

contains 1, μ^2 and

$$X_{0;1,0,0} + [2]_{\mathfrak{q}} X_{0;1,0,1} + X_{0;1,0,2} + [2]_{\mathfrak{q}} X_{0;1,1,2} + X_{0;1,2,2} = \mu F_{D_{2,0}-1} . \tag{12.5.23}$$

This candidate F is nice but not quite what we need: it behaves as the image of a negative charge 't Hooft loop in SQED_2 rather than SQED_3. Indeed, if we write $D_{1,0} = \zeta + \zeta^{-1}$, we find that the product with F_{u_+} factors as

$$(1 + \mathfrak{q}\mu\zeta)(1 + \mathfrak{q}\mu\zeta^{-1}) \tag{12.5.24}$$

Instead, we want the image of

$$u_+ u_- = (1 + \mathfrak{q}\mu\zeta)(1 + \mathfrak{q}\mu)(1 + \mu\zeta^{-1}) \tag{12.5.25}$$

as the $U(1)$ gauge fields couple to three hypermultiplets.

We can fix the problem by adding the $(1 + \mathfrak{q}\mu)$ factor by hand, setting

$$\begin{aligned} F_{u_-} = X_{-1;0,0,0} + X_{-1;1,0,0} + (\mathfrak{q} + \mathfrak{q}^{-1})X_{-1;1,0,1} + X_{-1;1,0,2} + X_{-1;1,1,1} + X_{-1;2,1,1} + \\ + (\mathfrak{q} + \mathfrak{q}^{-1})X_{-1;2,1,2} + (\mathfrak{q} + \mathfrak{q}^{-1})X_{-1;1,1,2} + X_{-1;1,2,2} + X_{-1;2,2,2} + \\ + (\mathfrak{q} + \mathfrak{q}^{-1})X_{-1;2,2,3} + X_{-1;2,3,3} + X_{-1;3,3,3} . \end{aligned} \tag{12.5.26}$$

We are now ready to impose an intertwining relation

$$\begin{aligned} X_{1;0,0,0}\cdot S = S\cdot(&X_{1;0,0,0}+X_{1;1,0,0}+(\mathfrak{q}+\mathfrak{q}^{-1})X_{1;1,1,0}+X_{1;1,1,1}+X_{1;2,1,1}+\\ &+(\mathfrak{q}+\mathfrak{q}^{-1})X_{1;2,2,1}+X_{1;1,2,0}+(\mathfrak{q}+\mathfrak{q}^{-1})X_{1;1,2,1}+X_{1;1,2,2}+\\ &+X_{1;2,2,2}+X_{1;2,3,1}+(\mathfrak{q}+\mathfrak{q}^{-1})X_{1;2,3,2}+X_{1;2,3,3}+X_{1;3,3,3})\,. \end{aligned} \tag{12.5.27}$$

This equation reproduces $\Sigma_{1,0,0}$ as well as $\Sigma_{1,1,0}$. It also fixes $\Sigma_{1,1,1}=\frac{2\mathfrak{q}^3-3\mathfrak{q}^5}{(1-\mathfrak{q}^2)^3}$. More importantly, the norm of the spherical vector now matches the Schur index of the theory.

If we had employed the naive F without the extra $(1+\mathfrak{q}\mu)$, the final answer for S would have missed an $E_{\mathfrak{q}}(\mu)$ factor and failed to reproduce the correct Schur index.

12.5.3 Partial RG flow

There is a natural RG flow relating this example to the pure $SU(2)$ example. We can identify

$$\mathrm{RG}(D_{1,0}) = w_1 \tag{12.5.28}$$

the Wilson lines in a natural way, as well as the action of the $(0,1,0)$ and $(0,0,1)$ mutations. Then we can identify

$$\begin{aligned} F^{\mathrm{IR}}(H_{-2}) &= X_{0,-\frac{1}{2},-1}+X_{0,-\frac{1}{2},0}\\ F^{\mathrm{IR}}(H_{-1}) &= X_{0,0,-\frac{1}{2}}\\ F^{\mathrm{IR}}(H_0) &= X_{0,\frac{1}{2},0}\\ F^{\mathrm{IR}}(H_1) &= X_{0,0,\frac{1}{2}}+X_{0,1,\frac{1}{2}} \end{aligned} \tag{12.5.29}$$

so that

$$\begin{aligned} \mathrm{RG}(D_{0,1}) &= \mu^{-\frac{1}{2}}H_0+\mu^{\frac{1}{2}}H_{-2}\\ \mathrm{RG}(D_{1,1}) &= \mu^{-\frac{1}{2}}H_1+\mu^{\frac{1}{2}}H_{-1} \end{aligned} \tag{12.5.30}$$

The spectrum generator for the partial RG flow will thus satisfy

$$\begin{aligned} w_1\cdot S &= S\cdot w_1\\ (\mu^{-\frac{1}{2}}H_0+\mu^{\frac{1}{2}}H_{-2})\cdot S &= S\cdot(\mu^{\frac{1}{2}}H_2+\mu^{-\frac{1}{2}}H_0)\\ (\mu^{-\frac{1}{2}}H_1+\mu^{\frac{1}{2}}H_{-1})\cdot S &= S\cdot(\mu^{\frac{1}{2}}H_3+\mu^{-\frac{1}{2}}H_1)\,. \end{aligned} \tag{12.5.31}$$

The first equation suggests that S should actually be built from w_1 and μ only. As $F^{\mathrm{IR}}(S)$ should contain $X_{1,0,0}$, S should contain $\ell_{1,0,0}=\mu w_2$, or more precisely,

$$S = 1-\frac{\mathfrak{q}}{1-\mathfrak{q}^2}w_2+\cdots \tag{12.5.32}$$

A "weak-coupling" expression for S_{UV} available in the literature (with a mild correction to include the flavour factor we computed above) is

$$E_{\mathfrak{q}}(X_{0,0,1})\cdots\left[E_{\mathfrak{q}}(X_{1,0,0})E_{\mathfrak{q}}(X_{1,1,1})E_{\mathfrak{q}}(X_{1,2,2})E_{\mathfrak{q}}^{-1}(-\mathfrak{q}^{-1}X_{0,1,1})E_{\mathfrak{q}}^{-1}(-\mathfrak{q}X_{0,1,1})\right]\cdots E_{\mathfrak{q}}(X_{0,1,0}) \tag{12.5.33}$$

It is not difficult to argue that acting with w_n on the left of the first semi-infinite sequence of operators is the same as inserting

$$\chi_n(X_{0,1,1}) \equiv X_{0,-\frac{n}{2},-\frac{n}{2}} + X_{0,1-\frac{n}{2},1-\frac{n}{2}} + \cdots X_{0,\frac{n}{2},\frac{n}{2}} \tag{12.5.34}$$

in the middle of the expression. Accordingly, if we decompose

$$E_{\mathfrak{q}}(\mu\zeta^{-1})E_{\mathfrak{q}}(\mu)E_{\mathfrak{q}}(\mu\zeta) = f_3(\mu, \chi_n(\zeta)) \tag{12.5.35}$$

we deduce that

$$S_{\rm UV} = \left[\sum_{m,n} c_{n,m}\mu^m F^{\rm IR}(w_n)\right] S_{\rm IR} \tag{12.5.36}$$

with $S_{\rm UV} = E_{\mathfrak{q}}(\gamma_2)E_{\mathfrak{q}}(\gamma_3)$, and in particular

$$S = f_3(\mu, w_n) \tag{12.5.37}$$

With some work, one can successfuly compare this solution to the recursive solution presented above.

A comparison with UV formulae for the Schur index is suprisingly simple, and can be recast as a direct derivation of $S_{\rm UV}$. We have

$$\langle 1; {\rm UV}|(F^{\rm UV}_{D_{1,0}})^n|1; {\rm UV}\rangle = \langle 1; {\rm IR}|(F^{\rm IR}_{w_1})^n \left[\sum_{m,n} c_{n,m}\mu^m F^{\rm IR}(w_n)\right]^2 |1; {\rm IR}\rangle \tag{12.5.38}$$

and thus it inserts the factor

$$E_{\mathfrak{q}}(\mu\zeta^{-1})E_{\mathfrak{q}}(\mu)E_{\mathfrak{q}}(\mu\zeta) \tag{12.5.39}$$

in the UV index contour integral formula, which precisely converts the pure $SU(2)$ calculation to $SU(2)$ $N = 2^*$.

12.6 The Spectrum Generator for RG flows triggered by large masses.

The example in the last Section suggests a broad generalization to any gauge theory $T[G, T^*N]$ with cotangent matter. The basic idea is that there is a natural RG flow $T[G, T^*N] \to T[G, 0]$ triggered by giving large masses to all of the matter fields.

We conjecture that this RG flow will send Wilson loops to Wilson loops for the same representation. As ρ acts on Wilson lines by conjugating the representation, the spectrum generator S for this flow should commute with Wilson loop operators. Accordingly, we also conjecture that S is a function of Wilson loop operators.

More precisely, consider the matter contribution to the UV formulae for Schur indices

$$\prod_{(w,w_f)\in T^*N} E_{\mathfrak{q}}(\mu^{w_f}\zeta^w) = \prod_{(w,w_f)\in N} E_{\mathfrak{q}}(\mu^{w_f}\zeta^w)E_{\mathfrak{q}}(\mu^{-w_f}\zeta^{-w}) \tag{12.6.1}$$

where w are the weights of the G Cartan torus action on T^*N and w_f are the weights of a flavor group action, say a $U(1)$ for each irreducible representation in N.

We can take the contribution of N and organize it into characters for G:

$$\prod_{(w,w_f)\in N} E_{\mathfrak{q}}(\mu^{w_f}\zeta^{w}) = f_N(\chi_R(\zeta),\mu) \tag{12.6.2}$$

We conjecture

$$S = f_N(w_R,\mu) \tag{12.6.3}$$

It is easy to see that such S reproduces the correct Schur index with Wilson loop insertions only:

$$\langle S|w_a|S\rangle = \langle 1|w_a \prod_{(w,w_f)\in N} E_{\mathfrak{q}}(\mu^{w_f}\zeta^{w})E_{\mathfrak{q}}(\mu^{-w_f}\zeta^{-w})|1\rangle \tag{12.6.4}$$

As Wilson loops contribute to the UV Schur index formulae by inserting characters in the contour integral, the product of $E_{\mathfrak{q}}$'s will simply reproduce the matter contribution to the UV index.

Ideally, we should also produce candidate RG flow images of 't Hooft-Wilson lines $D^N_{m,e}$ for the theory with matter, as linear combinations of the $D_{m',e'}$ loop operators of the pure gauge theory.

The $D^N_{m,e}$ loop operators are described in the UV by "Abelianized" formulae [377]. Essentially, one maps them to an extension of the algebra of loop operators for $T[H,T^*N]$, where H is the Cartan torus of G, which includes certain rational functions of Abelian Wilson generators v. A natural strategy is then to map the extended algebra for $T[H,T^*N]$ to the extended algebra for $T[H,0]$ by the RG flow map associated to the spectrum generator

$$\prod_{(w,w_f)\in N} E_{\mathfrak{q}}(\mu^{w_f}v^{w}) \tag{12.6.5}$$

We expect this map to descend to a map between $D_{m,e}$'s, compatible with our conjectural S.

If we have available any Coulomb RG flow for $T[G,0]$, with some spectrum generator $S_{\rm IR}$ and images $F^{\rm IR}_{w_R}$ for the Wilson loops, we can then predict a spectrum generator for $T[G,T^*N]$:

$$S_{\rm UV} = f_N(F^{IR}_{w_R},\mu)S_{\rm IR}\,. \tag{12.6.6}$$

with $F^{\rm UV}_{w_R} = F^{\rm IR}_{w_R}$ and appropriate images for more general $D_{m,e}$.

Furthermore, suppose that N is the direct sum of irreps N_i, associated to flavour parameters μ_i. Observe that the tropical labels of Wilson lines map the weight lattice of G into Γ. Then each factor of $f_{N_i}(\mu_i F^{IR}_{w_R})$ adds to the support of $S_{\rm UV}$ a collection of charges generated from the images of roots, which are already in $S_{\rm IR}$, and of the lowest weight w_i in N_i. This is also the tropical charge of w_{N_i}.

Accordingly, if we assume a cluster structure for both UV and IR theories, it appears that each N_i adds a new simple charge given by the image of w_i plus the flavour charge of μ_i. In the language of BPS quivers, each N_i adds a new node labelled by the tropical charge of w_N. This was clearly the case in the previous Section: γ_1 is the tropical charge

of w_2 in the IR theory. This principle has already been observed in the literature, with a focus on simple gauge groups [378–380].

We can broaden the conjecture further to a situation where we gauge the G flavour symmetry of any theory T, which may not be a gauge theory:

- Take the spectrum generator S_T as a function of the G flavour fugacities ζ.
- Expand it into characters $\chi_R(\zeta)$.
- Replace $\chi_R(\zeta)$ with Wilson loop operators w_R for a pure G gauge theory to obtain a candidate S.
- Define $S_{\rm UV} = F^{\rm IR}(S)S_{\rm IR}$ as before.

12.6.1 $SU(2)$ gauge theory with flavour

There are four more examples of well-defined gauge theories with gauge group $SU(2)$, coupled with a number N_f of fundamental hypermultiplets which goes from 1 to 4. In other words, $T[SU(2), T^*\mathbb{C}^{2N_f}]$.

The BPS quivers for these theories are known in an uniform manner: the pair of nodes from $SU(2)$, labeled by charges γ_1 and γ_2 with $\langle\gamma_1, \gamma_2\rangle = 2$, are augmented by N_f extra nodes γ_i, $i > 2$, such that $\langle\gamma_2, \gamma_i\rangle = \langle\gamma_i, \gamma_1\rangle = 1$ and all other pairings vanishing. As expected from the general conjecture, γ_i are precisely N_f copies of the tropical charge for w_1 in pure $SU(2)$ gauge theory.

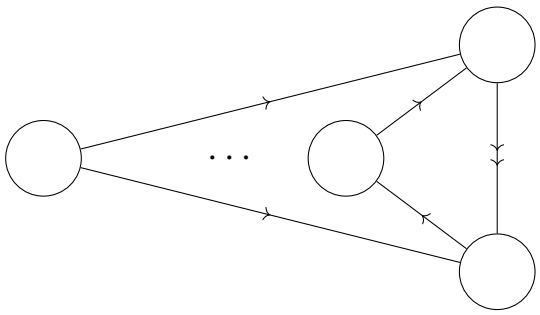


Figure 12.9: The BPS quiver for $SU(2)$ with N_f flavours. In a partial RG perspective, the rightmost nodes are inherited from pure $SU(2)$ gauge theory, with charges γ_1 and γ_2, and the collection of nodes on the left represent the N_f extra matter representations, with charges $\gamma_3, \cdots \gamma_{2+N_f}$.

These BPS quivers have loops, which makes a direct calculation of S complicated. For $N_f = 1, 2, 3$ there is a simple strategy to produce a candidate S: a sequence of mutations leads to quivers with no loops, for which S is known to be an ordered product of $E_{\mathfrak{q}}$ factors for each node of the quiver. We can then mutate back to the original BPS quiver and compare with our conjectural prescription for the quantum spectrum generator of gauge theories.

For $SU(2)$ $N_f = 4$ no such simplification is possible, but we can still compare our conjecture to known solutions for the spectrum generator and F's.

$N_f = 1$

A mutation at the γ_3 node gives a BPS quiver with nodes γ_1, $\gamma_2 + \gamma_3$ and $-\gamma_3$. The spectrum generator in this chamber is known to be

$$S' = E_{\mathfrak{q}}(X_{\gamma_1}) E_{\mathfrak{q}}(X_{-\gamma_3}) E_{\mathfrak{q}}(X_{\gamma_2+\gamma_3}) \tag{12.6.7}$$

The reader may observe the well-known RG flow to the $[A_1, A_2]$ theory, whose spectrum generator can e.g. be recognized in the last two factors.

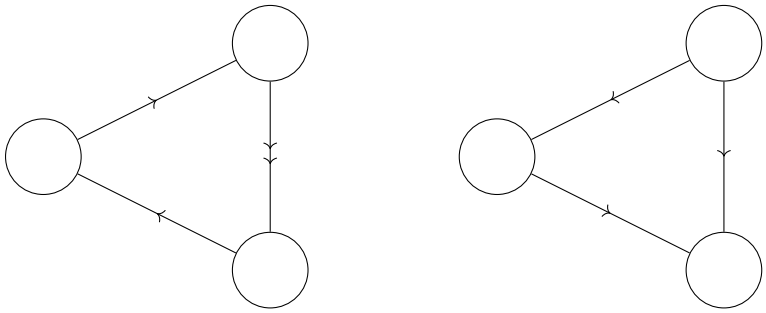


Figure 12.10: Left: the BPS quiver for the $N_f = 1$ theory computed from partial RG flow. Right: a mutation at the leftmost node (γ_3) gives a simpler quiver, with node labels γ_1, $-\gamma_3$, $\gamma_2 + \gamma_3$ used in the main text.

We can record some F's in this chamber:

$$\begin{aligned}
F'_{D_{1,2}} &= X_{\gamma_2+\gamma_3} + X_{\gamma_1+\gamma_2+\gamma_3} + X_{\gamma_2} + (\mathfrak{q} + \mathfrak{q}^{-1}) X_{\gamma_1+\gamma_2} + X_{2\gamma_1+\gamma_2} \\
F'_{D_{1,1}} &= X_{-\gamma_3} + X_{\gamma_1-\gamma_3} \\
F'_{D_{1,0}} &= X_{\gamma_1} \\
F'_{D_{1,-1}} &= X_{-\gamma_2-\gamma_3} \\
F'_{D_{1,-2}} &= X_{-\gamma_2} + X_{\gamma_3} \\
F'_{D_{1,-3}} &= X_{-\gamma_1-2\gamma_2-\gamma_3} + (\mathfrak{q} + \mathfrak{q}^{-1}) X_{-\gamma_1-\gamma_2} + X_{-\gamma_1-\gamma_2-\gamma_3} + X_{\gamma_3-\gamma_1} + X_{-\gamma_1} \\
F'_{D_{0,1}} &= X_{-\frac{1}{2}\gamma_1-\frac{1}{2}\gamma_2} + X_{-\frac{1}{2}\gamma_1+\frac{1}{2}\gamma_2+\gamma_3} + X_{-\frac{1}{2}\gamma_1+\frac{1}{2}\gamma_2} + X_{\frac{1}{2}\gamma_1+\frac{1}{2}\gamma_2}
\end{aligned} \tag{12.6.8}$$

Here we denoted as $D_{0,1}$ the Wilson line.

We can reorder the factors in S' to

$$S' = E_{\mathfrak{q}}(X_{\gamma_1}) E_{\mathfrak{q}}(X_{\gamma_2+\gamma_3}) E_{\mathfrak{q}}(X_{\gamma_2}) E_{\mathfrak{q}}(X_{-\gamma_3}) \tag{12.6.9}$$

and then (inverse) mutate to the desired spectrum generator:

$$S_{\rm UV} = E_{\mathfrak{q}}(X_{\gamma_3}) E_{\mathfrak{q}}(X_{\gamma_1}) E_{\mathfrak{q}}(X_{\gamma_2+\gamma_3}) E_{\mathfrak{q}}(X_{\gamma_2}) \tag{12.6.10}$$

A comparison with pure $SU(2)$ gauge theory is facilitated by a a further re-ordering:

$$S_{\rm UV} = E_{\mathfrak{q}}(X_{\gamma_3})E_{\mathfrak{q}}(X_{\gamma_2+\gamma_3})E_{\mathfrak{q}}(X_{\gamma_1+\gamma_2+\gamma_3})S_{\rm IR} \tag{12.6.11}$$

with the usual

$$S_{\rm IR} = E_{\mathfrak{q}}(X_{\gamma_1})E_{\mathfrak{q}}(X_{\gamma_2}) \tag{12.6.12}$$

Comparing with pure $SU(2)$ gauge theory, that can be written as

$$S_{\rm UV} = E_{\mathfrak{q}}(\mu X_{-\frac{1}{2}\gamma_1-\frac{1}{2}\gamma_2})E_{\mathfrak{q}}(\mu X_{-\frac{1}{2}\gamma_1+\frac{1}{2}\gamma_2})E_{\mathfrak{q}}(\mu X_{\frac{1}{2}\gamma_1+\frac{1}{2}\gamma_2})S_{\rm IR} \tag{12.6.13}$$

with $\mu = X_{\frac{1}{2}\gamma_1+\frac{1}{2}\gamma_2+\gamma_3}$.

The three arguments in the $E_{\mathfrak{q}}$ factors are the same as the summands in $\mu F^{\rm IR}_{w_1}$, as

$$F^{\rm IR}_{w_1} = X_{-\frac{1}{2}\gamma_1-\frac{1}{2}\gamma_2} + X_{-\frac{1}{2}\gamma_1+\frac{1}{2}\gamma_2} + X_{\frac{1}{2}\gamma_1+\frac{1}{2}\gamma_2} \tag{12.6.14}$$

Remarkably, it appears that the whole product can be written in terms of w_a's, and thus must satisfy:

$$E_{\mathfrak{q}}(\mu X_{-\frac{1}{2}\gamma_1-\frac{1}{2}\gamma_2})E_{\mathfrak{q}}(\mu X_{-\frac{1}{2}\gamma_1+\frac{1}{2}\gamma_2})E_{\mathfrak{q}}(\mu X_{\frac{1}{2}\gamma_1+\frac{1}{2}\gamma_2}) = f_2(\mu, w_a) \tag{12.6.15}$$

with

$$E_{\mathfrak{q}}(\mu\zeta^{-1})E_{\mathfrak{q}}(\mu\zeta) = f_2(\mu, \chi_a(\zeta))\,. \tag{12.6.16}$$

This verifies our conjecture about the spectrum generator of gauge theory.

We can record some F's in this chamber:

$$\begin{aligned}
F_{D_{1,2}} &= X_{\gamma_2} + (\mathfrak{q}+\mathfrak{q}^{-1})X_{\gamma_1+\gamma_2} + X_{2\gamma_1+\gamma_2} + X_{\gamma_1+\gamma_2+\gamma_3} + X_{2\gamma_1+\gamma_2+\gamma_3}\\
F_{D_{1,1}} &= X_{-\gamma_3} + X_{\gamma_1-\gamma_3} + X_{\gamma_1}\\
F_{D_{1,0}} &= X_{\gamma_1} + X_{\gamma_1+\gamma_3}\\
F_{D_{1,-1}} &= X_{-\gamma_2-\gamma_3} + X_{-\gamma_2}\\
F_{D_{1,-2}} &= X_{-\gamma_2} + X_{-\gamma_2+\gamma_3} + X_{\gamma_3}\\
F_{D_{1,-3}} &= X_{-\gamma_1-2\gamma_2-\gamma_3} + X_{-\gamma_1-2\gamma_2} + (\mathfrak{q}+\mathfrak{q}^{-1})X_{-\gamma_1-\gamma_2} + X_{-\gamma_1-\gamma_2-\gamma_3} + X_{-\gamma_1}\\
F_{D_{0,1}} &= X_{-\frac{1}{2}\gamma_1-\frac{1}{2}\gamma_2} + X_{-\frac{1}{2}\gamma_1+\frac{1}{2}\gamma_2} + X_{\frac{1}{2}\gamma_1+\frac{1}{2}\gamma_2}
\end{aligned} \tag{12.6.17}$$

and thus

$$\begin{aligned}
{\rm RG}(D_{1,2}) &= H_1^2 + \mathfrak{q}^{-\frac{1}{2}}\mu H_0 H_1\\
{\rm RG}(D_{1,1}) &= \mu^{-1}\mathfrak{q}^{-\frac{1}{2}}H_0 H_1 + H_0^2\\
{\rm RG}(D_{1,0}) &= H_0^2 + \mathfrak{q}^{-\frac{1}{2}}\mu H_{-1} H_0\\
{\rm RG}(D_{1,-1}) &= \mathfrak{q}^{-\frac{1}{2}}\mu^{-1}H_{-1}H_0 + H_{-1}^2\\
{\rm RG}(D_{1,-2}) &= H_{-1}^2 + \mathfrak{q}^{-\frac{1}{2}}\mu H_{-2}H_{-1}\\
{\rm RG}(D_{1,-3}) &= \mathfrak{q}^{-\frac{1}{2}}\mu^{-1}H_{-2}H_{-1} + H_{-2}^2\\
F_{D_{0,1}} &= w_1
\end{aligned} \tag{12.6.18}$$

The enthusiastic reader is invited to compare these relations with the Abelianized expressions, reviewed for example in [83]. For example, the right hand side of RG($D_{1,0}$) maps to

$$\begin{aligned}&(u_+ + u_-)^2 + \mu(u_+ v^{-1} + u_- v)(u_+ + u_-) = \\ &= (1 + \mathfrak{q}^{-1}\mu v^{-1})u_+^2 + \frac{\mathfrak{q} + \mathfrak{q}^{-1} + \mu(v + v^{-1})}{(\mathfrak{q}v - \mathfrak{q}^{-1}v^{-1})(\mathfrak{q}^{-1}v - \mathfrak{q}v^{-1})} + (1 + \mathfrak{q}^{-1}\mu v)u_-^2 \end{aligned} \quad (12.6.19)$$

This matches precisely the Abelianized expression (3.130) for $D_{1,0}$, after replacing $(1 + \mathfrak{q}^{-1}\mu v^{-1})u_+^2 \to u_+$ and $(1 + \mathfrak{q}^{-1}\mu v^{-1})u_+^2 \to u_-$, which up to naming conventions are the RG map one would encounter in the Abelian version $T[U(1), T^*\mathbb{C}^2]$ of the theory.

$N_f = 2$

A mutation of the canonical quiver at the γ_3 and γ_4 nodes gives a quiver with nodes γ_1, $\gamma_2 + \gamma_3 + \gamma_4$, $-\gamma_3$ and $-\gamma_4$. The spectrum generator in this chamber is known to be

$$S' = E_{\mathfrak{q}}(X_{\gamma_1})E_{\mathfrak{q}}(X_{-\gamma_3})E_{\mathfrak{q}}(X_{-\gamma_4})E_{\mathfrak{q}}(X_{\gamma_2+\gamma_3+\gamma_4}) \quad (12.6.20)$$

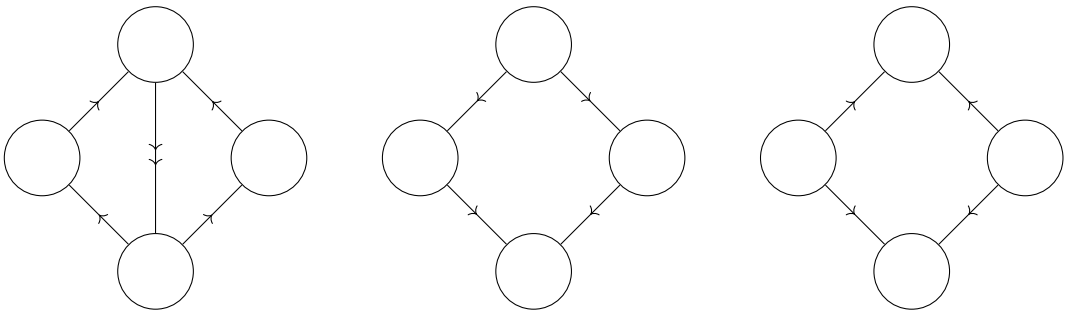


Figure 12.11: BPS quivers for $N_f = 2$. Left: The quiver associated to the partial RG flow to pure gauge theory. A mutation at the side nodes γ_3 and γ_4 gives the middle quiver, which admits a total order and allows for an immediate computation of the spectrum generator S'. A mutation at the top node γ_1 leads to the quiver on the right, which is particularly symmetric

We reorder the factors to

$$S' = E_{\mathfrak{q}}(X_{\gamma_1})E_{\mathfrak{q}}(X_{\gamma_2+\gamma_3+\gamma_4})E_{\mathfrak{q}}(X_{\gamma_2+\gamma_4})E_{\mathfrak{q}}(X_{\gamma_2+\gamma_3})E_{\mathfrak{q}}(X_{\gamma_2})E_{\mathfrak{q}}(X_{-\gamma_3})E_{\mathfrak{q}}(X_{-\gamma_4}) \quad (12.6.21)$$

and mutate back to

$$S_{\rm UV} = E_{\mathfrak{q}}(X_{\gamma_3})E_{\mathfrak{q}}(X_{\gamma_4})E_{\mathfrak{q}}(X_{\gamma_1})E_{\mathfrak{q}}(X_{\gamma_2+\gamma_3+\gamma_4})E_{\mathfrak{q}}(X_{\gamma_2+\gamma_4})E_{\mathfrak{q}}(X_{\gamma_2+\gamma_3})E_{\mathfrak{q}}(X_{\gamma_2}) \quad (12.6.22)$$

We can reorganize that to an RG flow form:

$$S_{\rm UV} = E_{\mathfrak{q}}(X_{\gamma_4})E_{\mathfrak{q}}(X_{\gamma_2+\gamma_4})E_{\mathfrak{q}}(X_{\gamma_1+\gamma_2+\gamma_4})E_{\mathfrak{q}}(X_{\gamma_3})E_{\mathfrak{q}}(X_{\gamma_2+\gamma_3})E_{\mathfrak{q}}(X_{\gamma_1+\gamma_2+\gamma_3})S_{\rm IR} \quad (12.6.23)$$

We recognize the factors in front as $f_2(\mu_1, w_a) f_2(\mu_2, w_a)$ with $\mu_1 = X_{\frac{1}{2}\gamma_1+\frac{1}{2}\gamma_2+\gamma_3}$ and $\mu_2 = X_{\frac{1}{2}\gamma_1+\frac{1}{2}\gamma_2+\gamma_4}$, as expected.

For future use, it is also useful to mutate the original expression at γ_1 to

$$S'' = E_{\mathfrak{q}}(X_{-\gamma_3}) E_{\mathfrak{q}}(X_{-\gamma_4}) E_{\mathfrak{q}}(X_{\gamma_2+\gamma_3+\gamma_4}) E_{\mathfrak{q}}(X_{-\gamma_1}) \tag{12.6.24}$$

This form of the spectrum generator makes manifest the full $\mathrm{Spin}(4) = SU(2) \times SU(2)$ symmetry of the system, which is hidden in the other chambers. Indeed, we can write the charges as

$$\begin{aligned} S'' = {} & E_{\mathfrak{q}}(\mu_+^{-1} X_{-\frac{1}{2}\gamma_3-\frac{1}{2}\gamma_4}) E_{\mathfrak{q}}(\mu_+ X_{-\frac{1}{2}\gamma_3-\frac{1}{2}\gamma_4}) \cdot \\ & \cdot E_{\mathfrak{q}}(\mu_- X_{-\frac{1}{2}\gamma_1+\frac{1}{2}\gamma_2+\frac{1}{2}\gamma_3+\frac{1}{2}\gamma_4}) E_{\mathfrak{q}}(\mu_-^{-1} X_{-\frac{1}{2}\gamma_1+\frac{1}{2}\gamma_2+\frac{1}{2}\gamma_3+\frac{1}{2}\gamma_4}) \end{aligned} \tag{12.6.25}$$

with $\mu_+ = X_{\frac{1}{2}\gamma_3-\frac{1}{2}\gamma_4}$ and $\mu_- = X_{\frac{1}{2}\gamma_1+\frac{1}{2}\gamma_2+\frac{1}{2}\gamma_3+\frac{1}{2}\gamma_4}$ being the flavor parameters for the two $SU(2)$ global symmetries.

We can transport the Wilson line image predicted by our conjecture

$$F^{\mathrm{UV}}_{D_{0,1}} = X_{-\frac{1}{2}\gamma_1-\frac{1}{2}\gamma_2} + X_{-\frac{1}{2}\gamma_1+\frac{1}{2}\gamma_2} + X_{\frac{1}{2}\gamma_1+\frac{1}{2}\gamma_2} \tag{12.6.26}$$

to

$$F'_{D_{0,1}} = X_{-\frac{1}{2}\gamma_1-\frac{1}{2}\gamma_2} + X_{-\frac{1}{2}\gamma_1+\frac{1}{2}\gamma_2} + X_{-\frac{1}{2}\gamma_1+\frac{1}{2}\gamma_2+\gamma_3} + X_{-\frac{1}{2}\gamma_1+\frac{1}{2}\gamma_2+\gamma_4} + X_{-\frac{1}{2}\gamma_1+\frac{1}{2}\gamma_2+\gamma_3+\gamma_4} + X_{\frac{1}{2}\gamma_1+\frac{1}{2}\gamma_2} \tag{12.6.27}$$

and then to

$$\begin{aligned} F''_{D_{0,1}} = {} & X_{\frac{1}{2}\gamma_1-\frac{1}{2}\gamma_2} + (X_{\frac{1}{2}\gamma_1+\frac{1}{2}\gamma_2+\gamma_3+\gamma_4} + X_{-\frac{1}{2}\gamma_1-\frac{1}{2}\gamma_2}) + X_{-\frac{1}{2}\gamma_1+\frac{1}{2}\gamma_2+\gamma_3+\gamma_4} + \\ & + (X_{-\frac{1}{2}\gamma_1+\frac{1}{2}\gamma_2+\gamma_3} + X_{-\frac{1}{2}\gamma_1+\frac{1}{2}\gamma_2+\gamma_4}) + X_{-\frac{1}{2}\gamma_1+\frac{1}{2}\gamma_2} \end{aligned} \tag{12.6.28}$$

Here we grouped terms which form doublets for the two $SU(2)$ global symmetries.

A simple guess for $\mathrm{RG}(D_{1,0})$ based on the UV formulae and the $N_f = 1$ example is

$$\mathrm{RG}(D_{1,0}) = H_0^2 + \mathfrak{q}^{-\frac{1}{2}}(\mu_1 + \mu_2) H_{-1} H_0 + \mathfrak{q}^{-1} \mu_1 \mu_2 H_{-2} H_0 \,, \tag{12.6.29}$$

though the definition of $D_{1,0}$, even in the UV, could be corrected by subtracting a multiple of 1 as was done in [83]. This would replace $\mathfrak{q}^{-1} H_{-2} H_0 \to H_{-1}^2$.

This gives

$$F^{\mathrm{UV}}_{D_{1,0}} = X_{\gamma_1} + X_{\gamma_1+\gamma_3} + X_{\gamma_1+\gamma_4} + X_{\gamma_1+\gamma_3+\gamma_4} \,, \tag{12.6.30}$$

which mutates to a very simple

$$F''_{D_{1,0}} = X_{\gamma_1} \,, \tag{12.6.31}$$

Another simple monomial F is

$$F''_{D_{1,-1}} = X_{\frac{1}{2}\gamma_1+\frac{1}{2}\gamma_2} \,, \tag{12.6.32}$$

i.e.

$$F^{\mathrm{UV}}_{D_{1,-1}} = X_{\frac{1}{2}\gamma_1+\frac{1}{2}\gamma_2} + X_{\frac{3}{2}\gamma_1+\frac{1}{2}\gamma_2} + X_{\frac{3}{2}\gamma_1+\frac{1}{2}\gamma_2+\gamma_3} + X_{\frac{3}{2}\gamma_1+\frac{1}{2}\gamma_2+\gamma_4} + X_{\frac{3}{2}\gamma_1+\frac{1}{2}\gamma_2+\gamma_3+\gamma_4} \,, \tag{12.6.33}$$

i.e.

$$\mathrm{RG}(D_{1,-1}) = H_0 H_1 + (\mu_1 + \mu_2) H_0^2 + \mu_1 \mu_2 H_0 H_{-1} \,. \tag{12.6.34}$$

$N_f = 3$

For brevity, we can start from the desired expression

$$S_{\rm UV} = f_2(\mu_1, w_a) f_2(\mu_2, w_a) f_2(\mu_3, w_a) S_{\rm IR} \tag{12.6.35}$$

together with

$$F_{w_1} = X_{-\frac{1}{2}\gamma_1 - \frac{1}{2}\gamma_2} + X_{-\frac{1}{2}\gamma_1 + \frac{1}{2}\gamma_2} + X_{\frac{1}{2}\gamma_1 + \frac{1}{2}\gamma_2} \tag{12.6.36}$$

and borrow some manipulations from the previous example,

$$\begin{aligned} S_{\rm UV} = {} & E_{\mathfrak{q}}(X_{\gamma_5}) E_{\mathfrak{q}}(X_{\gamma_4}) E_{\mathfrak{q}}(X_{\gamma_3}) E_{\mathfrak{q}}(X_{\gamma_2+\gamma_3+\gamma_4+\gamma_5}) E_{\mathfrak{q}}(X_{\gamma_1}) E_{\mathfrak{q}}(X_{\gamma_2+\gamma_4+\gamma_5}) E_{\mathfrak{q}}(X_{\gamma_2+\gamma_3+\gamma_5}) \cdot \\ & \cdot E_{\mathfrak{q}}(X_{\gamma_2+\gamma_5}) E_{\mathfrak{q}}(X_{\gamma_2+\gamma_3+\gamma_4}) E_{\mathfrak{q}}(X_{\gamma_2+\gamma_4}) E_{\mathfrak{q}}(X_{\gamma_2+\gamma_3}) E_{\mathfrak{q}}(X_{\gamma_2}) \end{aligned} \tag{12.6.37}$$

then mutate at the three nodes

$$\begin{aligned} S' = {} & E_{\mathfrak{q}}(X_{\gamma_2+\gamma_3+\gamma_4+\gamma_5}) E_{\mathfrak{q}}(X_{\gamma_1}) E_{\mathfrak{q}}(X_{\gamma_2+\gamma_4+\gamma_5}) E_{\mathfrak{q}}(X_{\gamma_2+\gamma_3+\gamma_5}) E_{\mathfrak{q}}(X_{\gamma_2+\gamma_5}) E_{\mathfrak{q}}(X_{\gamma_2+\gamma_3+\gamma_4}) \cdot \\ & \cdot E_{\mathfrak{q}}(X_{\gamma_2+\gamma_4}) E_{\mathfrak{q}}(X_{\gamma_2+\gamma_3}) E_{\mathfrak{q}}(X_{\gamma_2}) E_{\mathfrak{q}}(X_{-\gamma_3}) E_{\mathfrak{q}}(X_{-\gamma_5}) E_{\mathfrak{q}}(X_{-\gamma_4}) \end{aligned} \tag{12.6.38}$$

with

$$\begin{aligned} F'_{w_1} = {} & X_{-\frac{1}{2}\gamma_1 - \frac{1}{2}\gamma_2} + X_{-\frac{1}{2}\gamma_1 + \frac{1}{2}\gamma_2} + X_{-\frac{1}{2}\gamma_1 + \frac{1}{2}\gamma_2 + \gamma_3} + X_{-\frac{1}{2}\gamma_1 + \frac{1}{2}\gamma_2 + \gamma_4} + X_{-\frac{1}{2}\gamma_1 + \frac{1}{2}\gamma_2 + \gamma_3 + \gamma_4} + \\ & + X_{-\frac{1}{2}\gamma_1 + \frac{1}{2}\gamma_2 + \gamma_5} + X_{-\frac{1}{2}\gamma_1 + \frac{1}{2}\gamma_2 + \gamma_3 + \gamma_5} + X_{-\frac{1}{2}\gamma_1 + \frac{1}{2}\gamma_2 + \gamma_4 + \gamma_5} + X_{-\frac{1}{2}\gamma_1 + \frac{1}{2}\gamma_2 + \gamma_3 + \gamma_4 + \gamma_5} + X_{\frac{1}{2}\gamma_1 + \frac{1}{2}\gamma_2} \end{aligned} \tag{12.6.39}$$

reorganize

$$\begin{aligned} S' = {} & E_{\mathfrak{q}}(X_{\gamma_2+\gamma_3+\gamma_4+\gamma_5}) E_{\mathfrak{q}}(X_{\gamma_1}) E_{\mathfrak{q}}(X_{\gamma_2+\gamma_4+\gamma_5}) E_{\mathfrak{q}}(X_{-\gamma_3}) E_{\mathfrak{q}}(X_{\gamma_2+\gamma_3+\gamma_5}) \cdot \\ & \cdot E_{\mathfrak{q}}(X_{-\gamma_4}) E_{\mathfrak{q}}(X_{\gamma_2+\gamma_3+\gamma_4}) E_{\mathfrak{q}}(X_{-\gamma_5}) \end{aligned} \tag{12.6.40}$$

and mutate again at $\gamma_2 + \gamma_3 + \gamma_4 + \gamma_5$:

$$\begin{aligned} S'' = {} & E_{\mathfrak{q}}(X_{\gamma_1}) E_{\mathfrak{q}}(X_{\gamma_2+\gamma_4+\gamma_5}) E_{\mathfrak{q}}(X_{-\gamma_3}) E_{\mathfrak{q}}(X_{\gamma_2+\gamma_3+\gamma_5}) \cdot \\ & \cdot E_{\mathfrak{q}}(X_{-\gamma_4}) E_{\mathfrak{q}}(X_{\gamma_2+\gamma_3+\gamma_4}) E_{\mathfrak{q}}(X_{-\gamma_5}) E_{\mathfrak{q}}(X_{-\gamma_2-\gamma_3-\gamma_4-\gamma_5}) \end{aligned} \tag{12.6.41}$$

with

$$\begin{aligned} F''_{w_1} = {} & X_{-\frac{1}{2}\gamma_1 - \frac{1}{2}\gamma_2} + X_{-\frac{1}{2}\gamma_1 + \frac{1}{2}\gamma_2} + (\mathfrak{q} + \mathfrak{q}^{-1}) X_{-\frac{1}{2}\gamma_1 + \frac{3}{2}\gamma_2 + \gamma_3 + \gamma_4 + \gamma_5} + X_{-\frac{1}{2}\gamma_1 + \frac{5}{2}\gamma_2 + 2\gamma_3 + 2\gamma_4 + 2\gamma_5} + \\ & + X_{-\frac{1}{2}\gamma_1 + \frac{1}{2}\gamma_2 + \gamma_3} + X_{-\frac{1}{2}\gamma_1 + \frac{3}{2}\gamma_2 + 2\gamma_3 + \gamma_4 + \gamma_5} + X_{-\frac{1}{2}\gamma_1 + \frac{1}{2}\gamma_2 + \gamma_4} + X_{-\frac{1}{2}\gamma_1 + \frac{3}{2}\gamma_2 + \gamma_3 + 2\gamma_4 + \gamma_5} + \\ & + X_{-\frac{1}{2}\gamma_1 + \frac{1}{2}\gamma_2 + \gamma_3 + \gamma_4} + X_{-\frac{1}{2}\gamma_1 + \frac{1}{2}\gamma_2 + \gamma_5} + X_{-\frac{1}{2}\gamma_1 + \frac{3}{2}\gamma_2 + \gamma_3 + \gamma_4 + 2\gamma_5} + X_{-\frac{1}{2}\gamma_1 + \frac{1}{2}\gamma_2 + \gamma_3 + \gamma_5} + \\ & + X_{-\frac{1}{2}\gamma_1 + \frac{1}{2}\gamma_2 + \gamma_4 + \gamma_5} + X_{\frac{1}{2}\gamma_1 + \frac{1}{2}\gamma_2} + X_{\frac{1}{2}\gamma_1 + \frac{3}{2}\gamma_2 + \gamma_3 + \gamma_4 + \gamma_5} \end{aligned} \tag{12.6.42}$$

reorganized finally to

$$S'' = E_{\mathfrak{q}}(X_{\gamma_1})E_{\mathfrak{q}}(X_{-\gamma_2-\gamma_3-\gamma_4-\gamma_5})E_{\mathfrak{q}}(X_{\gamma_2+\gamma_4+\gamma_5})E_{\mathfrak{q}}(X_{\gamma_2+\gamma_3+\gamma_5})E_{\mathfrak{q}}(X_{\gamma_2+\gamma_3+\gamma_4}) \quad (12.6.43)$$

and mutated to a standard form:

$$S''' = E_{\mathfrak{q}}(X_{-\gamma_2-\gamma_3-\gamma_4-\gamma_5})E_{\mathfrak{q}}(X_{\gamma_2+\gamma_4+\gamma_5})E_{\mathfrak{q}}(X_{\gamma_2+\gamma_3+\gamma_5})E_{\mathfrak{q}}(X_{\gamma_2+\gamma_3+\gamma_4})E_{\mathfrak{q}}(X_{-\gamma_1}) \quad (12.6.44)$$

with a quadruplet of commuting factors on the right which makes manifest the $SU(4) =$ Spin(6) symmetry of the system.

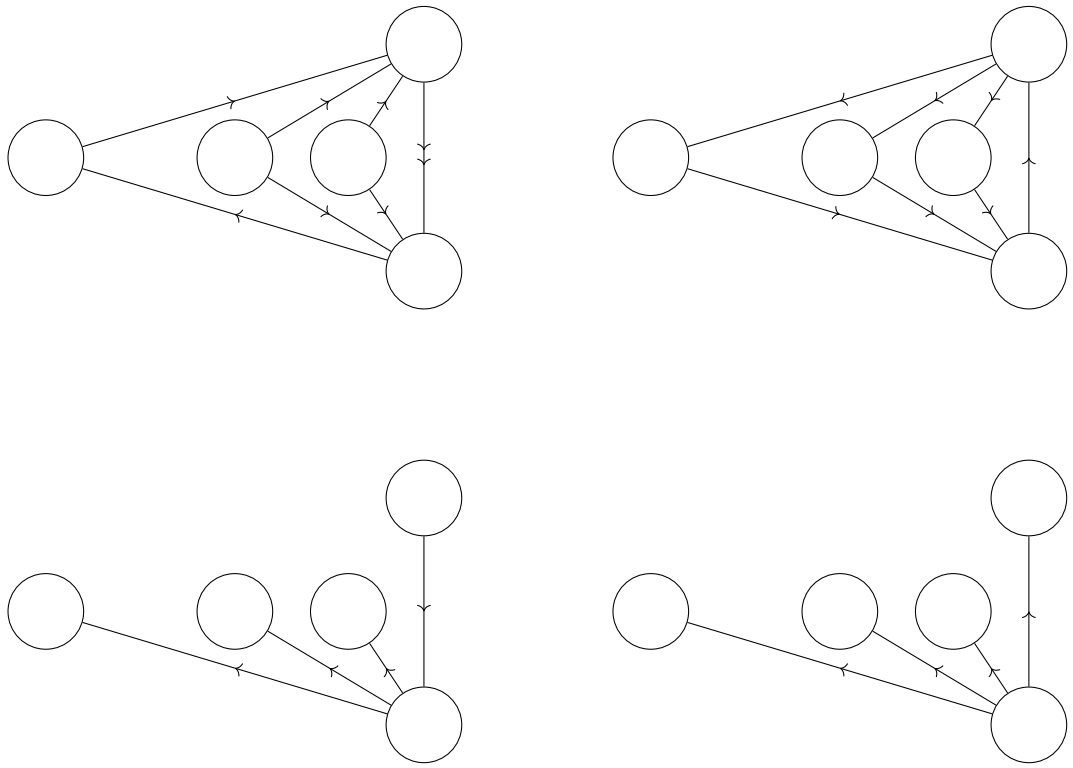


Figure 12.12: Top Left: the BPS quiver compatibl with the RG flow from $N_f = 3$ to pure $SU(2)$. Top Right: mutation at the three matter nodes gives this quiver. Bottom Left: Mutation at the bottom node simplifies the quiver drastically. Bottom Right: A final mutation at the top node makes a large symmetry manifest.

The final expression for the Wilson line is somewhat dreadful but $SU(4)$-covariant

$$\begin{aligned}F'''_{w_1} = {} & X_{\frac{1}{2}\gamma_1-\frac{1}{2}\gamma_2} + (X_{-\frac{1}{2}\gamma_1-\frac{1}{2}\gamma_2} + X_{\frac{1}{2}\gamma_1+\frac{1}{2}\gamma_2+\gamma_3+\gamma_4} + X_{\frac{1}{2}\gamma_1+\frac{1}{2}\gamma_2+\gamma_3+\gamma_5} + X_{\frac{1}{2}\gamma_1+\frac{1}{2}\gamma_2+\gamma_4+\gamma_5})+ \\ & + (X_{-\frac{1}{2}\gamma_1+\frac{1}{2}\gamma_2+\gamma_3+\gamma_4} + X_{-\frac{1}{2}\gamma_1+\frac{1}{2}\gamma_2+\gamma_3+\gamma_5} + X_{-\frac{1}{2}\gamma_1+\frac{1}{2}\gamma_2+\gamma_4+\gamma_5} + \\ & + X_{\frac{1}{2}\gamma_1+\frac{3}{2}\gamma_2+\gamma_3+2\gamma_4+\gamma_5} + X_{\frac{1}{2}\gamma_1+\frac{3}{2}\gamma_2+2\gamma_3+\gamma_4+\gamma_5} + X_{\frac{1}{2}\gamma_1+\frac{3}{2}\gamma_2+\gamma_3+\gamma_4+2\gamma_5})+ \\ & + (X_{-\frac{1}{2}\gamma_1+\frac{3}{2}\gamma_2+2\gamma_3+\gamma_4+\gamma_5} + X_{-\frac{1}{2}\gamma_1+\frac{3}{2}\gamma_2+\gamma_3+2\gamma_4+\gamma_5} + X_{-\frac{1}{2}\gamma_1+\frac{3}{2}\gamma_2+\gamma_3+\gamma_4+2\gamma_5} + X_{\frac{1}{2}\gamma_1+\frac{5}{2}\gamma_2+2\gamma_3+2\gamma_4+2\gamma_5}) \\ & + (X_{-\frac{1}{2}\gamma_1+\frac{1}{2}\gamma_2+\gamma_3} + X_{-\frac{1}{2}\gamma_1+\frac{1}{2}\gamma_2+\gamma_4} + X_{-\frac{1}{2}\gamma_1+\frac{1}{2}\gamma_2+\gamma_5} + X_{\frac{1}{2}\gamma_1+\frac{3}{2}\gamma_2+\gamma_3+\gamma_4+\gamma_5})+ \\ & + X_{-\frac{1}{2}\gamma_1+\frac{5}{2}\gamma_2+2\gamma_3+2\gamma_4+2\gamma_5} + (\mathfrak{q}+\mathfrak{q}^{-1})X_{-\frac{1}{2}\gamma_1+\frac{3}{2}\gamma_2+\gamma_3+\gamma_4+\gamma_5} + X_{-\frac{1}{2}\gamma_1+\frac{1}{2}\gamma_2}\end{aligned} \tag{12.6.45}$$

Conversely, starting from

$$F'''_{D_{1,0}} = X_{\gamma_1} \tag{12.6.46}$$

we get to

$$\begin{aligned}F^{\rm UV}_{D_{1,0}} = {} & X_{\gamma_1} + X_{\gamma_1+\gamma_3} + X_{\gamma_1+\gamma_4} + X_{\gamma_1+\gamma_5} + X_{\gamma_1+\gamma_3+\gamma_4} + \\ & + X_{\gamma_1+\gamma_3+\gamma_5} + X_{\gamma_1+\gamma_4+\gamma_5} + X_{\gamma_1+\gamma_3+\gamma_4+\gamma_5} + X_{\gamma_1+\gamma_2+\gamma_3+\gamma_4+\gamma_5}\end{aligned} \tag{12.6.47}$$

i.e.

$$\mathrm{RG}(D_{1,0}) = H_0^2 + (\mu_1+\mu_2+\mu_3)\mathfrak{q}^{-\frac{1}{2}}H_{-1}H_0 + (\mu_1\mu_2+\mu_2\mu_3+\mu_1\mu_3)H_{-1}^2 + \mu_1\mu_2\mu_3 H_{-2}H_{-1} \tag{12.6.48}$$

$N_f = 4$

We conjecture the expression

$$S_{\rm UV} = f_2(\mu_1, w_a) f_2(\mu_2, w_a) f_2(\mu_3, w_a) f_2(\mu_4, w_a) S_{\rm IR} \tag{12.6.49}$$

for the spectrum generator here, i.e.

$$\begin{aligned}S_{\rm UV} = {} & E_{\mathfrak{q}}(X_{\gamma_4})E_{\mathfrak{q}}(X_{\gamma_2+\gamma_4})E_{\mathfrak{q}}(X_{\gamma_1+\gamma_2+\gamma_4})E_{\mathfrak{q}}(X_{\gamma_3})E_{\mathfrak{q}}(X_{\gamma_2+\gamma_3})E_{\mathfrak{q}}(X_{\gamma_1+\gamma_2+\gamma_3})\cdot \\ & \cdot E_{\mathfrak{q}}(X_{\gamma_5})E_{\mathfrak{q}}(X_{\gamma_2+\gamma_5})E_{\mathfrak{q}}(X_{\gamma_1+\gamma_2+\gamma_5})E_{\mathfrak{q}}(X_{\gamma_6})E_{\mathfrak{q}}(X_{\gamma_2+\gamma_6})E_{\mathfrak{q}}(X_{\gamma_1+\gamma_2+\gamma_6})\cdot \\ & \cdot E_{\mathfrak{q}}(X_{\gamma_1})E_{\mathfrak{q}}(X_{\gamma_2})\end{aligned} \tag{12.6.50}$$

We are not aware of a finite chamber which makes the $SO(8)$ flavour symmetry of the theory manifest. A nice option is to mutate at γ_3, γ_4 and $\gamma_2+\gamma_3+\gamma_4$:

$$\begin{aligned}S' = {} & E_{\mathfrak{q}}(X_{\gamma_2+\gamma_4})E_{\mathfrak{q}}(X_{\gamma_1+\gamma_2+\gamma_4})E_{\mathfrak{q}}(X_{\gamma_2+\gamma_3})E_{\mathfrak{q}}(X_{\gamma_1+\gamma_2+\gamma_3})\cdot \\ & \cdot E_{\mathfrak{q}}(X_{\gamma_5})E_{\mathfrak{q}}(X_{\gamma_2+\gamma_5})E_{\mathfrak{q}}(X_{\gamma_1+\gamma_2+\gamma_5})E_{\mathfrak{q}}(X_{\gamma_6})E_{\mathfrak{q}}(X_{\gamma_2+\gamma_6})E_{\mathfrak{q}}(X_{\gamma_1+\gamma_2+\gamma_6})\cdot \\ & \cdot E_{\mathfrak{q}}(X_{\gamma_1})E_{\mathfrak{q}}(X_{\gamma_2})E_{\mathfrak{q}}(X_{-\gamma_4})E_{\mathfrak{q}}(X_{-\gamma_3})E_{\mathfrak{q}}(X_{-\gamma_2-\gamma_3-\gamma_4})\end{aligned} \tag{12.6.51}$$

The simple charges are now γ_1, $-\gamma_2-\gamma_3-\gamma_4$, $\gamma_2+\gamma_3$, $\gamma_2+\gamma_4$, γ_5, γ_6. This is an extremely symmetric collection: the BPS quiver is an octahedron. If S' is determined by the BPS

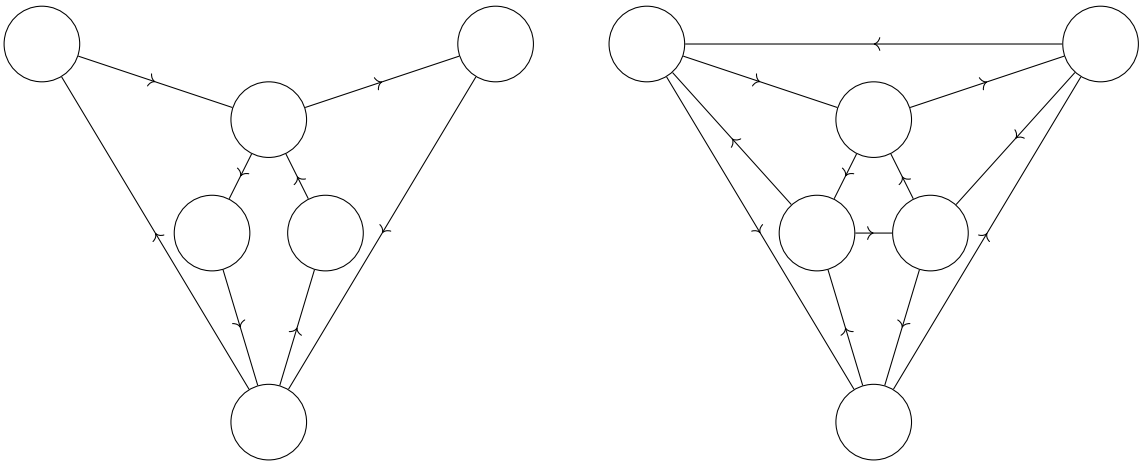


Figure 12.13: Mutating two matter nodes in the BPS quiver associated to the RG flow from pure $N_f = 4$ to pure $SU(2)$ produces the Left quiver. Mutation at the bottom node produces the octahedral form of the quiver.

quiver, it should have the same symmetry, though it is not manifest. In particular, this includes cyclic permutations of the three pairs of consecutive charges.

The Wilson loop in this chamber has the same general form as for $N_f = 2$

$$\begin{aligned} F'_{D_{0,1}} = & X_{-\frac{1}{2}\gamma_1-\frac{1}{2}\gamma_2} + (X_{-\frac{1}{2}\gamma_1+\frac{1}{2}\gamma_2+\gamma_3} + X_{-\frac{1}{2}\gamma_1+\frac{1}{2}\gamma_2+\gamma_4}) + X_{-\frac{1}{2}\gamma_1+\frac{3}{2}\gamma_2+\gamma_3+\gamma_4} + \\ & + (X_{-\frac{1}{2}\gamma_1+\frac{1}{2}\gamma_2} + X_{\frac{1}{2}\gamma_1+\frac{3}{2}\gamma_2+\gamma_3+\gamma_4}) + X_{\frac{1}{2}\gamma_1+\frac{1}{2}\gamma_2} \end{aligned} \tag{12.6.52}$$

If the expected symmetry holds, we should have two more simple F's:

$$\begin{aligned} F'_{D_{1,0}} = & X_{-\gamma_2-\frac{1}{2}\gamma_3-\frac{1}{2}\gamma_4-\frac{1}{2}\gamma_5-\frac{1}{2}\gamma_6} + (X_{-\gamma_2-\frac{1}{2}\gamma_3-\frac{1}{2}\gamma_4+\frac{1}{2}\gamma_5-\frac{1}{2}\gamma_6} + X_{-\gamma_2-\frac{1}{2}\gamma_3-\frac{1}{2}\gamma_4-\frac{1}{2}\gamma_5+\frac{1}{2}\gamma_6}) + \\ & + X_{-\gamma_2-\frac{1}{2}\gamma_3-\frac{1}{2}\gamma_4+\frac{1}{2}\gamma_5+\frac{1}{2}\gamma_6} + (X_{\frac{1}{2}\gamma_3-\frac{1}{2}\gamma_4+\frac{1}{2}\gamma_5+\frac{1}{2}\gamma_6} + X_{-\frac{1}{2}\gamma_3+\frac{1}{2}\gamma_4+\frac{1}{2}\gamma_5+\frac{1}{2}\gamma_6}) + X_{\gamma_2+\frac{1}{2}\gamma_3+\frac{1}{2}\gamma_4+\frac{1}{2}\gamma_5+\frac{1}{2}\gamma_6} \\ F'_{D_{1,1}} = & X_{-\frac{1}{2}\gamma_1+\frac{1}{2}\gamma_2+\frac{1}{2}\gamma_3+\frac{1}{2}\gamma_4-\frac{1}{2}\gamma_5-\frac{1}{2}\gamma_6} + (X_{\frac{1}{2}\gamma_1+\frac{1}{2}\gamma_2+\frac{1}{2}\gamma_3+\frac{1}{2}\gamma_4-\frac{1}{2}\gamma_5-\frac{1}{2}\gamma_6} + X_{-\frac{1}{2}\gamma_1-\frac{1}{2}\gamma_2-\frac{1}{2}\gamma_3-\frac{1}{2}\gamma_4-\frac{1}{2}\gamma_5-\frac{1}{2}\gamma_6}) + \\ & + X_{\frac{1}{2}\gamma_1-\frac{1}{2}\gamma_2-\frac{1}{2}\gamma_3-\frac{1}{2}\gamma_4-\frac{1}{2}\gamma_5-\frac{1}{2}\gamma_6} + (X_{\frac{1}{2}\gamma_1-\frac{1}{2}\gamma_2-\frac{1}{2}\gamma_3-\frac{1}{2}\gamma_4+\frac{1}{2}\gamma_5-\frac{1}{2}\gamma_6} + X_{\frac{1}{2}\gamma_1-\frac{1}{2}\gamma_2-\frac{1}{2}\gamma_3-\frac{1}{2}\gamma_4-\frac{1}{2}\gamma_5+\frac{1}{2}\gamma_6}) + \\ & + X_{\frac{1}{2}\gamma_1-\frac{1}{2}\gamma_2-\frac{1}{2}\gamma_3-\frac{1}{2}\gamma_4+\frac{1}{2}\gamma_5+\frac{1}{2}\gamma_6} \end{aligned} \tag{12.6.53}$$

As a test, we can mutate back,

$$\begin{aligned} F^{\rm UV}_{D_{1,1}} &= (\mu_1\mu_2\mu_3\mu_4)^{-\frac{1}{2}} X_{\frac{1}{2}\gamma_1+\frac{1}{2}\gamma_2} + (\mu_1\mu_2\mu_3\mu_4)^{-\frac{1}{2}} X_{\frac{3}{2}\gamma_1+\frac{1}{2}\gamma_2} + \\ &+ (\mu_1\mu_2\mu_3\mu_4)^{-\frac{1}{2}} X_{\gamma_1}(\mu_1+\mu_2+\mu_3+\mu_4) + \\ &+ (\mu_1\mu_2\mu_3\mu_4)^{-\frac{1}{2}} X_{\frac{1}{2}\gamma_1-\frac{1}{2}\gamma_2}\left(\sum_{i<j}\mu_i\mu_j\right) + \\ &+ (\mu_1\mu_2\mu_3\mu_4)^{\frac{1}{2}} X_{-\gamma_2}\left(\mu_1^{-1}+\mu_2^{-1}+\mu_3^{-1}+\mu_4^{-1}\right) + \\ &+ (\mu_1\mu_2\mu_3\mu_4)^{\frac{1}{2}} X_{-\frac{1}{2}\gamma_1-\frac{3}{2}\gamma_2} + (\mu_1\mu_2\mu_3\mu_4)^{\frac{1}{2}} X_{-\frac{1}{2}\gamma_1-\frac{1}{2}\gamma_2} \end{aligned} \tag{12.6.54}$$

i.e.

$$\begin{aligned} {\rm RG}(D_{1,1}) &= (\mu_1\mu_2\mu_3\mu_4)^{-\frac{1}{2}} \mathfrak{q}^{-\frac{1}{2}} H_0 H_1 + \\ &+ (\mu_1\mu_2\mu_3\mu_4)^{-\frac{1}{2}}(\mu_1+\mu_2+\mu_3+\mu_4) H_0^2 + \\ &+ (\mu_1\mu_2\mu_3\mu_4)^{-\frac{1}{2}}\left(\sum_{i<j}\mu_i\mu_j\right)\mathfrak{q}^{-\frac{1}{2}} H_{-1}H_0 + \\ &+ (\mu_1\mu_2\mu_3\mu_4)^{\frac{1}{2}}\left(\mu_1^{-1}+\mu_2^{-1}+\mu_3^{-1}+\mu_4^{-1}\right) H_{-1}^2 + \\ &+ (\mu_1\mu_2\mu_3\mu_4)^{\frac{1}{2}}\mathfrak{q}^{-\frac{1}{2}} H_{-2}H_{-1} \end{aligned} \tag{12.6.55}$$

as expected [83].

12.6.2 $SU(2) \times SU(2)$ quiver gauge theory

As a further example, we can consider an $SU(2) \times SU(2)$ gauge theory coupled to bi-fundamental matter. To do so, we need to expand

$$E_{\mathfrak{q}}(\mu\zeta_1\zeta_2)E_{\mathfrak{q}}(\mu\zeta_1/\zeta_2)E_{\mathfrak{q}}(\mu/\zeta_1\zeta_2)E_{\mathfrak{q}}(\mu/\zeta_1/\zeta_2) \tag{12.6.56}$$

into characters of the two gauge groups and replace them with two sets of Wilson loops. We can do it in two steps. First as in $SU(2)$ $N_f = 2$:

$$\begin{aligned} &E_{\mathfrak{q}}(\mu\zeta_2 X_{-\frac{1}{2}\gamma_1-\frac{1}{2}\gamma_2})E_{\mathfrak{q}}(\mu\zeta_2 X_{-\frac{1}{2}\gamma_1+\frac{1}{2}\gamma_2})E_{\mathfrak{q}}(\mu\zeta_2 X_{\frac{1}{2}\gamma_1+\frac{1}{2}\gamma_2})\cdot \\ &\cdot E_{\mathfrak{q}}(\mu/\zeta_2 X_{-\frac{1}{2}\gamma_1-\frac{1}{2}\gamma_2})E_{\mathfrak{q}}(\mu/\zeta_2 X_{-\frac{1}{2}\gamma_1+\frac{1}{2}\gamma_2})E_{\mathfrak{q}}(\mu/\zeta_2 X_{\frac{1}{2}\gamma_1+\frac{1}{2}\gamma_2}) \end{aligned} \tag{12.6.57}$$

We reorganize it to

$$\begin{aligned} &E_{\mathfrak{q}}(\mu\zeta_2 X_{-\frac{1}{2}\gamma_1-\frac{1}{2}\gamma_2})E_{\mathfrak{q}}(\mu/\zeta_2 X_{-\frac{1}{2}\gamma_1-\frac{1}{2}\gamma_2})E_{\mathfrak{q}}(\mu^2 X_{-\gamma_1})E_{\mathfrak{q}}(\mu\zeta_2 X_{-\frac{1}{2}\gamma_1+\frac{1}{2}\gamma_2})\cdot \\ &\cdot E_{\mathfrak{q}}(\mu/\zeta_2 X_{-\frac{1}{2}\gamma_1+\frac{1}{2}\gamma_2})E_{\mathfrak{q}}(\mu^2 X_{\gamma_2})E_{\mathfrak{q}}(\mu\zeta_2 X_{\frac{1}{2}\gamma_1+\frac{1}{2}\gamma_2})E_{\mathfrak{q}}(\mu/\zeta_2 X_{\frac{1}{2}\gamma_1+\frac{1}{2}\gamma_2}) \end{aligned} \tag{12.6.58}$$

and then we can readily do the replacement with a second set of Wilson lines:

$$E_{\mathfrak{q}}(\mu X_{-\frac{1}{2}\gamma_1-\frac{1}{2}\gamma_2-\frac{1}{2}\gamma_3-\frac{1}{2}\gamma_4})E_{\mathfrak{q}}(\mu X_{-\frac{1}{2}\gamma_1-\frac{1}{2}\gamma_2-\frac{1}{2}\gamma_3+\frac{1}{2}\gamma_4})E_{\mathfrak{q}}(\mu X_{-\frac{1}{2}\gamma_1-\frac{1}{2}\gamma_2+\frac{1}{2}\gamma_3+\frac{1}{2}\gamma_4})E_{\mathfrak{q}}(\mu^2 X_{-\gamma_1})\cdot$$
$$\cdot E_{\mathfrak{q}}(\mu X_{-\frac{1}{2}\gamma_1+\frac{1}{2}\gamma_2-\frac{1}{2}\gamma_3-\frac{1}{2}\gamma_4})E_{\mathfrak{q}}(\mu X_{-\frac{1}{2}\gamma_1+\frac{1}{2}\gamma_2-\frac{1}{2}\gamma_3+\frac{1}{2}\gamma_4})E_{\mathfrak{q}}(\mu X_{-\frac{1}{2}\gamma_1+\frac{1}{2}\gamma_2+\frac{1}{2}\gamma_3+\frac{1}{2}\gamma_4})E_{\mathfrak{q}}(\mu^2 X_{\gamma_2})\cdot$$
$$\cdot E_{\mathfrak{q}}(\mu X_{\frac{1}{2}\gamma_1+\frac{1}{2}\gamma_2-\frac{1}{2}\gamma_3-\frac{1}{2}\gamma_4})E_{\mathfrak{q}}(\mu X_{\frac{1}{2}\gamma_1+\frac{1}{2}\gamma_2-\frac{1}{2}\gamma_3+\frac{1}{2}\gamma_4})E_{\mathfrak{q}}(\mu X_{\frac{1}{2}\gamma_1+\frac{1}{2}\gamma_2+\frac{1}{2}\gamma_3+\frac{1}{2}\gamma_4}) \tag{12.6.59}$$

and possibly simplify a bit:

$$E_{\mathfrak{q}}(\mu X_{-\frac{1}{2}\gamma_1-\frac{1}{2}\gamma_2-\frac{1}{2}\gamma_3-\frac{1}{2}\gamma_4})E_{\mathfrak{q}}(\mu X_{-\frac{1}{2}\gamma_1-\frac{1}{2}\gamma_2-\frac{1}{2}\gamma_3+\frac{1}{2}\gamma_4})E_{\mathfrak{q}}(\mu X_{-\frac{1}{2}\gamma_1+\frac{1}{2}\gamma_2-\frac{1}{2}\gamma_3-\frac{1}{2}\gamma_4})\cdot$$
$$\cdot E_{\mathfrak{q}}(\mu X_{-\frac{1}{2}\gamma_1-\frac{1}{2}\gamma_2+\frac{1}{2}\gamma_3+\frac{1}{2}\gamma_4})E_{\mathfrak{q}}(\mu X_{-\frac{1}{2}\gamma_1+\frac{1}{2}\gamma_2-\frac{1}{2}\gamma_3+\frac{1}{2}\gamma_4})E_{\mathfrak{q}}(\mu X_{\frac{1}{2}\gamma_1+\frac{1}{2}\gamma_2-\frac{1}{2}\gamma_3-\frac{1}{2}\gamma_4})\cdot$$
$$\cdot E_{\mathfrak{q}}(\mu X_{-\frac{1}{2}\gamma_1+\frac{1}{2}\gamma_2+\frac{1}{2}\gamma_3+\frac{1}{2}\gamma_4})E_{\mathfrak{q}}(\mu X_{\frac{1}{2}\gamma_1+\frac{1}{2}\gamma_2-\frac{1}{2}\gamma_3+\frac{1}{2}\gamma_4})E_{\mathfrak{q}}(\mu X_{\frac{1}{2}\gamma_1+\frac{1}{2}\gamma_2+\frac{1}{2}\gamma_3+\frac{1}{2}\gamma_4}) \tag{12.6.60}$$

and combine into the final spectrum generator:

$$S = E_{\mathfrak{q}}(\mu X_{-\frac{1}{2}\gamma_1-\frac{1}{2}\gamma_2-\frac{1}{2}\gamma_3-\frac{1}{2}\gamma_4})E_{\mathfrak{q}}(\mu X_{-\frac{1}{2}\gamma_1-\frac{1}{2}\gamma_2-\frac{1}{2}\gamma_3+\frac{1}{2}\gamma_4})E_{\mathfrak{q}}(\mu X_{-\frac{1}{2}\gamma_1+\frac{1}{2}\gamma_2-\frac{1}{2}\gamma_3-\frac{1}{2}\gamma_4})\cdot$$
$$\cdot E_{\mathfrak{q}}(\mu X_{-\frac{1}{2}\gamma_1-\frac{1}{2}\gamma_2+\frac{1}{2}\gamma_3+\frac{1}{2}\gamma_4})E_{\mathfrak{q}}(\mu X_{-\frac{1}{2}\gamma_1+\frac{1}{2}\gamma_2-\frac{1}{2}\gamma_3+\frac{1}{2}\gamma_4})E_{\mathfrak{q}}(\mu X_{\frac{1}{2}\gamma_1+\frac{1}{2}\gamma_2-\frac{1}{2}\gamma_3-\frac{1}{2}\gamma_4})\cdot$$
$$\cdot E_{\mathfrak{q}}(\mu X_{-\frac{1}{2}\gamma_1+\frac{1}{2}\gamma_2+\frac{1}{2}\gamma_3+\frac{1}{2}\gamma_4})E_{\mathfrak{q}}(\mu X_{\frac{1}{2}\gamma_1+\frac{1}{2}\gamma_2-\frac{1}{2}\gamma_3+\frac{1}{2}\gamma_4})E_{\mathfrak{q}}(\mu X_{\frac{1}{2}\gamma_1+\frac{1}{2}\gamma_2+\frac{1}{2}\gamma_3+\frac{1}{2}\gamma_4})\cdot$$
$$\cdot E_{\mathfrak{q}}(X_{\gamma_1})E_{\mathfrak{q}}(X_{\gamma_2})E_{\mathfrak{q}}(X_{\gamma_3})E_{\mathfrak{q}}(X_{\gamma_4}) \tag{12.6.61}$$

with $\langle\gamma_1,\gamma_2\rangle = \langle\gamma_3,\gamma_4\rangle = 2$, which can be simplified further to

$$S = E_{\mathfrak{q}}(\mu X_{-\frac{1}{2}\gamma_1-\frac{1}{2}\gamma_2-\frac{1}{2}\gamma_3-\frac{1}{2}\gamma_4})E_{\mathfrak{q}}(\mu X_{-\frac{1}{2}\gamma_1-\frac{1}{2}\gamma_2-\frac{1}{2}\gamma_3+\frac{1}{2}\gamma_4})E_{\mathfrak{q}}(\mu X_{-\frac{1}{2}\gamma_1+\frac{1}{2}\gamma_2-\frac{1}{2}\gamma_3-\frac{1}{2}\gamma_4})\cdot$$
$$\cdot E_{\mathfrak{q}}(\mu X_{-\frac{1}{2}\gamma_1-\frac{1}{2}\gamma_2+\frac{1}{2}\gamma_3+\frac{1}{2}\gamma_4})E_{\mathfrak{q}}(\mu X_{\frac{1}{2}\gamma_1+\frac{1}{2}\gamma_2-\frac{1}{2}\gamma_3-\frac{1}{2}\gamma_4})E_{\mathfrak{q}}(X_{\gamma_1})E_{\mathfrak{q}}(X_{\gamma_3})E_{\mathfrak{q}}(\mu X_{-\frac{1}{2}\gamma_1+\frac{1}{2}\gamma_2-\frac{1}{2}\gamma_3+\frac{1}{2}\gamma_4})\cdot$$
$$\cdot E_{\mathfrak{q}}(X_{\gamma_2})E_{\mathfrak{q}}(X_{\gamma_4}) \tag{12.6.62}$$

The "simple" charges in the support of this spectrum generator appear to be γ_i and the charge γ_5 of $\mu X_{-\frac{1}{2}\gamma_1-\frac{1}{2}\gamma_2-\frac{1}{2}\gamma_3-\frac{1}{2}\gamma_4}$, which satisfies

$$\langle\gamma_5,\gamma_1\rangle = \langle\gamma_2,\gamma_5\rangle = \langle\gamma_5,\gamma_3\rangle = \langle\gamma_4,\gamma_5\rangle = 1 \tag{12.6.63}$$

which is indeed the known BPS quiver for this theory. See Figure 12.14.

For later use, we can also build an alternative conjectural spectrum generator from the Spin(4)-covariant spectrum generator of $SU(2)$ with $N_f = 2$, rewritten as

$$E_{\mathfrak{q}}(\mu^{-1}X_{\gamma_1})E_{\mathfrak{q}}(\mu X_{\gamma_1})E_{\mathfrak{q}}(\zeta X_{\gamma_2})E_{\mathfrak{q}}(\zeta^{-1}X_{\gamma_2}) \tag{12.6.64}$$

with $\langle\gamma_1,\gamma_2\rangle = 1$.

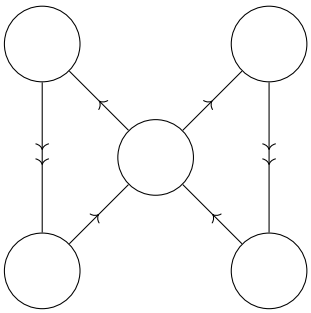


Figure 12.14: BPS quiver for $SU(2) \times SU(2)$ with bifundamental matter.

Promoting as usual the ζ dependence to a Wilson line expression for the new $SU(2)$ gauge theory:

$$S' = E_{\mathfrak{q}}(\mu^{-1}X_{\gamma_1})E_{\mathfrak{q}}(\mu X_{\gamma_1})E_{\mathfrak{q}}(X_{\gamma_2-\frac{1}{2}\gamma_3-\frac{1}{2}\gamma_4})E_{\mathfrak{q}}(X_{\gamma_2-\frac{1}{2}\gamma_3+\frac{1}{2}\gamma_4})E_{\mathfrak{q}}(X_{\gamma_2+\frac{1}{2}\gamma_3+\frac{1}{2}\gamma_4})E_{\mathfrak{q}}(X_{\gamma_3})E_{\mathfrak{q}}(X_{\gamma_4}) \tag{12.6.65}$$

with $\langle\gamma_3,\gamma_4\rangle = 2$, which makes manifest the additional $SU(2)$ flavour symmetry of the $SU(2) \times SU(2)$ gauge theory. The elementary charges are now $\mu^{\pm 1}\gamma_1$, $\gamma_2 - \frac{1}{2}\gamma_3 - \frac{1}{2}\gamma_4$, γ_3 and γ_4. This new BPS quiver is related to the original one by a lengthy sequence of mutations, which we will not attempt to record in detail. See Figure 12.15.

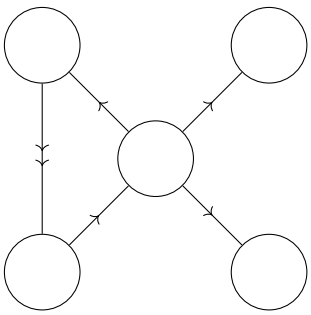


Figure 12.15: BPS quiver for $SU(2) \times SU(2)$ with bifundamental matter.

12.6.3 The trinion $SU(2)^3$ theory

We can now complete our sequence of examples by gauging the final $SU(2)$ flavour symmetry in the previous example:

$$\begin{aligned} S = {} & E_{\mathfrak{q}}(X_{\gamma_1-\frac{1}{2}\gamma_5-\frac{1}{2}\gamma_6})E_{\mathfrak{q}}(X_{\gamma_1-\frac{1}{2}\gamma_5+\frac{1}{2}\gamma_6})E_{\mathfrak{q}}(X_{\gamma_1+\frac{1}{2}\gamma_5+\frac{1}{2}\gamma_6})E_{\mathfrak{q}}(X_{\gamma_2-\frac{1}{2}\gamma_3-\frac{1}{2}\gamma_4})\cdot \\ & \cdot E_{\mathfrak{q}}(X_{\gamma_2-\frac{1}{2}\gamma_3+\frac{1}{2}\gamma_4})E_{\mathfrak{q}}(X_{\gamma_2+\frac{1}{2}\gamma_3+\frac{1}{2}\gamma_4})E_{\mathfrak{q}}(X_{\gamma_3})E_{\mathfrak{q}}(X_{\gamma_4})E_{\mathfrak{q}}(X_{\gamma_5})E_{\mathfrak{q}}(X_{\gamma_6}) \end{aligned} \tag{12.6.66}$$

This theory has three $SU(2)$ gauge groups acting symmetrically on eight half-hypermultiplets. The S_3 symmetry is not manifest in this spectrum generator, see Figure 12.16, but a judicious sequence of mutations can bring the quiver more symmetric forms, such as a

triangular prism with all side edges parallel and face edges ordered in opposite cyclic order. See Figure 12.17.

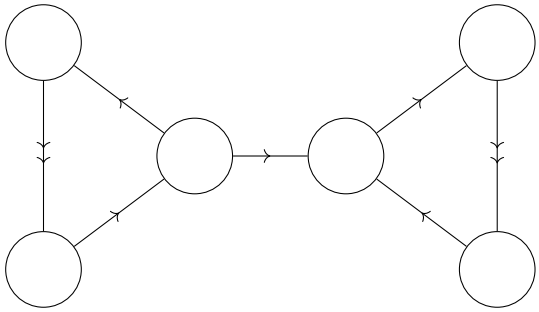


Figure 12.16: The BPS quiver for the $SU(2)^3$ theory obtained from our general strategy.

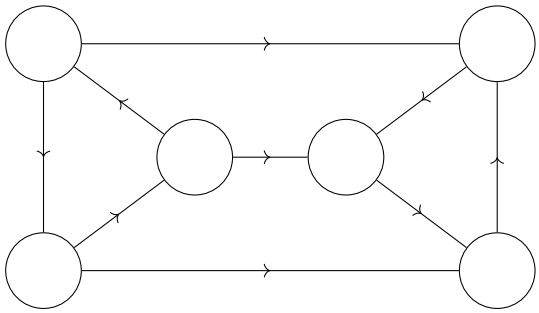


Figure 12.17: A more symmetric quiver for the $SU(2)^3$ theory.

12.7 Towards higher ranks: examples with $SU(3)$ gauge group

In the literature, the BPS spectrum of pure $SU(3)$ gauge theory is encoded into a BPS quiver with four nodes, with charges $\gamma_1, \cdots, \gamma_4$ such that

$$\begin{aligned} \langle \gamma_1, \gamma_2 \rangle &= 2 \\ \langle \gamma_2, \gamma_3 \rangle &= 1 \\ \langle \gamma_3, \gamma_4 \rangle &= 2 \\ \langle \gamma_4, \gamma_1 \rangle &= 1 \end{aligned} \tag{12.7.1}$$

and quantum spectrum generator

$$S = E_{\mathfrak{q}}(X_{\gamma_1}) E_{\mathfrak{q}}(X_{\gamma_3}) E_{\mathfrak{q}}(X_{\gamma_1+\gamma_4}) E_{\mathfrak{q}}(X_{\gamma_2+\gamma_3}) E_{\mathfrak{q}}(X_{\gamma_2}) E_{\mathfrak{q}}(X_{\gamma_4}) \tag{12.7.2}$$

See Figure 12.18.

Observe that a double mutation maps this to

$$E_{\mathfrak{q}}(X_{\gamma_1+\gamma_4}) E_{\mathfrak{q}}(X_{\gamma_2+\gamma_3}) E_{\mathfrak{q}}(X_{\gamma_2}) E_{\mathfrak{q}}(X_{\gamma_4}) E_{\mathfrak{q}}(X_{-\gamma_1}) E_{\mathfrak{q}}(X_{-\gamma_3}) \tag{12.7.3}$$

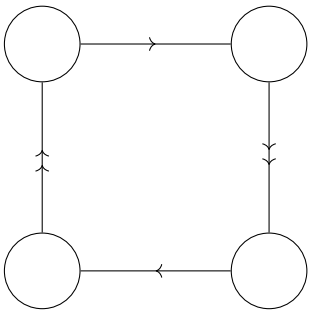


Figure 12.18: BPS quiver for pure $SU(3)$.

which is actually the same expression up to a charge re-definition. This is analogous to the γ_1 mutation in pure $SU(2)$ gauge theory.

Consider now a charge which has non-zero pairing only with γ_1 and γ_2 of the same form as the $SU(2)$ Wilson loop, such as $-\frac{2}{3}\gamma_1 - \frac{2}{3}\gamma_2 - \frac{1}{3}\gamma_4 - \frac{1}{3}\gamma_3$. We will look for a candidate F of the form

$$X_{-\frac{2}{3}\gamma_1-\frac{2}{3}\gamma_2-\frac{1}{3}\gamma_4-\frac{1}{3}\gamma_3} + \cdots \tag{12.7.4}$$

This behaves well under γ_1 and γ_3 mutations. The inverse γ_2 mutation requires an extra term

$$X_{-\frac{2}{3}\gamma_1-\frac{2}{3}\gamma_2-\frac{1}{3}\gamma_4-\frac{1}{3}\gamma_3} + X_{-\frac{2}{3}\gamma_1+\frac{1}{3}\gamma_2-\frac{1}{3}\gamma_4-\frac{1}{3}\gamma_3} + \cdots \tag{12.7.5}$$

and then the γ_1 mutation requires

$$X_{-\frac{2}{3}\gamma_1-\frac{2}{3}\gamma_2-\frac{1}{3}\gamma_4-\frac{1}{3}\gamma_3} + X_{-\frac{2}{3}\gamma_1+\frac{1}{3}\gamma_2-\frac{1}{3}\gamma_4-\frac{1}{3}\gamma_3} + X_{\frac{1}{3}\gamma_1+\frac{1}{3}\gamma_2-\frac{1}{3}\gamma_4-\frac{1}{3}\gamma_3} + \cdots \tag{12.7.6}$$

then inverse γ_4 requires

$$X_{-\frac{2}{3}\gamma_1-\frac{2}{3}\gamma_2-\frac{1}{3}\gamma_3-\frac{1}{3}\gamma_4} + X_{-\frac{2}{3}\gamma_1+\frac{1}{3}\gamma_2-\frac{1}{3}\gamma_3-\frac{1}{3}\gamma_4} + X_{\frac{1}{3}\gamma_1+\frac{1}{3}\gamma_2-\frac{1}{3}\gamma_3-\frac{1}{3}\gamma_4} + X_{\frac{1}{3}\gamma_1+\frac{1}{3}\gamma_2-\frac{1}{3}\gamma_3+\frac{2}{3}\gamma_4} + \cdots \tag{12.7.7}$$

and γ_3 requires the final correction:

$$\begin{aligned} F_{w_3} = {} & X_{-\frac{2}{3}\gamma_1-\frac{2}{3}\gamma_2-\frac{1}{3}\gamma_3-\frac{1}{3}\gamma_4} + X_{-\frac{2}{3}\gamma_1+\frac{1}{3}\gamma_2-\frac{1}{3}\gamma_3-\frac{1}{3}\gamma_4} + X_{\frac{1}{3}\gamma_1+\frac{1}{3}\gamma_2-\frac{1}{3}\gamma_3-\frac{1}{3}\gamma_4} + \\ & + X_{\frac{1}{3}\gamma_1+\frac{1}{3}\gamma_2-\frac{1}{3}\gamma_3+\frac{2}{3}\gamma_4} + X_{\frac{1}{3}\gamma_1+\frac{1}{3}\gamma_2+\frac{2}{3}\gamma_3+\frac{2}{3}\gamma_4} \end{aligned} \tag{12.7.8}$$

which we identify as a fundamental Wilson line. We also have an anti-fundamental candidate:

$$\begin{aligned} F_{w_{\bar{3}}} = {} & X_{-\frac{1}{3}\gamma_1-\frac{1}{3}\gamma_2-\frac{2}{3}\gamma_3-\frac{2}{3}\gamma_4} + X_{-\frac{1}{3}\gamma_1-\frac{1}{3}\gamma_2-\frac{2}{3}\gamma_3+\frac{1}{3}\gamma_4} + X_{-\frac{1}{3}\gamma_1-\frac{1}{3}\gamma_2+\frac{1}{3}\gamma_3+\frac{1}{3}\gamma_4} + \\ & + X_{-\frac{1}{3}\gamma_1+\frac{2}{3}\gamma_2+\frac{1}{3}\gamma_3+\frac{1}{3}\gamma_4} + X_{\frac{2}{3}\gamma_1+\frac{2}{3}\gamma_2+\frac{1}{3}\gamma_3+\frac{1}{3}\gamma_4} \end{aligned} \tag{12.7.9}$$

Another natural candidate for an F is the monomial

$$F_{H_0} = X_{\frac{2}{3}\gamma_1+\frac{1}{3}\gamma_3} \tag{12.7.10}$$

We can combine it with Wilson loops to get other candidates:

$$\begin{aligned}
F_{H_0}\cdot F_{w_3} &= \mathfrak{q}^{-\frac{2}{3}}X_{-\frac{2}{3}\gamma_2-\frac{1}{3}\gamma_4}+\mathfrak{q}^{\frac{1}{3}}(X_{\frac{1}{3}\gamma_2-\frac{1}{3}\gamma_4}+X_{\gamma_1+\frac{1}{3}\gamma_2-\frac{1}{3}\gamma_4}+X_{\gamma_1+\frac{1}{3}\gamma_2+\frac{2}{3}\gamma_4}+X_{\gamma_1+\frac{1}{3}\gamma_2+\gamma_3+\frac{2}{3}\gamma_4})\\
F_{H_0}\cdot F_{w_{\bar 3}} &= \mathfrak{q}^{-\frac{1}{3}}(X_{\frac{1}{3}\gamma_1-\frac{1}{3}\gamma_2-\frac{1}{3}\gamma_3-\frac{2}{3}\gamma_4}+X_{\frac{1}{3}\gamma_1-\frac{1}{3}\gamma_2-\frac{1}{3}\gamma_3+\frac{1}{3}\gamma_4}+X_{\frac{1}{3}\gamma_1-\frac{1}{3}\gamma_2+\frac{2}{3}\gamma_3+\frac{1}{3}\gamma_4})+\\
&\quad+\mathfrak{q}^{\frac{2}{3}}(X_{\frac{1}{3}\gamma_1+\frac{2}{3}\gamma_2+\frac{2}{3}\gamma_3+\frac{1}{3}\gamma_4}+X_{\frac{4}{3}\gamma_1+\frac{2}{3}\gamma_2+\frac{2}{3}\gamma_3+\frac{1}{3}\gamma_4})
\end{aligned}\tag{12.7.11}$$

etcetera. We can define a sequence of dyonic operators as

$$(\mathfrak{q}-\mathfrak{q}^{-1})H_{a+1}=\mathfrak{q}^{\frac{1}{3}}w_3H_a-\mathfrak{q}^{-\frac{1}{3}}H_aw_3\qquad\qquad(\mathfrak{q}-\mathfrak{q}^{-1})H_{a-1}=\mathfrak{q}^{\frac{1}{3}}H_aw_{\bar 3}-\mathfrak{q}^{-\frac{1}{3}}w_{\bar 3}H_a\tag{12.7.12}$$

These satisfy $H_{a+1}H_a=\mathfrak{q}^{\frac{4}{3}}H_aH_{a+1}$. We can also define

$$\bar H_a=\mathfrak{q}^{\frac{1}{3}}H_{a-1}H_{a+1}-\mathfrak{q}^{-1}H_a^2\tag{12.7.13}$$

and more. It would be nice to describe the full set of tropical generators.

We can also consider the RG flow from $SU(3)$ to $SU(2)$ gauge theory, mutating at γ_1 to

$$S'_{SU(3)}=E_{\mathfrak{q}}(X_{\gamma_3})E_{\mathfrak{q}}(X_{\gamma_1+\gamma_4})E_{\mathfrak{q}}(X_{\gamma_2+\gamma_3})E_{\mathfrak{q}}(X_{\gamma_4})E_{\mathfrak{q}}(X_{\gamma_2})E_{\mathfrak{q}}(X_{-\gamma_1})\tag{12.7.14}$$

and setting $S_{SU(2)}=E_{\mathfrak{q}}(X_{\gamma_2})E_{\mathfrak{q}}(X_{-\gamma_1})$, so that the RG flow is associated to the factors

$$E_{\mathfrak{q}}(X_{\gamma_3})E_{\mathfrak{q}}(X_{\gamma_2+\gamma_3})E_{\mathfrak{q}}(X_{\gamma_1+\gamma_4})E_{\mathfrak{q}}(X_{\gamma_4})=E_{\mathfrak{q}}(X_{\gamma_3}+X_{\gamma_2+\gamma_3})E_{\mathfrak{q}}(X_{\gamma_1+\gamma_4}+X_{\gamma_4})\tag{12.7.15}$$

which is the IR image of

$$S^{SU(2)}_{SU(3)}=E_{\mathfrak{q}}(X_{\gamma_3+\frac{1}{2}\gamma_1}H_1^{SU(2)})E_{\mathfrak{q}}(X_{\gamma_4+\frac{1}{2}\gamma_2}H_{-2}^{SU(2)})\,.\tag{12.7.16}$$

The Wilson lines mutate to

$$\begin{aligned}
F_{w_3} &= X_{-\frac{1}{6}\gamma_1-\frac{1}{6}\gamma_2-\frac{1}{3}\gamma_3-\frac{1}{3}\gamma_4}F^{\rm IR}_{w_1^{SU(2)}}+X_{-\frac{1}{6}\gamma_1+\frac{1}{3}\gamma_2-\frac{1}{3}\gamma_3+\frac{2}{3}\gamma_4}F^{\rm IR}_{H_{-1}^{SU(2)}}+X_{\frac{1}{3}\gamma_1+\frac{1}{3}\gamma_2+\frac{2}{3}\gamma_3+\frac{2}{3}\gamma_4}\\
F_{w_{\bar 3}} &= X_{-\frac{1}{3}\gamma_1-\frac{1}{3}\gamma_2-\frac{2}{3}\gamma_3-\frac{2}{3}\gamma_4}+X_{-\frac{1}{3}\gamma_1+\frac{1}{6}\gamma_2-\frac{2}{3}\gamma_3+\frac{1}{3}\gamma_4}F^{\rm IR}_{H_{-2}^{SU(2)}}+X_{\frac{1}{6}\gamma_1+\frac{1}{6}\gamma_2+\frac{1}{3}\gamma_3+\frac{1}{3}\gamma_4}F^{\rm IR}_{w_1^{SU(2)}}
\end{aligned}\tag{12.7.17}$$

It would be interesting to discuss a partial diagonalization of these operators in the $SU(2)$ theory. It should be implemented by the superconformal index for 3×2 3d chiral multiplets, a wavefunction written as the ratio of six $\mathfrak{q}^2$-factorials at numerator and six at denominator.

12.7.1 Adding fundamental flavour

We verified that the contribution of a fundamental representation,

$$E_{\mathfrak{q}}(\mu\zeta_1^{-\frac{2}{3}}\zeta_2^{-\frac{1}{3}})E_{\mathfrak{q}}(\mu\zeta_1^{\frac{1}{3}}\zeta_2^{-\frac{1}{3}})E_{\mathfrak{q}}(\mu\zeta_1^{\frac{1}{3}}\zeta_2^{\frac{2}{3}})=g_3(\mu,\zeta_1^{-\frac{2}{3}}\zeta_2^{-\frac{1}{3}}+\zeta_1^{\frac{1}{3}}\zeta_2^{-\frac{1}{3}}+\zeta_1^{\frac{1}{3}}\zeta_2^{\frac{2}{3}},\zeta_1^{-\frac{1}{3}}\zeta_2^{-\frac{2}{3}}+\zeta_1^{-\frac{1}{3}}\zeta_2^{\frac{1}{3}}+\zeta_1^{\frac{2}{3}}\zeta_2^{\frac{1}{3}})\tag{12.7.18}$$

factors nicely:

$$g_3(\mu, w_3, w_{\bar{3}}) = E_{\mathfrak{q}}(X_{-\frac{2}{3}\gamma_1-\frac{2}{3}\gamma_2-\frac{1}{3}\gamma_3-\frac{1}{3}\gamma_4})E_{\mathfrak{q}}(X_{-\frac{2}{3}\gamma_1+\frac{1}{3}\gamma_2-\frac{1}{3}\gamma_3-\frac{1}{3}\gamma_4})\cdot \\ \cdot E_{\mathfrak{q}}(X_{\frac{1}{3}\gamma_1+\frac{1}{3}\gamma_2-\frac{1}{3}\gamma_3-\frac{1}{3}\gamma_4})E_{\mathfrak{q}}(X_{\frac{1}{3}\gamma_1+\frac{1}{3}\gamma_2-\frac{1}{3}\gamma_3+\frac{2}{3}\gamma_4})E_{\mathfrak{q}}(X_{\frac{1}{3}\gamma_1+\frac{1}{3}\gamma_2+\frac{2}{3}\gamma_3+\frac{2}{3}\gamma_4}) \tag{12.7.19}$$

This leads to a prediction for the spectrum generator of $SU(3)$ with $N_f = 1$:

$$S = E_{\mathfrak{q}}(X_{-\frac{2}{3}\gamma_1-\frac{2}{3}\gamma_2-\frac{1}{3}\gamma_3-\frac{1}{3}\gamma_4})E_{\mathfrak{q}}(X_{-\frac{2}{3}\gamma_1+\frac{1}{3}\gamma_2-\frac{1}{3}\gamma_3-\frac{1}{3}\gamma_4})E_{\mathfrak{q}}(X_{\frac{1}{3}\gamma_1+\frac{1}{3}\gamma_2-\frac{1}{3}\gamma_3-\frac{1}{3}\gamma_4})\cdot \\ \cdot E_{\mathfrak{q}}(X_{\frac{1}{3}\gamma_1+\frac{1}{3}\gamma_2-\frac{1}{3}\gamma_3+\frac{2}{3}\gamma_4})E_{\mathfrak{q}}(X_{\frac{1}{3}\gamma_1+\frac{1}{3}\gamma_2+\frac{2}{3}\gamma_3+\frac{2}{3}\gamma_4})\cdot \\ \cdot E_{\mathfrak{q}}(X_{\gamma_1})E_{\mathfrak{q}}(X_{\gamma_3})E_{\mathfrak{q}}(X_{\gamma_1+\gamma_4})E_{\mathfrak{q}}(X_{\gamma_2+\gamma_3})E_{\mathfrak{q}}(X_{\gamma_2})E_{\mathfrak{q}}(X_{\gamma_4})\,. \tag{12.7.20}$$

12.7.2 Wild chambers

We now go back to pure $SU(3)$ and explore the potential mismatch between the mutation orbit of the original BPS quiver and the collection of physically realizable RG flows. The key observation is that if we mutate at γ_1 and then γ_2, the new BPS quiver has three edges between the first and last nodes. If an RG flow existed which allows decoupling of the remaining nodes, we will land on a BPS quiver which does not seem to correspond to a physical theory.

The node γ_3 does not really play a role in the sequence of mutations, so the problem would already manifest in a simpler model where we decoupled γ_3 from the very beginning. This leads to the question: is there a partial RG flow which eliminates a single node of the $SU(3)$ quiver?

The geometry of the space of vacua of pure $SU(3)$ gauge theory is intricate. The space of vacua is parameterized by two complex variables u and v. When u and v are both very large, instanton effects are suppressed and the space of vacua has an intuitive characterization: there is a weak-coupling discriminant $v^2 - u^3$ and near the vanishing locus of the discriminant the $SU(3)$ theory flows to a pure $SU(2) \times U(1)$ gauge theory first, and then to the IR description of the latter. This the RG flow we already discussed. The proposal of the partial spectrum generator capturing two BPS particles which behave as $H_1^{SU(2)}$ and $H_{-2}^{SU(2)}$ dressed by Abelian charges appears to be novel.

In order to find other interesting RG flows, we need to make one of these BPS particles light, possibly by exploring smaller values of u and v. The instanton-corrected discriminant, in units of the instanton action, is a more complicated polynomial in u^3 and v^2 which vanishes at loci where a BPS particle of the Seiberg-Witten description has vanishing mass. The loci are simply described as $v(u) = \pm u^{\frac{3}{2}} \pm 1$.

Another well-known RG flow goes to the $[A_1, A_2]$ Argyres-Douglas theory, say by dropping γ_2 and γ_3. This happens when, say, $1 - u^{\frac{3}{2}} = -1 + u^{\frac{3}{2}}$ and two branches of the vanishing locus meet. A partial RG flow dropping γ_3 would be a partial step in both known RG flows. It would essentially require one to keep three of the $v(u)$ values closer to each other than the fourth. This is manifestly impossible.

We conclude that an RG flow such as described by

$$S'_{SU(3)} = E_{\mathfrak{q}}(X_{\gamma_3})E_{\mathfrak{q}}(X_{\gamma_2+\gamma_3})S'_{\rm IR} \tag{12.7.21}$$

with

$$S'_{\rm IR} = E_{\mathfrak{q}}(X_{\gamma_1+\gamma_4})E_{\mathfrak{q}}(X_{\gamma_4})E_{\mathfrak{q}}(X_{\gamma_2})E_{\mathfrak{q}}(X_{-\gamma_1}) \tag{12.7.22}$$

should be unphysical. The candidate IR theory can be more concisely described in terms of the spectrum generator

$$S_{\rm IR} = E_{\mathfrak{q}}(X_{\gamma_4})E_{\mathfrak{q}}(X_{\gamma_1})E_{\mathfrak{q}}(X_{\gamma_2}) \tag{12.7.23}$$

This should be another example of BPS quiver which fails to lead to a consistent Schur quantization. As for the simpler example of the quiver with three arrows, we expect this to happen because some $\langle a|b\rangle$ inner products diverge.

12.8 Applications to the theory of quantum groups

The (central quotient of) the quantum groups $U_{\mathfrak{q}}(\mathfrak{g})$, presented as an algebra over $\mathbb{Z}[\mathfrak{q},\mathfrak{q}^{-1}]$ [11], is a special case of an algebra $\mathcal{A}$ which is expected to be associated to a 4d $\mathcal{N}=2$ gauge theory and thus amenable of our analysis. We will denote the theory as $T^{4d}[\mathfrak{g}]$, as it is a close relative of a 3d theory which plays an important role in S-duality.

In particular, there is a conjectural definition of $T^{4d}[\mathfrak{sl}_N]$ as a balanced quiver gauge theory with $N-1$ unitary nodes with rank increasing linearly from 1 to $N-1$. The identification with the central quotient of $U_{\mathfrak{q}}(\mathfrak{sl}_N)$ is well understood. It also has a class $\mathcal{S}$ description which makes contact with a known relation between $U_{\mathfrak{q}}(\mathfrak{sl}_N)$ and quantized character varieties.

Our results thus lead to a simple conjecture: the quantum spectrum generators S associated to such cluster parameterizations of $U_{\mathfrak{q}}(\mathfrak{g})$ must be normalizable and there is a well-defined complex cluster quantization of $U_{\mathfrak{q}}(\mathfrak{g})$ leading to spherical unitary representations with unitary central character μ. Gauging the Abelian flavour symmetry associated to μ should lead to representations of a larger algebra which decomposes into sectors with arbitrary μ with $|\mu| = \mathfrak{q}^k$ with integral k.

These theories are expected to be part of a more general family of theories $T^{4d}_{\rho}[\mathfrak{g}]$ for which we have a map $U_{\mathfrak{q}}(\mathfrak{g}) \to \mathcal{A}$ with special values of the Casimir generators of the quantum group. In particular, there is a conjectural definition of $T^{4d}_{\rho}[\mathfrak{sl}_N]$ as a balanced quiver gauge theories with $N-1$ unitary nodes but more general choices of rank.

These theories do have a class $\mathcal{S}$ description, but the corresponding character varieties do not have a known systematic cluster definition. The gauge theory description is thus a valuable tool to explore quantum group representations.

In this Section we would like to spell out some concrete examples of these statements. A full discussion would deserve a separate publication.

12.8.1 The central quotient of $U_{\mathfrak{q}}(\mathfrak{sl}_2)$ and SQED$_2$.

This case was discussed at some length in previous work. As the $U(1)$ gauge group is Abelian, the RG flow to a pure $U(1)$ gauge theory is very simple and the spectrum

[11] in a manner which does not seem to coincide with the Lusztig form

generator is written as

$$S = E_{\mathfrak{q}}(X_{0,1,1})E_{\mathfrak{q}}(X_{0,1,-1}) \tag{12.8.1}$$

with $\mu = X_{0,0,1}$ being a flavour parameter which will control the Casimir of $U_{\mathfrak{q}}(\mathfrak{sl}_2)$ and $\langle (1,0,0),(0,1,0)\rangle = 1$.

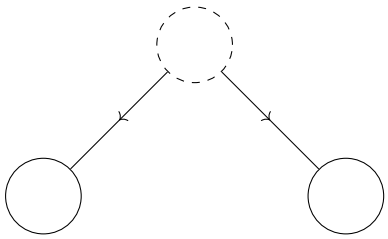


Figure 12.19: The BPS quiver for SQED_2.

The basic loop operators $D_{a,b}$ give the standard (divided powers of) quantum group generators up to a rescaling which makes the algebra over $\mathbb{Z}[\mathfrak{q},\mathfrak{q}^{-1}]$. In particular, we have multiplicative generators $u_+ = D_{1,0}$, $u_- = D_{-1,-1}$, $v^{\pm} = D_{0,\pm 1}$ and relations

$$\begin{aligned} u_+u_- &= \mathfrak{q}^{-1}v^{-1} + \mu + \mu^{-1} + \mathfrak{q}v \\ u_-u_+ &= \mathfrak{q}v^{-1} + \mu + \mu^{-1} + \mathfrak{q}^{-1}v \end{aligned} \tag{12.8.2}$$

with quadratic Casimir proportional to $\mu + \mu^{-1}$ and

$$\begin{aligned} F_v &= X_{0,1,0} \\ F_{u_+} &= X_{1,0,0} \\ F_{u_-} &= X_{-1,-1,0} + X_{-1,0,1} + X_{-1,0,-1} + X_{-1,1,0} \end{aligned} \tag{12.8.3}$$

In particular, $u_- = \ell_{-1,-1,0} = \rho(\mathfrak{q}u_+v^{-1})$ and $u_+ = \rho(\mathfrak{q}u_-v)$, $\rho(v) = v^{-1}$. So $\rho(u_+) = \mathfrak{q}v^{-1}u_-$ and $\rho(u_-) = \mathfrak{q}vu_+$.

We denote the associated representation on $\ell^2(\mathbb{Z}^2)$ as a spherical principal series representation.

12.8.2 The $\mathfrak{q}$ analogue of the $L^2(\mathbb{C}^2)$ spectral decomposition

If we gauge the $U(1)$ symmetry associated to μ, we embed A in a larger algebra A' where μ is now a non-trivial generator, a close relative of $\mathcal{W}^2$. We can roughly think about this as a $\mathfrak{q}$-oscillator representation of the quantum group.

In order to simplify the presentation, we will extend $\mathcal{W}$ to an algebra $\mathcal{W}_2$ over $\mathbb{Z}[\mathfrak{q}^{\frac{1}{2}},\mathfrak{q}^{-\frac{1}{2}}]$. We will denote the generators of $\mathcal{W}_2$ as $p_\pm$ and x, with

$$\begin{aligned} p_\pm v &= \mathfrak{q}^{\pm} x p_\pm \\ p_+p_- &= \mathfrak{q}^{\frac{1}{2}}x + \mathfrak{q}^{-\frac{1}{2}}x^{-1} \\ p_-p_+ &= \mathfrak{q}^{-\frac{1}{2}}x + \mathfrak{q}^{\frac{1}{2}}x^{-1} \end{aligned} \tag{12.8.4}$$

Then given two copies of the algebra we write

$$\begin{aligned} v &= x_1 x_2 \\ \mu &= x_1 x_2^{-1} \\ u_+ &= p_{1,+} p_{2,+} \\ u_- &= p_{1,-} p_{2,-} \end{aligned} \tag{12.8.5}$$

Then $\mathcal{W}_2$ can be represented on $\ell^2(\mathbb{Z} \oplus \frac{1}{2}\mathbb{Z})$, say by

$$\begin{aligned} F_x &= X_{0,\frac{1}{2}} \\ F_{p_+} &= X_{1,0} \\ F_{p_-} &= X_{-1,\frac{1}{2}} + X_{-1,-\frac{1}{2}} \end{aligned} \tag{12.8.6}$$

Accordingly, we represent $\mathcal{A}$ on $\ell^2(\mathbb{Z} \oplus \frac{1}{2}\mathbb{Z}) \otimes \ell^2(\mathbb{Z} \oplus \frac{1}{2}\mathbb{Z})$.

The image of the spherical vector under A is obviously supported on $(m, a; m, b)$. Summands of the Hilbert space supported on $(m, a; m + k, b)$ are eigenspaces of $|\mu|^2 = \mathfrak{q}^k$. Each can be further decomposed into distributional eigenspaces for μ which can be identified as non-spherical principal series representations of $\mathcal{A}$. These are literally $\mathfrak{q}$-deformed versions of familiar representations of $SL(2, \mathbb{C})$ appearing in a spectral decomposition of $L^2(\mathbb{C}^2)$, wavefunctions on $\mathbb{C}^2$ with $GL(2)$ acting as holomorphic rotations.

12.8.3 $U(2)$ with $N_f = 1$

The $SU(2)$ $N_f = 1$ theory has a $U(1)$ flavour symmetry acting on two hypermultiplets. Gauging the $U(1)$ will thus enlarge the operator algebra to include a copy of $U_{\mathfrak{q}}(\mathfrak{sl}_2)$, with Casimir equal to the Wilson loop $D_{0,1}$.

A possible application of this structure is to give a first example of the relation between quantum group representation theory and the diagonalizing $D_{0,1}$.

Add an Abelian magnetic charge γ_m with $\langle \gamma_m, \gamma_3 \rangle = 1$ and other vanishing. In the RG chamber, we can set $F_v = \mu = X_{\frac{1}{2}\gamma_1 + \frac{1}{2}\gamma_2 + \gamma_3}$,

$$F_{u_+} = X_{\gamma_m} \,. \tag{12.8.7}$$

Then $u_+ u_- = \mathfrak{q} v + D_{0,1} + \mathfrak{q}^{-1} v^{-1}$ gives

$$F_{u_-} = X_{-\gamma_m - \frac{1}{2}\gamma_1 - \frac{1}{2}\gamma_2 - \gamma_3} + X_{-\gamma_m - \frac{1}{2}\gamma_1 - \frac{1}{2}\gamma_2} + X_{-\gamma_m - \frac{1}{2}\gamma_1 + \frac{1}{2}\gamma_2} + X_{-\gamma_m + \frac{1}{2}\gamma_1 + \frac{1}{2}\gamma_2} + X_{-\gamma_m + \frac{1}{2}\gamma_1 + \frac{1}{2}\gamma_2 + \gamma_3} \tag{12.8.8}$$

We thus get a spherical representation of (the $*$-double of) $U_{\mathfrak{q}}(\mathfrak{sl}_2)$ on $\ell^2(\mathbb{Z}\gamma_m \oplus \Gamma)$ which can be decomposed into principal series representations by diagonalizing $F_{D_{1,0}}$. The diagonalization gives the UV presentation of Schur quantization, so each representation should occur once (in the distributional sense) and the UV presentation makes the decomposition of individual $|a\rangle$ vectors very explicit. Conversely, diagonalizing v gives representations of the $N_f = 1$ algebra.

In the primed chamber, the quantum group generators are simpler:

$$\begin{aligned} F'_v &= X_{\frac{1}{2}\gamma_1+\frac{1}{2}\gamma_2+\gamma_3} \\ F'_{u_+} &= X_{\gamma_m} + X_{\gamma_m+\gamma_3} \\ F'_{u_-} &= X_{-\gamma_m-\frac{1}{2}\gamma_1-\frac{1}{2}\gamma_2-\gamma_3} + X_{-\gamma_m-\frac{1}{2}\gamma_1+\frac{1}{2}\gamma_2} + X_{-\gamma_m+\frac{1}{2}\gamma_1+\frac{1}{2}\gamma_2} \end{aligned} \tag{12.8.9}$$

but the Casimir generator is a bit more complicated.

Again, formulae will be a bit simpler if we enlarge the relevant algebras slightly at the price of allowing powers of $\mathfrak{q}^{\frac{1}{2}}$. We can include operators which have half-integral magnetic charges for both gauge groups:

$$\begin{aligned} F'_{D_{\frac{1}{2},\frac{1}{2};0,0}} &= X_{\frac{1}{2}\gamma_m+\frac{1}{2}\gamma_1} \\ F'_{D_{\frac{1}{2},\frac{1}{2};-1,0}} &= X_{\frac{1}{2}\gamma_m-\frac{1}{2}\gamma_2} \\ F'_{D_{\frac{1}{2},-\frac{1}{2};0,0}} &= X_{-\frac{1}{2}\gamma_m+\frac{1}{2}\gamma_1} \\ F'_{D_{\frac{1}{2},-\frac{1}{2};-1,0}} &= X_{-\frac{1}{2}\gamma_m-\frac{1}{2}\gamma_2} + X_{-\frac{1}{2}\gamma_m+\frac{1}{2}\gamma_2+\gamma_3} \end{aligned} \tag{12.8.10}$$

which have a nice interplay with the quantum group generators $u_\pm$.

12.8.4 Glued quantum groups

We will only look briefly at the next example, mostly in light of a possible application to real versions of Schur quantization. The idea is to start from $SU(2)$ with $N_f = 2$ and gauge both $U(1)$ flavour symmetries, to get an extended algebra with two $U_\mathfrak{q}(\mathfrak{sl}_2)$ sub-algebras. The Casimir of both sub-algebras coincide with the Wilson loop $D_{0,1}$.

If we add charges γ_m and γ_n dual to γ_3 and γ_4 respectively, the F's for the two sets of quantum group generators are identical to these in the previous example, one literally and the other under $\gamma_3 \to \gamma_4$, $\gamma_m \to \gamma_n$.

Mutating to the primed chamber, one can do a partial RG flow preserving a doublet of simple charges, mapping the algebra to a combination of two $\mathcal{W}$'s and a quantum torus algebra. This does not seem particularly illuminating, so we will omit it.

We expect this algebra to be a $\mathfrak{q}$-deformed version of the algebra of holomorphic vectorfields on $SL(2,\mathbb{C})$, with $U(\mathfrak{sl}_2)$ acting by left- and right- vectorfields. Again, we leave the details to the enthusiastic reader.

By construction, the diagonalization of the Wilson line $D_{0,1}$ will decompose the Schur quantization representation into a direct integral of products of principal series representations for the two $U_\mathfrak{q}(\mathfrak{sl}_2)$'s with the same character, each appearing once.

12.8.5 The $U_\mathfrak{q}(\mathfrak{sl}_2)$ coproduct as a partial RG flow

The $SU(2)$ $N_f = 3$ theory can be maximally enlarged by gauging three $U(1)$ flavour groups. The resulting algebra has three $U_\mathfrak{q}(\mathfrak{sl}_2)$ sub-algebras, with coincident Casimirs given by $D_{0,1}$.

A crucial feature is the possibility of an RG flow to four copies of $\mathcal{W}_2$, represented by the four symmetric nodes in the last BPS quiver presentation of the theory given above. This should be an $\mathfrak{q}$-deformation of the embedding of three $U(\mathfrak{sl}_2)$ in a Weyl algebra with 8 generators, which has interesting Langlands applications.

Furthermore, we will argue that if we focus on a single copy of $U_\mathfrak{q}(\mathfrak{sl}_2)$ in the extended algebra, the map to $\mathcal{W}_2^4$ coincides with a well-known realization of the $U_\mathfrak{q}(\mathfrak{sl}_2)$ coproduct, composed with the maps to $\mathcal{W}_2^2$ we discussed above. Accordingly, if we diagonalize μ_2 and μ_3 we will find the coproduct of principal series representations with the corresponding Casimirs.

The diagonalization of $D_{1,0}$ then solves the problem of decomposing the coproduct of two principal series representations of $U_\mathfrak{q}(\mathfrak{sl}_2)$ into principal series representations and the UV formulae for the Scur index essentially provide the Clebsh-Gordon coefficients. This is an $\mathfrak{q}$-deformation of an analogous statement about $SL(2,\mathbb{C})$ actions on $L^2(\mathbb{C}^4)$.

In order to builg the appropriate lattice for this example, we add charges γ_m, γ_n, γ_o dual to $\gamma_{4,5,6}$ respectively, as we did in simpler examples. Hence

$$\begin{aligned}
F_{v_1} &= \mu_1 = X_{\frac{1}{2}\gamma_1+\frac{1}{2}\gamma_2+\gamma_3} \\
F_{u_{1,+}} &= X_{\gamma_m} \\
F_{u_{1,-}} &= X_{-\gamma_m-\frac{1}{2}\gamma_1-\frac{1}{2}\gamma_2-\gamma_3} + X_{-\gamma_m-\frac{1}{2}\gamma_1-\frac{1}{2}\gamma_2} + X_{-\gamma_m-\frac{1}{2}\gamma_1+\frac{1}{2}\gamma_2} + X_{-\gamma_m+\frac{1}{2}\gamma_1+\frac{1}{2}\gamma_2} \\
&\quad + X_{-\gamma_m+\frac{1}{2}\gamma_1+\frac{1}{2}\gamma_2+\gamma_3}
\end{aligned} \tag{12.8.11}$$

etcetera. We can now perform a series of mutations:

$$\begin{aligned}
F'_{v_1} &= \mu_1 = X_{\frac{1}{2}\gamma_1+\frac{1}{2}\gamma_2+\gamma_3} \\
F'_{u_{1,+}} &= X_{\gamma_m} + X_{\gamma_m+\gamma_3} \\
F'_{u_{1,-}} &= X_{-\gamma_m-\frac{1}{2}\gamma_1-\frac{1}{2}\gamma_2-\gamma_3} + X_{-\gamma_m-\frac{1}{2}\gamma_1+\frac{1}{2}\gamma_2} + X_{-\gamma_m-\frac{1}{2}\gamma_1+\frac{1}{2}\gamma_2+\gamma_4} + X_{-\gamma_m-\frac{1}{2}\gamma_1+\frac{1}{2}\gamma_2+\gamma_5} \\
&\quad + X_{-\gamma_m-\frac{1}{2}\gamma_1+\frac{1}{2}\gamma_2+\gamma_4+\gamma_5} + X_{-\gamma_m+\frac{1}{2}\gamma_1+\frac{1}{2}\gamma_2}
\end{aligned} \tag{12.8.12}$$

and

$$\begin{aligned}
F''_{v_1} &= \mu_1 = X_{\frac{1}{2}\gamma_1+\frac{1}{2}\gamma_2+\gamma_3} \\
F''_{u_{1,+}} &= X_{\gamma_m} + X_{\gamma_m+\gamma_2+\gamma_3+\gamma_4+\gamma_5} + X_{\gamma_m+\gamma_3} \\
F''_{u_{1,-}} &= X_{-\gamma_m-\frac{1}{2}\gamma_1-\frac{1}{2}\gamma_2-\gamma_3} + X_{-\gamma_m-\frac{1}{2}\gamma_1+\frac{1}{2}\gamma_2} + X_{-\gamma_m-\frac{1}{2}\gamma_1+\frac{3}{2}\gamma_2+\gamma_3+\gamma_4+\gamma_5} + X_{-\gamma_m-\frac{1}{2}\gamma_1+\frac{1}{2}\gamma_2+\gamma_4} \\
&\quad + X_{-\gamma_m-\frac{1}{2}\gamma_1+\frac{1}{2}\gamma_2+\gamma_5} + X_{-\gamma_m+\frac{1}{2}\gamma_1+\frac{1}{2}\gamma_2}
\end{aligned} \tag{12.8.13}$$

to finally obtain:

$$\begin{aligned}
F'''_{v_1} &= \mu_1 = X_{\frac{1}{2}\gamma_1+\frac{1}{2}\gamma_2+\gamma_3} \\
F'''_{u_{1,+}} &= X_{\gamma_m} + X_{\gamma_m+\gamma_2+\gamma_3+\gamma_4+\gamma_5} + X_{\gamma_m+\gamma_1+\gamma_2+\gamma_3+\gamma_4+\gamma_5} + X_{\gamma_m+\gamma_3} + X_{\gamma_m+\gamma_1+\gamma_3} \\
F'''_{u_{1,-}} &= X_{-\gamma_m-\frac{1}{2}\gamma_1-\frac{1}{2}\gamma_2-\gamma_3} + X_{-\gamma_m-\frac{1}{2}\gamma_1+\frac{1}{2}\gamma_2} + X_{-\gamma_m-\frac{1}{2}\gamma_1+\frac{3}{2}\gamma_2+\gamma_3+\gamma_4+\gamma_5} + \qquad (12.8.14) \\
&\quad + X_{-\gamma_m-\frac{1}{2}\gamma_1+\frac{1}{2}\gamma_2+\gamma_4} + X_{-\gamma_m-\frac{1}{2}\gamma_1+\frac{1}{2}\gamma_2+\gamma_5}\,.
\end{aligned} \tag{12.8.15}$$

In this chamber, we would like to have an RG flow from

$$S''' = E_{\mathfrak{q}}(X_{-\gamma_2-\gamma_3-\gamma_4-\gamma_5})E_{\mathfrak{q}}(X_{\gamma_2+\gamma_4+\gamma_5})E_{\mathfrak{q}}(X_{\gamma_2+\gamma_3+\gamma_5})E_{\mathfrak{q}}(X_{\gamma_2+\gamma_3+\gamma_4})E_{\mathfrak{q}}(X_{-\gamma_1}) \tag{12.8.16}$$

to

$$S_{\rm IR} = E_{\mathfrak{q}}(X_{\gamma_2+\gamma_4+\gamma_5})E_{\mathfrak{q}}(X_{\gamma_2+\gamma_3+\gamma_5})E_{\mathfrak{q}}(X_{\gamma_2+\gamma_3+\gamma_4})E_{\mathfrak{q}}(X_{-\gamma_1}) \tag{12.8.17}$$

The arguments will be the x_i^2 for the four copies of $\mathcal{W}_2$. We can identify dual variables:

$$\begin{aligned}
F^{\rm IR}_{p_{1,+}} &= X_{-\frac{1}{2}\gamma_m+\frac{1}{2}\gamma_n+\frac{1}{2}\gamma_o} \\
F^{\rm IR}_{p_{1,-}} &= X_{\frac{1}{2}\gamma_m-\frac{1}{2}\gamma_n-\frac{1}{2}\gamma_o-\frac{1}{2}\gamma_2-\frac{1}{2}\gamma_4-\frac{1}{2}\gamma_5} + X_{\frac{1}{2}\gamma_m-\frac{1}{2}\gamma_n-\frac{1}{2}\gamma_o+\frac{1}{2}\gamma_2+\frac{1}{2}\gamma_4+\frac{1}{2}\gamma_5} \\
F^{\rm IR}_{p_{2,+}} &= X_{\frac{1}{2}\gamma_m-\frac{1}{2}\gamma_n+\frac{1}{2}\gamma_o} \\
F^{\rm IR}_{p_{2,-}} &= X_{-\frac{1}{2}\gamma_m+\frac{1}{2}\gamma_n-\frac{1}{2}\gamma_o-\frac{1}{2}\gamma_2-\frac{1}{2}\gamma_3-\frac{1}{2}\gamma_5} + X_{-\frac{1}{2}\gamma_m+\frac{1}{2}\gamma_n-\frac{1}{2}\gamma_o+\frac{1}{2}\gamma_2+\frac{1}{2}\gamma_3+\frac{1}{2}\gamma_5} \\
F^{\rm IR}_{p_{3,+}} &= X_{\frac{1}{2}\gamma_m+\frac{1}{2}\gamma_n-\frac{1}{2}\gamma_o} \\
F^{\rm IR}_{p_{3,-}} &= X_{-\frac{1}{2}\gamma_m-\frac{1}{2}\gamma_n+\frac{1}{2}\gamma_o-\frac{1}{2}\gamma_2-\frac{1}{2}\gamma_3-\frac{1}{2}\gamma_4} + X_{-\frac{1}{2}\gamma_m-\frac{1}{2}\gamma_n+\frac{1}{2}\gamma_o+\frac{1}{2}\gamma_2+\frac{1}{2}\gamma_3+\frac{1}{2}\gamma_4} \\
F^{\rm IR}_{p_{4,+}} &= X_{-\frac{1}{2}\gamma_m-\frac{1}{2}\gamma_n-\frac{1}{2}\gamma_o-\frac{1}{2}\gamma_1+\frac{1}{2}\gamma_2} \\
F^{\rm IR}_{p_{4,-}} &= X_{\frac{1}{2}\gamma_m+\frac{1}{2}\gamma_n+\frac{1}{2}\gamma_o+\gamma_1-\frac{1}{2}\gamma_2} + X_{\frac{1}{2}\gamma_m+\frac{1}{2}\gamma_n+\frac{1}{2}\gamma_o-\frac{1}{2}\gamma_2}
\end{aligned} \tag{12.8.18}$$

so that e.g.

$$\begin{aligned}
{\rm RG}(v_1) &= x_1^{-1}x_2x_3x_4^{-1} \\
{\rm RG}(u_{1,+}) &= p_{2,+}p_{3,+} + x_2x_3p_{4,-}p_{1,-} \\
{\rm RG}(u_{1,-}) &= p_{1,+}p_{4,+} + x_1x_4p_{2,-}p_{3,-}
\end{aligned} \tag{12.8.19}$$

which is a nice coproduct of two sets of bilinear generators embedded in two copies of $\mathcal{W}_2^2$. The relative spectrum generator is $E_{\mathfrak{q}}(\mathfrak{q}^2\prod_i x_i^{-1}p_{i,+})$.

Notice that the Casimirs of the two sets of bilinear quantum group generators are controlled by $\mu_2\mu_3$ and μ_2/μ_3, as expected from the character variety interpretation of the coproduct.

12.9 Partial RG flows and $SL(2)$ character varieties

In this Section we will very briefly discuss a geometric perspective on partial RG flows in for theories of class $\mathcal{S}$ associated to $\mathfrak{sl}_2$. Recall that the theories are labeled by a compact surface C, possibly decorated by punctures which can be regular or irregular.

Regular punctures are associated to an $SU(2)$ flavour symmetry factor. Irregular punctures are labeled by an half-integral rank and for integral rank they are associated to a $U(1)$ factor of the flavour group, which we will often weakly gauge.

As long as ranks are bounded by 1, the class $\mathcal{S}$ theories will have multiple equivalent Lagrangian descriptions. Higher rank punctures can be defined by partial RG flow from multiple punctures of lower rank.

When discussing the associated algebra $\mathcal{A}$, it is useful to formally replace irregular singularities of rank $k/2$ with small holes with k marked points. The algebra is a variant of the familiar Skein algebra for $\mathfrak{sl}_2$ Chern-Simons theory, where lines are allowed to end at marked points. The roles governing these marked points are a bit complicated and we will not attempt to review them here.

As long as C has at least one puncture, typical Coulomb RG flows are labelled by triangulations of C, with vertices at punctures or marked points [327].

In that context, the resulting BPS quiver has nodes associated to internal edges and arrows associated to vertices of individual triangles, joining the corresponding pairs of edges counterclockwise. Each of the $SU(2)$ examples discussed in the previous Sections can be recovered in this manner.

It was observed (see e.g. [367]) that each edge of the triangulation can be thought of as capturing some part of the RG flow. Indeed, from the perspective of this Chapter we would consider partial triangulations of C as representing partial RG flows to an IR theory which includes both $U(1)$ gauge fields and matter theories associated to the surface C_{IR} obtained from C by cutting along edges. We also expect the RG flow map on the Skein algebra to be "local", with precise rules on how to break lines which cross the edges.

If this perspective is correct, the minimal RG flow step consists of adding an edge and cutting along it, and more general RG flows can be expressed in multiple ways as sequences of minimal flows.

We can give some concrete justifications for this proposal. For example, consider a surface with two regular punctures and an edge between them. The two theories have very similar Lagrangian descriptions, when available: the UV theory includes an $SU(2)$ gauge group acting on $T^*\mathbb{C}^4$, the IR theory is obtained by replacing $T^*\mathbb{C}^4$ with $T^*\mathbb{C}^2$. The corresponding RG flow is naturally triggered by giving a large mass to the $T^*\mathbb{C}^2$ matter fields we want to remove.

Skeins with lines which pass between the two punctures map to line defects with magnetic charge under $SU(2)$ and the "cutting" rules are associated to the behavior of these 't Hooft operators when some matter is removed. If we use our "gauging" technology to decompose S_{UV} and S_{IR} in terms of the spectrum generator of pure $SU(2)$ gauge theory, we see that they will differ by a simple factor of $f_2(\mu, w_1)$ as in our examples. Here w_1 is the algebra element associated to a loop around the two punctures.

Similarly, we can consider an edge which joins a puncture to itself, going around a non-trivial loop on the surface. Then cutting along the edge leaves behind two irregular punctures of rank $\frac{1}{2}$ on C_{IR}. In a gauge theory description, we have two $SU(2)$ gauge fields acting on bi-fundamental hypermultiplets. Giving a mass to these and removing them leaves the expected gauge theory description associated to C_{IR}. Conversely, we would build S_{UV} from S_{IR} by adding $f_{2\times 2}(\mu, w_1, w_1')$. Here w_1 and w_1' are the loops just to the left and just to the right of the cut.

A progressive decomposition of C will at some point require cutting along edges with at least one end on a marked point. In turn, this will require increasingly complex RG flows which we have not explored at this point.

An interesting exception is an edge which joins the two marked points of a rank 1 singularity along some non-trivial path. We can pick a duality frame such that the whole gadget is captured by an $SU(2)$ $N_f = 3$ theory coupled to the rest by gauging an $SO(4)$ subgroup of the flavour symmetry. The RG flow we studied in the context of the quantum group coproduct then breaks the curve into two IR curves both with a regular puncture, coupled by a diagonal $U(1)$ gauge field. The spectrum generator for this flow was described above.

Accordingly, as soon as a singe rank 1 irregular singularity appears, the curve can be rapidly decomposed until no non-trivial loops connecting the two marked points of a rank 1 singularity exist. This leaves building blocks which we have already studied as $SU(2)$ gauge theory examples. In all these situations, we can thus verify the expected IR BPS quiver and even build the spectrum generator systematically. It would be interesting to compare the result with other approaches, such as the construction of Strebel spectral networks [381].

12.10 Quantization of the Teichmüller space

In this section we address the quantization of the Teichmüller space associated to punctured Riemann surfaces. In the regime $|\mathfrak{q}|^2 = 1$ this subject has a long history [299–304,304–306], both in the infinite dimensional representations for generic $\mathfrak{q}$, and more recently in the finite dimensional case where $\mathfrak{q}$ is a root of unity [382]. Our goal here is extend this construction to the Schur quantization regime, where the moduli space of flat connection is quantized for $0 < |\mathfrak{q}|^2 < 1$. This question naturally arises in our work as the Teichmüller space corresponds to the phase space of $\mathfrak{sl}_2(\mathbb{C})$ Chern-Simons theory in its Schur quantization[83], and therefore to the phase space [312] of Lorentzian de Sitter 3d gravity[12]. As we see shortly, the construction of the Teichmüller space follows from the IR Schur quantization applied to theories of class $\mathcal{S}$, and it is deeply connected to the theory of quantum groups and cluster algebras [341,343].

Let us briefly summarize the construction before delving into the details. Providing a quantization of the Teichmüller space accounts to constructive a (projective) representation of the (dotted) Ptolemy groupoid, whose objects consist of ideal (decorated) triangulations and its morphisms are *flips* among them corresponding to the Mapping Class Group action. Concretely in Kashaev's construction, one defines coordinates on the Teichmüller space associating to each (marked) triangulations a vector space, spanned by a quantization of Kashaev's coordinates, onto which the flip morphisms act as linear operators generating quantum coordinate change. For $|\mathfrak{q}| = 1$, these linear operators are constructed based on the Faddeev non-compact quantum dilogarithm [307]. In our $-1 < \mathfrak{q} < 1$ story, we find that this crucial ingredients is replaced by (a version of) the

[12] In this regards, it would be very interesting to compare our approach to the one advocated in [383,384]

corresponding quantum exponential function(C.2.5)[309]:

$$\Phi_{\mathfrak{q}}(z) = \frac{(\mathfrak{q}^2 z;\mathfrak{q}^2)_\infty}{(\overline{z};\mathfrak{q}^2)_\infty}\,, \qquad |z| \in \mathfrak{q}^{\mathbb{Z}} \tag{12.10.1}$$

at values $|\mathfrak{q}| < 1$, that, as expected, produces the intertwiner for the diagonalization of the Wilson Line on the annulus[13]. We find that this special function is the one giving the multiplicative unitary operator associated with the $U_{\mathfrak{q}}(\mathfrak{sl}_2)$ quantum group in the Schur regime. This elucidates the relation to the Teichmüller quantization[305] based on the quantization of cluster varieties proposed by Fock and Goncharov [302,304,341,343] for the case $|\mathfrak{q}| = 1$, that we extended here for the Schur regime.

The quantization of Teichmüller space provides a realization of the Schur quantization developed in Section 12.3 for the case of Class $\mathcal{S}$ theories. The Hilbert space is realized explicitly by $L^2(\Gamma/\Gamma_f)$ where the generators are naturally associated with the cluster basis given by Fock-Goncharov coordinates associated to the surface $\mathcal{S}$ as discussed below in 12.10.2. Indeed, the Fock-Goncharov quantization produces precisely the cluster structure presented in 12.3.5. The algebra $\mathcal{A}$ is the Skein algebra $\mathrm{Sk}(\mathfrak{g},\mathcal{S})$ and is realized canonically within Teichmüller theory via the "traffic rules" construction[367,385].

12.10.1 Representation of Ptolemy groupoid

Let us consider an ideal triangulation Δ of a compact Riemann surface Σ equipped with a set of marked points. A dotted triangulation $\dot{\Delta}$ is an ideal triangulation equipped with the a map choosing a particular vertex of each triangle $\Delta_v \in \Delta$. The dotted Ptolemy groupoid of Σ is the full groupoid over the set of dotted ideal triangulations of Σ. This decoration of the Ptolemy groupoid accounts to specifying a particular polarization in assigning Weyl commuting variables to each triangle in the triangulation Its morphisms are generated by the two elementary moves[300,303–305]: the dot rotation A_v and the flip T_{vw} reported in Figure 12.20. A_v acts on a triangulation by rotating the marked vertex of the v-th triangle, and corresponds to the elementary move generating the change of polarization. The T_{vw} morphism acts by *flipping* the diagonal of two triangles in as in Figure 12.20.



Figure 12.20: Elementary moves.

[13] That is the diagonalization of the Dehn Twist for this surface.

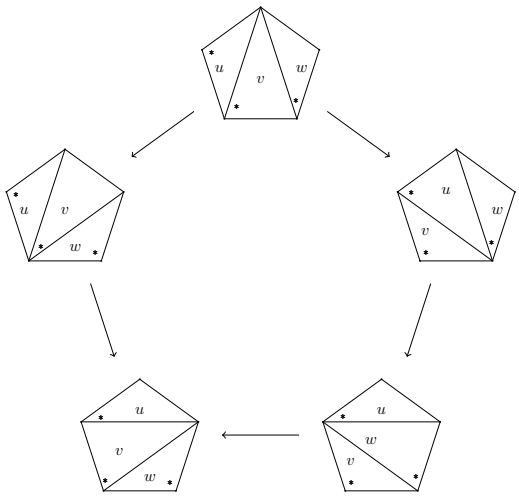


Figure 12.21: Pentagon equation

The elementary moves are subjected to the following set of relations[303]:

$$A_v^3 = \mathbf{1} \tag{12.10.2}$$
$$T_{uv}\, T_{uw}\, T_{vw} = T_{vw}\, T_{uv} \tag{12.10.3}$$
$$T_{uv}\, T_{wz} = T_{wz}\, T_{uv} \tag{12.10.4}$$
$$A_v\, T_{vw}\, A_w = A_w\, T_{wv}\, A_v \tag{12.10.5}$$
$$T_{vw}\, A_v\, T_{wv} = A_v\, A_w\, P_{vw} \tag{12.10.6}$$

where P_{vw} denotes the permutation of v and w. The second of those identities is the famous pentagon equation in Figure 12.21. Clearly under the forgetful functor dropping the marked points, $\dot{\Delta} \to \Delta$, the dot rotation descends to the identity morphism $A_v \to \mathbf{1}$ and the Ptolemy groupoid consist only of flip relation.

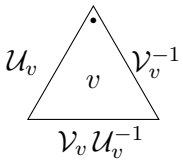
Now, let us fix a polarization by quantizing Kashaev coordinates[14] by assigning to each dotted triangle $\dot{t}_v \in \dot{\Delta}$ of any given triangulation $\mathfrak{q}$-Weyl commuting coordinates for the $*$-algebra double $\mathcal{W}_v \times \mathcal{W}_v^{\mathrm{op}}$ satisfying the Schur commutation relations(cfr. with related discussion in Section 5.1 of [83])[15]:

$$\mathcal{U}_v\, \mathcal{V}_v = \mathfrak{q}\, \mathcal{V}_v\, \mathcal{U}_v\,, \quad \overline{\mathcal{U}}_v\, \overline{\mathcal{V}}_v = \mathfrak{q}^{-1}\, \overline{\mathcal{V}}_v\, \overline{\mathcal{U}}_v\,, \tag{12.10.7}$$

[14] It is standard how to recover Penner/shear/Fock coordinates from the Kashaev ones and we defer the reader to [303–306] for the details

[15] In the case of Class $\mathcal{S}$ the ρ is the trivial automorphism of the doubled algebra and $\mathcal{U}_v^\dagger = \overline{\mathcal{U}}_v, \mathcal{V}_v^\dagger = \overline{\mathcal{V}}_v$

and commuting otherwise, in such a way that the variables are associated to the edges as:



(12.10.8)

and analogously for the adjoint generators. Then, it is clear that over the Schur representation the operator A_v is simply the unitary operator implementing the change of polarization as[16]:

$$A_v\,\mathcal{U}_v\,A_v^{-1}=\mathcal{V}_v\,\mathcal{U}_v^{-1}\,,\qquad A_v\,\mathcal{V}_v\,A_v^{-1}=\mathcal{U}_v^{-1}\,. \tag{12.10.9}$$

and analogously on the $\overline{\mathcal{U}}_v,\overline{\mathcal{V}}_v$ pair. We found that the operator:

$$T_{uv}=\Phi_{\mathfrak{q}}(\mathcal{U}_u\,\mathcal{V}_v\,\mathcal{U}_v^{-1})\,\chi(\mathcal{U}_v,\mathcal{V}_u) \tag{12.10.10}$$

where we used the standard tensor product notation, and $\chi(\mathcal{U}_v,\mathcal{V}_u)$ is the bi-character:

$$\chi(\mathcal{U}_v,\mathcal{V}_u):=\chi(\mathbf{1}\otimes\mathcal{U}_v,\mathcal{V}_u\otimes\mathbf{1})=\left(\frac{\mathcal{U}_v}{\overline{\mathcal{U}}_v}\right)^{-N_u}\otimes\mathbf{1},\qquad |\mathcal{V}_u|=\left|\overline{\mathcal{V}}_u\right|=\mathfrak{q}^{N_u} \tag{12.10.11}$$

gives a representation of the flip operator (see also related discussions in [308,309,341,386]). This can be proven by showing that (12.10.3)-(12.10.6) are satisfied. In particular, the pentagon identity can be shown by observing that:

$$T_{uv}\,T_{uw}\,T_{vw}=\Phi_{\mathfrak{q}}(\mathcal{U}_u\,\mathcal{V}_v\,\mathcal{U}_v^{-1})\Phi_{\mathfrak{q}}(\mathcal{U}_u\,\mathcal{U}_v^{-1}\,\mathcal{U}_w^{-1}\,\mathcal{V}_w)\,\Phi_{\mathfrak{q}}(\mathcal{U}_v\,\mathcal{V}_w\,\mathcal{U}_w^{-1})\,\chi(\mathcal{U}_v,\mathcal{V}_u)\,\chi(\mathcal{U}_w,\mathcal{V}_u)\,\chi(\mathcal{U}_w,\mathcal{V}_v) \tag{12.10.12}$$

a direct computations gives the pentagon identity for the characters

$$\chi(\mathcal{U}_v,\mathcal{V}_u)\,\chi(\mathcal{U}_w,\mathcal{V}_u)\,\chi(\mathcal{U}_w,\mathcal{V}_v)=\chi(\mathcal{U}_w,\mathcal{V}_v)\,\chi(\mathcal{U}_v,\mathcal{V}_u)\,, \tag{12.10.13}$$

while the non trivial relation for the special function $\Phi_{\mathfrak{q}}(-)$ over the Schur representation:

$$\Phi_{\mathfrak{q}}(\mathcal{U}_u\,\mathcal{V}_v\,\mathcal{U}_v^{-1})\Phi_{\mathfrak{q}}(\mathcal{U}_u\,\mathcal{U}_v^{-1}\,\mathcal{U}_w^{-1}\,\mathcal{V}_w)\,\Phi_{\mathfrak{q}}(\mathcal{U}_v\,\mathcal{V}_w\,\mathcal{U}_w^{-1})=\Phi_{\mathfrak{q}}(\mathcal{U}_v\,\mathcal{V}_w\,\mathcal{U}_w^{-1})\,\Phi_{\mathfrak{q}}(\mathcal{U}_u\,\mathcal{V}_v\,\mathcal{U}_v^{-1}) \tag{12.10.14}$$

follows from Theorem 2.2 and 4.1 in [309]. (12.10.4), (12.10.5) follow directly from the definitions, while the inversion (12.10.6) is a consequence of the inversion relation for the function $F_{\mathfrak{q}}(z)$ (C.2.9). Indeed, after basic algebra, one finds that the operator:

$$\Pi_{vw}=A_w^{-1}\,A_v^{-1}\,T_{vw}\,A_v T_{wv}=A_w^{-1}\,\chi(\mathcal{U}_2\,\mathcal{V}_1^{-1},\mathcal{U}_2\,\mathcal{V}_1^{-1})\chi(\mathcal{V}_1\,\mathcal{U}_2^{-1},\mathcal{V}_2)\,\chi(\mathcal{U}_2,\mathcal{V}_1) \tag{12.10.15}$$

coincides with the permutation operator $\Pi_{vw}=P_{vw}$. This is different compared to the case $|\mathfrak{q}|^2=1$ where the representation of the Ptolemy groupoid is projective and extended by the central charge of Liouville theory.

[16]The explicit expression for A_v is identical to the one in e.g. [303].

12.10.2 Relation to cluster algebra quantization

In the previous section we found that the representation of the Ptolemy groupoid is not Projective over the Schur quantization Hilbert space. This suggest we could have avoided to first fix a particular polarization, and then showing compatibility with the flip operation. This is a rather expected result in lieu of the works[302,341,343] where it was shown that in the construction of quantum double already in the regime $|\mathfrak{q}|^2 = 1$ there is no dependence on the polarization choice. Here we will we schematically extend to the Schur case their argument, and we refer to their work, and in particular to [341] for more details. From this perspective, the Schur Teichmüller quantization can be thought as following from the quantization of the underlying quantum doubled cluster variety.

We associate to the triangulation Δ (not it does not need to have any marking) a quantum torus algebra $\mathcal{X}_\Delta$ by assigning a generator $\left(X_\alpha^\Delta\right)^{\pm 1}$ for each α being an edge in Δ, satisfying the relation:

$$X_\alpha^\Delta \, X_\beta^\Delta = \mathfrak{q}^{2\epsilon_{\alpha\beta}^\Delta} X_\beta^\Delta \, X_\alpha^\Delta \tag{12.10.16}$$

where $\epsilon_{\alpha\beta}^\Delta$ is a skewsymmetric pairing obtained if the following way: for each vertex between α and β, $\epsilon_{\alpha\beta}^\Delta$ is the number of angular sectors between the edges α and β, with positive sign if counterclockwise or with negative sign if clockwise around the vertex. Then a basis for the Schur quantum double is given by the generators (12.10.16) together with their counterpart in the opposite algebra $\mathcal{X}_\Delta^{\rm op}$:

$$\overline{X}_\alpha^\Delta \, \overline{X}_\beta^\Delta = \mathfrak{q}^{-2\epsilon_{\alpha\beta}^\Delta} \overline{X}_\beta^\Delta \, \overline{X}_\alpha^\Delta \tag{12.10.17}$$

with $\overline{X}_\alpha \, X_\beta = X_\beta \, \overline{X}_\alpha$.

Mutations μ_γ of the quantum double along the direction γ correspond to flips of the underlying triangulation at the edge γ and the corresponding pairings are related by:

$$\mu_\gamma : \mathcal{X}_\Delta \times \mathcal{X}_\Delta^{\rm op} \to \mathcal{X}_{\Delta'} \times \mathcal{X}_{\Delta'}^{\rm op} \,, \tag{12.10.18}$$

$$\mu_\gamma : \epsilon_{\alpha\beta}^\Delta \mapsto \epsilon_{\alpha\beta}^{\Delta'} = \begin{cases} -\epsilon_{\alpha\beta}^\Delta & \text{if} \quad \alpha = \gamma \quad \text{or} \quad \beta = \gamma \\ \epsilon_{\alpha\beta}^\Delta & \text{if} \quad \epsilon_{\alpha\gamma}^\Delta \, \epsilon_{\gamma\beta}^\Delta \leq 0 \\ \epsilon_{\alpha\beta}^\Delta + \left|\epsilon_{\alpha\gamma}^\Delta\right| \epsilon_{\beta\gamma}^\Delta & \text{if} \quad \epsilon_{\alpha\gamma}^\Delta \, \epsilon_{\gamma\beta}^\Delta > 0 \end{cases} \tag{12.10.19}$$

Note that graphically, these exactly correspond to quiver mutations, where $\epsilon_{\alpha\beta}$ is the number of arrows between the node α, β with corresponding sign. The mutation induce corresponding rational maps between the cluster tori that we indicate with μ_γ^* by:

$$\mu_\gamma^* \, X_\alpha = \begin{cases} X_\alpha^{-1} & \text{if} \quad \gamma = \alpha \\ X_\alpha \left(1 + X_\gamma^{-\text{sgn}(\epsilon_{\alpha\gamma}^\Delta)}\right)^{-\epsilon_{\alpha\gamma}^\Delta} & \text{if} \quad \gamma \neq \alpha \end{cases} \tag{12.10.20}$$

$$\mu_\gamma^* \, \overline{X}_\alpha = \begin{cases} \overline{X}_\alpha^{-1} & \text{if} \quad \gamma = \alpha \\ \overline{X}_\alpha \left(1 + \overline{X}_\gamma^{\text{sgn}(\epsilon_{\alpha\gamma}^\Delta)}\right)^{\epsilon_{\alpha\gamma}^\Delta} & \text{if} \quad \gamma \neq \alpha \end{cases} \tag{12.10.21}$$

and analogously on $\mathcal{X}_\Delta^{\rm op}$. As advocated in [341] the quantum version of the mutation maps may be decomposed in a composition:

$$\mu_\gamma^{\mathfrak{q}} = \mu_\gamma^{\#} \circ \mu'_k \tag{12.10.22}$$

while the "monomial" part is universal and given by:

$$\mu'_\gamma(X_\alpha) = \begin{cases} X_\alpha^{-1} & \text{if} \quad \alpha = \gamma \\ X_\alpha \, (X_\gamma)^{[\epsilon^\Delta_{\alpha\gamma}]_+} & \text{if} \quad \alpha \neq \gamma \end{cases}, \quad \mu'_\gamma(\overline{X}_\alpha) = \begin{cases} \overline{X}_\alpha^{-1} & \text{if} \quad \alpha = \gamma \\ \overline{X}_\alpha \left(\overline{X}_\gamma\right)^{-[\epsilon^\Delta_{\alpha\gamma}]_+} & \text{if} \quad \alpha \neq \gamma \end{cases} \tag{12.10.23}$$

where $[a]_+ = \max(a, 0)$, as in the case of $|q|^2 = 1$. The "automorphism" part $\mu_\gamma^{\#}$ is instead governed by the quantum dilogarithm. For the quantization on the unit circle the automorphism part is shown be be conjugation by the Faddeev non-compact quantum dilog, as expected. In our regime[17] of interested, is it given by the corresponding adjoint action by the Schur multiplicative unitarity "quantum dilogorithm" $F_{\mathfrak{q}}(X_\gamma)$:

$$\mu_\gamma^{\#}(A) = F_{\mathfrak{q}}^{-1}(X_\gamma)\, A F_{\mathfrak{q}}(X_\gamma)\,, \qquad F_{\mathfrak{q}}(X_\gamma) = \frac{(X_\gamma; \mathfrak{q}^2)_\infty}{\left(\overline{X}_\gamma; \mathfrak{q}^2\right)_\infty} \tag{12.10.24}$$

where $A = X_\alpha, \overline{X}_\alpha$.

Consider the $\star$-algebra representation of $(\mathcal{X}_\Delta \times \mathcal{X}_\Delta^{\rm op})$ over a Hilbert space of L^2 functions on the quantum torus[18]. Then mutation $\mu^{\mathfrak{q}}$ descends to an unitary intertwiner $K^k_{\Delta,\Delta'} := K^{\#} \circ K'$ between the Schwartz spaces $\mathcal{S}_\Delta$ and $\mathcal{S}_{\Delta'}$ introduced in section 12.3.1, where Δ and Δ' differ by a mutation along k. Explicitly, $K^{\#}$ acts as multiplication operator by $\Phi_{\mathfrak{q}}(X_k)$ and K' acts the bi-character (12.10.11) $\chi(X_k \otimes \mathbf{1}, \mathbf{1} \otimes X_k)$. Then, the intertwiner satisfies the pentagon relation as follows from the discussion in the previous subsection.

Henceforth, from the quantization of the cluster variety we inherit a quantization of the Teichmüller space. To clarify the relation with the discussion in the previous subsection, one can embed $\mathcal{X}_\Delta$ into the star representation of the dotted Ptolemy groupoid by just associating to each triangle Δ_v in Δ coordinates in $\mathcal{W}_v \times \mathcal{W}_v^{\rm op}$ denoted by $W_{\alpha,v}$, $\overline{W}_{\alpha,v}$ for the dual graph [305] as in (12.10.8) and 12.22 , where one of the corners inherits the decoration of $\dot{\Delta}_v$; explicitly one associates $W_{1,v} = \mathcal{U}_v$, $W_{2,v} = \mathcal{V}_v \mathcal{U}_v^{-1}$, $W_{3,v} = \mathcal{V}_v^{-1}$, to the triangle in (12.10.8), and analogously for $\overline{\mathcal{W}}$. Then, the embedding :

$$X_\alpha^\Delta \mapsto W_{\alpha,v}\, W_{\alpha,w}\,, \qquad \overline{X}_\alpha^\Delta \mapsto \overline{W}_{\alpha,v}\, \overline{W}_{\alpha,w} \tag{12.10.25}$$

[17] It was already observed in [341] that this ration of quantum dilogarithm provides the correct qunatum mutation action. Yet, in that work they were interested in the quantization at $|\mathfrak{q}|^2 = 1$, where the ratio can merely be understood as a formal power series. They indeed replace it by its convergent version being the Faddeev one.

[18] E.g. for a single pair of cluster coordinates this is just a representation[83] where $X_1\, X_2 = \mathfrak{q}^2\, X_2\, X_1$ and the Hilbert space is just $L^2(\mathbb{Z} \times S^1)$ where $X_1 g_n(\theta) = g_{n+1}(\theta - i\hbar)$, $X_2 g_n(\theta) = \mathfrak{q}^n\, e^{i\theta} g_n(\theta)$ where $\mathfrak{q}^2 = e^{-\hbar}$.

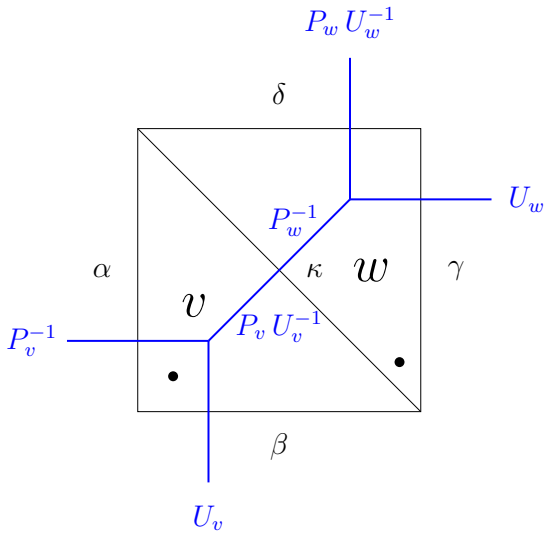


Figure 12.22: Dual graph associated to a triangulation $\Delta = \Delta_v \oplus \Delta_w$ and coordinates as prescribed in (12.10.8). Here $W_{\alpha,v} = P_v^{-1}$, $W_{\beta,v} = U_v$, $W_{\kappa,v} = P_v\,U_v^{-1}$ etc...

is the unique[382] algebra embedding of $\mathcal{X}_\Delta$ in the dotted torus algebra, where $W_{\alpha,w}$, $W_{\alpha,w}$ are the coordinates in Δ_v and Δ_w associated to the same edge α of Δ. It is then straightforward to verify that the quantum mutation maps constructed above descend to the operators T_{uv} in the previous subsection (12.10.10) under the above embedding.

Chapter 13

Outlook

In Part III, we explored various aspects of Schur quantization of the K-theoretic Coulomb branch of 4d $\mathcal{N} = 2$ SQFTs, along with the (quantum) Analytic Langlands correspondence. In Chapter 11, we leveraged the deep connection between analytic Langlands and integrable systems to present a preliminary proof of the correspondence in genus zero, i.e. for $\mathcal{C} = \mathcal{C}_{0,n}$. This was achieved using the SoV (Separation of Variables) method, which provides a unitary transform $\mathsf{SoV} : \mathcal{H}_0 \to \mathcal{H}_1$, allowing us to establish the Hecke eigenvalue property.

In Chapter 12, we studied the renormalization group (RG) flow of Schur indices and fusion algebras of BPS line defects. Due to wall-crossing phenomena in the IR, Schur indices are not preserved under RG flows $T_1 \to T_2$, but are instead intertwined by an object called the spectrum generator:

$$I^{(2)}_{\mathrm{RG}(a)\cdot S,\mathrm{RG}(b)\cdot S} = I^{(1)}_{a,b}.$$

The spectrum generator S induces an isometry between the Hilbert spaces associated to the two quantum mechanical systems. This key observation allowed us to derive a formula for the spectrum generator associated with RG flows triggered by large masses. Furthermore, we studied the Wilson Line spectral problem on the annulus providing the building block for the dictionary between UV and IR Schur quantization. Moreover, the IR quantization furnishes an explicit realization of the quantum complex Teichmüller space in the regime $0 < |\mathfrak{q}|^2 < 1$.

We now highlight several open directions that we leave for future work.

Stratified structure. The moduli stack of Higgs bundles admits a natural stratification by the maximal degree k of sub-line bundles. The automorphism group dimension grows with k, and in each stratum, a corresponding SoV transform can be defined. In this thesis, we focused on the dense, open stratum with minimal automorphism group. However, there is a rich interplay between Hecke action and SoV over this stratified stack. This is the subject of ongoing work with J. Teschner.

Higher rank and higher genus. Our analysis has been limited to the rank-one case of analytic Langlands. Yet, the conjecture extends to arbitrary (split reductive) Lie groups.

It is therefore natural to ask whether the SoV framework extends coherently to higher rank. For example, in the case of $G = \mathrm{PGL}_N$, the associated CFT is expected to be the N-Toda theory, a non-compact CFT with extended $\mathcal{W}_N$ symmetry (see also Chapter 9). A comprehensive discussion of the higher-rank SoV transform is still lacking.[1]
The first nontrivial case–SL_3 opers and PGL_3 Hitchin eigenstates–would involve a correspondence between $\mathfrak{sl}_3$ KZ equations and the third-order BPZ equations for degenerate fields with null vectors at levels 1, 2, and 3. While similar ideas have been explored in [387], the perspective of analytic Langlands and its CFT realization motivates a renewed investigation.

The generalization of the H_3^+–Liouville SoV correspondence to higher-genus Riemann surfaces was achieved shortly after [82] in [388]. The relevant integrable structure for the higher-genus moduli space has recently been explored in [389]. These results should lay the groundwork for extending our proof of Langlands to higher genus.

Relations to 3d Gravity. There is a key connection between Schur quantization and 3D de Sitter gravity (dS_3). Although dS_3 gravity is not strictly equivalent to CS theory, they are closely related. In the first-order formalism, the Einstein–Hilbert action can be written in CS form using the complexified connection:

$$\mathcal{A}^a = \omega^a + \frac{i}{\ell_{\mathrm{dS}}} e^a,$$

leading to a $\mathrm{PSL}_2(\mathbb{C})$ connection and action [390]:

$$S_{\mathrm{EH}}[g] = S_{\mathrm{CS}}(\mathcal{A}) - S_{\mathrm{CS}}(\bar{\mathcal{A}}), \qquad \text{with level} \quad k = \frac{i\ell_{\mathrm{dS}}}{4G_N}.$$

Yet, not all flat connections correspond to geometries with invertible metrics, and large diffeomorphisms are not gauge symmetries in CS theory; therefore the two theories are not exactly equivalent in the de Sitter regime. Interestingly, recent developments in dS_3 gravity have been obtained via the *complex Liouville string* [384,391–394]. These works reveal connections to IR Schur quantization. This non-critical string theory couples complex-conjugate copies of Liouville CFTs with $c = 13 + i\lambda$ and an appropriate $\mathfrak{bc}$ ghost system to cancel anomalies. This is exactly the regime relevant for Schur quantization. Indeed,[2] genus-g, n-point amplitudes of complex Liouville string have been related to Schur indices for class $\mathcal{S}$ theories on $\mathcal{C}_{g,n}$ [393, Section 3.6]. This connection motivates a deeper reconsideration of the relation between CS theory and dS_3 gravity through the lens of Schur quantization. We hope to return to this in future work.

DSSYK. Another intriguing avenue is the triality discovered in [311] between Schur quantization, complex CS theory, and the double-scaled SYK (DSSYK) model. Section 6 of [311] already outlines several open problems in this direction. More recently, extensions

[1] We acknowledge discussions with J. Teschner on this topic and for sharing a set of unpublished notes.

[2] We thank J. Teschner for pointing this out to us and relevant discussions.

of the triality to include matter fields and higher-rank analogues of the DSSYK chordal algebra have been proposed in [395,396].

Yet, many questions remain. For example, it is important to clarify the relation between the quantum group structures discussed in this thesis [5,83] and those arising in DSSYK [397]. Additionally, the holographic interpretation in terms of 3d gravity remains open. Motivated by recent work [395], it would be very interesting to investigate whether microscopic fermionic models can realize the higher-rank skein algebras.[3]

Finally, the recent incorporation of matter fields into the triality [396] raises the question of if our formalism may be applied as well to DSSYK. We leave this and related explorations for future work.

[3]We acknowledge discussions with H. Verlinde and H. Lin on this topic.

Appendix C

Supplement to Part III

C.1 A primer on H_3^+ and Liouville CFT

Here we give a lightning account of relevant fact about the H_3^+ model and Liouville theory that we use in the rest of our discussion. For a more thorough discussion the reader may want to refer to classical references e.g. [398–400].

C.1.1 Liouville CFT

Liouville theory is a 2D CFT defined at the classical level by the action:

$$S = \int \mathrm{d}^2 z \left((\partial\phi)^2 + \frac{b^2}{\pi^2} e^{2b\phi} \right)$$

Liouville theory is the simplest possible nontrivial theory with a continuous spectrum of primaries and central charge $c \in \mathbb{C}$

$$c = 1 + 6Q^2 \,, \qquad Q = b + b^{-1}$$

Representations of the symmetry algebra $\mathfrak{Vir} \times \overline{\mathfrak{Vir}}$ have multiplicities zero or one, and the correlation functions are meromorphic functions of the coupling constant b (and are symmetric under $b \leftrightarrow b^{-1}$) and of the fields' momentums $\alpha \in \mathbb{C}$. Virasoro primaries $V_\alpha(z)$ reduce to simple exponential in the classical limit $V_\alpha(z) \xrightarrow{b\to 0} e^{2\alpha z}$ and are normalizable for $\alpha = Q/2 + i\mathbb{R}$. The conformal weight of the primary V_α is:

$$\Delta_\alpha = \alpha(Q - \alpha)$$

Primary fields enjoy the reflection relation:

$$V_\alpha(z) = R(\alpha) V_{Q-\alpha}(z)$$

where $R(\alpha)$ is a the reflection amplitude (e.g. [82, (2.10)]).

2- and 3- points correlation functions are known exactly[398,401,402]:

$$\langle V_{\alpha_2}(z_2)V_{\alpha_1}(z_1)\rangle = 2\pi\left(\delta(Q-\alpha_2-\alpha_1)+R(\alpha_1)\delta(\alpha_2-\alpha_1)\right)\times|z_2-z_1|^{-4\Delta_{\alpha_1}}, \tag{C.1.1}$$

$$\langle V_{\alpha_3}(z_3)V_{\alpha_2}(z_2)V_{\alpha_1}(z_1)\rangle = |z_3-z_2|^{-2\Delta^1_{32}}|z_3-z_1|^{-2\Delta^2_{31}}|z_2-z_1|^{-2\Delta^3_{21}}\times C(\alpha_3,\alpha_2,\alpha_1), \tag{C.1.2}$$

where the structure constant may be found in e.g. [82, (2.9)], and higher point functions are reconstructed via the OPE[1,2]:

$$V_{\alpha_2}(z_2)V_{\alpha_1}(z_1) = \frac{1}{2\pi}\int_{\frac{Q}{2}+i\mathbb{R}_+} d\alpha_3\ \langle V_{\alpha_3}(\infty)V_{\alpha_2}(z_2-z_1)V_{\alpha_1}(0)\rangle\times\left(V_{Q-\alpha_3}(z_1)+(\text{desc. })\right)$$

Degenerate fields

Representation of the Virasoro algebra with momentum $\alpha=\frac{-1}{2b}$ are degenerate Verma module of the $(1,2)$ kind. The presence of a null vector at level 2 implies that correlation functions involving primaries $V_{\frac{-1}{2b}}$ satisfy a second order differential operator obtained by inserting $(L_{-2}+L_{-1}^2/b^2)$ into correlation functions. A the Liouville conformal block:

$$\mathcal{Z}_{\rm L}(\boldsymbol{y},\boldsymbol{z};\boldsymbol{\alpha}) = \left\langle V_{\alpha_1}(z_1)\cdots V_{\alpha_n}(z_n)V_{\frac{-1}{2b}}(y_1)\cdots V_{\frac{-1}{2b}}(y_m)\right\rangle$$

satisfies m BPZ differential equations:

$$\mathcal{D}_i^{\rm BPZ}\,\mathcal{Z}_{\rm L}(\boldsymbol{y},\boldsymbol{z};\boldsymbol{\alpha}) = 0\,,\qquad i=1,\cdots,m$$

where:

$$\mathcal{D}_i^{\rm BPZ} = b^2\frac{\partial^2}{\partial y_r^2}+\sum_{s\neq r}\left(\frac{1}{y_r-y_s}\frac{\partial}{\partial y_s}+\frac{\Delta_{-\frac{1}{2b}}}{(y_r-y_s)^2}\right)+\sum_s\left(\frac{1}{y_r-z_s}\frac{\partial}{\partial z_s}+\frac{\Delta_{\alpha_s}}{(y_r-z_s)^2}\right). \tag{C.1.3}$$

This implies that the OPE between with the degenerate (1,2) field, truncates only to 2 primaries:

$$[V_\alpha]\times[V_{-1/2b}] = [V_{\alpha+1/2b}]+[V_{\alpha-1/2b}]\,.$$

C.1.2 H_3^+ WZW model

The H_3^+ Wess–Zumino–Witten (WZW) model is a two-dimensional conformal field theory (CFT) based on the non-compact Lie group $\mathrm{SL}(2)/\mathrm{SU}(2)\simeq \mathrm{H}_3^+$, (that is Euclidean AdS_3). It is a key object in the study of string theory in AdS backgrounds, especially AdS_3 and for its relation to the Euclidean Black Hole CFT.

[1]The integration over $\mathbb{R}_+$ is due to the reflection symmetry.

[2]The insertion at infinity is defined in such a way correlation functions are finite $V_\alpha(\infty) = \lim_{z\to\infty} z^{4\Delta(\alpha)}V_\alpha(z)$.

H_3^+ field values matrices are parametrized by $\left(\begin{smallmatrix} e^{-\phi}+e^{\phi}|\gamma|^2 & e^{\phi}\bar\gamma \\ e^{\phi}\gamma & e^{\phi}\end{smallmatrix}\right) : z \mapsto H_3^+$, so that the coset is defined by the WZW action:

$$S = k\int d^2z\left(\partial\phi\,\bar\partial\phi + e^{2\phi}\,|\bar\partial\gamma|^2\right) \tag{C.1.4}$$

where k is the level. This defines at the quantum level a conformal field theory enjoying an affine $(\widehat{\mathfrak{sl}_2})_k \times (\widehat{\mathfrak{sl}_2})_k$ current algebra generated by the currents $J^a(z), \bar J^a(\bar z)$. Primary operators $\Phi^j(x;z)$ are labeled by a complex $\mathfrak{sl}_2$ spin j and correspond to the quantization of the classical fields:

$$\Phi^j(x;z) \to \Phi^j_{\rm cl}(x;z) \equiv \frac{2j+1}{\pi}\left(|\gamma - x|^2 e^{\phi} + e^{-\phi}\right)^{-2j}\,, \qquad x, z \in \mathbb{P}^1$$

having conformal weight

$$\Delta_j = \frac{j(j+1)}{k+2}\,.$$

The spectrum of the H_3^+ model correspond to the spherical principal series (corresponding to delta-function normalizable primaries)[3] of $\mathfrak{sl}_2$

$$j = -\frac{1}{2} + i\mathbb{R} \tag{C.1.5}$$

but we will also consider meromorphic continuation of H_3^+ correlates to accommodate for representation with generic spin j (in particular we are interested in null vectors with $j = k/2$).

From the Sugawara construction, one deduces that correlation functions

$$\mathcal{Z}_{\rm WZW}(\boldsymbol{x}, \boldsymbol{z}; \boldsymbol{j}) = \langle \Phi^{j_1}(x_1, z_1)\cdots\Phi^{j_n}(x_n, z_n)\rangle$$

with affine symmetry satisfy the following KZ differential equation:

$$\begin{aligned}(k+2)\tfrac{\partial}{\partial z_r}\mathcal{Z}_{\rm WZW}(\boldsymbol{x}, \boldsymbol{z}; \boldsymbol{j}) &= \mathrm{H}_r\,\mathcal{Z}_{\rm WZW}(\boldsymbol{x}, \boldsymbol{z}; \boldsymbol{j}) \\ (k+2)\tfrac{\partial}{\partial \bar z_r}\mathcal{Z}_{\rm WZW}(\boldsymbol{x}, \boldsymbol{z}; \boldsymbol{j}) &= \overline{\mathrm{H}}_r\,\mathcal{Z}_{\rm WZW}(\boldsymbol{x}, \boldsymbol{z}; \boldsymbol{j})\end{aligned} \qquad r = 1, \cdots, n \tag{C.1.6}$$

where $\mathrm{H_r}$ are the quantum Hitchin Hamiltonians (11.1.12) as above, defining a system of coupled partial differential equations of the second order in x's and first in the positions of the punctures $z \in \mathbb{P}^1$. The representations j are $-j-1$ are isomorphic [400] via the reflection (or shadow transform)

$$\int d^2x'\,|x-x'|^{-4j-4}\,\Phi^j(x';z) = -\frac{\pi}{2j+1}\,R(b(j+1) - 1/(2b))\,\Phi^{-j-1}(x;z) \tag{C.1.7}$$

R is the reflection in Liouville theory, cfr. [82, (2.31), (3.5)]

[3] We may distinguish primary fields generating *lowest* weight vectors, $\lim_{x,z\to 0}\Phi^j_l(x,z)|0\rangle = |j\rangle_l$, $J_0^-|j\rangle_l = 0$, $J_0^0|j\rangle_l = -j|j\rangle_l$ from primary fields generating *highest* weight vectors, $\lim_{\substack{x\to\infty\\ z\to 0}} x^{-2j}\Phi^j_h(x,z)|0\rangle = |j\rangle_h$, $J_0^+|j\rangle_h = 0$, , $J_0^0|j\rangle_h = +j|j\rangle_h$. Whenever unspecified we intend lowest weight Verma modules.

Null vectors

Primaries with $j = \frac{k}{2}$ define lowest Verma modules $\left|\frac{k}{2}\right\rangle = \lim_{z,x\to 0} \Phi^{\frac{k}{2}}(x;z)$ containing the null vector J^-_{-1} as following from the standard computation using the modes of the currents J^a:

$$J^+_1 J^-_{-1} \left|\tfrac{k}{2}\right\rangle = \left(2J^0_0 + k\right)\left|\tfrac{k}{2}\right\rangle = 0, \qquad J^0_1 J^-_{-1}\left|\tfrac{k}{2}\right\rangle = -J^-_0\left|\tfrac{k}{2}\right\rangle = 0\,.$$

All together this implies that the OPE with J^- of a $k/2$ field has a zero of order one: $J^-(z)\Phi^{\frac{k}{2}}(x;z) = \mathcal{O}(z-w)$ Then, correlation functions including a $k/2$ puncture, satisfies the additional null vector decoupling equation in addition to the KZ equations:

$$\begin{aligned} &\mathcal{D}^{\text{nvd}}\,\langle \Phi^{\frac{k}{2}}(x;z)\Phi^{j_1}(x_1;z_1)\cdots\Phi^{j_n}(x_n;z_n)\rangle = 0 \\ &\mathcal{D}^{\text{nvd}} = \sum_{r=1}^{n} \frac{1}{z-z_r}\left[(x-x_r)^2\partial_{x_r} - 2j_r(x-x_r)\right] \end{aligned} \tag{C.1.8}$$

Momentum space

SoV acts naturally in the Fourier space of momenta $x \to k$:

$$\begin{aligned} \Phi^j(k;z) &= |k|^{2j+2}\int_{\mathbb{P}^1} d^2x\, e^{kx-\bar{k}\bar{x}}\,\Phi^j(x,z)\,, \\ \widetilde{\mathcal{Z}}_{\text{WZW}}(\boldsymbol{k},\boldsymbol{z};\boldsymbol{j}) &= \prod_{i=1}^{n}|k_i|^{2j+2}\int_{(\mathbb{P}^1)^n} \mathrm{d}^{2n}\boldsymbol{x}\,\mathcal{Z}_{\text{WZW}}(\boldsymbol{x},\boldsymbol{z};\boldsymbol{j})\,e^{-2i\sum_{r=1}^{n}\mathrm{Im}(k_r x_r)} \end{aligned}$$

In this basis Hitchin Hamiltonians are differential operators $\mathrm{H}_r = \sum_{r\neq s}\frac{\eta_{ab}\mathcal{D}^a_s\mathcal{D}^b_s}{z_r-z_s}$ in k_r with:

$$\mathcal{D}^0_r = -k_r\partial_{k_r}\,, \qquad \mathcal{D}^+_r = -k_r\,, \qquad \mathcal{D}^-_r = k_r\partial^2_{k_r} - \frac{j(j+1)}{k_r}\,. \tag{C.1.9}$$

This is the momentum basis we will use in the following.
Note that in mometum representation, the reflection is diagonal

$$\Phi^j(k;z) = \widetilde{R}(j)\Phi^{-j-1}(k;z)$$

.

C.2 Spectral problem on the annulus

In this appendix we discuss the spectral problem associated to the Discrete Liouville difference operator that we report here for convenience:

$$F[w_1]\,g_n(\zeta) = g_{n+1}(\mathfrak{q}\,\zeta) + g_{n-1}(\mathfrak{q}^{-1}\,\zeta) + \mathfrak{q}^{-n}\zeta\,g_n(\zeta) \tag{C.2.1}$$

corresponding to the diagonalization of the Wilson line operator $F[w_1]$ on the annulus. This problem was solved in [310] in the case $|\mathfrak{q}|^2 = 1$; here we extend their discussion to the Schur quantization regime.

Let us go in the Fourier space representation over $\mathbb{L}^2(\mathbb{Z}\times\mathbb{Z})$:

$$\widetilde{F}[w_1]\, g_{n,m} = \mathfrak{q}^m g_{n+1,m} + \mathfrak{q}^{-m} g_{n-1,m} + \mathfrak{q}^{-n} g_{n,m+1}\,. \tag{C.2.2}$$

Now, this operator is non-diagonal in both copies of $\mathbb{Z}$. We parametrize the eingevalues as $\lambda+\lambda^{-1}$ and study the eigenproblem:

$$\mathfrak{q}^m g_{n+1,m} + \mathfrak{q}^{-m} g_{n-1,m} + \mathfrak{q}^{-n} g_{n,m+1} - (\lambda+\lambda^{-1}) g_{n,m} = 0\,, \quad |\lambda|^2 \in \mathfrak{q}^{\mathbb{Z}}\,. \tag{C.2.3}$$

It is convenient to parametrize

$$\lambda = \mathfrak{q}^k \kappa$$

with $k\in\mathbb{Z}, \kappa\in S^1$. Let us further consider a second Fourier transformation $\mathbb{L}^2(\mathbb{Z}\times S^1) \xrightarrow{\mathcal{F}_1\circ\mathcal{F}_2} \mathbb{L}^2(S^1\times\mathbb{Z})$:

$$(\widehat{F}[w_1] - \lambda - \lambda^{-1})\widehat{g}_m(\theta) = \left(\mathfrak{q}^m\zeta + \mathfrak{q}^{-m}\zeta^{-1} - \mathfrak{q}^k\kappa + \mathfrak{q}^{-k}\kappa^{-1}\right)\widehat{g}_m(\zeta) + \widehat{g}_{m+1}(\mathfrak{q}\,\zeta) = 0 \tag{C.2.4}$$

This is again the analogous of the recursion relation in [310].

C.2.1 Solutions of the difference equation

Now, let us introduce the $0<\mathfrak{q}^2<1$ version of the Faddeev Quantum dilogarithm introduced by Woronowicz [309]:

$$F_{\mathfrak{q}}(z) = \prod_{k=0}^{\infty} \frac{1-\mathfrak{q}^{2k} z^\dagger}{1-\mathfrak{q}^{2k} z}\,, \tag{C.2.5}$$

that is continuous for

$$\zeta \in \mathbb{C}^{\mathfrak{q}} = \{\zeta\in\mathbb{C} : \log_{\mathfrak{q}}(|\zeta|)\in\mathbb{Z}\}\,. \tag{C.2.6}$$

This special function has a natural representation on the Schur quantization Hilbert space $\mathbb{L}^2(\mathbb{Z}\times S^1)$:

$$F_{\mathfrak{q}}(n,\zeta) = \prod_{k=0}^{\infty} \frac{1-\mathfrak{q}^{2k+n}\,\zeta}{1-\mathfrak{q}^{2k+n}\,\zeta^{-1}}\,, \qquad \zeta\in S^1\,. \tag{C.2.7}$$

$F_{\mathfrak{q}}(n,\zeta)$ admits a meromorphic continuation to the complex plane with poles and zeros respectively at: $\zeta=\mathfrak{q}^{-2k-n}$ and $\zeta=\mathfrak{q}^{2k+n}$ for $k\in\mathbb{Z}$ It enjoys the reality condition:

$$\overline{F_{\mathfrak{q}}(n,\zeta)} F_{\mathfrak{q}}(n,\zeta) = F_{\mathfrak{q}}(n,\zeta^\dagger) F_{\mathfrak{q}}(n,\zeta) = 1\,, \tag{C.2.8}$$

and the inversion formula:

$$F_{\mathfrak{q}}(n+2,\zeta) F_{\mathfrak{q}}(-n,\zeta^{-1}) = (-\zeta)^{-n-1}\,. \tag{C.2.9}$$

This special function satisfies the important shift-property:

$$F_{\mathfrak{q}}(n+1,\mathfrak{q}^{-1}\,\zeta) = \left(1-\mathfrak{q}^n\zeta^{-1}\right) F_{\mathfrak{q}}(n,\zeta)\,, \tag{C.2.10}$$

as illustrated by the direct computation:

$$\frac{F_{\mathfrak{q}}(n+1,\mathfrak{q}^{-1}\,\zeta)}{F_{\mathfrak{q}}(n,\zeta)}=\prod_{k=0}^{\infty}\frac{1-\mathfrak{q}^{2k+n}\zeta^{-1}}{1-\mathfrak{q}^{2k+n+2}\zeta^{-1}}=1-\mathfrak{q}^{n}\zeta^{-1} \tag{C.2.11}$$

The property (C.2.10) is crucial to show that:

$$\begin{aligned}\psi_m(\zeta;\lambda)&=(-\zeta)^{m-1}F_{\mathfrak{q}}(m+k+1,\mathfrak{q}\zeta\kappa^{-1})\,F_{\mathfrak{q}}(m-k+1,\mathfrak{q}\zeta\kappa)\\&=(-\zeta)^{m-1}\frac{(\mathfrak{q}^{2+m}\lambda^{\dagger}\zeta;\mathfrak{q}^2)_\infty}{(\mathfrak{q}^{m}\lambda\zeta^{-1};\mathfrak{q}^2)_\infty}\frac{(\mathfrak{q}^{2+m}(\lambda^{\dagger})^{-1}\zeta;\mathfrak{q}^2)_\infty}{(\mathfrak{q}^{m}\lambda^{-1}\zeta^{-1};\mathfrak{q}^2)_\infty}\end{aligned} \tag{C.2.12}$$

provides a general solution of the recurrence relation in (C.2.4), an anticipated in (12.4.49). One can recognize the two factors be one one of pair of chiral multiplets to the 3d superconformal index. The shift by a semi-period guarantees that when $m\pm k=0$, $\kappa=\zeta^{\mp 1}$ is a pole, that will be crucial for the following. Also, note that this solution satisfies the reality condition:

$$\psi_m(\zeta^{-1};\lambda^{\dagger})=\overline{\psi_m(\zeta;\lambda)} \tag{C.2.13}$$

C.2.2 Scattering solution

From $\psi_m(\zeta;\lambda)$, one constructs the scattering solution by anti-Fourier transforming it:

$$\begin{aligned}\varphi_n(\zeta;\lambda)&=\frac{1}{2\pi}\sum_{m\in\mathbb{Z}}\int_{S^1}\mathrm{d}\xi\,\xi^n\,\zeta^m\,\psi_m(\xi;\lambda)\,,\qquad n\in\mathbb{Z}\,,\quad \zeta\in S^1\\\widetilde{\varphi}_{n,m}(\lambda)&=\frac{1}{2\pi}\int_{S^1}\mathrm{d}\xi\,\xi^n\,\psi_m(\xi;\lambda)\,,\qquad n,m\in\mathbb{Z}\end{aligned} \tag{C.2.14}$$

$\varphi_n(\zeta;\lambda)$ admits analytical continuation in $\mathbb{C}^{\mathfrak{q}}$ by contour deformation of the Fourier transform. By standard contour manipulation, it is straightforward to show that indeed (C.2.14) provide solutions to (C.2.3).

Since $\forall m\in\mathbb{Z}$,$\psi_m(\zeta;\lambda)$ is an analytical function on $\zeta\in S^1$, then its Fourier transform decays exponentially at infinity:

$$\lim_{n\to\pm\infty}\widetilde{\varphi}_{n,m}(\lambda)=\lim_{n\to\pm\infty}\varphi_n(\zeta;\lambda)=0 \tag{C.2.15}$$

Explicitly, let us parametrize $\xi=e^{-i\theta}$, $\kappa=e^{-i\chi}$, so that the Fourier transform is an integral $\frac{1}{2\pi}\sum_{m\in\mathbb{Z}}\int_0^{2\pi}\mathrm{d}\theta\,e^{-in\theta}\,\zeta^m\,\psi_m(e^{-in\theta};\lambda)$. The closest poles to the real axis of $\psi_m(\xi;\lambda)$ are located at:

$$\theta=\mp\chi+i(m\pm k)\hbar\qquad m\pm k=0,\cdots,\infty\,,\quad \hbar=-\log\mathfrak{q} \tag{C.2.16}$$

That are located in the upper or lower half plane depending on the sign of $(m\pm k)$. Let us assume for now that $m\pm k>0$, as the situation is analogous for the opposite case. To determine the behavior at $n\to-\infty$, on can consider a box contour in the upper half plane as in Figure C.1. The contributions due to the contour along the imaginary

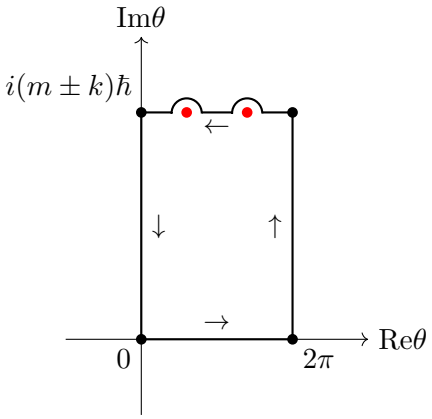


Figure C.1: Integration contour in the complex θ-plane

axis is suppressed exponentially at $n \to -\infty$: $\pm \int_0^{\hbar(m\pm k)} e^{n\theta}(\cdots)\mathrm{d}\theta \to 0$ as well as the contribution from the top straight part of the contour $\int_{2\pi}^{0} \mathrm{d}\theta e^{n\hbar(m\pm k)} e^{-in\theta}(\cdots) \xrightarrow{n\to-\infty} 0$. The dominant contribution comes from the two residue terms located at the points (C.2.16). The residue of $F_{\mathfrak{q}}(n,\zeta)$ there, can be computed recursively:

$$i\mathrm{Res}_{\zeta=\mathfrak{q}^{-n}}\left(F_{\mathfrak{q}}(n,\zeta)\right) = \frac{1}{(\mathfrak{q}^2;\mathfrak{q}^2)_n}\,, \qquad n = 0, \infty \tag{C.2.17}$$

So that, at $n \to -\infty$, one obtains the following asymptotic expansion:

$$\widetilde{\varphi}_{n,m}(\lambda) \asymp M_m(\lambda^{-1})\mathfrak{q}^{-n(m+k)}\kappa^{-n} + M_m(\lambda)\mathfrak{q}^{n(k-m)}\kappa^{n}\,, \tag{C.2.18}$$

that, at $n \to -\infty$, is non zero only for:

$$\begin{aligned}\widetilde{\varphi}_{n,m}(\lambda) &\asymp \delta_{m,-k} M_m(\lambda^{-1})\kappa^{-n} + \delta_{m,k} M_m(\lambda)\kappa^{n} \\ &:= M_+(\lambda)\,\kappa^n \delta_{m,k} + M_-(\lambda^{-1})\,\kappa^{-n}\delta_{m,-k}\,.\end{aligned} \tag{C.2.19}$$

This is analogous to what found in [310]. One can compute explicitly the functions $M_\pm(\lambda)$:

$$M_\pm(\lambda) = \frac{(-\mathfrak{q})^{\pm k}}{(\mathfrak{q}^2;\mathfrak{q}^2)_0} F_{\mathfrak{q}}(\mp 2k+1, \mathfrak{q}\kappa^{\pm 2}) = (-\mathfrak{q})^{\pm k}\frac{(\mathfrak{q}^{2\mp 2k}\kappa^{\pm 2};\mathfrak{q}^2)_\infty}{(\mathfrak{q}^{\mp 2k}\kappa^{\mp 2};\mathfrak{q}^2)_\infty} \tag{C.2.20}$$

that satisfy:

$$M_\mp(\lambda) = M_\pm(\lambda^{-1}) \tag{C.2.21}$$

Furthermore, one has that:

$$\frac{1}{M_+(\lambda)M_-(\lambda)} = 4\mathfrak{q}^{-2k}(\lambda-\lambda^{-1})(\lambda-\lambda^{-1})^\dagger \tag{C.2.22}$$

That is the equivalent of the result of [310].

C.2.3 Jost solutions

As $n \to -\infty$ the Fourier tranform of operator (C.2.3) reduces to the "free" operator:

$$\mathfrak{q}^m g_{n+1,m} + \mathfrak{q}^{-m} g_{n-1,m} - 2(\lambda + \lambda^{-1}) g_{n,m} \,. \tag{C.2.23}$$

The free operator, admits the Jost solutions:

$$f_{\pm}^{\text{free}}(n, m; \lambda) = \kappa^{\mp n} \delta_{\pm m,k} \,. \tag{C.2.24}$$

It is then natural to look for Jost solutions $f_{\pm}$ of the "interacting" operator, having the following asymptotic behavior:

$$f_{\pm}(n, m; \lambda) \xrightarrow{n \to -\infty} \kappa^{\pm n} \delta_{\mp m,k} + o(1) \,, \tag{C.2.25}$$

Consider the functions (remember $\kappa = e^{i\chi}$):

$$f_{\pm}(n, m; \lambda) = \frac{1}{4\pi \sinh\left(\mp \frac{2\pi\chi}{\hbar}\right) M_{\pm}(\lambda)} \int_0^{2\pi} \mathrm{d}\theta e^{-in\theta} \varphi_m(e^{i\theta}; \lambda) \left(\sinh\left(\frac{2\pi\theta}{\hbar}\right) + \sinh\left(\mp \frac{2\pi\chi}{\hbar}\right) \right) . \tag{C.2.26}$$

To show that $\lim_{n\to-\infty} f_{\pm}(n, m; \lambda) = e^{\pm in\kappa} \delta_{m,\mp k} + o(1)$, one uses the same contour as in Figure C.1. Yet, due to the term further quasi-constant piece $\left(\sinh\left(\frac{2\pi\theta}{\hbar}\right) + \sinh\left(\mp \frac{2\pi\kappa}{\hbar}\right) \right)$, only one between the two poles of $\widehat{\varphi}$ at $\theta = \pm\kappa$ for $i\hbar(m \pm k) = 0$ is a singularity of each of the integrands in (C.2.26).

The functions (C.2.26) solve (C.2.3) in its representation over $L^2(\mathbb{Z} \times \mathbb{Z})$ (C.2.2). This can be shown by noting that:

$$f_{\pm}(n, m; \lambda) = \frac{1}{4\pi \sinh\left(\mp \frac{2\pi\chi}{\hbar}\right) M_{\pm}(\lambda)} \left(\widetilde{\varphi}_{n+\frac{2\pi i}{\hbar},m}(\lambda) - \widetilde{\varphi}_{-\frac{2\pi i}{\hbar},m}(\lambda) + \sinh\left(\mp \frac{2\pi\chi}{\hbar}\right) \widetilde{\varphi}_{n,m}(\lambda) \right) \tag{C.2.27}$$

And, since $\mathfrak{q}^{-n \pm \frac{2\pi i}{\hbar}} = \mathfrak{q}^{-n}$, then also $\widetilde{\varphi}_{n \pm \frac{2\pi i}{\hbar},m}$ are solutions of (C.2.2).

Then, it follows that:

$$\widetilde{\varphi}_{n,m}(\lambda) = M_+(\lambda) f_+(n, m; \lambda) + M_-(\lambda) f_-(n, m; \lambda) \tag{C.2.28}$$

C.2.4 Casorati determinant

It is important for the following to compute the discrete version of the Wronskian, known as *Casorati* determinant. Given two solutions f, g, the Casorati determinant is defined by:

$$C(f, g)(n, m; \lambda) = \mathfrak{q}^m \, f(n, -m; \lambda) \, g(n+1, m; \lambda) - \mathfrak{q}^m \, f(n+1, m; \lambda) \, g(n, -m; \lambda) \tag{C.2.29}$$

Let us take the Casorati determinant between f_- and f_+. We have that:

$$\lim_{n \to -\infty} C(f_+, f_-)(n, m; \lambda) = \lambda - \lambda^{-1} + o(1) \tag{C.2.30}$$

One has

$$C(f_+, f_-)(n, m; \lambda) = \lambda - \lambda^{-1} \tag{C.2.31}$$

Note that:

$$C(f_+, f_-)(n, -m; \lambda) = \left(\lambda - \lambda^{-1}\right)^\dagger \tag{C.2.32}$$

Clearly, one has:

$$C(f_+, \widetilde{\varphi})(n, m; \lambda) = 2M_-(\lambda)\left(\lambda - \lambda^{-1}\right) \tag{C.2.33}$$

C.2.5 Resolvent

The resolvent of $\widetilde{F}[w_1]$ is, by definition,

$$R(\lambda) = (\widetilde{F}[w_1] - \lambda)^{-1}$$

, i.e. the operator such that:

$$\sum_{n,m\in\mathbb{Z}} R(n, m; n', m'|\lambda) g_{n',m'} = h_{n,m} \in \mathcal{D}(\widetilde{F}[w_1])\,, \qquad \left(\widetilde{F}[w_1] - (\lambda + \lambda^{-1})\right) h_{n,m} = g_{n,m}\,. \tag{C.2.34}$$

This, for $g \in \mathcal{D}(\widetilde{\mathcal{H}})$, is equivalent to verify that:

$$\left(\widetilde{F}[w_1] - (\lambda + \lambda^{-1})\mathbb{1}_{n,m}\right) R(n, m; n', m'|\lambda) = \delta_{n,n'}\delta_{m,m'} \tag{C.2.35}$$

or, explicitly:

$$\begin{aligned}\mathfrak{q}^m\, R(n+1, m; n', m'|\lambda) + \mathfrak{q}^{-m} R(n-1, m; n', m'|\lambda) + \mathfrak{q}^{-n} R(n, m+1; n', m'|\lambda) + \\ -(\lambda + \lambda^{-1}) R(n, m; n', m'|\lambda) = \delta_{n,n'}\delta_{m,m'}\end{aligned} \tag{C.2.36}$$

Define the operator:

$$R(n, m; n', m'|\lambda) = \frac{\pi}{(\lambda - \lambda^{-1})M_-(\boldsymbol{k})}\left[\frac{f_+(n, m; \lambda)\widetilde{\varphi}(n', -m')(\lambda)}{1 - e^{2\pi i(n-n')}e^{-2\pi i(m-m')}} + \frac{f_+(n', -m'; \lambda)\widetilde{\varphi}_{n,m}(\lambda)}{1 - e^{-2\pi i(n-n')}e^{2\pi i(m-m')}}\right] \tag{C.2.37}$$

Given that both f_- and $\widetilde{\varphi}$ are solutions of $(\widetilde{F}[w_1] - (\lambda + \lambda^{-1})) = 0$ and the denominators are invariant under shifts of n, m by integers, it is clear that (C.2.37) satisfies (C.2.36) whenever $R(n, m; n', m'|\lambda)$ is not singular, so that (C.2.36) is trivially satisfied whenever $n \neq n'$ and $m \neq m'$. At $n = n' \wedge m = m'$, where the distribution R is singular, one receives the following divergent contribution:

$$\begin{aligned}\lim_{\epsilon\to 0^+} \frac{\pi}{(\lambda - \lambda^{-1})M_-(\lambda)} \frac{1}{2\pi}\Bigg[\mathfrak{q}^m \frac{f_+(n+1, m; \lambda)\widetilde{\varphi}_{n',-m'}(\lambda) - f_+(n', -m'; \lambda)\widetilde{\varphi}_{n+1,m}(\lambda)}{(n-n') - (m-m') + i\epsilon} \\ + \mathfrak{q}^{-m} \frac{f_+(n-1, m; \lambda)\widetilde{\varphi}_{n',-m'}(\lambda) - f_+(n', -m'; \lambda)\widetilde{\varphi}_{n-1,m}(\lambda)}{(n-n') - (m-m') - i\epsilon}\Bigg] \\ = \delta_{n,n'}\delta_{m,m'} \frac{C(f_+, \widetilde{\varphi})(n, n; \lambda)}{2(\lambda - \lambda^{-1})M_-(\lambda)} = \delta_{n,n'}\delta_{m,m'}\end{aligned} \tag{C.2.38}$$

that coincides with the r.h.s. of (C.2.36).

C.2.6 Eigenfunctions expansion theorem

Let us denote the spectrum domain as:

$$\mathcal{I} = \left\{ \mathrm{Im}\,(\lambda + \lambda^{-1})\,,\ |\lambda| \in \mathfrak{q}^{\mathbb{Z}} \right\} \tag{C.2.39}$$

For $\psi \in \mathbb{L}^2(\mathbb{Z}\times\mathbb{Z})$, define the operator $\mathcal{U}$ by:

$$\mathcal{U} : \mathbb{L}^2(\mathbb{Z}\times\mathbb{Z}) \to \mathbb{L}^2(\mathcal{I})\,, (\mathcal{U}\psi)(\boldsymbol{k}) = \sum_{n,m\in\mathbb{Z}} \psi(n,m)\widetilde{\varphi}_{n,m}(\lambda) = \langle \psi, \widetilde{\varphi}(\lambda)\rangle\,, \tag{C.2.40}$$

then, $\mathcal{U}$ maps isometrically $\mathbb{L}^2(\mathbb{Z}\times\mathbb{Z})$ onto $\mathbb{L}^2(\mathcal{I})$ with spectral measure:

$$\rho(\lambda) = \frac{\pi \mathfrak{q}^{-2k}}{2M_+(\lambda)M_-(\lambda)} = \frac{\pi}{2}(\lambda - \lambda^{-1})(\lambda - \lambda^{-1})^\dagger \tag{C.2.41}$$

To show that, we claim that the following identity holds:

$$\psi(n,m) = \int_{\mathcal{I}} \mathrm{d}\lambda \sum_{n',m'\in\mathbb{Z}} \psi(n',m')\widetilde{\varphi}_{n',m'}(\lambda)\overline{\widetilde{\varphi}_{n,m}(\lambda)}\rho(\lambda) = \int_{\mathcal{I}} \mathrm{d}\lambda (\mathcal{U}\psi)(\lambda)\overline{\widetilde{\varphi}_{n,m}(\lambda)}\rho(\lambda) \tag{C.2.42}$$

The starting point to prove this, is the *Stone's theorem* relating a resolution of the identity to the jump of the resolvent on the absolutely continuum spectrum:

$$\mathbb{1}_{n,n'}\mathbb{1}_{n,m'} = \lim_{\epsilon\to 0^+} \int_{\mathcal{I}} \mathrm{d}\lambda\,(\lambda - \lambda^{-1}) \left(R(n,n',m,m'|\lambda e^{i\epsilon}) - (R(n,n',m,m'|\lambda e^{-i\epsilon}) \right) \tag{C.2.43}$$

taking $\lambda e^{-i\epsilon}$ corresponds to sending $\lambda \to \lambda^{-1}$. We can compute explicitly the discontinuity of the resolvent across the continuous spectrum. To do that, let first write the resolvent in the form:

$$R(n,m;n',m'|\lambda) = \pi \frac{f_+(n,m;\lambda)\widetilde{\varphi}_{n',-m'}(\lambda)e^{-i\pi(n-n'+m-m')} - f_+(n',-m';\lambda)\widetilde{\varphi}_{n,m}(\lambda)e^{i\pi(n-n'+m-m')}}{2(\lambda-\lambda^{-1})M_-(\lambda)\sinh(i\pi(n-n'+m-m'))}\,. \tag{C.2.44}$$

Using (C.2.21), (C.2.28) and (C.2.13) and the definition of $\widetilde{\varphi}$ in (C.2.14), one computes:

$$R(n,n',m,m'|\lambda) - R(n,n',m,m'|\lambda^{-1}) = \frac{\pi}{2(\lambda-\lambda^{-1})} \frac{\mathfrak{q}^{-2k}\widetilde{\varphi}_{n',m'}(\lambda)\,\overline{\widetilde{\varphi}_{n,m}(\lambda)}}{M_+(\lambda)M_-(\lambda)}\,, \tag{C.2.45}$$

and therefore:

$$\mathbb{1}_{n,n'}\mathbb{1}_{n,m'} = \int_{\mathcal{I}} \mathrm{d}\lambda\rho(\lambda)\widetilde{\varphi}_{n',m'}(\lambda)\,\overline{\widetilde{\varphi}_{n,m}(\lambda)}\,. \tag{C.2.46}$$

Then, we obtain (C.2.42) by simply inserting this resolution of the identity:

$$\begin{aligned}\psi(n,m) &= \sum_{n',m'\in\mathbb{Z}} \mathbb{1}_{n,n'}\mathbb{1}_{n,m'}\,\psi(n',m') = \sum_{n',m'\in\mathbb{Z}} \int_{\mathcal{I}} \mathrm{d}\lambda\rho(\lambda)\psi(n',m'\widetilde{\varphi}_\lambda(n',m')\,\overline{\widetilde{\varphi}_{n,m}(\lambda)} \\ &= \int_{\mathcal{I}} \mathrm{d}\lambda\rho(\lambda)\,(\mathcal{U}\psi)(\lambda)\,\overline{\widetilde{\varphi}_{n,m}(\lambda)}\end{aligned} \tag{C.2.47}$$

From this identity, by taking the inner product with $\overline{\psi(n,m)}$ follows the Plancharel theorem:

$$\|\mathcal{U}\psi\|^2_{\mathbb{L}^2(\mathcal{I})} = \|\psi\|^2_{\mathbb{L}^2(\mathbb{Z}\times\mathbb{Z})} \tag{C.2.48}$$

Where the Hilbert space $\mathbb{L}^2(\mathcal{I})$ is equipped with spectral measure $\rho(\lambda)\mathrm{d}\lambda$. From this isometric property of the operator, follows that $\mathcal{U}^{-1}\mathcal{U} = \mathbb{1}_{\mathbb{L}^2(\mathbb{Z}\times\mathbb{Z})}$. To show that $\mathcal{U}\mathcal{U}^{-1} = \mathbb{1}_{\mathbb{L}^2(\mathcal{I})}$, it is enough to show that the image of $\mathcal{U}$ coincides with $\mathbb{L}^2(\mathcal{I})$. This follows, as customary by the observation that since:

$$\mathcal{U}R(\lambda)\mathcal{U}^{-1} = \widehat{R}(\lambda) \Rightarrow \mathcal{U}(F[w_1] - \lambda - \lambda^{-1})\mathcal{U}^{-1} = \widehat{F}[w_1] - \lambda - \lambda^{-1}\,, \tag{C.2.49}$$

then $\widehat{F}[w_1]$ coincides on $\mathbb{L}^2(\mathcal{I})$ with the multiplication operator $(\lambda + \lambda^{-1})$.

Bibliography

[1] F. Ambrosino and S. Komatsu, *2d QCD and integrability. Part I. 't Hooft model*, *JHEP* **02** (2025) 126, [arXiv:2312.15598].

[2] F. Ambrosino and S. Komatsu, *2d QCD and Integrability, Part II: Generalized QCD*, arXiv:2406.11078.

[3] F. Ambrosino and S. Negro, *Minimal Model Renormalization Group Flows: Noninvertible Symmetries and Nonperturbative Description*, *Phys. Rev. Lett.* **135** (2025), no. 2 021602, [arXiv:2501.07511].

[4] F. Ambrosino, I. Runkel, and G. M. T. Watts, *Non-local charges from perturbed defects via SymTFT in 2d CFT*, arXiv:2504.05277.

[5] F. Ambrosino and D. Gaiotto, *Renormalization Group flow in Schur quantization*, arXiv:2503.16685.

[6] F. Ambrosino and J. Teschner, *Analytic Langlands correspondence from SoV*, arXiv:2510.06991.

[7] F. Ambrosino, R. Luo, Y.-N. Wang, and Y. Zhang, *Understanding fermionic generalized symmetries*, *Phys. Rev. D* **110** (2024), no. 10 105020, [arXiv:2404.12301].

[8] P. A. Lee, N. Nagaosa, and X.-G. Wen, *Doping a mott insulator: Physics of high temperature superconductivity*, 2004.

[9] E. Dagotto, *Correlated electrons in high-temperature superconductors*, *Rev. Mod. Phys.* **66** (Jul, 1994) 763–840.

[10] J. Bardeen, L. N. Cooper, and J. R. Schrieffer, *Microscopic theory of superconductivity*, *Phys. Rev.* **106** (Apr, 1957) 162–164.

[11] L. Susskind, *The World as a hologram*, *J. Math. Phys.* **36** (1995) 6377–6396, [hep-th/9409089].

[12] J. M. Maldacena, *The Large N limit of superconformal field theories and supergravity*, *Adv. Theor. Math. Phys.* **2** (1998) 231–252, [hep-th/9711200].

[13] P. Candelas, X. C. De La Ossa, P. S. Green, and L. Parkes, *A pair of calabi-yau manifolds as an exactly soluble superconformal theory*, *Nuclear Physics B* **359** (1991), no. 1 21–74.

[14] M. Kontsevich, *Homological Algebra of Mirror Symmetry*, alg-geom/9411018.

[15] K. Hori, S. Katz, A. Klemm, R. Pandharipande, R. Thomas, C. Vafa, R. Vakil, and E. Zaslow, *Mirror Symmetry*, vol. 1 of *Clay Mathematics Monographs*. American Mathematical Society, Providence, RI, 2003.

[16] A. Beilinson and V. Drinfeld, *Opers*, 2005.

[17] A. Kapustin and E. Witten, *Electric-Magnetic Duality And The Geometric Langlands Program*, *Commun. Num. Theor. Phys.* **1** (2007) 1–236, [hep-th/0604151].

[18] E. Frenkel, *Lectures on the Langlands program and conformal field theory*, in *Les Houches School of Physics: Frontiers in Number Theory, Physics and Geometry*, pp. 387–533, 2007. hep-th/0512172.

[19] J. Teschner, *Quantisation conditions of the quantum Hitchin system and the real geometric Langlands correspondence*, arXiv:1707.07873.

[20] P. Etingof, E. Frenkel, and D. Kazhdan, *Analytic Langlands correspondence for PGL_2 on $\mathbb{P}^1$ with parabolic structures over local fields*, *Geom. Funct. Anal.* **32** (2022), no. 4 725–831, [arXiv:2106.05243].

[21] D. Gaiotto and E. Witten, *Gauge Theory and the Analytic Form of the Geometric Langlands Program*, *Annales Henri Poincare* **25** (2024), no. 1 557–671, [arXiv:2107.01732].

[22] D. Gaiotto and J. Teschner, *Quantum analytic Langlands correspondence*, *SciPost Phys.* **18** (2025), no. 4 144, [arXiv:2402.00494].

[23] P. Di Francesco, P. Mathieu, and D. Senechal, *Conformal Field Theory*. Graduate Texts in Contemporary Physics. Springer-Verlag, New York, 1997.

[24] R. Rattazzi, V. S. Rychkov, E. Tonni, and A. Vichi, *Bounding scalar operator dimensions in 4D CFT*, *JHEP* **12** (2008) 031, [arXiv:0807.0004].

[25] S. El-Showk, M. F. Paulos, D. Poland, S. Rychkov, D. Simmons-Duffin, and A. Vichi, *Solving the 3D Ising Model with the Conformal Bootstrap*, *Phys. Rev. D* **86** (2012) 025022, [arXiv:1203.6064].

[26] C.-H. Chang, V. Dommes, R. S. Erramilli, A. Homrich, P. Kravchuk, A. Liu, M. S. Mitchell, D. Poland, and D. Simmons-Duffin, *Bootstrapping the 3d Ising stress tensor*, *JHEP* **03** (2025) 136, [arXiv:2411.15300].

[27] A. A. Belavin, A. M. Polyakov, and A. B. Zamolodchikov, *Infinite Conformal Symmetry in Two-Dimensional Quantum Field Theory*, *Nucl. Phys. B* **241** (1984) 333–380.

[28] N. Seiberg, *Exact results on the space of vacua of four-dimensional susy gauge theories*, *Physical Review D* **49** (1994), no. 10 6857–6863, [hep-th/9402044].

[29] E. Witten, *Dyons of charge $e\theta/2\pi$*, *Physics Letters B* **86** (1979), no. 3-4 283–287.

[30] N. Seiberg, *Electric - magnetic duality in supersymmetric nonAbelian gauge theories*, *Nucl. Phys. B* **435** (1995) 129–146, [hep-th/9411149].

[31] C. Montonen and D. I. Olive, *Magnetic Monopoles as Gauge Particles?*, *Phys. Lett. B* **72** (1977) 117–120.

[32] N. Seiberg and E. Witten, *Electric - magnetic duality, monopole condensation, and confinement in N=2 supersymmetric Yang-Mills theory*, *Nucl. Phys. B* **426** (1994) 19–52, [hep-th/9407087]. [Erratum: Nucl.Phys.B 430, 485–486 (1994)].

[33] J. H. Schwarz, *Lectures on superstring and m theory dualities*, *Nuclear Physics B - Proceedings Supplements* **55** (1997), no. 1-2 1–32, [hep-th/9607201].

[34] S. Coleman, R. Jackiw, and H. D. Politzer, *Spontaneous symmetry breaking in the o(n) model for large n*, *Physical Review D* **10** (1974), no. 8 2491–2499.

[35] G. Hooft, *A planar diagram theory for strong interactions*, *Nuclear Physics B* **72** (1974), no. 3 461–473.

[36] E. Witten, *Baryons in the 1/n Expansion*, *Nucl. Phys. B* **160** (1979) 57–115.

[37] S. Hellerman, D. Orlando, S. Reffert, and M. Watanabe, *On the CFT Operator Spectrum at Large Global Charge*, *JHEP* **12** (2015) 071, [arXiv:1505.01537].

[38] L. F. Alday and J. M. Maldacena, *Comments on operators with large spin*, *JHEP* **11** (2007) 019, [arXiv:0708.0672].

[39] Z. Komargodski and A. Zhiboedov, *Convexity and Liberation at Large Spin*, *JHEP* **11** (2013) 140, [arXiv:1212.4103].

[40] A. L. Fitzpatrick, J. Kaplan, D. Poland, and D. Simmons-Duffin, *The Analytic Bootstrap and AdS Superhorizon Locality*, *JHEP* **12** (2013) 004, [arXiv:1212.3616].

[41] E. Witten, *Instantons, the quark model, and the 1/n expansion*, *Nuclear Physics B* **149** (1979) 285–320.

[42] D. J. Gross and A. Neveu, *Dynamical symmetry breaking in asymptotically free field theories*, *Physical Review D* **10** (1974), no. 10 3235–3253.

[43] G. 't Hooft, *A Two-Dimensional Model for Mesons*, *Nucl. Phys. B* **75** (1974) 461–470.

[44] E. Witten, *Constraints on supersymmetry breaking*, *Nuclear Physics B* **202** (1982), no. 2 253–316.

[45] S. Sachdev and J. Ye, *Gapless spin-fluid ground state in a random, quantum heisenberg magnet*, *Physical Review Letters* **70** (1993), no. 21 3339–3342.

[46] A. Kitaev, "A simple model of quantum holography." http://online.kitp.ucsb.edu/online/entangled15/kitaev/, 2015. Talks at KITP, February and April 2015.

[47] H. Bethe, *Zur theorie der metalle. eigenwerte und eigenfunktionen der linearen atomkette*, *Zeitschrift für Physik* **71** (1931) 205–226.

[48] J. Hubbard, *Electron correlations in narrow energy bands*, *Proceedings of the Royal Society of London. Series A. Mathematical and Physical Sciences* **276** (1963), no. 1365 238–257.

[49] N. Beisert et al., *Review of AdS/CFT Integrability: An Overview*, *Lett. Math. Phys.* **99** (2012) 3–32, [arXiv:1012.3982].

[50] A. B. Zamolodchikov and A. B. Zamolodchikov, *Factorized s-matrices in two dimensions as the exact solutions of certain relativistic quantum field theory models*, *Annals of Physics* **120** (1979), no. 2 253–291.

[51] C. N. Yang, *Some exact results for the many-body problem in one dimension with repulsive delta-function interaction*, *Physical Review Letters* **19** (1967) 1312–1315.

[52] R. J. Baxter, *Exactly Solved Models in Statistical Mechanics*. Academic Press, 1982.

[53] A. B. Zamolodchikov, *Tba equations for integrable perturbed conformal field theories and their large volume limit*, *Nuclear Physics B* **342** (1991) 695–720.

[54] M. F. Paulos, J. Toledo, B. C. van Rees, and P. Vieira, *S-matrix bootstrap in two dimensions*, *Journal of High Energy Physics* **2017** (2017), no. 11 1–40, [arXiv:1607.06109].

[55] A. B. Zamolodchikov, *Mass scale in the sine-gordon model and its reductions*, *International Journal of Modern Physics A* **10** (1995), no. 8 1125–1150.

[56] J. Kondo, *Resistance minimum in dilute magnetic alloys*, *Progress of Theoretical Physics* **32** (1964), no. 1 37–49.

[57] I. Affleck, *Conformal field theory approach to the kondo effect*, *Acta Physica Polonica B* **26** (1995) 1869–1932, [cond-mat/9512099].

[58] A. Kapustin, *Wilson-'t Hooft operators in four-dimensional gauge theories and S-duality*, *Phys. Rev. D* **74** (2006) 025005, [hep-th/0501015].

[59] O. Aharony, N. Seiberg, and Y. Tachikawa, *Reading between the lines of four-dimensional gauge theories*, *JHEP* **08** (2013) 115, [arXiv:1305.0318].

[60] D. Gaiotto, G. W. Moore, and A. Neitzke, *Framed BPS States*, *Adv. Theor. Math. Phys.* **17** (2013), no. 2 241–397, [arXiv:1006.0146].

[61] S. Gukov and E. Witten, *Gauge Theory, Ramification, And The Geometric Langlands Program*, hep-th/0612073.

[62] E. Frenkel, S. Gukov, and J. Teschner, *Surface Operators and Separation of Variables*, *JHEP* **01** (2016) 179, [arXiv:1506.07508].

[63] M. Billò, V. Gonçalves, E. Lauria, and M. Meineri, *Defects in conformal field theory*, *JHEP* **04** (2016) 091, [arXiv:1601.02883].

[64] J. L. Cardy, *Conformal invariance and surface critical behavior*, *Nuclear Physics B* **240** (1984), no. 4 514–532.

[65] J. Fröhlich, J. Fuchs, I. Runkel, and C. Schweigert, *Duality and defects in rational conformal field theory*, *Nucl. Phys. B* **763** (2007) 354–430, [hep-th/0607247].

[66] D. Gaiotto, A. Kapustin, N. Seiberg, and B. Willett, *Generalized Global Symmetries*, *JHEP* **02** (2015) 172, [arXiv:1412.5148].

[67] S. Schafer-Nameki, *ICTP lectures on (non-)invertible generalized symmetries*, *Phys. Rept.* **1063** (2024) 1–55, [arXiv:2305.18296].

[68] S.-H. Shao, *What's Done Cannot Be Undone: TASI Lectures on Non-Invertible Symmetries*, arXiv:2308.00747.

[69] E. Witten, *On s-duality in abelian gauge theory*, *Selecta Mathematica* **1** (1995) 383–410, [hep-th/9505186].

[70] J. Polchinski, *Dirichlet-branes and ramond-ramond charges*, *Physical Review Letters* **75** (1995) 4724–4727, [hep-th/9510017].

[71] A. Giveon and D. Kutasov, *Brane dynamics and gauge theory*, *Reviews of Modern Physics* **71** (1999), no. 4 983–1084, [hep-th/9802067].

[72] A. Hanany and E. Witten, *Type iib superstrings, bps monopoles, and three-dimensional gauge dynamics*, *Nuclear Physics B* **492** (1997), no. 1-2 152–190, [hep-th/9611230].

[73] A. Giveon, M. Porrati, and E. Rabinovici, *Target space duality in string theory*, *Physics Reports* **244** (1994), no. 2-3 77–202, [hep-th/9401139].

[74] P. Goddard, J. Nuyts, and D. I. Olive, *Gauge Theories and Magnetic Charge*, *Nucl. Phys. B* **125** (1977) 1–28.

[75] J. Teschner, ed., *New Dualities of Supersymmetric Gauge Theories*. Mathematical Physics Studies. Springer, Cham, Switzerland, 2016.

[76] N. Seiberg and E. Witten, *Monopoles, duality and chiral symmetry breaking in N=2 supersymmetric QCD*, *Nucl. Phys. B* **431** (1994) 484–550, [hep-th/9408099].

[77] D. Gaiotto, *N=2 dualities*, *JHEP* **08** (2012) 034, [arXiv:0904.2715].

[78] L. F. Alday, D. Gaiotto, and Y. Tachikawa, *Liouville Correlation Functions from Four-dimensional Gauge Theories*, *Lett. Math. Phys.* **91** (2010) 167–197, [arXiv:0906.3219].

[79] P. Etingof, E. Frenkel, and D. Kazhdan, *An analytic version of the Langlands correspondence for complex curves*, arXiv:1908.09677.

[80] P. Etingof, E. Frenkel, and D. Kazhdan, *Hecke operators and analytic Langlands correspondence for curves over local fields*, *Duke Math. J.* **172** (2023), no. 11 2015–2071, [arXiv:2103.01509].

[81] T. Figiel, *Quantization of the Hitchin system from loop operator expectation values*. PhD thesis, U. Hamburg (main), 2020.

[82] S. Ribault and J. Teschner, *H+(3)-WZNW correlators from Liouville theory*, *JHEP* **06** (2005) 014, [hep-th/0502048].

[83] D. Gaiotto and J. Teschner, *Schur Quantization and Complex Chern-Simons theory*, arXiv:2406.09171.

[84] G. W. Moore and N. Seiberg, *Classical and Quantum Conformal Field Theory*, *Commun. Math. Phys.* **123** (1989) 177.

[85] G. Moore and A. Strominger, *The wall crossing formula and the spectrum of bps states*, . unpublished.

[86] M. Kontsevich and Y. Soibelman, *Stability structures, motivic Donaldson-Thomas invariants and cluster transformations*, arXiv:0811.2435.

[87] A. Gadde, L. Rastelli, S. S. Razamat, and W. Yan, *The 4d Superconformal Index from q-deformed 2d Yang-Mills*, *Phys. Rev. Lett.* **106** (2011) 241602, [arXiv:1104.3850].

[88] C. Córdova and A. Neitzke, *Line Defects, Tropicalization, and Multi-Centered Quiver Quantum Mechanics*, *JHEP* **09** (2014) 099, [arXiv:1308.6829].

[89] C. Cordova and S.-H. Shao, *Schur Indices, BPS Particles, and Argyres-Douglas Theories*, *JHEP* **01** (2016) 040, [arXiv:1506.00265].

[90] C. Cordova, D. Gaiotto, and S.-H. Shao, *Infrared Computations of Defect Schur Indices*, *JHEP* **11** (2016) 106, [arXiv:1606.08429].

[91] G. 't Hooft, *A two-dimensional model for mesons*, *Nuclear Physics B* **75** (1974), no. 3 461–470.

[92] V. A. Fateev, S. L. Lukyanov, and A. B. Zamolodchikov, *On mass spectrum in 't Hooft's 2D model of mesons*, *J. Phys. A* **42** (2009) 304012, [arXiv:0905.2280].

[93] A. Litvinov and P. Meshcheriakov, *Meson mass spectrum in QCD_2 't Hooft's model*, arXiv:2409.11324.

[94] A. Artemev, A. Litvinov, and P. Meshcheriakov, *QCD2 't Hooft model: Two-flavor mesons spectrum*, *Phys. Rev. D* **111** (2025), no. 12 125001, [arXiv:2504.12081].

[95] M. R. Douglas, K. Li, and M. Staudacher, *Generalized two-dimensional QCD*, *Nucl. Phys. B* **420** (1994) 118–140, [hep-th/9401062].

[96] A. Kaushal, N. S. Prabhakar, and S. R. Wadia, *Meson spectrum of $SU(2)$ QCD_{1+1} with Quarks in Large Representations*, arXiv:2307.15015.

[97] F. Ambrosino and T. Procházka, *RG flows of minimal $\mathcal{W}$-algebra CFTs via non-invertible symmetries*, arXiv:2601.18667.

[98] Y. Nakayama and T. Tanaka, *Infinitely many new renormalization group flows between Virasoro minimal models from non-invertible symmetries*, *JHEP* **11** (2024) 137, [arXiv:2407.21353].

[99] I. Runkel, *Perturbed Defects and T-Systems in Conformal Field Theory*, *J. Phys. A* **41** (2008) 105401, [arXiv:0711.0102].

[100] I. Runkel, *Non-local conserved charges from defects in perturbed conformal field theory*, *J. Phys. A* **43** (2010), no. 36 365206, [arXiv:1004.1909].

[101] D. Bücher and I. Runkel, *Integrable perturbations of conformal field theories and Yetter-Drinfeld modules*, *J. Math. Phys.* **55** (2014) 111705, [arXiv:1211.4726].

[102] J. Teschner, *Quantization of the Hitchin moduli spaces, Liouville theory, and the geometric Langlands correspondence I*, *Adv. Theor. Math. Phys.* **15** (2011), no. 2 471–564, [arXiv:1005.2846].

[103] C. Beem, M. Lemos, P. Liendo, W. Peelaers, L. Rastelli, and B. C. van Rees, *Infinite chiral symmetry in four dimensions*, *Commun. Math. Phys.* **336** (2015) 1359–1433, [arXiv:1312.5344].

[104] C. Beem, M. Lemos, L. Rastelli, and B. C. van Rees, *The (2, 0) superconformal bootstrap*, *Phys. Rev. D* **93** (2016), no. 2 025016, [arXiv:1412.7541].

[105] J. Teschner, *(quantum) analytic langlands correspondence, complex chern-simons theory, and susy qft, Talk at ICBS 2025.*

[106] N. A. Nekrasov and S. L. Shatashvili, *Quantization of Integrable Systems and Four Dimensional Gauge Theories*, in *16th International Congress on Mathematical Physics*, pp. 265–289, 2010. arXiv:0908.4052.

[107] E. Abdalla and M. Abdalla, *Updating QCD2*, *Physics Reports* **265** (feb, 1996) 253–368.

[108] S. Dalley and I. R. Klebanov, *String spectrum of (1+1)-dimensional large N QCD with adjoint matter*, *Phys. Rev. D* **47** (1993) 2517–2527, [hep-th/9209049].

[109] D. Kutasov, *Two-dimensional QCD coupled to adjoint matter and string theory*, *Nucl. Phys. B* **414** (1994) 33–52, [hep-th/9306013].

[110] J. Boorstein and D. Kutasov, *Symmetries and mass splittings in QCD in two-dimensions coupled to adjoint fermions*, *Nucl. Phys. B* **421** (1994) 263–277, [hep-th/9401044].

[111] G. Bhanot, K. Demeterfi, and I. R. Klebanov, *(1+1)-dimensional large N QCD coupled to adjoint fermions*, *Phys. Rev. D* **48** (1993) 4980–4990, [hep-th/9307111].

[112] K. Demeterfi, I. R. Klebanov, and G. Bhanot, *Glueball spectrum in a (1+1)-dimensional model for QCD*, *Nucl. Phys. B* **418** (1994) 15–29, [hep-th/9311015].

[113] A. V. Smilga, *Instantons and fermion condensate in adjoint QCD in two-dimensions*, *Phys. Rev. D* **49** (1994) 6836–6848, [hep-th/9402066].

[114] F. Lenz, M. A. Shifman, and M. Thies, *Quantum mechanics of the vacuum state in two-dimensional QCD with adjoint fermions*, *Phys. Rev. D* **51** (1995) 7060–7082, [hep-th/9412113].

[115] E. Katz, G. Marques Tavares, and Y. Xu, *Solving 2D QCD with an adjoint fermion analytically*, *JHEP* **05** (2014) 143, [arXiv:1308.4980].

[116] E. Katz, G. Marques Tavares, and Y. Xu, *A solution of 2D QCD at Finite N using a conformal basis*, arXiv:1405.6727.

[117] A. Cherman, T. Jacobson, Y. Tanizaki, and M. Ünsal, *Anomalies, a mod 2 index, and dynamics of 2d adjoint QCD*, *SciPost Phys.* **8** (2020), no. 5 072, [arXiv:1908.09858].

[118] Z. Komargodski, K. Ohmori, K. Roumpedakis, and S. Seifnashri, *Symmetries and strings of adjoint QCD_2*, *JHEP* **03** (2021) 103, [arXiv:2008.07567].

[119] R. Dempsey, I. R. Klebanov, and S. S. Pufu, *Exact symmetries and threshold states in two-dimensional models for QCD*, *JHEP* **10** (2021) 096, [arXiv:2101.05432].

[120] F. K. Popov, *Supersymmetry in QCD2 coupled to fermions*, *Phys. Rev. D* **105** (2022), no. 7 074005, [arXiv:2202.04017].

[121] R. Dempsey, I. R. Klebanov, L. L. Lin, and S. S. Pufu, *Adjoint Majorana QCD_2 at finite N*, *JHEP* **04** (2023) 107, [arXiv:2210.10895].

[122] R. Dempsey, I. R. Klebanov, S. S. Pufu, and B. T. Søgaard, *Lattice Hamiltonian for Adjoint QCD_2*, arXiv:2311.09334.

[123] D. J. Gross, I. R. Klebanov, A. V. Matytsin, and A. V. Smilga, *Screening versus confinement in (1+1)-dimensions*, *Nucl. Phys. B* **461** (1996) 109–130, [hep-th/9511104].

[124] F. Antonuccio and S. Pinsky, *On the transition from confinement to screening in QCD(1+1) coupled to adjoint fermions at finite N*, *Phys. Lett. B* **439** (1998) 142–149, [hep-th/9805188].

[125] S. Dubovsky, *A Simple Worldsheet Black Hole*, *JHEP* **07** (2018) 011, [arXiv:1803.00577].

[126] J. C. Donahue and S. Dubovsky, *Confining Strings, Infinite Statistics and Integrability*, *Phys. Rev. D* **101** (2020), no. 8 081901, [arXiv:1907.07799].

[127] J. C. Donahue and S. Dubovsky, *Classical Integrability of the Zigzag Model*, *Phys. Rev. D* **102** (2020), no. 2 026005, [arXiv:1912.08885].

[128] J. C. Donahue and S. Dubovsky, *Quantization of the zigzag model*, *JHEP* **08** (2022) 047, [arXiv:2202.11746].

[129] M. Asrat, *(1+1)D QCD with heavy adjoint quarks*, *Phys. Rev. D* **107** (2023), no. 10 106022, [arXiv:2212.02162].

[130] C. G. Callan, N. Coote, and D. J. Gross, *Two-dimensional yang-mills theory: A model of quark confinement*, *Phys. Rev. D* **13** (Mar, 1976) 1649–1669.

[131] N. Anand, A. L. Fitzpatrick, E. Katz, and Y. Xin, *Chiral Limit of 2d QCD Revisited with Lightcone Conformal Truncation*, arXiv:2111.00021.

[132] R. Brower, J. Ellis, M. Schmidt, and J. Weis, *Hadron scattering in two-dimensional qcd: (i). formalism and leading order calculations*, *Nuclear Physics B* **128** (1977), no. 1 131–174.

[133] M. Marino and P. Putrov, *ABJM theory as a Fermi gas*, *J. Stat. Mech.* **1203** (2012) P03001, [arXiv:1110.4066].

[134] J. Kallen and M. Marino, *Instanton Effects and Quantum Spectral Curves*, *Annales Henri Poincare* **17** (2016), no. 5 1037–1074, [arXiv:1308.6485].

[135] A. Grassi, Y. Hatsuda, and M. Marino, *Topological strings from quantum mechanics*, 2015.

[136] M. Marino and S. Zakany, *Exact eigenfunctions and the open topological string*, *J. Phys. A* **50** (2017), no. 32 325401, [arXiv:1606.05297].

[137] M. Marino and S. Zakany, *Wavefunctions, integrability, and open strings*, *JHEP* **05** (2019) 014, [arXiv:1706.07402].

[138] A. Litvinov, P. Meshcheriakov, and E. Shestopalov, *Meson mass spectrum in Ising Field Theory*, arXiv:2507.15766.

[139] N. Muskhelishvili, *Singular Integral Equations: Boundary Problems of Function Theory and Their Application to Mathematical Physics*. Dover Books on Mathematics. Dover Publications, 2013.

[140] R. C. Brower, W. L. Spence, and J. H. Weis, *Bound States and Asymptotic Limits for QCD in Two-dimensions*, *Phys. Rev. D* **19** (1979) 3024.

[141] R. Narayanan and H. Neuberger, *The quark mass dependence of the pion mass at infinite n*, *Physics Letters B* **616** (jun, 2005) 76–84.

[142] D. Correa, J. Henn, J. Maldacena, and A. Sever, *The cusp anomalous dimension at three loops and beyond*, *JHEP* **05** (2012) 098, [arXiv:1203.1019].

[143] M. Kim, N. Kiryu, S. Komatsu, and T. Nishimura, *Structure Constants of Defect Changing Operators on the 1/2 BPS Wilson Loop*, *JHEP* **12** (2017) 055, [arXiv:1710.07325].

[144] A. Cavaglià, N. Gromov, and F. Levkovich-Maslyuk, *Quantum spectral curve and structure constants in $\mathcal{N} = 4$ SYM: cusps in the ladder limit*, *JHEP* **10** (2018) 060, [arXiv:1802.04237].

[145] W. Hackbusch, *Integral equations : theory and numerical treatment*, vol. 120 of *International series of numerical mathematics*. Birkhäuser, Basel, 1995.

[146] E. W. Weisstein, "Fredholm integral equation of the second kind. From MathWorld—A Wolfram Web Resource."

[147] J. Kallen and M. Marino, *Instanton Effects and Quantum Spectral Curves*, *Annales Henri Poincare* **17** (2016), no. 5 1037–1074, [arXiv:1308.6485].

[148] A. Zamolodchikov, *Painlevé III and 2d polymers*, *Nuclear Physics B* **432** (dec, 1994) 427–456.

[149] J. Kallen, *The spectral problem of the abj fermi gas*, arXiv:1407.0625.

[150] G. Bonelli, A. Grassi, and A. Tanzini, *Seiberg–Witten theory as a Fermi gas*, *Lett. Math. Phys.* **107** (2017), no. 1 1–30, [arXiv:1603.01174].

[151] P. Fonseca and A. Zamolodchikov, *Ising spectroscopy i: Mesons at $t < t_c$*, 2006.

[152] C. A. Tracy and H. Widom, *Proofs of two conjectures related to the thermodynamic bethe ansatz*, *Communications in Mathematical Physics* **179** (sep, 1996) 667–680.

[153] A. Dhar, G. Mandal, and S. R. Wadia, *String field theory of two dimensional qcd: a realization of w∞ algebra*, *Physics Letters B* **329** (June, 1994) 15–26.

[154] S. Caron-Huot, *Analyticity in Spin in Conformal Theories*, *JHEP* **09** (2017) 078, [arXiv:1703.00278].

[155] I. A. I. A.R., K. V.E., and S. N.A., *Differential equations for quantum correlation function*, *Int. J. Mod. Phys. B4* (1990).

[156] V. E. Korepin, N. M. Bogoliubov, and A. G. Izergin, *Quantum Inverse Scattering Method and Correlation Functions*. Cambridge Monographs on Mathematical Physics. Cambridge University Press, 1993.

[157] A. Zamolodchikov, *On Confining Interactions in 1+1,*, *Conference in Memory of Aliosha Zamolodchikov, Saclay/ENS, 2009*.

[158] P. Dorey and R. Tateo, *Excited states by analytic continuation of TBA equations*, *Nucl. Phys. B* **482** (1996) 639–659, [hep-th/9607167].

[159] N. D. Mermin and H. Wagner, *Absence of ferromagnetism or antiferromagnetism in one-dimensional or two-dimensional isotropic Heisenberg models*, *Phys. Rev. Lett.* **17** (1966) 1133–1136.

[160] S. R. Coleman, *There are no Goldstone bosons in two-dimensions*, *Commun. Math. Phys.* **31** (1973) 259–264.

[161] D. J. Gross and A. Neveu, *Dynamical Symmetry Breaking in Asymptotically Free Field Theories*, *Phys. Rev. D* **10** (1974) 3235.

[162] D. Delmastro, J. Gomis, and M. Yu, *Infrared phases of 2d QCD*, *JHEP* **02** (2023) 157, [arXiv:2108.02202].

[163] I. Affleck, *On the realization of chiral symmetry in (1+1) dimensions*, *Nuclear Physics B* **265** (1986), no. 3 448–468.

[164] W. Krauth and M. Staudacher, *Non-integrability of two-dimensional QCD*, *Physics Letters B* **388** (nov, 1996) 808–812.

[165] M. Abramowitz and I. A. Stegun, *Handbook of Mathematical Functions with Formulas, Graphs, and Mathematical Tables*. Dover, New York, ninth dover printing, tenth gpo printing ed., 1964.

[166] D. Delmastro and J. Gomis, *RG flows in 2d QCD*, *JHEP* **09** (2023) 158, [arXiv:2211.09036].

[167] A. Bourget, D. Rodriguez-Gomez, and J. G. Russo, *A limit for large R-charge correlators in $\mathcal{N} = 2$ theories*, *JHEP* **05** (2018) 074, [arXiv:1803.00580].

[168] G. Arias-Tamargo, D. Rodriguez-Gomez, and J. G. Russo, *The large charge limit of scalar field theories and the Wilson-Fisher fixed point at $\epsilon = 0$*, *JHEP* **10** (2019) 201, [arXiv:1908.11347].

[169] G. Arias-Tamargo, D. Rodriguez-Gomez, and J. G. Russo, *Correlation functions in scalar field theory at large charge*, *JHEP* **01** (2020) 171, [arXiv:1912.01623].

[170] G. Badel, G. Cuomo, A. Monin, and R. Rattazzi, *The Epsilon Expansion Meets Semiclassics*, *JHEP* **11** (2019) 110, [arXiv:1909.01269].

[171] M. Watanabe, *Accessing large global charge via the ϵ-expansion*, *JHEP* **04** (2021) 264, [arXiv:1909.01337].

[172] S. Giombi and J. Hyman, *On the large charge sector in the critical O(N) model at large N*, *JHEP* **09** (2021) 184, [arXiv:2011.11622].

[173] J. a. Caetano, S. Komatsu, and Y. Wang, *Large Charge 't Hooft Limit of $\mathcal{N} = 4$ Super-Yang-Mills*, arXiv:2306.00929.

[174] G. Cuomo, Z. Komargodski, M. Mezei, and A. Raviv-Moshe, *Spin impurities, Wilson lines and semiclassics*, *JHEP* **06** (2022) 112, [arXiv:2202.00040].

[175] O. Aharony, G. Cuomo, Z. Komargodski, M. Mezei, and A. Raviv-Moshe, *Phases of Wilson Lines in Conformal Field Theories*, *Phys. Rev. Lett.* **130** (2023), no. 15 151601, [arXiv:2211.11775].

[176] O. Aharony, G. Cuomo, Z. Komargodski, M. Mezei, and A. Raviv-Moshe, *Phases of Wilson Lines: Conformality and Screening*, arXiv:2310.00045.

[177] D. Rodriguez-Gomez and J. G. Russo, *Wilson loops in large symmetric representations through a double-scaling limit*, *JHEP* **08** (2022) 253, [arXiv:2206.09935].

[178] M. Beccaria, S. Giombi, and A. A. Tseytlin, *Wilson loop in general representation and RG flow in 1D defect QFT*, *J. Phys. A* **55** (2022), no. 25 255401, [arXiv:2202.00028].

[179] D. Rodriguez-Gomez and J. G. Russo, *Defects in scalar field theories, RG flows and dimensional disentangling*, *JHEP* **11** (2022) 167, [arXiv:2209.00663].

[180] I. Carreño Bolla, D. Rodriguez-Gomez, and J. G. Russo, *RG flows and stability in defect field theories*, *JHEP* **05** (2023) 105, [arXiv:2303.01935].

[181] C. M. Bender and S. Boettcher, *Real spectra in non-hermitian hamiltonians having pt symmetry*, *Physical Review Letters* **80** (jun, 1998) 5243–5246.

[182] C. M. Bender, *Introduction to pt-symmetric quantum theory*, *Contemporary Physics* **46** (jul, 2005) 277–292.

[183] C. M. Bender, D. C. Brody, and H. F. Jones, *Extension of PT symmetric quantum mechanics to quantum field theory with cubic interaction*, *Phys. Rev. D* **70** (2004) 025001, [hep-th/0402183]. [Erratum: Phys.Rev.D 71, 049901 (2005)].

[184] M. Lencsés, A. Miscioscia, G. Mussardo, and G. Takács, *Multicriticality in Yang-Lee edge singularity*, *JHEP* **02** (2023) 046, [arXiv:2211.01123].

[185] M. Lencsés, A. Miscioscia, G. Mussardo, and G. Takács, *$\mathcal{PT}$ breaking and RG flows between multicritical Yang-Lee fixed points*, *JHEP* **09** (2023) 052, [arXiv:2304.08522].

[186] M. Lencsés, A. Miscioscia, G. Mussardo, and G. Takács, *Ginzburg-Landau description for multicritical Yang-Lee models*, arXiv:2404.06100.

[187] R. J. Eden, P. V. Landshoff, D. I. Olive, and J. C. Polkinghorne, *The analytic S-matrix*. Cambridge Univ. Press, Cambridge, 1966.

[188] I. Pesando, *Generalized QCD in two-dimensions via the bilocal method*, *Mod. Phys. Lett. A* **9** (1994) 2927–2936, [hep-th/9408018].

[189] A. DHAR, G. MANDAL, and S. R. WADIA, *$W\infty$ coherent states and path-integral derivation of bosonization of non-relativistic fermions in one dimension*, *Modern Physics Letters A* **08** (Dec., 1993) 3557–3568.

[190] B. Gabai, D. Mazáč, A. Shieber, P. Vieira, and Y. Zhou, *No Particle Production in Two Dimensions: Recursion Relations and Multi-Regge Limit*, *JHEP* **02** (2019) 094, [arXiv:1803.03578].

[191] I. V. Kochergin, *$1/N$ Corrections in QCD_2: Small Mass Limit and Threshold States*, arXiv:2405.04031.

[192] C. Cordova, D. García-Sepúlveda, and N. Holfester, *Particle-Soliton Degeneracy in 2D Quantum Chromodynamics*, arXiv:2412.21153.

[193] R. Dempsey, S. S. Pufu, B. T. Søgaard, and I. R. Klebanov, *More About the Lattice Hamiltonian for Adjoint QCD_2*, arXiv:2409.19164.

[194] I. R. Klebanov, S. S. Pufu, B. Søgaard, and E. Witten, *Supercurrents and (Partial) Supersymmetry in Adjoint QCD_2 and Its Generalizations*, arXiv:2507.17138.

[195] A. B. Zamolodchikov, *'FISHNET' DIAGRAMS AS A COMPLETELY INTEGRABLE SYSTEM*, *Phys. Lett. B* **97** (1980) 63–66.

[196] O. Gürdoğan and V. Kazakov, *New Integrable 4D Quantum Field Theories from Strongly Deformed Planar $\mathcal{N} = 4$ Supersymmetric Yang-Mills Theory*, *Phys. Rev. Lett.* **117** (2016), no. 20 201602, [arXiv:1512.06704]. [Addendum: Phys.Rev.Lett. 117, 259903 (2016)].

[197] J. a. Caetano, O. Gürdoğan, and V. Kazakov, *Chiral limit of $\mathcal{N} = 4$ SYM and ABJM and integrable Feynman graphs*, *JHEP* **03** (2018) 077, [arXiv:1612.05895].

[198] D. Kutasov, *Two-dimensional qcd coupled to adjoint matter and string theory*, *Nuclear Physics B* **414** (Feb., 1994) 33–52.

[199] A. Homrich, D. Simmons-Duffin, and P. Vieira, *Light-Ray Wave Functions and Integrability*, arXiv:2409.02160.

[200] S. E. Derkachov, G. P. Korchemsky, and A. N. Manashov, *Separation of variables for the quantum SL(2,R) spin chain*, *JHEP* **07** (2003) 047, [hep-th/0210216].

[201] C.-M. Chang, Y.-H. Lin, S.-H. Shao, Y. Wang, and X. Yin, *Topological Defect Lines and Renormalization Group Flows in Two Dimensions*, *JHEP* **01** (2019) 026, [arXiv:1802.04445].

[202] J. Frohlich, J. Fuchs, I. Runkel, and C. Schweigert, *Kramers-Wannier duality from conformal defects*, *Phys. Rev. Lett.* **93** (2004) 070601, [cond-mat/0404051].

[203] J. Fuchs, M. R. Gaberdiel, I. Runkel, and C. Schweigert, *Topological defects for the free boson CFT*, *J. Phys. A* **40** (2007) 11403, [arXiv:0705.3129].

[204] D. Aasen, P. Fendley, and R. S. K. Mong, *Topological Defects on the Lattice: Dualities and Degeneracies*, arXiv:2008.08598.

[205] C. Copetti, L. Cordova, and S. Komatsu, *S-Matrix Bootstrap and Non-Invertible Symmetries*, arXiv:2408.13132.

[206] C. Copetti, L. Cordova, and S. Komatsu, *Noninvertible Symmetries, Anomalies, and Scattering Amplitudes*, *Phys. Rev. Lett.* **133** (2024), no. 18 181601, [arXiv:2403.04835].

[207] C. Cordova, D. García-Sepúlveda, and N. Holfester, *Particle-soliton degeneracies from spontaneously broken non-invertible symmetry*, 2024.

[208] A. Antunes and C. Behan, *Coupled minimal models revisited II: Constraints from permutation symmetry*, arXiv:2412.21107.

[209] A. Antunes and J. Rong, *Irrational CFTs from coupled anyon chains with non-invertible symmetries?*, arXiv:2507.14280.

[210] S. Fredenhagen, M. R. Gaberdiel, and C. Schmidt-Colinet, *Bulk flows in Virasoro minimal models with boundaries*, *J. Phys. A* **42** (2009), no. 49 495403, [arXiv:0907.2560].

[211] D. Gaiotto, *Domain Walls for Two-Dimensional Renormalization Group Flows*, *JHEP* **12** (2012) 103, [arXiv:1201.0767].

[212] L. Bhardwaj, L. E. Bottini, D. Pajer, and S. Schäfer-Nameki, *Gapped Phases with Non-Invertible Symmetries: (1+1)d*, *SciPost Phys.* **18** (2025) 032, [arXiv:2310.03784].

[213] C. Cordova, D. García-Sepúlveda, and N. Holfester, *Particle-soliton degeneracies from spontaneously broken non-invertible symmetry*, *JHEP* **07** (2024) 154, [arXiv:2403.08883].

[214] V. Benedetti, H. Casini, and J. M. Magan, *Selection rules for RG flows of minimal models*, arXiv:2412.16587.

[215] O. Delouche, J. Elias Miro, and J. Ingoldby, *Testing the RG-flow* $M(3,10)+\phi_{1,7}\to M(3,8)$ *with Hamiltonian Truncation*, arXiv:2412.09295.

[216] A. Katsevich, *The spectrum of perturbed (3, 10) minimal model*, arXiv:2410.18069.

[217] A. Katsevich, I. R. Klebanov, and Z. Sun, *Ginzburg-Landau description of a class of non-unitary minimal models*, arXiv:2410.11714.

[218] A. Antunes and C. Behan, *Coupled Minimal Conformal Field Theory Models Revisited*, *Phys. Rev. Lett.* **130** (2023), no. 7 071602, [arXiv:2211.16503].

[219] K. Kikuchi, *RG flows from WZW models*, arXiv:2212.13851.

[220] K. Kikuchi, *Rational RG flow, extension, and Witt class*, arXiv:2412.08935.

[221] A. B. Zamolodchikov and A. B. Zamolodchikov, *Factorized s Matrices in Two-Dimensions as the Exact Solutions of Certain Relativistic Quantum Field Models*, *Annals Phys.* **120** (1979) 253–291.

[222] V. A. Fateev and A. B. Zamolodchikov, *Conformal field theory and purely elastic S matrices*, *Int. J. Mod. Phys. A* **5** (1990) 1025–1048.

[223] P. Dorey, *Exact S matrices*, in *Eotvos Summer School in Physics: Conformal Field Theories and Integrable Models*, pp. 85–125, 8, 1996. hep-th/9810026.

[224] A. B. Zamolodchikov, *Thermodynamic Bethe Ansatz in Relativistic Models. Scaling Three State Potts and Lee-yang Models*, *Nucl. Phys. B* **342** (1990) 695–720.

[225] C. Destri and H. J. De Vega, *Unified approach to thermodynamic Bethe Ansatz and finite size corrections for lattice models and field theories*, *Nucl. Phys. B* **438** (1995) 413–454, [hep-th/9407117].

[226] A. Klumper, M. T. Batchelor, and P. A. Pearce, *Central charges of the 6- and 19-vertex models with twisted boundary conditions*, *J. Phys. A* **24** (1991) 3111.

[227] M. J. Martins, *Renormalization group trajectories from resonance factorized S matrices*, *Phys. Rev. Lett.* **69** (1992) 2461–2464, [hep-th/9205024].

[228] M. J. Martins, *Exact resonance A-D-E S matrices and their renormalization group trajectories*, *Nucl. Phys. B* **394** (1993) 339–355, [hep-th/9208011].

[229] A. B. Zamolodchikov, *Thermodynamics of imaginary coupled sine-Gordon: Dense polymer finite size scaling function*, *Phys. Lett. B* **335** (1994) 436–443.

[230] D. Fioravanti, A. Mariottini, E. Quattrini, and F. Ravanini, *Excited state Destri-De Vega equation for Sine-Gordon and restricted Sine-Gordon models*, *Phys. Lett. B* **390** (1997) 243–251, [hep-th/9608091].

[231] G. Feverati, F. Ravanini, and G. Takacs, *Nonlinear integral equation and finite volume spectrum of minimal models perturbed by $\phi_{(1,3)}$*, *Nucl. Phys. B* **570** (2000) 615–643, [hep-th/9909031].

[232] P. Fendley, H. Saleur, and A. B. Zamolodchikov, *Massless flows. 1. The Sine-Gordon and O(n) models*, *Int. J. Mod. Phys. A* **8** (1993) 5717–5750, [hep-th/9304050].

[233] P. Fendley, H. Saleur, and A. B. Zamolodchikov, *Massless flows, 2. The Exact S matrix approach*, *Int. J. Mod. Phys. A* **8** (1993) 5751–5778, [hep-th/9304051].

[234] P. Dorey, C. Dunning, and R. Tateo, *New families of flows between two-dimensional conformal field theories*, *Nucl. Phys. B* **578** (2000) 699–727, [hep-th/0001185].

[235] V. P. Yurov and A. B. Zamolodchikov, *TRUNCATED CONFORMAL SPACE APPROACH TO SCALING LEE-YANG MODEL*, *Int. J. Mod. Phys. A* **5** (1990) 3221–3246.

[236] C. Cordova, N. Holfester, and K. Ohmori, *Representation Theory of Solitons*, arXiv:2408.11045.

[237] O. A. Castro-Alvaredo, B. Doyon, and F. Ravanini, *Irreversibility of the renormalization group flow in non-unitary quantum field theory*, *J. Phys. A* **50** (2017), no. 42 424002, [arXiv:1706.01871].

[238] A. B. Zamolodchikov, *Irreversibility of the Flux of the Renormalization Group in a 2D Field Theory*, *JETP Lett.* **43** (1986) 730–732.

[239] F. A. Smirnov, *Exact S matrices for phi(1,2) perturbated minimal models of conformal field theory*, *Int. J. Mod. Phys. A* **6** (1991) 1407–1428.

[240] A. B. Zamolodchikov, *Renormalization Group and Perturbation Theory Near Fixed Points in Two-Dimensional Field Theory*, *Sov. J. Nucl. Phys.* **46** (1987) 1090.

[241] F. A. Smirnov, *The Perturbated $C < 1$ Conformal Field Theories as Reductions of Sine-Gordon Model*, *Int. J. Mod. Phys. A* **4** (1989) 4213–4220.

[242] A. LeClair, *Restricted Sine-Gordon Theory and the Minimal Conformal Series*, *Phys. Lett. B* **230** (1989) 103–107.

[243] F. A. Smirnov, *Reductions of the sine-Gordon model as a perturbation of minimal models of conformal field theory*, *Nucl. Phys. B* **337** (1990) 156–180.

[244] M. J. Martins, *Constructing a S matrix from the truncated conformal approach data*, *Phys. Lett. B* **262** (1991) 39–42.

[245] C. J. Efthimiou, *Quantum group symmetry for the Phi(12) perturbed and Phi(21) perturbed minimal models of conformal field theory*, *Nucl. Phys. B* **398** (1993) 697–740.

[246] G. Takacs, *A New RSOS restriction of the Zhiber-Mikhailov-Shabat model and phi (1,5) perturbations of nonunitary minimal models*, *Nucl. Phys. B* **489** (1997) 532–556, [hep-th/9604098].

[247] J. L. Cardy, *Operator Content of Two-Dimensional Conformally Invariant Theories*, *Nucl. Phys. B* **270** (1986) 186–204.

[248] A. B. Zamolodchikov, *Painleve III and 2-d polymers*, *Nucl. Phys. B* **432** (1994) 427–456, [hep-th/9409108].

[249] T. R. Klassen and E. Melzer, *The Thermodynamics of purely elastic scattering theories and conformal perturbation theory*, *Nucl. Phys. B* **350** (1991) 635–689.

[250] A. B. Zamolodchikov, *Thermodynamic Bethe ansatz for RSOS scattering theories*, *Nucl. Phys. B* **358** (1991) 497–523.

[251] L. Fei, S. Giombi, I. R. Klebanov, and G. Tarnopolsky, *Three loop analysis of the critical O(N) models in 6-ε dimensions*, *Phys. Rev. D* **91** (2015), no. 4 045011, [arXiv:1411.1099].

[252] I. R. Klebanov, V. Narovlansky, Z. Sun, and G. Tarnopolsky, *Ginzburg-Landau description and emergent supersymmetry of the (3, 8) minimal model*, *JHEP* **02** (2023) 066, [arXiv:2211.07029].

[253] V. V. Bazhanov, S. L. Lukyanov, and A. B. Zamolodchikov, *Integrable structure of conformal field theory, quantum KdV theory and thermodynamic Bethe ansatz*, *Commun. Math. Phys.* **177** (1996) 381–398, [hep-th/9412229].

[254] D. Fioravanti, F. Ravanini, and M. Stanishkov, *Generalized KdV and quantum inverse scattering description of conformal minimal models*, *Phys. Lett. B* **367** (1996) 113–120, [hep-th/9510047].

[255] V. V. Bazhanov, S. L. Lukyanov, and A. B. Zamolodchikov, *Integrable structure of conformal field theory. 2. Q operator and DDV equation*, *Commun. Math. Phys.* **190** (1997) 247–278, [hep-th/9604044].

[256] V. V. Bazhanov, S. L. Lukyanov, and A. B. Zamolodchikov, *Integrable quantum field theories in finite volume: Excited state energies*, *Nucl. Phys. B* **489** (1997) 487–531, [hep-th/9607099].

[257] V. V. Bazhanov, A. N. Hibberd, and S. M. Khoroshkin, *Integrable structure of W(3) conformal field theory, quantum Boussinesq theory and boundary affine Toda theory*, *Nucl. Phys. B* **622** (2002) 475–547, [hep-th/0105177].

[258] M. Lüscher, *Quantum Nonlocal Charges and Absence of Particle Production in the Two-Dimensional Nonlinear Sigma Model*, *Nucl. Phys. B* **135** (1978) 1–19.

[259] A. B. Zamolodchikov, *Fractional spin integrals of motion in perturbed conformal field theory*, in *CCAST Symposium / Workshop on Fields, Strings and Quantum Gravity*, pp. 349–372, 1989.

[260] D. Bernard and A. Leclair, *Quantum group symmetries and nonlocal currents in 2-D QFT*, *Commun. Math. Phys.* **142** (1991) 99–138.

[261] L. Kong, T. Lan, X.-G. Wen, Z.-H. Zhang, and H. Zheng, *Algebraic higher symmetry and categorical symmetry – a holographic and entanglement view of symmetry*, *Phys. Rev. Res.* **2** (2020), no. 4 043086, [arXiv:2005.14178].

[262] D. Gaiotto and J. Kulp, *Orbifold groupoids*, *JHEP* **02** (2021) 132, [arXiv:2008.05960].

[263] F. Apruzzi, F. Bonetti, I. García Etxebarria, S. S. Hosseini, and S. Schäfer-Nameki, *Symmetry TFTs from String Theory*, *Commun. Math. Phys.* **402** (2023), no. 1 895–949, [arXiv:2112.02092].

[264] D. S. Freed, G. W. Moore, and C. Teleman, *Topological symmetry in quantum field theory*, arXiv:2209.07471.

[265] J. Kaidi, K. Ohmori, and Y. Zheng, *Symmetry TFTs for Non-invertible Defects*, *Commun. Math. Phys.* **404** (2023), no. 2 1021–1124, [arXiv:2209.11062].

[266] L. Bhardwaj and S. Schäfer-Nameki, *Generalized Charges, Part II: Non-Invertible Symmetries and the Symmetry TFT*, arXiv:2305.17159.

[267] L. Bhardwaj, L. E. Bottini, L. Fraser-Taliente, L. Gladden, D. S. W. Gould, A. Platschorre, and H. Tillim, *Lectures on generalized symmetries*, *Phys. Rept.* **1051** (2024) 1–87, [arXiv:2307.07547].

[268] N. Carqueville, M. Del Zotto, and I. Runkel, *Topological defects*, in *Encyclopedia of Mathematical Physics (Second Edition)*, vol. 5, pp. 621–647. Academic Press, 2025. arXiv:2311.02449.

[269] G. Felder, J. Fröhlich, J. Fuchs, and C. Schweigert, *Correlation functions and boundary conditions in RCFT and three-dimensional topology*, *Compos. Math.* **131** (2002) 189–237, [hep-th/9912239].

[270] J. Fuchs, I. Runkel, and C. Schweigert, *TFT construction of RCFT correlators 1. Partition functions*, *Nucl. Phys. B* **646** (2002) 353–497, [hep-th/0204148].

[271] I. Romaidis and I. Runkel, *CFT Correlators and Mapping Class Group Averages*, *Commun. Math. Phys.* **405** (2024), no. 10 247, [arXiv:2309.14000].

[272] D. Manolopoulos and I. Runkel, *A Monoidal Category for Perturbed Defects in Conformal Field Theory*, *Commun. Math. Phys.* **295** (2010) 327–362, [arXiv:0904.1122].

[273] V. B. Petkova and J. B. Zuber, *Generalized twisted partition functions*, *Phys. Lett. B* **504** (2001) 157–164, [hep-th/0011021].

[274] A. B. Zamolodchikov, *Integrable field theory from conformal field theory*, *Adv. Stud. Pure Math.* **19** (1989) 641–674.

[275] A. Kapustin and N. Saulina, *Surface operators in 3d Topological Field Theory and 2d Rational Conformal Field Theory*, arXiv:1012.0911.

[276] J. Fuchs, C. Schweigert, and A. Valentino, *Bicategories for boundary conditions and for surface defects in 3-d TFT*, *Commun. Math. Phys.* **321** (2013) 543–575, [arXiv:1203.4568].

[277] N. Carqueville, I. Runkel, and G. Schaumann, *Line and surface defects in Reshetikhin–Turaev TQFT*, *Quantum Topol.* **10** (2018), no. 3 399–439, [arXiv:1710.10214].

[278] V. Koppen, V. Mulevičius, I. Runkel, and C. Schweigert, *Domain Walls Between 3d Phases of Reshetikhin–Turaev TQFTs*, *Commun. Math. Phys.* **396** (2022), no. 3 1187–1220, [arXiv:2105.04613].

[279] R. Konik and A. LeClair, *Purely transmitting defect field theories*, *Nucl. Phys. B* **538** (1999) 587–611, [hep-th/9703085].

[280] C. Bachas and M. R. Gaberdiel, *Loop operators and the kondo problem*, *Journal of High Energy Physics* **2004** (12, 2004) 065, [hep-th/0411067].

[281] M. Kormos, I. Runkel, and G. M. T. Watts, *Defect flows in minimal models*, *JHEP* **11** (2009) 057, [arXiv:0907.1497].

[282] I. Brunner, D. Roggenkamp, and S. Rossi, *Defect Perturbations in Landau-Ginzburg Models*, *JHEP* **03** (2010) 015, [arXiv:0909.0696].

[283] V. S. Dotsenko and V. A. Fateev, *Four Point Correlation Functions and the Operator Algebra in the Two-Dimensional Conformal Invariant Theories with the Central Charge $c < 1$*, *Nucl. Phys. B* **251** (1985) 691–734.

[284] P. Furlan, A. C. Ganchev, and V. B. Petkova, *Fusion Matrices and $C < 1$ (Quasi)local Conformal Theories*, *Int. J. Mod. Phys. A* **5** (1990) 2721–2736. [Erratum: Int.J.Mod.Phys.A 5, 3641 (1990)].

[285] K. Graham, I. Runkel, and G. M. T. Watts, *Minimal model boundary flows and c=1 CFT*, *Nucl. Phys. B* **608** (2001) 527–556, [hep-th/0101187].

[286] I. Runkel, *Boundary structure constants for the A series Virasoro minimal models*, *Nucl. Phys. B* **549** (1999) 563–578, [hep-th/9811178].

[287] T. Quella, I. Runkel, and G. M. T. Watts, *Reflection and transmission for conformal defects*, *JHEP* **04** (2007) 095, [hep-th/0611296].

[288] B. Feigin and E. Frenkel, *Free field resolutions in affine Toda field theories*, *Phys. Lett. B* **276** (1992) 79–86.

[289] A. Milas, M. Penn, and C. Sadowski, *S3-permutation orbifolds of Virasoro vertex algebras*, *J. Pure Appl. Algebra* **227** (2023) 107378.

[290] Z. Bajnok, L. Holló, and G. Watts, *Defect scaling Lee–Yang model from the perturbed DCFT point of view*, *Nucl. Phys. B* **886** (2014) 93–124, [arXiv:1307.4536].

[291] P. Dorey, A. Pocklington, R. Tateo, and G. Watts, *TBA and TCSA with boundaries and excited states*, *Nucl. Phys. B* **525** (1998) 641–663, [hep-th/9712197].

[292] H. Poghosyan and R. Poghossian, *RG flows between W_3 minimal models*, *PoS* **Regio2021** (2022) 039.

[293] D. Delmastro, A. Sharon, and Y. Zheng, *Non-Local Conserved Currents and Continuous Non-Invertible Symmetries*, arXiv:2507.22976.

[294] A. Kuniba, T. Nakanishi, and J. Suzuki, *Functional relations in solvable lattice models. 1: Functional relations and representation theory*, *Int. J. Mod. Phys. A* **9** (1994) 5215–5266, [hep-th/9309137].

[295] A. Konechny, *Open topological defects and boundary RG flows*, *J. Phys. A* **53** (2020), no. 15 155401, [arXiv:1911.06041].

[296] Y.-H. Lin, M. Okada, S. Seifnashri, and Y. Tachikawa, *Asymptotic density of states in 2d CFTs with non-invertible symmetries*, *JHEP* **03** (2023) 094, [arXiv:2208.05495].

[297] T. Bartsch, M. Bullimore, and A. Grigoletto, *Representation theory for categorical symmetries*, arXiv:2305.17165.

[298] C. Córdova, K. Ohmori, S.-H. Shao, and F. Yan, *Decorated $\mathbb{Z}_2$ symmetry defects and their time-reversal anomalies*, *Phys. Rev. D* **102** (2020), no. 4 045019, [arXiv:1910.14046].

[299] H. L. Verlinde, *Conformal Field Theory, 2-D Quantum Gravity and Quantization of Teichmuller Space*, *Nucl. Phys. B* **337** (1990) 652–680.

[300] R. M. Kashaev, *Quantization of teichmüller spaces and the quantum dilogarithm*, 1997.

[301] R. M. Kashaev, *Liouville central charge in quantum Teichmuller theory*, hep-th/9811203.

[302] L. Chekhov and V. V. Fock, *Quantum Teichmuller space*, *Theor. Math. Phys.* **120** (1999) 1245–1259, [math/9908165].

[303] R. M. Kashaev, *On the spectrum of Dehn twists in quantum Teichmuller theory*, math/0008148.

[304] J. Teschner, *On the relation between quantum Liouville theory and the quantized Teichmuller spaces*, *Int. J. Mod. Phys. A* **19S2** (2004) 459–477, [hep-th/0303149].

[305] J. Teschner, *An Analog of a modular functor from quantized teichmuller theory*, math/0510174.

[306] N. Aghaei, M. Pawelkiewicz, and J. Teschner, *Quantisation of super Teichmüller theory*, *Commun. Math. Phys.* **353** (2017), no. 2 597–631, [arXiv:1512.02617].

[307] L. D. Faddeev and R. M. Kashaev, *Quantum Dilogarithm*, *Mod. Phys. Lett. A* **9** (1994) 427–434, [hep-th/9310070].

[308] S. Woronowicz, *Quantum e(2) group and and its pontryagin dual*, *Letters in Mathematical Physics* **23** (Jan., 2025).

[309] S. L. Woronowicz, *Operator equalities related to the quantume(2) group*, *Communications in Mathematical Physics* **144** (Feb, 1992) 417–428.

[310] L. D. Faddeev and L. A. Takhtajan, *On the spectral theory of one functional-difference operator from conformal field theory*, 2014.

[311] D. Gaiotto and H. Verlinde, *SYK-Schur duality: Double scaled SYK correlators from $N = 2$ supersymmetric gauge theory*, arXiv:2409.11551.

[312] E. Witten, *Quantization of Chern-Simons Gauge Theory With Complex Gauge Group*, *Commun. Math. Phys.* **137** (1991) 29–66.

[313] N. Drukker, J. Gomis, T. Okuda, and J. Teschner, *Gauge Theory Loop Operators and Liouville Theory*, *JHEP* **02** (2010) 057, [arXiv:0909.1105].

[314] L. F. Alday, D. Gaiotto, S. Gukov, Y. Tachikawa, and H. Verlinde, *Loop and surface operators in N=2 gauge theory and Liouville modular geometry*, *JHEP* **01** (2010) 113, [arXiv:0909.0945].

[315] N. Nekrasov, V. Pestun, and S. Shatashvili, *Quantum geometry and quiver gauge theories*, *Commun. Math. Phys.* **357** (2018), no. 2 519–567, [arXiv:1312.6689].

[316] J. Teschner, *Quantization of moduli spaces of flat connections and Liouville theory*, in *International Congress of Mathematicians*, 5, 2014. arXiv:1405.0359.

[317] N. Reshetikhin and A. Varchenko, *Quasiclassical asymptotics of solutions to the KZ equations*, hep-th/9402126.

[318] P. T. Gressman and E. M. Stein, *Regularity of the fourier transform on spaces of homogeneous distributions*, *Journal d'Analyse Mathématique* **100** (2006), no. 1 211–222.

[319] E. K. Sklyanin, *Separation of variables in the Gaudin model*, *Zap. Nauchn. Semin.* **164** (1987) 151–169.

[320] I. M. Gelfand and G. E. Shilov, *Generalized Functions, Volume I: Properties and Operations*. Academic Press, New York, 1964.

[321] V. S. Dotsenko, *LECTURES ON CONFORMAL FIELD THEORY*, .

[322] E. Witten, *Monopoles and four manifolds*, *Math. Res. Lett.* **1** (1994) 769–796, [hep-th/9411102].

[323] P. C. Argyres and M. R. Douglas, *New phenomena in SU(3) supersymmetric gauge theory*, *Nucl. Phys. B* **448** (1995) 93–126, [hep-th/9505062].

[324] R. Donagi and E. Witten, *Supersymmetric Yang-Mills theory and integrable systems*, *Nucl. Phys. B* **460** (1996) 299–334, [hep-th/9510101].

[325] N. A. Nekrasov, *Seiberg-Witten prepotential from instanton counting*, *Adv. Theor. Math. Phys.* **7** (2003), no. 5 831–864, [hep-th/0206161].

[326] S. Cecotti and C. Vafa, *BPS Wall Crossing and Topological Strings*, arXiv:0910.2615.

[327] D. Gaiotto, G. W. Moore, and A. Neitzke, *Wall-crossing, Hitchin systems, and the WKB approximation*, *Adv. Math.* **234** (2013) 239–403, [arXiv:0907.3987].

[328] T. Dimofte, S. Gukov, and Y. Soibelman, *Quantum Wall Crossing in N=2 Gauge Theories*, *Lett. Math. Phys.* **95** (2011) 1–25, [arXiv:0912.1346].

[329] D. Gaiotto, G. W. Moore, and A. Neitzke, *Wall-Crossing in Coupled 2d-4d Systems*, *JHEP* **12** (2012) 082, [arXiv:1103.2598].

[330] D. Gaiotto, G. W. Moore, and A. Neitzke, *Four-dimensional wall-crossing via three-dimensional field theory*, *Commun. Math. Phys.* **299** (2010) 163–224, [arXiv:0807.4723].

[331] J. Manschot, B. Pioline, and A. Sen, *Wall Crossing from Boltzmann Black Hole Halos*, *JHEP* **07** (2011) 059, [arXiv:1011.1258].

[332] M. Alim, S. Cecotti, C. Cordova, S. Espahbodi, A. Rastogi, and C. Vafa, *BPS Quivers and Spectra of Complete N=2 Quantum Field Theories*, *Commun. Math. Phys.* **323** (2013) 1185–1227, [arXiv:1109.4941].

[333] A. Kapustin and N. Saulina, *The Algebra of Wilson-'t Hooft operators*, *Nucl. Phys. B* **814** (2009) 327–365, [arXiv:0710.2097].

[334] T. Dimofte, D. Gaiotto, and S. Gukov, *3-Manifolds and 3d Indices*, *Adv. Theor. Math. Phys.* **17** (2013), no. 5 975–1076, [arXiv:1112.5179].

[335] A. Braverman, M. Finkelberg, and H. Nakajima, *Towards a mathematical definition of Coulomb branches of* 3*-dimensional* $\mathcal{N} = 4$ *gauge theories, II*, *Adv. Theor. Math. Phys.* **22** (2018) 1071–1147, [arXiv:1601.03586].

[336] J. Gomis, T. Okuda, and V. Pestun, *Exact Results for 't Hooft Loops in Gauge Theories on* S^4, *JHEP* **05** (2012) 141, [arXiv:1105.2568].

[337] A. Braverman, G. Dhillon, M. Finkelberg, S. Raskin, and R. Travkin, *Coulomb branches of noncotangent type (with appendices by Gurbir Dhillon and Theo Johnson-Freyd)*, arXiv:2201.09475.

[338] M. Kontsevich and Y. Soibelman, *Wall-Crossing Structures in Donaldson–Thomas Invariants, Integrable Systems and Mirror Symmetry*, pp. 197–308. Springer International Publishing, Cham, 2014.

[339] R. M. Kashaev, *Quantization of teichmüller spaces and the quantum dilogarithm*, 1997.

[340] V. V. Fock and A. B. Goncharov, *Cluster x-varieties, amalgamation and poisson-lie groups*, 2006.

[341] V. Fock and A. Goncharov, *The quantum dilogarithm and representations of quantum cluster varieties*, *Inventiones mathematicae* **175** (Sept., 2008) 223–286.

[342] I. LE, *Cluster structures on higher teichmuller spaces for classical groups*, *Forum of Mathematics, Sigma* **7** (2019).

[343] V. V. Fock and A. B. Goncharov, *Moduli spaces of local systems and higher teichmuller theory*, 2006.

[344] V. V. Fock and A. B. Goncharov, *Cluster ensembles, quantization and the dilogarithm*, 2009.

[345] D. Gaiotto, G. W. Moore, A. Neitzke, and F. Yan, *Commuting Line Defects At* $q^N = 1$, arXiv:2307.14429.

[346] S. Fomin and A. Zelevinsky, *Cluster algebras i: Foundations*, 2001.

[347] S. Fomin and A. Zelevinsky, *Cluster algebras ii: Finite type classification*, *Inventiones mathematicae* **154** (May, 2003) 63–121.

[348] S. Fomin and A. Zelevinsky, *Cluster algebras iv: Coefficients*, 2006.

[349] E. Witten, *Solutions of four-dimensional field theories via M-theory*, *Nucl. Phys. B* **500** (1997) 3–42, [hep-th/9703166].

[350] P. Longhi, *The structure of BPS spectra.* PhD thesis, Rutgers U., Piscataway, 2015.

[351] A. Neitzke and F. Yan, *q-nonabelianization for line defects*, *JHEP* **09** (2020) 153, [arXiv:2002.08382].

[352] A. Neitzke and F. Yan, *The quantum UV-IR map for line defects in* $\mathfrak{gl}$*(3)-type class S theories*, *JHEP* **09** (2022) 081, [arXiv:2112.03775].

[353] M. Kontsevich and Y. Soibelman, *Cohomological Hall algebra, exponential Hodge structures and motivic Donaldson-Thomas invariants*, *Commun. Num. Theor. Phys.* **5** (2011) 231–352, [arXiv:1006.2706].

[354] M. Cirafici, *Quivers, Line Defects and Framed BPS Invariants*, *Annales Henri Poincare* **19** (2018), no. 1 1–70, [arXiv:1703.06449].

[355] D. Gaiotto, N. Grygoryev, and W. Li, *Categories of Line Defects and Cohomological Hall Algebras*, arXiv:2406.07134.

[356] B. Davison, *The generic Markov CoHA is not spherically generated*, arXiv:2502.05009.

[357] P. Bousseau, *Holomorphic Floer theory and Donaldson-Thomas invariants*, in *String-Math 2022*, vol. 107 of *Proc. Sympos. Pure Math.*, pp. 45–78. Amer. Math. Soc., Providence, RI, [2024] ©2024.

[358] A. Kapustin, *Holomorphic reduction of N=2 gauge theories, Wilson-'t Hooft operators, and S-duality*, hep-th/0612119.

[359] D. Gaiotto, G. W. Moore, and E. Witten, *Algebra of the Infrared: String Field Theoretic Structures in Massive* $\mathcal{N} = (2,2)$ *Field Theory In Two Dimensions*, arXiv:1506.04087.

[360] S. Cautis and H. Williams, *Canonical bases for coulomb branches of 4d* $\mathcal{N} = 2$ *gauge theories*, 2023.

[361] W. Niu, *Local operators of* $4d\mathcal{N} = 2$ *gauge theories from the affine Grassmannian*, *Adv. Theor. Math. Phys.* **26** (2022), no. 9 3207–3247, [arXiv:2112.12164].

[362] D. Gaiotto, *Sphere quantization of Higgs and Coulomb branches and Analytic Symplectic Duality*, *JHEP* **01** (2025) 188, [arXiv:2307.12396].

[363] D. Gaiotto, J. Hilburn, J. Redondo-Yuste, B. Webster, and Z. Zhou, *Twisted traces on abelian quantum Higgs and Coulomb branches*, arXiv:2308.15198.

[364] S. Cecotti and C. Vafa, *Classification of complete N=2 supersymmetric theories in 4 dimensions*, arXiv:1103.5832.

[365] M. Alim, S. Cecotti, C. Cordova, S. Espahbodi, A. Rastogi, and C. Vafa, $\mathcal{N} = 2$ *quantum field theories and their BPS quivers*, *Adv. Theor. Math. Phys.* **18** (2014), no. 1 27–127, [arXiv:1112.3984].

[366] S.-J. Lee, Z.-L. Wang, and P. Yi, *BPS States, Refined Indices, and Quiver Invariants*, *JHEP* **10** (2012) 094, [arXiv:1207.0821].

[367] M. Gabella, P. Longhi, C. Y. Park, and M. Yamazaki, *BPS Graphs: From Spectral Networks to BPS Quivers*, *JHEP* **07** (2017) 032, [arXiv:1704.04204].

[368] H. Derksen, J. Weyman, and A. Zelevinsky, *Quivers with potentials and their representations i: Mutations*, 2008.

[369] M. Cirafici, *Line defects and (framed) BPS quivers*, *JHEP* **11** (2013) 141, [arXiv:1307.7134].

[370] S. Cecotti and M. Del Zotto, *Y systems, Q systems, and 4D* $\mathcal{N} = 2$ *supersymmetric QFT*, *J. Phys. A* **47** (2014), no. 47 474001, [arXiv:1403.7613].

[371] S. Cecotti, A. Neitzke, and C. Vafa, *R-Twisting and 4d/2d Correspondences*, arXiv:1006.3435.

[372] B. Keller, *On cluster theory and quantum dilogarithm identities*, 2011.

[373] T. Dimofte, D. Gaiotto, and R. van der Veen, *RG Domain Walls and Hybrid Triangulations*, *Adv. Theor. Math. Phys.* **19** (2015) 137–276, [arXiv:1304.6721].

[374] Y. Imamura and S. Yokoyama, *Index for three dimensional superconformal field theories with general R-charge assignments*, *JHEP* **04** (2011) 007, [arXiv:1101.0557].

[375] N. Hama, K. Hosomichi, and S. Lee, *SUSY Gauge Theories on Squashed Three-Spheres*, *JHEP* **05** (2011) 014, [arXiv:1102.4716].

[376] T. Dimofte, D. Gaiotto, and S. Gukov, *Gauge Theories Labelled by Three-Manifolds*, *Commun. Math. Phys.* **325** (2014) 367–419, [arXiv:1108.4389].

[377] M. Bullimore, T. Dimofte, and D. Gaiotto, *The Coulomb Branch of 3d* $\mathcal{N} = 4$ *Theories*, *Commun. Math. Phys.* **354** (2017), no. 2 671–751, [arXiv:1503.04817].

[378] S. Cecotti and M. Del Zotto, *Half-Hypers and Quivers*, *JHEP* **09** (2012) 135, [arXiv:1207.2275].

[379] S. Cecotti and M. Del Zotto, *4d N=2 Gauge Theories and Quivers: the Non-Simply Laced Case*, *JHEP* **10** (2012) 190, [arXiv:1207.7205].

[380] S. Cecotti, *The quiver approach to the BPS spectrum of a 4d N=2 gauge theory*, *Proc. Symp. Pure Math.* **90** (2015) 3–18, [arXiv:1212.3431].

[381] P. Longhi, *Wall-Crossing Invariants from Spectral Networks*, *Annales Henri Poincare* **19** (2018), no. 3 775–842, [arXiv:1611.00150].

[382] T. Ishibashi, *Cyclic quantum teichmüller theory*, 2025.

[383] S. Collier, L. Eberhardt, and B. Mühlmann, *The complex Liouville string: the gravitational path integral*, arXiv:2501.10265.

[384] S. Collier, L. Eberhardt, B. Mühlmann, and V. A. Rodriguez, *The complex Liouville string*, arXiv:2409.17246.

[385] D. Gaiotto, G. W. Moore, and A. Neitzke, *Spectral networks*, *Annales Henri Poincare* **14** (2013) 1643–1731, [arXiv:1204.4824].

[386] A. Jacobs, *The quantum e(2) group*, 2005-11-09.

[387] S. Ribault, *On sl(3) Knizhnik-Zamolodchikov equations and W(3) null-vector equations*, *JHEP* **10** (2009) 002, [arXiv:0811.4587].

[388] Y. Hikida and V. Schomerus, *H+(3) WZNW model from Liouville field theory*, *JHEP* **10** (2007) 064, [arXiv:0706.1030].

[389] D. Dinh and J. Teschner, *Classical limit of the geometric Langlands correspondence for* $SL(2,\mathbb{C})$, arXiv:2312.13393.

[390] E. Witten, *(2+1)-Dimensional Gravity as an Exactly Soluble System*, *Nucl. Phys. B* **311** (1988) 46.

[391] S. Collier, L. Eberhardt, B. Mühlmann, and V. A. Rodriguez, *The complex Liouville string: the worldsheet*, arXiv:2409.18759.

[392] S. Collier, L. Eberhardt, B. Mühlmann, and V. A. Rodriguez, *The complex Liouville string: worldsheet boundaries and non-perturbative effects*, arXiv:2410.09179.

[393] S. Collier, L. Eberhardt, B. Mühlmann, and V. A. Rodriguez, *The complex Liouville string: the matrix integral*, *SciPost Phys.* **18** (2025) 154, [arXiv:2410.07345].

[394] S. Collier, L. Eberhardt, and B. Mühlmann, *A microscopic realization of* dS_3, *SciPost Phys.* **18** (2025), no. 4 131, [arXiv:2501.01486].

[395] O. Lewis, M. Mezei, M. Sacchi, and S. Schafer-Nameki, *Schur Connections: Chord Counting, Line Operators, and Indices*, arXiv:2506.17384.

[396] M. Berkooz, T. Kukolj, and J. Seitz, *Comments on Class S(YK)*, arXiv:2507.12524.

[397] H. W. Lin and D. Stanford, *A symmetry algebra in double-scaled SYK*, *SciPost Phys.* **15** (2023), no. 6 234, [arXiv:2307.15725].

[398] J. Teschner, *Liouville theory revisited*, *Class. Quant. Grav.* **18** (2001) R153–R222, [hep-th/0104158].

[399] Y. Nakayama, *Liouville field theory: A Decade after the revolution*, *Int. J. Mod. Phys. A* **19** (2004) 2771–2930, [hep-th/0402009].

[400] J. Teschner, *On structure constants and fusion rules in the SL(2,C) / SU(2) WZNW model*, *Nucl. Phys. B* **546** (1999) 390–422, [hep-th/9712256].

[401] H. Dorn and H. J. Otto, *Two and three point functions in Liouville theory*, *Nucl. Phys. B* **429** (1994) 375–388, [hep-th/9403141].

[402] A. B. Zamolodchikov and A. B. Zamolodchikov, *Structure constants and conformal bootstrap in Liouville field theory*, *Nucl. Phys. B* **477** (1996) 577–605, [hep-th/9506136].